Forensic Medicine of the Lower Extremity

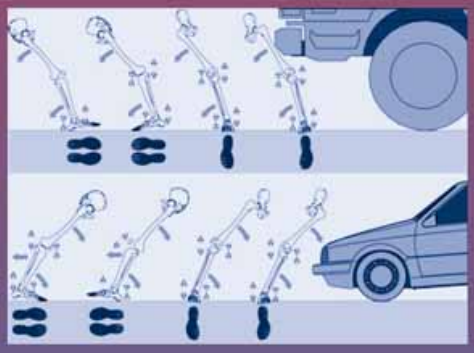

Human Identification and Trauma Analysis of the Thigh, Leg, and Foot

EDITED BY

JEREMY RICH, DPM

DOROTHY E. DEAN, MD

ROBERT H. POWERS, PhD

HUMANA PRESS

Forensic Medicine of the Lower Extremity

FORENSIC SCIENCE AND MEDICINE

Steven B. Karch, MD, SERIES EDITOR

FORENSIC MEDICINE OF THE LOWER EXTREMITY: *HUMAN IDENTIFICATION AND TRAUMA ANALYSIS OF THE THIGH, LEG, AND FOOT,*
edited by ***Jeremy Rich, Dorothy E. Dean, and Robert H. Powers,*** *2005*

FORENSIC AND CLINICAL APPLICATIONS OF SOLID PHASE EXTRACTION,
by ***Michael J. Telepchak, Thomas F. August, and Glynn Chaney,*** *2004*

HANDBOOK OF DRUG INTERACTIONS: *A CLINICAL AND FORENSIC GUIDE,*
edited by ***Ashraf Mozayani and Lionel P. Raymon,*** *2004*

DIETARY SUPPLEMENTS: *TOXICOLOGY AND CLINICAL PHARMACOLOGY,*
edited by ***Melanie Johns Cupp and Timothy S. Tracy,*** *2003*

BUPRENOPHINE THERAPY OF OPIATE ADDICTION,
edited by ***Pascal Kintz and Pierre Marquet,*** *2002*

BENZODIAZEPINES AND GHB: *DETECTION AND PHARMACOLOGY,*
edited by ***Salvatore J. Salamone,*** *2002*

ON-SITE DRUG TESTING,
edited by ***Amanda J. Jenkins and Bruce A. Goldberger,*** *2001*

BRAIN IMAGING IN SUBSTANCE ABUSE: *RESEARCH, CLINICAL, AND FORENSIC APPLICATIONS,*
edited by ***Marc J. Kaufman,*** *2001*

TOXICOLOGY AND CLINICAL PHARMACOLOGY OF HERBAL PRODUCTS,
edited by ***Melanie Johns Cupp,*** *2000*

CRIMINAL POISONING: *INVESTIGATIONAL GUIDE FOR LAW ENFORCEMENT, TOXICOLOGISTS, FORENSIC SCIENTISTS, AND ATTORNEYS,*
by ***John H. Trestrail, III,*** *2000*

A PHYSICIAN'S GUIDE TO CLINICAL FORENSIC MEDICINE,
edited by ***Margaret M. Stark,*** *2000*

Forensic Medicine of the Lower Extremity

Human Identification and Trauma Analysis of the Thigh, Leg, and Foot

Edited by

Jeremy Rich, DPM
Department of Medicine, Brigham and Women's Hospital, Harvard Medical School, Boston, MA

Dorothy E. Dean, MD
Office of the Medical Examiner, County of Summit, Akron, OH

Robert H. Powers, PhD
Division of Scientific Services, Controlled Substances/Toxicology Laboratory, Connecticut Department of Public Safety, Hartford, CT

Foreword by

Kathleen J. Reichs, PhD, DABFA
Office of the Chief Medical Examiner, Chapel Hill, NC and Laboratoire des Sciences Judiciaires et de Médecine Légale, Quebec, Canada

Humana Press
Totowa, New Jersey

999 Riverview Drive, Suite 208
Totowa, New Jersey 07512

www.humanapress.com

Production Editor: Nicole E. Furia
Cover design by Patricia F. Cleary
Cover Illustration: Figures 23 and 29 from Chapter 10, "Injuries of the Thigh, Knee, and Ankle as Reconstructive Factors in Road Traffic Accidents," by Grzegorz Teresinski.

For additional copies, pricing for bulk purchases, and/or information about other Humana titles, contact Humana at the above address or at any of the following numbers: Tel.: 973-256-1699; Fax: 973-256-8341; E-mail: humana@humanapr.com or visit our website: http://humanapress.com

This publication is printed on acid-free paper. ♾
ANSI Z39.48-1984 (American National Standards Institute) Permanence of Paper for Printed Library Materials.

Printed in the United States of America. 10 9 8 7 6 5 4 3 2 1

eISBN 1-59259-897-8

Library of Congress Cataloging-in-Publication Data

Forensic medicine of the lower extremity : human identification and trauma analysis of the thigh, leg, and foot / edited by Jeremy Rich, Dorothy E. Dean, Robert H. Powers ; foreword by Kathleen Reichs.
p. cm.
Includes bibliographical references and index.
ISBN 1-58829-269-X (alk. paper)
1. Forensic osteology. 2. Leg. I. Rich, Jeremy II. Dean, Dorothy E. III. Powers, Robert H.
RA1059.F675 2005
614'.17--dc22

2004017442

Foreword

Publius Syrus stated back in 42 B.C.,

"You cannot put the same shoe on every foot." (Maxim 596)

Though written long before the advent of forensic science, Syrus' maxim summarizes the theme of *Forensic Medicine of the Lower Extremity: Human Identification and Trauma Analysis of the Thigh, Leg, and Foot*.

Put simply, the lower extremity is a tremendously variable anatomic region. This variation is beneficial to forensic experts. Differences in the leg and foot can be used to establish individual identity. Analysis of damage to the lower limb can be used to reconstruct antemortem, perimortem, and postmortem trauma.

As a forensic anthropologist, I analyze cases involving decomposed, burned, mummified, mutilated, and skeletal remains. Many of the corpses I examine are incomplete. Occasionally, I receive nothing but the legs and feet; a lower torso dragged from a river; a foot recovered in a city park; dismembered drug dealers in plastic bags; victims of bombings and airline disasters; and the dead commingled in common graves.

Though the leg and foot contain much that is useful in forensic analysis, before this publication, investigators faced a twofold problem. Little research that focused on the lower extremity was available in the literature, and the existing research was published in diverse sources, making its location and synthesis a daunting task.

Recognizing this difficulty, Jeremy Rich, Dorothy E. Dean, and Robert H. Powers brought together into one volume articles addressing a broad range of topics specific to the forensic examination of the lower limb. Each chapter deals with a technique or research area in terms of methodology, reliability, and interpretive import.

Included in these chapters are descriptions of the biochemical events of decomposition; discussions of osteology, emphasizing the implications of skeletal anatomy for age, sex, race, and height estimation; and extensive outlines of the role of radiology. They also include thorough explorations of trauma analysis and reconstruction, including details on such specialty areas as slip-and-fall incidents, and impact, traffic, and pediatric injuries, as well as considerations of foot and footprint identification.

As an active practitioner, I greet the publication of this volume with thankful appreciation. *Forensic Medicine of the Lower Extremity: Human Identification and Trauma Analysis of the Thigh, Leg, and Foot* will simplify my task. The book is, appropriately, a major step forward.

Kathleen J. Reichs, ***PhD, DABFA***

Preface

There remains a paucity of text literature regarding forensic implications of the lower extremity. *Forensic Medicine of the Lower Extremity: Human Identification and Trauma Analysis of the Thigh, Leg, and Foot* encompasses human identification, biomechanics, trauma analysis, and new areas for potential forensic research with regard to the thigh, knee, leg, ankle, and foot. Initially, the reader may question what makes the lower extremity different enough from other anatomic regions that it merits a separate text. Simply put, the lower extremity can provide a plethora of forensically useful information from an identification and biomechanical perspective.

The anatomic regions used for identification may include the dentition, skull, lumbar spine, and pelvis. If the remains are from an isolated body part as may be frequently encountered in violent deaths, mass disasters, and/or cases of human rights abuse including torture, the task of positive identification and trauma analysis may represent a significant and daunting task for forensic experts. Moreover, the aforementioned anatomic regions may be unavailable or too destroyed to be of forensic value.

Forensic Medicine of the Lower Extremity: Human Identification and Trauma Analysis of the Thigh, Leg, and Foot focuses on the use of the lower extremity to facilitate the identification of decomposed, mutilated, incinerated, and/or fragmented human remains. Additionally, trauma analysis is discussed with an emphasis on accident reconstruction and the biomechanics underlying the trauma from both a theoretical and practical perspective. The book is meant not as an all-inclusive discussion of forensic aspects of the lower extremity, but rather as a treatise on topics specific to the potential of this region relative to investigations involving human identification and trauma analysis. Areas for future research are presented, and each chapter is followed by references for further study.

Forensic Medicine of the Lower Extremity: Human Identification and Trauma Analysis of the Thigh, Leg, and Foot is divided into three parts. Part I of the text lays the groundwork for the applied forensic processes detailed in later chapters. The biochemical decomposition processes of human remains are discussed to help develop a greater appreciation of the mechanistic events surrounding a death scene. Perhaps the most challenging task of the forensic team is the positive identification of the remains. A discussion of human development, skeletal variations, and forensic analysis is included. Forensic radiology is explored, with emphasis on the use of radiographs to facilitate

identification and evaluate trauma. This section also discusses the practical aspects and processes of identification from the lower extremity.

Part II focuses on ante- and postmortem processes that can produce identifiable markers in the remains. Soft tissue and skeletal injuries and their implications for accident investigation and reconstruction are reviewed. A discussion of the physics of skeletal trauma is also presented. These chapters translate the theoretical considerations of the preceding chapters into practical information relevant to clinical observation and/or forensic inference.

Part III discusses case studies involving the foot and ankle and presents potential areas of investigation that may offer promise in medicolegal contexts. Specific identification processes and ongoing research are reviewed including the forensic potential of feet and footwear and barefoot impression evidence.

Forensic Medicine of the Lower Extremity: Human Identification and Trauma Analysis of the Thigh, Leg, and Foot serves as a comprehensive review of both the theoretical and practical aspects of the lower limb for the forensic expert. The readership may include physicians, physical anthropologists, engineers, and criminalists, along with other forensic investigators.

We are indebted to all the authors who contributed to this text. It was a privilege to have worked with such a distinguished group. The editors and authors also extend their appreciation to Nicole Furia, Elyse O'Grady, and the staff at Humana Press for assisting in the preparation of this book.

Jeremy Rich, ***DPM***
Dorothy E. Dean, ***MD***
Robert H. Powers, ***PhD***

Contents

Foreword v
Preface vi
Contributors xi

PART I ANALYSIS, DEVELOPMENT, AND IDENTIFICATION MARKERS

Chapter 1: The Decomposition of Human Remains:
A Biochemical Perspective 3
Robert H. Powers

Chapter 2: Forensically Significant Skeletal Anatomy 17
Nancy E. Tatarek and Dorothy E. Dean

Chapter 3: Normal Osteology of the Knee Joint and Markers
of Stress and Injury 33
Emily A. Craig

Chapter 4: Anthropological Analysis of the Lower Extremity:
Determining Sex, Race, and Stature From Skeletal Elements 69
Nancy E. Tatarek and Paul W. Sciulli

Chapter 5: Estimating Age at Death 99
Douglas H. Ubelaker

Chapter 6: Radiology of the Lower Extremity 113
B. G. Brogdon

PART II TRAUMA ANALYSIS AND RECONSTRUCTION

Chapter 7: Injuries to Children: *A Surgeon's Perspective* 241
Jonathan I. Groner

Chapter 8: Skeletal Trauma Analysis of the Lower Extremity 253
Alison Galloway and Lauren Zephro

Chapter 9: Biomechanics of Impact Injury 279
David J. Porta

Chapter 10: Injuries of the Thigh, Knee, and Ankle as Reconstructive Factors in Road Traffic Accidents 311
Grzegorz Teresiński

Chapter 11: Biomechanical Analysis of Slip, Trip, and Fall Accidents 343
Scott D. Batterman and Steven C. Batterman

PART III FOOT IDENTIFICATION CASE STUDIES, PEDAL EVIDENCE, AND ONGOING RESEARCH

Chapter 12: "The Game is Afoot": *Feet Help Solve Forensic Puzzles in the United States and Overseas* 359
Julie Mather Saul and Frank P. Saul

Chapter 13: The Role of Feet and Footwear in Medicolegal Investigations 375
John A. DiMaggio

Chapter 14: Ongoing Research Into Barefoot Impression Evidence 401
Robert B. Kennedy

Index 415

Contributors

Scott D. Batterman, PhD • Batterman Engineering, LLC, Cherry Hill, NJ

Steven C. Batterman, PhD • Batterman Engineering, LLC, Cherry Hill, NJ and Professor Emeritus of Bioengineering, School of Engineering and Applied Science and Professor Emeritus of Bioengineering in Orthopaedic Surgery, School of Medicine, University of Pennsylvania, Philadelphia, PA

B. G. Brogdon, MD • University Distinguished Professor Emeritus of Radiology, Department of Radiology, University of South Alabama College of Medicine, Mobile, AL

Emily A. Craig, PhD, DABFA • Kentucky Cabinet for Justice and Public Safety, Office of the Medical Examiner, Frankfort, KY

Dorothy E. Dean, MD • Office of the Medical Examiner, County of Summit, Akron, OH

John A. DiMaggio, DPM • Forensic Podiatry Consulting Services, Tempe, AZ

Alison Galloway, PhD, DABFA • Department of Anthropology, University of California, Santa Cruz, CA

Jonathan I. Groner, MD • Department of Surgery, Children's Hospital, The Ohio State University College of Medicine and Public Health, Columbus, OH

Robert B. Kennedy • Forensic Identification Research Services, Royal Canadian Mounted Police, Ottawa, Canada

David J. Porta, PhD • Department of Biology, Bellarmine University and Department of Anatomy, University of Louisville School of Medicine, Louisville, KY

Robert H. Powers, PhD • Division of Scientific Services, Controlled Substances/ Toxicology Laboratory, Connecticut Department of Public Safety, Hartford, CT

Jeremy Rich, DPM • Department of Medicine, Brigham and Women's Hospital, Research Fellow in Medicine, Harvard Medical School, Boston, MA

Frank P. Saul, PhD, DABFA • Associate Dean Emeritus and Professor Emeritus, Anatomy, Medical College of Ohio, Toledo, OH and Commander, United States Department of Homeland Security, Disaster Mortuary Operational Response Team, Region V.

Julie Mather Saul, BA • Lucas County Coroner's Office, Toledo, OH and Wayne County Medical Examiner's Office, Detroit, MI

Paul W. Sciulli, PhD • Department of Anthropology, The Ohio State University, Columbus, OH

Nancy E. Tatarek, PhD • Department of Sociology and Anthropology, Ohio University, Athens, OH

Grzegorz Teresiński, MD • Department of Forensic Medicine, Medical University of Lublin, Lublin, Poland

Douglas H. Ubelaker, PhD, DABFA • Department of Anthropology, Smithsonian Institution, National Museum of Natural History, Washington, DC

Lauren Zephro, MA • Monterey County Sheriff's Office, Monterey, CA and University of California, Santa Cruz, CA

Color Plates

Color Plates 1–4 appear as an insert following p. 240.

Color Plate 1:
Chapter 7, Figure 1. Epidermolysis bullosa mimics scalded skin from a hot liquid in this infant. The distribution of this disease mimics injury patterns that are usually found in children struggling to get away from the heat source. A bulla (blister) is also seen on the proximal thigh. *See* discussion on pp. 247–248.

Color Plate 2:
Chapter 7, Figure 2 A,B. Stevens-Johnson syndrome in the distal lower extremity intraoperatively **(A)** and showing healed lesions **(B)**. These lesions mimic thermal trauma, such as that caused by cigarette burns or wounds induced with a heated implement. *See* discussion on pp. 248–250.

Color Plate 3:
Chapter 10, Figure 22. The pattern of hip dislocation in a frontal collision depends on the initial sitting position of vehicle occupants. *See* discussion on pp. 326–327,333.

Color Plate 4:
Chapter 10, Figure 29. The direction of knee joint dislocation and rotation of the saddle in car–bicycle collisions in relation to the direction of the impact. *See* discussion on p. 333.

Part I

Analysis, Development, and Identification Markers

Chapter 1

The Decomposition of Human Remains

A Biochemical Perspective

Robert H. Powers, PhD

1. Introduction

The end result of decomposition of humans is more intimately familiar and perhaps of greater interest to forensic pathologists than to any other group whose duties include the evaluation and investigation of postmortem remains on a routine basis. From such remains, the forensic pathologist may be asked to make an evaluation of the cause and manner of death and, perhaps, how long the body had been *in situ*. These determinations may be challenging, even for the experienced investigator, depending on the condition and location of the remains. The extent, pattern, and nature of decomposition in a specific circumstance may be of great significance and utility in the forensic investigation of a death. Conclusions and inferences drawn from the investigation can be the subject of scrutiny, consideration, and documentation.

Clearly, an understanding of the processes of decomposition can be of benefit for such purposes as estimation of the postmortem interval, recognition of postmortem artifacts, and in an overall evaluation of the death scene. For the forensic pathologist faced with the even more complex issues associated with partial remains, such as the lower extremity, knowledge of the mechanistic processes of decomposition may facilitate an understanding of the specific circumstances of the death in question.

Because the physical appearance and sequence of decomposition events has been extensively detailed and reviewed in the forensic literature, the focus of this chapter is to explore the biochemical reactions and processes that provide the ultimate basis for

From: *Forensic Science and Medicine*
Forensic Medicine of the Lower Extremity: Human Identification and Trauma Analysis of the Thigh, Leg, and Foot
Edited by: J. Rich, D. E. Dean, and R. H. Powers © The Humana Press Inc., Totowa, NJ

the visible (or otherwise detectable) evidence of the decomposition with which we regularly deal with in medicolegal contexts.

There are many macroscopic processes or events that can impact the fate of postmortem remains in an unpredictable and variable nature, such as physical disruption, scavenging, and deliberate or accidental burial. However, the common underlying sequence of biochemical events provides a basis for understanding decomposition as a logical progression of natural processes. It is anticipated that an enhanced understanding of the biochemistry of decomposition of human remains will be useful to some investigators, and facilitate the evaluation, and extraction of useful information from the seemingly unpredictable and chaotic processes lying at the center of a crime or death scene.

Life can be viewed in its essence, as an energy-utilizing sequence of interrelated chemical reactions whereby order and structure, of truly magnificent scope and complexity, is derived from an intricate and multifaceted process of breakdown, combination, synthesis, and modification or rebuilding of biomolecules from an otherwise random or partially organized collection of both simple and more complex available molecules, ions, and atoms. The maintenance of life—or more accurately, the maintenance of the underlying order, as reflected in molecular and macromolecular structures—requires the continued input and utilization of energy. The interlinked reactions of life comprise overall, an endothermic process both in total and on an individual basis. Clearly, the termination of a life results in the cessation of the flow of energy available to maintain, support, and reproduce the molecules, structures, and biochemical processes of the organism.

Organic biomolecules are—as considered from the temporal perspective of days, months, or years—extremely fragile and ethereal constructions, readily broken apart by relatively small amounts of thermal, electrochemical, or electromagnetic energy. Within living organisms, the molecules of life are primarily "reduced," in the chemical sense, in that they are hydrogen-rich and able to react with molecular oxygen either directly or via intermediate molecules as electron donors or "reducing agents." Indeed, a major form of energy storage in living cells is long-chain carbohydrate molecules. The energy potential of such molecules, which is released upon oxidation, is readily demonstrable in the burning wax of a candle, the fat stores of animals preparing for winter hibernation, and the utilization of geochemical (although essentially biological in origin) oil and its refinement product, gasoline.

Despite the reduced state of most biomolecules, our earthly environment provides an oxidizing atmosphere and (generally) oxygenated aqueous ecosystems. In such a system, the ultimate fate of organic molecules is the corresponding oxidation products of component atoms. Hydrogen yields water and other oxidized products such as hydrogen sulfide. Carbon ultimately yields carbon dioxide. Nitrogen and other elements yield corresponding oxide forms. The facility with which organic molecules are able to transfer single electrons to molecular oxygen provides the underlying basis for aerobic life, given that the energy of that transfer is captured and made available to the organism in the form of high-energy molecules, such as adenosine triphosphate (ATP).

The relative fragility of organic molecules necessitates active biological structures to maintain some degree of flux at the molecular level, in that the molecules from which such structures are comprised are always degrading (albeit at different rates). Damaged or degraded molecules are then constantly being replaced by newly synthesized (or otherwise

acquired) versions of the same molecule (with the rate of repair dependent to an extent on the health and age of the individual). Complex and elegant enzymatic systems exist to perform the functions of evaluation, repair, and/or replacement of biomolecules.

As a consequence of death, the molecules created by the organism that serve as the building blocks of its corporeal body, internal structures, and organs—both on the macro and micro scale—must, as noted above, ultimately undergo oxidation and degradation in an environment where the normal repair and replacement mechanisms are no longer operative. The process in total, whereby the structures and biomolecules of an organism become less organized or broken down—either by chemical or biochemical processes—and the constituent molecules and atoms are made available to new life, is referred to as "decomposition." The extent to which this process is dependent on the chemical nature of the surroundings is readily illustrated by the recovery of well-preserved specimens—both human and otherwise—from bogs (or, more accurately, peat excavations of ancient bogs). The subsurface ecosystem of a bog is severely oxygen depleted and acidic, resulting—for any unfortunate individual trapped therein—in a preservative entombment that precludes normal molecular oxidative degradation and will not support the aerobic life forms (nor many anaerobes) necessary for a complete decomposition process.

In contrast to the synthetic functions of the living organism, postmortem decomposition of the body is reflective of a collection of physical and degradative biochemical processes that will be situationally dependent for any given body. To an extent, the temporal sequence, and even occurrence, of particular decomposition events in a specific situation will be the result of the combined effects of environmental conditions and the physical setting of the body, as well as the physical actions associated with death. Similarly, the rate at which changes will occur—correlating with the physical state of the remains at any point—will also be a function of those circumstances. With the exception of physically disruptive processes, decomposition is essentially a biological and biochemical phenomenon, mediated by enzymes that are already present in the body, by digestive enzymes and the activities of exogenous flora and fauna colonizing the remains. All of the processes are driven by the stored chemical energy that the decomposing body represents. This chapter is devoted to understanding—in a general but mechanistic and biochemical sense—the nature of the decomposition processes to which remains of the lower extremity may be subjected.

2. *The Decomposition Sequence*

In the absence of physical disruption and in unfrozen, unpreserved tissue, the processes of decomposition follow a reasonably predictable pattern. The breakdown of body tissues consists primarily of two processes: autolysis and putrefaction. *Autolysis* is an aseptic phenomenon caused by the release and subsequent uncontrolled activity of intracellular enzymes that hydrolytically break down cellular constituents that may serve as catalytic substrates. The autolytic process sets the stage for the subsequent massive transformation of previously (more or less) solid tissue to gas, liquid, and salt products during the septic process of putrefaction.

In contrast to autolysis, *putrefaction* is the consequence of a "population explosion" of xenobiota in the body, as various organisms (both micro- and macrobiological

endogenous and invasive plants, animals, and fungi) compete for the available energy the decomposing tissues represent. Although the difference between autolysis and putrefaction may be relatively clear and definable on a molecular level, the distinction between the processes in an actively decaying corpse may be considerably less so, with both functions occurring to some extent simultaneously.

Although recognizing that there may be significant variations in the time course of the decompositional process within any specific corpse, generally five stages of decomposition have been identified in unpreserved bodies:

1. Fresh (~0–2 d): Begins at the moment of death and includes the autolytic processes. Usually relatively few changes are readily observable on a macrobiologic scale. This stage ends with the beginning of putrefaction. Generally, insect infestation and utilization of the corpse is not extensive at this stage.
2. Bloated (~2–6 d): Begins as the processes of putrefaction start to produce enough gaseous byproducts to start inflating the abdomen and other soft tissue. This activity reflects the geometric rates of growth of invasive and/or opportunistic organisms—primarily anaerobic bacteria—in the corpse. Insect activity may be significant during this stage and particularly enhanced as fluids start to seep from the body.
3. Decay (~5–11 d): Begins as the skin of the abdominal wall ruptures or is otherwise breached, thereby allowing the release of trapped putrefactive gases. This process may be facilitated by insect feeding or other scavenger activities. The body may appear moist and blackened. During this stage, a significant loss of soft-tissue mass will occur, primarily as a consequence of maggot feeding activity. Toward the end of the decay stage, the body will begin to dry and the insect population may shift somewhat toward scavenging and predatory beetles.
4. Postdecay (~10–25 d): The nature of the postdecay process is a function of the degree of moisture available in the immediate surroundings of the body. In dry climates, remains will be primarily bones, dried skin, and cartilaginous materials. In moist regions, byproducts of decomposition may remain in the vicinity of the body (e.g., in adjacent soil) for an extended period of time.
5. Dry state (~>25 d): This is generally defined as the stage at which only bones and hair remain, and no significant odor distinct from normal soil or forest duff is readily discernable.

2.1. Autolysis

Autolysis is the "self-digestion" of the cell. In the context of postmortem decomposition, it refers to the process by which catabolically active enzymes are able to act on cellular organelles and molecular components that would not normally serve as substrates. The release of these enzymes from their subcellular locations marks the beginning of an irreversible process that will eventually result in the complete reduction of the newly dead organism to the remnants of decomposition, available to serve as food for other life forms that can derive energy and nutrients from the decaying corpse. The potential for the autolytic, enzymatic breakdown of cellular biomolecules exists in every cell as a consequence of the presence of the biochemical machinery necessary to process nutrients, degrade toxic species, and recycle structural and functional molecules and, indeed, entire cellular organelles. That tissues differ in rates of autolytic processes can be understood in terms of differential enzyme complements and reflects the functional

distinctions of the tissues. Hence the liver, with a broad spectrum of highly active catabolic enzymes, undergoes rapid autolysis, whereas tissues with more limited biochemical activity, e.g., muscle, tend to degrade more slowly.

Interestingly, the essentially aseptic nature of the autolytic process can be understood on reflection that the "aging" process used to enhance the flavor and texture of certain meats and game produce a tenderized yet not microbially contaminated product. The operation of autolytic processes in a manner that is protected from either infection or other means of contamination is primarily responsible for the change in physical properties of the muscle mass.

Clearly some mechanism for isolating or segregating the activities of catabolic enzymes with generalized substrate capability is required in the cell, because the maintenance of intracellular structures is in the interest of the organism. The primary segregating elements for catabolic enzymes and processes within the cell are the lysosomes, peroxisomes, and, to a lesser extent, mitochondria. An understanding of autolysis and hence of the entire decomposition process requires familiarity with the enzymatic complements and mechanism for the release of enzymes from these subcellular organelles after the death of the organism *(1,2)*.

Subcompartmentalization of catabolic enzymes within the lysosomes, peroxisomes, and other subcellular vesicles protects the operating molecular machinery of the cell from the degradative potential of these enzymes. In addition to the limitation of activity by intracellular segregation, there is elegant additional protection of intracellular constituents. The activity of the lysosomal hydrolases is optimal at an acidic pH (~5.0), which is significantly distinct from the somewhat more basic pH (~7.2) of the surrounding cytosol.

With the death of the organism and the associated circulatory failure, there is a concomitant failure of oxygen transport and delivery to cells. Molecular oxygen serves as the terminal electron acceptor in the electron transport chain in biochemical reactions known collectively as oxidative phosphorylation. This sequence of connected reactions is the primary source of high-energy ATP molecules in the body, which in turn provide the energy for a multiplicity of cellular functions by hydrolysis of phosphate ester linkages *(3)*. A consequence of oxygen deprivation is the failure of oxidative phosphorylation to take place, causing a shift in cellular metabolism favoring anaerobic glycolysis, a fermentative process which acts to compensate for the energy deficit. Anaerobic glycolysis results in the conversion of glucose to pyruvate and eventually to lactate. The elevation in lactic and pyruvic acid levels in the cell causes the intracellular pH to decline and the intracellular buffering capacity to become quickly overwhelmed. As the glycolytic process continues, intracellular glucose is rapidly depleted, as is the glucose polysaccharide glycogen; thus, it eventually deprives the cell of even this limited resource of ATP production. Anaerobic glycolysis is less efficient than oxidative phosphorylation, in that it leaves an incompletely oxidized product (lactate) and it is further limited to the available substrate, endogenous glucose, and molecules that can be readily converted to glucose, e.g., glycogen *(3)*.

The consequences of the limitation in ATP synthesis are multifaceted and ultimately devastating for the cell. Many cellular transport mechanisms depend on ATP to provide the energy required to drive energetically unfavorable processes. Many nutrients and other molecules essential to the life of the cell are actively transported across

cellular membranes by mechanisms that require ATP hydrolysis. The cellular membrane potential, ranging from approx –10 mV to as much as –90 mV (depending on the tissue or cell type) is also maintained by the action of the sodium–potassium ATPase pump; termination of the activity of this structure allows intracellular sodium to accumulate while potassium diffuses out of the cell through permanent membrane ion channels *(4)*. As the membrane potential disappears, calcium ions enter the cell (a key indicator and perhaps contributor to the impending death of the cell). The intracellular accumulation of solute ions occurs concomitantly with cell swelling, a function of an increase in the intracellular water content, which is driven by osmotic pressure. Typical necrotic changes in the cell, such as vacuolization and dissociation of cellular organelles, further characterize the cellular demise. Of major significance for autolysis is the disruption of the lysosomal membrane consequential to intracellular acidification and ionic changes. The leakage of the lysosomal acid hydrolases into an acidic environment at a now near-optimal pH for hydrolytic activity facilitates the enzymatic breakdown of cellular components and membranes.

Lysosomes have a single limiting membrane, and the intravesicular pH is maintained at approx 5.0 (corresponding to the optimal pH for hydrolytic enzymes) by a membrane-bound hydrogen ion pump. Lysosomes typically contain a broad spectrum of enzymes capable of hydrolytically cleaving polysaccharides, proteins, nucleic acids, lipids, phosphoric acyl esters and sulfates (Tables 1 and 2). Lysosomal action is primarily mediated as a consequence of the fusing of a primary lysosome with an intracellular vesicle produced via phagocytosis (for extracellular materials) or by the analogous budding of an intracellular membrane (for intracellular materials). The fused product is referred to as a *digestive vacuole*, and it is in this protected environment that complex biomolecules are hydrolytically "de-constructed" *(5)*.

As previously noted, the capability of the cell to rapidly degrade molecules of significant size and complexity requires compartmentalization and segmentation of the process. The integrity of the lysosomal membrane also prevents the unwanted destruction of other intracellular components, the loss of which could have a negative impact on the viability of the cell. Clearly a loss of lysosomal membrane integrity can result in the appearance within the cytosol of a significant and indiscriminant hydrolytic function with the potential to damage cellular organelles, membranes, and other important biomolecules.

Peroxisomes function primarily in the breakdown of lipids, with long chain fatty acids (>20 CH_2 groups) processed essentially exclusively within these organelles. Medium-chain fatty acids (~10–20 CH_2 groups) may be degraded in either mitochondria or peroxisomes. Although the reactions of the mitochondria and peroxisome are similar in many respects, some significant differences serve to point out the functional distinctions. The mitochondrial oxidative phosphorylation process oxidizes flavin adenine dinucleotide, reduced $(FADH)_2$, to yield FAD, with $FADH_2$ regenerated by the oxidation of a fatty acyl CoA molecule. In contrast peroxisomal $FADH_2$ is generated by the same enzyme-catalyzed reaction but oxidized in the process of the reduction of molecular oxygen to hydrogen peroxide, a potentially cytotoxic molecule *(1)*.

Peroxisomes contain significant quantities of the protective enzyme catalase, the activity of which breaks hydrogen peroxide down to water and oxygen. In the peroxisome, unsaturated fatty acyl CoA molecules are converted to the hydroxy analogs, which

Table 1
Lysosomal Enzyme Classes: Examples and Typical Substrates

Enzyme Type	Typical Substrate
Lipid Hydrolases:	
Lipases	Triacylglycerol esters
	Cholesterol esters
Esterases	Fatty acyl esters
Phospholipases	Phospholipids
Nucleic Acid Hydrolases:	
Ribonuclease	Ribonucleic acids
Deoxyribonuclease	Deoxyribonucleic acids
Phosphatases:	
Phosphatase	Phosphomonoesters
Phosphodiesterase	Phosphodiesters
Polysaccharide Hydrolases:	
α-*Glucosidase*	Glycogen
α-*Flucosidase*	Membrane fucose
β-*Galactosidase*	Galactosides
α-*Mannosidase*	Mannosides
β-*Glucuronidase*	Glucuronides
Hyaluronidase	Hyaluronic acid
	Chondroitin sulfates
Arylsulfatase	Organic sulfates
Lysozyme	Bacterial cell walls
Protein Hydrolases:	
Cathepsins	Proteins
Collagenase	Collagen
Elastase	Elastin
Peptidases	Peptides
Sulfatases:	
	Heparan sulfate
	Dermatan sulfate

are subsequently oxidized to their corresponding ketones by means of hydroxy fatty acyl dehydrogenase with the concomitant formation of NADH. In the absence of an active electron-transport chain and associated cellular synthetic processes, there is no metabolic "sink" for the reducing equivalents and nicotinamide adenine dinucleotide is exported to the cytosol. Therefore, peroxisomal catabolism of fatty acids represents a source of both acetyl CoA and reducing equivalents in the form of

Table 2
Autolytic Events: Cellular Death

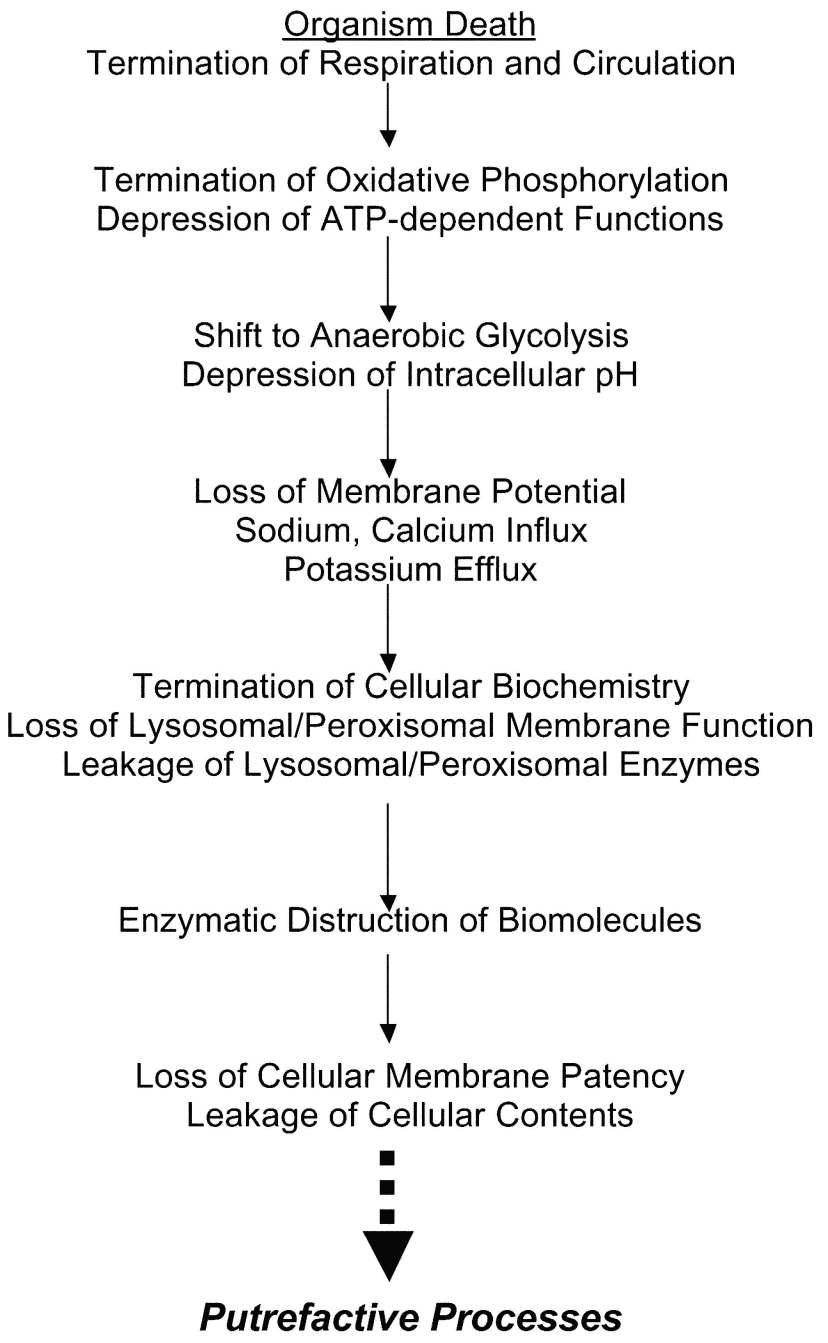

nicotinamide adenine dinucleotide. Significant for the autolytic process, the enzymatic systems contained in the peroxisome represent the catabolic potential for fatty acids and also for the production of active oxygen species, e.g., hydrogen peroxide. The peroxisomal membrane suffers the same fate in the necrotic cell as the lysosome, with the leakage of its enzymatic machinery into the cytosol, where it becomes available to further catalyze the destruction of cellular components.

Failure of respiration and hence, cellular oxidative phosphorylation, is therefore the key trigger in the autolytic process. Termination of the availability of high-energy molecules that are routinely required to maintain the integrity of the cell, key cellular components and processes (e.g., membranes), synthetic capability, and ion and molecular pumps causes significant changes in the biochemical operation of the cell. This process ultimately leads to the lysis of intracellular organelles, of particular significance being lysosomes and peroxisomes, and the release of their constituent enzymes into the cytosol, where their catalytic actions can break down and destroy the very molecules that had previously served to define the living cell and functions in it.

2.2. Rigor Mortis

The postmortem depletion of cellular energy stores leading to autolysis also produces a well-recognized macro-scale phenomenon characterized by the stiffening of voluntary and involuntary muscles, known as rigor mortis. Mechanistically, this process is the result of association of the muscle proteins actin and myosin as intracellular pH decreases to less than approx 6.5 and calcium—normally sequestered in the sarcoplasmic reticulum (SR)—leaks into the cytosol as the SR membrane is compromised during autolysis. Cytosolic calcium then binds to troponin, causing a conformational change that results in the "unmasking" of myosin binding sites on the actin molecule. In living cells, the subsequent dissociation of the actin–myosin complex is promoted by ATP as part of the normal sequence of events that results in muscle contraction *(6)*. However, in the ATP-deficient postmortem environment in dead or dying cells, the actin–myosin complex remains until it is either denatured or enzymatically degraded *(7)*. The process causes the "death stiffness" of muscles, or rigor mortis. In contrast to active muscle contraction, there is no process of actin–myosin translocation in rigor mortis and, hence, no shortening of muscle fibers. Thus, rigor is characterized by muscles that are stiff but not contracted. Although rigor mortis occurs in the muscles, it is readily detectable only when the affected muscles are connected to central joints, such as the knees.

2.3. Livor Mortis

Lividity is a discoloration of the skin—generally to a dark purple—that results from the pooling of deoxygenated blood in the veins and capillary beds of the body as circulation fails. This process occurs in direct response to gravitational forces. The blood remains fluid after death as a consequence of the release of plasmin, a fibrinolytic enzyme, from the vasculature and serous surfaces. This process depletes the blood of fibrinogen, thereby eventually rendering the blood permanently incoagulable (~30–60 min after death, depending on the ambient temperature). Blood, by providing an ideal liquid growth medium, facilitates the rapid growth of xenobiotics during the putrefaction stage and serves as a conduit for the spread of microbes throughout the body.

The characteristic color of body surfaces during lividity is reminiscent of cyanosis, i.e., the bluish discoloration of skin, nail beds, and mucous membranes that develops in clinical settings as a consequence of inadequate oxygenation. In the postmortem environment, the continued kinetically driven dissociation of oxygen from the hemoglobin molecule continues, changing the absorption spectra of the blood and producing the characteristic and readily observable change in color *(7)*.

2.4. Putrefaction

The result of autolysis is the development of a slightly acidic, anaerobic, nutrient-rich environment, with significant degradation of biomolecules at the cellular level. In this fertile milieu, devoid of normally protective and defensive cells and barriers, the proliferation of both invasive and opportunistic endogenous micro-organisms can be rapid and extensive. Ultimately, bacterial growth can affect and transform all the tissues in the body, being limited only by environmental factors, such as temperature and humidity.

The decomposition processes that begins as bacteria proliferate results in the production of gases and other metabolic products. These consequences of microbial growth result in some of the characteristic color changes, bloating, and odor changes that are universally recognized as the hallmarks of a decaying body and are collectively referred to as *putrefaction.* On the molecular level, the actions of microbial degradation transform the complex biomolecules of the body into gases, liquids, and simple molecules. Putrefaction results in the complete (albeit gradual) loss of structural integrity and recognizability of tissues and, indeed, the ultimate reduction of those tissues into their component molecules, molecular fragments, and atoms.

The primary source for the opportunistic microbiological colonization in the decomposing body is the microbially rich environment of the gastrointestinal tract. These enteric micro-organisms can cross the failing membrane barriers, a process that is facilitated by the autolytic degradation of body tissues, and migrate and proliferate throughout the body. Hence, the pronounced impact of autolytic processes on the structural integrity of the cellular membranes and the end of the viability of regular "defensive" or protective cells (e.g. macrophages and neutrophils) as a function of pH changes and the loss of available oxygen, provides the basis for the population explosion the putrefactive period represents. Characteristic microbial species observed during putrefaction include various Bacilli and *Pseudomonas, Bacterioides fragilis, Eschericia coli, Clostridium perfringens, Proteus mirabilis, Staphylococcus epidermidis,* and *Staphylococcus faecalis (8).*

Although the primary source of anaerobes in decomposition processes is the intestinal tract, other organisms—such as those found in the respiratory tree—may be present and able to take advantage of the conditions for growth. Naturally, any significant antemortem infection (e.g., septicemia or pneumonia) will give the causative agent a "head start" on the putrefactive process and may therefore result in an unusual microbiological population, at least during the initial stages of decomposition. The rate of putrefaction will vary with temperature, which will affect primarily the rate of enzymatic activity, with acceleration occurring until temperatures become inconsistent with the maintenance of protein structures.

In the absence of a septic condition, putrefaction begins in the stomach and intestines. The gastric mucosa and intestines acquire a dark purple-brownish color as a

result of the release of heme compounds. The mucosal epithelium of the airways becomes deep red, and a hemolytic plum coloration may be noted in the myocardium and large blood vessels, again a result of the release of heme. Changes in organ structure are readily apparent, as seen in the thinning and softening of the myocardium. The liver develops a honeycomb pattern as a result of extensive gas formation. The brain similarly goes through a structural disintegration process that may proceed to complete liquefaction. The spleen becomes exceptionally soft and may extrude through its delineating capsule. The lungs become filled with and surrounded by fluid.

Putrefactive processes are generally first represented by the generation of a greenish color—a consequence of the formation and accumulation of sulphhemoglobin in the abdominal wall where it coincides with the large intestine. Eventually, the discoloration spreads over the entire abdominal wall and may extend over the entire body. Coincident with this color change is the appearance of the superficial veins of the skin as a pattern of lines often described as "marbling." As the process continues, the skin eventually acquires a dark pigmentation that may range from a red-tinged greenish color through purple to black.

The skin color changes are accompanied by structural disintegration of the tissue that results in the characteristic skin-slippage that accompanies the process of decomposition. Large sections of epidermis may be dislodged as a consequence of even a small amount of shear. The newly exposed basal layers appear moist and pinkish and may take on a yellow–tan parchment appearance when they dry. Blisters as large as 20 cm may develop. These blisters are generally filled with a dark fluid and gases of putrefaction and may be easily disrupted to expose a dermal surface similar to that seen as a result of skin-slip.

Putrefaction is often characterized by pronounced bloated, distended bodies as a consequence of the formation of gas in the stomach, intestine, and abdominal cavity. The gas, a consequence of microbial action, is composed of hydrogen sulfide, methane, carbon dioxide, ammonia, and hydrogen, and is responsible for the characteristic odor of putrefaction, along with low molecular-weight organic compounds, including mercaptans, indoles, and the aptly named cadaverine and putrescine. This gas invades all body tissues and causes a generalized swelling to occur, which is characteristically crepitant to palpation. The pressure generated by the evolution of this gas may contribute to the separation of necrotic tissue layers.

At the molecular level, it is the ability of the bacterial species to secrete enzymes into their immediate environment that provides both the basis for the delivery of nutrients back to the microbe, yet also results in the degradation of biomolecules in the vicinity of the organism. These *exoenzymes* are responsible for the significant denaturation and breakdown of proteins into their constituent amino acids, which may be taken up and utilized, or further catabolized by the microbial population. The gas that characterizes the putrefactive process arises as a direct consequence of protein breakdown. Sulfur-containing amino acids are readily reduced to yield hydrogen sulfide, which plays a significant role in the production of the greenish sulfhemoglobin pigmentation and the reaction with reduced (ferrous) iron (released from the iron transport protein transferrin or the iron storage protein ferritin) that produces a black precipitate of ferrous sulfide. Ornithine—a four-carbon diamine amino acid—and lysine, its five-carbon

analog, are readily decarboxylated to produce carbon dioxide, but more significantly for humans and "cadaver dogs" results in the production of the four-carbon "putrescine" and five-carbon "cadaverine," which are associated with a decomposing body.

2.5. Formation of Adipocere

Adipocere is a decomposition product of adipose tissue and may be an extensively formed a consequence of the putrefactive process in the presence of appropriate environmental conditions—generally high humidity or an aqueous environment coupled with relatively warm temperatures, conducive to the growth of putrefactive organisms. The formation of adipocere is a specific consequence of bacterial action, in which triacyl glycerols and other fatty esters are enzymatically hydrolyzed to produce both fatty acids and salts *(9,10)*. Other bacterial reactions that will subsequently affect the chemical composition and physical nature of the final product are hydrogenation, stereoisomerization, hydration, and dehydrogenation *(11)*. The physical nature of the material (increasingly hydrophobic as a consequence of the reactions noted above) limits additional breakdown and utilization of the high-energy molecules. The final nature of adipocere varies with the extent of hydration and the fatty acyl cation. Sodium salts produce a relatively soft material, whereas potassium salts are harder. Replacement of sodium with calcium creates an insoluble, somewhat brittle material *(7)*. Hence, the adipocere may vary from a grayish white, relatively soft, greasy substance to a crumbly, friable material as the water content is reduced *(9)*.

2.6. Mummification

Mummification (or dehydration of tissues) is neither a direct consequence of autolysis or putrefaction but is, in a sense, a competing process. As a function of environmental conditions, the rate at which water evaporates from the body or from exposed sections of the body can be rapid enough to reach a point where dehydration of individual tissues precludes the bacterial action of putrefaction. However, such tissues are subjected to slow oxidative processes that result in the characteristic darkening of the tissues. Internal organs in circumstances of mummification may be somewhat preserved, but usually have undergone some degree of autolysis and putrefactive changes because of the relatively protected and hydrated conditions. Clearly, conditions favoring the dehydration of bodies will facilitate mummification, but the effects of cold should not be discounted. When microbial activity is sufficiently slowed by temperature, the evaporation (or sublimation from frozen tissues) of water in a low-humidity environment may provide conditions for partial or complete mummification.

3. Factors Affecting Decomposition Processes

The dependence of the processes of decomposition on physical environmental factors, such as humidity and temperature, was noted previously in this chapter. However, the "contamination" or poisoning of the decomposing remains—either deliberately via an embalming process or accidentally by leaching of adjacent metal ions or the deposition of the body in a matrix that is unable to support microbial growth—can severely inhibit or effectively preclude any appreciable amount of decomposition.

REFERENCES

1. Lodish H, Berk A, Matsudaira P, et al. Biomembranes and cell architecture. In: Lodish H, Berk A, Matsudaira P et al. Molecular Cell Biology. NewYork, NY: WH Freeman and Company, 2004; pp. 165–173.
2. Devlin TM. Eukaryotic cell structure. In: Devlin TM, ed. Textbook of Biochemistry with Clinical Correlations. 5th ed. New York, NY: Wiley-Liss, 2002; pp. 16–23.
3. Beattie DS. Bioenergetics and oxidative metabolism In: Devlin, TM, ed. Textbook of Biochemistry with Clinical Correlations. 5th ed. New York, NY: Wiley-Liss, 2002; pp. 1021–1027.
4. Lodish H, Berk A, Matsudaira P, et al. Transport of ions and small molecules across cell membranes In: Lodish H, Berk A, Matsudaira P, et al., eds. Molecular Cell Biology. New York: WH Freeman and Company, 2004; 252–258.
5. Lodish H, Berk A, Matsudaira P, et al. Receptor-mediated eulocytosis and the sorting of internalized proteins. In: Lodish H, Berk A, Matsudaira P, et al., eds. Molecular Cell Biology. New York: WH Freeman and Company, 2004; 727–732.
6. Smith TE Molecular cell biology. In: Devlin, TM. ed. Textbook of Biochemistry with Clinical Correlations. 5th ed. New York, NY: Wiley-Liss, 2002; pp. 1021–1027.
7. Gill-King H. Chemical and ultrastructural aspects of decomposition. In: Haglund WD, Sorg MH, eds. Forensic Taphonomy. Boca Raton, FL: CRC Press, 1996; pp. 98.
8. Corry JEL. Possible sources of ethanol ante- and post-mortem: its relationship to the biochemistry and microbiology of decomposition. J Appl Bacteriol 1978; 44:1–56.
9. Perper JA. Time of death and changes after death. In: Spitz WU, ed. Spitz and Fisher's Medicolegal Investigation of Death. 3rd ed. Springfield Ill: Charles C. Thomas, 1993: pp. 14–49.
10. Forbes SL, Stuart BH, Dadour IR, Dent BB. A preliminary investigation of the states of adipocere formation. J Forensic Sci 2004;49:566–574.
11. Yan F, McNally R, Kontanis E, Sadic, OA. Preliminary quantitative investigation of postmortem adipocere formation. J Forensic Sci 2001;46:609–614.

Chapter 2

Forensically Significant Skeletal Anatomy

Nancy E. Tatarek, PhD and Dorothy E. Dean, MD

1. Introduction

Forensically significant cases are those in which remains are recovered that have come from humans who died violently or unexpectedly, or for which the cause of death or manner of death is potentially a legal or otherwise significant issue (this may exclude very old or prehistoric remains). This text discusses the subset of forensically significant remains that are partially or completely decomposed, fragmented, or unidentified. This chapter is not meant to reiterate what other experts have described. Rather, we present the authors' philosophy regarding the evaluation of cases in which the lower extremities, or parts thereof, represent the majority of the forensically significant and useful remains recovered. Results expected from the analysis of such remains form a biological profile that is potentially capable of providing positive identification (which is discussed further in later chapters) leading to and perhaps facilitating the determination of the cause and manner of death, a task that usually requires the integration of data from multiple sources and which is outside the scope of this book.

Fragmentary or partial remains, such as a single lower extremity, clearly pose a somewhat more daunting task than a more complete set of remains. Human anatomy is easily recognizable when complete, fleshed remains are involved. Skeletonized remains are less familiar and can be confused with nonhuman skeletal elements or even wood or rocks. The lower extremity is composed of the thigh, the knee, the leg, the ankle, and the foot. Basic familiarity with the overall skeletal anatomy of the femur, tibia, fibula, patella, and foot bones can aid investigators in determining exactly which segments are present (and of course, those that are missing) in medicolegal investigations involving lower extremity remains. This chapter is a summary of some of the more forensically

From: *Forensic Science and Medicine*
Forensic Medicine of the Lower Extremity: Human Identification and Trauma Analysis of the Thigh, Leg, and Foot
Edited by: J. Rich, D. E. Dean, and R. H. Powers © The Humana Press Inc., Totowa, NJ

Fig. 1. Anterior view of femoral proximal end. The "ball-and-socket" of the ball and socket hip joint.

important skeletal landmarks and is intended to aid in the identification of the bone to which they belong. Readers interested in a more detailed account should consult one of the several excellent human osteology books available.

2. *Forensically Significant Skeletal Anatomy*

The thigh contains the largest bone in the human body: the femur. The proximal end of the femur consists of a rounded head made of spongy bone that forms the ball of the ball-and-socket hip joint (Fig. 1). This head is distinctive in shape and size; the femur is the only bone in the human body with this skeletal configuration. The distal epiphysis forms part of the knee and is made up of two large condyles. Anteriorly the femur is devoid of significant landmarks. Posteriorly, the linea aspera is the point of muscle attachment for the short head of the biceps femoris, and next to it is a nutrient foramen. In heavily muscled individuals, the linea aspera can be quite large, forming a large bony ridge that runs the length of the femur. Juvenile and adult femoral morphology is largely similar, with the exception that unfused juvenile femora consist of multiple segments and adult femora (barring trauma or abnormal development) consist of a single segment.

The patella (knee cap) is the largest sesamoid (bone nodule) in the human body. It lies anteriorly to the lower extremity of the distal end of the femur and slightly superior to the proximal tibia. The patella has two articular surfaces posterior—a larger lateral and slightly smaller medial surface. Multiple nutrient foramina on the anterior surface may be mistaken by the inexperienced as rocks with pits caused by erosion. If the entire patella is covered with mud, it may be mistaken at the forensic scene for a clump of mud or a rock. Variation in the patella is common; triangular, elliptical, circular, and oblique shapes have been documented *(1)*. A comprehensive discussion of markers of stress and injury in the knee joint is provided in Chapter 3.

The lower leg contains two bones, the tibia and the fibula. The tibia is the larger and is commonly known as the "shin bone." (Fig. 2). The tibial shaft is somewhat triangular compared with the relatively more rounded femoral shaft. The proximal posterior

Fig. 2. Lateral view of tibial proximal end.

shaft is marked by the popliteal line, which forms a boundary for insertion of the popliteus muscle. A nutrient foramen also appears at the same location lateral to the popliteal line and nearly always slopes distally, exiting the bone proximally *(1)* (Fig. 3). The proximal epiphyseal end is formed by two large, flat condyles and the tibial tuberosity on the proximal anterior side. The distal epiphyseal end is characterized by the medial malleolus, a projection of bone that is felt on the medial aspect of the ankle.

The fibula is the smaller of the two leg bones and its distal end forms the outside part of the ankle. In contrast to the relatively wider tibia, the fibula is irregular and narrow in shape. The proximal epiphysis consists of a slightly rounded formation with a styloid process (posterior projection of bone), and its the distal end consists of a lateral malleolus, which forms the outside part of the ankle. The fibular shaft is largely unremarkable, offering no distinguishing features because it bears no weight. Unlike the femur, it is not expected to be significantly larger in well-muscled individuals.

The human foot is made up of 14 phalanges, 5 metatarsals, and 7 tarsals (calcaneus, talus, cuboid, navicular, and the first, second, and third cuneiforms). Additionally, two sesamoids sit inferiorly on the distal first metatarsal. The calcaneus forms the heel and the talus articulates with the distal tibia, forming the medial aspect of the ankle. The human foot is unique amongst mammalian extremities, because it is constructed for upright walking. The four toes are in line with the first (big) toe (the hallux), unlike the toes of other apes (humans are considered apes), in which the hallux is offset from the remaining toes. To a large extent, the human foot has lost its grasping ability, which is characteristic of the other apes. In humans, the tarsals usually form an arch—an ideal structure for weight-bearing in a bipedal animal. The relatively large number of skeletal elements and articular surfaces results in a number of unique skeletal features, including trabecular patterns and osteophytes, which may be useful within forensic contexts, e.g., for comparing radiographs *(2,3)*. Similar to the patella, the tarsals also exhibit foramina for blood vessels that may be confused with surface erosion by the untrained eye. Additionally, the foot may often be well preserved when it remains in footwear, frequently surviving intact for forensic analysis.

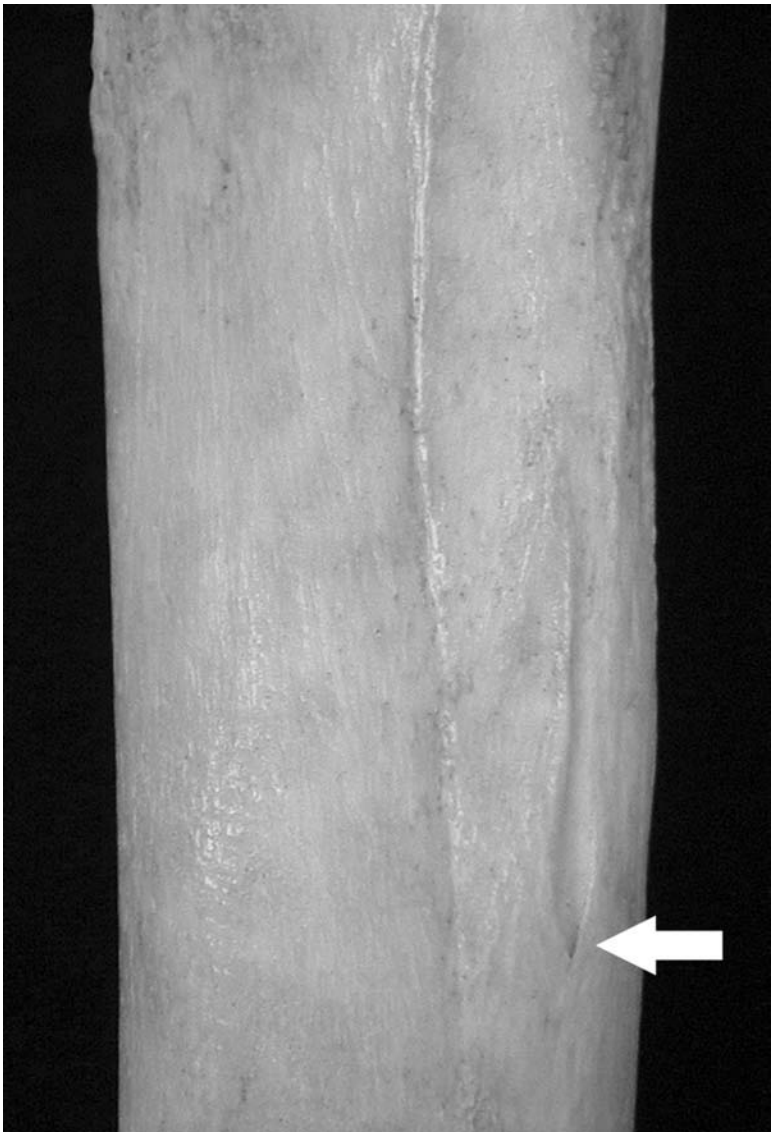

Fig. 3. Arrow denotes tibial nutrient foramen.

3. *Embryology*

The development of the human is complex, yet orderly. There are critical periods of human development during which certain major elements are formed. For the lower extremity, the critical period begins during the third week after fertilization with the formation of the cardiovascular system, including vessels for limbs. During the third and fourth weeks, limb buds appear. By the end of the eighth week, all the major organ systems have begun to develop. It is between the third and eighth weeks of gestation that *in utero* exposure to toxins (teratogens) may cause abnormal development of the limbs persisting into extrauterine (postnatal) life *(4)*. Examples of such toxins are numerous and include thalidomide and cocaine. However harmful teratogens are, their

Fig. 4. Anterior views of six adult femora, illustrating variation in size.

effects may become useful when evaluating forensically significant case material. For example, fetal malformations caused by maternal substance abuse may provide anatomic features unique to that individual that can be used to assist identification efforts. Alcohol consumption by the mother can cause fetal alcohol syndrome, and cocaine use may cause vascular malformations. Both of these teratogens may result in potentially unique anatomic features that can be used for premortem and postmortem comparisons.

Normal bone growth involves the development of blood vessels that penetrate the cortices via nutrient canals. Both the location and angle of entry of vascular elements into the bony cortex are highly variable from person to person and even from one side of the bone to the other in the same individual. This variation may be of significant forensic utility. For example, the nutrient artery for the femur arises from the deep femoral artery and enters the femur posteriorly along the linea aspera, but the location of entry of the vessel is somewhat variable. If two femora are recovered whose general physical characteristics indicate that they are from the same individual, the disparate positions of the nutrient canals should not dissuade the examiner from the concluding that they are from the same person.

Because muscles attach to bone, the absence of one or more muscles can cause limb deformities. Any muscle of the body may fail to develop. If the opposing muscle is present, the limb contracts at the joint. Such deformities can be corrected with braces or surgical repair. Although functionally insignificant, slight variations in muscle development or attachment can be used forensically. Additionally, population differences in skeletal development can cause a slight variation in limb appearance, especially with regard to limb length (Figs. 4, 5). The ratio between the lengths of the tibia

Fig. 5. Anterior views of five adult tibiae, illustrating variation in size.

and femur varies and may provide clues to ethnicity *(1)*. (Postnatal aberrations will be discussed in a later chapter.)

4. Procedural Approaches

When confronted with decomposed or partial human remains, attention to anatomical detail, careful consideration of the available human remains, and scrutiny of the surrounding scene or environment are important for identification and trauma analysis purposes. Because of the complexity of procedures involved in examining human remains within various contexts, the authors advocate a multidisciplinary team approach to the recovery and analysis of suspected human remains. Thus, when remains are discovered, securing the scene and maintaining it in an undisturbed fashion until all appropriate personnel (e.g., medical examiner/coroner's agent, law enforcement, forensic anthropologist, odontologist, and radiologist) are present is important. Although it may seem obvious, the authors cannot emphasize enough that human remains can look remarkably like sticks, rocks, or chunks of mud or dirt. The following figure presents a summary list of questions that may be of use in the analysis of suspected human remains (Fig. 6).

Fragmentary, burned, mummified, or partial lower extremities can resemble wood, rock, or other features of the surrounding scene, such as foam or asbestos (Figs. 7, 8).

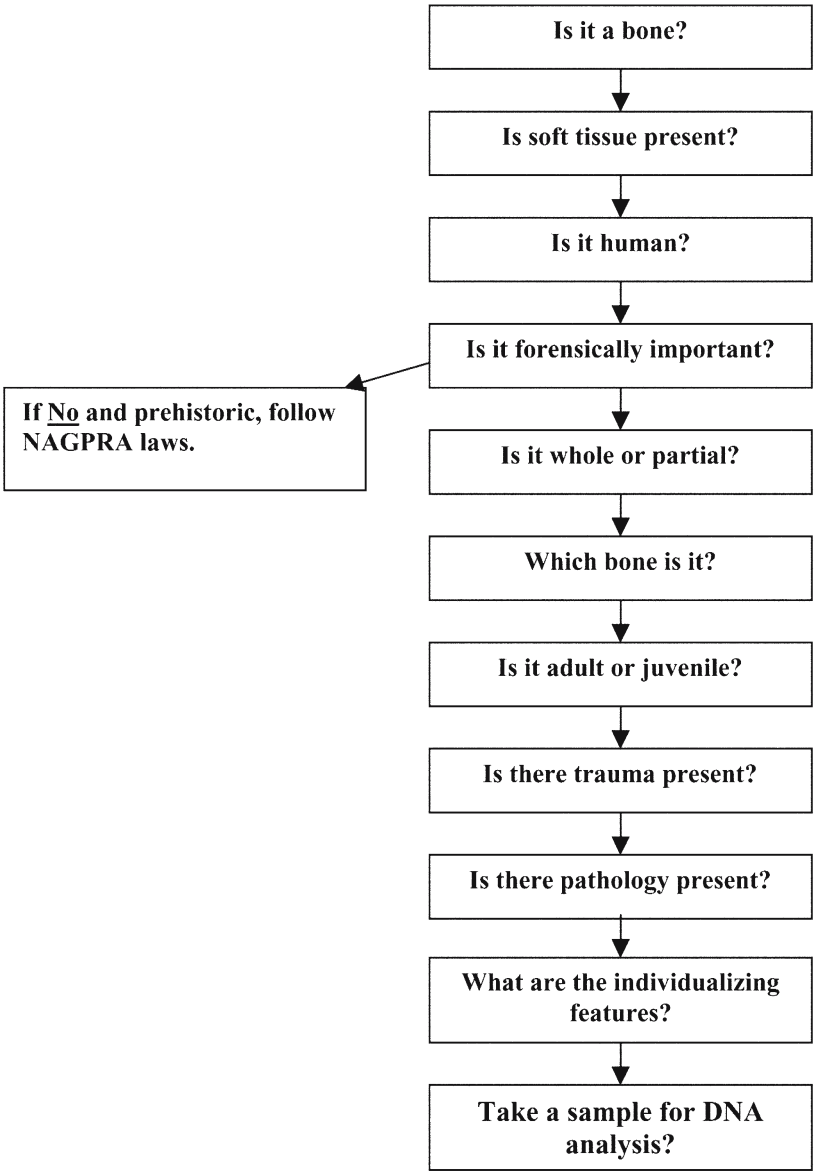

Fig. 6. Chart used to illustrate an algorithm in the analysis of fragmentary remains.

Juvenile remains—being smaller in size and having unfused epiphyses—are more likely to be confused with wood or mud than are whole adult remains. Adult tarsals, metatarsals, phalanges, and sesamoids are also likely to resemble wood, rocks, or mud due to their irregular shapes (Figs. 9, 10). Shafts of the infant femur, tibia, and fibula may be confused with small twigs or animal bones, while the epiphyseal ends may be confused with lumps of mud, dirt, or clay, particularly in outdoor settings (Fig. 11). Within an archaeological context, juvenile remains are sometimes not recovered due to preservation issues or, more commonly, lack of recognition by individuals who are

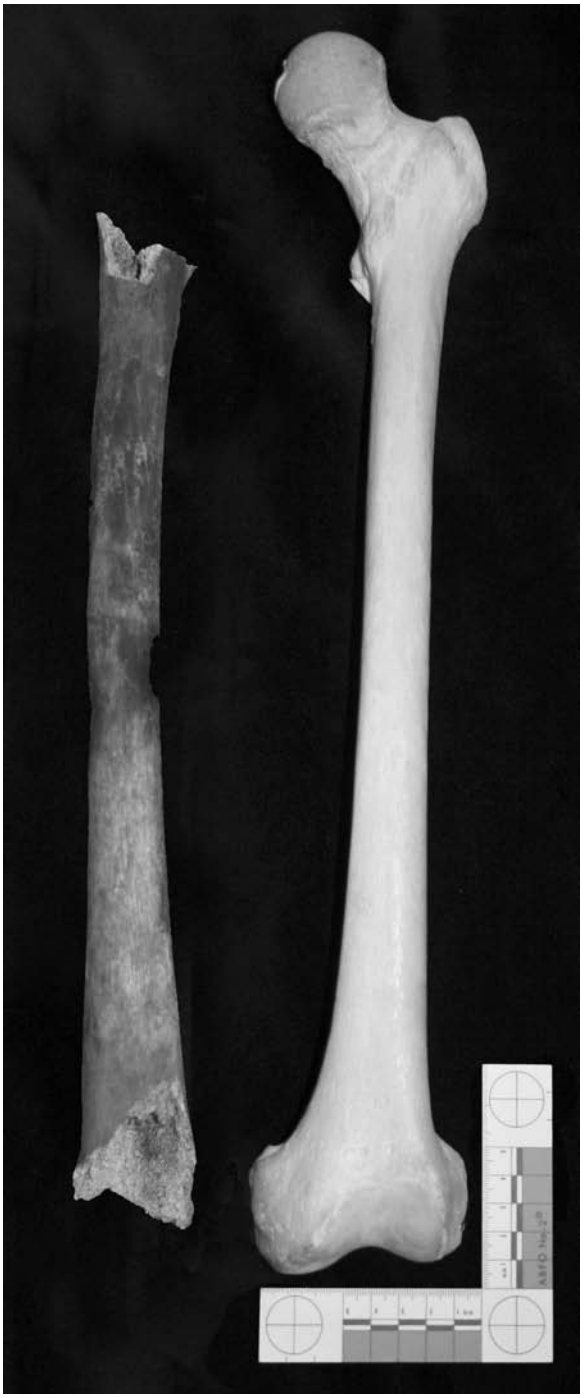

Fig. 7. Anterior views of fragmentary and whole femora.

Fig. 8. Anterior views of fragmentary and whole tibiae.

Fig. 9. Photograph comparing a human first metatarsal (left) to a small twig.

inexperienced with children's skeletons. Within a forensic context, recognition of various juvenile segments and fragmentary adult segments is vital to facilitate recovery and subsequent analyses.

The next step in the analysis is to determine whether the remains are human. Numerous authors have documented similarities between both adult and juvenile human remains and those of various animals, particularly with respect to the lower extremity *(5,6)*. Adult animals—such as dogs, sheep, goats, and rabbits—have smaller extremities than adult humans. The skeletal remains of adult cattle, horses, or other larger animals will exhibit limbs that are larger than those of adult humans. Differences in morphology and bone texture can yield clues as to species (Fig. 12). For example, human infant remains can be confused with avian skeletal remains; however; the lighter, hollow bones of birds help distinguish these materials from human skeletal remains. Comparative mammalian skeletal collections are also useful during this stage of the analysis. Extremely fragmented remains may not contain enough diagnostic features to assign a species designation.

If the remains are determined to be human, the next step is to consider their potential forensic significance. Human remains may be found within many contexts, not all of which necessitate forensic investigation or personal identification. Commonly, information gained from the context of the remains and the condition of the remains themselves

Fig. 10. A photograph similar to that of Fig. 9; with a closer color match.

will aid in the determination. The accompanying presence of archaeologically significant materials such as arrowheads or pottery may indicate ancient remains. Tombstones, coffin hardware, buttons, and clothing may provide data with respect to the time frame. Extreme drying of remains, with little adherent soft tissue, often indicates remains of no forensic significance. In the United States, Native American Graves Protection and Repatriation Act (NAGPRA) laws dictate that law enforcement agencies, coroners, and medical examiners must identify the nearest Native American group and notify them of any finds before proceeding with removal *(7)*. Experienced forensic or physical anthropologists will need to examine the remains *in situ*. In some situations, the determination of forensic significance can be made before any further investigative effort is undertaken.

The discovery of forensically significant remains should culminate in a recovery using standard archaeological procedures to maximize the preservation of information and maintain the chain of custody at the scene. A thorough search of the scene as well as detailed photography, mapping, packaging, and transporting of human remains are necessary to optimize the forensic recovery and subsequent evaluation. Scene context (indoor or outdoor, size of the scene, landscape, weather), available personnel, budget, resources, and legal issues all contribute to the nature of a recovery operation *(7)*. Forensic anthropologists can often be located by contacting the nearest university with an anthropology department. These individuals, who have

Fig. 11. Photograph illustrating similarities between non-human skeletal elements (left and right) and human infant or fetal skeletal elements (center).

advanced degrees and training in archaeology and human osteology, are typically best equipped to handle the recovery and analysis of fragmentary human remains. Following the team approach, the forensic anthropologist should be consulted early in the investigation and ideally would participate in recovery efforts.

Suspected and known human remains should be transported to a laboratory. All remains should be photographed immediately—*in toto* and each element separately—upon their arrival at the laboratory. Traditionally, 35-mm film cameras can provide a high level of resolution. However, high-quality digital cameras can also achieve high resolution. Inclusion of an American Board of Forensic Odontology standard grey scale in photographs is essential for accurate measurements and dimensions. Radiography is a routine procedure in forensic examinations and is useful for separating human from nonhuman and nonskeletal materials. Radiographs should be performed prior to the

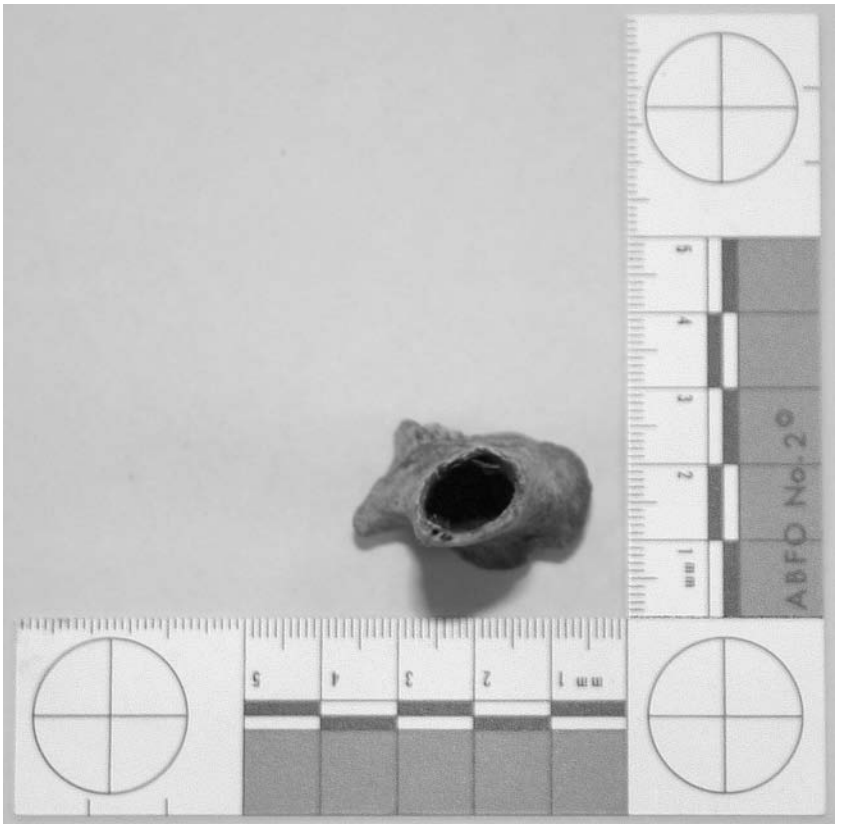

Fig. 12. Photograph of broken bird bone to illustrate the thin walls of the medullary cavity.

removal of any clothing, soft tissue (if defleshing is desired), debris, or other adherent material. Highly decomposed remains frequently result in variable soft tissue density, which may obscure skeletal detail in the radiograph. Therefore, we recommend that the examiner who requires fine skeletal detail on radiograph remove the soft tissue and radiograph the remains again with various image orientations (e.g, anterior-posterior, lateral, medial, and oblique views). The authors have had success in macerating soft tissue using an enzymatic detergent followed by a wash in household ammonia, as described by Fenton et al. *(8)*.

Radiographically, bone may demonstrate a discernable medullar cavity and trabecular latticework. Radiographs will also highlight potential features for individual identification (described in Chapter 6). It should be noted that prior to defleshing, tissue samples should be preserved in case of a need for pathological, DNA, or toxicological analysis. Thorough documentation of the soft tissue should be accomplished prior to tissue removal, and photographs should be taken and any individual characteristics noted.

Subsequent to radiography, an inventory of the remains should be made. This serves two purposes: first, a permanent inventory of the collected and any missing

remains can be maintained and distributed to other agencies and is vital for comparison with any subsequent discoveries; second, information regarding the remains present also dictates the next steps of the analysis, i.e., determination of race, age, sex, and stature (which constitutes the biological profile). Investigators should make notes of any signs of pathology or disease processes, such as osteomyelitis or antemortem fractures, which can be compared with antemortem medical records for presumptive identification.

Documentation of any and all individualizing characteristics present on the soft tissue or skeletal elements can also aid in making a positive identification. Soft tissue characteristics may include tattoos, scars, birthmarks, or concentrations of melanin; characteristics intrinsic to the bone itself include the trabecular pattern *(2)*. Fractures in various stages of healing can be compared with medical records, leading to a positive identification. Surgical alterations or implants such as rods, pins, or hip replacements can also be useful. Some implants are imprinted with serial numbers, which are recorded at the time of surgery and can be linked to an individual using available antemortem medical records.

Comparison with records of missing individuals is the final stage in the process. However, there is the possibility of finding no match between the remains and an individual, given the fragmentary nature of the skeletal materials. For example, a small segment of a human fibula may be forensically significant but otherwise unidentifiable. Some jurisdictions may choose not to treat the remains as forensically significant, because the removal of all or part of a skeletal element in the lower extremity is theoretically compatible with life (e.g., surgery). Fragmentary remains can be scattered across great geographical distances because of a traumatic event or animal scavenging; therefore, communicating with other agencies regarding the inventory of the remains is vital.

5. Summary

The process of recovering, analyzing, and positively identifying forensically significant skeletal remains is enhanced by adherence to the procedures outlined in this chapter and by focusing on an integrated multidisciplinary approach.

References

1. Scheuer L, Black S. Developmental juvenile osteology. New York, NY: Academic Press; 2000.
2. Rich J, Tatarek NE, Powers RH, Brogdon BG, Lewis BJ, Dean DE. Using pre- and post-surgical foot and ankle radiograph for identification. J Forensic Sci 2002;47:1319–1322.
3. Sudimack J, Lewis BJ, Rich J, Dean DE, Fardal PM. Identification of decomposed human remains from radiographic comparisons of an unusual foot deformity. J Forensic Sci 2002;47:218–220.
4. Moore KL, The Developing Human, Clinically Oriented Embryology. Philadelphia, PA: WB Saunders, 1988.
5. Bass WM. Human osteology: a laboratory and field manual of the human skeleton. 4th ed. Columbia, MO: Missouri Archaeological Society, 1995.
6. White TD. Human osteology. New York, NY: Academic Press, 2000.

7. Nafte M. Flesh and bone. An introduction to forensic anthropology. Durham, NC: Carolina Academic Press, 2000.
8. Fenton TW, Birkby WH, Cornelison, J. A fast and safe non-bleaching method for forensic skeletal preparation. J Forensic Sci 2003;48:274–276.

Further Reading

Byers D. Introduction to forensic anthropology. Boston: Allyn & Bacon, 2001.

Ortner DJ, Identification of pathological conditions in human skeletal remains, 2nd ed. New York, NY: Academic Press, 2003.

Reichs KJ. Forensic Ostelogy: advances in the identification of human remains. Reichs KJ, ed. Springfield: Charles C. Thomas, 1998.

Chapter 3

Normal Osteology of the Knee Joint and Markers of Stress and Injury

Emily A. Craig, PhD

1. Introduction

Analysis of the knee for forensic identification has often been overlooked in favor of studies of skeletal elements that have more individualizing features than the knee. However, there may be instances when careful analysis of the knee can provide clues to a person's identity.

All the musculoskeletal tissue at the knee should be examined carefully for evidence of antemortem injuries, repetitive stress, and surgical modifications, which, it is hoped, correlate with a specific overuse syndrome or ideally with a putative victim's medical record. In skeletonized remains, osteologic evidence (and perhaps some nonabsorbable sutures) may be the only evidence remaining for analysis. In other cases, analysis of the connecting ligaments and capsular structures often can provide answers to the puzzle of victim identification. Therefore, these structures should never be removed during hasty attempts to expose the bone.

This chapter will help forensic experts become familiar with the most common anatomic terminology and conditions involving the knee and provide a condensed anatomy atlas of that region. All illustrations depict the right knee.

2. Osteology

2.1. Femur

The femur is the longest bone of the human body. It consists of a rounded proximal head that articulates with the acetabulum at the hip, a nearly cylindrical shaft, and a distal metaphysis that forms two large rounded condyles that articulate with the tibia.

From: *Forensic Science and Medicine*
Forensic Medicine of the Lower Extremity: Human Identification and Trauma Analysis of the Thigh, Leg, and Foot
Edited by: J. Rich, D. E. Dean, and R. H. Powers © The Humana Press Inc., Totowa, NJ

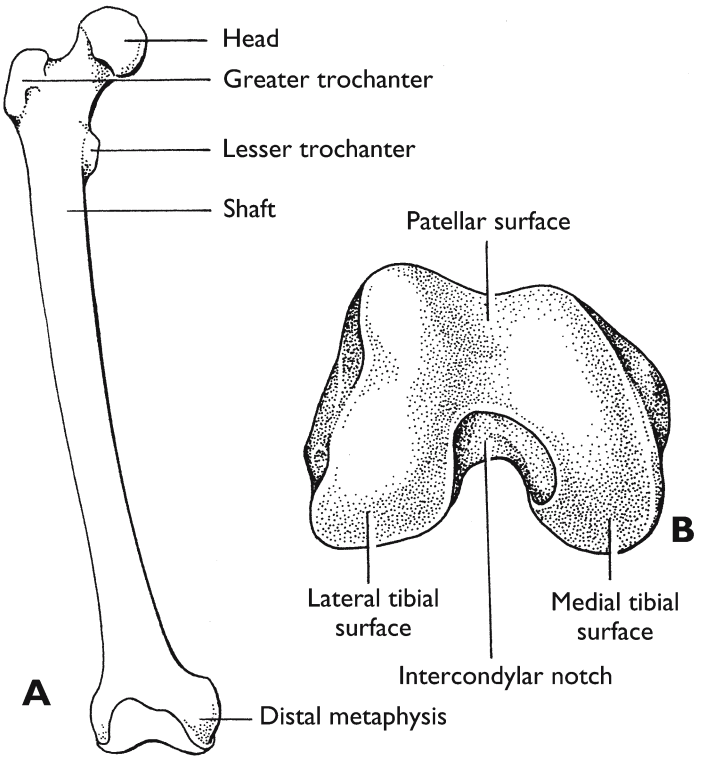

Fig. 1. Anterior femur: **(A)** Anterior view of the entire femur; **(B)** The distal articular surface shows how the patellar surface blends into the medial and lateral tibial surfaces.

Because of its relationship with the osteology of the knee, the distal portion of the femur will be the focus of this section. This distal portion is widely expanded to provide a large surface for the transmission of body weight to the top of the tibia. It is made up of two large condyles that are partially covered by articular cartilage. These two condyles are separated posteriorly by the intercondylar notch but are united anteriorly, where they provide an articular surface for the patella.

2.1.1. Articular Surfaces

The patellar and the tibial surfaces are the two major divisions of the distal articular surface. The patellar surface is concave from side to side and has a groove along its long axis. It is higher on the lateral side and is separated from the tibial surfaces by two relatively indistinct grooves. The tibial surface is further divided into medial and lateral parts. Anteriorly the tibial surfaces are continuous with the patellar surface, but posteriorly they are separated by the intercondylar notch or fossa (Figs. 1, 2). Normally, all of these articular surfaces are covered with a thick layer of cartilage that protects the underlying bone.

2.1.2. Condyles

The femoral condyles are convex from side to side and front to back, and both project posteriorly past the plane of the posterior shaft of the femur. The medial femoral

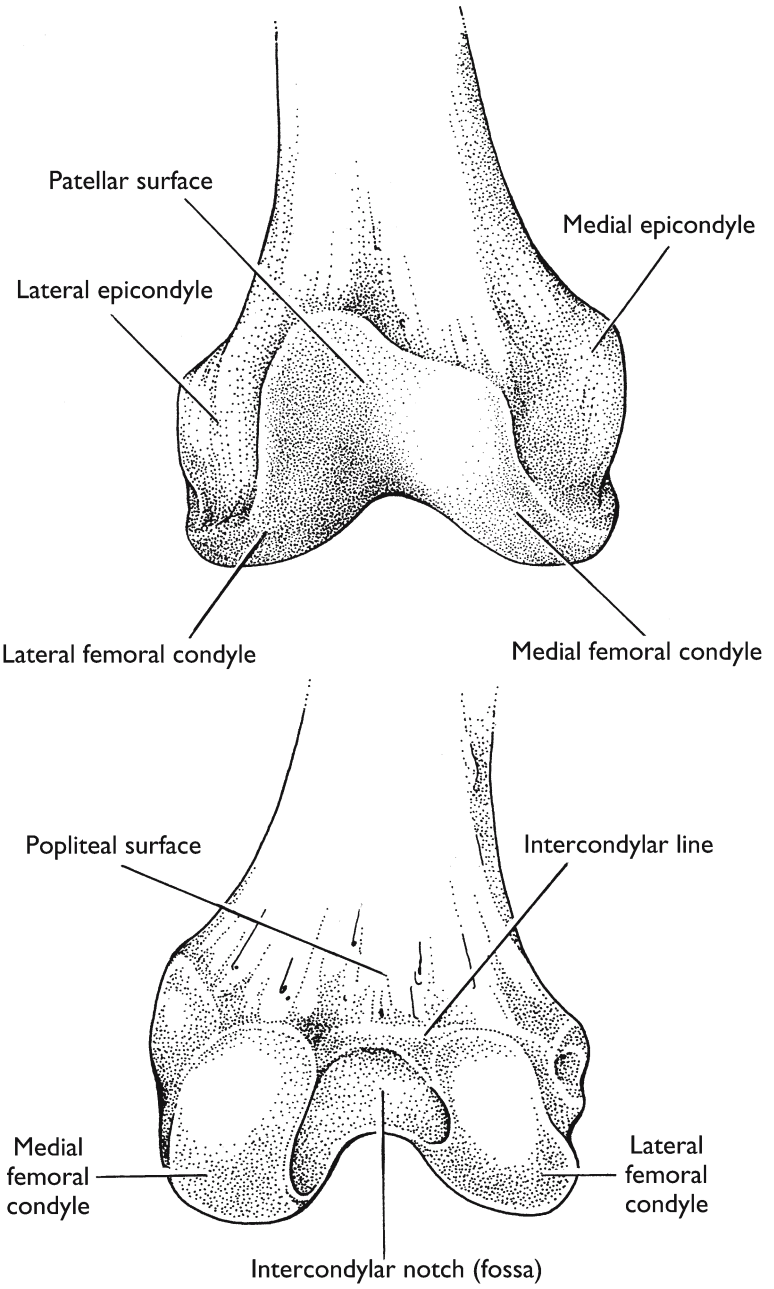

Fig. 2. Anterior and posterior views of the distal femur.

condyle is larger and rounder than the lateral condyle and projects downward and medially to such an extent that the lower surface of the lower end of the bone appears to be practically horizontal when seen from the side (Fig. 3). The lateral femoral condyle is less prominent but is longer from front to back. It is wide and steeply sloped medially to laterally, where it creates a large weight-bearing surface against the interspinous eminence

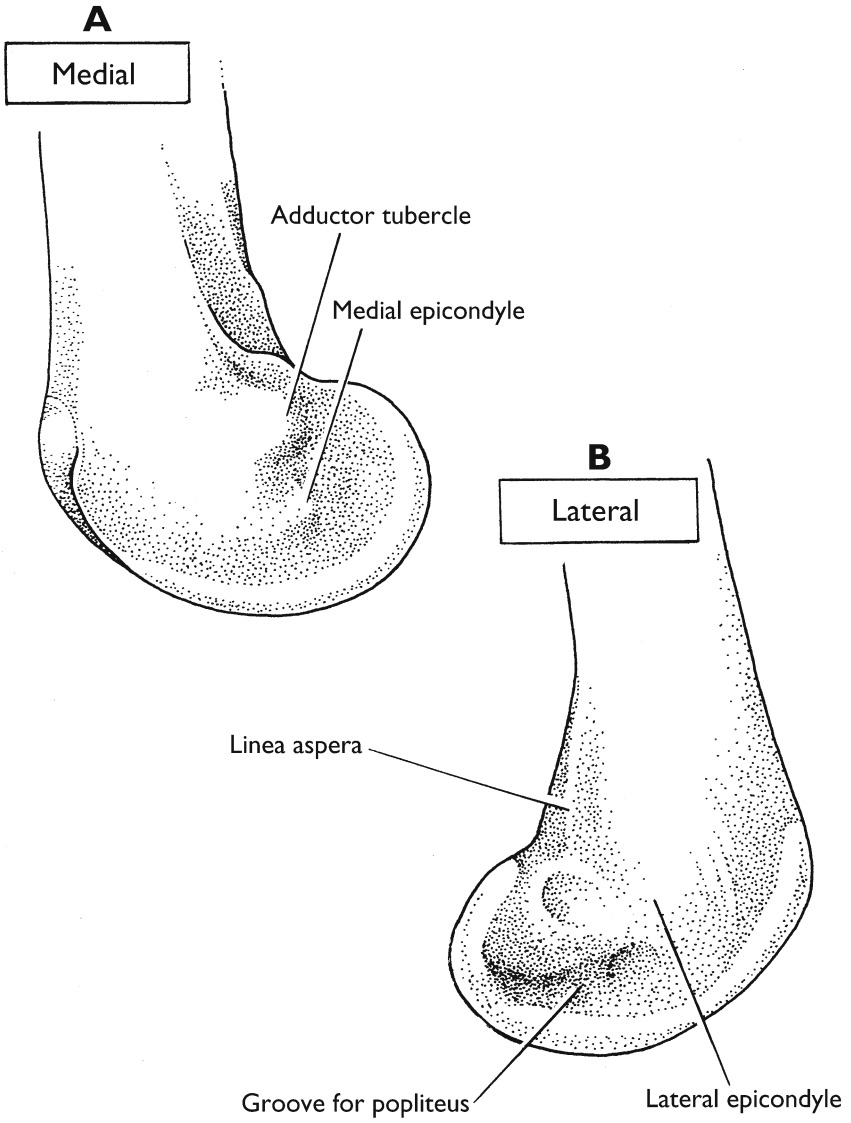

Fig. 3. The epicondyles of the femur: lateral and medial views.

of the lateral tibial plateau. The lateral femoral condyle is comparatively narrow posteriorly, where it is not in weight-bearing apposition with the tibia.

2.1.3. Epicondyles

Immediately superior to the femoral condyles are the epicondyles and their tubercles, which provide attachments for many muscles, tendons, and capsular ligaments (Fig. 4). Some of these attachment sites are well defined on the bone, but others are much more subtle. The attachment site of the tibial collateral ligament on the medial femoral epicondyle is a distinct raised area immediately anterior and inferior

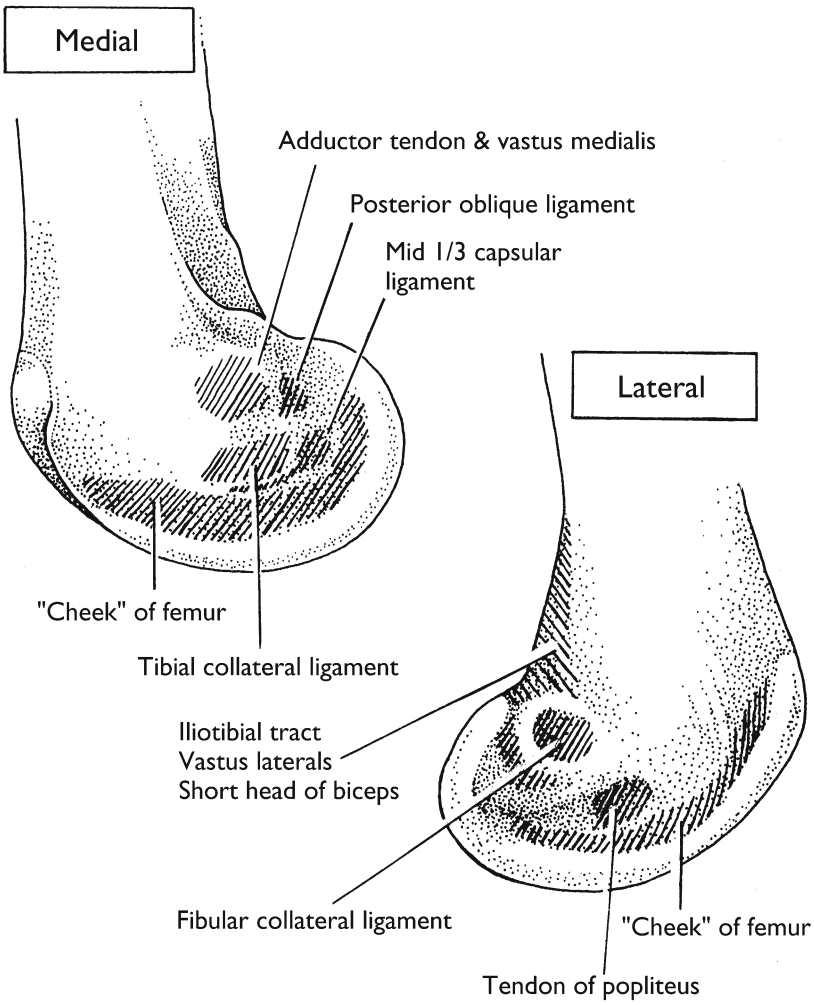

Fig. 4. Attachment sites for soft tissues. Just above the articular surfaces, the distal femur has numerous sites of attachment for periarticular soft tissues *(10,11)*.

to the adductor tubercle, which in turn is the attachment site for the adductor tendon as well as for the vastus medialis obliquus muscle. Just inferior to the medial epicondyle is the attachment site for the mid third of the medial capsular ligament; slightly posterior to this is the insertion site of the posterior oblique ligament and capsular arm of the semimembranosus (Fig. 5).

The lateral epicondyle provides attachment sites for the fibular collateral ligament, the tendon of the popliteus muscle, fibers of the iliotibial tract, and the lateral capsular ligament. Just superior and posterior to the epicondyle is the most distal extent of the linea aspera. This raised area of bone provides attachment sites for the iliotibial tract, the vastus lateralis, and the short head of the biceps. Between the lateral epicondyle and the linea aspera is the attachment site for the lateral head of the gastrocnemius.

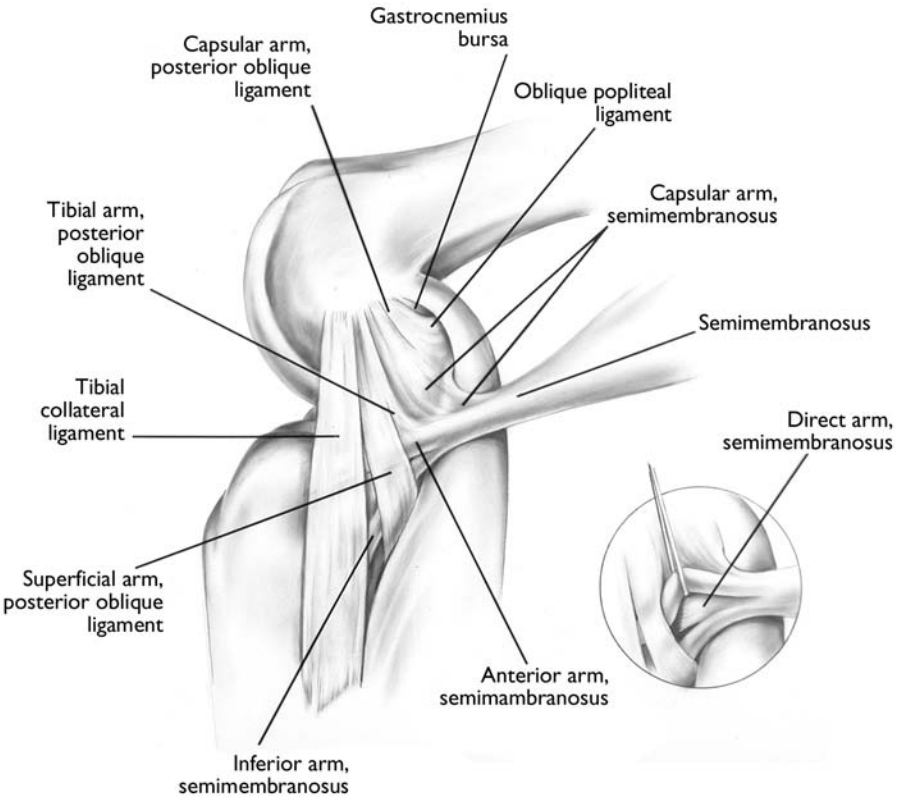

Fig. 5. The capsular expanse of the semimembranosus covers the entire posteromedial corner of the knee joint (illustration by the author, reproduced with permission from ref. *1*; Hughston Sports Medicine Foundation, Inc., Columbus, Georgia).

The so-called "cheek" of the femur *(1)* provides an attachment site for the synovial membrane and separates both medial and lateral epicondylar areas of bone from the articular surfaces.

2.1.4. Intercondylar Notch

The intercondylar notch separates the medial and lateral femoral condyles and is the attachment site for the cruciate ligaments, the ligaments of Wrisberg and Humphrey, and the frenulum of the patellar fat pad (Figs. 1, 6–8). A large portion of the notch is rough and pitted by vascular foramina, but it is relatively smooth where it provides attachment for ligaments. To accommodate the ligaments, the notch is widened posteriorly where it is not in apposition with the tibia. In the most posterior superior portion, the notch connects to the intercondylar line, a distinct ridge of bone that provides attachments for the oblique popliteal ligament and the posterior portion of the arcuate ligament (Fig. 9).

2.1.5. Popliteal Surface

A large portion of the posterior distal femur is described as the popliteal surface. It is the floor of the upper part of the popliteal fossa of the knee and is covered by fat,

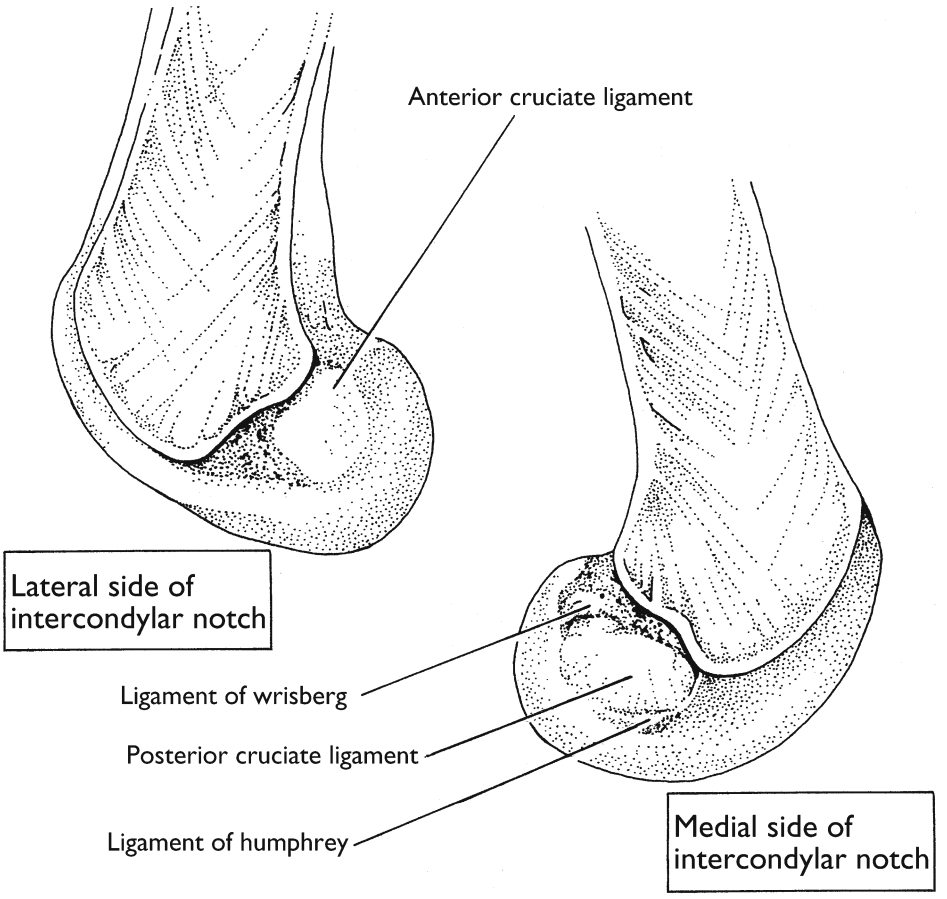

Fig. 6. Sagittal sections of the femur expose medial and lateral sides of the intercondylar notch and show the attachment sites for the cruciate ligaments as well as the ligaments of Humphrey and Wrisberg *(12)*. The frenulum of the infrapatellar fat pad, shown in Fig. 8, also inserts in the notch but the bony landmarks are ambiguous and variable *(1)*.

which separates it from the popliteal artery. It is a relatively flat, slightly concave surface that is deeply pitted with vascular foramina. Lateral to this is a raised area of bone where the plantaris, the lateral head of the gastrocnemius, and the arcuate ligament attach. At the most medial edge of the popliteal surface, the bone expands to provide an attachment site for the medial head of the gastrocnemius, the adductor aponeurosis, and the semimembranosus retinaculum (Figs. 2, 9,10).

2.2. Tibia

The tibia is the larger of the two bones of the lower leg and, except for the femur, is the longest bone of the skeleton. The proximal end is flattened and expanded to provide a large surface for bearing body weight transmitted through the lower end of the femur. The shaft is prismoid in section, especially in the proximal third. The distal end is smaller than the proximal end, and there is a stout process—the medial malleolus—at the end. The proximal end forms a large portion of the knee joint.

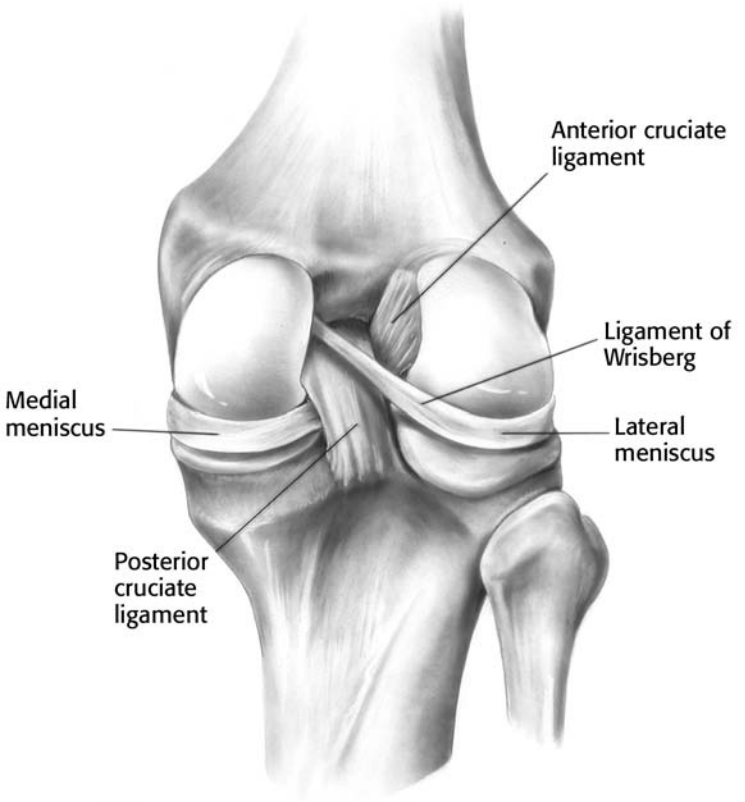

Fig. 7. The intercondylar notch is widened posteriorly to accommodate the proximal attachments of the posterior cruciate, the anterior cruciate, and the ligament of Wrisberg. (illustration by the author, reproduced with permission from ref. *1*; Hughston Sports Medicine Foundation, Inc., Columbus, Georgia).

2.2.1. Articular Surfaces

The uppermost portion of the tibia is expanded, especially in the transverse axis, into two prominent condyles. The articular surface of the larger medial condyle is concave and essentially ovoid. It is flattened where it comes in contact with the medial meniscus, and the imprint of the medial meniscus can frequently be seen on the bone. The articular surface of the lateral tibial condyle is more circular in outline and likewise bears a flattened imprint of the corresponding lateral meniscus (Fig. 11). Both articular surfaces are normally covered with thick cartilage, and they rise sharply in the center of the joint to form their respective sides of the intercondylar eminence.

As the anterior articular margins of the two articular surfaces recede from each other, the middle of the tibial plateau broadens into a fairly flat, smooth area that is devoid of cartilage. The infrapatellar fat pad covers this portion and separates it from

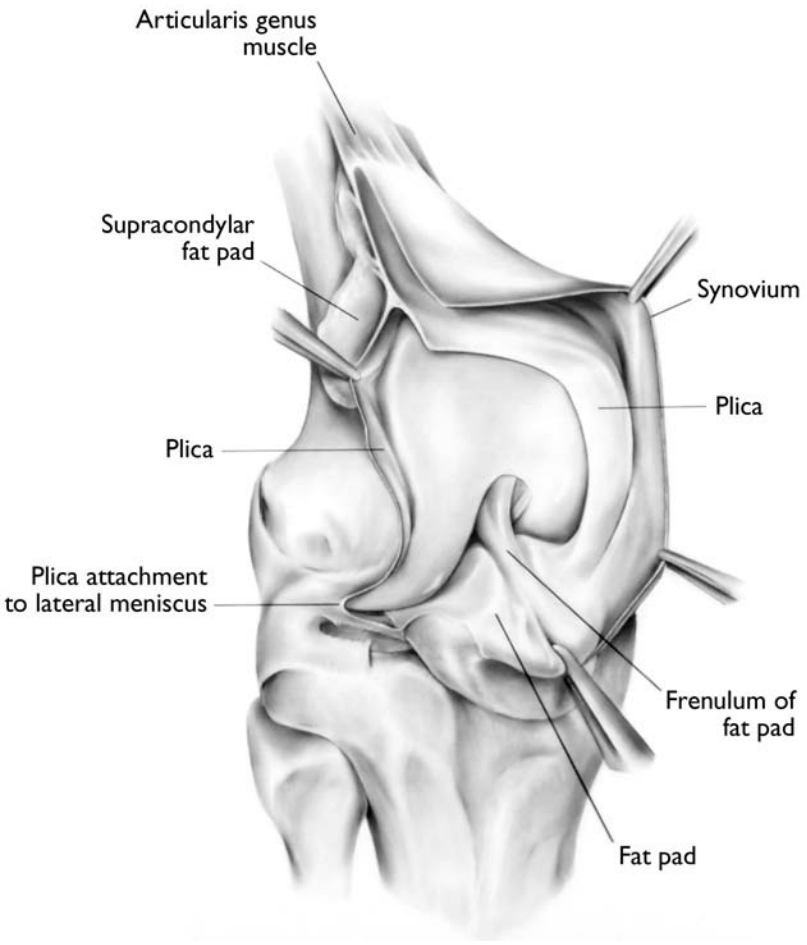

Fig. 8. Suprapatellar plica. The suprapatellar plica is a fold of the normal synovium surrounding the knee. It originates superolaterally over the supracondylar fat pad. It is tethered superiorly by the articularis genu. When healthy and smooth, it glides over the medial articular surface and inserts distally into the infrapatellar fat pad (illustration by the author, reproduced with permission from ref. *1;* Hughston Sports Medicine Foundation, Inc., Columbus, Georgia).

the patellar ligament. The medial and lateral menisci insert between this smooth, flat area and the articular surfaces just posterior to this fat pad. The area of attachment for the anterior cruciate ligament fits between the meniscal attachments and the intercondylar spines or eminences. Immediately posterior to the intercondylar eminences are attachment sites for the posterior horns of the medial and lateral menisci. Behind these, the posterior intercondylar area slopes sharply downward into a fovea and provides an attachment site for the lower end of the posterior cruciate ligament. The posterior intercondylar area ends in a ridge to which the posterior capsular structures are attached (Figs. 10, 11).

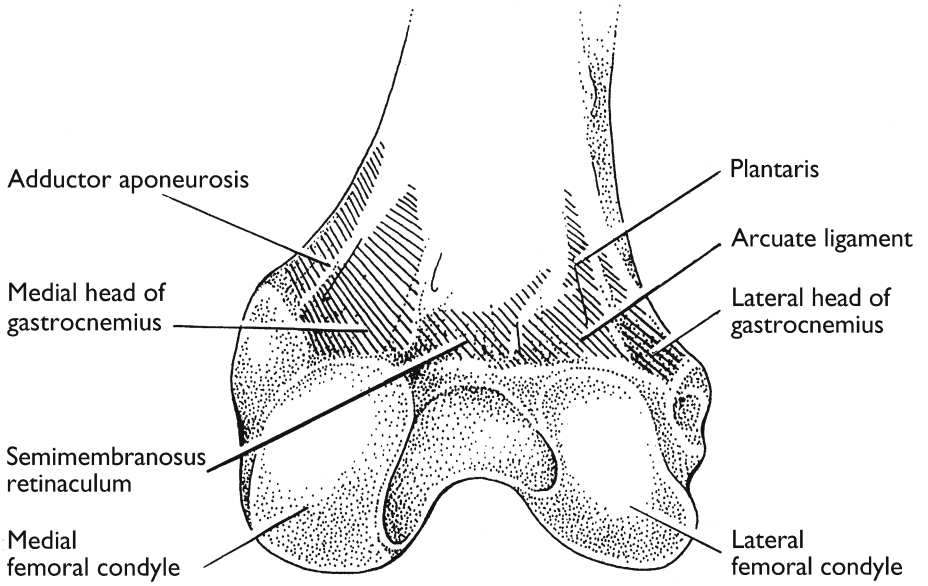

Fig. 9. The posterior portion of the distal femur consists of a central popliteal surface with attachments for periarticular structures across almost the entire distal expanse. These periarticular structures are shown in Figs. 5, 9, 10, 16, 17).

2.2.2. Tibial Tuberosity

A large tuberosity that is divided into a lower roughened region and a smooth upper region is present on the anterior surface of the proximal tibial shaft. The patella ligament inserts on the lower region. The upper surface of this tuberosity is tilted backward relative to the long axis of the shaft, but the inferior surface projects forward in a triangular protuberance (Fig. 12).

2.2.3. Condyles

On the lateral side of the tuberosity, the tibia first forms a ridge that provides attachment sites for the lateral capsule and fibers from the iliotibial tract (Figs. 12, 13). The strongest, direct attachment for the iliotibial tract, however, is on the lateral tibial tubercle. A prominent ridge just posterior to the tubercle provides an attachment site for the lateral capsular ligaments. The lateral tibial condyle is somewhat flattened below and articulates with the head of the fibula posteriorly. The fibular facet is directed downward and laterally to match the articular surface of the head of the fibula. The posterior edge of the fibular facet is on the posterolateral portion of the proximal tibia, just below the posterolateral tibial plateau. The most posterior third of the lateral condyle has an acute posterior slope just medial to the plateau (Figs. 12, 14, 15).

The medial tibial condyle projects much farther posteriorly than does the lateral condyle, and the entire nonarticular surface provides an extensive attachment site for the tendon and retinaculum of the semimembranosus. The superior posteromedial edge of this condyle has a distinct groove for the direct arm of the semimembranosus, and the tibial attachment for the posterior oblique ligament and the mid third of the medial

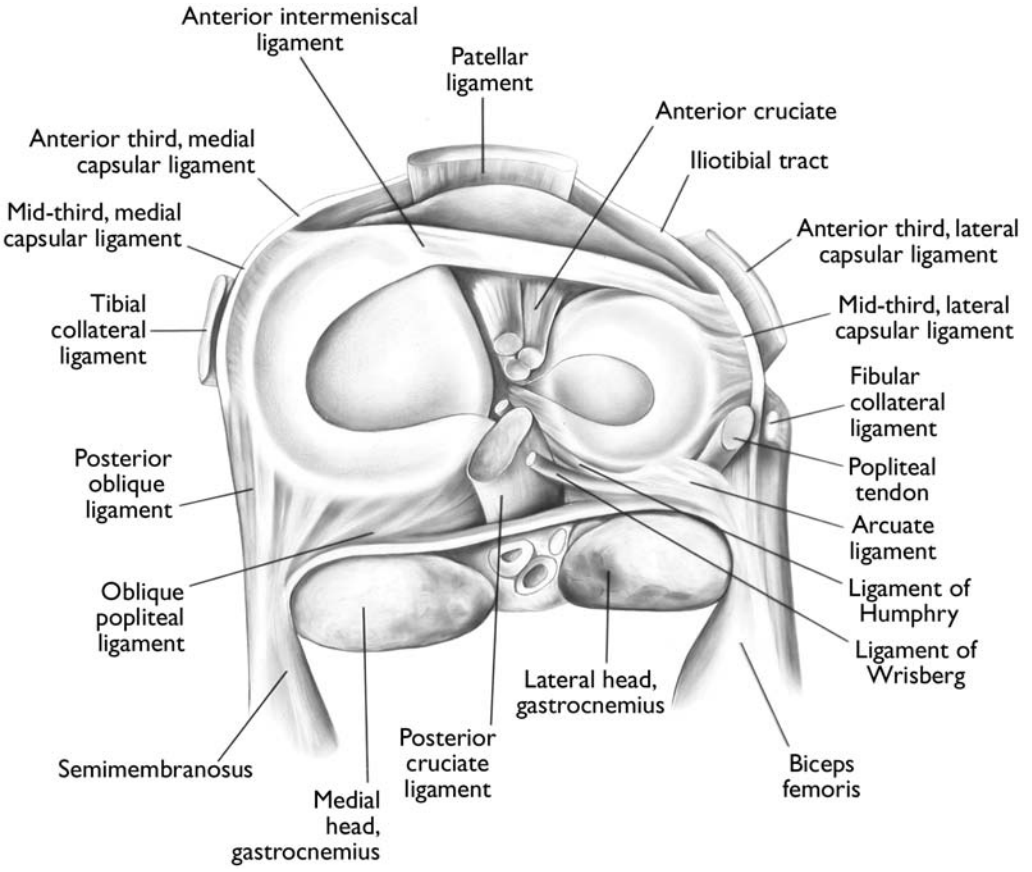

Fig. 10. Proximal surface of the tibia with associated soft tissues: superior view (illustration by the author, reproduced with permission from ref. *1*; Hughston Sports Medicine Foundation, Inc., Columbus, Georgia).

capsular ligament is just above this groove. The most medial portion of the medial tibial condyle is raised to create a smooth projection that secures a bursa over which the tibial collateral ligament glides. This ligament produces a distinct ridge that extends down the medial shaft of the tibia. As the distal condyle blends into the shaft, it drops off sharply and angles anteriorly to produce the medial surface of the tibial tuberosity and provide an attachment site for the tendons of the sartorius, gracilis and semitendinosus (Figs. 14, 16–18).

2.2.4. Posterior Surface

The proximal tibia expands posteriorly and angles obliquely from the medial to lateral direction. Distally it ends abruptly as the shaft drops off to form a deep depression to accommodate the bulk of the popliteus muscle. Medial and posterior to the fibular facet, the tendon of the popliteus produces a distinct groove on the bone. The posterior border of the tibial plateau ends in a sharp ridge medial to this popliteal groove, and the posterior popliteal ligament inserts in the area inferior to the ridge.

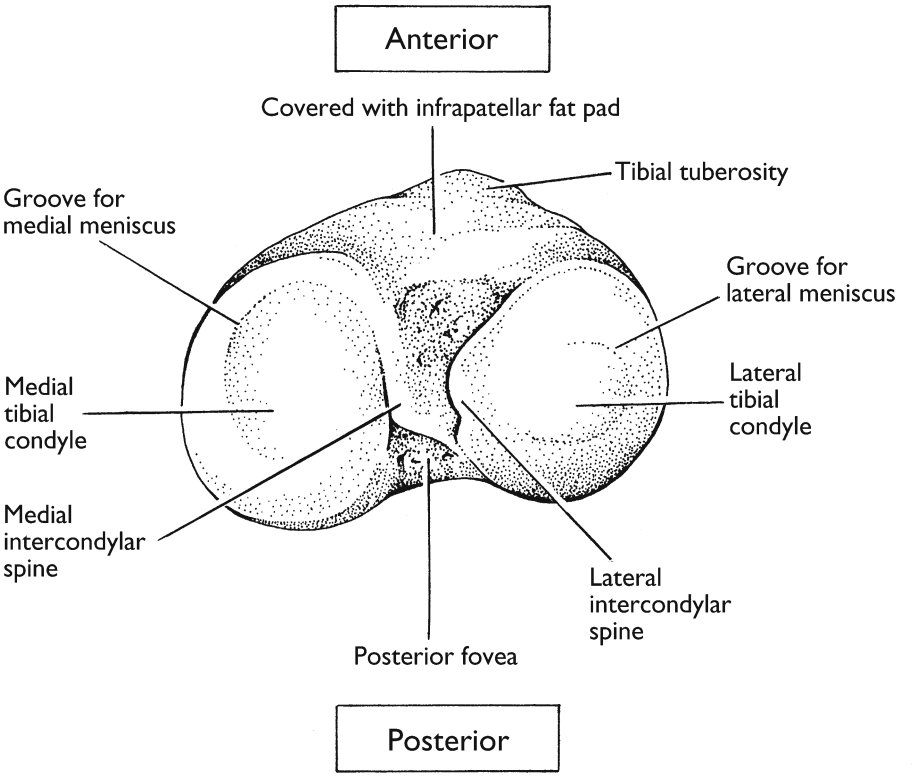

Fig. 11. Proximal surface of the tibia: superior view.

A deep fovea in the central part of the posterior proximal tibia marks the lower site of attachment for the posterior cruciate ligament. A distinct osseous ridge extends from just below the posterolateral tibial plateau and runs obliquely toward the medial border of the tibial shaft, the bony origin of the soleus muscle (Figs. 7, 11, 14, 18).

2.3. Fibula

The fibula, the lateral bone of the leg, is more slender than the tibia. It does not share in the transmission of body weight but functions primarily as an anchor for the muscles of the lower leg. The shaft, which has a variable shape that is molded by the muscles to which it gives attachment, ends distally as the lateral malleolus.

The head of the fibula is the only portion that contributes to the structure of the knee joint. The shape of the head is extremely variable, and all its diameters are expanded in relation to the shaft. Its upper surface contains an articular facet that joins onto the inferior lateral tibial condyle, but the exact location of the articulation with the tibia is not constant. The styloid process projects upwards from the lateral part of the superior surface of the head and is the site of attachment for the arcuate ligament. Anterior to this is a small depression that marks the attachment of the fibular collateral ligament. Short, strong ligaments totally surround the tibiofibular articular surfaces and create what is an almost immovable "plane joint" between the two bones. The tendon of the combined long and short heads of the biceps femoris inserts on the anterior surface of the head of the fibula (Fig. 15).

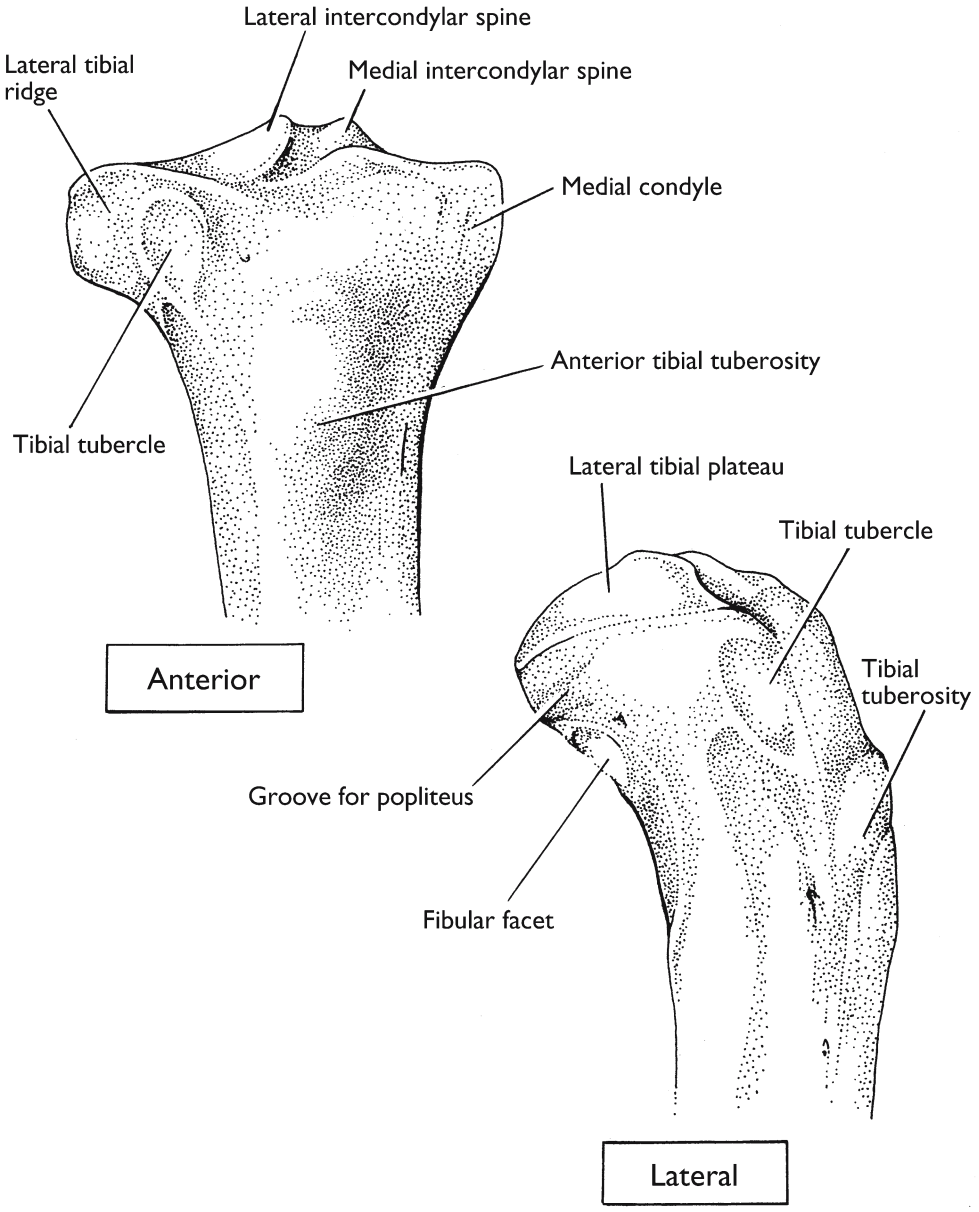

Fig. 12. Proximal tibia: anterior and lateral views.

2.4. Patella

The patella is a large sesamoid bone within the quadriceps femoris tendon that articulates with the patellar surface of the distal femur. The anterior surface is flattened, with just a slight convex curve. The surface is perforated with many nutrient foramina and is marked with numerous rough, longitudinal striae. The inferior half is roughly triangular and the superior border is rounded. The medial and lateral borders are relatively

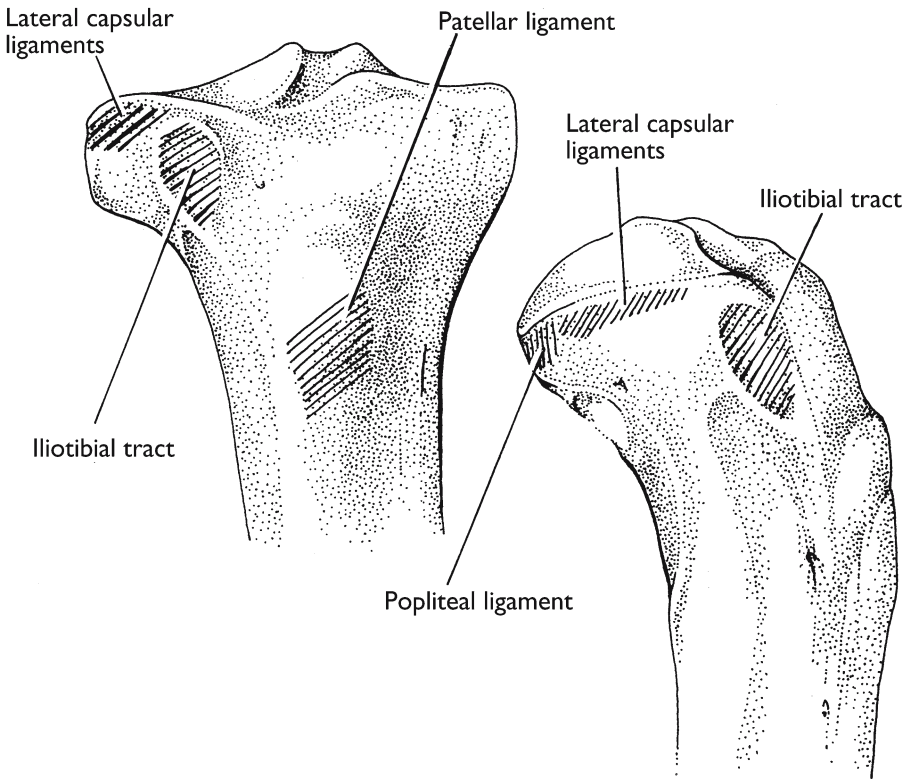

Fig. 13. Anterior and lateral views of the proximal tibia showing soft tissue attachment sites.

thin but provide substantial areas for musculotendinous attachments. The superolateral border is the site of attachment of the vastus lateralis tendon, where a distinct notch often is present or even an accessory ossification center.

An articular surface covers most of the posterior patella and molds to fit smoothly against the femur. It made up of a large medial and lateral facet; a central ridge; and a single, small, medial facet that is sometimes referred to as the "odd" facet *(2)*. The lateral facet is the largest and deepest of the three facets.

Just inferior to the articular surface is an area known as the apex. The inferior border of the apex is roughened and provides attachment for the patellar ligament. Its superior surface is covered by the infrapatellar fat pad and an extension of synovium termed the ligamentum mucosum or frenulum (Fig. 19).

2.5. Fabella

Fabella, a term derived from the Latin word for "little bean," is a sesamoid bone buried in the lateral head of the gastrocnemius muscle near the musculotendinous junction. The fabella is approximately 13.5 mm long and 3.5 mm wide on average but can be as large as 22 mm × 14 mm *(3–5)*. Data on the occurrence of a fabella vary greatly; the reported frequency ranges from 9.8 to 22% in the normal population and up to 35% in

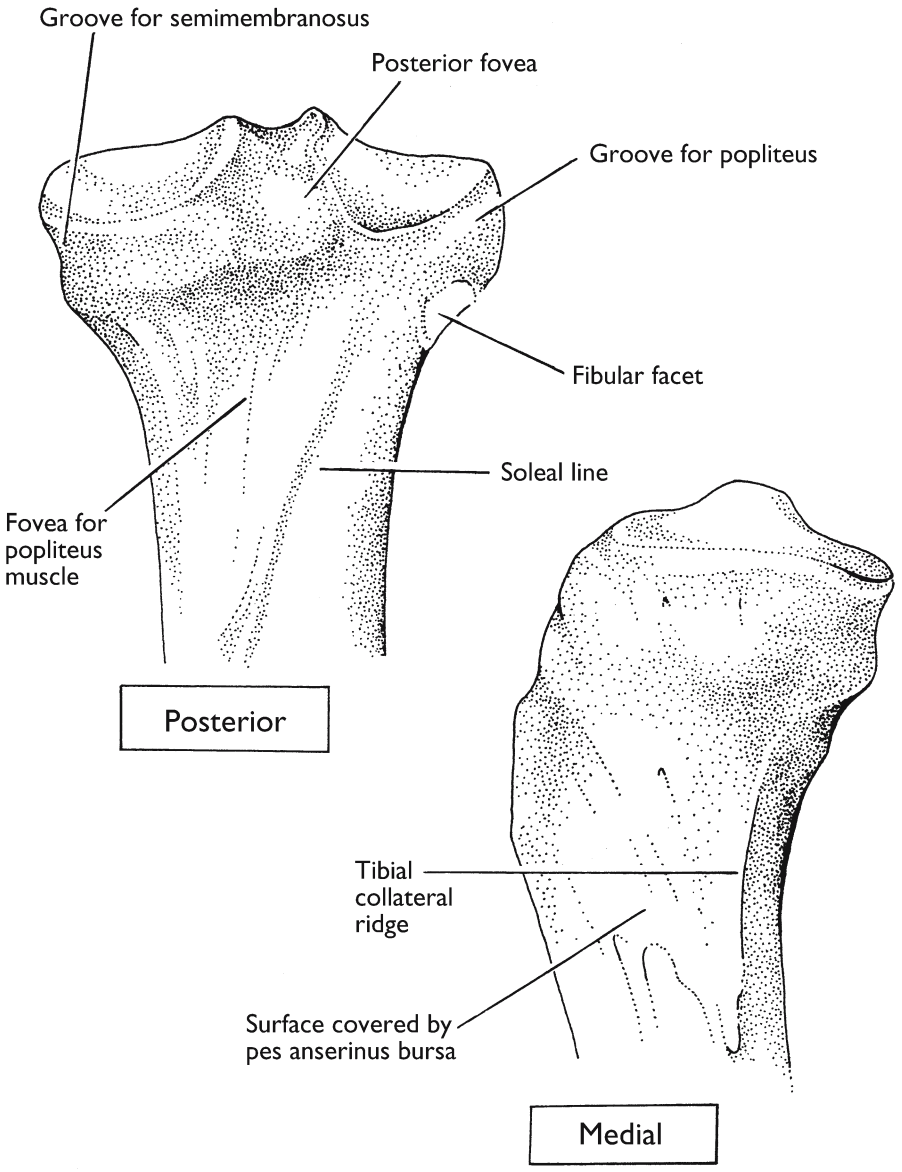

Fig. 14. Bony topography of the posterior and medial proximal tibia.

patients with clinically significant osteoarthritis of the knee *(3,4,6)*. Among individuals who have a fabella, it is bilateral in 71 to 85% *(6,7)*.

The anterior surface of the fabella is covered with cartilage and forms an articulation with the posterior surface of the lateral femoral condyle. The fabella articulates with only a portion of the lateral femoral condyle when the knee is in extension, and the concave curve of the fabella touches only a small arc of the condyle. This limited contact area produces a fabella articular surface that curves very gently in both a superior–inferior and a medial–lateral direction. The overall shape of the fabella is variable, but the curve of the

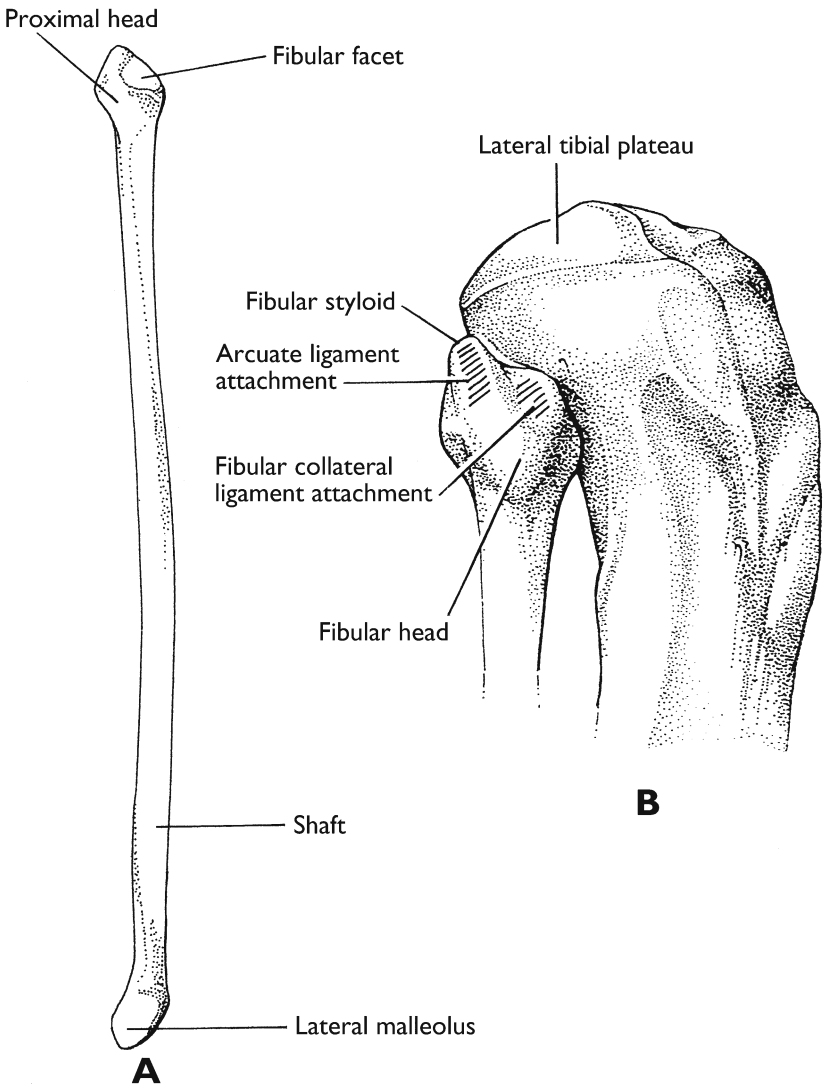

Fig. 15. The fibula: **(A)** Anterior view of the entire fibula; **(B)** Lateral view of the fibula and its relation to the tibia.

anterior articular surface is very consistent and its most distinguishing feature. This curve distinguishes a fabella from a toe sesamoid. Where the toe sesamoid forms a joint with the first metatarsal, the curve is opposite that of the fabella–femur articulation *(8)* (Fig. 20).

3. *Skeletal Evidence of Knee Injury and Stress*

The knee is the largest and one of the strongest joints in the human body. It is a major weight-bearing joint and is subjected to stress and injury even during sedentary daily living. During athletic competition and other strenuous activity, the stress is increased

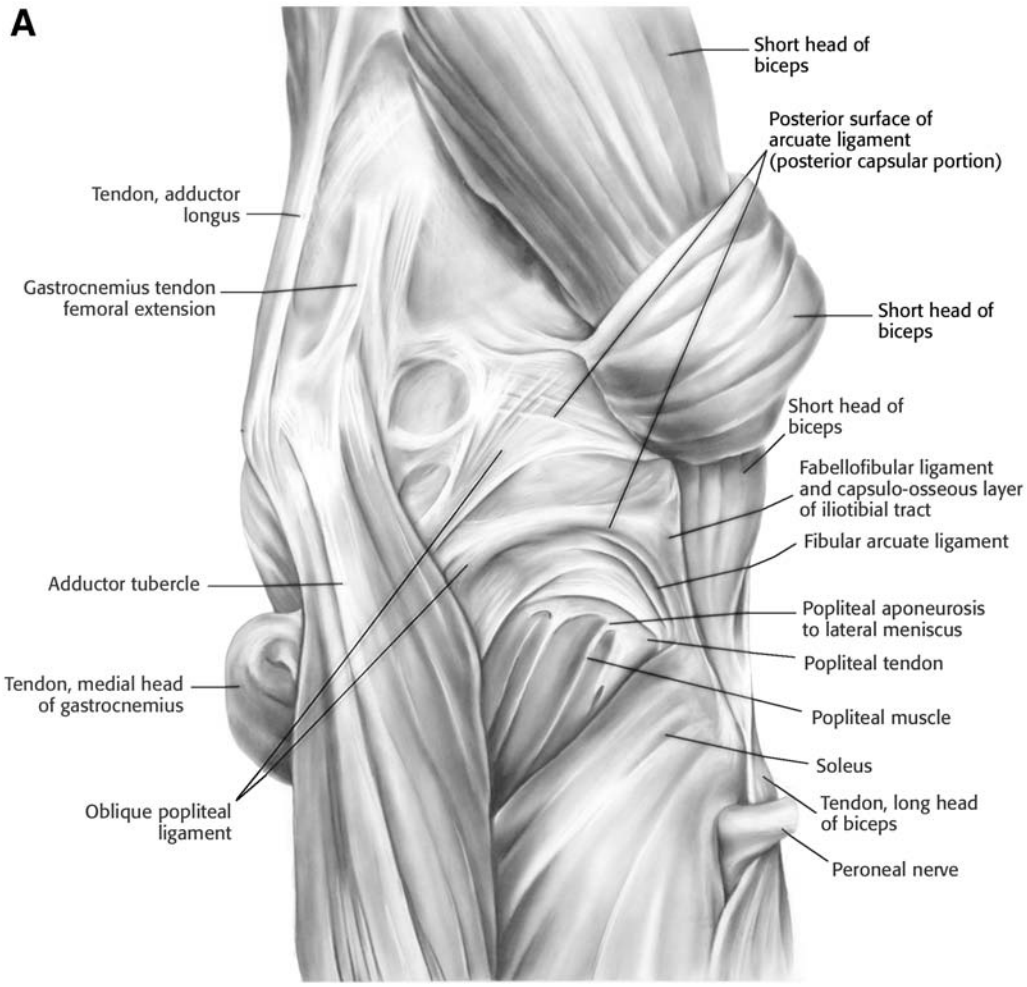

Fig. 16. These thick, strong tendons and capsular structures that cover the posterior aspect of the knee help mold the contours of the underlying bone (illustration by the author, reproduced with permission from ref. *1*; Hughston Sports Medicine Foundation, Inc., Columbus, Georgia).

to incredible levels. Some of these injuries and stresses can produce changes in the bone that become part of the permanent osteological evidence and thus can be used to recreate a pattern of activity. In forensic cases, this type of analysis can lead to a correlation with a medical record and possibly a positive identification. It is important to be able to recognize changes in the bone that are due to injury and to the stresses caused by such factors as misalignment and other mechanical forces.

The process of bone remodeling is controlled by an intricate system of bone deposition and resorption. The biomechanical principles that apply to long-bone response and remodeling are not quite the same as those that apply to synovial weight-bearing joints such as the knee, but the physiological principles are similar.

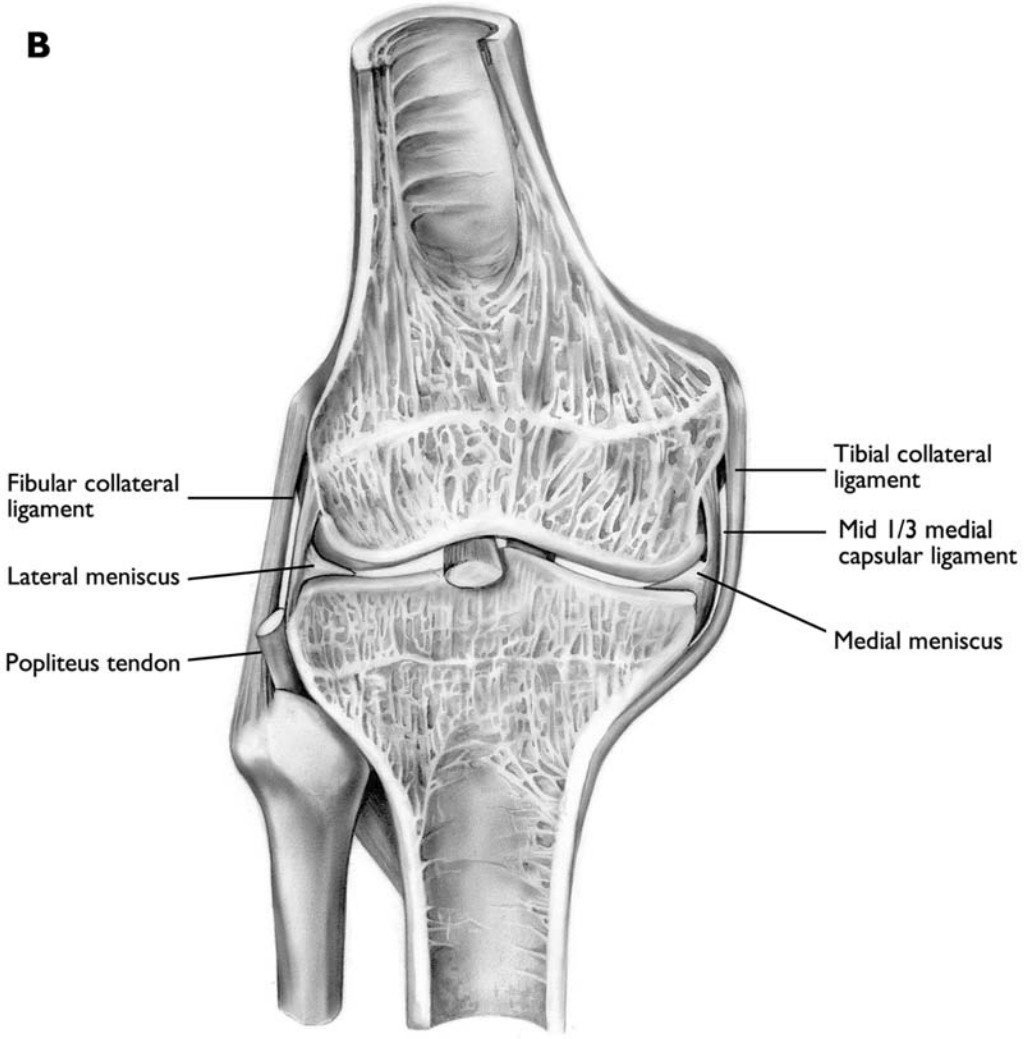

Fig. 16. *Continued.*

At the ends of the femur and tibia, the trabeculae are arranged to resist both tensile and compressive forces. When a change occurs in overall body weight, biomechanical forces, or both, there is a corresponding thickening or thinning of the trabeculae. This change in trabecular thickness, rather than cortical bone remodeling, is the primary stress response at the joint.

Other forces and factors in and around the articular surfaces of weight-bearing joints affect the response to injury and stress. In addition to bone, cartilage is the primary connective tissue involved in and around large synovial joints. Articular cartilage covers the gliding and load-bearing surfaces of the bones; fibrocartilage attaches ligaments and tendons to the bones, and fibroelastic cartilage constitutes the bulk of the interarticular menisci.

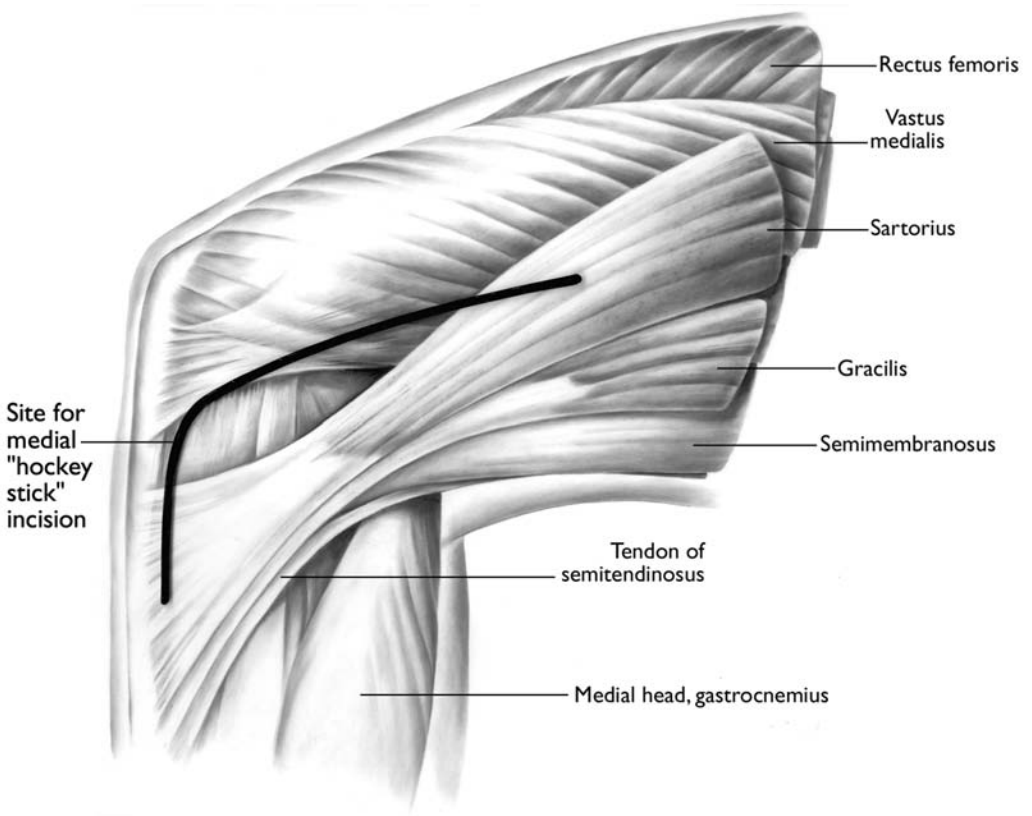

Fig. 17. The tendons of the sartorius, gracilis, and semitendinosus muscles come together as the *pes anserinus* tendon group. Here the large distal retinacular portion of the vastus medialis is also evident (illustration by the author, reproduced with permission from ref. *1*; Hughston Sports Medicine Foundation, Inc., Columbus, Georgia).

The articular cartilage is continuous with the synovium, or synovial membrane. This synovium is a vascular mesenchymal tissue that lines the joint space and produces the joint fluid that serves to lubricate, nourish, and remove cellular debris within the joint capsule.

Trauma to a large synovial joint affects primarily the ligamentous, capsular, and cartilaginous structures, but these in turn can affect the osseous structures because of the action and interaction of all anatomic and biomechanical parts. Trauma to the synovial membrane and cartilaginous surfaces is a contributory factor to the later onset of degenerative arthritis. Miltner et al. *(9)* pointed out that this synovial membrane becomes congested with small hemorrhages, resulting in the formation of pannus at the osteocartilaginous junction. This causes fibrillar degeneration of the surface layers of cartilage on the side of injury and cell damage and fissuring of the intermediate layer of cells on the opposite side. This latter change is the primary culprit in the onset of late traumatic arthritis.

Ligament injuries may be complete or incomplete. Complete ligament injury will result in demonstrable instability that if left untreated may become permanent and cause

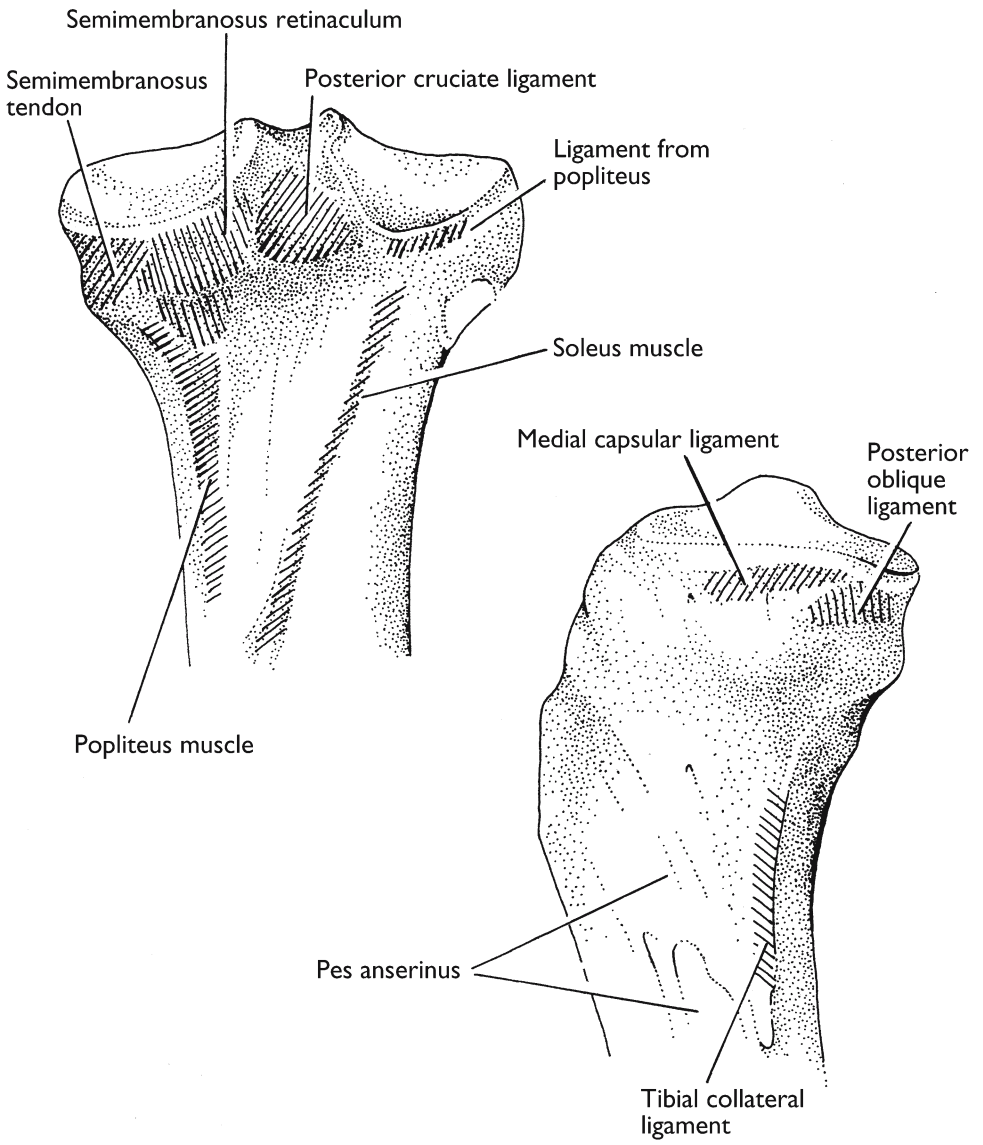

Fig. 18. Proximal view of the posterior and medial tibia showing the soft tissue attachment sites.

irreparable damage to cartilaginous and osseous structures. Repeated microtrauma can lead to the same sequence of hemorrhage, pannus, and fibrillar degeneration.

Postmortem evidence of these injuries and instabilities can be seen in and around the ends of long bones. They are sometimes overlooked or attributed to the general condition of "arthritis." For forensic identification experts, however, it is important to be able to recognize and classify evidence of knee injuries and specific stress that may offer clues leading to identification of the victim.

As a consequence of diagnostic coding protocols that have been established by the health insurance industry, the recognition and exact classification of an injury is often

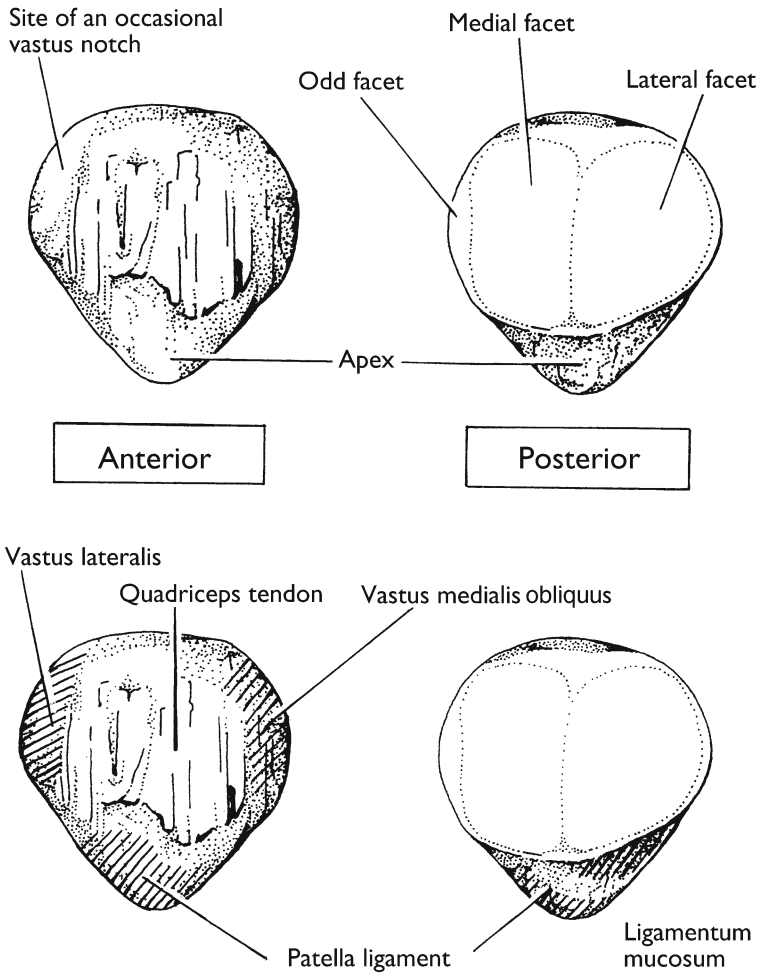

Fig. 19. Anterior and posterior views of a right patella. The top two views show the bony topography of the patella. The bottom two views indicate the attachment sites of soft tissues.

necessary to trace an individual's medical history. The ability to provide autopsy documentation that an individual at one time likely sustained an "acute avulsion of the anterior cruciate ligament" or a "lateral tibial plateau fracture" will prove to be an advantage when attempting to match damaged, decomposed, or skeletal remains with the medical records of missing persons.

This section will illustrate the typical appearance of bones that have incurred repeated mechanical stress and some of the most common knee injuries.

Femur: STRESS RELATED:

Age-related gonarthrosis (Fig. 21)
Injury-related gonarthrosis (Fig. 22)
Suprapatellar plica anatomy (Fig. 8)
Suprapatellar plica defect on bone (Fig. 23)

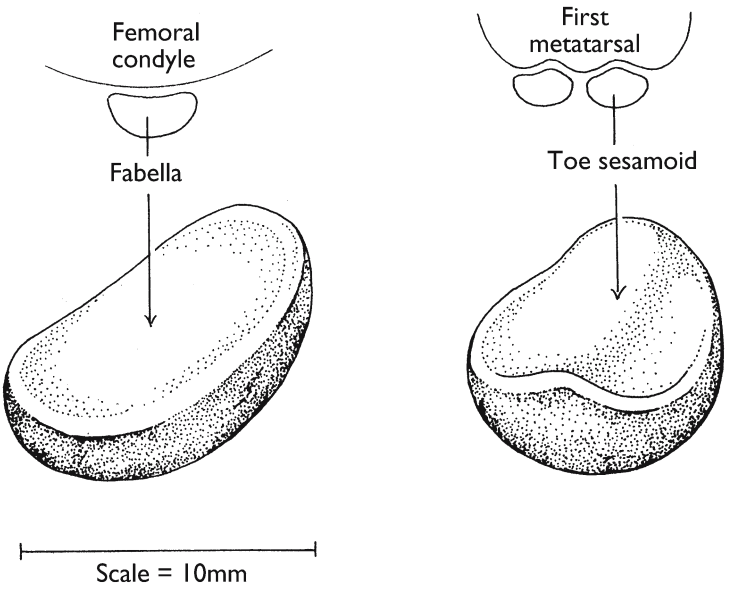

Fig. 20. Articular surfaces of a fabella and a toe sesamoid. The articular surface of the fabella is gently concave in superior–inferior and medial–lateral directions. There is a central convex curve in a toe sesamoid *(7)*.

Fabella articulation (Fig. 24)
Subluxing patella (Fig. 25)
Osteochondritis dissecans (Fig. 26)
Pellegrini–Steida disease (Fig. 27)

INJURY RELATED:
Supracondylar and condylar fractures (Fig. 28)
Ligament avulsions (Fig. 29)

Tibia: STRESS RELATED:
Meniscal wear (Fig. 30)
Age-related gonarthrosis (Fig. 31)

INJURY RELATED:
Condylar fractures (Fig. 32)
Tibial plateau fractures (Fig. 33)
Avulsion fractures (Fig. 34)
Osgood–Schlatter disease (Fig. 35)

Patella: Patellar injuries (Fig. 36)

4. Conclusions

Evidence of antemortem injuries and stress usually remains as permanent osteological features in the bone. If recognized and correctly classified, this evidence can become a critical element in the process of victim identification.

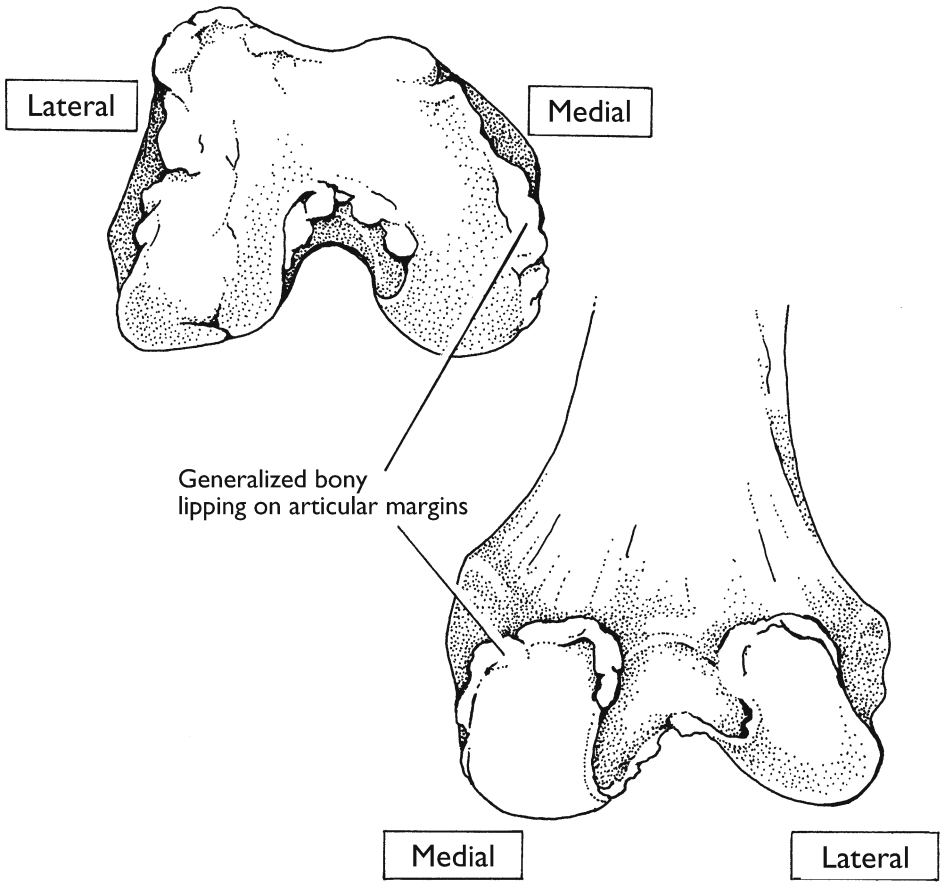

Fig. 21. Age-related gonarthrosis. Age-related, degenerative gonarthrosis is undoubtedly the most commonly encountered abnormality in the distal femur. It first appears as a general increase of bony lipping of the articular margins and can eventually involve all articular surfaces.

The first step is to recognize the anatomic or mechanical causation of the defect to identify individual clinical diagnoses that can perhaps be linked to these defects. The second step is to correlate these findings with the medical histories or medical records of suspected missing persons who match the additional criteria of age, race, sex, and stature.

The ultimate goal in forensic analysis is, of course, to identify the skeletal remains, and more often than not the final identification will be based on dentition or DNA. Sometimes, however, evidence from the postcranial skeleton can provide critical clues leading to putative identification based on clinical history. In some cases, individual features of the knee can provide the investigator with enough evidence to make a positive identification if there is comparative documentation such as a radiograph, computed tomography, or magnetic resonance imaging.

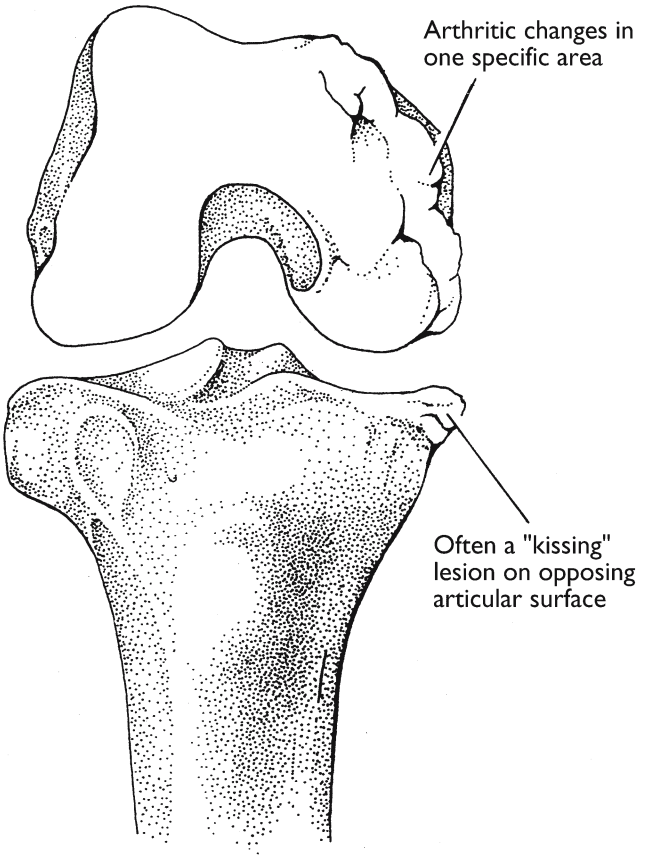

Fig. 22. Injury-related gonarthrosis. When a single specific injury to the knee results in gonarthrosis, the pattern can differ from degenerative changes. A fracture or a significant ligamentous injury can start a series of events that lead to significant arthritic changes in only one joint. This may or may not lead to generalized gonarthrosis.

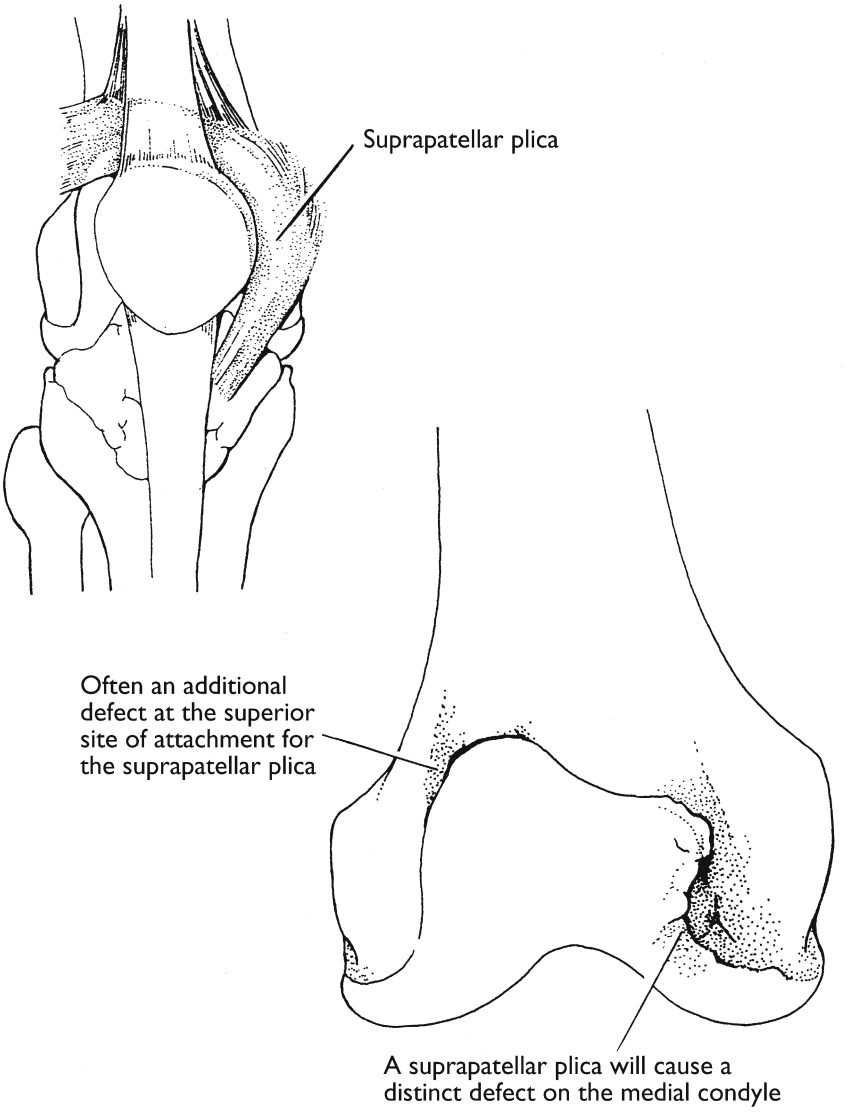

Fig. 23. Suprapatellar plica. Trauma or repetitive irritation can produce fibrosis of the plica, which in turn creates distinct scars on the femur *(1)*.

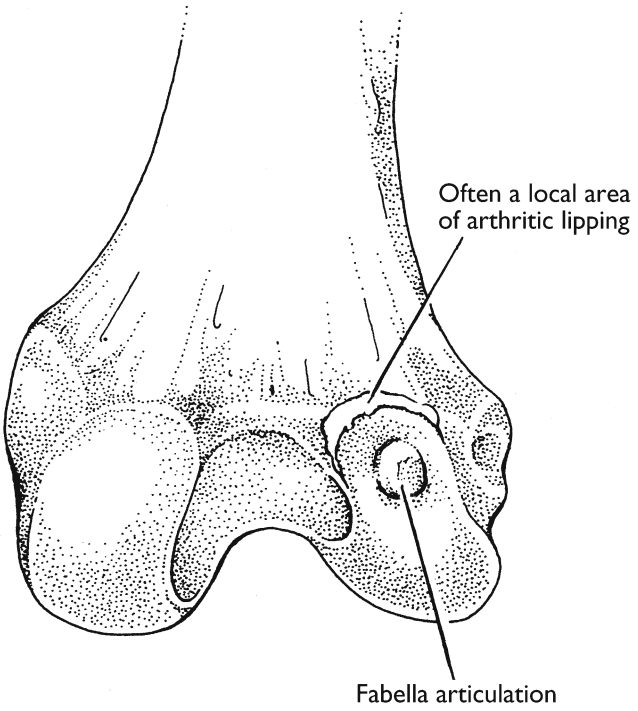

Fig. 24. Fabella articulation. The fabella articulates with a very small portion of the posterior lateral femoral condyle. This often causes chondromalacia that can lead to a discrete bony lesion *(13,14)*.

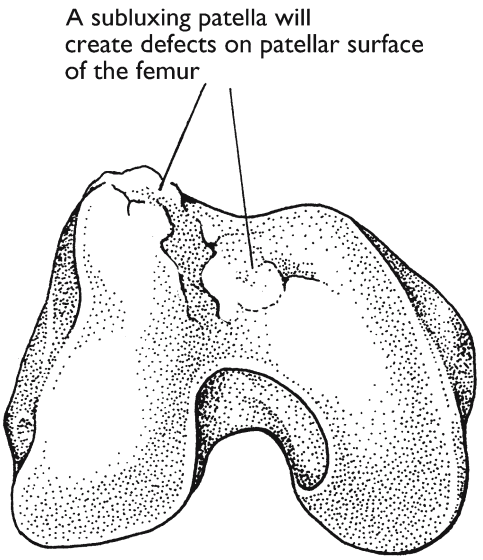

Fig. 25. Subluxing patella. Evidence of chronic patellar subluxation presents as significant degenerative arthritis on the patellar articular surface *(15)*.

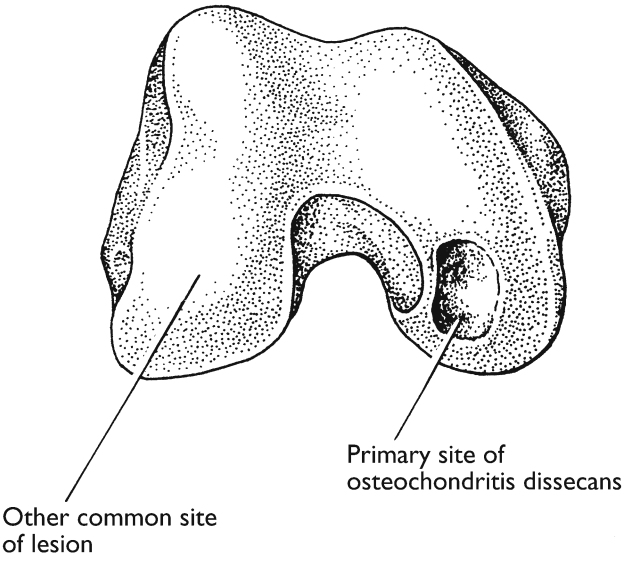

Fig. 26. Osteochondritis dessicans. Osteochondritis dissecans creates a discrete lesion on the tibial articular surface. An area of subchondral bone undergoes avascular necrosis, and degenerative changes occur in the cartilage overlying it. The lesion is usually located on the medial femoral condyle, where weight is born against the medial eminence, but it can occur elsewhere on this articular surface and also on the lateral femoral condyle *(16)*.

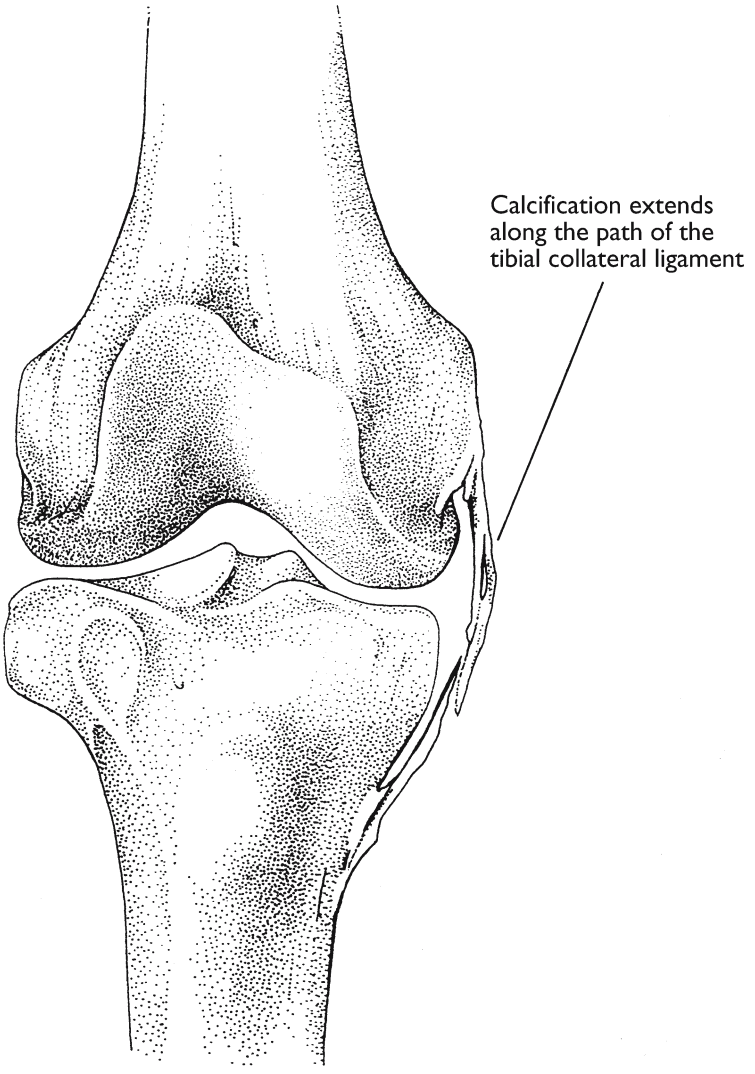

Fig. 27. Pelligrini–Stieda disease. Pelligrini–Stieda disease is characterized by a bony formation that starts in the superior portion of the tibial collateral ligament and can extend to the tibia in severe cases. It is due to previous trauma to the medial capsular structures of the knee *(1,17)*.

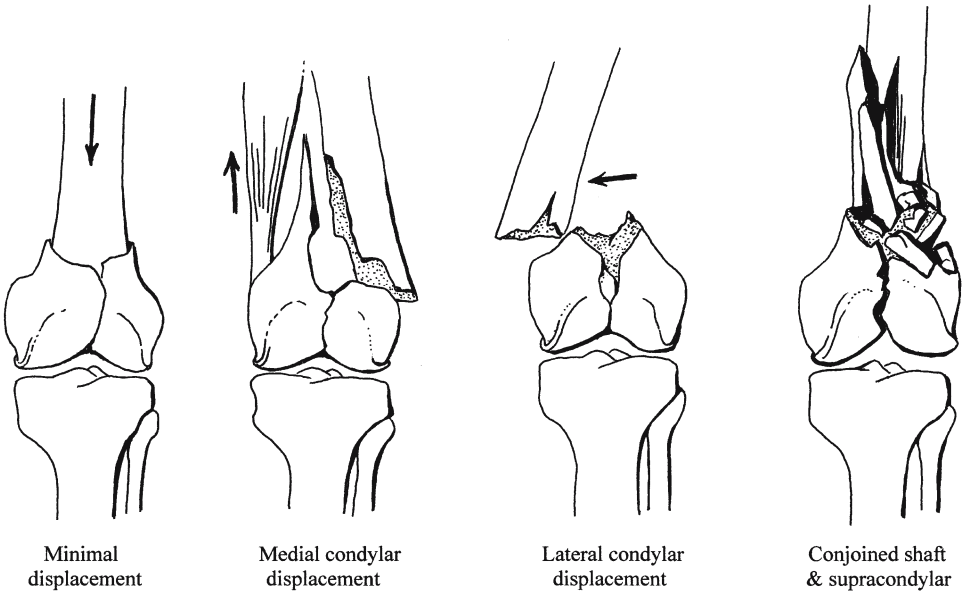

Fig. 28. Condylar and supracondylar fractures. Condylar and supracondylar fractures of the femur can take many forms, and Neer et al. proposed a useful classification of these *(18)*, which are redrawn here. Severe displaced fractures are now most likely to be treated with open reduction and internal fixation (Left knee).

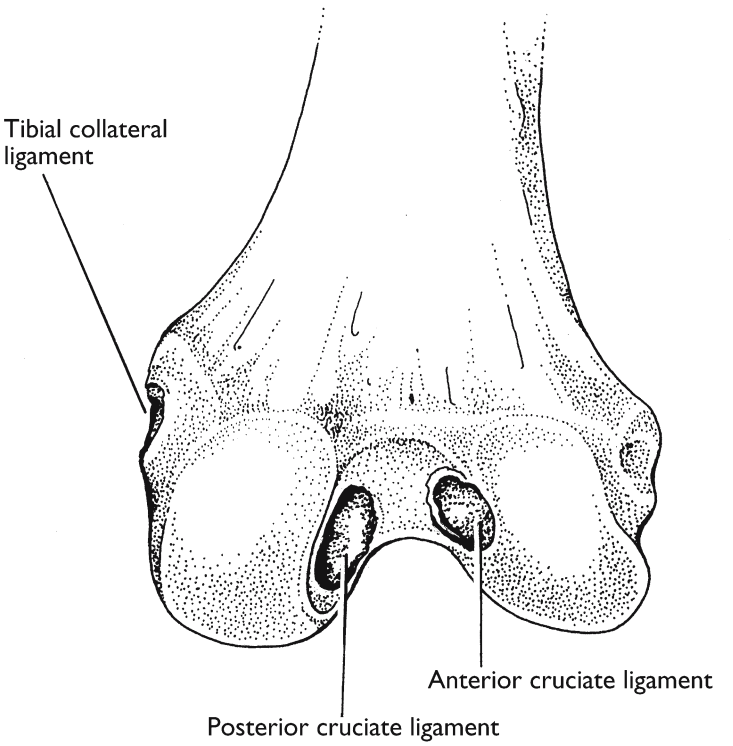

Fig. 29. Avulsion fractures. Avulsion fractures always occur at the site of attachment of a muscle, ligament, or tendon. By referring to the osteology section, one can determine the associated soft-tissue component of any avulsion fracture *(16,19)*. Three of the most common sites of avulsion fracture are shown here: **(A)** Posterior cruciate ligament; **(B)** anterior cruciate ligament; **(C)** tibial collateral ligament.

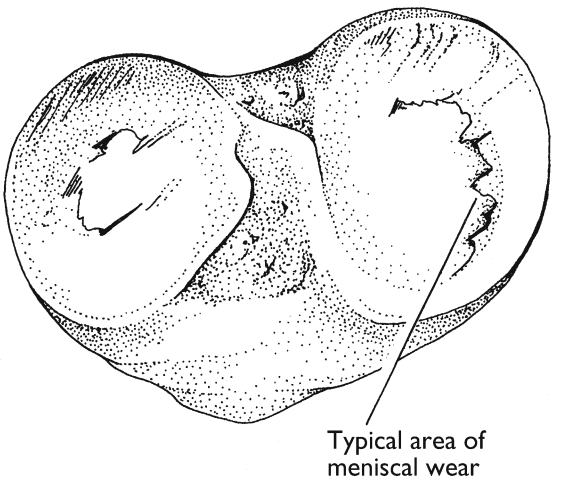

Fig. 30. Meniscal wear. Tears of the menisci create distinctive patterns of wear on the articular cartilage, and in severe cases, these torn menisci can permanently scar the articular surfaces of the bone.

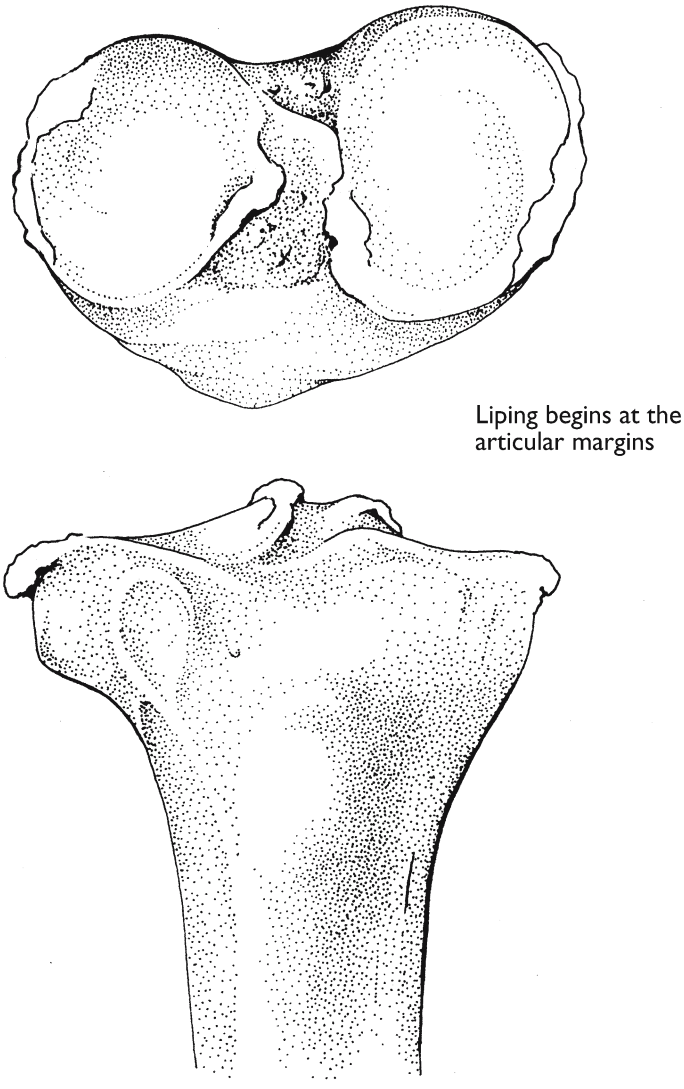

Fig. 31. Age-related gonarthrosis. Age-related degenerative gonarthrosis of the tibia is a very common finding. It generally starts on the outer edge of the articular margins and against the intercondylar eminences. It slowly progresses until the entire articular surfaces are involved.

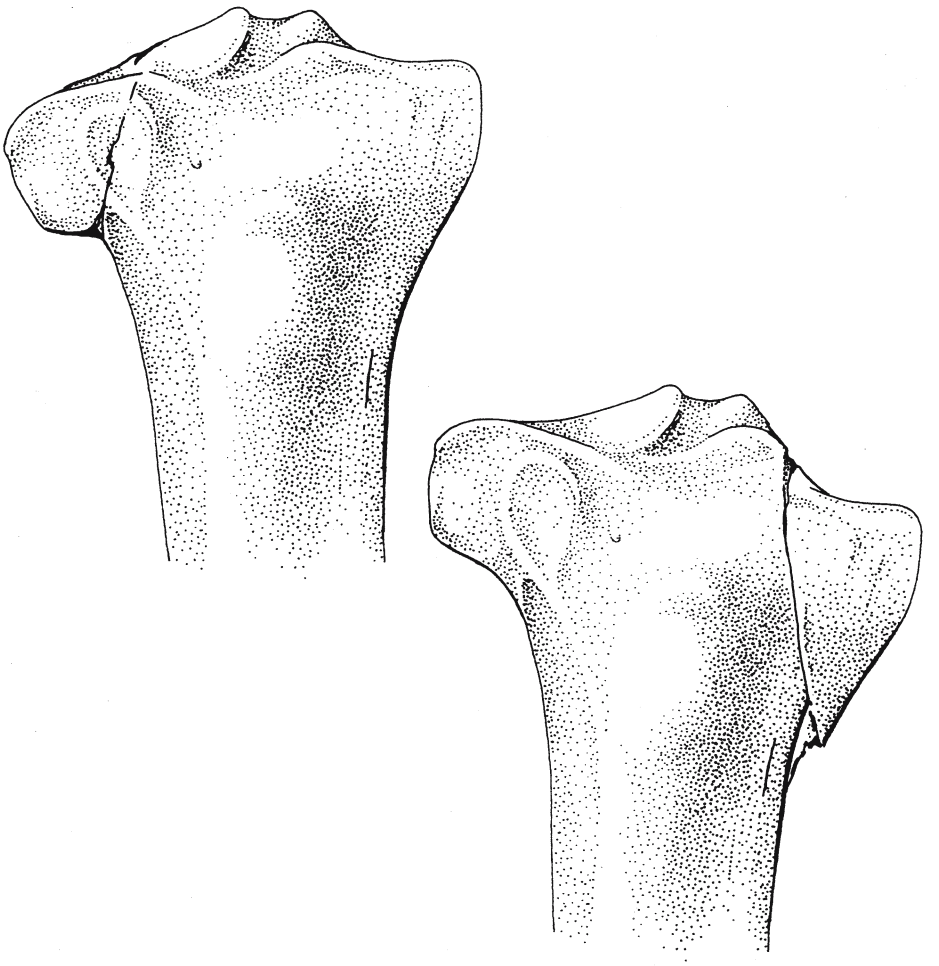

Fig. 32. Condylar fractures. Fractures of the tibial condyles often heal with displacement. This can change the position of the weight-bearing surfaces to valgus or varus weight-bearing alignment, an increase in joint space, and usually some rotational deformity *(20)*. The most commonly used classification for tibial condylar fractures is that described by Hohl *(21)*.

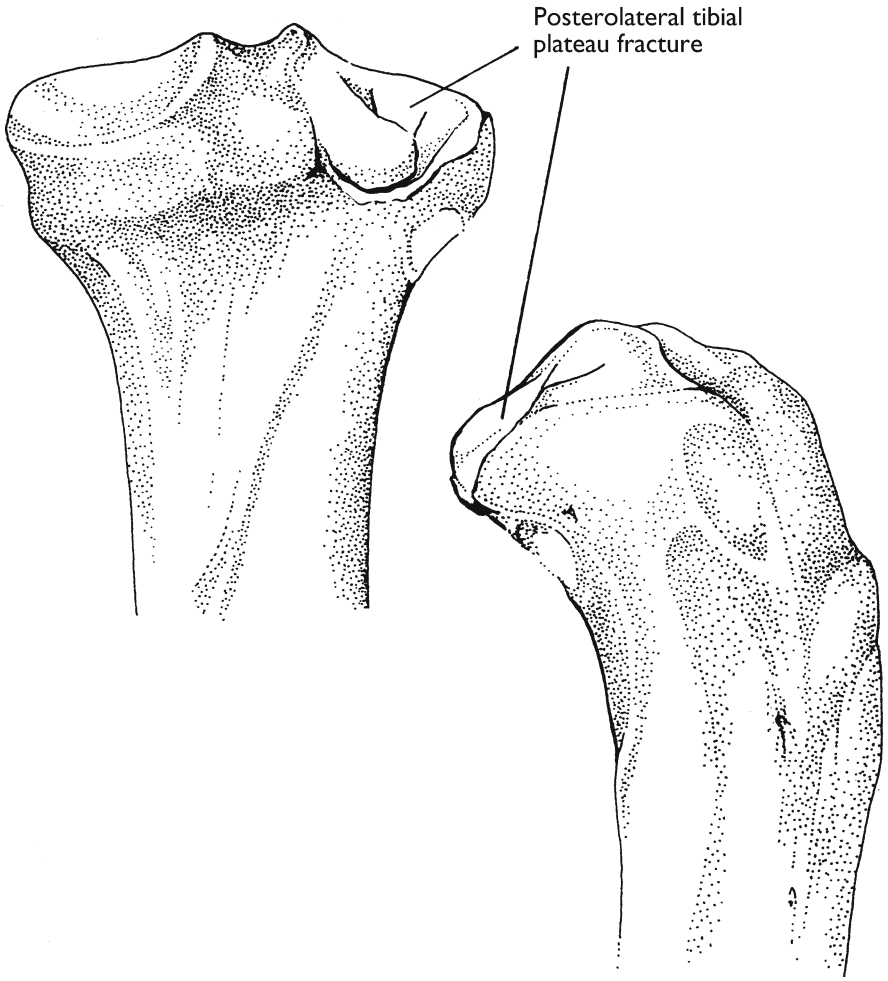

Fig. 33. Tibial plateau fractures. Tibial plateau fractures are technically just variations of tibial condylar fractures, but they are much more subtle in the clinical situation and are more difficult to recognize and classify *(1)*.

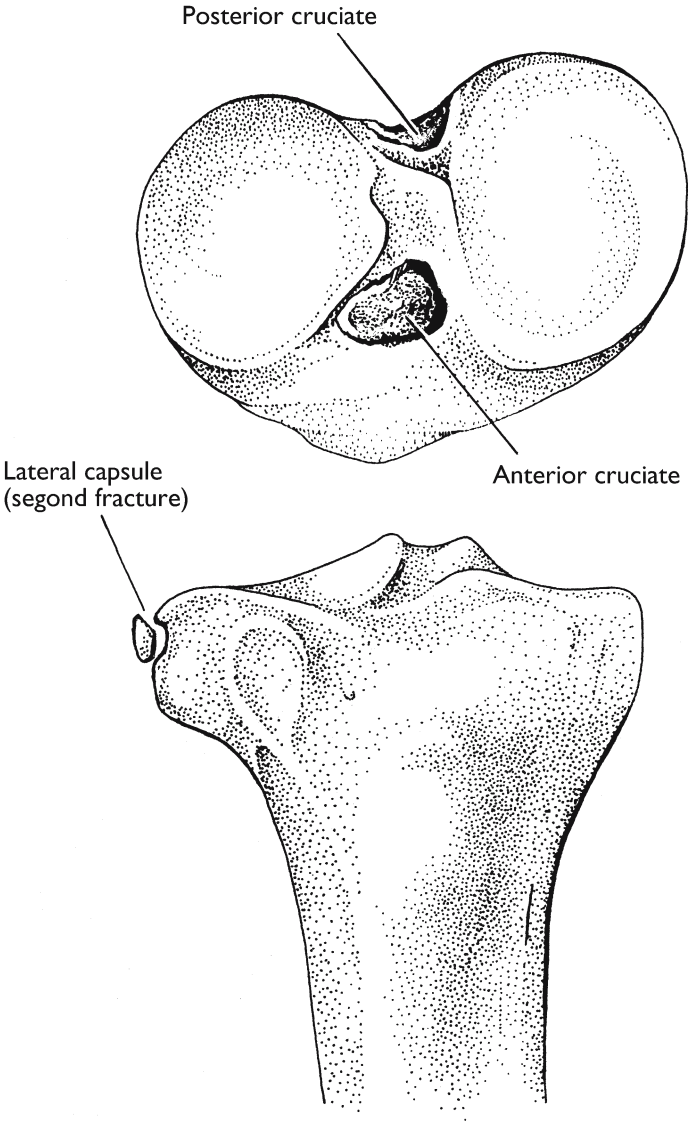

Fig. 34. Avulsion fractures. Just as on the femur, avulsion fractures of the tibia occur at the attachment site of ligaments and tendons. Three of the most common sites of avulsion fractures are shown here: **(A)** Segond fracture (lateral capsular ligament); **(B)** Anterior cruciate; **(C)** Posterior cruciate.

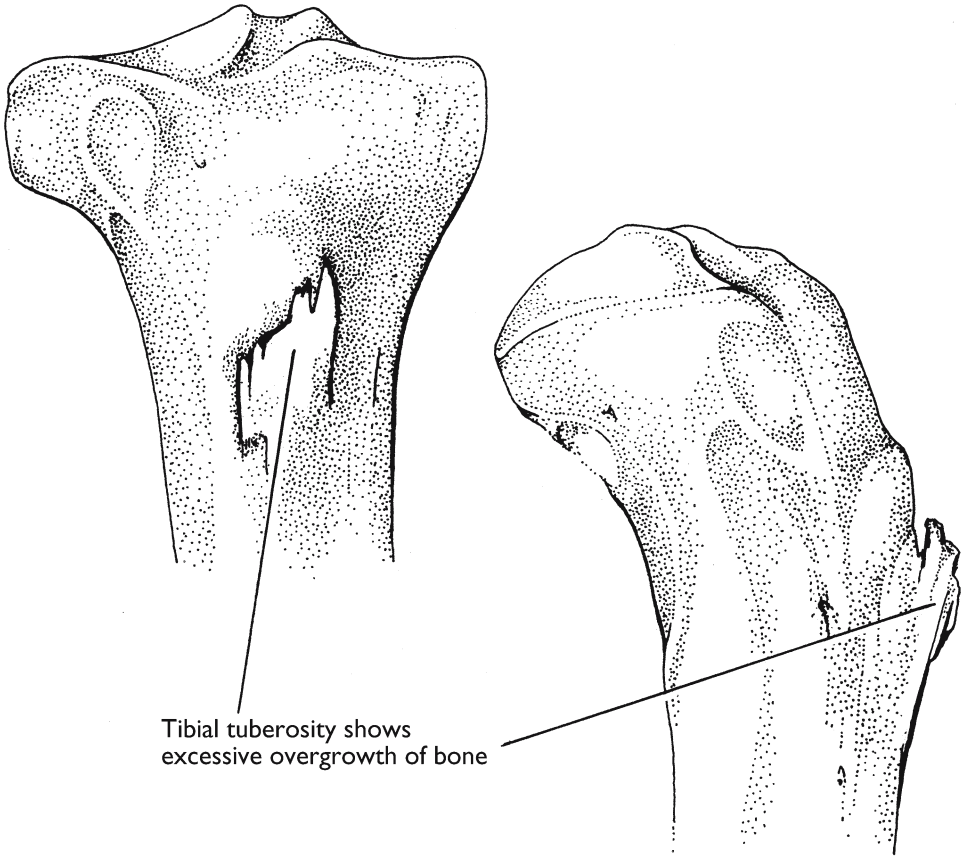

Fig. 35. Osgood–Schlatter disease and tibial tuberosity avulsion fracture. The tibial tuberosity is the insertion site of the patellar ligament, and as such is subjected to stresses from the quadriceps femoris. An overgrowth of bone here can develop following repeated microtrauma to the growing epiphysis. The tuberosity occasionally fractures as a result of forceful contraction of the quadriceps *(22,23)*.

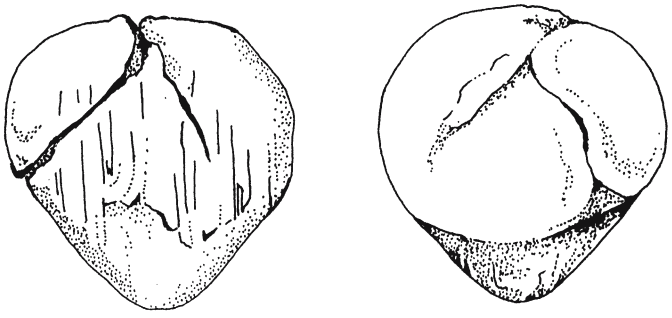

Fig. 36. Patellar injuries. Injuries and stress to the patella can leave significant evidence on the cartilage and bone Patellar fractures sometimes heal without surgical intervention, but the original fracture patterns may remain evident for years *(2)*.

Acknowledgment

All illustrations are by the author.

References

1. Hughston JC. Knee ligaments, repair, and reconstruction. St. Louis, Mo: Mosby Yearbook, Inc., 1993.
2. Hughston JC, Walsh WM, Puddu G. Patella subluxation and dislocation. Saunders Monographs in Clinical Orthopaedics. Volume V. Philadelphia, Pa: WB Saunders, 1994.
3. Frey C, Biorkengen A, Sartoris D, Resnick D. Knee dysfunction secondary to dislocation of the fabella. Clin Orthop 1987;222:223–227.
4. Sutro CJ, Pomeranz MM, Simon SM. Fabella (sesamoid in the lateral head of the gastrocnemius). Arch Surg 1935;30:777–782.
5. Mangieri JV. Peroneal nerve injury from an enlarged fabella: a case report. J Bone Joint Surg 1973;55:395–397.
6. Pritchett JW. The incidence of fabella in osteoarthritis of the knee. J Bone Joint Surg 1984;66a:1379–1380.
7. Friedman AC, Naidich TP. The fabella sign: fabella displacement in synovial effusion and popliteal fossa masses—normal and abnormal fabello-femoral and fabello-tibial distances. Radiology 1978;127:113–121.
8. Craig EA. Bones of the knee joint and individual features that can be used for forensic identification [dissertation]. University of Tennessee, 1994.
9. Miltner LJ, Hu MD, Fang HC. Experimental joint strain. Arch Surg 1937;38:232.
10. Blackburn, TA, Craig, EA. Knee anatomy: a brief review. In: The knee: athletic injuries. Washington, DC: American Physical Therapy Association, 1981, pp. 8–12.
11. Fulkerson, JP, Gossling, HR. Anatomy of the knee joint lateral retinaculum. Clin Orthop 1980;153:183–188.
12. Hefzy MS, Grood ES, Noyes FR. Factors affecting the region of most isometric femoral attachments. Part II: the anterior cruciate ligament. Am J Sports Med 1989;17:208–215.
13. Goldenberg RR, Wild. EL. Chondromalacia fabellae. J Bone Joint Surg 1952;34A:688–690.
14. Weiner, D, Macnab, I, Turner, M. The fabella syndrome. Clin Orthop 1977;126:213–215.
15. Jacobson KE, Flandry FC. Diagnosis of anterior joint pain. Clin Sports Med 1989;8:179–195.
16. Sisk TD. Fractures. In: Campbell's orthopaedics. Edmonson AS, Crenshaw AH, eds. St. Louis, Mo: CV Mosby Company, 1980, p. 587.
17. Smith R, Russell RGG, Woods CG. Myositis ossificans progressiva: clinical features of eight patients and their response to treatment. J Bone Joint Surg 1976;58B:48.
18. Neer CS II, Grantham SA, Shelton ML. Supracondylar fracture of the adult femur: a study of one hundred and ten cases. J Bone Joint Surg 1967;49B:591.
19. Hughston JC, Andrews JR, Cross MJ, Moschi A. Classification of knee ligament instabilities. Part I: the medial compartment and cruciate ligaments. J Bone Joint Surg 1976;58A:159–172.
20. Smith H. Malunited fractures. In: Campbell's orthopaedics. Edmonson AS, Crenshaw AH, eds. St. Louis, Mo: C.V. Mosby Company, 1980, pp. 726–734.
21. Hohl M. Tibial condylar fractures. J Bone Joint Surg 1967;49A:1455.
22. Hand WL, Hand CR, Dunn AW. Avulsion fractures of the tibial tubercle. J Bone Joint Surg 1971;53A:1579.
23. Rockwood CA, Green DP. Fractures in adults. Philadelphia: Lippincott, 1975.

Chapter 4

Anthropological Analysis of the Lower Extremity

Determining Sex, Race, and Stature From Skeletal Elements

Nancy E. Tatarek, PhD and Paul W. Sciulli, PhD

1. Introduction

Human remains in an advanced state of decomposition, fragmentation or incineration, or remains that are comingled often present challenges for coroners, pathologists, and law enforcement agencies. These agencies often turn to anthropologists for their expertise in the analysis of human remains. For a variety of reasons—including coverage with clothing and footwear, the amount of tissue, and the large size of the bones—the leg and foot are frequently preserved and recovered in even the most extreme circumstances (e.g., from a shark's stomach) *(1)*. The human lower extremity possesses at least 30 skeletal elements, including sesamoid bones. If these remains are analyzed thoroughly, they can be used to assess an individual's age at death, sex, ancestry, and stature. This baseline biological information, known by physical anthropologists as the *biological profile,* can narrow the search for missing persons. Methods of determining the age at death are discussed elsewhere in this volume. The focus of this chapter is on the remaining three aspects of the biological profile: sex, ancestry, and stature. Some anthropologists complete the biological profile in the following order: ancestry, sex, age, and stature, whereas others prefer the order of age, sex, ancestry, and stature. In all probability, most analyses occur in an integrated manner as the experienced anthropologist examines a set of skeletal remains. In this chapter, both morphological and metric methods of analysis are addressed and problems and pitfalls associated with some of the approaches are discussed.

From: *Forensic Science and Medicine*
Forensic Medicine of the Lower Extremity: Human Identification and Trauma Analysis of the Thigh, Leg, and Foot
Edited by: J. Rich, D. E. Dean, and R. H. Powers © The Humana Press Inc., Totowa, NJ

2. Sex Estimation

English speakers increasingly use the term *gender* when describing males and females *(2)*. In anthropological terms, *sex* refers to the biological status of a human being—either an XX chromosomal constitution for a female or an XY for a male. Gender applies to the roles that individuals take on within a cultural context. Sex can be estimated from a set of human skeletal remains; establishing gender requires material cultural goods, such as clothing, jewelry, and accessories. This chapter will follow the anthropological parlance.

Compared with some nonhuman primates, especially gorillas and baboons, humans exhibit relatively little sexual dimorphism (differences between males and females). The range of sexual dimorphism among humans usually falls within a normal distribution, with an overlap of the ranges for males and females. The degree of overlap varies with a number of variables, including ancestry, environment, nutrition, and activity *(3)*. In well-nourished populations, it is reasonable to expect that some females might manifest either a mixture of male and female features or even that their features will fall well within the range of male traits *(3)*. Such cases are both the bane of the anthropologist and a testament to the plasticity of human development. In any event, those traits that exhibit the greatest sexual dimorphism are the most useful for estimating sex.

2.1. Sex Estimation Before Adulthood

Any degree of sexual dimorphism discernable in the lower extremity, as in the entire human skeleton, is best developed after individuals go through puberty. Thus, it is difficult to assign sex to infant and juvenile skeletons. No extensive and reliable studies currently exist on postcranial morphological or metric sex differences in prepubescent children.

2.2. Morphological Sex Estimation in Adults

Osteologists consider sexual dimorphism in the adult human skeleton (postpubertal individuals may also fall into this category) to be both well documented and less consistent than metric or measurable differences *(4)*. Generally, males are larger and more robust, with heavier lower extremities *(5,6)*. For example, in males the femoral heads and condyles are larger and the femoral midshaft is broader and thicker in cross -section than in females *(5)*. Hrdlicka reported that males display longer and heavier muscle attachments, specifically the linea aspera of the femur *(6)*. Boyd and Trevor *(7)* noted that regions of articulation can indicate sex, with males generally possessing larger joint surfaces; however, these authors cautioned that this feature is best applied in an analysis of a series of skeletons (i.e., a population) and is not as useful in forensic contexts in which the population specifics are largely unknown. Walsh-Haney *(8)* suggested that it is necessary to avoid a general size description in morphological analyses of skeletal remains and that assessment of all available characteristics (muscle attachments, shaft circumference, head diameter) is important to ensure a complete evaluation.

2.3. Estimating Sex From Metrics of Skeletal Elements in the Lower Extremities

Human populations generally exhibit some degree of sexual dimorphism. Although the degree of sexual dimorphism varies somewhat among human populations, its presence

and the observation that males are on average larger than females allows the sizes of skeletal elements to be used to estimate sex *(9)*.

In the simplest case, investigators might take into consideration that in a given population in which the size of a single measure (X) of a bone from the lower extremity differs in males and females and that the mean measurement in males is u_2 and in females it is u_1. These investigators may determine further that the measure has a normal distribution in both sexes and that the sexes share a common variance for that measure. If we are presented with a bone from an individual of this population that measures X_1, how do we determine whether that individual is male or female?

If the mean is larger for males than for females (i.e., $u_2 > u_1$), then it may be reasonable to designate the individual as male if X_1 is greater than $(u_1 + u_2)/2$, and as female if X_1 is less than $(u_1 + u_2)/2$, where $(u_1 + u_2/2)$ is the average for males and females and serves as the cut-off or sectioning point for the assignment to sex.

An example of this method is given by a study of the circumference of the tibia at the nutrient foramen *(10)*, which was measured on 40 male and female African-American skeletons obtained from the Terry collection housed at the Smithsonian Institute. The mean and variance for this measure in males were 100.43 mm and 43.96 mm^2, respectively, and for females were 90.08 mm and 37.09 mm^2, respectively. The sectioning point (average of the sexes) is as follows:

$$(100.43 + 90.08)/2 = 95.26 \text{ mm}$$

and the sex assignment rule is as follows:

$$\text{If } X > 95.26 \text{ mm, assign to males}$$

$$\text{If } X < 95.26 \text{ mm, assign to females}$$

where X represents the circumference of the tibia at the nutrient foramen. In this sample, the assignment rule correctly identified 77.5% of males and 82.5% of females.

More complex cases involve multiple measures of a bone or bones taken in the lower extremity. Suppose we have such multiple measures of a lower extremity bone in the two sexes, the measures differ between the sexes, the measures have a multivariate normal distribution in each sex, and the variance–covariance matrices are equal between the sexes.

Then $\bar{\boldsymbol{x}}_i$ and $\mathbf{S}_i$ are the sample mean vectors and variance–covariance matrices of the sexes ($i = 1,2$). The sample discriminant rule is then to assign an individual of unknown sex with a vector of measures, $\mathbf{x}$, to males if

$$h(\boldsymbol{x}) = \mathbf{S}^{-1}(\bar{\boldsymbol{x}}_m - \bar{\boldsymbol{x}}_F)[\mathbf{x} - (\tfrac{1}{2}[\bar{\boldsymbol{x}}_m + \bar{\boldsymbol{x}}_F])] > 0$$

and to females if this quantity is greater than 0. Here $\mathbf{S}^{-1}$ is the inverse of the pooled variance–covariance matrices with the pooled matrix:

$$\mathbf{S} = (\sum n_i \mathbf{S}_i)/(n-2)$$

The vectors $\bar{\boldsymbol{x}}_m$ and $\bar{\boldsymbol{x}}_F$ are the mean vectors of males and females, respectively, and $\mathbf{x}$ is the vector of measures of the individual to be assigned to a sex.

An example of this type of analysis is given in a study of Japanese skeletons by Hanihara *(11)*. As part of a larger study, Hanihara presented data on the bicondylar

length and the distal breadth of the femur in 48 males and 40 females. The mean vectors and the variance–covariance matrices were as follows:

$\bar{\boldsymbol{x}}_{\boldsymbol{m}} = (411.00, 8.53)$ $\bar{\boldsymbol{x}}_{\boldsymbol{F}} = (372.85, 70.45)$ (length, breadth)

$$\mathbf{S}_m = \begin{pmatrix} 408.13 & 35.79 \\ 35.79 & 18.31 \end{pmatrix} \quad \mathbf{S}_F = \begin{pmatrix} 356.46 & 44.99 \\ 44.99 & 14.86 \end{pmatrix}$$

The pooled variance–covariance matrix was as follows:

$$\mathbf{S} = \begin{pmatrix} 393.59 & 40.90 \\ 40.90 & 17.13 \end{pmatrix}$$

The sample discriminant rule would assign an individual of unknown sex to male if the following were true:

$$h(x) = \begin{pmatrix} .0485 & .4640 \end{pmatrix} \begin{pmatrix} L - 361.98 \\ B - 75.42 \end{pmatrix} > 0$$

$$h(x) = 0.0485L + 0.4640B - 54.0 > 0$$

An unknown individual with measurements equal to those of the male mean vector would have $h(x) = 3.22$ and would be assigned to males while an unknown individual with measures equal to the female mean vector would have $h(x) = -3.22$ and would be assigned to females.

This type of analysis can be extended to additional measures with the main complication that the sample discriminant rule becomes longer: one factor for each measure plus the final constant.

In the following presentation, sample discriminant rules will be provided for skeletal elements of the lower extremity along with measures of the success of the rules in discriminating between males and females (*see* Appendix).

3. Estimation of Ancestry (Race)

Anthropologists agree that humans comprise a single species, *Homo sapiens*. However, they differ with respect to their views on race. In general, physical anthropologists disavow the use of racial categories to describe humans (e.g., *12,13*). In contrast, forensic anthropologists are faced with a paradox: the idea of the nonexistence of race along with the need to estimate race for law enforcement agencies. As aptly put by Norman Sauer in a 1992 article *(14)*:

> The race controversy in anthropology is a debate about natural groupings of human biological diversity, a question of taxonomy. Forensic anthropologists, when they assign a race label to a skeleton, are involved in a process that uses a narrowly defined set of biological variables for a very specific end, that is, to construct a biological profile that will match a missing person report.

Essentially, forensic anthropologists apply biological characteristics to socially meaningful labels, a process that is necessary to operate within the cultural labeling system prevalent in the United States. Again quoting from Sauer *(14)*:

> Rather it is a prediction, based upon skeletal morphology, that a particular label would have been assigned to a particular individual when that individual was alive.

Of all the tasks a forensic anthropologist must perform, determination of ancestry is perhaps the most difficult. Migration, immigration, admixture, and changes in social construction of racial identity impact attempts to link biological traits to social labels. For example, an individual may exhibit skeletal traits associated with individuals of African or African-American descent, but the individual may self-identify as white or Caucasian, and this identity may be recorded on the individual's driver's license or physician's medical reports. In addition, individuals of mixed heritage may choose to identify with one rather than the other yet possess skeletal traits representative of both.

The lack of complete random mating in our species, coupled with variation in the environment, results in a discontinuous distribution of human populations. Humans are not evenly spread over the landscape but are usually grouped into populations that often show some degree of biological differentiation. Obviously not all populations differ to the same degree and not all biological features show the same amount of differentiation. The degree of differentiation results from the complex historical processes that have affected and are continuing to affect the populations. If differences among populations do occur in biological features, and if part of the identification of an individual is the population to which they belong or from which they are descended, then the use of those features will provide an important practical service in forensic identification.

Most of the highly discriminant morphological or metrically identifiable skeletal characteristics in humans are confined to the skull *(9,15)*. Certain studies (e.g., *16*) highlight an anterior curvature to the femur that is linked to a difference in race. However, with respect to ancestry, postcranial differences are largely nonexistent.

Skeletally, human ancestral groups do differ with respect to their limb proportion *(17)*; ratios of limb length to stature, intramembranal ratios (crural index: leg length:femur length) and intermembranal ratios (arm length:leg length). The crural index is calculated as follows:

$$(\text{Tibial length} \times 100)/\text{femoral length} \quad (17)$$

The intermembranal ratio is calculated as follows:

$$(\text{humeral length} + \text{radial length}) \times (100/[\text{femoral length} + \text{tibial length}]) \quad (17)$$

Although considered largely nondiscriminatory, the crural indices were larger for individuals of African or African-American descent because of relatively longer tibiae *(17)*. These indices can best be utilized to corroborate an estimation constructed from other skeletal indicators.

3.1 Ancestry Estimation Before Adulthood

As with sex characteristics, skeletal traits linked to different ancestral groups do not fully develop until after puberty. Traits commonly used to estimate sex in adults in metric analyses have not yet been determined in juveniles.

3.2. Morphological Ancestry Estimation in Adults

As reviewed by St. Hoyme and Iscan *(18)*, osteological studies in the 1960s and 1970s demonstrated a visual difference in the anterior curvature of the femur. Individuals identified as Caucasian possessed a curvature nearer the midshaft and less straight than did those identified as African Americans (maximum curvature between trochanter and midshaft). Native Americans and Aleutian femora possessed the greatest degree of curvature.

3.3. Estimating Ancestry From Lower Extremity Metrics

The primary method of estimating the ancestry of individuals from skeletal elements of the lower extremity is discriminant analysis. Because the method is the same as that used to determine sex and was presented in the section on estimating sex, only an example of this type of analysis will be presented here.

Iscan and Cotton *(19)* investigated the utility of a variety of measures of the pelvis, tibia, and femur for distinguishing between African-Americans and European Americans.

The sample consisted of 111 European Americans and 113 African-Americans from the Hamman–Todd collection. Here we present the results for females (55 European Americans and 61 African-Americans) using only femur and tibia measurements.

Nine measures (five from the femur and four from the tibia) were used: femur length (FL), femur anterior–posterior (AP) diameter (FAP), femur mid-length diameter (FML), femur midshaft diameter (FMS), femur head diameter (FH), tibia length (TL), tibia AP diameter (TAP), tibia distal epiphyseal breadth (TDE), and tibia circumference at the nutrient foramen (TNF). The allocation rule is to classify the individual as African-American if the following were true:

$$+ 0.024(FL) + 0.249(FAP) - 0.188(FML) - 0.102(FMS) - 0.133(FH)$$
$$+ 0.062(TL) - 0.154(TAP) + 0.164(TDE) + 0.073(TNF) = > 0$$

and as European American if the result is less than zero. Misallocation to ancestral group occurred in 20.5% of the cases.

4. Estimation of Stature

Stature or height estimation is defined in anthropological terms as the estimation of living height from skeletal remains, which, in this context, refers specifically to the lower extremity. Anthropologists thus distinguish between living stature and skeletal stature. Living stature is that measured in the living person and may reflect reported stature. Skeletal stature applies to stature estimated from whole or part of a human skeleton. (Some texts use the term *cadaver stature* to indicate a height taken from a deceased but fully fleshed individual.)

The height or stature of any adult can be separated into the contributions of five body segments: head, thorax, pelvic region, leg, and foot. If the skeletal elements representing those parts of the body are present (i.e., skull, vertebrae, sacrum, femur, tibia, and calcaneus and talus), stature can be estimated by measuring each element and adding the measures to yield skeletal height, then correcting this estimate to account for missing soft tissue, which will then yield an estimate of stature *(20,21,22)*. By using all the body segments that contribute to stature, the *Fully method* is generally believed to provide accurate estimates of stature. This method also has the advantages of not requiring information about sex and ancestry to obtain an estimate of stature (*see* **Subheading 4.1.**).

One drawback of the Fully method is the assumption that the correction for soft tissue thickness, which is derived from French males, is applicable to individuals from all populations.

4.1. Fully Method of Stature Estimation

Thomas Dwight published a paper in 1894 *(23)* on what he termed the *anatomical method* of stature estimation. Dwight's method involved articulating the entire skeleton on a measuring board and correcting for the curvature of the spine and thus estimating stature. During the mid-1950s, Georges Fully *(20)* developed his own anatomical method—a much simpler version of Dwight's method. Because Fully's anatomical method involves the lower extremity, it is included here. Fully's anatomical method requires the observer to take the following measurements from the skeleton:

- Skull: basion to bregma height
- Second cervical to the fifth lumbar vertebrae: maximum body height
- First sacral element: anterior height
- Femur: oblique length
- Tibia: length without tibial spine
- Foot height: talus and calcaneus articulated

Fully used the following factors to correct for the loss of vertebral disk tissue:

- For skeletal heights of 153.5 cm or less, add 10.0 cm
- For skeletal heights of 153.6–165.4 cm, add 10.5 cm
- For skeletal heights of 165.5 cm or more, add 11.0 cm

Stewart *(21)* expressed doubt about the applicability of this method across populations because the formula was developed based on measurements of Europeans. However, other researchers *(24,25)* have found that both the method and the correction factors are satisfactory for population areas as diverse as those found in South Africa and North America. Lundy *(26)* tested Fully's method against Trotter and Glesar's equations and found the two to be in close agreement.

4.2. Estimating Adult Stature From Skeletal Elements of the Lower Extremity

If the full skeleton is present, the Fully method will likely provide the best estimate of stature. However, skeletal elements are missing or damaged in many cases and thus cannot be measured. In these cases, separate skeletal elements or some combination of elements must suffice as a source of data from which the estimate of stature is to be made.

The most common method used to obtain stature estimates from separate skeletal elements is linear regression *(27,28)*. With this technique, the known statures of adults in a given population are plotted against the lengths of skeletal elements and the best lines are fitted to the scatter plots. Because of size differences between the sexes, the analyses are performed separately for males and females. Because different populations often have different bodily proportions, individuals from only the specified population are used. The resulting linear regression equations (representing the best-fit lines) are *population- and sex-specific.* The regression equations are in the form of

$$\hat{y} = a + bx$$

where $\hat{y}$ is the estimated stature (the value that falls on the line, given a skeletal element length), a is the *y*-intercept, *b* is the slope of the line, and *x* is the length of a skeletal element. For example, Genoves *(29)* provides a stature reconstruction formula by sex

for indigenous Mesoamericans. The formula for stature reconstruction is based on the total (maximum) length in centimeters of the femur of Mesoamerican males is:

$$\text{stature} = 66.38 + (2.26 \times \text{femur length})\ \text{cm} \quad (1)$$

Thus, the estimated stature of a Mesoamerican male with a total femur length of 43.0 cm is:

$$\begin{aligned}\text{stature} &= 66.38 + 2.26\ (43.0)\ \text{cm}\\ &= 66.38 + 97.18\ \text{cm}\\ &= 163.56\ \text{cm}\end{aligned}$$

In the United States, stature is usually recorded in English measurement units. The following formula can be used to convert this stature estimate to feet and inches:

$$\left(\frac{163.56\,\text{cm}}{1}\right)\times\left(\frac{1\,\text{in.}}{2.54\ \text{cm}}\right)\times\left(\frac{1\,\text{ft}}{12\,\text{in.}}\right)=5.37\,\text{ft}$$

$$\left(\frac{0.37\,\text{ft}}{1}\right)\times\left(\frac{12\,\text{in.}}{1\,\text{ft}}\right)=4.5\ \text{in.}$$

Thus, the estimate of 163.56 cm equals approx 5 feet 4.5 in.

Although $\hat{y}$ (163.56 cm) is the best estimate of stature, given the data on which the equation is based, it is still only an estimate. We need some information about the precision of this estimate, especially if the estimate is to be used for personal identification. We can express the precision of this estimate by calculating the confidence interval (CI). To calculate the CI for a given estimate we need to be furnished with or must be able to calculate from the data presented the following quantities:

- S^2_{y*x}: the residual mean square (the variance of the statures after taking into account the dependence of stature on skeletal element length), or
- S_{y*x}: the standard error of the estimate (or standard error of regression). This is the square root of the residual mean square.
- n: the number of individuals on which the regression equation is based.
- $\bar{x}$: the average value of the skeletal element in the populations on the estimate was made (in this case, the total femur length).
- x_i: the value obtained from the individual for which stature is to be estimated (in this case, 43 cm).
- $\sum x_i^2$: the sum of squares of x_i (the values of the skeletal elements length squared and summed). This is also written as $\sum(x_i - \bar{x})^2$, the numerator of the variance of x.

Given these quantities, we can calculate a number of standard errors and CIs. Assume, for example, that our question is as follows: "What is the *mean* stature of all Mesoamerican males with a total femur length of 43 cm, and what is the CI for this estimate?" The following calculation would be appropriate:

$$\text{Given } \hat{y} = 66.38 + 2.26\ (43.0)$$

$$\hat{y} = 163.56\ \text{cm}$$

The standard error for this estimate is:

$$S_{yi} = \sqrt{S^2_{y*x}\left[\left(\frac{1}{n}\right)+\left[\frac{(x_i-\bar{x})^2}{\sum x^2}\right]\right]} \tag{2}$$

Based on the data presented in the Genoves *(29)* study for a sample of 22 individuals, the standard error is as follows:

$$S_{yi} = \sqrt{11.68\times\left[\left(\frac{1}{22}\right)+\frac{(43.0-43.21)^2}{93.49}\right]} = \sqrt{0.54}$$
$$= 0.73$$

and the 95% confidence interval (CI) can be obtained from

$$95\%\ \text{CI} = (\hat{y}_i \pm t_{0.05(20)})\times\left(S_{\hat{Y}i}\right) = \hat{y}_i \pm 2.086\times 0.73 \tag{3}$$
$$= 163.56 \pm 1.53$$

where the lower limit (L_1) and upper limit (L_2) are as follows:

$$L_1 = 163.56 - 1.53 = 162.0 \text{ cm}$$
$$L_2 = 163.56 + 1.53 = 165.1 \text{ cm}$$

In equation 3, $t_{0.05(20)}$ is the value of the *t* distribution for 20 degrees of freedom (N-2) with probability set at 0.05.

By contrast, consider the following question: "If 20 Mesoamerican males with a total femur length of 43.0 cm were taken from the population, what would their *mean* stature be and what is the CI for this calculation?" In this case, the following calculation would be appropriate:

$$\hat{Y} = 66.38 + (2.26\times 43.0) \text{ cm}$$
$$\hat{Y} = 163.56 \text{ cm}$$

The standard error for this estimate is as follows:

$$(S_{yi})_{20} = \sqrt{S^2_{y*x}\left[\left(\frac{1}{n_i}\right)+\left(\frac{1}{n}\right)+\left[\frac{(x_i-\bar{x})^2}{\sum x^2}\right]\right]} \tag{4}$$
$$= \sqrt{11.68\left[\left(\frac{1}{22}\right)+\left(\frac{1}{20}\right)+\frac{(43.0-43.21)^2}{93.49}\right]} = \sqrt{1.12}$$
$$= 1.06$$

and the 95% CI for this estimate is as follows:

$$95\%\ \text{CI} = \hat{Y}_i \pm t_{0.05(20)}\times(S_{yi})_{20} = \hat{y}_i \pm 2.086\times 1.06$$
$$= 163.56 \pm 2.21$$

where

$$L_1 = 163.56 - 2.21 = 161.35$$
$$L_2 = 163.56 + 2.21 = 165.77$$

Finally, consider the kind of question that is commonly asked in forensic settings: "What is the stature of a *single* Mesoamerican male with a maximum femur length of 43.0 cm, and what is the CI?" The following estimate would be appropriate:

$$\hat{Y} = 66.38 + 2.26\ (43.0)\ \text{cm}$$
$$= 163.56\ \text{cm}$$

The standard error for this estimate is:

$$(S\hat{Y}_i)_1 = \sqrt{S^2_{y*x}\left[\left(\frac{1}{n_i}\right)+\left(\frac{1}{n}\right)+\left(\frac{x_i-\bar{x}}{\sum x^2}\right)\right]} \tag{5}$$

$$(S_{\hat{Y}i})_1 = \sqrt{11.68\left[\left(1+\left(\frac{1}{22}\right)+\left(\frac{[43.0-43.21]^2}{93.49}\right)\right)\right]}$$
$$= \sqrt{12.22}$$
$$= 3.50$$

and the 95% CI for this estimate is as follows:

$$95\%\ \text{CI} = (\hat{y}_i \pm t_{0.05(20)}) \times \left(S_{\hat{Y}i}\right) = \hat{y}_i \pm 2.086 \times 0.73$$
$$= 2.08 \times 3.50$$
$$= 7.30$$

where

$$L_1 = 163.56 - 7.30 = 156.26\ \text{cm}$$
$$L_2 = 163.56 + 7.30 = 170.86\ \text{cm}$$

The CI using equation 5 is often referred to as the *prediction interval* and should be used in forensic cases involving single individuals.

As one can see from these hypothetical questions, the accuracy of prediction increases with the amount of data upon which the prediction is based. For the entire sample (equation 2), the CI is 3.06 cm; for 20 individuals (equation 4), the CI is 4.42 cm; and for a single individual (equation 5)—the most common situation in forensic cases—the CI is 14.6 cm or almost 6 in.

Konigsberg et al. *(30)* have shown on the basis of both theoretical arguments and practical examples that this method of inverse calibration (regression of stature based on bone length) is generally the preferred method when there is some *a priori* reason for presuming that the individual whose stature is to be estimated comes from the group with the same stature distribution as is represented within the reference sample, i.e., the same sex and ancestral group or a group with the same relationship between stature and long bone length. If this is not the case, Konigsberg et al. *(30)* provide recommendations for estimating stature.

The following presentation contains a discussion of stature reconstruction formulas for lower extremity skeletal elements, along with the data required to calculate prediction intervals (Tables 1–6; Appendix).

Table 1
Confidence Interval Calculations for Stature Estimation in European Males

Source	Bone	N	Mean	SD[a]	SE[b]	$\sum(x - \bar{x})^2$
Simmons (1990)	Femur, VHA	200	99.10	5.87	6.10	6856.92
	Femur, LCH	200	41.35	2.91	6.24	1685.15
	Femur, VHD	200	48.27	3.17	6.77	1999.73
Holland (1992)[c]	Tibia, BB	29	75.78	3.36	2.41	316.11
	Tibia, MCL	29	47.93	3.95	5.24	436.87
Trotter and Gleser (1958)	Femur, R	2227	47.077	2.382	4.04	13197.55
	Femur, L	2345	47.150	2.345	3.987	12889.71
	Tibia, R	2483	38.429	2.226	3.97	12298.50
	Tibia, L	2482	38.457	2.214	3.95	12161.36
	Fibula, R	2207	38.258	2.084	3.84	9580.78
	Fibula, L	2217	38.276	2.058	3.80	9385.57

Femur VHA, upper breadth of femur; femur LCH, lateral condyle height; femur VHD, vertical diameter of femoral head; Tibia BB, biarticular breadth; Tibia MCL, medial collateral ligament.

[a]Standard deviation.

[b]Standard estimate of regression.

[c]Measurements in mm (all other measurements in cm).

4.3. Stature Estimation From Fragmentary Bone

Taphonomy, trauma, excavation, and transport of skeletal remains can cause skeletal elements to become fragmented. Several authors *(31–35)* have developed methodologies for compensating when remains are fragmentary. Of relevance here are the methods based on the femur and the tibia. Stature is estimated in two ways. In one method, a direct relationship is made using a segment or fragment of bone as a basis for estimating bone length, which, in turn, is used to estimate stature. The second method involves a two-step estimation process and, therefore, will have a higher rate of error. To estimate stature, follow guidelines for measuring the appropriate fragment or segment. Holland *(34)* and Simmons et al *(33)* are good references for the methods commonly used when dealing with fragments of skeletal elements.

4.4. Issues to Consider in Stature Estimation

During the last decade, anthropological research into stature estimation methods focused on refining techniques and fully delineating factors that affect terminal stature in human populations around the world. Although concentrating primarily on mathematical refinements, such as the use of regression formulas, researchers have also begun to understand more completely how biocultural influences, such as secular trends and errors in stature reporting methods, impact the job of the forensic scientist in analyzing skeletal remains.

Height is always included in reports on a missing person. Several studies examined sources of errors in reported stature *(36,37)*. In the United States (and many other countries) there are four primary sources of stature measurement and reporting: self,

Table 2
Confidence Interval Calculations for Stature Estimation in European Females

Source	Bone	N	Mean	SD[a]	SE[b]	$\sum(x - \bar{x})^2$
Simmons	Femur, VHA	200	88.24	5.18	6.67	5339.65
(1990)	Femur, LCH	200	36.30	2.53	6.91	1157.98
	Femur, VHD	200	42.54	2.50	6.92	1243.75
Holland	Tibia, BB	29	67.85	3.25	4.71	295.75
(1992)[c]	Tibia, MCL	29	43.09	3.47	4.29	337.15
	Tibia, LCL	29	36.87	3.32	4.62	308.63

Femur VHA, upper breadth of femur; femur LCH, lateral condyle height; femur VHD, vertical diameter of femoral head; tibia BB, biarticular breadth; tibia MCL, medial collateral ligament; tibia LCL, lateral collateral ligament.

[a]Standard deviation.

[b]Standard estimate of regression.

[c]Measurement in mm (all other measurements in cm).

Table 3
Confidence Interval Calculations for Stature Estimation in African-American Males

Source	Bone	N	Mean	SD[a]	SE[b]	$\sum(x - \bar{x})^2$
Simmons	Femur, VHA	200	98.99	5.77	6.60	6625.29
(1990)	Femur, LCH	200	42.33	3.00	5.77	1791.00
	Femur, VHD	200	47.65	2.69	7.16	1439.98
Holland	Tibia, BB	29	77.62	2.75	4.88	211.75
(1992)[c]	Tibia, MCL	29	48.81	2.96	5.11	245.32
	Tibia, LCL	29	42.98	2.89	5.11	233.86
Trotter and Gleser	Femur, R	343	48.200	2.511	3.83	2156.35
(1958)	Femur, L	338	48.338	2.552	3.99	2194.78
	Tibia, R	346	40.337	2.323	3.88	1861.73
	Tibia, L	342	40.318	2.426	4.04	2006.95
	Fibula, R	301	40.029	3.183	3.96	3039.45
	Fibula, L	306	39.968	2.229	4.09	1515.37

Femur VHA, upper breadth of femur; femur LCH, lateral condyle height; femur VHD, vertical diameter of femoral head; tibia BB, biarticular breadth; tibia MCL, medial collateral ligament; tibia LCL, lateral collateral ligament.

[a]Standard deviation.

[b]Standard estimate of regression.

[c]Measurement in mm (all other measurements in cm).

spouse or partner, physician's offices, and the Division of Motor Vehicles. Himes and Roche found that males overreported their stature by at least an inch, while females (especially tall women) underreported their stature by the same amount *(37)*. In addition, spouses or partners tend to overreport the stature of their loved ones. These erroneous reports introduce the first of the errors into stature estimation. Measurements

Table 4
Confidence Interval Calculations for Stature Estimation in African-American Females

Source	Bone	N	Mean	SD[a]	SE[b]	$\sum(x - \bar{x})^2$
Simmons	Femur, VHA	200	88.98	5.24	6.00	5464.06
(1990)	Femur, LCH	200	37.05	2.34	5.47	1089.64
	Femur, VHD	200	41.95	2.35	5.59	1098.98
Holland	Tibia, MCW	29	29.03	1.82	4.64	92.75
(1992)[c]	Tibia, MCL	29	42.76	2.14	4.35	128.23
	Tibia, LCL	29	36.28	2.25	4.62	141.75

Femur VHA, upper breadth of femur; femur LCH, lateral condyle height; femur VHD, vertical diameter of femoral head; tibia MCW, medial condyle articular width; tibia MCL, medial collateral ligament; tibia LCL, lateral collateral ligament.

[a]Standard deviation.

[b]Standard estimate of regression.

[c]Measurement in mm (all other measurements in cm).

at physician's offices or by individuals at motor vehicle licensing agencies further confound the issue.

Variables such as the time of day an individual is measured, the training and consistency of those taking the measurements, the type of equipment used, the individual's posture, and whether the individual removed his or her shoes before being measured affect the resulting stature. Individuals are shorter later in the day owing to the gradual compression of the intervertebral disks while walking and sitting upright. Poor training and inconsistent measurement methods, as well as interobserver errors in measurement, can occur in physician's offices and licensing agencies. At some agencies, the measurement is obtained while the individual stands next to a measuring tape on the wall. Slumped posture (as occurs in with aging or ill health) and the wearing of footwear potentially will also alter the final stature measurement.

Stature changes as an individual goes through the life cycle, increasing with growth and development then leveling off for several decades and finally decreasing during passage through older adulthood. Aging is thus an important consideration in estimating stature. The 2000 census estimated the number of individuals aged 65 or more years in the United States to be greater than 33 million; thus, studies examining the decline in stature with age are particularly germane *(38,39)*. These researchers have reported on the necessary corrections that must be made when estimating the stature of individuals older than 45 yr of age. Galloway found an average reduction in height of 0.16 cm and indicates that the stature of older individuals can be estimated using the following formula:

$$\text{Height loss (cm)} = 0.16\ (\text{age} - 45\ \text{yr}).$$

Galloway also suggests providing both the corrected and uncorrected stature estimates to law enforcement officials, because aging individuals might not acknowledge a decline in stature.

Table 5
Confidence Interval Calculations for Stature Estimation in Miscellaneous Males

Source	Bone	N	Mean	SD[a]	SE[b]	$\sum(x - \bar{x})^2$
Mohanty-Oriya (India)(1998)	PCTL	500	37.08	2.34	2.8735	2732.32
Munoz-Spanish (2001)	Femur	52	47.00	2.42	3.605	298.68
	Tibia	52	38.85	2.29	4.010	267.45
	Fibula	52	36.90	2.06	3.667	216.42
Genoves-"I" (1967)	Femur	22	43.21	2.11	3.417	93.49
	Tibia	22	35.89	2.43	2.812	124.00
Trotter and Gleser Mongoloid[c] (1958)	Femur, R	67	44.246	2.479	3.92	405.60
	Femur, L	60	44.640	2.476	3.67	361.70
	Tibia, R	68	36.038	2.092	3.26	140.16
	Tibia, L	67	36.503	2.349	3.28	364.17
	Fibula, R	61	36.146	2.170	3.20	282.53
	Fibula, L	62	36.340	2.273	3.28	315.16
Trotter and Gleser Mexican (1958)[c]	Femur, R	50	45.138	2.316	3.10	230.55
	Femur, L	57	45.596	2.474	2.88	342.76
	Tibia, R	51	37.30	2.356	3.59	277.54
	Tibia, L	52	37.487	2.401	3.88	294.00
	Fibula, R	52	37.154	2.221	3.32	251.57
Trotter and Gleser Puerto Rican (1958)[c]	Femur, R	40	44.758	2.150	3.18	180.28
	Femur, L	44	44.820	2.136	3.19	196.19
	Tibia, R	43	37.142	2.00	3.61	168.00
	Tibia, L	42	37.024	2.174	3.80	193.78
	Fibula, R	41	36.956	2.021	3.48	163.38
	Fibula, L	42	36.867	2.051	3.79	172.47
	Fibula, L	45	37.342	2.150	3.72	203.39

PCTL, percutaneous tibial length.
I, indigenous MesoAmerican.
[a]Standard deviation.
[b]Standard estimate of regression.
[c]Measurement in mm (all other measurements in cm).

Along with age-related changes in stature, recent height data suggest changes in terminal stature across time *(40–43)*. Several studies have shown that variations in adult stature occur over successive generations and highlight that data as recent as from the 1940s may not reflect current population heights. Regression techniques employed by many anthropologists are based on reference populations from the early to mid 1900s. The most frequently quoted and used regression equations—e.g., the Trotter and Glesar equations *(44)*—were based primarily on data taken from recruits during the second World War and The Korean War. Increasingly, anthropologists are recognizing that nutritional, medical, and technological improvements contribute to the change in the average stature *(45–47)*.

Table 6
Confidence Interval Calculations for Stature Estimation in Miscellaneous Females

Source	Bone	N	Mean	SD[a]	SE[b]	$\sum(x - \bar{x})^2$
Mohanty-Oriya (India) (1998)	PCTL	500	35.03	2.60	3.4423	3373.24
Munoz-Spanish (2001)	Femur	52	43.04	2.35	3.270	281.65
	Tibia	52	39.05	2.26	3.033	260.49
	Fibula	52	33.46	1.96	3.129	195.92
Genoves "I" and "IM" (1967)	Femur	15	39.63	2.16	3.816	65.32
	Tibia	15	32.54	2.13	3.513	63.52
Holland (1992)[c]	Tibia, MCL	58	42.93	2.86	4.25	466.24
	Tibia, LCL	58	36.58	2.82	4.63	453.29

I, Indigenous MesoAmerican; IM, Indigenous with some mestizo.
[a]Standard deviation.
[b]Standard estimate of regression.
[c]Measurement in mm (all other measurements in cm).

Decompositional processes may also affect bone length and subsequent stature estimations. As skeletal elements lose their organic components and are reduced to primarily mineral or inorganic components, a certain amount of bone shrinkage can occur. Exposure to repeated cycles of saturation and desiccation or extreme temperature fluctuations can also change the bone length. Exposure to high temperatures, such as in a fire, can significantly shrink skeletal material up to 25%, depending on the skeletal elements affected *(48)*. These factors should be taken into consideration when estimating stature. No studies exist estimating the amount of shrinkage that occurs during a fire and exactly how this impacts stature estimation.

As internal structural changes have been shown to alter stature estimates, so to have observer errors been demonstrated to influence the process *(49)*. Interobserver and intraobserver differences in measurement techniques and the use of measurements that differ from those used in the construction of a stature formula increase the error in estimation. Jantz et al. reviewed the methods and formulas presented by Trotter and Gleser in a 1958 article *(50)*. Their discovery that the tibia lengths were too short compared with those used in other data sets highlighted the need for careful and consistent attention to measurement methods. Although it is difficult to reconstruct some of the data from Trotter and Gleser's work, comparisons that could be made indicated that the problem was with the medial malleolus of the tibia. Some measurements included this length, whereas some did not. The authors conclude that formulas presented in a 1970 article are best substituted for those established with the questionable measuring techniques. To that recommendation these authors add another: careful reading and practicing of measurement techniques associated with stature regression formulas is essential.

Appendix: Formulas, Equations, and Sectioning Points

Sex Estimation

Chart 1

Source	Element	Population	Sex	Sectioning Point
Asala (2001) South Africa (based on significant differences at $p < 0.001$ for means)	Vertical femoral head diameter (left bone)	White	Males	48.40 mm*
			Females	42.28 mm*
		Black	Males	44.45 mm*
			Females	39.64 mm*
	Transverse femoral head diameter	White	Males	46.85 mm*
			Females	41.00 mm*
		Black	Males	44.20 mm*
			Females	39.20 mm*
King, et al. (1998) Thailand	Maximum femoral head diameter (91.3% accurate)	Thai	Males	>42.18 mm
			Females	<42.18 mm
	Femoral midshaft circumference (85.6% accurate)	Thai	Males	>79.55 mm
			Females	<79.55 mm
	Femoral bicondylar breadth (93.3% accurate)	Thai	Males	<74.81 mm
			Females	<74.81 mm

*Measurement is the mean.

Chart 2

Stojanowski and Seidemann (1999), supero-inferior femoral neck diameter (SID):

Sex = 0.387*SID-12.462 (Caucasian specific) (84% accurate)
Sex = 0.415*SID-13.422 (African-American specific) (82% accurate)
Sex = 0.379*SID-12.174 (combined equation) (85% accurate)

Scores above zero are considered male; scores below zero are considered female.

Chart 3

Source	Equation	Functions and Variables	Raw Coefficient	Sectioning Point
Iscan and Shihai (1995) China. Femur	1 (92.3%)	Distal breadth	0.20277340	0.04
		Maximum length	0.01041030	
		Anteroposterior diameter	0.8912650	
		Constant	−21.98602	
	2 (84.2%)	Midshaft circumference	0.08765310	0.03
		Head diameter	0.23995960	
		Constant	−17.49596	
	3 (94.7%)	Midshaft circumference	0.02085637	0.03
		Distal breadth	0.24609700	
		Constant	−20.21629	
	4 (81.7%)	Midshaft circumference	0.1834105	0.09
		Constant	−14.72835	
		Females <80.4	< males*	
	5 (94.9%)	Distal breadth	0.2660647	0.03
		Constant	−20.04588	
		Females <75.5	< males*	
	6 (83.1%)	Head diameter	0.3804008	0.03
		Constant	−20.21629	
		Females <43.6	< males*	
Iscan et al. (1994) Japan, Tibia.	1 (87.2%)	Prox. epiphyseal br	0.1529167	−0.15
		Distal epiphyseal br	0.2284790	
		Constant	−20.5825300	
	2 (87.3%)	Prox. epiphyseal br	0.2447224	−0.13
		Circumference @nutrient foranen	0.0213940	
		Constant	−19.02956	
	3 (83.8%)	Distal epiphyseal br	0.3659270	−0.13
		Min. circumference	0.0449891	
		Constant	−18.94278	
	4 (88.6%)	Prox. epiphyseal br	0.2683954	−0.13
		Constant	−18.81521	
			females <69.5 < males*	
	5 (83.8%)	Distal epiphyseal br	0.4260344	−0.13
		Constant	−18.39048	
			females <42.5 < males*	
	6 (80.0%)	Circumference @nutrient foranen	0.1536506	−0.09
		Constant	−13.452822	
			females <87 < males*	
	7 (80.3%)	Min. circumference	0.4260344	−0.14
		Constant	−18.39048	
			females <69.5 < males*	

(Continued)

Chart 3 *(continued)*

Source	Equation	Functions and Variables	Raw Coefficient	Sectioning Point
Steyn and Iscan (1997) South Africa, Femur and Tibia.	1 (88.6%)	Femoral head diameter	0.16363890	–0.09389
		Femoral transverse diameter	0.09093376	
		Femoral distal breadth	0.13420310	
		Constant	–20.80771000	
	2 (90.6%)	Prox. tibial breadth	0.10786020	–0.10170
		Tibial A/P diameter	0.15334320	
		Tibial transverse diameter	0.06750036	
		Min. circumference	–0.09845310	
		Distal tibial epiphysis breadth	0.24325580	
		Constant	–19.48625000	
	3 (91.4%)	Femoral head diameter	0.09752152	–0.108495
		Femoral transverse breadth	0.13898700	
		Distal femoral breadth	0.08792625	
		Tibial A/P diameter	0.16188040	
		Min. circumference	–0.10122840	
		Tibial physeal length	–0.00937566	
		Distal tibial epiphysis breadth	0.2215850	
		Constant	–20.83820000	
	4 (85.9%)	Femoral head diameter	0.40482060	–0.086700
		Constant	–18.57893000	
			females <45.8 < males*	
	5 (90.5%)	Distal femoral breadth	0.24411720	–0.089390
		Constant	–19.58571000	
			females <79.9 < males*	
	6 (88.6%)	Distal femoral breadth	0.14677350	–0.092675
		Femoral head diameter	0.18175910	
		Constant	–20.11745000	
	7 (86.8%)	Proximal tibial breadth	0.23434210	–0.085625
		Constant	–17.51482000	
			females <74.5 < males*	
	8 (88.7%)	Distal tibial epiphyseal breadth	0.38066440	–0.087630
		Constant	–18.06326000	
			females <47.29 < males*	
	9 (90.6%)	Proximal tibial breadth	0.12370260	–0.096260
		Distal tibial epiphyseal breadth	0.22181770	
		Constant	–19.77125000	

A discriminant score less than the sectioning point indicates female.
% Accuracy follows equation number in parentheses.
*These values can also be used to determine sex.

Chart 4

Source	Variable	1	2	3	4	5
Steele (1969):	Body height-calc.	0.36061				0.23126
Terry Collection:	Load arm width-calc.	0.41828				
Tarsals	Max. talus length		0.42002	0.84693	0.38368	0.31859
	Max. talus width		0.41096		0.42741	
	Body height: talus				0.13722	
	Width/length of talus			27.92377		
	Trochlear width/length			10.35583	9.29162	
	Male $\bar{x}$	33.57	40.87	79.09	52.41	49.88
	Section point	32.0	38.75	75.44	50.05	47.30
	Female $\bar{x}$	30.42	36.62	73.84	47.68	44.72

Accuracy ranges from 83% to 89%; *see* Steele, 1970. PhD dissertation.

Race Estimation

Source	Element	Population	Sex	Demarking Point
Craig (1995)	Intercondylar shelf angle (degrees)	African American	NA	>141°
		Caucasian	NA	<141°
	Intercondylar angle is a measurement of the angle between intercondylar shelf of the femur and the posterior shaft of the femur. 85% accuracy for the entire sample.			
Gill (2001)	Femoral notch height	African American	Males (79.2%)	≥34 mm
			Females (82.5%)	≥31 mm
		Caucasian	Males (76.9%)	≤32 mm
			Females (76.9%)	≤29 mm
	Notch height is the measurement taken from the surface upon which the femoral condyles rest to the highest point of the rim of the anterior outlet of the intercondylar notch. % accuracy follows sex in parentheses.			

Stature Estimation

Bidmos (2003), South Africa

Calcaneus
Males
St = 0.38 (MAXL) + 0.35 (MAXH) + 0.59 (MIDB) + 0.56 (DAFB) + 68.17 ± 4.9
St = 0.43 (MAXL) + 0.41 (MAXH) + 0.59 (MIDB) + –0.19 (DAFL) + 0.65 (DAFB) + 64.42 ± 4.94
St = 0.42 (MAXL) + 0.16 (BH) + 0.33 (MAXH) + 0.59 (MIDB) + –0.22 (DAFL) + 0.63 (DAFB) + 64.06 ± 4.98
Females
St = 0.81 (MAXL) + –0.73 (LAL) + 1.41 (DAFL) + 75.22
St = 0.69 (MAXL) + –0.67 (LAL) + 0.37 (BH) + 1.27 (DAFL) + 72.24 ± 4.01
St = 0.67 (MAXL) + –0.67 (LAL) + 0.35 (MAXH) + 1.35 (DAFL) + 70.13 ± 4.01

MAXL, maximum length; CFH, cuboidal facet height; LAL, load arm length; BH, body height; MAXH, maximum height; MIDB, middle breadth; DAFB, dorsal articular facet breadth; DAFL, dorsal articular facet length; MINB, minimum breadth. Measurements are in mm.

Boldsen (1984)

Males	Females
St = 2.519 × femur length + 52.85	St = 2.528 × femur length + 50.76
St = 2.406 × tibia length + 82.37	St = 2.869 × tibia length + 60.85

Maximum length of femur and tibia. Measurements in mm.

Byers (1989), Metatarsals

First Metatarsal:	
Combined data:	St = 634 + 16.8 (Met. 1) ± 65.4
All males:	St = 815 + 14.3 (Met. 1) ± 64.2
Euro-American males:	St = 768 + 15.2 (Met. 1) ± 63.2
Euro-American females:	St = 656 + 16.3 (Met. 1) ± 49.6
African-American males:	St = 556 + 17.6 (Met. 1) ± 51.0
Second Metatarsal:	
Combined data:	St = 675 + 13.4 (Met. 2) ± 65.4
All females:	St = 791 + 11.5 (Met. 2) ± 54.8
Euro-American females:	St = 712 + 12.8 (Met. 2) ± 52.0
African-American males:	St = 605 + 14.0 (Met. 2) ± 56.8
African-American females:	St = 783 + 10.9 (Met. 2) ± 39.9
Third Metatarsal:	
Combined data:	St = 720 + 13.6 (Met. 3) ± 67.6
African-American males:	St = 706 + 13.3 (Met. 3) ± 42.2
African-American females:	St = 904 + 9.9 (Met. 3) ± 44.9
Fourth Metatarsal:	
Combined data:	St = 715 + 14.0 (Met. 4) ± 68.5
Euro-American females:	St = 719 + 13.8 (Met. 4) ± 57.5
African-American males:	St = 759 + 13.0 (Met. 4) ± 46.5
African-American females:	St = 961 + 9.3 (Met. 4) ± 46.5
Fifth Metatarsal (functional):	
African-American males:	St = 761 + 14.7 (Met. 5F) ± 68.0
African-American females:	St = 979 + 10.2 (Met. 5F) ± 47.4

Length from the apex of the capitulum to the midpoint of the articular surface of the base parallel to the longitudinal axis of the bone. For MT5, the functional length is measured from the dorsoplantar midpoint of the intersection between the fourth metatarsal and cuboid facets. Measurements are in mm.

De Mendonca (2000), Femur

Males	Females
St = (47.18 + 0.2663 × PhLF) ± 6.90	St = (55.63 + 0.2428 PhLF) ± 5.92
St = (46.89 + 0.2657 × PLF) ± 6.96	St = (57.86 + 0.2359 PLF) ± 5.96

PhLF, physiological length of the femur; PLF, perpendicular length of the femur. Measurements are in mm.

Dupertuis (1959)

White Males:

St = 77.048 + 2.116 × femur ± 0.2308
St = 92.766 + 2.178 × tibia ± 0.2436
St = 84.898 + 1.072 (femur + tibia) ± 0.2508
St = 76.201 + 1.330 femur + 0.991 tibia ± 0.2173

White Females:

St = 62.872 + 2.322 × femur ± 0.2256
St = 71.652 + 2.635 × tibia ± 0.2433
St = 57.872 + 1.354 (femur + tibia) ± 0.2016
St = 60.377 + 1.472 femur + 1.133 tibia ± 0.2063

Femur, greatest length from the internal condyle resting against vertical wall of measuring board, with bone lying on its dorsal surface, to the extreme point of the head; Tibia, greatest length from end of malleolus against vertical wall of osteometric board to the anterior edge of the lateral condyle external to the tibial spine. The bone rests on its dorsal surface with its long axis parallel to the long axis of the board. All measurements are in mm.

Genoves (1967), Mesoamerican

Males	Females
St = 2.26 femur + 66.379 ± 3.417	St = 2.59 femur + 49.742 ± 3.816
St = 1.96 tibia + 93.752 ± 2.812	St = 2.72 tibia + 63.781 ± 3.513

Subtract 2.5 cm for living stature; femur, maximum length; tibia, length without the tuberosity. Measurements are in cm.

Holland (1992), Proximal Tibia

White Males:
St = 1.031 (MCL) + 122.38 ± 5.24
St = 1.149 (MCW) + 0.992 (MCL) + 85.87 ± 4.51
St = 0.867 (MCL) + 0.606 (LCL) + 104.56 ± 4.88
St = 0.947 (MCW) + 0.911 (MCL) + 0.325 (LCL) + 82.73 ± 4.48

Black Males:
St = 1.313 (BB) + 75.36 ± 4.88
St = 1.115 (MCL) + 122.80 ± 5.11
St = 1.14 (LCL) + 128.26 ± 5.11
St = 0.836 (MCL) + 0.853 (LCL) + 99.79 ± 4.62

Black or White Males:
St = 1.145 (MCL) + 119.14 ± 5.56
St = 1.054 (LCL) + 129.55 ± 5.92
St = 0.924 (MCL) + 0.742 (LCL) + 98.17 ± 5.11
St = 0.966 (MCW) + 1.012 (MCL) + 93.12 ± 5.19
St = 0.641 (BB) + 0.806 (MCL) + 0.352 (LCL) + 71.39 ± 4.95
St = 0.621 (MCW) + 0.896 (MCL) + 0.549 (LCL) + 86.86 ± 5.01

White Females:
St = 1.64 (MCL) + 91.77 ± 4.29
St = 1.642 (LCL) + 101.89 ± 4.62
St = 1.66 (BB) + 50.27 ± 4.71
St = 1.062 (MCL) + 0.854 (LCL) + 85.19 ± 3.86
St = 1.032 (LCW) + 1.149 (LCL) + 89.22 ± 4.41
St = 0.950 (MCL) + 0.578 (LCW) + 0.661 (LCL) + 79.84 ± 3.84

Black Females:
St = 1.318 (MCL) + 105.82 ± 4.35
St = 0.905 (LCL) + 129.05 ± 4.62
St = 1.142 (MCW) + 128.78 ± 4.64
St = 1.174 (MCL) + 0.962 (LCL) + 68.44 ± 3.77
St = 0.742 (MCW) + 1.089 (MCL) + 94.02 ± 4.24
St = 0.613 (MCW) + 1.182 (MCL) + 0.916 (LCL) + 60.50 ± 3.69

Black or White Females:
St = 1.085 (MCL) + 0.904 (LCL) + 83.01 ± 4.47
St = 0.296 (BB) + 0.261 (MCW) + 0.894 (MCL) + 0.562 (LCL) + 75.87 ± 4.34

BB, biarticular breadth—maximum breadth of the proximal articular surface of the tibia as measured from the lateral edge of the lateral condyle to the medial edge of the medial condyle (calipers should be positioned only on the articular surfaces of the condyles); MCW, medial condyle articular width—maximum transverse width of the medial condyle as measured from lateral to medial edges (calipers should be placed on the slight rim located on the condyle surface); MCL, medial condyle articular length—perpendicular to width (maximum length from the anterior edge of the medial condyle to the posterior margin); LCW, similar to width of the medial condyle, but measured on the lateral condyle; LCL, similar to length of medial condyle, but made on the lateral condyle. All measurements are in mm.

Lundy (1983), South Africa

Males:

St = 2.79 (femur max) + 28.12 ± 2.80
St = 2.43 (femur) + 44.64 ± 3.39
St = 2.43 (tibia) + 60.86 ± 3.44
St = 2.48 (fibula) + 60.29 ± 3.67
St = 1.46 (femur max + tibia) + 32.51 ± 2.56
St = 1.23 (femur + tibia) + 51.76 ± 3.06

Females:

St = 2.07 (femur max) + 56.27 ± 3.77
St = 2.67 (femur) + 32.00 ± 3.80
St = 2.38 (tibia) + 59.96 ± 4.13
St = 2.65 (fibula) + 51.70 ± 4.19
St = 1.10 (femur max + tibia) + 26.83 (femur max + tibia) 3.60
St = 1.33 (femur + tibia) + 41.38 (femur max + tibia) 4.27

Measurements are in cm. Maximum length of femur follows Hrdlicka; measurement of tibia is without spines (bicondylar length of Hrdlicka). For heights ≤153.5 cm, add 10.0 cm; for heights 153.6–165.4 cm, add 10.5 cm; for heights ≥165.5, add 11.5 cm. To estimate the age of older individuals, subtract 0.06 cm for every year of age >30: (age in yr –30 cm).

Lundy: Revised (1987)

Males:

St = 2.403 (femur max) + 45.721 ± 2.777
St = 2.427 (tibia) + 60.789 ± 2.78
St = 2.515 (fibula) + 58.999 ± 2.98
St = 1.288 (femur max + tibia) + 46.543 ± 2.371

Females:

St = 2.769 (femur max) + 27.424 ± 2.789
St = 2.485 (tibia) + 55.968 ± 3.056
St = 2.761 (fibula) + 47.575 ± 3.168
St = 1.41 (femur max + tibia) + 34.617 (femur max + tibia) 2.497

Measurements are in cm. Maximum length of femur follows Hrdlicka; measurement of tibia is without spines (bicondylar length of Hrdlicka). For heights ≤153.5, add 10.0 cm; for heights 153.6–165.4 cm, add 10.5 cm; for heights ≥165.5, add 11.5 cm. To estimate the age of older individuals, subtract 0.06 cm for every year of age >30: (age in yr –30 cm).

Mohanty (1998), Percutaneous Tibial Length

Males: St = 22.8325 + 3.7500 × PCTL ± 2.8735
Females: St = 27.3032 + 3.5587 × PCTL ± 3.4423

Tibial length is measured by surface anatomical landmarks between the most prominently palpable part of the medial condyle of tibia and tip of the medial malleolus. Measurements are in cm.

PCTL, Percutaneous tibial length.

Munoz et al. (2001) Spanish Sample

Males:

St = 62.92 + 2.39 (femur) ± 3.605
St = 81.70 + 2.40 (tibia) ± 4.010
St = 72.23 + 2.79 (fibula) ± 3.667
St = 60.498 + 1.590 (femur) + 1.030 (tibia) ± 3.370

Females:

St = 64.01 + 2.25 (femur) ± 3.270
St = 76.53 + 2.41 (tibia) ± 3.033
St = 69.22 + 2.74 (fibula) ± 3.620
St = 68.192 + 0.863 (femur) + 1.592 (tibia) ± 2.944

Unknown Sex:

St = 40.68 + 2.83 (femur) ± 4.006
St = 59.15 + 2.95 (tibia) ± 4.006
St = 50.70 + 3.34 (fibula) ± 4.083
St = 44.479 + 1.56 (femur) + 1.439 (tibia) ± 3.543

All measurements are in cm. Measurements were taken in an AP radiograph. Draw a line between the most distal points of both femoral condyles. Draw a second line perpendicular to that which crosses the farthest point of femoral head. The femur is measured by between the most distal points of both femoral condyles and also along the perpendicular plane crossing the farthest point of the femoral head. The femoral length is the distance between this latter point of and the intersection of the two lines. The tibia is measured between the most proximal and internal point of the medial condyle and the tip of the medial malleolus. The fibula is measured by the distance between the most external points of the fibular head and the tip of the malleolus.

Ross and Konigsberg (2002): Balkans

Femur:	St = 634.56 + 2.3622 × femur ± 40.3
Tibia:	St = 751.85 + 2.5712 × tibia ± 33.9

Maximum femur and tibia length. Measurements are in mm.

Simmons et al. (1990)

Femur: VHA	
White Males:	St = 0.78 (VHA) + 89.64 ± 6.10
Black Males:	St = 0.79 (VHA) + 91.70 ± 6.60
White Females:	St = 0.73 (VHA) + 91.54 ± 6.67
Black Females:	St = 0.59 (VHA) + 107.10 ± 6.00
Femur: LCH	
White Males:	St = 1.47 (LCH) + 107.09 ± 6.24
Black Males:	St = 1.34 (LCH) + 113.23 ± 6.91
White Females:	St = 1.94 (LCH) + 86.10 ± 5.77
Black Females:	St = 1.59 (LCH) + 100.07 ± 5.47
Femur: VHD	
White Males:	St = 1.11 (VHD) + 113.89 ± 6.77
Black Males:	St = 1.51 (VHD) + 97.82 ± 6.92
White Females:	St = 1.35 (VHD) + 99.22 ± 7.16
Black Females:	St = 1.59 (VHD) + 92.43 ± 5.59

Femur VHA, upper breadth of femur; femur LCH, lateral condyle height; femur VHD, vertical diameter of the femoral head. Measurements are in cm.

Trotter (1970)

White Males:	White Females:
St = 2.38 (femur) + 61.41 ± 3.27	St = 2.47 (femur) + 54.10 ± 3.72
St = 2.52 (tibia) + 78.62 ± 3.37	St = 2.90 (tibia) + 61.53 ± 3.66
St = 2.68 (fibula) + 71.78 ± 3.29	St = 2.93 (fibula) + 59.61 ± 3.57
St = 1.30 (femur + tibia) + 53.20 ± 2.99	St = 1.39 (femur + tibia) + 53.20 ± 3.55
Black Males:	Black Females:
St = 2.11 (femur) + 70.35 ± 3.94	St = 2.28 (femur) + 59.76 ± 3.41
St = 2.19 (tibia) + 86.02 ± 3.78	St = 2.45 (tibia) + 72.65 ± 3.70
St = 2.19 (fibula) + 85.65 ± 4.08	St = 2.49 (fibula) + 70.90 ± 3.80
St = 1.15 (femur + tibia) + 71.04 ± 3.53	St = 1.26 (femur + tibia) + 59.72 ± 3.28
Mongoloid Males:	
St = 2.15 (femur) + 72.57 ± 3.80	
St = 2.39 (tibia) + 81.45 ± 3.27	
St = 2.40 (fibula) + 80.56 ± 3.24	
St = 1.22 (femur + tibia) + 70.37 ± 3.24	
Mexican Males:	
St = 2.44 (femur) + 58.67 ± 2.99	
St = 2.36 (tibia) + 80.62 ± 3.73	
St = 2.50 (fibula) + 75.44 ± 3.52	

Measurements are in cm. To estimate stature of older individuals, subtract 0.06 × (age in yr –30 cm). To estimate cadaver stature, add 2.5 cm.

Measurements are bone maximums; tibia measurement does not include medial malleolus.

REFERENCES

1. Rathbun TA, Rathbun BC. Human remains recovered from a shark's stomach in South Carolina. In: Haglund WD, Sorg MH, ed. Forensic taphonomy: the postmortem fate of human remains. Boca Raton, Fla: CRC Press, 1997:449–458.
2. Cook DC, Walker PL. Brief communication: gender and sex—vive la difference. Am J Phys Anthropol 1998;106:255–259.
3. Saunders SR and Yang D. Sex determination: XX or XY from the human skeleton. In: Fairgrieve SI, ed. Forensic Osteological Analysis: A Book of Case Studies. Springfield, Ill: Charles C. Thomas, 1999: 36–59.
4. Ubelaker DH. Human Skeletal Remains: Excavation, Analysis, Interpretation, 2nd ed. Washington, DC: Taraxacum, 1989, pp. 52–55.
5. Brothwell DR. Digging Up Bones. 3rd ed. Ithaca, NY: Cornell University Press, 1981, pp. 59–63.
6. Stewart TD. Hrdlicka's Practical Anthropometry. 3rd ed. Editor. Philadelphia, Pa: Wistar Institute, 1947.
7. Boyd JD, Trevor JC. Problems in reconstruction. In: Modern Trends in Forensic Medicine. Simpson, K., ed. London: Butterworth, 1953, pp. 133–153.
8. Walsh-Haney H, Katzmarzk C, Falsetti AB. Identification of human skeletal remains: was he a she or she a he? In: Fairgrieve SI, ed. Forensic Osteological Analysis: A Book of Case Studies. Springfield: Charles C. Thomas, 1999, pp. 17–35.
9. White TD. Human Osteology. New York, NY: Academic Press, 2000.
10. Iscan MY, Miller-Shaivitz P. Determination of sex from the tibia. Am J Phys Anthropol 1984;64:53–59.
11. Hanihara K. Sexual diagnosis of Japanese long bones by means of discriminant function. J Anthrop Soc Nippon 1958;66:187–196. (In Japanese, English summary).
12. Brace CL. Region does not mean 'race': reality versus convention in forensic anthropology. J Forensic Sci 1995;40:171–175.
13. Belcher R, Williams F and Armelagos GJ. Misidentification of meroitic Nubians using FORDISC 2.0. Paper presented (April 2002) at: the American Association of Physical Anthropology, 2002; Buffalo, NY.
14. Sauer NJ. Forensic anthropology and the concept of race: if races don't exist, why are forensic anthropologists so good at identifying them? Soc Sci Med 1992;34:107–111.
15. Giles E. Discriminant function sexing of the human skeleton. In: Personal Identification in Mass Disasters. Stewart TD, ed. Washington, DC: National Museum of Natural History, 1970, pp. 99–107.
16. Gilbert BM. Anterior femoral curvature: its probable basis and utility as a criterion of racial assessment. Am J Phys Anthropol 1976;45:601–604.
17. Krogman WM, Iscan MY. The Human Skeleton In Forensic Medicine. Springfield: Charles C. Thomas, 1986.
18. St. Hoyme LE, Iscan MY. Determination of sex and race: accuracy and assumptions. In: Reconstruction of Life From the Skeleton. Krogman WM, Iscan MY, eds. New York: Alan R. Liss, 1989, pp. 53–94.
19. Iscan MY, Cotton TS. Race determination from the post cranial skeleton. In: Skeletal Race and Identification: New Approaches in Forensic Anthropology. Gill GW, Rhine JS, eds Albuquerque, NM: Maxwell Museum Technical Services, University of New Mexico Press, 1986, pp. 74–106.
20. Fully G. Une Nouvelle Methode de Determination de la Taille. Annales de Medecine Legale 1956;35:266–273.
21. Stewart TD. Essentials of Forensic Anthropology. Springfield: Charles C. Thomas, 1979.
22. El-Najjar MY, McWilliams KR. Forensic Anthropology. Springfield: Charles C. Thomas, 1978.
23. Dwight T. Methods of estimating the height from parts of the skeleton. Med Rec NY 1894;46:293–296.
24. Sciulli PW, Schneider KN, Mahaney MC. Stature estimation in prehistoric Ohio Native Americans. Am J Phys Anthropol 1991;83:275–280.

25. Lundy JK. Regression equations for estimating living stature from long limb bones in the South African Negro. S Afr J Sci 1983;79:337–338.
26. Lundy JK. A report on the use of Fully's anatomical method to estimate stature in military skeletal remains. J Forensic Sci 1988;33:534–539.
27. Sokal RR, Rohlf FJ. Biometry. New York, NY: WH Freeman and Co, 1981.
28. Zar JH. Biostatistical Analysis. Upper Saddle River, NJ: Prentice Hall, 1999.
29. Genoves S. Proportionality of long bones and their relation to stature among Mesoamericans. Am J Phys Anthropol 1967;26:67–78.
30. Konigsberg LW, et al. Stature estimation and calibration: Bayesian and maximum likelihood perspectives in physical anthropology. Yearbook of Phys Anthropol 1998;41:65–91.
31. Steele DG, McKern TW. A method for assessment of maximum long bone length and living stature from fragmentary long bones. Am J Phys Anthropol 1969;31:215–228.
32. Steele DG. Estimation of stature from fragments of long limb bones. Personal Identification in Mass Disasters. Washington, DC: Smithsonian Institute, 1970, pp. 85–97.
33. Simmons T, et al. Stature estimation from fragmentary femora: a revision of the Steele method. J Forensic Sci 1990;35:628–636.
34. Holland T. Estimation of adult stature from fragmentary tibias. J Forensic Sci 1992;37:1223–1229.
35. Jacobs K. Estimating femur and tibia length from fragmentary bones: an evaluation of Steele's (1970) method using a prehistoric European sample. Am J Phys Anthropol 1992;89:333–345.
36. Giles E, Hutchinson D. Stature and age-related bias in self-reported stature. J Forensic Sci 1991;36: 765–780.
37. Himes JH, Roche AF. Reported versus measured adult statures. Am J Phys Anthropol 1982;58: 335–341.
38. Galloway A. Estimating actual height in the older individual. J Forensic Sci 1988;33:126–136.
39. McCullough JM, McCullough CS. Age-specific variation in the secular trend for stature: a comparison of samples from industrialized and nonindustrialized regions. Am J of Phys Anthropol 1984;65:169–180.
40. Jantz LM, Jantz RL. Secular change in long bone length and proportion in the United States: 1800–1970. Am J Phys Anthropol 1999;110:57–67.
41. Klepinger LL. Stature, maturation, variation, and secular trends in forensic anthropology. J Forensic Sci 2001;46:788–790.
42. Meadows L, Jantz R. Allometric secular change in the long bones from the 1800s to the present. J Forensic Sci 1995;40:762–767.
43. Ulijasek SJ. Secular trends in growth: the narrowing of ethnic differences in stature. Nutrition Bulletin: 2001;26:43–51.
44. Trotter M. Estimation of stature from intact long limb bones. In: Personal Identification in Mass Disasters. Stewart, TD, ed. Washington, DC: Smithsonian Institute, 1970, pp. 71–83.
45. Costa DL, Steckel RH. Long term trends in health, welfare and economic growth in the United States. In: Health and Welfare During Industrialization. Steckel RH, Floud R, eds. Chicago: University of Chicago Press, 1997, pp. 47–89.
46. Kirby R. Human heights and the standard of living. School of Social and International Studies: Sunderland University. 2000. Available at:http://humanities.uwe.ac.uk/corehistorians/social/cores/kirbycor.htm.
47. Steckel RH. Height and health in the United States: 1710–1950. In: Stature, Living Standards and Economic Development: Essays in Anthropometric History. Komlos J, ed. Chicago: University of Chicago Press, 1994, pp. 153–170.
48. McKinley J. The analysis of cremated bone. In: Human Osteology in Archaeology and Forensic Science. Cox M, Mays S, eds. London: Greenwich Medical Media Ltd., 2002, pp. 403–424.
49. Jantz RL, Hunt DR, Meadows L. The measure and mismeasure of the tibia: implications for stature estimation. J Forensic Sci 1995;40:758–761.
50. Trotter M, Gleser G. A re-evaluation of estimation of stature based on measurements of stature taken during life and of long bones after death. Am J Phys Anthropol 1958;16:79–123.

FURTHER READING

Equations, Formulas, and Other Sources

Asala SA. Sex determination from the head of the femur of South African whites and blacks. Forensic Sci Int 2001;117:15–22.

Alunni-Perret V. et al. Reexamination of a measurement for sexual determination using the supero–inferior femoral neck diameter in a modern European population. J Forensic Sci 2003;48:1–4.

Bidmos MA, Asala SA. Discriminant function sexing of the calcaneus of the South African white population. J Forensic Sci 2003;48:1213–1218.

Bidmos MA, Dayal MR. Sex determination from the talus of South African whites by discriminant function analysis. Am J Forensic Med & Pathol 2003;24:322–328.

Bidmos MA, Asala SA. Adult stature estimation from the calcaneus of South African blacks. Poster presented at: 72nd meeting of the American Association of Physical Anthropologists; Tempe, Arizona; April 25, 2003.

Boldsen JA. Statistical evaluation of the basis for predicting stature from lengths of long bones in European populations. Am J Phys Anthropol 1984;65:305–311.

Byers S, Akoshima K, Curran B. Determination of adult stature from metatarsal length. Am J Phys Anthropol 1989;79:275–281.

Craig E. Intercondylar shelf angle: a new method to determine race from the distal femur. J Forensic Sci 1995;40:777–782.

De Mendonca MC. Estimation of height from the length of long bones in a Portuguese adult population. Am J Phys Anthropol 2000;112:39–48.

Dupertuis CW, Hadden JA. On the reconstruction of stature from long bones. Am J Phys Anthropol 1959;9:15–54.

Feldesman M, Fountain R. 'Race' specificity and the femur/stature ratio. Am J Phys Anthropol 1996; 100:207–224.

Giles E. Corrections for age in estimating older adults' stature from long bones. J Forensic Sci 1991; 36:898–901.

Giles E. Modifying stature estimation from the femur and tibia. J Forensic Sci 1993;38:758–760.

Giles E, Klepinger L. Confidence intervals for estimates based on linear regression in forensic anthropology. J Forensic Sci 1988;33:1218–1222.

Gill G. Racial variation in the proximal and distal femur: heritability and forensic utility. J Forensic Sci 2001;46:791–799.

Gill G. Challenge on the frontier: discerning American Indians from whites osteologically. J Forensic Sci 1995;40:783–788.

Gonzalez-Reimers E et al. Sex determination by discriminant function analysis of the right tibia in the prehistoric populations of the Canary Islands. Forensic Sci Int 2000;108:165172.

Holliday TW, Falsetti AB. A new method for discriminating African-American from European-American skeletons using postcranial osteometrics reflective of body shape. J Forensic Sci 1999;44:926–930.

Introna F Jr, et al. Sex determination by discriminant analysis of calcanei measurements. J Forensic Sci 1997;42:725–728.

Iscan MY. Discriminant function sexing of the tibia. J Forensic Sci 1984;29:1087–1093.

Iscan, MY, et al. Sex determination from the tibia: standards for contemporary Japan. J Forensic Sci 1994;39:785–792.

Iscan MY, Shihai D. Sexual dimorphism in the Chinese femur. Forensic Sci Int 1995;74:79–87.

Jantz RL. Modification of the Trotter and Glesar female stature estimation formulae. J Forensic Sci 1992; 37:1230–1235.

King CA, et al. Metric and comparative analysis of sexual dimorphism in the Thai femur. J Forensic Sci 1998;43:954–958.

Lundy JK, Feldesman MR. Revised equations for estimating living stature from the long bones of the South African Negro. S Afr J Sci 1987;83:54–55.

Manouvrier L. Determination de la Taille D'apres Les Grands os des Membres. Revue Mensuelle L'Ecole D'Anthropologie de Paris 1892;2:225–233.

Mohanty NK. Prediction of height from percutaneous tibial length amongst Oriya population. Forensic Sci Int 1998;98:137–141.

Munoz J, et al. Stature estimation from radiographically determined long bone length in a Spanish population sample. J Forensic Sci 2001;46:363–366.

Murphy AMC. The talus: sex assessment of prehistoric New Zealand Polynesian skeletal remains. Forensic Sci Int 2002;128:155–158.

Murphy AMC. The calcaneus: sex assessment of prehistoric New Zealand Polynesian skeletal remains. Forensic Sci Int 2002;129:205–208.

Ousley S. Should we estimate biological or forensic stature? J Forensic Sci 1995; 40:768–773.

Pelin IC, Duyar I. Estimating stature from tibia length: a comparison of methods. J Forensic Sci 2003; 48:1–5.

Reipert T. et al. Estimation of sex on the basis of radiographs of the calcaneus. Forensic Sci Int 1996; 77:133–140.

Robling AG, Ubelaker DH. Sex estimation from the metatarsals. J Forensic Sci 1997;42:1062–1069.

Ross AH, Konisgsberg L. New formulae for estimating stature in the Balkans. J Forensic Sci 2002; 47:165–167.

Safont S, et al. Sex assessment on the basis of long bone circumference. Am J Phys Anthropol 2000; 113:317–328.

Seidemann R, et al. The use of the supero–inferior femoral neck diameter as a sex assessor. Am J Phys Anthropol 1998;107:305–313.

Singh S, Singh SP. Identification of sex from tarsal bones. Acta Anat. 1975;93:568–573.

Smith SL. Attribution of foot bones to sex and population groups. J Forensic Sci 1997;42:186–195.

Steyn M, Iscan MY. Sex determination from the femur and tibia in South African whites. Forensic Sci Int 1997;90:111–119.

Stojanowski CM, Seidemann RM. A reevaluation of the sex prediction accuracy of the minimum supero–inferior femoral neck diameter for modern individuals. J Forensic Sci 1999;44:1215–1218.

Taylor JV, et al. Metropolitan forensic anthropology team (MFAT): studies in identification: 1. Race and sex assessment by discriminant function analysis of the postcranial skeleton. J Forensic Sci 1984;29:798–805.

Trotter M, Gleser G. The effect of aging on stature. Am J Phys Anthropol 1951;9:311–324.

Trudell MB. Anterior femoral curvature revisited: race assessment from the femur. J Forensic Sci 1999; 44:700–707.

Wright LE, Vasquez MA. Estimating the length of incomplete long bones: forensic standards from Guatemala. Am J Phys Anthropol 2003;120:233–251.

Chapter 5

Estimating Age at Death

Douglas H. Ubelaker, PhD

1. Introduction

The estimation of age at death based on anatomical information from the lower extremity involves an assessment of physiological age and an attempt to correlate it with chronological age. Specific techniques employed in this process vary with the sample available for analysis as well as the general age of the individual *(1,2)*. Some techniques are specific to particular bones or even parts of bones. Techniques that would be ideal to use to estimate age at death in fetal remains are irrelevant in adults. Some consideration also must be given to sex and population differences and their impact on age indicators. In this chapter, the relevant literature will be reviewed and recommendations for appropriate procedures will be provided. In recognition of the focus of this volume, this discussion will be limited to the lower extremity, although workers should be aware that additional and perhaps more accurate techniques may be available when other anatomical areas are present. General reviews of techniques for estimating age at death based on all parts of the body have been published by Bass *(3)*, Krogman and Iscan *(4)*, Scheuer and Black *(5)*, Steele and Bramblett *(6)*, Stewart *(7)*, Sundick *(8)*, Ubelaker *(9)*, White *(10)*, and the Workshop of European Anthropologists *(11)*.

The complex processes of growth, maturation, and subsequent degeneration associated with aging produce changes in the lower extremity that can prove useful in the estimation of age at death *(12,13)*. Such changes include the increase in external dimensions *(14–16)*, the appearance and union of epiphyses and other ossification centers *(17)*, remodeling, bone loss, arthritic changes, and shifts in chemical composition. Information regarding growth, epiphyseal appearance, and union is most useful for immature individuals and has even been used to predict future growth in living individuals *(18)*. The remaining processes provide information that is most useful for estimating age at death in adults.

From: *Forensic Science and Medicine*
Forensic Medicine of the Lower Extremity: Human Identification and Trauma Analysis of the Thigh, Leg, and Foot
Edited by: J. Rich, D. E. Dean, and R. H. Powers © The Humana Press Inc., Totowa, NJ

2. Fetal Body Measurements

Fetal measurements provide useful information about changes with aging in forensic cases in which a sufficient amount of soft tissue is present.

According to pediatric literature (e.g., refs. *19,20*) the measurements most commonly used in the fetus are total body length and crown rump length; however, anthropometric information from the lower extremity is useful. Scammon *(19)* describes methods of using data from the lower extremity, including leg length, thigh length (trochanter to knee), and foot length. Age is listed in terms of lunar months (i.e., calculated from the beginning of the last menstruation of the mother). De Vasconcellos et al. provide additional data on foot length *(21)*.

2.1. Bone Formation and Growth

The formation and development of bone is a complex process *(22–25)*. As noted by Gardner and Gray *(26)*, prenatal development of the femur (as well as other long bones) involves the formation and subsequent erosion of a primary bone collar and calcification of cartilage with subsequent destruction of cartilage, endochondral ossification, periosteal bone formation, trabeculation of the bone collar, fusion of endochondral trabeculae with the inner aspect of the periosteal shell, and formation of a central medullary cavity free of trabeculae. Of course, variations of the normal ossification pattern may occur *(27)*.

The increase in the dimensions of bones of the lower extremity provides a major source of information regarding age at death for immature individuals *(28–30)*. With increasing age, differences between the sexes, among populations, and among individuals within populations lead to an increase in such variation, thereby limiting the accuracy of age estimation. The many factors that influence growth (genetics, nutrition, morbidity, etc.) also affect the correlation of bone size with chronological age *(31–33)*. Accuracy diminishes with increasing age, even if these variables can be controlled (known sex, population, etc.). Such data are the most accurate and reliable sources of information in fetal remains.

Estimates of age at death can also be generated using measurements of skeletal remains *(34–39)*. Scheuer et al. *(40)* provide regression equations to estimate fetal age on the basis of limb bone length. Their study included measurements taken from radiographs of the femur and tibia from British fetuses aged 24 to 46 wk. Regressions are published separately for each sex as well as for both sexes combined.

Fazekas and Kósa *(41)* provide a method for estimating chronological age at death from fetal remains through their analysis of a large Hungarian sample *(42)*. They examined 138 fetuses (71 males and 67 females) with ages at death ranging from the third to the tenth lunar month and body lengths ranging from 9 to 55 cm. Measurements of bones in the lower extremity included femur length and width, tibia length, fibula length, and length of the first metatarsal. Regression equations for calculating body length from long bones in the lower extremity generated from this study consist of the following:

$$\text{femur length (cm)} \times 6.44 + 4.51$$
$$\text{femur width (cm)} \times 22.63 + 7.57$$
$$\text{tibia length (cm)} \times 7.24 + 4.90$$
$$\text{fibula length (cm)} \times 7.59 + 4.68 \quad (41)$$

The formula for the maximum length of the first metatarsal is as follows:

$$\text{body length (cm)} = \text{length (cm)} \times 29.38 + 12.69 \textit{ (41)}$$

This approach differs from the method of Scheuer et al. *(40)*, in that it relies on body length, which must then be converted to chronological age.

One issue in assessing age at death based on fetal remains concerns differences in bone size as it appears in radiographs vs direct measurements of bone in a skeletonized condition. For example, the Scheuer et al. study *(40)*, whose findings are summarized above, reported measurements from radiographs with soft tissue present.

The Fazekas and Kósa *(41)* measurements were taken directly from the bones (no soft tissue).

Similarly, the solution to forensic problems may involve measurements of recovered bones or radiographs of fetal remains with soft tissue present.

A discussion of methodologies used to correlate measurements of bones that are taken under a variety of conditions are provided by Adalian et al. *(43)*, Huxley *(44)*, and Huxley and Kósa *(45)*.

3. Growth: Infancy Through Adolescence

After birth, the complex growth process causes the dimensions of bones in the lower limbs to continue to increase until maturity *(46)*. The most accurate data correlating long bone length with chronological age at death originate from radiographic studies of the living. Data on long-bone growth from such studies are provided by Anderson and Green *(47)*; Anderson, Green, and Messner, *(48)*; Anderson, Messner, and Green *(49)*; as well as Francis *(50)*, Ghantus *(51)*, Gindhart *(52)*, Hoffman *(53)*, Maresh *(37,38)*, and Maresh and Deming *(39)*.

Comparative data from samples of archeological origin are available in publications by Hoppa *(54)*, Hoppa and Gruspier, *(55)*, Johnston *(56)*, Merchant and Ubelaker, *(57)* Miles and Bulman, *(58)*, Stewart *(59)*, Steyn and Henneberg *(60)*, Sundick *(61,62)*, and Walker *(63)*. These studies generally involve measurements of long bones and other skeletal data compared with estimates of age at death, usually derived from assessment of dental formation. Although age at death cannot be calculated as precisely after death as with tissue samples obtained from living individuals, these references provide valuable comparable data about long-bone growth in different populations.

Although bone size can provide important information regarding age at death *(64)*, it is important to consider sex and population origin whenever possible. The comparative studies discussed above suggest considerable population variation, as well as considerable individual variation within populations. This variation increases with age. For example, given an individual of unknown sex, a maximum femur length of approx 310 mm would suggest an age at death of just under 8 yr if the individual was originally a member of an American population of European ancestry, but just under 12 yr if the individual was originally a member of an Eskimo population *(9)*. These data reflect mean values; the actual variation among individuals could present even greater variation.

Humphrey *(65)* demonstrated that the timing and expression of sexual dimorphism varies in different parts of the skeleton. Sex differences are apparent at birth in

the maximum and minimum diameter of the diaphyseal femur. They are apparent at age 2.3 yr in the maximum diameter of the fibula diaphysis, 4.2 yr in the maximum diameter of the tibia diaphysis, 5.3 yr in the minimum diameter of the tibia diaphysis, 11.2 yr in the minimum diameter of the fibula diaphysis, and between 16.1 and 17.6 yr in the maximum lengths of the femur, tibia, and fibula.

If soft tissue is present, measurements can provide useful data on age. Several studies provide information on the growth of the foot *(66–71)*. Correlations between age and calf circumference in different populations are available in Eveleth and Tanner *(72)*.

4. Ossification Center Appearance and Epiphyseal Union

The appearance and union of the epiphyses associated with bones of the lower extremity can also provide useful information for estimating age at death *(73–79)*, especially during adolescence. Epiphyses are the bony caps on the ends of long bones and on certain other bony structures. Their appearance and size in radiographic studies of bones with associated soft tissue are particularly useful in determining age at death *(80,81)*.

In examinations of recovered skeletal remains, the small developing epiphyses can prove difficult to recognize and recover, and it can be difficult to identify their location within the skeleton.

This limitation also applies to newly formed ossification centers in general. Although formation data are available *(82–110)*, they are most useful in radiographic studies when soft tissue is present, the anatomical location can be determined, and the sex is known *(111)*.

Through their study of 136 human embryos, Noback and Robertson *(112)* note the order of appearance of ossification centers in major bones of the lower extremity as follows: (1) femur, (2) tibia, (3) fibula, (4) metatarsals, (5) distal phalanges, (6) proximal phalanges, and (7) middle phalanges. Kraus *(113)* adds more detailed data on the sequence of 18 centers in the bones of the foot, beginning with the first distal phalanx and ending with the fourth intermediate phalanx. Additional supportive data are provided by O'Rahilly and Gardner *(114)*, who note that ossification begins in the femur and tibia prior to the fibula.

Epiphyses are most useful in skeletal age estimation procedures when they are approximately fully formed and in the process of uniting with the associated diaphysis. The epiphyses of the lower extremity that are most useful in age estimation are those of the proximal femur, greater trochanter of the femur, distal femur, proximal tibia, distal tibia, proximal fibula, distal fibula, and the metatarsals and foot phalanges. Radiographically, ununited epiphyses can be recognized by a clear line of non-union between the epiphysis and the adjacent aspect of the bone. As the epiphyses unite, these lines diminish or disappear altogether. With bones devoid of soft tissue, evidence of non-articulation consists of an uneven and fracture-free articular surface (on the articular surfaces of both the epiphysis and the diaphysis or associated bone).

It is important to remember that a considerable length of time can elapse between the beginning and end of epiphyseal closure for each epiphysis *(115)*. Thus, when using information from the literature to interpret observations on closure, attention must be paid to the definitions of closure that are used. Definitions of radiographic closure may differ slightly from those describing bones lacking soft tissue.

Since adolescent females mature earlier than males, sex should be considered in estimating age at death from epiphyseal union. Because many sources report data for the two sexes separately, sex-specific data should be consulted if the sex is known. If the sex is not known, the age range under consideration should be expanded to include the possibility of either sex. According to Lewis and Garn *(116)*, many ossification centers occur approx 25% earlier in girls than in boys (e.g., approx 19% earlier in the knee area). Sex differences in the timing of union in epiphyses of the lower extremity can be in the magnitude of 1 to 2 yr *(7,117)*.

Correlations between age at death and the timing of epiphyseal appearance and union is presented in many general references. Pyle and Hoerr *(118)* provide a radiographic atlas for age progression in the knee region; a similar atlas is available for the foot and ankle *(119)*. The Hoerr et al. radiographic atlas presents information and radiographic images of the foot and ankle of males and females between the ages of 38 fetal wk to adulthood.

McKern and Stewart *(120)* present evidence for union in skeletal remains devoid of soft tissue, although for males of military age, only. Their study offers important data on the variation of epiphyseal union, rather than just the mean values. They found that among the epiphyses of the lower extremity, the head and distal end of the femur were especially useful.

Of course, the value of epiphyseal union for age estimation lies in the fact that all epiphyses do not unite simultaneously in any individual but vary considerably. Within the lower extremity, the epiphyses of the ankle and hip unite before those in the knee region. Note also that variations can occur *(121)*, including "pseudo-epiphyses," which are diaphyseal extensions into the cartilaginous extremity of the bone *(122)*. Individuals with a leg-length discrepancy show increased age-related variation *(123)*.

Osborne et al. *(124)* call attention to age changes in immature trabecular bone. Their radiological study of children aged newborn to 15 yr documents such changes in the proximal femur.

5. *Bone Remodeling*

The normal process of remodeling of compact bone in the long bones of the lower extremity provides histological information that can prove useful in estimating age at death, especially in adults *(125–128)*. Bone remodeling involves the conversion of primary bone (i.e., that formed during the initial ossification of the bone) to secondary bone. Bone turnover is accomplished through the action of osteoclasts to create resorption spaces, which are subsequently filled in to form secondary osteons. This process begins early in life and continues until death. With increasing age, the original components of diaphyseal compact bone are gradually replaced by the new structures. Preexisting structures, such as lines of increased density, may be altered or removed *(129)*. With advancing age, resorption spaces are created not only at the expense of the original circumferential lamellar bone and primary osteons but pre-existing secondary osteons as well, thereby forming secondary osteon fragments.

In 1965, Kerley introduced a histological technique based on the examination of thin cross-sections of undecalcified ground tissue removed from the mid shaft of the femur,

tibia, and fibula. This technique calls for the examination of four circular fields, each measuring approximately 1.62 mm in diameter and located adjacent to the periosteal edge of the bone on its anterior, posterior, medial, and lateral surfaces *(130–132)*. Within each of these fields, the numbers of primary osteons, secondary osteons, and osteon fragments must be counted, as well as the percentage remaining of the original circumferential lamellar bone. The technique recognizes that circumferential lamellar bone and primary osteons were formed during the original formation process. Secondary osteons and osteon fragments are created during the remodeling process. Thus with increasing age, the percentage of circumferential lamellar bone and the number of primary osteons decrease while the number of secondary osteons and osteon fragments increases. The Kerley system allows the age at death to be estimated through the use of a "profile chart" or regression equations. The profile chart is created by plotting age distribution data for each variable and then observing the age at which they overlap. The regression equations allow direct estimation of age for each variable.

The Kerley method is useful if complete cross-sections are available, but is limited if the external (periosteal) surface is damaged or otherwise missing. Error is introduced if visual fields are used other than those defined, because the histology of the bone cortex varies *(133)*.

Several modified or alternative methods have been introduced since Kerley introduced this technique. Ahlqvist and Damsten *(134)* offered a modification of this technique in which the combined frequencies of secondary osteons and osteon fragments within fields located between those used by Kerley are examined. These field locations were chosen because they avoid Kerley's posterior field on the linea aspera, a site of muscle attachment and potential activity-induced change unrelated to age. However, their sample was more restricted than Kerley's, in terms of size and composition, and by combining two of Kerley's variables, they sacrificed some useful sources of information *(135)*.

Another modification, suggested by Singh and Gunberg *(136)*, examines the number of secondary osteons, the average number of lamellae per osteon, and the average shortest diameter between Haversian canals in two randomly selected fields within the periosteal third of the cortex. Regression equations are available from their study of 59 individuals aged 40 to 88 yr. These equations include those applicable to the femur and tibia.

In 1979, Thompson *(137)* published a technique that utilizes only a small core of bone (4 mm in diameter) removed from the anterior mid shaft of the femur and the medial mid shaft of the tibia, as well as other bones. His complex method employing 19 variables was based on a sample of 116 adults. Although the method examines only one area of the bone cortex, it has the advantage of not requiring a cross section.

Watanabe et al. *(138)* studied stained ground thin sections taken from the mid-shaft of the femur in 72 Japanese males aged 43 to 92 yr and 26 females aged 2 and 88 yr. They examined the area, maximum diameter, minimum diameter, and perimeter of intact osteons and Haversian canals, as well as type II osteons, fragments, and the triangular area of associated osteons. The osteon dimensions displayed a higher correlation with age than the Haversian canals.

Walker et al. *(139)* reported that in individuals aged more than 50 yr, the density of osteons and osteon fragments correlated with cortical mass but not with age.

These researchers urged caution in the use of these attributes to estimate histological age in individuals in this age bracket.

Of course, all of the histological methods are by nature destructive and require the necessary equipment. Experience with these techniques is also important to ensure correct identification of the structures involved *(140)*. For general reviews of histological approaches, see Robling and Stout *(125)* and Ubelaker *(127,128)*.

5.1. Radiographic Approaches

A 1953 study by Hansen *(141)* revealed that among adults, the medullary cavity increases in size with age. At the proximal end of the femur, the cavity advances (at the expense of trabecular bone) to the level of the surgical neck during the fourth decade and reaches the epiphyseal line between 61 and 74 yr. The medullary cavity also increases in width with aging, creating a loss of cortical bone and thickness in advanced years.

Walker and Lovejoy *(142)* present radiographic data on age progression in the proximal femur and calcaneus in 130 individuals from the Hamann–Todd collection. For the femur, they present radiographic standards comprised of eight phases. Radiographic images of each phase are accompanied by descriptive narrative. The first of the eight phases has a suggested age range of 18 to 24 yr, and the final one is listed at 60 yr or more.

Ruff and Jones *(143)* add that adult remodeling can alter asymmetry in cortical bone. With aging, patterns of adult cortical remodeling correlate with activity levels. Their study of mature tibiae indicates that the loss of cortical bone with remodelling likely produces shifts in asymmetry.

In older adults, bone density decreases with age. Note, however, that Atkinson and Weatherell found that within the femoral diaphysis, bone density varied at several locations in the diaphysis but was greatest at mid shaft *(144)*. Density also varied at sites around the circumference of the diaphysis. The reader is encouraged to review the chapter entitled *Radiology of the Lower Extremity* for a comprehensive treatise on evaluating ossification centers from radiographs.

5.2. Arthritic Changes

General changes associated with arthritis provide an additional source of age information from bones in the lower extremity *(131)*. Obviously, as adults age, the frequency and probability of arthritis-associated changes in the joints increases. Generalized changes provide clues to advancing age, but pathological conditions can produce such evidence prematurely or with varied expressions in different anatomical areas.

5.3. Chemical Changes

Ohtani et al. *(145)* report that aspartic acid racemization ratios in the human femur may provide some information that is useful in age determination procedures. The normal L form of amino acids change to the D form with aging. Their study of femoral compact bone revealed that sex differences were apparent, with males demonstrating the greater increase in the D/L ratio with aging. They recommend using the total amino-acid fractions instead of the acid-insoluble collagen fraction.

6. Summary

A variety of techniques *(146)* are available to estimate age at death based on information obtained from the lower extremity. The nature and accuracy of these techniques vary with the general age of the material examined and the particular anatomical areas available for analysis. Generally, all available evidence should be evaluated to determine the age at death *(140,147)*.

In the fetus, priority should be given first to long-bone lengths, then to whatever other measurable bones are available or for which data exist. Whether measurements are obtained through radiography or direct measurement of isolated bones, it is important to use appropriate data, conversion methodology, or both. Long-bone diaphyseal lengths and other bone measurements continue to be important in age determination procedures through childhood, although measurements of soft tissue can also be useful. With increasing age, the appearance, growth, and union of epiphyses can prove important sources of information in juveniles, especially in soft tissue cases. Also, with increasing age during adolescence, information about sex and population variation become significant factors and must be considered when available.

With maturity, the criteria for age determination shifts toward histological and degenerative alterations. Histological age determination techniques (especially the Kerley method and its modifications) offer the most accuracy if appropriate tissues are preserved and available. Chemical and radiological approaches also show some promise in this age range, but more research is needed.

References

1. Kerley ER. Forensic anthropology and crimes involving children. J Forensic Sci 1976;21:333–339.
2. Ubelaker DH. Methodological considerations in the forensic applications of human skeletal biology. In: Biological anthropology of the human skeleton. Katzenberg MA, Saunders SR, eds. New York, NY: Wiley-Liss, 2000: pp. 41–67.
3. Bass WM. Human osteology: a laboratory and field manual. 3rd ed. Columbia, Mo: Missouri Archaeological Society, Inc., 1987.
4. Krogman WM, Işcan MY. The human skeleton in forensic medicine. 2nd ed. Springfield, Ill: Charles C. Thomas, 1986.
5. Scheuer L, Black S. Developmental Juvenile Osteology. New York, NY: Academic Press, 2000.
6. Steele DG, Bramblett CA. The anatomy and biology of the human skeleton. College Station, Tex: Texas A & M University Press, 1988.
7. Stewart TD. Essentials of forensic anthropology. Springfield, Ill: Charles C. Thomas, 1979.
8. Sundick RI. Age and sex determination of subadult skeletons. J Forensic Sci 1977;22:141–144.
9. Ubelaker DH. Human skeletal remains: excavation, analysis, interpretation. 3rd ed. Manuals on Archeology. Washington, DC: Taraxacum, 1999.
10. White TD. Human osteology. New York, NY: Academic Press, Inc., 1991.
11. Workshop of European Anthropologists (WEA). Recommendations for age and sex diagnoses of skeletons. J Hum Evol 1980;9:517–549.
12. Acheson RM. Maturation of the skeleton. In: Human Development. Falkner F, ed. Philadelphia: WB Saunders, 1966, pp. 465–502.
13. Acheson RM, Hewitt D. Oxford Child Health Survey: stature and skeletal maturation in the preschool child. Brit J Prev Soc Med 1954;8:59–65.
14. Pritchett JW. Longitudinal growth and growth-plate activity in the lower extremity. Clin Orthop Relat R 1992;275:274–279.

15. Saunders SR. Subadult skeletons and growth-related studies. In: Skeletal Biology of Past Peoples: Research Methods. Saunders SR, Katzenberg MA, eds. New York: Wiley-Liss, 1992, pp. 1–20.
16. Saunders SR. Subadult skeletons and growth-related studies. In: Skeletal biology of past peoples: research methods. Saunders SR, Katzenberg MA, eds. New York: Wiley-Liss, 2000, pp.135–161.
17. MacLaughlin-Black S, Gunstone A. Early fetal maturity assessed from patterns of ossification in the hand and foot. Int J Osteoarchaeol 1995;5:51–59.
18. Gill GG, Abbott LC. Practical method of predicting the growth of the femur and tibia in the child. Arch Surg 1942;45:286–315.
19. Scammon RE. Two simple nomographs for estimating the age and some of the major external dimensions of the human fetus. Anat Rec 1937;68:221–225.
20. Scammon RE, Calkins LA. New empirical formulae for determining the age of human fetus. Anat Rec 1923;25:148–149.
21. de Vasconcellos HA, Prates JC, Belo de Moraes LG. A study of human foot length growth in the early fetal period. Ann Anat 1992;174:473–474.
22. Moss ML, Noback CR, Robertson GG. Critical developmental horizons in human fetal long bones. Am J Anat 1955;97:155–175.
23. Beals RK, Skyhar M. Growth and development of the tibia, fibula, and ankle joint. Clin Orthop Relat R 1984;182:289–292.
24. Felts WJL. The prenatal development of the human femur. Am J Anat 1954;94:1–44.
25. Hall BK. The embryonic development of bone. Am Sci 1988;76:174–181.
26. Gardner E, Gray DJ. The prenatal development of the human femur. Am J Anat 1970;129:121–140.
27. Burkus JK, Ogden JA. Bipartite primary ossification in the developing human femur. J Pediatr Orthop 1982;2:63–65.
28. de Vasconcellos HA, Ferreira E. Metatarsal growth during the second trimester: a predictor of gestational age? J Anat 1998;193:145–149.
29. Ubelaker DH. Estimating age at death from immature human skeletons: an overview. J Forensic Sci 1987;32:1254–1263.
30. Ubelaker DH. The estimation of age at death from immature human bone. In: Age Markers in the Human Skeleton. Işcan MY, ed. Springfield: Charles C. Thomas, 1989, pp. 55–70.
31. Johnston FE, Zimmer LO. Assessment of growth and age in the immature skeleton. In: Reconstruction of life from the skeleton. Işcan MY, Kennedy KAR, eds. New York: Alan R. Liss, 1989, pp. 11–21.
32. Lampl M, Johnston FE. Problems in the aging of skeletal juveniles: perspectives from maturation assessments of living children. Am J Phys Anthropol 1996;101:345–355.
33. Weaver DS. Forensic aspects of fetal and neonatal skeletons. In: Forensic osteology: advances in the identification of human remains. Reichs KJ, ed. Springfield: Charles C. Thomas, 1986.
34. Deutsch D, Goultschin J, Anteby S. Determination of human fetal age from the length of femur, mandible, and maxillary incisor. Growth 1981;45:232–238.
35. Hesdorffer MB, Scammon RE. Growth of long-bones of human fetus as illustrated by the tibia: proceedings of the Society for Experimental Biology and Medicine 1928;25:638–641.
36. Kelemen E, Jánossa M, Calvo W, Fliedner TM. Developmental age estimated by bone-length measurement in human fetuses. Anat Rec 1984;209:547–552.
37. Maresh MM. Growth of major long bones in healthy children. Am J Dis Child 1943;89:227–257.
38. Maresh MM. Linear growth of long bones of extremities from infancy through adolescence. Am J Dis Child 1955;89:725–742.
39. Maresh MM, Deming J. The growth of long bones in 80 infants. Child Dev 1939;10:91–106.
40. Scheuer JL, Musgrave JH, Evans SP. The estimation of late fetal and perinatal age from limb bone length by linear and logarithmic regression. Ann Hum Biol 1980;7:257–265.
41. Fazekas IG, Kósa F. Forensic fetal osteology. Budapest: Akadémiai Kiadó, 1978, pp. 232–256.
42. Kósa F. Age estimation from the fetal skeleton. In: Age markers in the human skeleton. Işcan MY, ed. Springfield: Charles C. Thomas, 1989, pp. 21–54.

43. Adalian P, Piercecchi-Marti MD, Bourliere-Najean B, et al. Postmortem assessment of fetal diaphyseal femoral length: validation of a radiographic methodology. J Forensic Sci 2001;46:215–219.
44. Huxley AK. Analysis of shrinkage in human fetal diaphyseal lengths from fresh to dry bone using Petersohn and Köhler's data. J Forensic Sci 1998;43:423–426.
45. Huxley AK, Kósa F. Calculation of percent shrinkage in human fetal diaphyseal lengths from fresh bone to carbonized and calcined bone using Petersohn and Köhler's data. J Forensic Sci 1999;44:577–583.
46. Sinclair D. Human growth after birth. 3rd ed. London: Oxford University Press, 1978.
47. Anderson M, Green WT. Lengths of the femur and tibia: norms derived from orthoentgenograms of children from five years of age until epiphyseal closure. Am J Dis Child 1948;75:279–290.
48. Anderson M, Green WT, Messner MB. Growth and predictions of growth in the lower extremities. J Bone Joint Surg 1963;45:1–14.
49. Anderson M, Messner MB, Green WT. Distribution of lengths of the normal femur and tibia in children from one to eighteen years of age. J Bone Joint Surg 1964;46:1197–1202.
50. Francis CC. Growth of the human tibia. Am J Phys Anthropol 1939;25:323–331.
51. Ghantus M. Growth of the shaft of the human radius and ulna during the first two years of life. Am J Roentgenol 1951;65:784–786.
52. Gindhart PS. Growth standards for the tibia and radius in children aged one month through eighteen years. Am J Phys Anthropol 1973;39:41–48.
53. Hoffman JM. Age estimations from diaphyseal lengths: two months to twelve years. J Forensic Sci 1979;24:461–469.
54. Hoppa RD. Evaluating human skeletal growth: an Anglo-Saxon example. Int J Osteoarchaeol 1992;2:275–288.
55. Hoppa RD, Gruspier KL. Estimating diaphyseal length from fragmentary subadult skeletal remains: implications for paleodemographic reconstructions of a southern Ontario ossuary. Am J Phys Anthropol 1996;100:341–345.
56. Johnston FE. Growth of long bones of infants and young children at Indian Knoll. Am J Phys Anthropol 1962;20:249–254.
57. Merchant VL, Ubelaker DH. Skeletal growth of the Protohistoric Arikara. Am J Phys Anthropol 1977;46:61–72.
58. Miles AEW, Bulman JS. Growth curves of immature bones from a Scottish island population of sixteenth to mid-nineteenth century: limb-bone diaphyses and some bones of the hand and foot. Int J Osteoarchaeol 1994;4:121–136.
59. Stewart TD. Identification by the skeletal structures. In: Gradwohl's Legal Medicine. 2nd ed. Camps, FE, ed. Bristol: Wright, 1968, pp. 123–154.
60. Steyn M, Henneberg M. Skeletal growth of children from the Iron Age site at K2 (South Africa). Am J Phys Anthropol 1996;100:389–396.
61. Sundick RI. Human skeletal growth and dental development as observed in the Indian Knoll population. PhD dissertation. University of Toronto, 1972.
62. Sundick RI. Human skeletal growth and age determination. Homo 1979;29:228–249.
63. Walker PL. The linear growth of long bones in Late Woodland Indian children: proceedings of the Indiana Academy of Science 1969;78:83–87.
64. Hunt EE, Hatch JW. The estimation of age at death and ages of formation of transverse lines from measurements of human long bones. Am J Phys Anthropol 1981;54:461–469.
65. Humphrey LT. Growth patterns in the modern human skeleton. Am J Phys Anthropol 1998; 105:57–72.
66. Anderson M, Blais M, Green WT. Growth of the normal foot during childhood and adolescence: length of the foot and interrelations of foot, stature and lower extremity as seen in serial records of children between 1–18 years of age. Am J Phys Anthropol 1956;14:287–308.
67. Blais MM, Green WT, Anderson M. Lengths of the growing foot. J Bone Joint Surg 1956;38: 998–1000.

68. Davenport CB. The growth of the human foot. Am J Phys Anthropol 1932;17:167–211.
69. Hill LM. Changes in the proportions of the female foot during growth. Am J Phys Anthropol 1958;16:349–366.
70. Mercer BM, Sklar S, Shariatmadar A, Gillieson MS, D'Alton ME. Fetal foot length as a predictor of gestational age. Am J Obstet Gynecol 1987;156:350–355.
71. Meredith HV. Human foot length from embryo to adult. Hum Biol 1944;16:207–282.
72. Eveleth PB, Tanner JM. Worldwide variation in human growth. 2nd ed. Cambridge: Cambridge University Press, 1990.
73. Blechschmidt E. The early stages of human limb development. In: Limb development and deformity: problems of evaluation and rehabilitation. Swinyard CA, ed. Springfield: Charles. C. Thomas, 1969, pp. 24–56.
74. Burkus JK, Ogden JA. Development of the distal femoral epiphysis: a microscopic morphological investigation of the Zone of Ranvier. J Pediatr Orthop 1984;4:661–668.
75. Davies DA, Parsons FG. The age order of the appearance and union of the normal epiphyses as seen by x-rays. J Anat 1927;62:58–71.
76. Flecker H. Roentgenographic observations of the times of appearance of epiphyses and their fusion with the diaphyses. J Anat 1932–1933;67:118–164.
77. Menees TO, Holly LE. The ossification in the extremities of the new-born. Am J Roentgenol 1932;28:389–390.
78. Roche AF, Sunderland S. Multiple ossification centres in the epiphyses of the long bones of the human hand and foot. J Bone Joint Surg 1959;41:375–383.
79. Siegling JA. Growth of the epiphyses. J Bone Joint Surg 1941;23:23–36.
80. Love SM, Ganey T, Ogden JA. Postnatal epiphyseal development: the distal tibia and fibula. J Pediatr Orthop 1990;10:298–305.
81. Paterson RS. A radiological investigation of the epiphyses of the long bones. J Anat 1929;64:28–46.
82. Acheson RM. The Oxford method of assessing skeletal maturity. Clin Orthop Relat R 1957;10:19–39.
83. Adair FL, Scammon RE. A study of the ossification centers of the wrist, knee, and ankle at birth, with particular reference to the physical development and maturity of the newborn. Am J Obstet Gynecol 1921;2:35–60.
84. Bagnall KM, Harris PF, Jones PRM. A radiographic study of the longitudinal growth of primary ossification centers in limb long bones of the human fetus. Anat Rec 1982;203:293–299.
85. Camp JD, Cilley EIL. Diagrammatic chart showing time of appearance of the various centers of ossification and period of union. Am J Roentgenol 1931;26:905.
86. Christie A. Prevalence and distribution of ossification centers in the newborn infant. Am J Dis Child 1949;77:355–361.
87. Ellis FG, Joseph J. Time of appearance of the centres of ossification of the fibular epiphyses. J Anat 1954;88:533–536.
88. Francis CC. The appearance of centers of ossification from 6 to 15 years. Am J Phys Anthropol 1940;27:127–138.
89. Francis CC, Werle PP. The appearance of centers of ossification from birth to five years. Am J Phys Anthropol 1939;24:273–299.
90. Gardner E, Gray DJ, O'Rahilly, R. Prenatal development of the skeleton and joints of the human foot. J Bone Joint Surg 1959;41:847–876.
91. Girdany BR, Golden R. Centers of ossification of the skeleton. Am J Roentgenol 1952;68:922–924.
92. Hansman CF. Appearance and fusion of ossification centers in the human skeleton. Am J Roentgenol 1962;88:476–482.
93. Harding VSV. A method of evaluating osseous development from birth to 14 years. Child Dev 1952;23:247–271.
94. Harding VV. Time schedule for the appearance and fusion of a second accessory center of ossification of the calcaneus. Child Dev 1952;23:181–184.

95. Hill AH. Fetal age assessment by centers of ossification. Am J Phys Anthropol 1939;24:251–272.
96. Kelly HJ, Reynolds L. Appearance and growth of ossification centers and increases in the body dimensions of White and Negro infants. Am J Roentgenol 1947;57:477–516.
97. Kjar I. Skeletal maturation of the human fetus assessed radiographically on the basis of ossification sequences in the hand and foot. Am J Phys Anthropol 1974;40:257–276.
98. Mall FP. On ossification centers in human embryos less than one hundred days old. Am J Anat 1906;5:433–458.
99. Meyer DB, O'Rahilly R. Multiple techniques in the study of the onset of prenatal ossification. Anat Rec 1958;132:181–193.
100. Meyer DB, O'Rahilly R. The onset of ossification in the human calcaneus. Anat Embryol 1976; 150:19–33.
101. O'Rahilly R. The human foot. Part 1: Prenatal development. In: Foot disorders: medical and surgical management, 2nd ed. Giannestras NJ, ed. Philadelphia: Lea and Febiger, 1973, pp. 16–23.
102. O'Rahilly R, Meyer DB. Roentgenographic investigation of the human skeleton during early fetal life. Am J Roentgenol 1956;76:455–468.
103. O'Rahilly R, Gardner E, Gray DJ. The skeletal development of the foot. Clin Orthop Relat R 1960; 16:7–14.
104. Pryor JW. Roentgenographic investigation of the time element in ossification. Am J Roentgenol 1933;28:798–804.
105. Pyle I, Sontag LW. Variability in onset of ossification in epiphyses and short bones of the extremities. Am J Roentgenol 1943;49:795–798.
106. Roche AF. Epiphyseal ossification and shaft elongation in human metatarsal bones. Anat Rec 1964;149:449–451.
107. Sawtell RO. Ossification and growth of children from one to eight years of age. Am J Dis Child 1929;37:61–87.
108. Selby S. Separate centers of ossification of the tip of the internal malleolus. Am J Roentgenol 1961;86:496–501.
109. Sontag LW, Snell D, Anderson M. Rate of appearance of ossification centers from birth to the age of five years. Am J Dis Child 1939;58:949–956.
110. Walmsley R. The development of the patella. J Anat 1940;74:360–368.
111. Pryor JW. Difference in the ossification of the male and female skeleton. J Anat 1927–1928; 62:499–506.
112. Noback CR, Robertson GG. Sequences of appearance of ossification centers in the human skeleton during the first five prenatal months. Am J Anat 1951;89:1–28.
113. Kraus BS. Sequence of appearance of primary centers of ossification in the human foot. Am J Anat 1961;109:103–115.
114. O'Rahilly R, Gardner E. The initial appearance of ossification in staged human embryos. Am J Anat 1972;134:291–301.
115. Dvonch VM, Bunch WH. Pattern of closure of the proximal femoral and tibial epiphyses in man. J Pediatr Orthop 1983;3:498–501.
116. Lewis AB, Garn SM. The relationship between tooth formation and other maturational factors. Angle Orthod 1960;30:70–77.
117. Krogman WM. The human skeleton in forensic medicine. 2nd ed. Springfield: Charles C. Thomas, 1962.
118. Pyle SI, Hoerr NL. Radiographic atlas of skeletal development of the knee. Springfield: Charles C. Thomas, 1955.
119. Hoerr NL, Pyle SI, Francis CC. Radiographic atlas of skeletal development of the foot and ankle. Springfield: Charles C. Thomas, 1962.
120. McKern TW, Stewart TD. Skeletal age changes in young American males. Natick, Mass: Headquarters, Quartermaster Research, and Development Command Technical Report EP-45, 1957.

121. Colwell HA. Case showing abnormal epiphyses of metatarsals and first metacarpals. J Anat 1927; 62:183.
122. Posener K, Walker E, Weddell G. Radiographic studies of the metacarpal and metatarsal bones in children. J Anat 1939;74:76–79.
123. Cundy P, Paterson D, Morris L, Foster B. Skeletal age estimation in leg length discrepancy. J Pediatr Orthop 1988;8:513–515.
124. Osborne D, Effmann E, Broda K, Harrelson J. The development of the upper end of the femur, with special reference to its internal architecture. Radiology 1980;137:71–76.
125. Robling AG, Stout SD. Histomorphometry of human cortical bone: applications to age estimation. In: Biological anthropology of the human skeleton. Katzenberg MA, Saunders SR, eds. New York: Wiley-Liss, 2000, pp. 187–213.
126. Strandh J, Diffang CH, Saldeen T. Age determination of bone tissue by microscopical studies on microradiograms of thin saw-cut slices from femur. Swed Soc Forensic Med 1972;1:116.
127. Ubelaker DH. Estimation of age at death from histology of human bone. In: Dating and age determination of biological materials. Zimmerman MR, Angel JL, eds. London: Croom Helm, 1986, pp. 240–247.
128. Ubelaker DH. The evolving role of the microscope in forensic anthropology. In: Forensic osteology: advances in the identification of human remains. 2nd ed. Reichs KJ, ed. Springfield: Charles C. Thomas, 1998, pp. 514–532.
129. Garn SM, Schwager PM. Age dynamics of persistent traverse lines in the tibia. Am J Phys Anthropol 1967;27:375–378.
130. Kerley ER. The microscopic determination of age in human bone. Am J Phys Anthrop 1965;23:149–163.
131. Kerley ER. Estimation of skeletal age: after about age thirty. In: Personal identification in mass disasters. Stewart TD, ed. Washington, DC: National Museum of Natural History, Smithsonian Institution, 1970, pp. 57–70.
132. Kerley ER, Ubelaker DH. Revisions in the microscopic method of estimating age at death in human cortical bone. Am J Phys Anthropol 1978;49:545–546.
133. Saunders SR. Growth remodeling of the human femur. Can Rev Phys Anthropol 1987; :20–30.
134. Ahlqvist J, Damsten O. A modification of Kerley's method for the microscopic determination of age in human bone. J Forensic Sci 1969;14:205–212.
135. Bouvier M, Ubelaker DH. A comparison of two methods for the microscopic determination of age at death. Am J Phys Anthropol 1977;46:391–394.
136. Singh IJ, Gunberg DL. Estimation of age at death in human males from quantitative histology of bone fragments. Am J Phys Anthropol 1970;33:373–381.
137. Thompson DD. The core technique in the determination of age at death in skeletons. J Forensic Sci 1979;24:902–915.
138. Watanabe Y, Konishi M, Shimada M, Ohara H, Iwamoto, S. Estimation of age from the femur of Japanese cadavers. Forensic Sci Int 1998;98:55–65.
139. Walker RA, Lovejoy CO, Meindl RS. Histomorphological and geometric proportions of human femoral cortex in individuals over 50: implications for histomorphological determination of age at death. Am J Hum Biol 1994;6:659–667.
140. Baccino E, Ubelaker DH, Hayek LC, Zerilli A. Evaluation of seven methods of estimating age at death from mature human skeletal remains. J Forensic Sci 1999;44:931–936.
141. Hansen G. Die altersbestimmung am proximalen humerus-und femurende in rahmen der identifizierung menschlicher skelettreste. Wissenschaftliche Zeitschrift der Humboldt–Universität zu Berlin, Mathematish–Naturwissenschaftliche Reihe 1953;3:1–73.
142. Walker RA, Lovejoy CO. Radiographic changes in the clavicle and proximal femur and their use in the determination of skeletal age at death. Am J Phys Anthropol 1985;68:67–78.
143. Ruff CB, Jones HH. Bilateral asymmetry in cortical bone of the humerus and tibia—sex and age factors. Hum Biol 1981;53:69–86.

144. Atkinson PJ, Weatherell JA. Variation in the density of the femoral diaphysis with age. J Bone Joint Surg 1967;49:781–788.
145. Ohtani S, Matsushima Y, Kobayashi Y, Kishi K. Evaluation of aspartic acid racemization ratios in the human femur for age estimation. J Forensic Sci 1998;43:949–953.
146. Jackes M. Building the bases for paleodemographic analysis: adult age determination. In: Biological anthropology of the human skeleton. Katzenberg MA, Saunders SR, eds. New York: Wiley-Liss, 2000, pp. 417–466.
147. Saunders SR, Fitzgerald C, Rogers T, Dudar C, McKillop H. A test of several methods of skeletal age estimation using a documented archaeological sample. Can Soc Forensic Sci J 1992;25:97–118.

Chapter 6

Radiology of the Lower Extremity

B. G. Brogdon, MD

1. Introduction and Historical Review

1.1. Introduction

While the field of forensic medicine is said to have begun at some indefinite time five or six centuries ago, the origins of forensic radiology can be described more precisely. Wilhem Conrad Röntgen (Fig. 1)—professor of physics, director of the Physics Institute, and Rector of the University of Würzburg—observed an unusual phenomenon while experimenting with cathode ray tubes on November 8, 1895. After 50 d of intensive investigation, he determined that he had discovered a new kind of ray ("eine neue Arte von Strahlen"), one that could penetrate solid, opaque materials and produce photographic representations of their contents. He called them "X-rays" because "x" was the symbol of the unknown. A manuscript was produced and immediately accepted for presentation at the January 23, 1896, meeting of the Würzburg Physical Medicine Society *(1)*. As sometimes happens today, word of his findings were "leaked" to the popular press and flashed by telegraph and cable throughout the electrified world, reaching New York on January 8, 1896 *(2)*. The potential for applying this new ray to the task of forensic problem solving was recognized almost immediately.

Professor Arthur William Wright, director of the Sloan Physics Laboratory at Yale University, is accorded primacy in the production of X-ray images (of inanimate objects) in the United States on January 28, 1896. A few days later, he bought a rabbit at a market and exposed the carcass to an X-ray beam for an hour. Examination of the photographic plate revealed lead shot within the body *(3)*. Professor Wright had, for the first time, established a cause of death through radiography—put another way, by forensic radiology!

In consonance with the purpose of this book, we will attempt a chronology of early forensic applications of radiology limited to the lower extremity.

From: *Forensic Science and Medicine*
Forensic Medicine of the Lower Extremity: Human Identification and Trauma Analysis of the Thigh, Leg, and Foot
Edited by: J. Rich, D. E. Dean, and R. H. Powers © The Humana Press Inc., Totowa, NJ

Fig. 1. WC Röntgen, MD: the discoverer of X-rays.

1.2. A Chronology of Early Forensic Radiology of the Lower Extremity

On a cold Christmas Eve in Montreal, George Holden shot Tolson Cunning in the leg. The wound healed, but the injured limb remained symptomatic. His surgeon, Dr. R. C. Kirkpatrick, requested an X-ray photograph of the area to be taken by Professor John Cox of the Physics Department at McGill University. This was accomplished on February 7, 1896 and showed the bullet lodged between the tibia and fibula (Fig. 2). This image was submitted to the court during Mr. Holden's trial for attempted murder. Successful prosecution resulted in a sentence of 14 yr in the penitentiary *(3–5)*.

In England, during September 1895, a burlesque and comedic actress known to us now only as Miss Folliott fell on the steps leading to her dressing room in the Nottingham Theater. Her foot injury kept her bedfast for a month, after which she was still unable to tread the boards. Dr. Frankish sent her to University College Hospital, where both feet were "photographed" by X-rays (perhaps the first comparison of films?) and the films demonstrated that the left cuboid clearly was displaced. This finding could be appreciated by both judge and jury when the negatives were displayed in court. The conviction of the theater owners for maintaining an unsafe workplace was somewhat

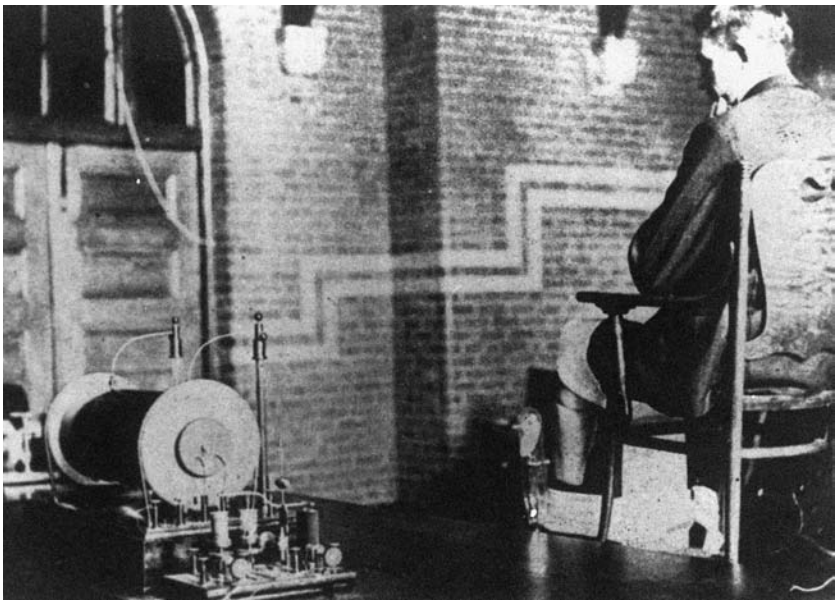

Fig. 2. The X-ray examination of Tolson Cunning's leg took place on February 7, 1896 and resulted in the first X-ray plate to be admitted to a court in North America. From the American College of Radiology Archives, with permission.

mitigated by the charge that Miss Folliott was guilty of contributory carelessness *(4,6)*. Because this case was commented on in British publications as early as April 1896 *(7)*, the actual radiography must be almost contemporaneous with the Holden case.

On September 2, 1895, Frank B. Bolling was thrown from his buggy "while driving a fractious horse" on the streets of Chicago and sustained a fracture of his right ankle. The fracture was set by two surgeons, and Mr. Bolling was able to return to work by May 1, 1896, but his ankle still hurt. To evaluate this persistent pain, Dr. Otto L. Smith and Professor W. C. Fuchs examined the offending ankle with 35 to 40 min of exposure to an X-ray tube placed just 5 in. from the ankle. Subsequent radiation damage and pain led to an amputation in November 1896 and two more amputations later because of pain and recurrent infections. Bolling filed the first malpractice suit for radiation damage and was awarded $10,000 *(4,8)*. (Images of the initial injury—the fractures—were not submitted to the court.)

The first trial in which X-ray evidence was accepted by a United States Court took place in Denver in the waning months of 1896 *(4,8–10)*. The case began on June 15, 1895, when James Smith fell from a ladder while pruning a tree and injured his hip. Perhaps for pecuniary reasons, he waited almost a month before soliciting the professional services of Dr. W. W. Grant, who was widely known and well respected and a founder of the American College of Surgeons. He is credited with performing the first appendectomy in the United States, in 22-yr-old Mary Gartside *(11)*.

Dr. Grant found no evidence of a fracture and did not restrict Mr. Smith's activity, but requested that he return in 1 wk. The diagnosis of "no fracture" was again asserted. Dr. Grant heard no more about Mr. Smith until April 1896, when the poorly paid law clerk

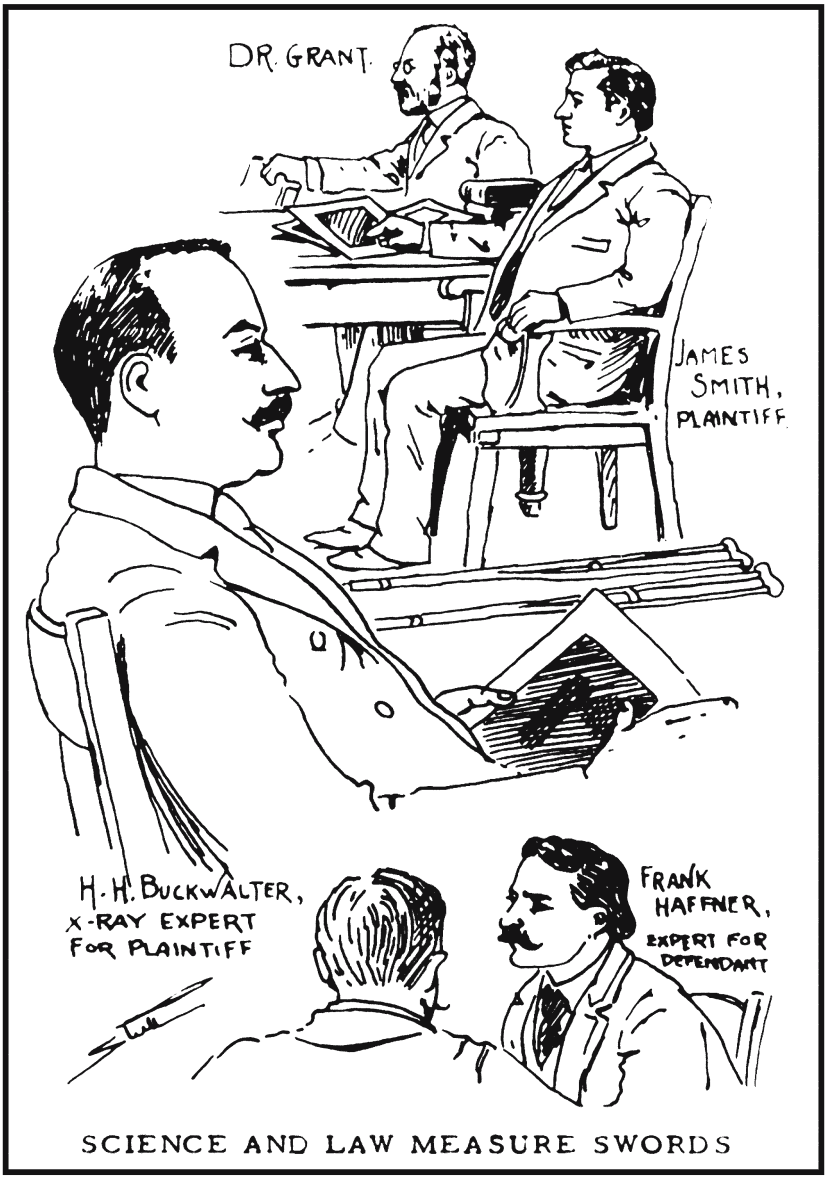

Fig. 3. Some of the principles and witnesses in *Smith v. Grant* illustrated in the *Daily News,* December 3, 1896. Reprinted from ref. *8* with permission from Charles C. Thomas.

engaged two of the best young lawyers in Colorado to file a $10,000 civil action against Dr. Grant, claiming limb shortening and disability as a result of his failure to diagnose a femoral fracture (Fig. 3). Quick to take advantage of new technology, these bright young attorneys had engaged the services of Dr. Chauncey Tennent Jr, MD, of Denver Homeopathic College and a local photojournalist, Harry H. Buchwalter, to examine their client with X-rays (Fig. 4). On four occasions between November 7 and 29, 1896, several

Fig. 4. Chauncey Tennant, MD, (right) and HH Buckwalter (left) made the first clinical radiograph in Colorado in the spring of 1896. The patient, Marshal Kehler, had been shot by a miner. Tennant and Buckwalter later performed the radiography on Mr. Smith's broken femur, the first X-ray admitted into evidence in the United States. Reprinted from ref. *9* with permission from the American Roentgen Ray Society.

attempts to obtain an image of Mr. Smith's hip (with exposures ranging up to 80 min) were finally successful in showing the outlines of an impacted fracture of the proximal femur. (It is not clear whether this was a femoral neck fracture or an intertrochanteric fracture.)

The fundamental legal issue was admission of a radiograph as evidence. Photographs were already recognized for their ability to show something a witness could testify to as an accurate representation of what had actually been seen. The X-ray image revealed structures or objects hidden from the eye and had been refused admission in some jurisdictions, which felt that it was "like offering the photograph of a ghost." The argument raged all day before District Judge Owen E LeFuvre who, after sleeping on the matter, handed down his decision, eloquently phrased in the elegant language of those days:

> We... have been presented with a photograph taken by means of a new scientific discovery... it knocks for admission at the temple of learning. What shall be do or say? Close fast the door or open wide the portals? These photographs are offered in evidence to show the present condition of the head and neck of the femur bone, which is entirely hidden from the eye of the surgeon... Modern science has made it possible to look beneath the tissues of the human body, and has aided the surgeon in telling of the hidden mysteries. We believe it is our duty to be the first... in admitting in evidence a process known and acknowledged as a determinate science. The exhibits will be admitted in evidence.

The first appellate decision regarding the admission of radiographs as evidence in a US courtroom was rendered in 1897 *(4,12)*. It involved the case of Mr. Beall, who was in an elevator in the warehouse of WS Bruce and Company when it fell five stories. He sustained injuries to his leg and sued for compensation, claiming negligence in the construction and maintenance of the elevator. A witness, Dr. Saltman, testified that "overlapping bones of one of the plaintiff's legs, at the point where it was broken by this fall" were shown on a radiograph he was permitted to submit to the jury. The defense objected to admission of the radiograph and appealed. The Supreme Court of Tennessee ruled "...no sound reason was assigned at the bar why a civil court should not avail itself of this invention, when it is apparent that it would serve to throw light on the matter in controversy."

Dr. H. Graeme Anderson was one of the pioneer physicians assigned to the British Royal Flying Corps during World War I. He also became a licensed pilot, hence, one of the earliest flight surgeons. In his 1919 book, *The Medical and Surgical Aspects of Aviation (13)*, Dr. Anderson devoted several pages to 17 cases of injuries to the talus that had been sustained during aircraft accidents. He termed this generic injury "Aviator's Astralagus" and illustrated it with radiographs. This probably is the first recognition of "pattern injuries," of which more will be said later.

(It surely is worth mentioning that Dr. Anderson also reported that "Nemirovsky and Tilmant have lately organized an aeroplane...to carry a pilot, a surgeon, and a radiographer who can act as an assistant surgeon.... The elective current from the aeroplane can be used...to work the X-ray apparatus." Surely this is a first—and maybe the last—example of in-flight radiography. The author will welcome information about other examples).

Feet played an important role in solving the infamous Ruxton murder *(14,15)*. On September 15, 1935, the wife of a Dr. Ruxton and her nursemaid disappeared from the family home in Lancaster and were never again seen alive. Two weeks later, a discovery of human remains triggered a search that began in the surrounding area and continued for another month until most of two female bodies could be reassembled. However, the faces had been mutilated, the teeth extracted, the terminal digits of the hands amputated, and other distinguishing topographical features had been excised from soft tissues, all to preclude identification.

Three feet were recovered. Casts were made and fitted into the shoes of the missing women (Fig. 5). The presumptive left foot of Mrs. Ruxton was mutilated where she was known to have had a bunion and elsewhere (perhaps as a distraction), but a radiograph showed an exostosis of the first metatarsal head consistent with the bunion deformity (Fig. 6). Other identifying anatomic features were found, and this case featured an early use of the photographic superimposition of facial features on a skull. Incriminating evidence also was found in the Ruxton home. The doctor was convicted and hanged for the murders.

In 1946, Dr. John Caffey MD, (Fig. 7)—self-taught radiologist at New York's Babies Hospital (and the father of Pediatric Radiology)—published the first of several papers alerting the profession (and the public) to the peculiar concatenation of unusual skeletal injuries in the extremities of children that had often been associated with skull injuries, subdural hematomas, or both in the absence of any history of trauma *(16)*. This led to the now widespread recognition of the intentional physical abuse of children—perhaps radiology's greatest contribution to forensic medicine.

Fig. 5. Casts of the left feet of Mrs. Ruxton and her housekeeper. The tips of Mrs. Ruxton's toes have been amputated.

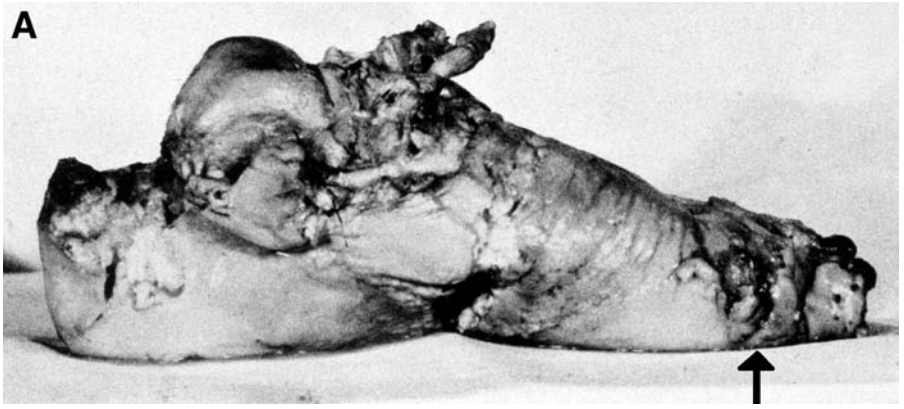

Fig. 6. **(A)** and **(B)**: Photographs of the top and medial side of Mrs. Ruxton's left foot show mutilations performed in an attempt to prevent identification. **(C)** Radiograph of Mrs. Ruxton's left foot showing amputated phalanges and hypertrophic changes on the head of the first metatarsal corresponding to the excised bunion.

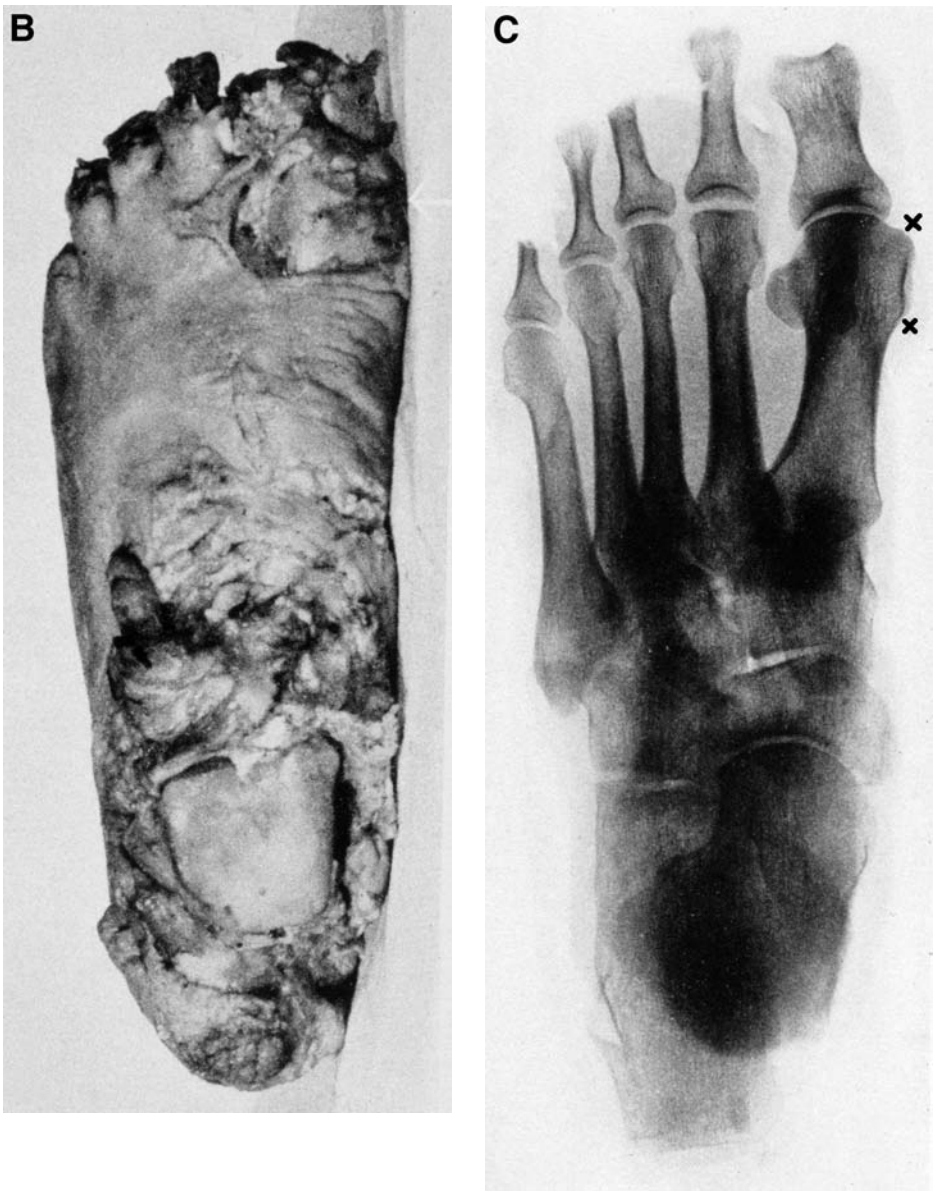

Fig. 6. *Continued.*

In 1949, the Great Lakes liner Noronic caught fire and burned in Toronto, with many fatalities. Dr. Arthur C Singleton, a professor and head of the Radiology Department at the University of Toronto, was asked by the Attorney General of Ontario to assist in the identification of the bodies, thus becoming the father of mass casualty radiology. He was able to positively identify 24 of 119 fatalities by radiologic comparison alone. One of the illustrations in his paper on the matter *(17)* showed comparison radiographs of a dismembered foot, noting similar features (Fig. 8).

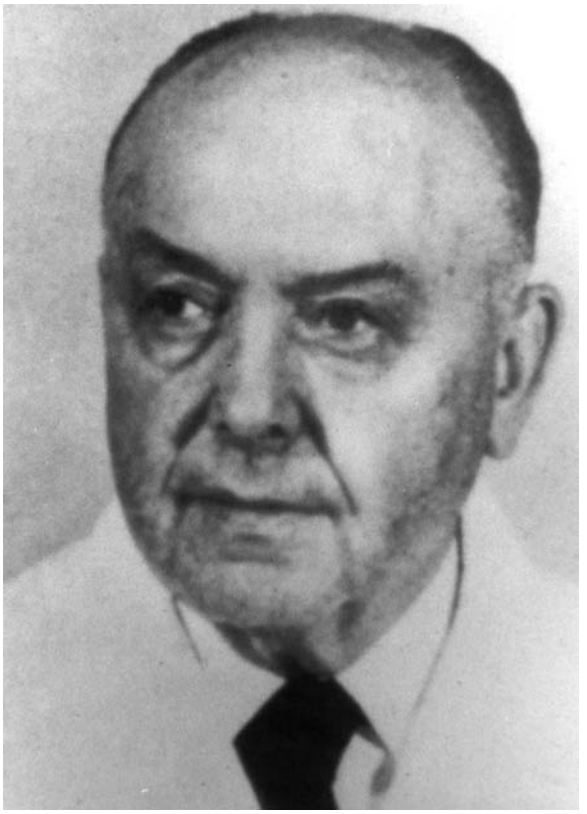

Fig. 7. John Caffey, MD, the father of pediatric radiology. From the American College of Radiology Archives, with permission.

In 1981, Evans and Knight's book, *Forensic Radiology,* became available to the English-speaking world *(18)*. It described applications of radiology for the purpose of identification and to identify evidence of abuse, mishaps, and malpractice, as well as for age determination and other anthropological conditions and correlation with forensic pathology, gunshot wounds, and other inflicted trauma. Unfortunately, of the more than 100 radiographs reproduced in this small but fairly comprehensive volume, only six were of the lower extremity.

In the ensuing quarter century, the utilization of radiology in the forensic sciences has increased and now includes some applications of newer modalities—nuclear radiology, ultrasonography, magnetic resonance imaging, and computed tomography (CT). Still, the great potential for radiology in forensics that was predicted by enthusiasts in the first couple of years after Röntgen's discovery remains largely unrealized *(19)*.

2. *Anthropological Considerations*

It was recognized early after Röntgen's discovery that the X-ray could greatly assist in the identification of human remains, especially those in which superficial identifying features were distorted or destroyed by fire, immersion, decomposition, mutilation, or

Fig. 8. (A) Antemortem and **(B)** postmortem radiographs of the foot of a victim of the Noronic disaster. Corresponding points were numbered by Dr. Singleton. Reprinted from ref. *17* with permission from the American Roentgen Ray Society.

fragmentation. The first step in the procedure is the establishment of certain anthropological parameters, sometimes called the "biologic profile": age, sex, stature, and race or population ancestry. When the body or its parts are skeletonized, or when there are time and available facilities to remove flesh from the remains, the physical anthropologist can do the job with equal or sometimes superior accuracy. Otherwise, the radiologic method must suffice. In either event, it is useful to radiograph the remains for purposes of subsequent comparison with antemortem examinations.

First, one must determine whether the remains are human or animal. Skeletal similarities (Fig. 9) can be confusing to the inexperienced viewer.

Next, it must be determined whether the remains are those of a single human or commingled with other humans or animals—a sometimes difficult and time-consuming task. Only then can a biologic profile be established. For the purposes of this discussion, it is assumed that human body parts from the lower extremities are being analyzed.

2.1. Age Determination

The radiologic determination of maturity or prematurity at birth is based on the ossification of secondary centers at the knee. The distal femoral epiphysis will be

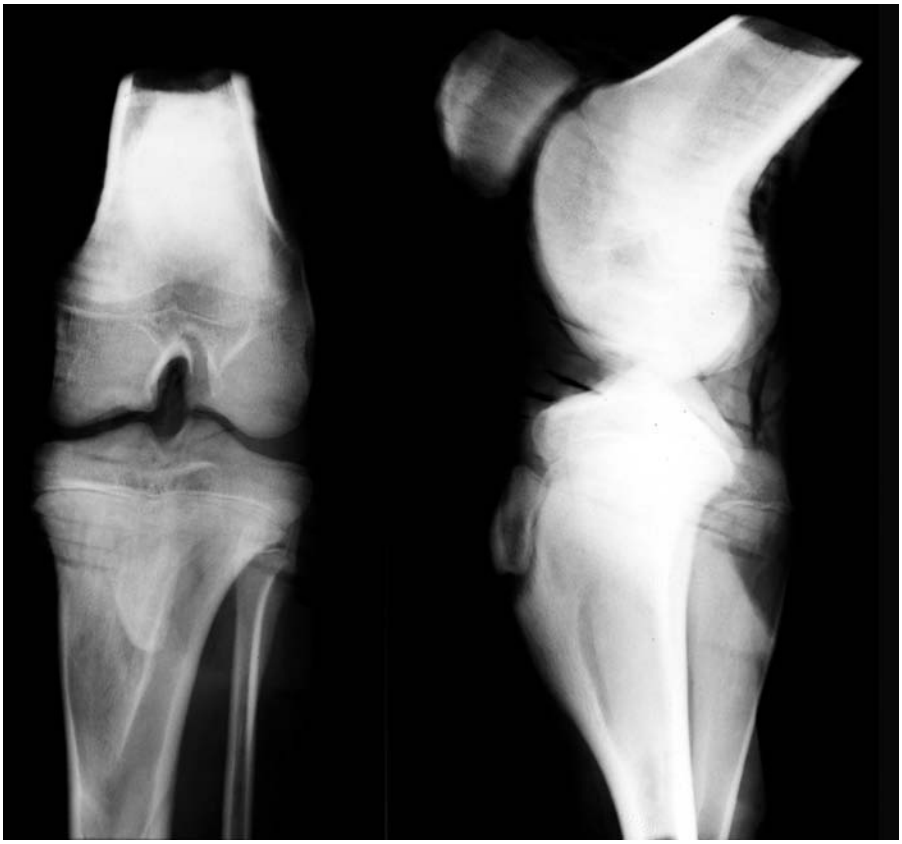

Fig. 9. Frontal and lateral views of a honey-baked ham.

partially ossified in 90% or more of full-term fetuses. The proximal tibial epiphysis will be similarly visible in 80% or more of mature neonates (Fig. 10). Thereafter, chronological age is estimated according to skeletal maturation, as indicated by the appearance, growth, and ultimate fusion of epiphyses and apophyses (non-articulating secondary ossification centers). Detailed tables and schematic representations of skeletal maturation are amply provided in the literature *(20–25)*. Some examples that are particularly useful in the lower extremity are included here (Table 1, Figs. 11, 12).

Between mid-adolescence and middle age, the fusion line of the physis gradually disappears, tendinous attachments may become more prominent, and degenerative change insidiously commences. Estimation of skeletal age by radiologic evaluation of the lower extremities during these decades is fraught with difficulty and inaccuracy.

The effects of advancing age become more apparent with advancing degenerative change and skeletal demineralization, but even then the use of radiology to estimate age may result of an error of a decade or so *(26)*.

2.2. Sex Determination

Skeletal maturation accelerates in females at a greater rate than in males after the third or fourth year of life. However, this difference is not a useful determinant.

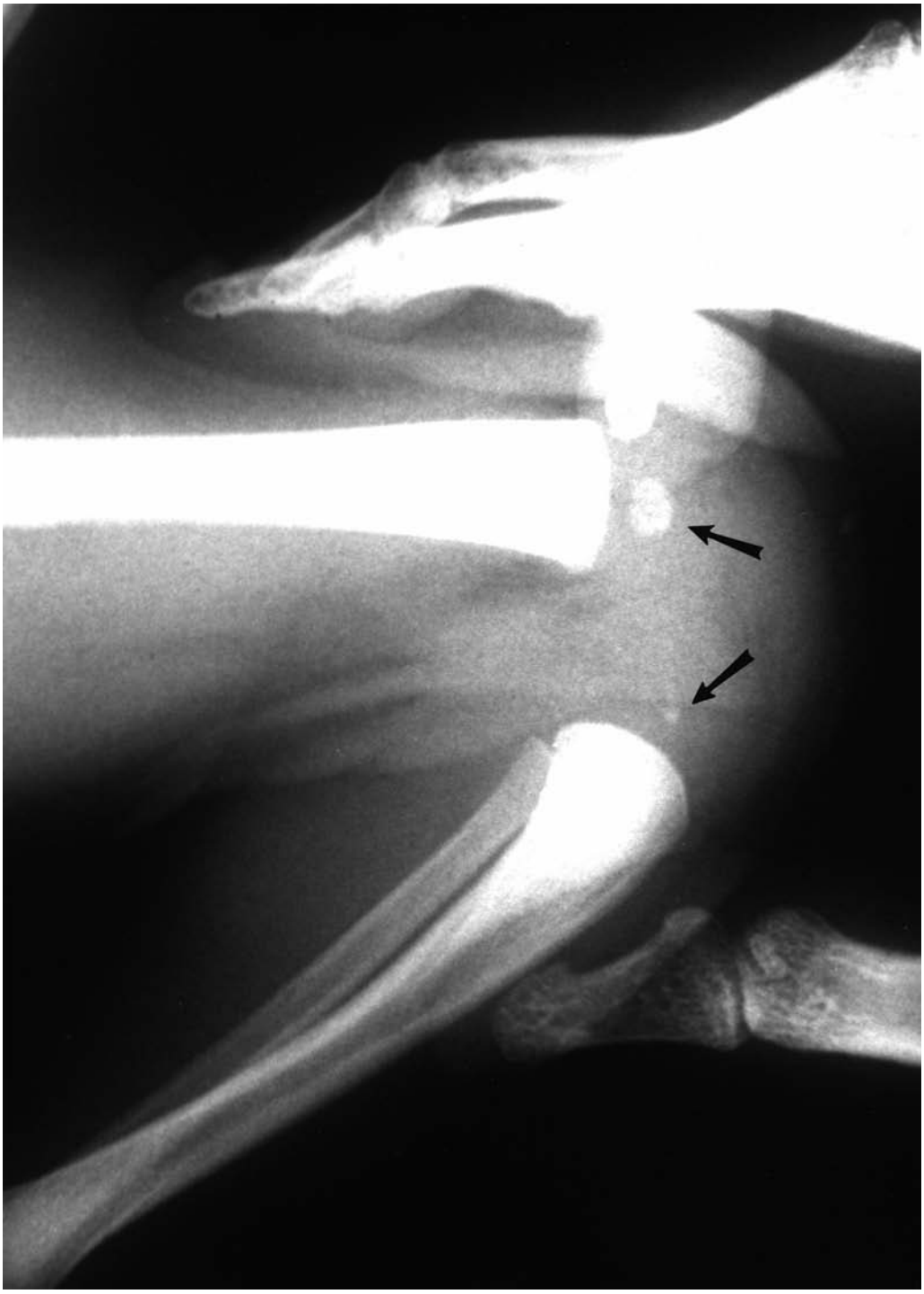

Fig. 10. Mature newborn knee showing calcified distal femoral and proximal tibial epiphyses. Reprinted from Brogdon, BG, Forensic radiology (1998) with permission from CRC Press.

Table 1
Percentiles for Age at Appearance (Years-Months) of Selected Ossification Centers

	Boys Percentile			Girls Percentile		
Centers	5th	50th	95th	5th	50th	95th
1. Tibia, proximal	–	0–0	0–1	–	0–0	0–0
2. Cuboid	–	0–1	0–4	–	0–1	0–2
3. Femur, head	**0–1**	**0–4**	**0–8**	**0–0**	**0–4**	**0–7**
4. Cuneiform 3	**0–1**	**0–6**	**1–7**	**–**	**0–3**	**1–3**
5. Toe phalanx 5 M	–	1–0	3–10	–	0–9	2–1
6. Toe phalanx 1 D	0–9	1–3	2–1	0–5	0–9	1–8
7. Toe phalanx 4 M	0–5	1–3	2–11	0–5	0–11	3–0
8. Toe phalanx 3 M	0–5	1–5	4–3	3–0	1–0	2–6
9. Toe phalanx 3 P	0–11	1–7	2–6	0–6	1–1	1–11
10. Toe phalanx 4 P	0–11	1–8	2–8	0–7	1–3	2–1
11. Toe phalanx 2 P	1–0	1–9	2–8	0–8	1–2	2–1
12. Toe phalanx 2 M	0–11	2–0	4–1	0–6	1–2	2–3
13. Cuneiform 1	**0–11**	**2–2**	**3–9**	**0–6**	**1–5**	**2–10**
14. Metatarsal 1	1–5	2–2	3–1	1–0	1–7	2–3
15. Toe phalanx 1 P	1–5	2–4	3–4	0–11	1–7	2–6
16. Toe phalanx 5 P	1–6	2–5	3–8	1–0	1–9	2–8
17. Cuneiform 2	**1–2**	**2–8**	**4–3**	**0–10**	**1–10**	**3–0**
18. Metatarsal 2	1–11	2–10	4–4	1–3	2–2	3–5
19. Femur, greater trochanter	1–11	3–0	4–4	1–0	1–10	3–0
20. Navicular foot	**1–1**	**3–0**	**5–5**	**0–9**	**1–11**	**3–7**
21. Fibular, proximal	**1–10**	**3–6**	**5–3**	**1–4**	**2–7**	**3–11**
22. Metatarsal 3	2–4	3–6	5–0	1–5	2–6	3–8
23. Toe phalanx 5 D	2–4	3–11	6–4	1–2	2–4	4–1
24. Patella	**2–7**	**4–0**	**6–0**	**1–6**	**2–6**	**4–0**
25. Metatarsal 4	**2–11**	**4–0**	**5–9**	**1–9**	**2–10**	**4–1**
26. Toe phalanx 3 D	3–0	4–4	6–2	1–4	2–9	4–1
27. Metatarsal 5	3–1	4–4	6–4	2–1	3–3	4–11
28. Toe phalanx 4 D	2–11	4–5	6–5	1–4	2–7	4–1
29. Toe phalanx 2 D	3–3	4–8	6–9	1–6	2–11	4–6
30. Calcaneal apophysis	**5–2**	**7–7**	**9–7**	**3–6**	**5–4**	**7–4**
31. Tibial tubercle	**9–11**	**11–10**	**13–5**	**7–11**	**10–3**	**11–10**

Note: P, proximal; M, middle; D, distal. Important events at various ages are in bold. Reprinted from ref. *20,* with permission from Elsevier.

In general, the male skeleton becomes more robust and heavier with aging and develops more prominent attachments for muscles and tendons. With further aging, there is a tendency for more degenerative hyperostotic changes in the male. Male long bones are approx 110% longer than their female counterparts. The male femoral head is larger. All of these findings are helpful but not definitive in establishing the sex of unidentified remains.

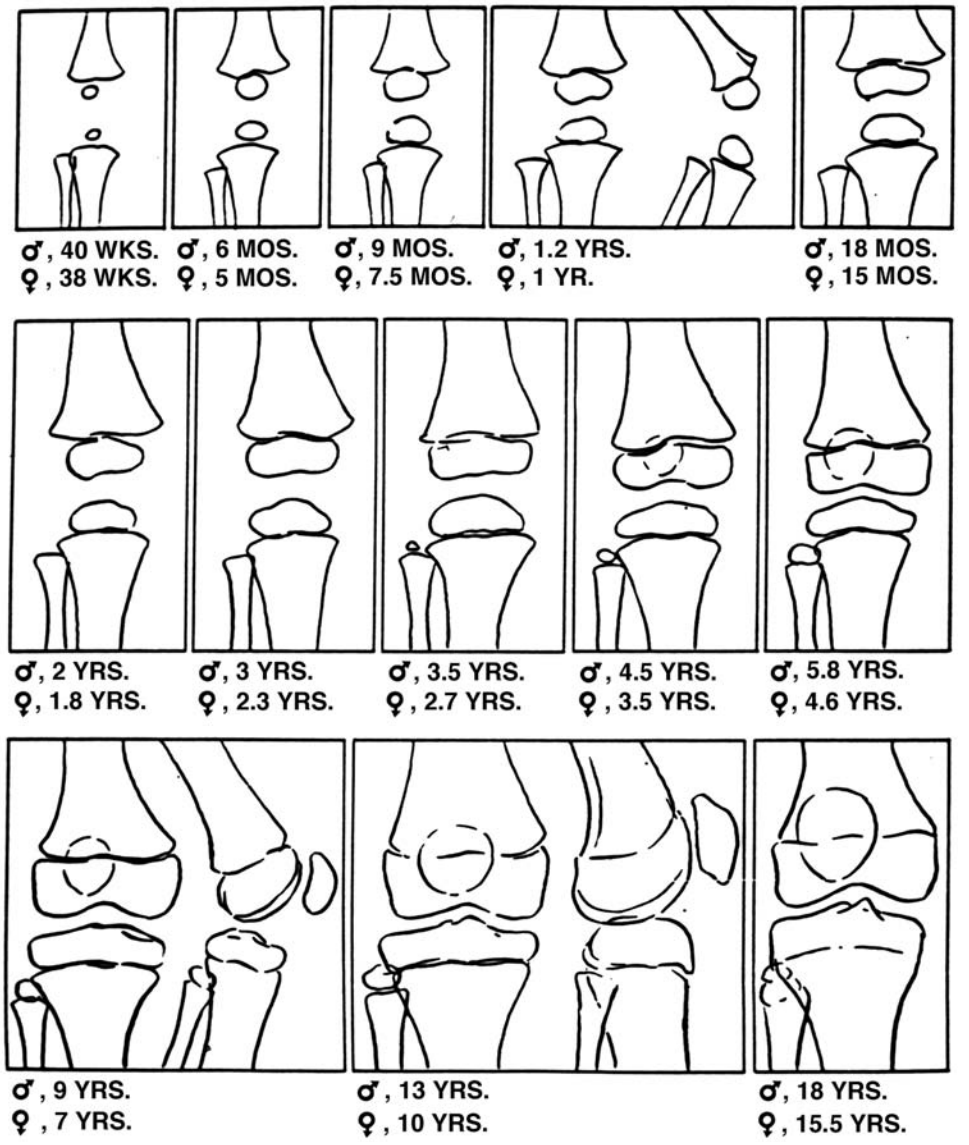

Fig. 11. Chronological development of the knee. Reprinted from ref. *25* with permission from Charles C. Thomas. Tracings reprinted from ref. *25* with permission from Elsevier.

Other parts of the skeleton are far more helpful than those of the extremities. Bipartite patella, an anatomical variant occurring in approx 2% of the adolescent population, is nine times more common in boys than in girls *(27)*.

In individuals of African ancestry, the tibia is long relative to the femur, but the ratios vary and overlap in US populations, probably due to racial mixing. The femoral shaft is bowed anteriorly in white and Asian populations compared with black populations; however, there is still considerable variability. However, a markedly bowed femur is unlikely to belong to a black decedent *(28)*.

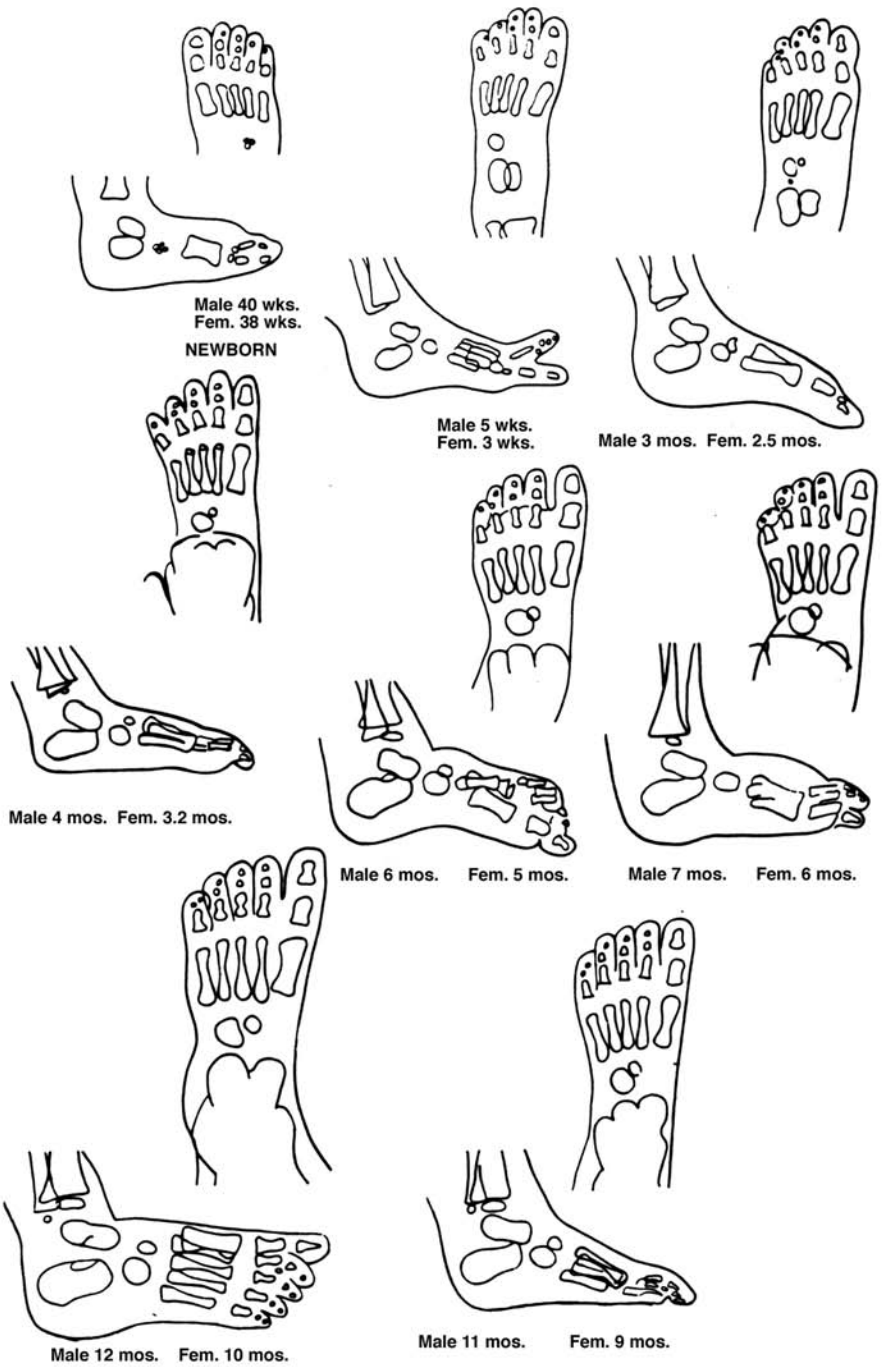

Fig. 12. Chronological development of the foot and ankle. Reprinted from ref. *26* with permission from Charles C. Thomas. Tracings reprinted from ref. *25* with permission from Elsevier.

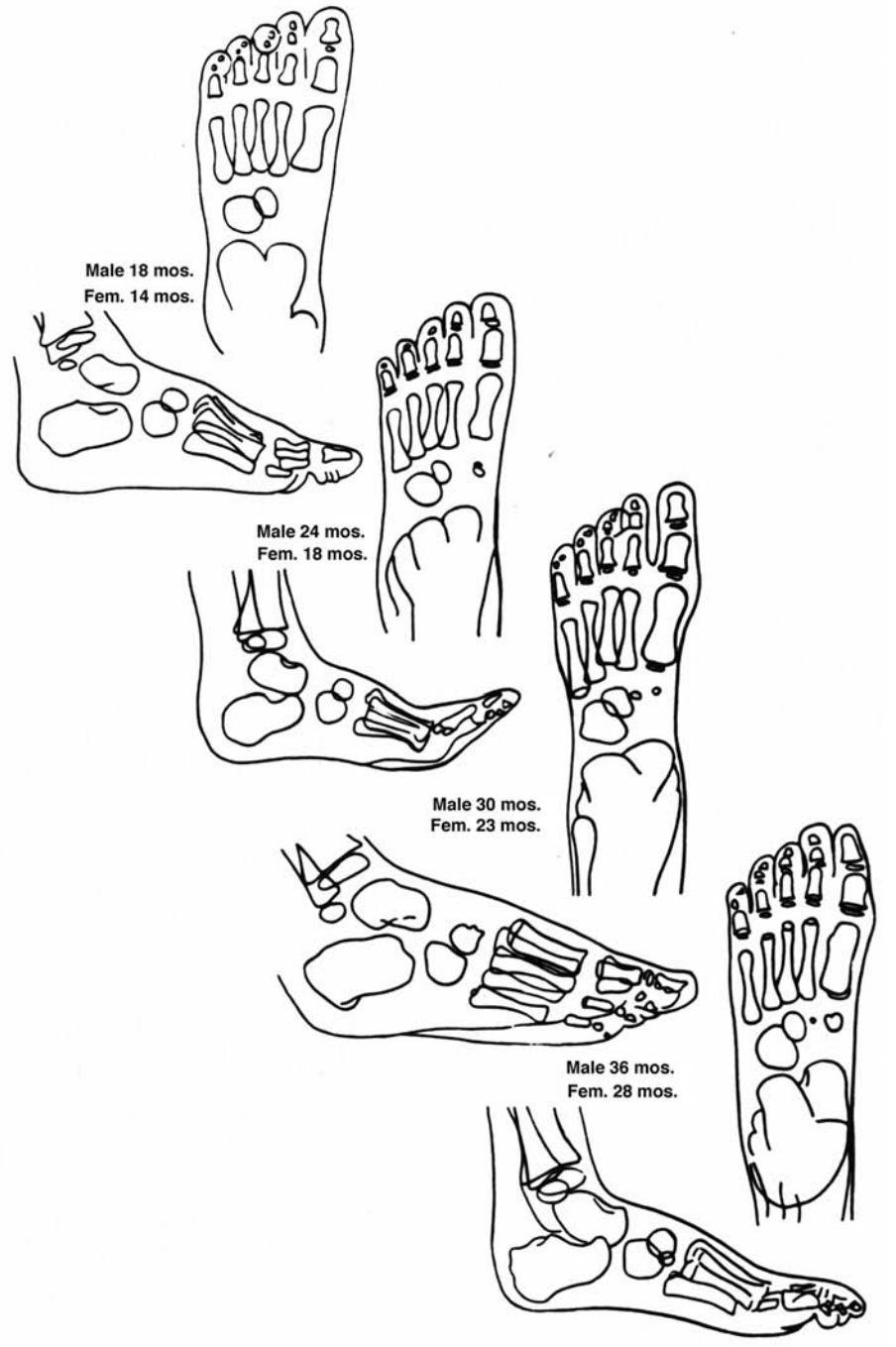

Fig. 12. *Continued.*

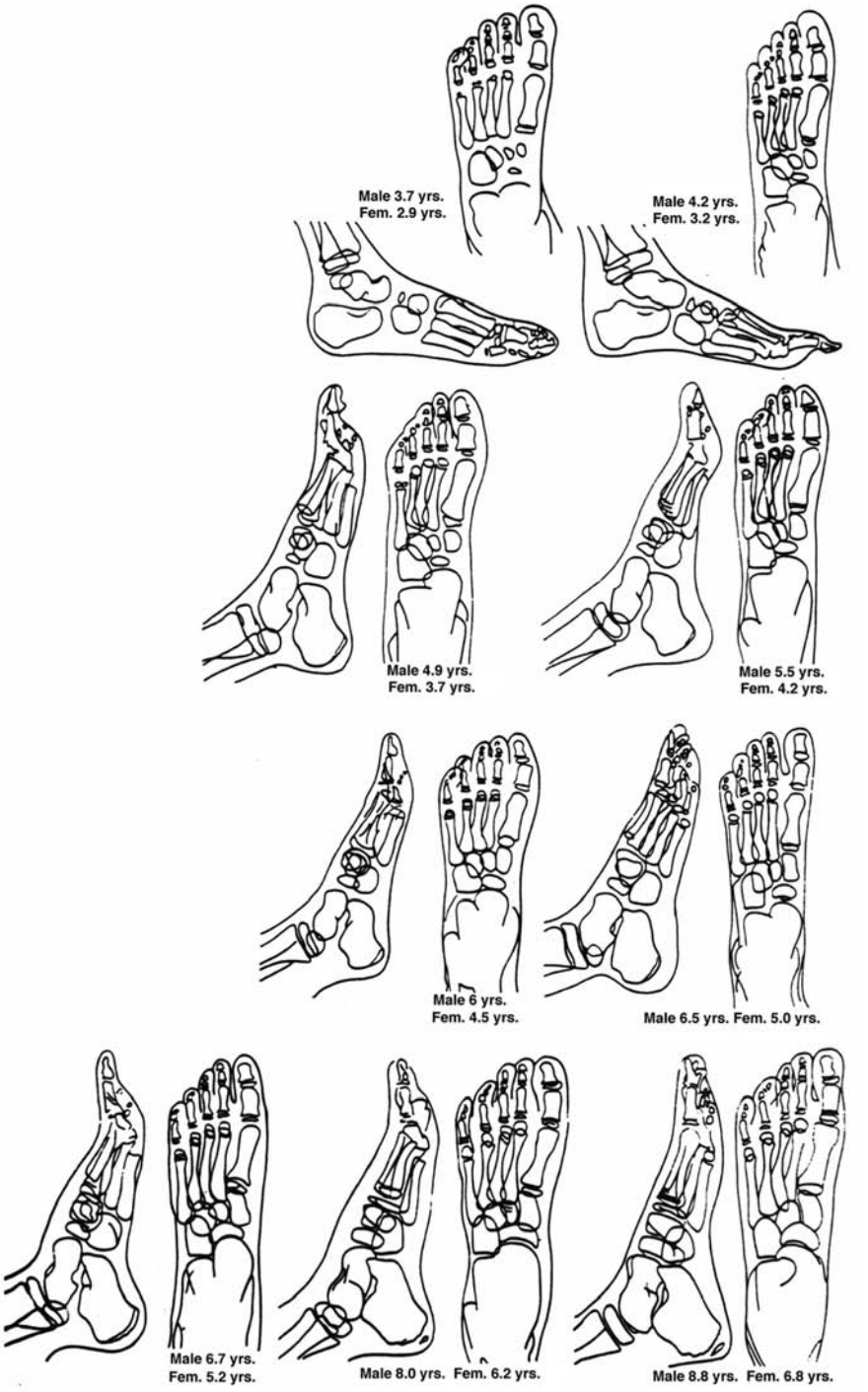

Fig. 12. *Continued.*

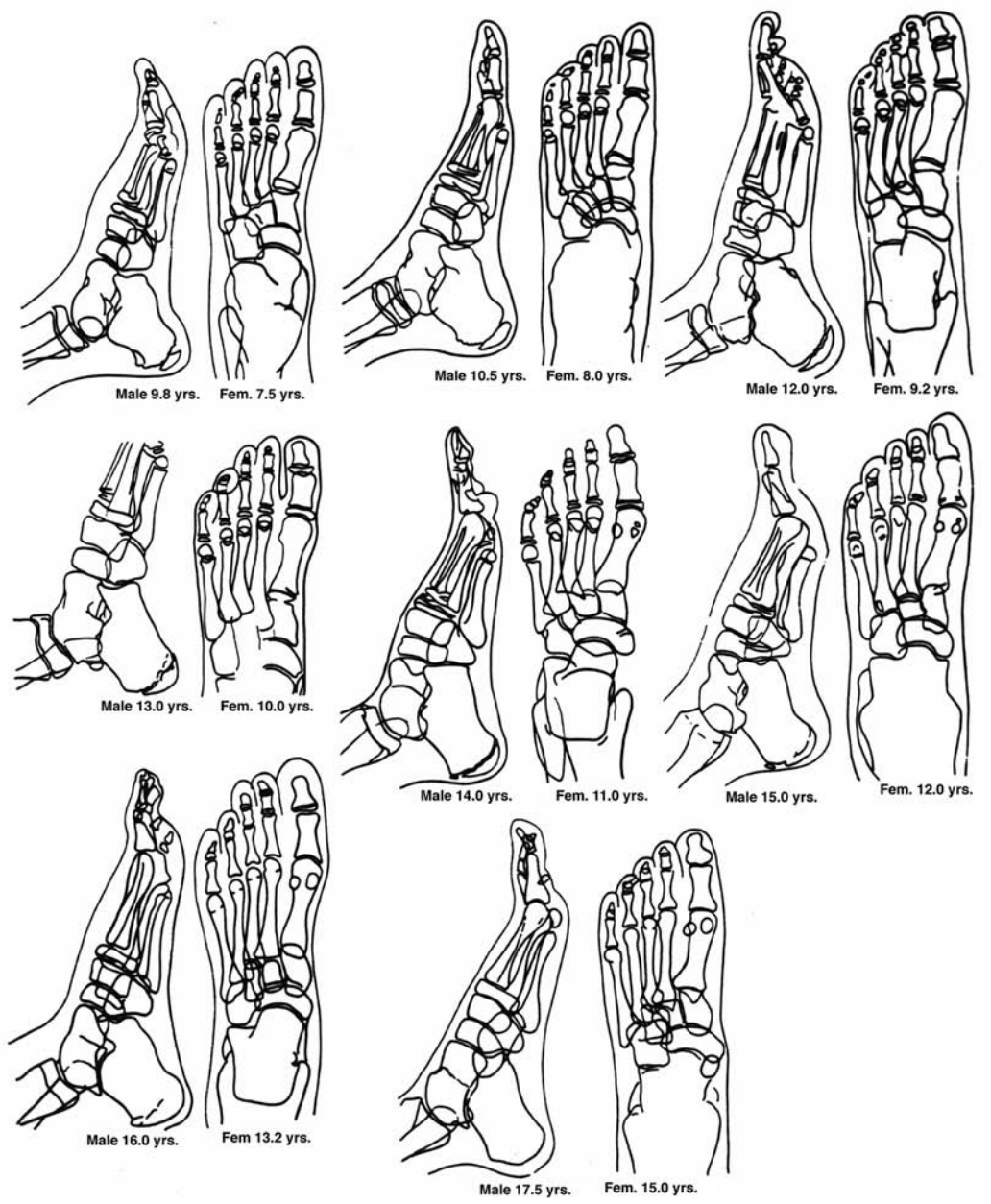

Fig. 12. *Continued.*

Craig *(29)* developed a method of determining race based on the angle of the intercondylar shelf on the femur that can be used with either skeletal or fleshed remains (Fig. 13). It requires radiography with true lateral positioning of the distal femur. The angle between the roof of the intercondylar notch (or intercondylar shelf) and the long axis of the femoral shaft are measured. Figure 14 shows the bimodal nature of the racial curves, indicating a fairly narrow overlap between the sectioning points. Thus, this may serve as a fairly useful determinant for assigning race or population ancestry.

Fig. 13. Lateral radiograph of the knee illustrating method of measuring the intercondylar shelf angle. Reprinted from Brogdon, BG, Forensic radiology (1998) with permission from CRC Press.

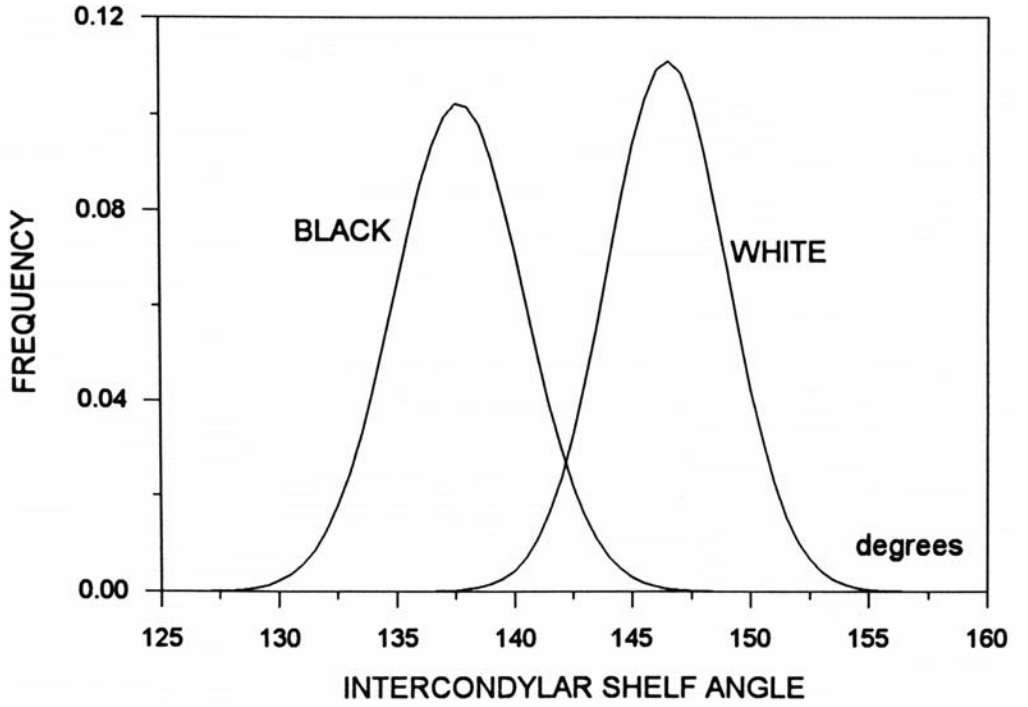

Fig. 14. Graphic representation of racial distribution of intercondylar shelf angles. Courtesy of Michael D Harpen, PhD. Reprinted from Brogdon, BG, Forensic radiology (1998) with permission from CRC Press.

Steinbach and Russell *(30)* suggested that a measurement of the soft tissue in the heel pad that exceeds 21 mm is a reasonably accurate indication of acromegaly (Fig. 15). However, the fallibility of this diagnostic indicator has been described by Puckett and Seymour *(31)*, who demonstrated a greater-than-"average" heel pad measurement in Blacks, 40% of whom had heel pads exceeding 21 mm compared with only 9% of Caucasians. Local soft-tissue swelling can skew this measurement even further. Hence, heel pad thickness is of doubtful value in the process of determining race or population ancestry in unidentified body parts.

2.3. Determination of Stature

Extensive research on World War II and Korean War casualties *(32)* has enabled investigators to develop methods of estimating stature based on measurements of long bones. The length of the femur is the most reliable basis for calculating stature *(28)*. The tibia is also useful, but there has been some controversy over the accuracy of tibial measurements, particularly the most appropriate location of the more distal measuring point. Apparently, the plafond of the tibia is the preferred site of measurement rather than the tip of the medial malleolus *(33)*. The tables and equations furnished to estimate stature from long-bone measurements are based on direct measurements of defleshed or skeletonized specimens (Table 2). However, measurements from radiographs can be

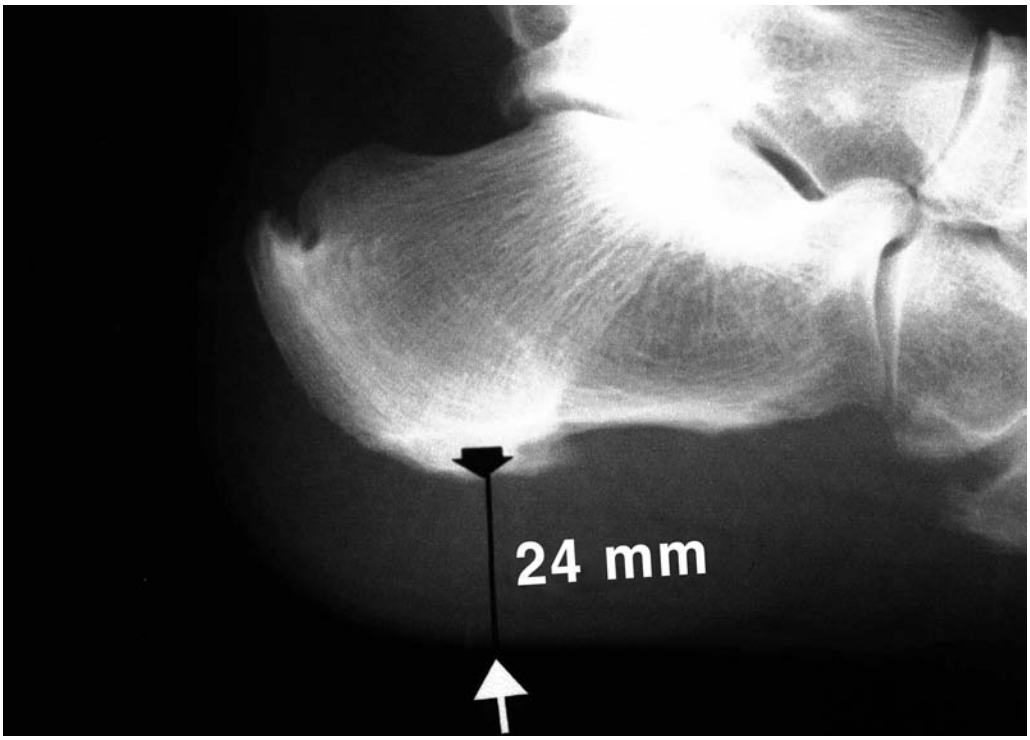

Fig. 15. Illustration of measurement of the heel pad thickness.

Table 2
Equations for Estimating Living Stature From the Long Bones of American Aged 18 to 30 Years[a]

White Males, cm		**African-American Males, cm**	
2.38 Femur + 61-41	±3.27	2.11 Femur + 70.35	±3.94
2.52 Tibia + 78.62	±3.37	2 .19 Tibia + 86.02	±3.78
2.68 Fibula + 71.78	±3.29	2.19 Fibula + 85.65	±4.08
1.30 (Femur + Tibia) + 63.29	±2.99	1.15 (Femur + Tibia) + 71.04	±3.53
White Females, cm		**African-American Females, cm**	
2.47 Femur + 54.10	±3.72	2.28 Femur + 59.76	±3.41
2.90 Tibia + 61.53	±3.66	2.45 Tibia + 72.65	±3.70
2.93 Fibula + 59.61	±3.57	2.49 Fibula + 70.90	±3.80
1.39 (Femur + Tibia) + 53.20	±3.55	1.26 (Femur + Tibia)+59.72	±3.28
Asian Males, cm		**Mexican-American Males, cm**	
2.15 Femur + 72.57	±3.80	2.44 Femur + 58.67	±2.99
2.39 Tibia + 81.45	±3.27	2.36 Tibia + 80.62	±3.73
2.40 Fibula + 80.56	±3.24	2.50 Fibula + 75.44	±3.52
1.22 (Femur + Tibia) + 70.37	±3.24		

[a]To estimate stature in older individuals, subtract 0.06 × (age in years –30) cm; to estimate cadaver stature, add 2.5 cm. Reprinted from ref. *33a*, with permission.

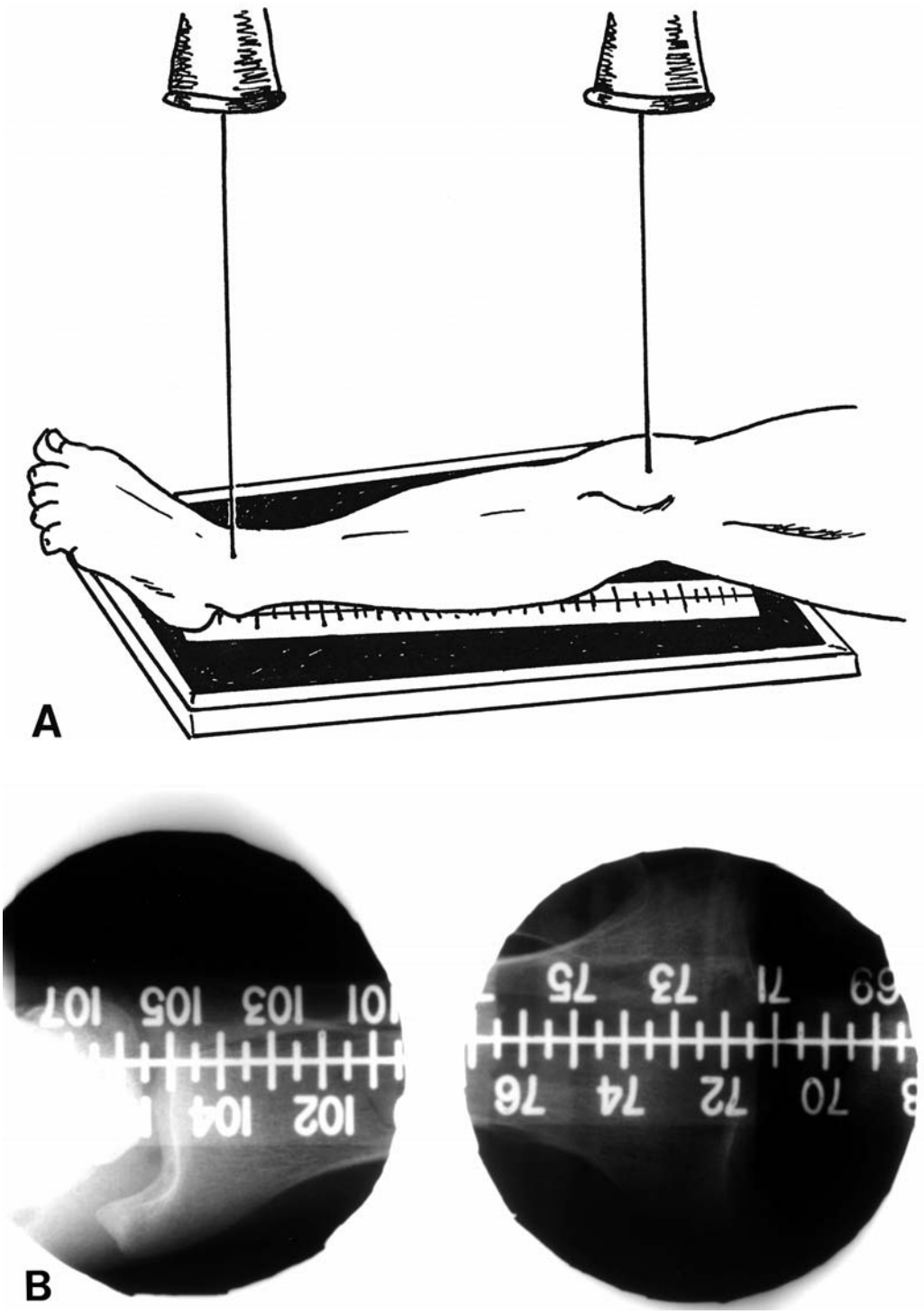

Fig. 16. **(A)** Schematic representation of the scanogram method of obtaining magnification-free measurements of long bone length using collimated, nondivergent X-rays over the bone ends with a partially radiopaque ruler in the field of exposure. **(B)** Resultant scanogram of the leg.

equally useful if corrections for magnification are applied. The effect of magnification can be nullified with an extremely long distance between the X-ray tube and the object–film combination (≥6 ft), but this is impractical in most laboratory settings. An old but useful technique for measuring long bones involves the use of X-ray beams from conventional tube–object distances (36–40 in.) that are carefully collimated so that only nondivergent central rays are used. A partially opaque ruler can be used for direct measurements (Fig. 16). Finally, if CT equipment is available, direct measures can be easily obtained from the image with a cursor.

3. IDENTIFICATION

3.1. General Considerations

The accuracy of radiology when used to identify human remains depends on the ability to find identical points of comparison between antemortem diagnostic radiological studies and postmortem images obtained with similar techniques. Hence, postmortem studies must be obtained with the parts positioned to simulate the routine radiologic positions and projections used in medical diagnostic studies. Equipment and technical factors employed in the production of such postmortem radiologic images will be discussed later in this chapter. Unless identity is readily established, it is wise to obtain radiographic studies of all available body parts prior to their release, because it is not easy to predict which body regions will be represented on the antemortem radiographs subsequently acquired.

3.2. Statistical Considerations Related to Body Parts

The abdominal trunk—particularly the soft tissue and bony structures of the back, including the spine and pelvis—are most likely to survive the rigors of separation, incineration, decomposition, and the activities of carnivores. The extremities are susceptible to damage by all of these factors. Further, the odds of finding antemortem studies of the extremities are less than those of some other body parts. In a survey of films in a large university hospital radiology department *(34)*, investigators found that the lower extremity accounted for only 11% of all roentgenograms and an even smaller percentage of studies using other radiologic modalities. In the Bass and Driscoll study of incomplete skeleton retrieval in Tennessee *(35)*, the femur was the second most common skeletal element found in 58 fragmented skeletons; the tibia ranked fifth, the fibula eighth, and the patella 13th. In a series of 30 cases in which the identification of the victim was established by comparing antemortem and postmortem radiologic findings, Murphy and coworkers found that the extremities contributed to 20% of cases *(36)*.

3.3. Identification of Individual Skeletal Elements

Individual bones can be matched on antemortem and postmortem radiographs by comparing overall configurations or comparable abnormalities associated with (1) anomalous, congenital, or developmental lesions; (2) disease or tissue degeneration; (3) tumors or tumor-like conditions; (4) trauma; (5) iatrogenic lesions; and (6) trabecular patterns and vascular grooves *(34)*.

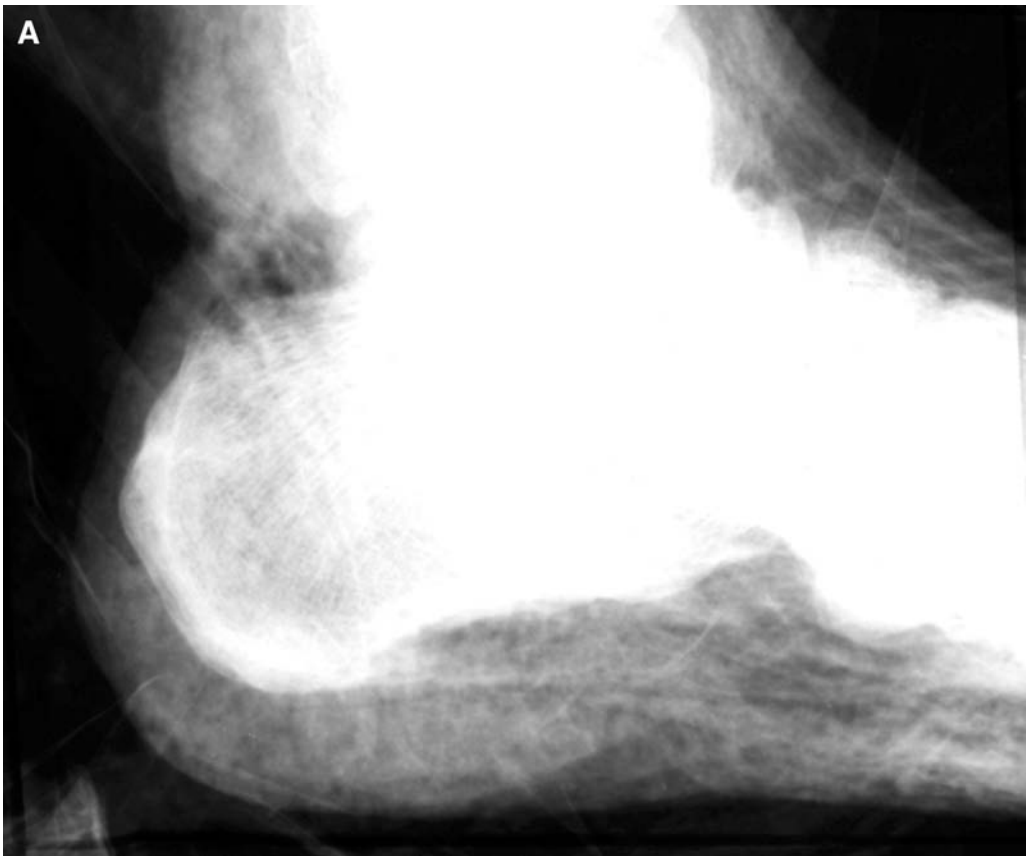

Fig. 17. Postmortem **(A)** and antermortem **(B)** radiographs of the os calcis allowing comparison of the total configuration of the bone. The quality of the postmortem radiograph does not permit confident comparison of trabecular pattern, although some areas of similarity can be identified.

Again, the position of the postmortem specimen must duplicate that of the antemortem radiograph. This may require trial and error or the "shadow positioning technique" of Fitzpatrick and Mascaluso *(37)*.

Figure 17 contains an example of a match made by comparing several points along the general outline of the bone, even though good detail is not present on the postmortem radiograph. A recent investigation confirms the value of comparing configuration *(38)*, which surpassed all other features in that study for establishing a match.

3.4. Anomalous, Developmental, and Congenital Variations

Riddick et al. *(39)* were able to identify the charred remains of a kidnapped murder victim on the basis of a developmental anomaly in a patella—a "dorsal defect" found in only 1% of the population *(40)* (Fig. 18).

Clubfoot deformities were discovered in one examination of decomposed human remains *(41)*. Finding custom-made orthopedic shoes in the room, investigators were able to locate the vendor who, in turn, helped them antemortem radiographs of the feet. These were successfully compared with postmortem studies (Fig. 19).

Fig. 17. *Continued.*

Other conditions in this category that may prove useful in future cases are illustrated in Figs. 20–24.

3.5. Disease or Degenerative Change

Degenerative changes are frequently helpful or even definitive in the identification of unknown remains. We have already seen examples in the Ruxton case *(14,15)* and in the case of heel spurs of the calcaneus. Judging from the literature, it is rare to be able to match skeletal remains by lesions that arise secondary to disease processes. However, certain diseases have such distinctive features that they could be used for identification purposes. Several examples are shown in Figs. 25–29.

3.5.1. Tumors and Tumor-Like Lesions

Malignant tumors may change so rapidly that they are of little use for comparison studies, especially when the films were obtained over a long interval of time (Fig. 30). Other such lesions, however, are relatively stable and may be useful on occasion. Examples are shown in Figs. 31–33.

3.5.2. Trauma

Dr. Fovau d'Courmelles accurately predicted in the October 1898 *American X-Ray Journal* that

> "knowing the existence of a fracture in a person, who has been burned or mutilated beyond recognition, we can hope to identify him by the X-ray".

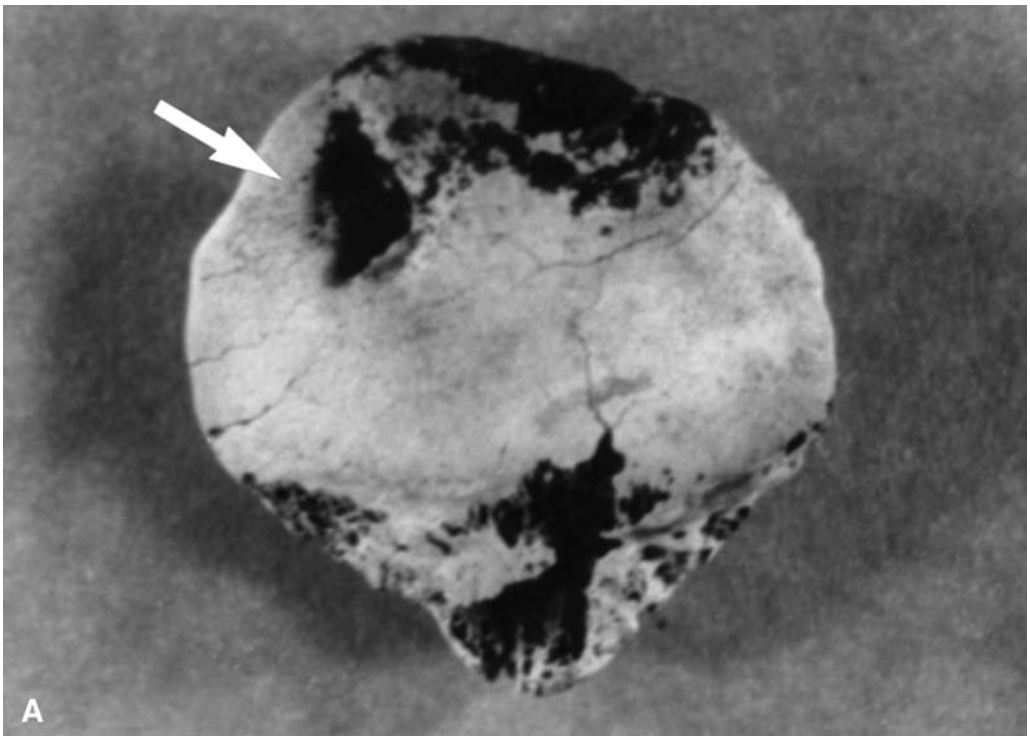

Fig. 18. (A). Photograph of the posterior surface of the left patella showing the "dorsal defect" (arrow). **(B,C).** The isolated, incinerated patella can be successfully compared radiographically with a clinical examination obtained 2 yr earlier after an automobile accident. Reprinted from ref. *39* with permission. © ASTM International.

Residual deformities from fractures, retained bullets, embedded knife blades, or posttraumatic calcifications can all provide identification if appropriate comparative radiographs become available (Figs. 34–35).

3.5.3. Iatrogenic Alterations

Residual findings from previous treatments or manipulations can be helpful in using radiology for identification purposes. Orthopedic hardware, prostheses, drill holes and drill bits, osteotomies, fusions, and manipulations may all leave recognizable traces that can be seen on the radiograph (Figs. 36–39).

3.6. Trabecular Patterns and Vascular Grooves

The trabecular pattern of some bones can be quite distinctive and can be matched on antemortem and postmortem films. Weight-bearing or stress-bearing large trabeculae in the femur, tibia, and os calcis are particularly useful. Kahana and Hiss *(43)* have described a computerized system of matching trabecular patterns by superimposing densitographs and reported a case identified by that system using only the bones of a thumb. However, we find that in most cases, one can satisfactorily match the pattern by sight alone while manipulating the specimen.

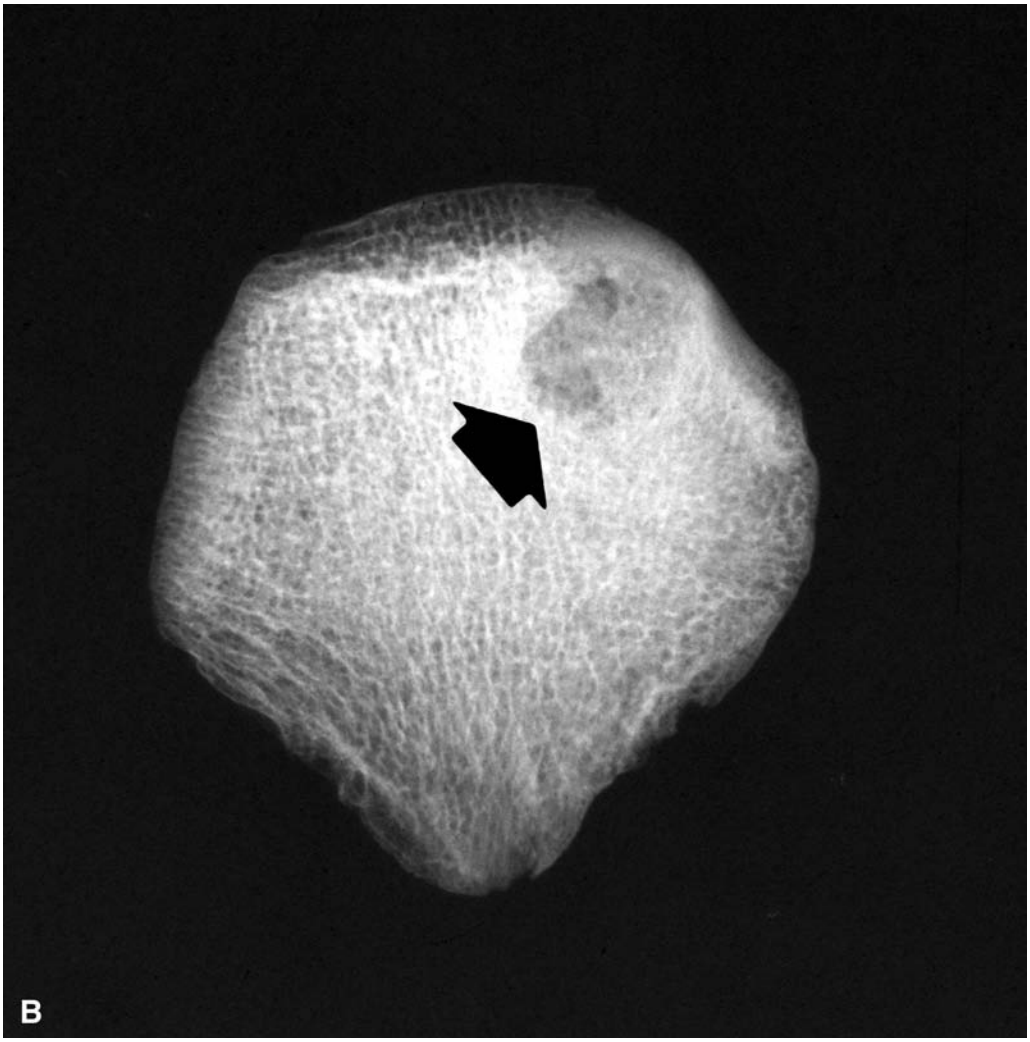

Fig. 18. *Continued.*

4. Identification in Mass Casualty Situations

The same techniques and variables that are taken into consideration when identifying individual skeletal elements apply to mass casualty situations, except for the logistical problems that are complicated by the size of the matrix (i.e., the number of remains involved and the fact that they are sometimes commingled and often fragmented). Most mass casualty operations take on the characteristics of a field exercise, because a fear of contaminated blood and body fluids has closed the doors of most hospitals to mass casualty remains *(44,45)*. The organization of a mass casualty operation is beyond the scope of this chapter, but there is extensive literature on the subject. Apart from obtaining radiographs of mass casualty victims for identification purposes, it is also useful to look for foreign bodies (Fig. 40) that may provide valuable information,

Fig. 18. *Continued.*

such as serial or part numbers, sources of bombs or weapons, trace evidence of explosives or chemicals, or even an unexploded bomb.

5. *Pattern Injuries*

Some traumatic episodes result in radiologically demonstrable lesions that are relatively consistent. These are called *pattern injuries,* and they can frequently be used to predict or deduce the mechanism of injury, the offending agent, or both.

5.1. Abuse

5.1.1. Child Abuse

In Caffey's first paper on the subject, he remarked on a pattern of skeletal lesions found in children who also had a subdural hematoma. The pattern was one of metaphyseal fragmentation, another finding he called "involucrum," and fractures in different stages of healing *(16)* (Figs. 41–44). Later, Caffey added other components to the pattern: "bowing fractures" (Fig. 45), metaphyseal cupping (Fig. 46), and "ectopic ossification centers,"

Fig. 19. Postmortem **(A,B)** and antemortem **(C,D)** radiographs of a decedent with bilateral club foot deformities, which were used to establish a positive identification. Matching points are indicated with arrows. Reprinted from ref. *41* with permission. © ASTM International.

which nowadays translates to epiphyseal separation (Fig. 47). Caffey and others added still more observations to the total pattern, including transverse and spiral fractures of long bones that are inappropriate to the age and activity of the child *(46,47)* (Figs. 48–51).

The interpretation of pediatric radiographs requires considerable training and experience. Radiographically, it is quite true that "children are not just little adults." Other conditions, both normal and abnormal, may be confused with child abuse. One of the best examples of this is the so-called "toddler's fracture" (Fig. 52)—an undisplaced spiral fracture of the tibia that is the common result of the somewhat uncoordinated, often pigeon-toed effort at locomotion by children in this age group—which is not an indication of abuse. By contrast, a spiral fracture of the tibia in a nonambulatory child is almost invariably an indication of child abuse.

Fig. 19. *Continued.*

A single thin line of periosteal calcification may exist in normal healthy infants up to age 4 mo. However, it is bilateral, symmetrical, unilamellar, and asymptomatic and is not indicative of child abuse (Fig. 53). A number of other conditions may be confusing, including that darling of defense attorneys: osteogenesis imperfecta (Figs. 54–62).

It must be remembered that the most important feature of radiologic findings in child abuse is that the injury is inconsistent with the age, development, and activity of the child.

5.1.2. Physical Abuse of Adults

Spousal abuse or abuse of intimate partners does not usually involve the lower extremity. Abusive blows to women are almost exclusively directed to the head, neck, and face *(49,50)*. Domestic violence and automobile accidents are the most common causes of facial injury in women. Patterns emerge here: automobile accident victims tend to show massive and multiple injuries to the facial bones and mandible, whereas battered women show mostly fractures of the mandibular body or angle and the contralateral mandibular ramus. Of course, nasal, orbital, zygomaticofacial, and dental fractures are seen along with dislocations of the mandible. Defensive injuries of the upper extremity (fending fractures) are seen, but the lower extremities are rarely involved. Blows to the body are uncommon except in pregnant women, where the breast and abdomen may be pummeled.

Fig. 19. *Continued.*

5.1.3. Abuse of the Aged

Here, the patterns of injury are somewhat like those seen in child abuse, i.e., twisting, pulling, and squeezing injuries of the extremities as a result of punishment or attempts at restraint. However, blows to the head may simulate those seen in spousal abuse. Senile osteoporosis complicates the diagnostic issue in the elderly—particularly in the extremities, where routine handling, lifting, turning, and restraint may produce fractures *(50,51)*.

5.2. Pedal Injury Patterns

This topic is something of a double entendre, because it refers to injuries to the pedal extremity—which are caused mostly by pedals, either brake or rudder!

Dr. Andrew's collection of "aviator's astragalus" cases was amassed from air crashes, and he believed that the mechanism was one of dorsiflexion against the rudder pedal during impact *(13)*. More contemporary studies have suggested a spectrum of injuries caused by this mechanism *(52)*. In Group 1 injuries of this type, there is a relatively

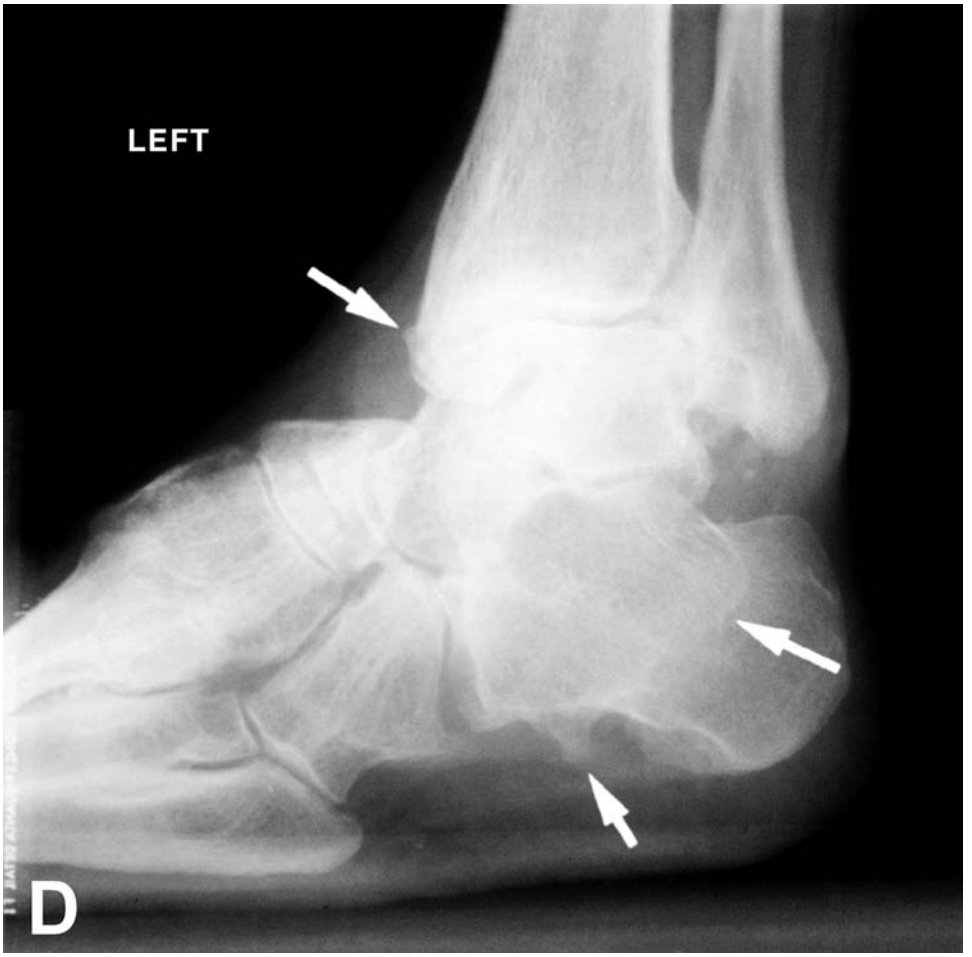

Fig. 19. *Continued.*

undisplaced fracture of the neck of the astragalus or talus (Fig. 63). In Group 2, there is fracture of the talar neck with displacement of the body of the talus into equinous deformity. In Group 3, there is a posterior dislocation of the talus, which may involve the entire bone or only a major portion of the body of the talus, with the anterior fragment remaining roughly in place between the tibial plafond and the navicular. True posterior extrusion of the talus is quite rare, because it requires rupture of the Achilles tendon (Fig. 64). Talar dislocations and extrusions also occur in plantar flexion *(53)* in association with either pronation or supination, in which case the soft tissue injury and extrusion will be either anteromedial or anterolateral, respectively. Figures 65 and 66 show additional examples of talar fracture/dislocation and extrusion.

According to Simson *(54)*, flight surgeons during World War II recognized a lesion they called "Aviator's fracture"—a pattern of dorsally displaced mid-foot metatarsal fractures that occur as a result of impact against a rudder pedal (Fig. 67). It is impossible to tell from the rather poorly reproduced roentgenogram the extent of additional injuries to the tarsal bones. It appears that there are fractures of not only the

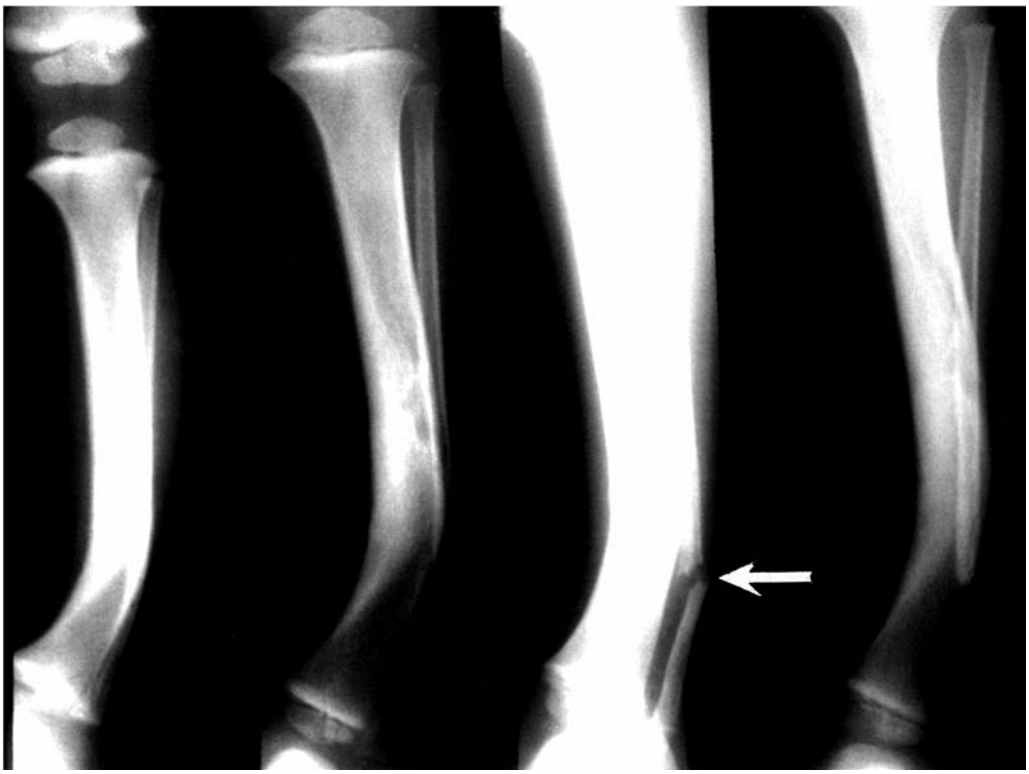

Fig. 20. Serial radiographs of a patient with kyphoscoliosis of the tibia in association with neurofibromatosis. Pseudoarthrosis of the fibula (arrow) develops over the course of time.

metatarsals but also fracture/dislocations in the hind foot. Figure 68 shows deformity of a reinforced flying boot from impact on the rudder pedal indicating the direction of force that would produce the injuries described by Simson.

Tarsometatarsal fracture/dislocation (the so-called Lisfranc lesion) can be acquired through a variety of mechanisms, with dislocations occurring in both the dorsal and plantar direction *(55)*. It is not uncommon for the history to include the fact that the foot was forced against or trapped beneath a brake or gas pedal. However, such injuries can also occur as a result of a fall, the foot being run over by a vehicle, or a heavy weight being dropped on the foot. Thus, the pattern is not specific. The key injury is disruption of the locking mechanism of the base of the second metatarsal between the first, second, and third cuneiforms. Ordinarily the lateral metatarsals are displaced both laterally and dorsally. Figure 69 shows a case that resulted when the right foot was jammed forcibly against a brake or gas pedal during an accident. There is a divergent Lisfranc deformity involving a fracture of the base of the second metatarsal and lateral subluxation of the four lateral metatarsals.

5.2.1. The Bumper Fracture

The bumper fracture has been recognized for years as a well-established pattern suggesting the injury, the object, the direction in which it was traveling, and the position of the victim (Fig. 70).

Fig. 21. Typical "dripping candle wax" hyperostosis of melorheostosis in the tibia **(A)** and several bones of the ipsilateral foot **(B).**

Fig. 21. *Continued.*

5.3. Patterns of Torture and Terrorism

Physical beating is a widespread form of torture *(56)*. Palmatoria is a form of localized torture virtually unique to the small West African country Guinea–Bissau. Palmatoria involve repetitive blows by a slender rod to the shin, where the tibia lies closest beneath the skin. Ordinary radiographs (of somewhat limited quality) have shown a periosteal reaction, presumably as a result of subperiosteal hemorrhage and hematoma. Somewhat peculiar endosteal and medullary changes have also been seen (Fig. 71). Recent case reports in the United States and France *(57,58)* have shown that this specific injury can produce a hidden endosteal fracture that is likely to be undetected on plain films but becomes obvious on a CT scan (Figs. 72, 73). It seems possible (perhaps likely) that some of the cases that took place in Guinea–Bissau would show similar findings when more sophisticated imaging modalities were used.

Falaca is a form of torture characterized by beating the foot, primarily the sole of the foot *(56)*. This is a widespread form of torture in the Middle East, especially in Turkey and Iraq, as well as in Asia and in some Spanish-speaking areas (where it is called bastinado). Substantial injuries can be produced by this form of torture, including edema, hematoma, fractures, and injuries to ligaments, tendons, fascia, and aponeuroses. The clinical findings are usually diagnostic if they are made immediately after such torture. Radiography can confirm or exclude fractures and allows the investigator to estimate the extent of soft tissue injury and the time interval since torture. Early nuclear medicine studies show a massive increased uptake in the affected areas. Later radiographic studies demonstrate bone and soft tissue injury and evidence of subsequent healing (Figs. 74–76).

Fig. 22. Focal deposits of compact bone in a knee. Diagnostic of osteopoikilosis.

5.3.1. Knee Capping

The punitive destruction of a major joint by gunshot wound was originally thought to be the signature injury of certain criminal elements in the United States. More recently, it has been seen as an act of terrorism in other parts of the world, especially

Fig. 23. Neurogenic destruction in the ankle and hindfoot of a 7-yr-old female with congenital insensitivity to pain. Reprinted from Brogdon BG, Vogel H, McDowell JD, eds. A radiologic atlas of abuse, torture, terrorism, and inflicted trauma (2003) with permission from CRC Press.

Northern Ireland *(59)*. The punishment is not limited to the knee; other major joints have also been targeted (Figs. 77–80).

6. Gunshot Wounds

From the day that Professor Wright examined his rabbit *(3)*, radiology has played an important role in the evaluation of gunshot wounds. The number, location, and caliber of bullets; the angle and direction of fire; the discovery of concealed gunshot wounds; weapon ballistics; types of bullets; and unconventional loads all fall within the purview of modern radiologic investigation *(60–64)*.

6.1. Number of Bullets

Since more than one bullet can enter through a single entrance wound, it is important to determine the number of bullets and correlate them with entrance and exit wounds. Any discrepancy requires a search for spent bullet casings at the scene, additional entrance wounds, or radiographic investigation.

6.2. Caliber of Bullets

The use of radiographs to estimate the caliber of a bullet can be fraught with difficulty, particularly because the range of bullet sizes among calibers that are commonly used in handguns, for instance, is quite minimal (Fig. 81). The magnification factor

Fig. 24. Residual deformity of the femoral head and neck in healed Legg-Calvé-Perthe disease.

further confuses the picture and increases the risk of comprising the accuracy of the findings.

6.3. Location

Locating the bullet would seem to be a rather simple task. However, bullets may end up at sites quite distant from the entrance wound. They may be diverted from their

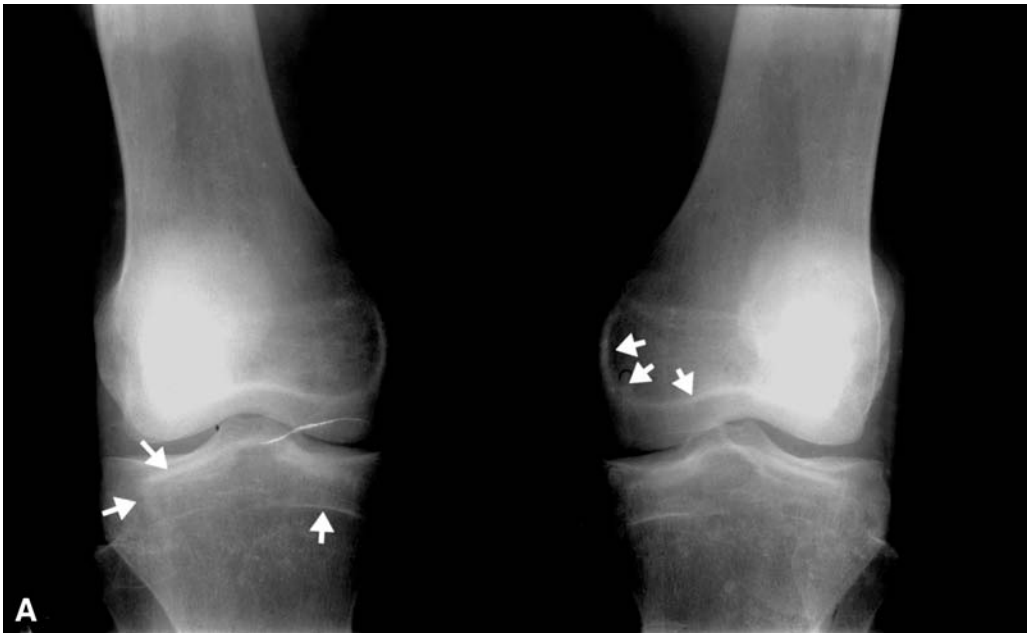

Fig. 25. A, B, and **C**: Radiographs of the knee and ankle show the "bone-in-bone" phenomenon, which can result from heavy metal poisoning or serious illness during bone growth. One can see the faint outline of the smaller bone at the time of the insult encased in the larger mature bone. This individual had ingested phosphorus during bone growth because of a habit of chewing matches. We have seen similar changes following severe childhood typhoid fever. A somewhat similar appearance can be seen in osteopetrosis or treated histiocytosis X.

expected path by striking bone or tissue. They may migrate great distances through blood vessels, the alimentary tract, the genitourinary tract, the spinal canal, the tracheobronchial tree, or within pleural and peritoneal spaces (Figs. 82, 83).

6.4. Types of Bullets

The ordinary load for handguns and rifles is a bullet made of lead. The lead may be fully or partially covered by another metal, called a jacket, which has several purposes: it protects the barrel of the weapon from leading; it hardens and lubricates the bullet, thereby somewhat diminishing the possibility of bullet deformity when it strikes tissue, particularly bone; and it may be shed as the bullet traverses tissues in the body. Each weapon has grooves inside the barrel that leave identifiable marks on the bullet as it passes through. This is important for ballistics identification. In the unjacketed bullet, the pattern will be on the lead itself; in semi- or fully-jacketed bullets, the ballistic markings will be on the jacket. Hence, it is important to identify and retrieve the separated jacket for ballistic purposes (Fig. 84). Copper jacketing is usually quite easily identified. The so-called silvertip load, which has become quite popular in the United States, is jacketed with aluminum and can be quite difficult or impossible to locate with conventional radiography.

Fig. 25. *Continued.*

Fig. 26. Massive destruction of the bones and soft tissues in Madura foot.

Fig. 27. Calcification at the site of the secondary attachment of the plantar fascia. It has no clinical significance and is not be to be confused with plantar fasciitis.

Fig. 28. Typical diaphyseal sclerosing osteomyelitis of Garré.

Fig. 29. "Burned out" juvenile rheumatoid arthritis in a 22-year-old woman. The onset of disease was at age 6. Typical changes at the knee include massive overgrowth of the epiphyseal ends of the bones with atrophic osteoporotic shafts and joint destruction.

Military weapons tend to have high-velocity characteristics and, according to the Hague Piece Conference of 1899, must be fully jacketed. "Civilian" weapons and loads are mostly of a lower velocity (Figs. 85, 86). Some of the bullets used in civilian handguns and rifles have identifying characteristics, including the following:

Fig. 29. *Continued.*

Fig. 30. Osteogenic sarcoma in the distal metaphyseal-diaphyseal of the femur in an adolescent male.

Fig. 31. Typical fibrous dysplasia in the first metatarsal with expansion of the bone and "ground-glass" appearance of bone in a fibrous matrix.

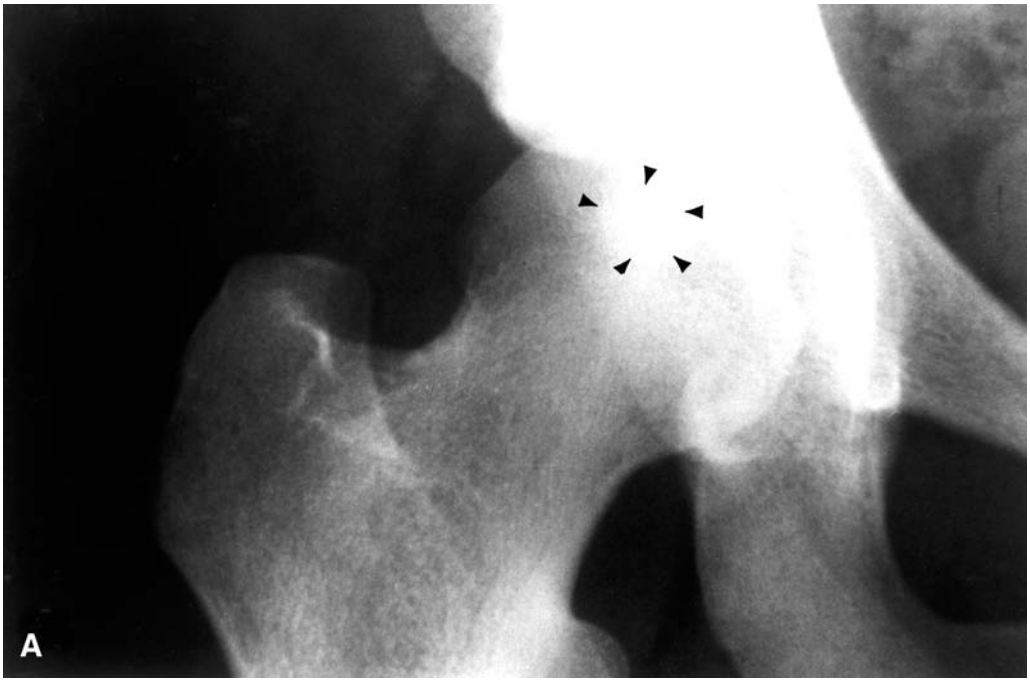

Fig. 32. **(A)** Typical "bone island" composed of normal compact bone in the head of the femur. **(B)** Bone island in the head of the femur in a T-1 weighted MRI. **(C)** Bone island in the head of the femur of a victim of the Air India disaster. None of the individuals in these three images are related. This points out the difficulty involved in trying to match common lesions in images obtained using different modalities. Reprinted from Brogdon, BG, Forensic radiology (1998) with permission from CRC Press.

- The unjacketed bullet commonly used in high-velocity hunting ammunition fragments so extensively that the resulting pattern is called a "lead snowstorm."
- The Black Talon mushrooms into a characteristic six-petal flower or star configuration.
- The Glaser safety slug carries multiple small lead pellets in a copper cup, producing an unusual mixed pattern of densities.
- The Winchester Western .25 caliber cartridge contains a copper-coated lead hollow-point bullet filled with a single no. 4 steel pellet and, thus, produces the unusual finding of a single small bullet accompanied by a single small shot.

Finally, unconventional loads—plastic bullets, rubber bullets, and ceramic bullets (Figs. 87,88)—are being seen with increasing frequency because they are used in crowd control.

7. Technical Considerations: Production of the Radiograph

As previously mentioned, it has become increasingly difficult to use hospital or clinical radiologic installations for forensic investigation. The medical examiner's office, whether a one-room morgue or a separate building, needs its own in-house radiologic facility. The basic requirements are functional radiographic equipment and space

Fig. 32. *Continued.*

to store and use it; X-ray films, cassettes, film storage space; a dark room and film processing facility, a film identification system; and envelopes and storage space for archival radiographs *(66)*.

7.1. X-Ray Equipment

Either mobile or fixed X-ray equipment will suffice. The mobile X-ray unit is entirely self-contained and mounted on wheels for easy maneuverability. Stand-alone units may also be used; these are mounted on the floor, wall, or ceiling. A disadvantage lies in the fact that the staff must bring the body or body parts to the machine. An advantage is that high-performance X-ray equipment is not required, because there is no need to overcome the problem of physical or physiologic motion in the body or body part being examined. Thus, adequate equipment can be obtained at fairly reasonable cost, particularly because second-hand equipment has been made available as a result of recent technological advances and the introduction of new modalities to the field of clinical radiology.

Fig. 32. *Continued.*

Fig. 33. (A) Frontal radiograph of the knee shows fibrous cortical defects of the distal femur. **(B)** T-1 weighted MR shows the identical lesions in the same patient. This combination of lesions is sufficiently unequivocal to allow a match. Reprinted from Brogdon, BG, Forensic radiology (1998) with permission from CRC Press.

Fig. 33. *Continued.*

Fig. 34. **(A)** Postmortem view of the proximal femur shows evidence of an old healed fracture with residual deformity. **(B)** Antemortem views of the same area show a similar entity, but differences in positioning prevent a precise match, thus allowing only a presumptive identification. Reprinted from ref. *42* with permission from ecomed verlagsgesellschaft mbH.

Fig. 34. *Continued.*

7.1.1. Film

X-ray film is sensitive not only to X-rays but almost every color of light. It is packaged in light-proof cardboard boxes and must be handled in a darkroom equipped with an approved X-ray safety light. X-ray film is also sensitive to heat, low humidity, and stray

Fig. 35. A murder victim found beside an interstate highway had fatal large-caliber gunshot wounds in the head and chest. Incidental finding of a small-caliber bullet in the thigh could be historically linked to a gunshot wound made years earlier at the hands of a barkeep during an attempted robbery.

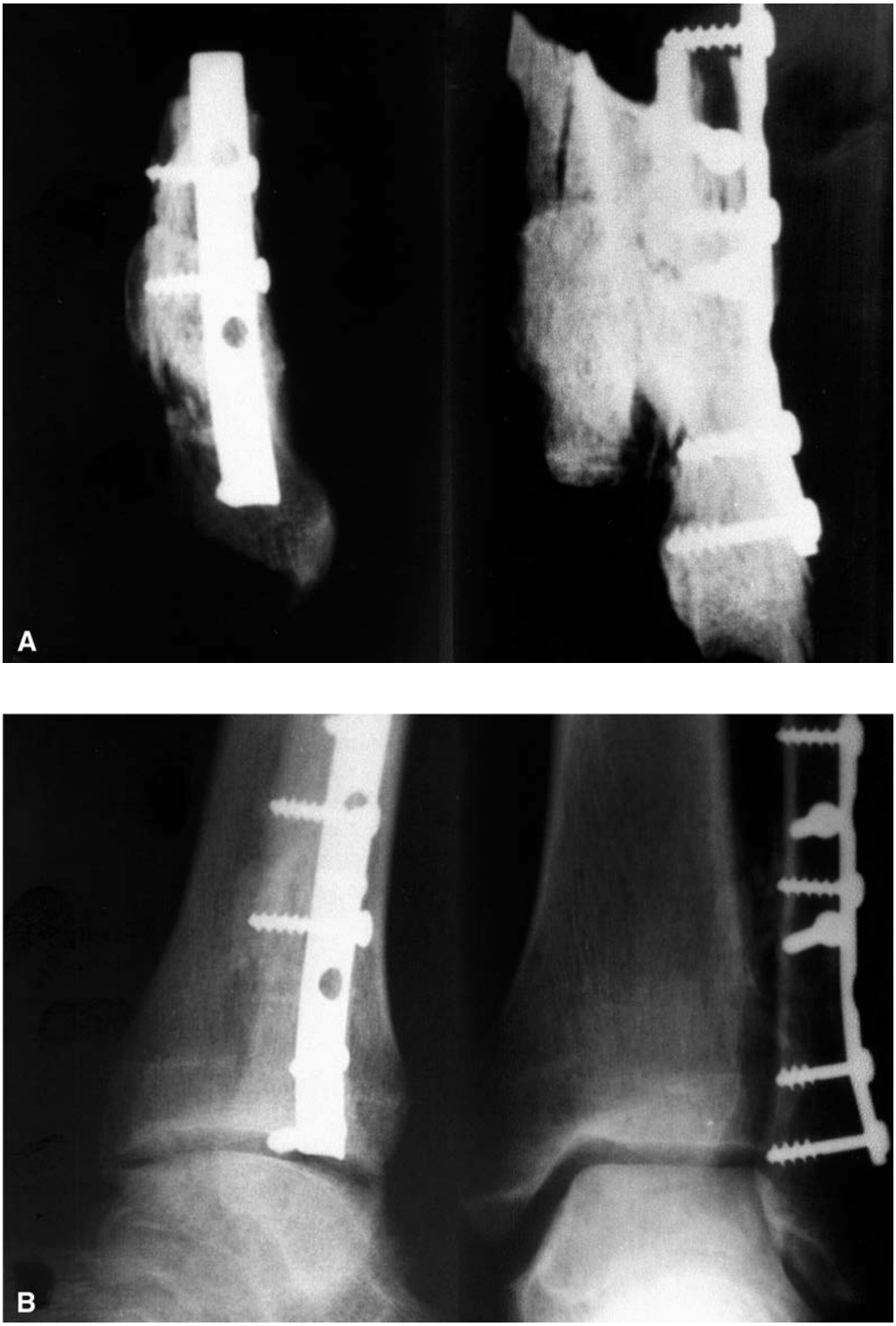

Fig. 36. A fragment of the tibia containing an orthopedic plate and screws **(A)** that could be matched eventually with antemortem radiographs **(B)** showing the identical fixation device. Reprinted from ref. *42* with permission from ecomed verlagsgesellschaft mbH.

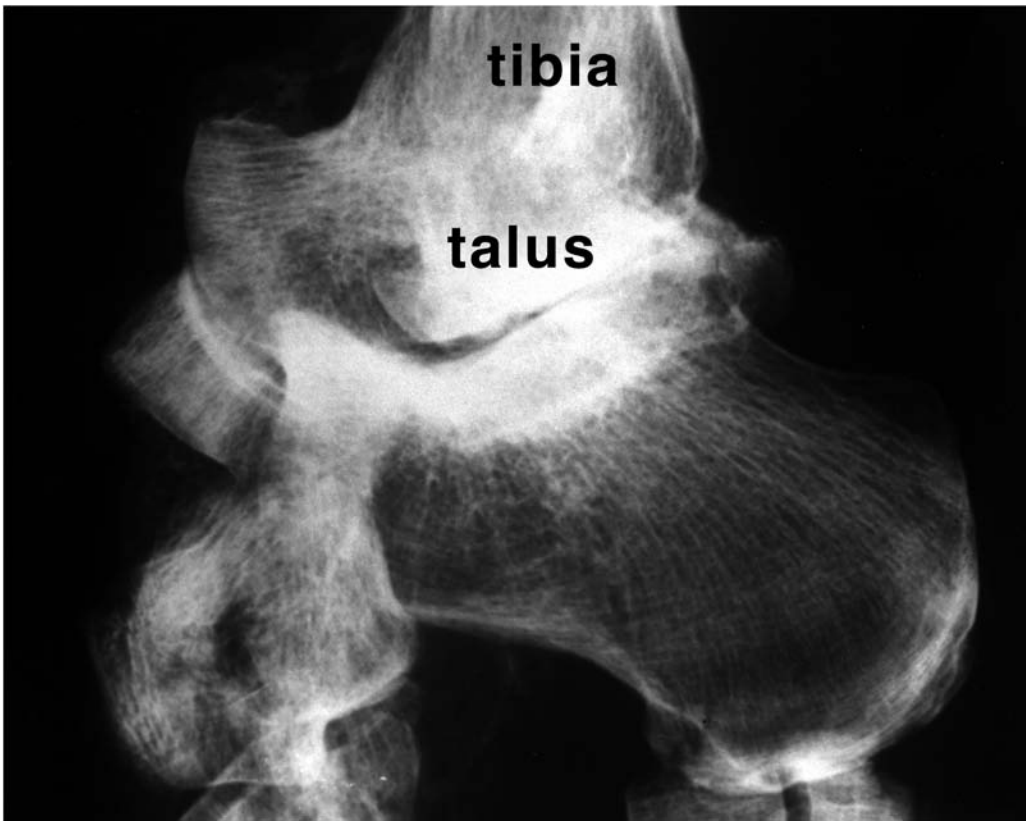

Fig. 37. A fragment of an incinerated ankle shows evidence of talo-tibial fusion. The kidnapped murder victim eventually identified by the patellar lesion (Fig. 18) had undergone such a procedure, but the postoperative films were not available. Hence, this could only be used to provide a presumptive identification until the patellar match was established. Reprinted from Brogdon, BG, Forensic radiology (1998) with permission from CRC Press.

radiation; hence, it must be carefully stored. X-ray film comes in a variety of sizes. It is easier for the forensic facility to employ one standard size; 14- × 17-inch film is recommended.

7.1.2. Film Cassettes

Unexposed film is loaded in the darkroom onto rigid holders called cassettes, which are made of plastic and metal. The cassettes are flat, rectangular structures that are hinged at one end. The unexposed film is sandwiched between two fluorescent intensifying screens, which help reduce the amount of X-ray exposure required. Some cassettes come with a built-in grid of parallel lead lines, which improves the quality of images made of thick body parts. Both grid and non-grid cassettes are required for different examinations.

7.1.3. Film Processing

Exposed films must be unloaded from a cassette in the dark and processed. There are many small automatic processors on the market, and these are highly recommended.

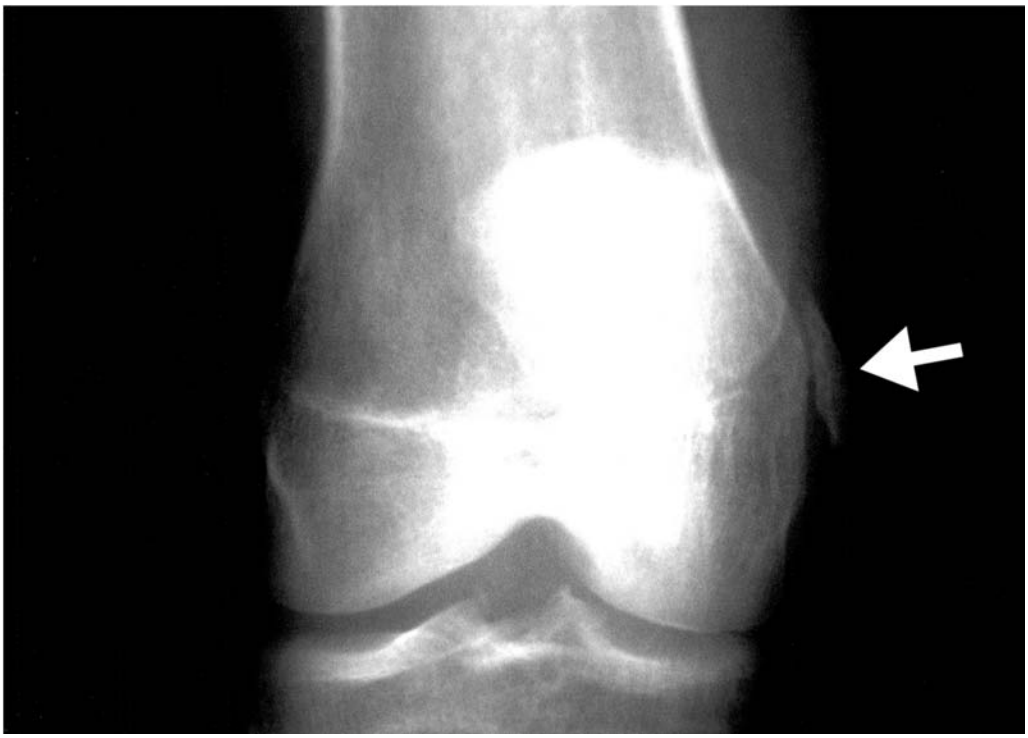

Fig. 38. Posttraumatic calcification of the medial collateral ligament of the knee—so-called *Pellegrini-Stieda* disease.

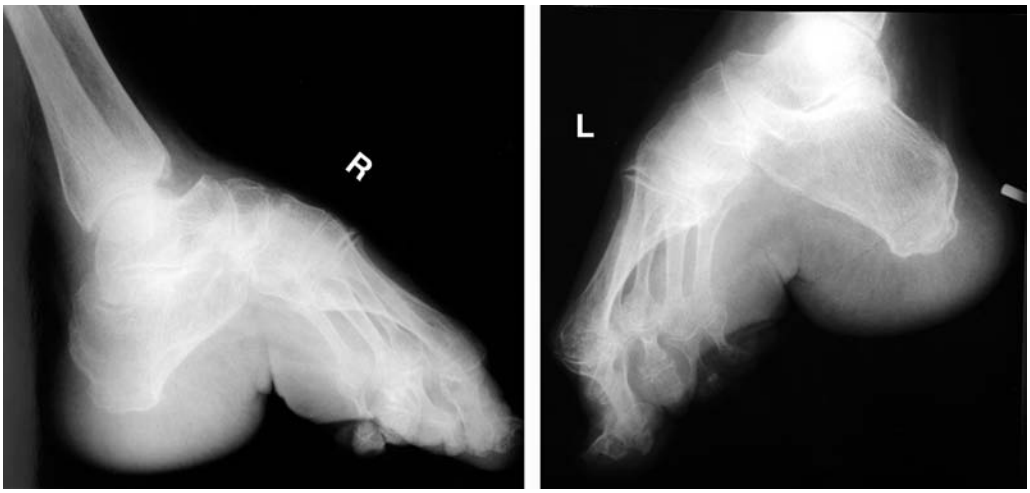

Fig. 39. A and **B**: Chinese bound-foot deformity. Reprinted from Brogdon BG, Vogel H, McDowell JD, eds. A radiologic atlas of abuse, torture, terrorism, and inflicted trauma (2003) with permission from CRC Press.

Fig. 40. Foreign material in a burned and fragmented foot and ankle. Examination of such material may give important information Reprinted from Brogdon BG, Vogel H, McDowell JD, eds. A radiologic atlas of abuse, torture, terrorism, and inflicted trauma (2003) with permission from CRC Press.

Fig. 41. Bilateral metaphyseal fractures of the femur in a case of child abuse. These are large "corner fractures." Reprinted from Brogdon BG, Vogel H, McDowell JD, eds. A radiologic atlas of abuse, torture, terrorism, and inflicted trauma (2003) with permission from CRC Press.

If available, a nearby hospital or clinic processing facility may be a satisfactory alternative to in-house processing.

7.2. Film Identification

If the radiographic output is quite low, one can successfully write the name or other identifier of the body or body parts directly on the film with an indelible marker after the film has been processed. A better and more dependable method involves affixing readily available lead letters and numbers on the exposable surface of the cassette with adhesive tape, thus putting identification on the film at the same time as the exposure *(67)*.

7.3. Exposure Factors

All radiographic equipment will have a control panel allowing the technician to select exposure factors—milliamperes (ma), exposure time(s), and kilovoltage (kVp)—appropriate for the body part and its thickness. Milliamperage and time may be combined as milliampere-seconds (mAs) *(68)*.

Table 3 is a simplified exposure chart, which is suggested as a starting point for the production of useable images. Suggested milliampere-seconds, kilovoltage settings,

Fig. 42. Metaphyseal fracture of the so-called "bucket-handle" type in an abused infant. Actually, these metaphyseal fractures cross the metaphysis just beneath the growth plate in a fairly straight line. They appear as corner fractures or bucket handles due to slight differences in the positioning of the bone relative to the central beam of the X-ray. Reprinted from Brogdon BG, Vogel H, McDowell JD, eds. A radiologic atlas of abuse, torture, terrorism, and inflicted trauma (2003) with permission from CRC Press.

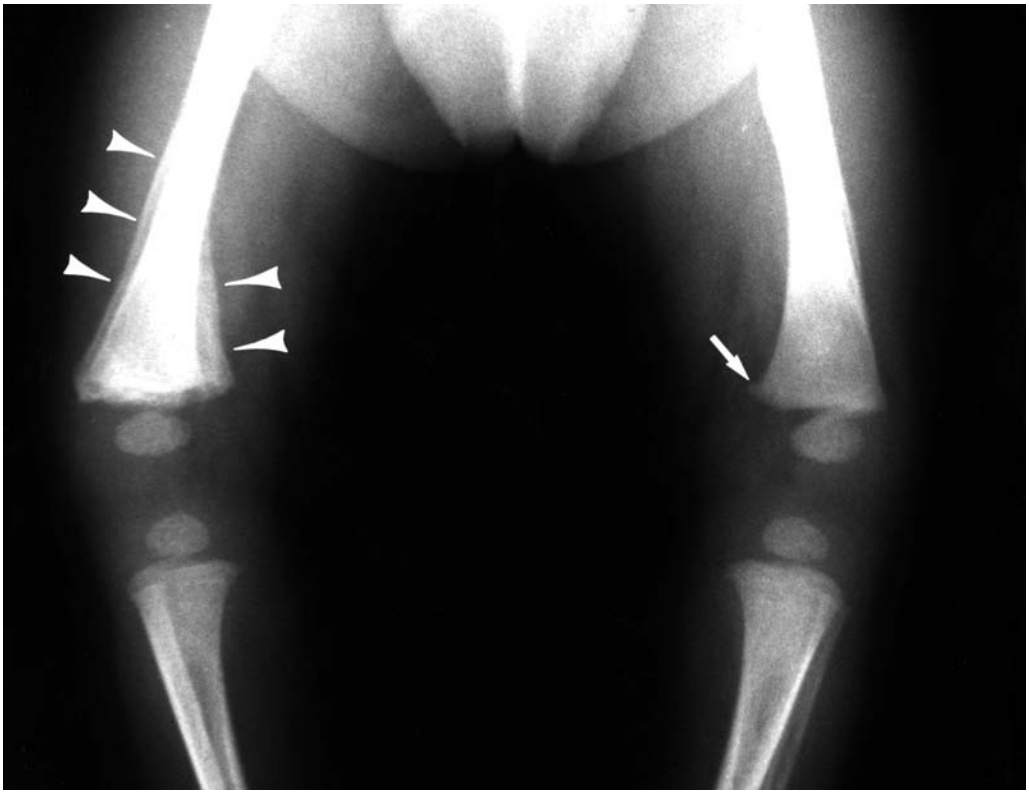

Fig. 43. Abused infant showing a corner fracture (arrow) in the distal left femoral metaphysis. The right femur shows what Caffey called "involucrum" (arrowheads). This is posttraumatic calcification caused by stripping of the periosteum by twisting action on the extremity. Reprinted from Brogdon BG, Vogel H, McDowell JD, eds. A radiologic atlas of abuse, torture, terrorism, and inflicted trauma (2003) with permission from CRC Press.

and the selection of a grid or non-grid cassette are supplied for different body parts and tissue thicknesses. It is recommended that the X-ray tube be 40 in. from the film or cassette holder. A ruler or simple aluminum caliper should be used to measure the thickness of the part to be examined.

The chart supplied in Table 3 assumes a screen/film system speed of 400 (your supplier can help you set this up) and 8:1 grid ratios (again furnished by your supplier).

7.4. Positioning

Standard radiographic positions for the lower extremity are required in order to match features on antemortem radiographs *(68)*. Figures 89 through 96 provide information that can be used to determine how to position the body part and central beam of the X-ray for each standard position. Each positioning photo is accompanied by a sample of the image to be expected from it.

Fig. 44. Old periosteal new bone around the distal femur from earlier trauma (arrows). Reprinted from ref. *42* with permission from ecomed verlagsgesellschaft mbH.

Fig. 45. Infantile ankle showing what Caffey called traumatic bowing, actually a green stick fracture of the metaphyses (arrows). Reprinted from Brogdon, BG, Forensic radiology (1998) with permission from CRC Press.

Fig. 46. "Metaphyseal cupping" secondary to epiphyseal injury which blights the growth process. Reprinted from Brogdon BG, Vogel H, McDowell JD, eds. A radiologic atlas of abuse, torture, terrorism, and inflicted trauma (2003) with permission from CRC Press.

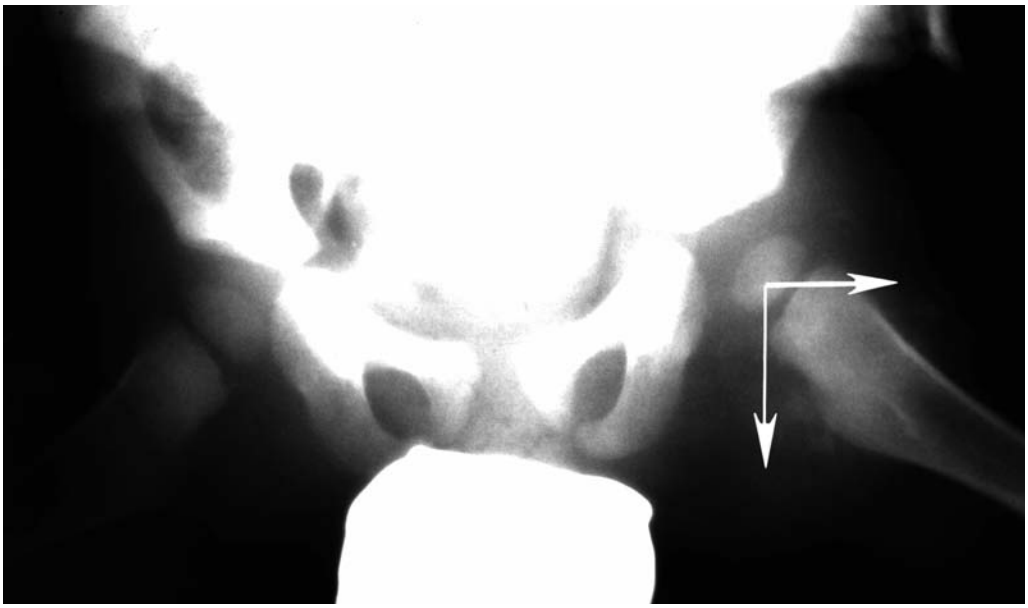

Fig. 47. Subluxation of the left femoral epiphysis due to intracapsular blood or effusion. This child had massive trauma elsewhere and was probably swung by this extremity. Compare with the right hip to see the widened joint. Reprinted from Brogdon BG, Vogel H, McDowell JD, eds. A radiologic atlas of abuse, torture, terrorism, and inflicted trauma (2003) with permission from CRC Press.

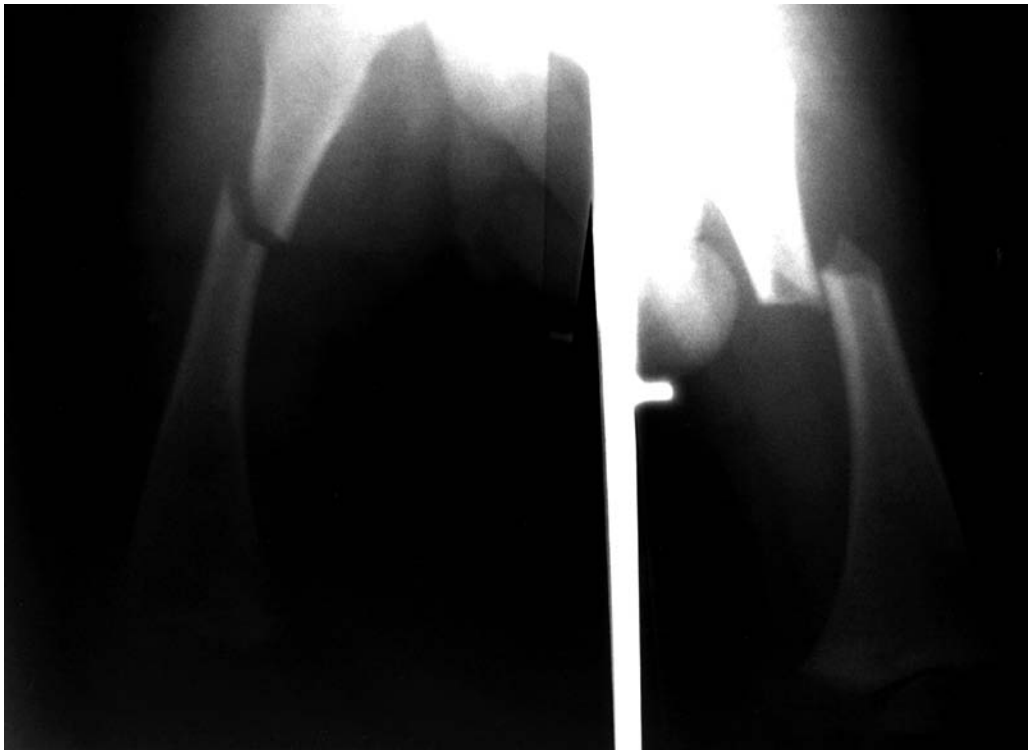

Fig. 48. Bilateral transverse fractures of the femora in a non-ambulatory child. Reprinted from Brogdon BG, Vogel H, McDowell JD, eds. A radiologic atlas of abuse, torture, terrorism, and inflicted trauma (2003) with permission from CRC Press.

Fig. 49. Transverse fracture of the tibial diaphysis with an associated plastic or bowing fracture of the fibula in an abused neonate.

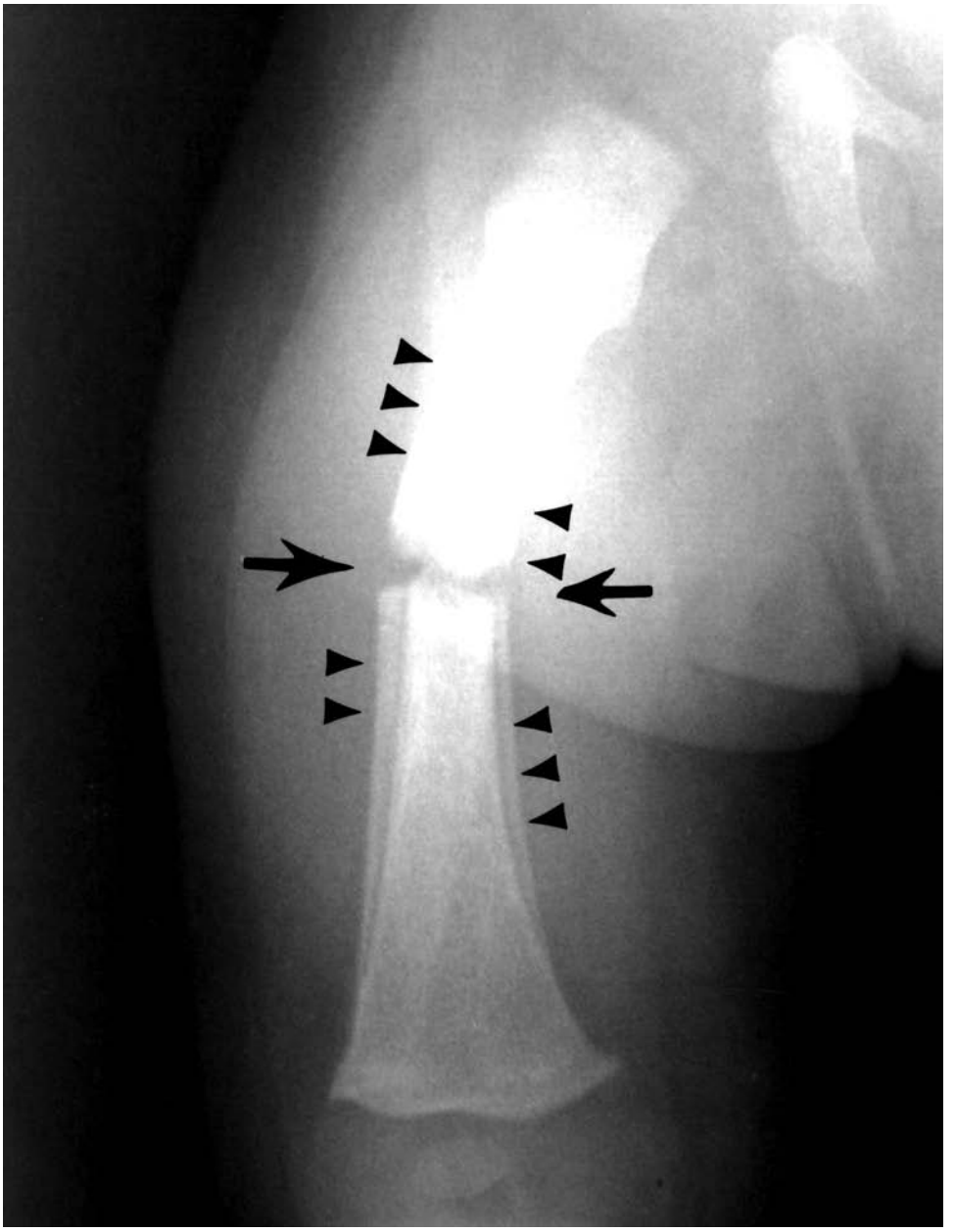

Fig. 50. Evidence of serial injuries on a single radiograph. There is fairly mature periosteal new bone from a previous twisting injury to the femur (arrowheads) which now shows a new transverse fracture (arrows) through both the shaft of the femur and the pre-existing periosteal new bone. Reprinted from ref. *48* with permission from CC Thomas.

Fig. 51. Another example of multiple injuries. This 11-mo-old female from a communal house had 30% burns and multiple injuries. (**A)** The toes were completely destroyed by fire (arrow). **(B)** There was a healing fracture of the left distal femoral metaphysis (arrow). (**C)** An older healing fracture of the distal tibial metaphysis (arrow) with injury to the physis and metaphyseal cupping of the epiphyseal center. Reprinted from Brogdon BG, Vogel H, McDowell JD, eds. A radiologic atlas of abuse, torture, terrorism, and inflicted trauma (2003) with permission from CRC Press.

Fig. 51. *Continued.*

Fig. 51. *Continued.*

Fig. 52. "Toddler's fracture." A common result of normal activity in young children as they first learn to walk. The same fracture in a nonambulatory infant or child indicates probable child abuse.

Fig. 53. Physiologic periosteal elevation and calcification in a 4-mo-old male. The bilateral symmetry and the single thin lamina of subperiosteal calcification is typical of this normal process. Reprinted from Brogdon, BG, Forensic radiology (1998) with permission from CRC Press.

Fig. 54. Thin, gracile, osteoporotic bone with healed fractures typical of osteogensis imperfecta.

Fig. 55. Intrauterine infection with rubella (German measles) produced these linear radiolucencies in the metaphyses. This is sometimes called a "celery stalk" appearance. It is not specific for rubella; other intrauterine infections may produce a similar appearance. Reprinted from Brogdon, BG, Forensic radiology (1998) with permission from CRC Press.

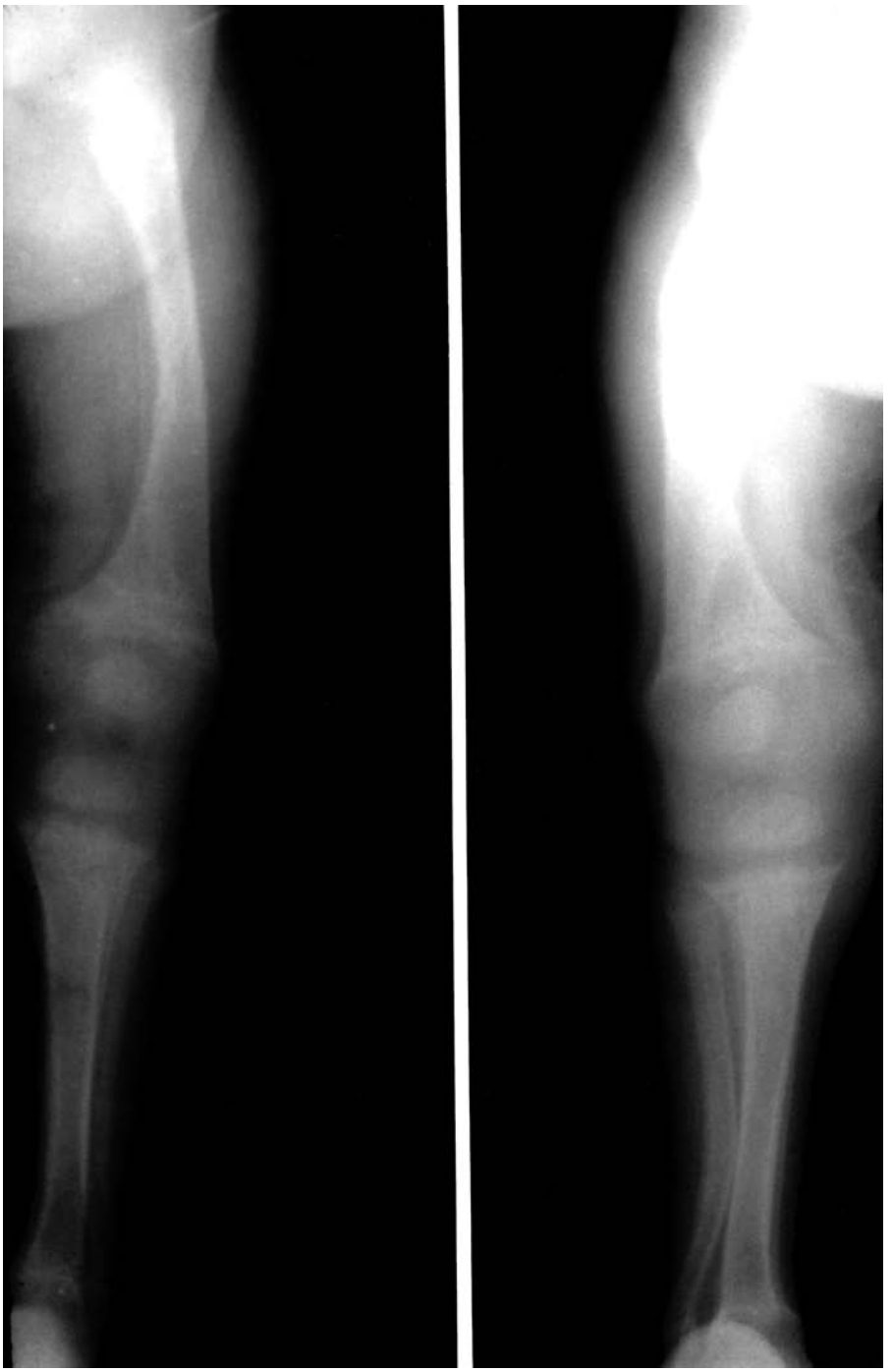

Fig. 56. Typical rachetic appearance with softened osteomalacic bone with periosteal reaction, bending fractures, and widened, frayed metaphyses with absence of the zone of provisional calcification.

Fig. 57. Scurvy. A dense ringlike band surrounds the epiphyses (Winberger's sign). There are beak-like projections at the corners of the metaphyses (Pelken's sign). The zone of provisional calcification is dense and wide. On the shaft side of that is a zone of increased radiolucency (the scurvy zone) and another white line of trabecular fragmentation. The overall quality of the bone indicates osteoporosis. A subperiosteal hemorrhage may eventually form periosteal calcification (not shown).

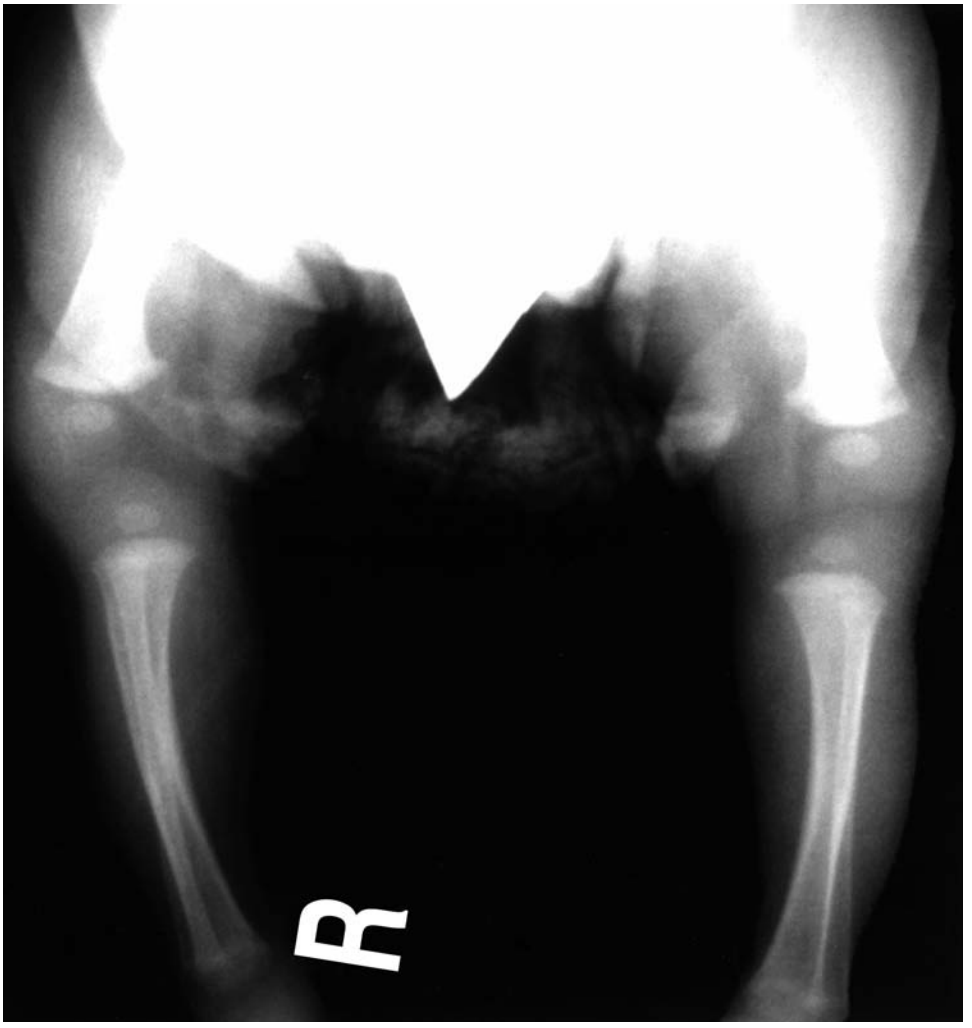

Fig. 58. Menkes disease (kinky hair syndrome). Rachetic-like bone changes are related to copper deficiency in this degenerative disease, which is also characterized by mental and motor retardation, clonic seizures, and peculiarly kinky hair. Reprinted from Brogdon, BG, Forensic radiology (1998) with permission from CRC Press.

Fig. 59. Osteomyelitis. Involucrum (arrowheads) encloses the deformed and partially destroyed bone. Those particularly bright white areas of the bone are necrotic and represent sequestra. Reprinted from Brogdon, BG, Forensic radiology (1998) with permission from CRC Press.

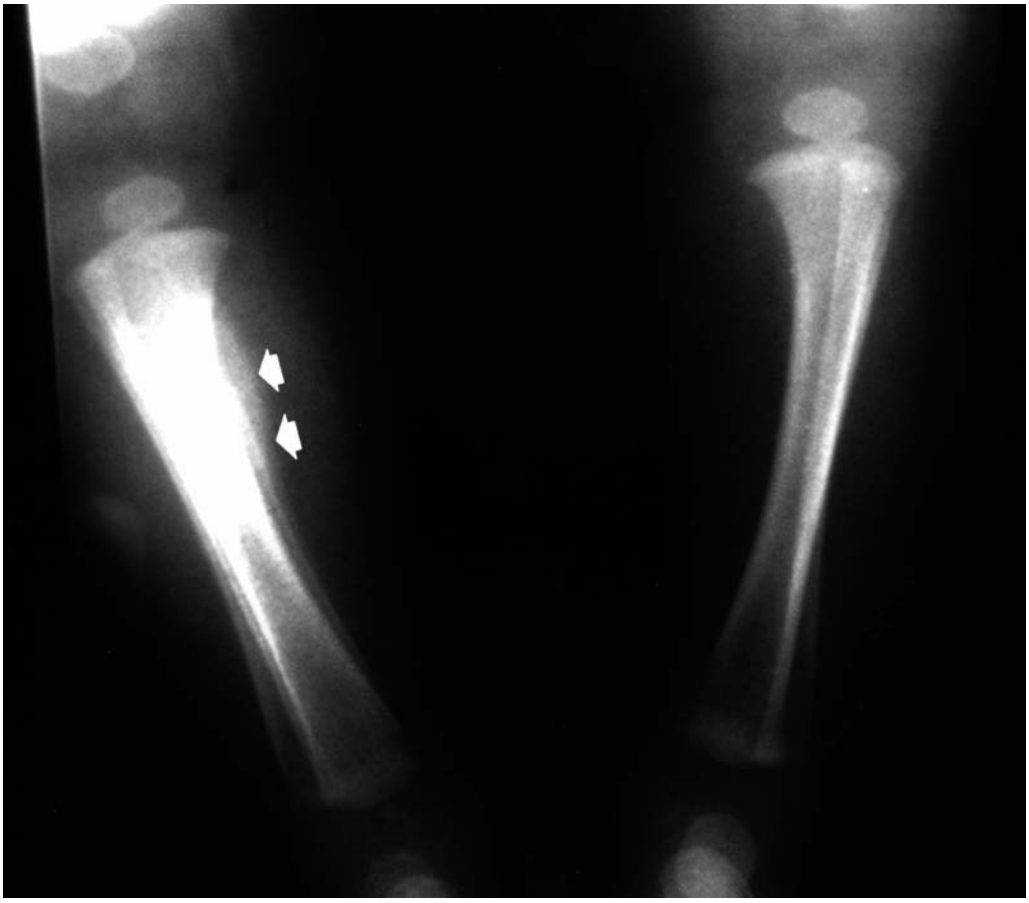

Fig. 60. Tibial periostitis in a case of Caffey's disease. Reprinted from Brogdon, BG, Forensic radiology (1998) with permission from CRC Press.

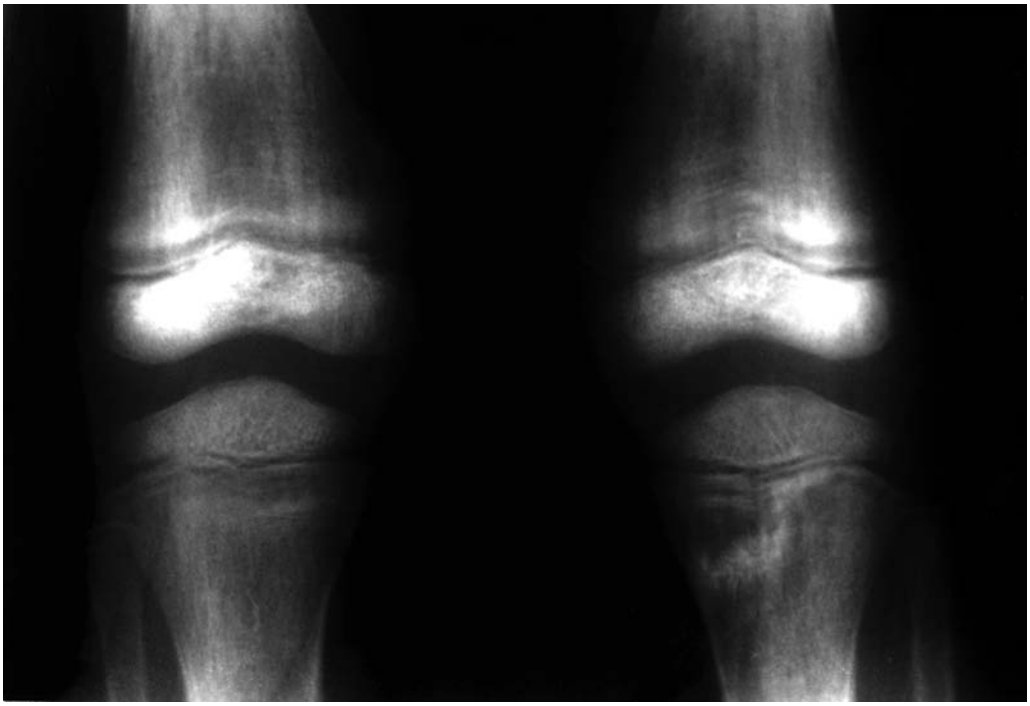

Fig. 61. Leukemic bone changes in a child, characterized by rarifaction just beneath the zone of provisional calcification, as well as periostitis. Reprinted from Brogdon, BG, Forensic radiology (1998) with permission from CRC Press.

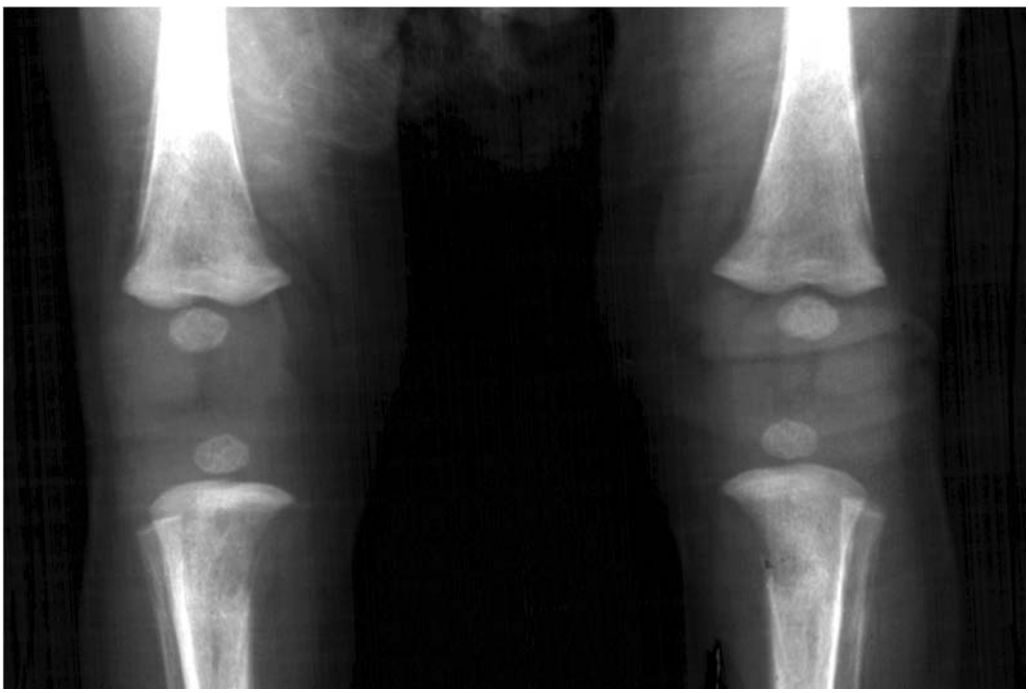

Fig. 62. Congenital syphilis with periostitis and focal destructive lesions in the metaphysis.

Fig. 63. Fracture of the talar neck in a young woman who had a head-on collision while driving an automobile. She believed she jammed her foot against the brake pedal.

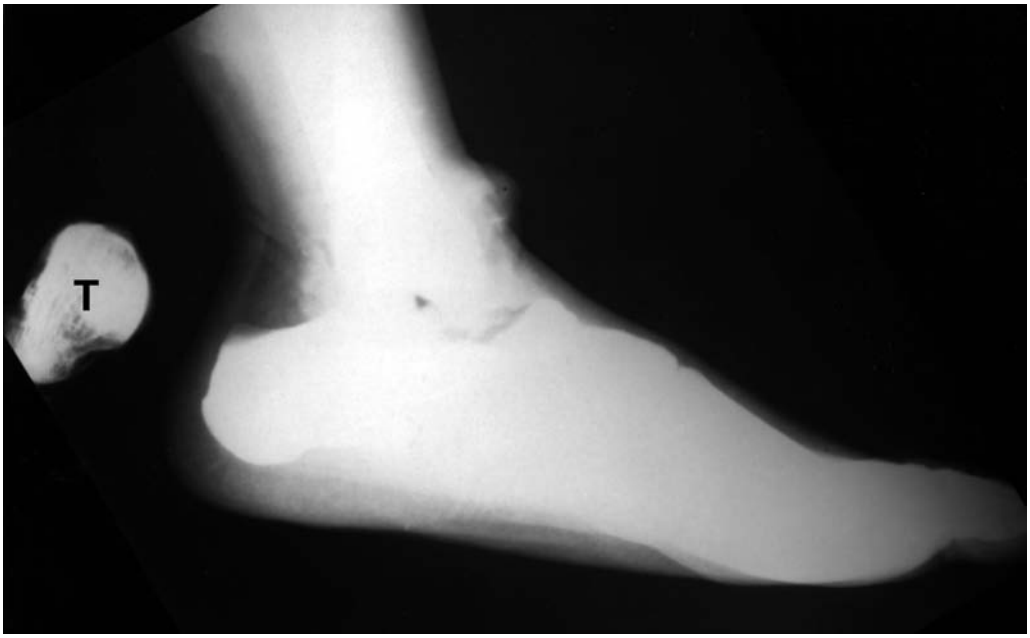

Fig. 64. Extrusion of the talus in a man who was driving a beverage truck that became involved in a collision. The X-ray technologist noted a peculiar bulge in his sock and took the radiograph without removing it. It shows a nearly complete talus with perhaps a minor fragment remaining in situ. This was reported informally as a posterior extrusion. We have not been able to confirm this but believe it likely, because the Achilles tendon shadow is not observed on the radiograph. If so, this is the rarest form of talar extrusion. Reprinted from ref. *48* with permission from CC Thomas.

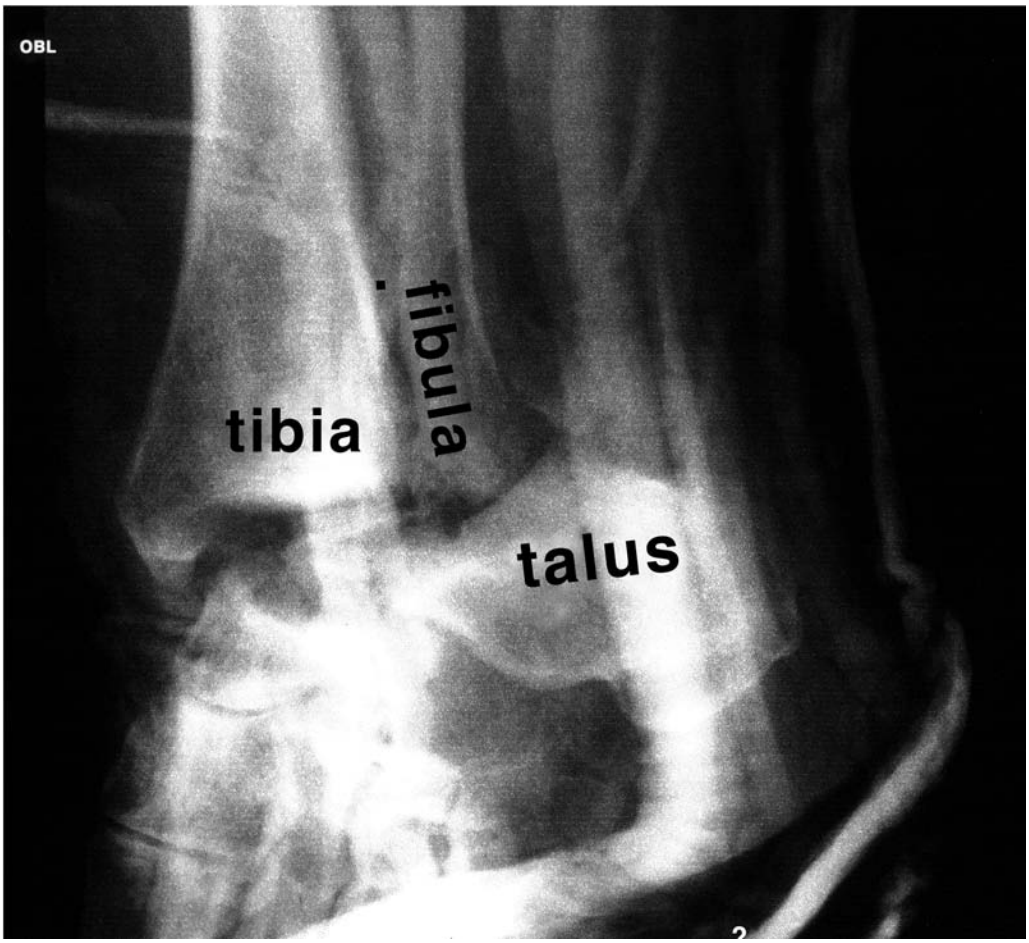

Fig. 65. Anterolateral fracture/extrusion of the talus in a driver involved in a roll-over automobile accident. Anterolateral extrusion indicates supination and extension of the foot. Courtesy Jeremy Rich, DPM.

Fig. 66. Total absence of the talus, which was extruded anteromedially during a motorcycle accident. Courtesy Christopher Cenac, MD.

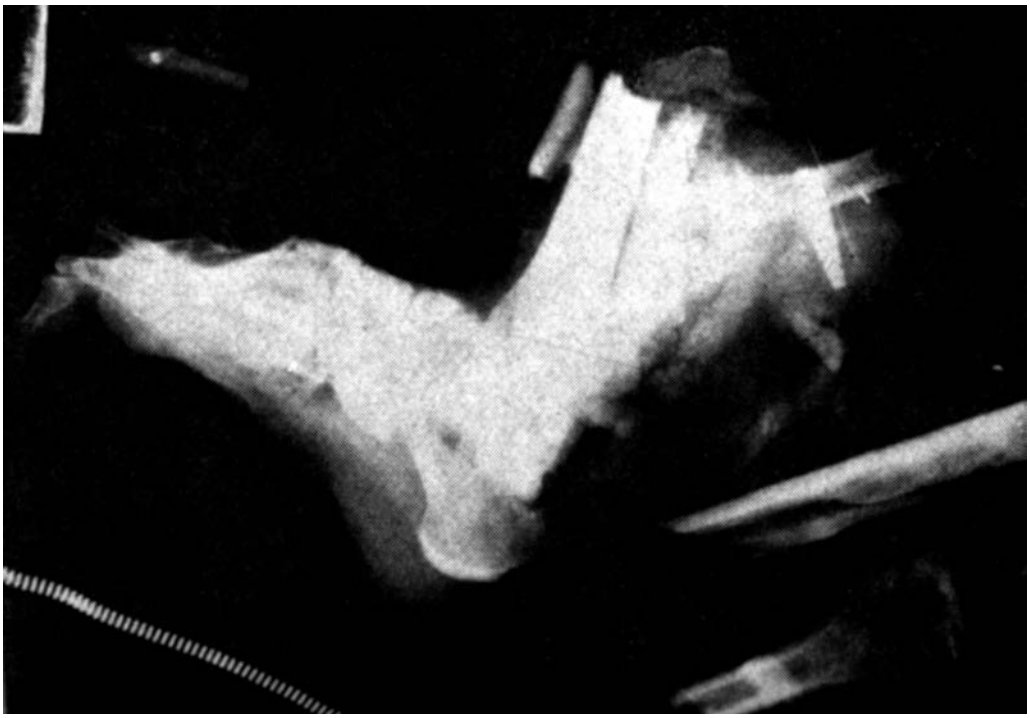

Fig. 67. "Aviator's foot." Plantar invagination of the foot, with multiple fracture dislocations of the midfoot and hindfoot caused by impact with the rudder bar at the time of a crash that was the result of an inverted spin. Reprinted from ref. *54* with permission.

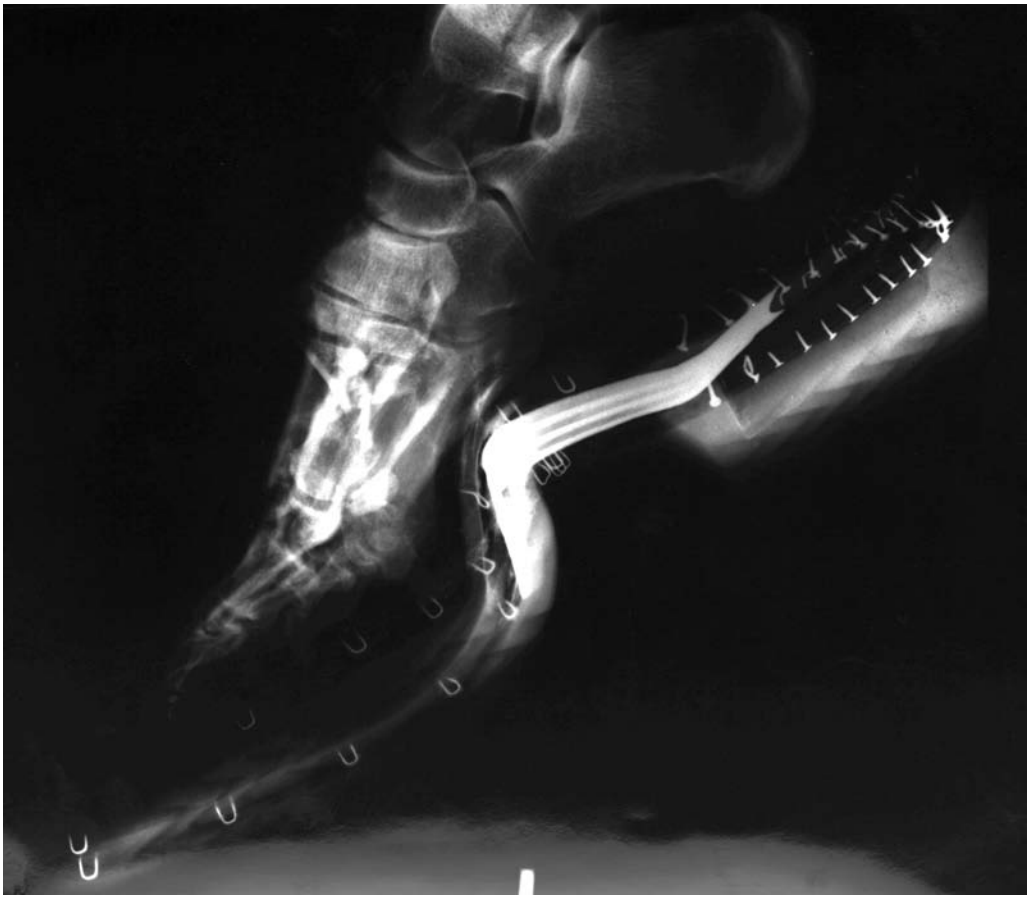

Fig. 68. This heavy flying boot was deformed by the rudder pedal at the time of a crash but protected the flyer from "aviator's foot."

Fig. 69. Divergent Lisfranc fracture/dislocation, with fractures and subluxation of the lateral rays away from the first metatarsal.

Fig. 70. "Bumper fracture." This pedestrian was struck from the right side by an automobile. The impact produced angulated fractures pointing away from the point of impact. The level of the fractures is consistent with the height of the bumper.

Fig. 71. Close-up of the midshafts of the tibia and fibula of a victim of palmatoria. The anterior cortex of the tibia is thickened by periostitis and there are peculiar endosteal and intramedullary changes. Reprinted from Brogdon BG, Vogel H, McDowell JD, eds. A radiologic atlas of abuse, torture, terrorism, and inflicted trauma (2003) with permission from CRC Press.

Fig. 72. A young man was struck on the shin with a metal rod. He sustained a laceration that was irrigated and sutured. **(A)** A worrisome finding on the radiograph prompted his being recalled to the hospital, where the wound was reopened and explored to reveal an intact periosteum. **(B)** A CT scan revealed a cone-shaped endosteal fracture fragment beneath an intact, slightly dimpled outer cortex. Reprinted from ref. *58* with permission from the American Roentgen Ray Association.

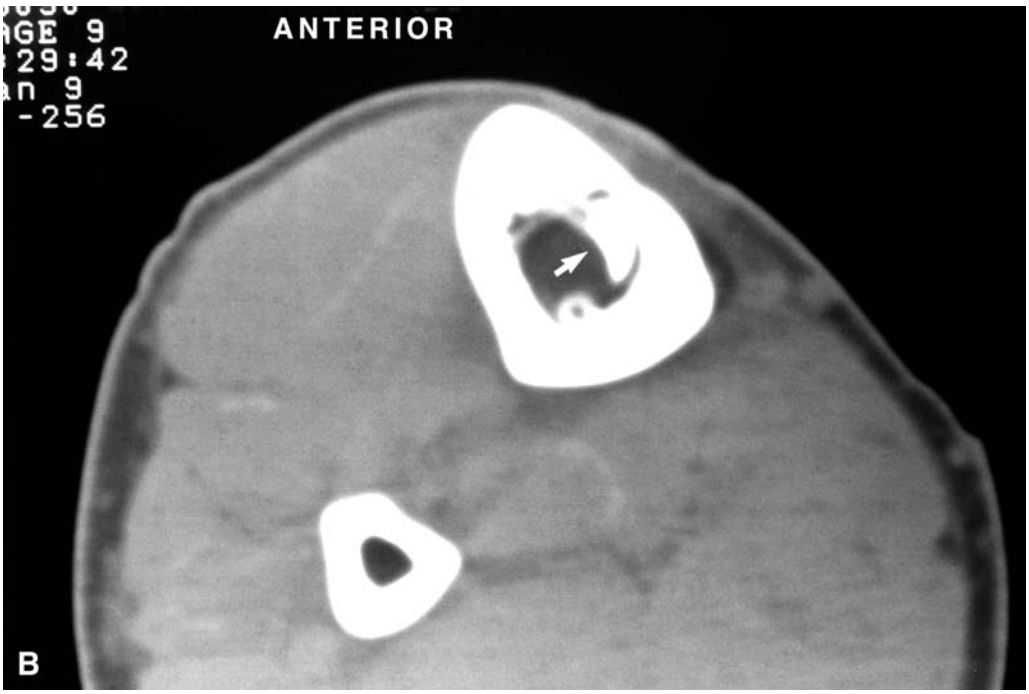

Fig. 72. *Continued.*

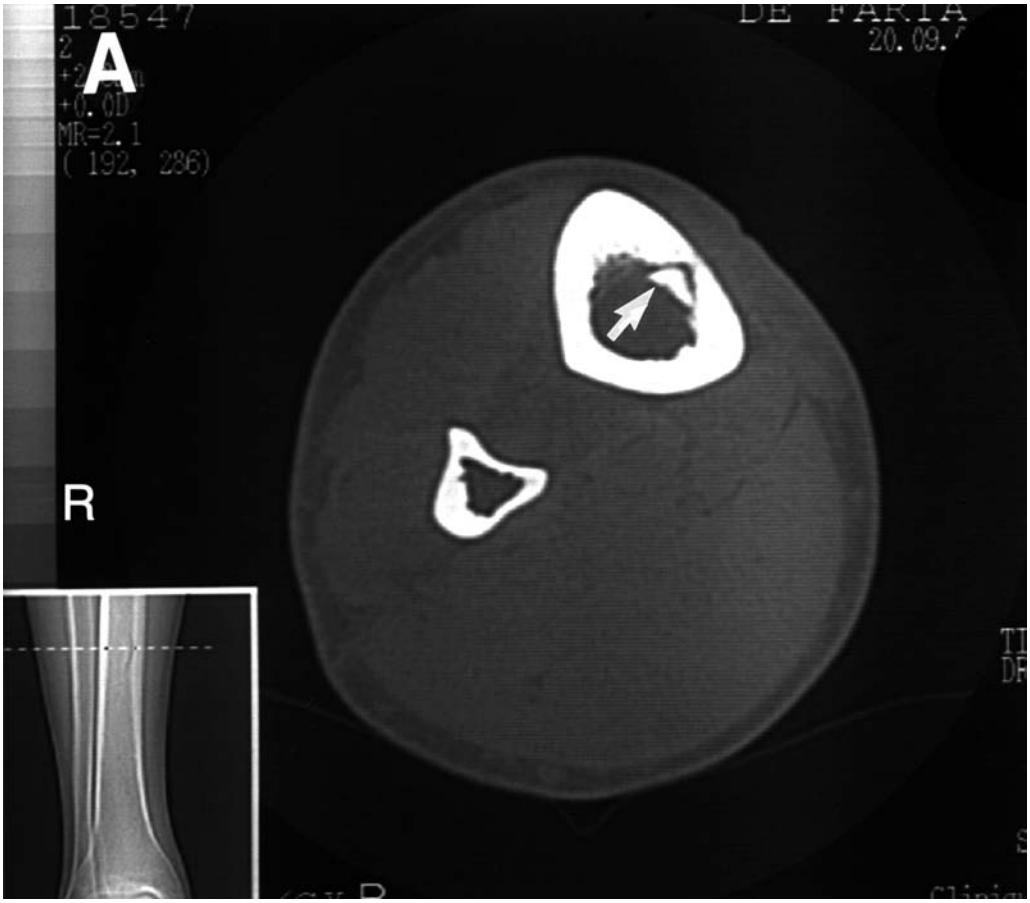

Fig. 73. Another young man struck on the shin with a metal rod. This presents findings identical to those in Fig. 72. **A.** Internal endosteal fracture fragment (arrow). **B.** Longitudinal reconstruction demonstrating the endosteal fragment (arrow). Courtesy of Daniel Vanel, MD. Reprinted from ref. *57* with permission from the American Roentgen Ray Society.

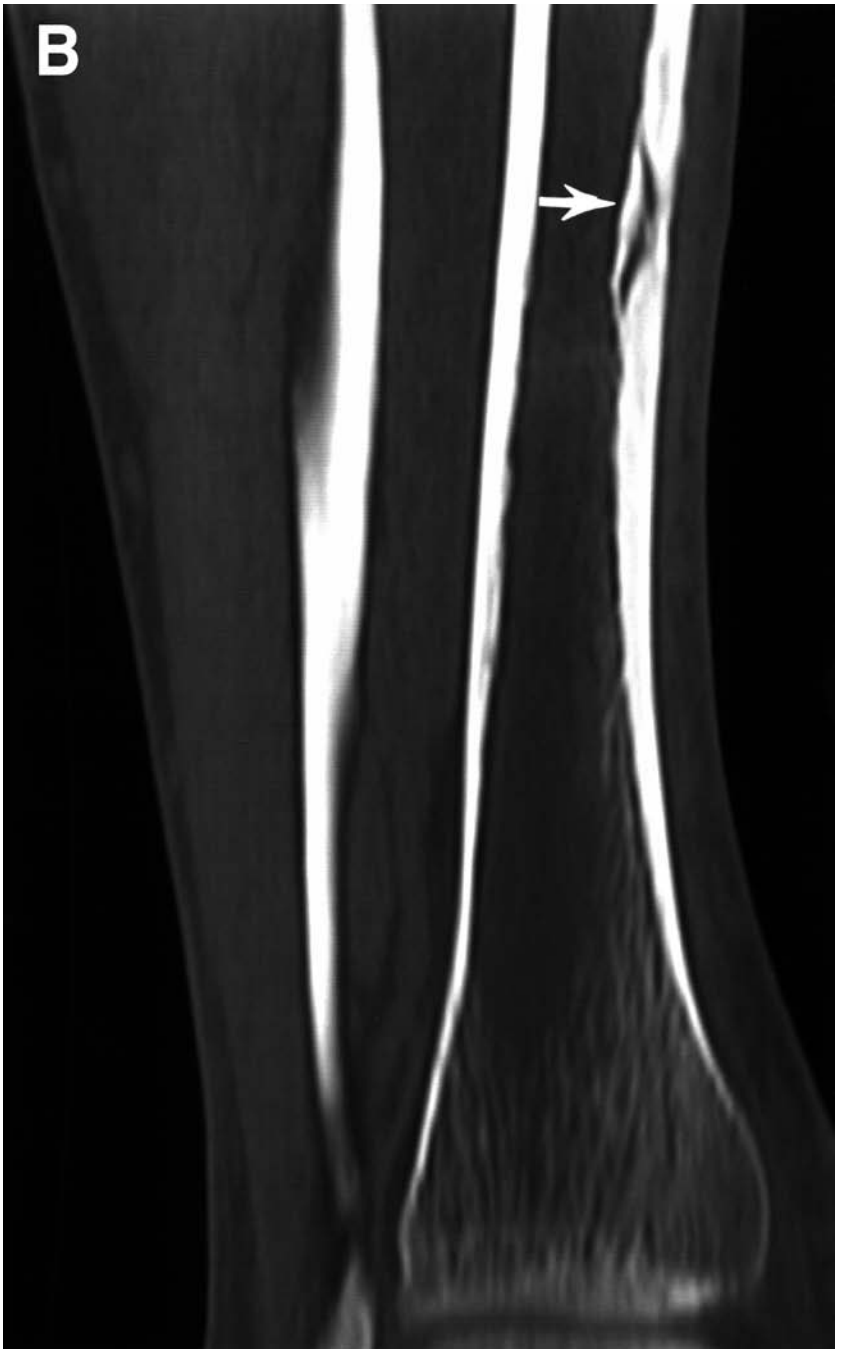

Fig. 73. *Continued.*

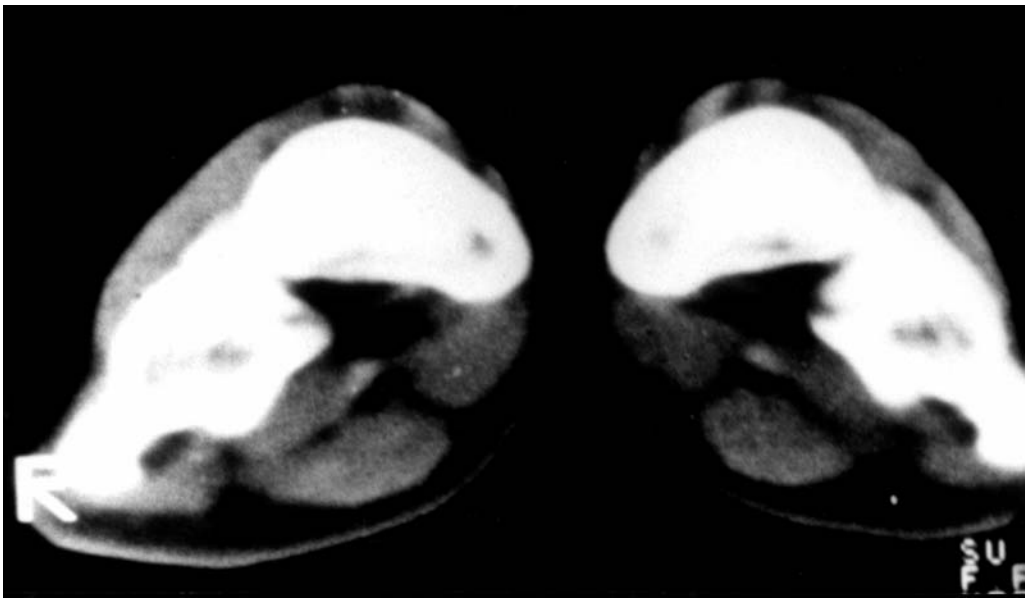

Fig. 74. Bilateral plantar edema and hematomas of the feet after falaca, as demonstrated by CT. Reprinted from ref. *42* with permission from ecomed verlagsgesellschaft mbH.

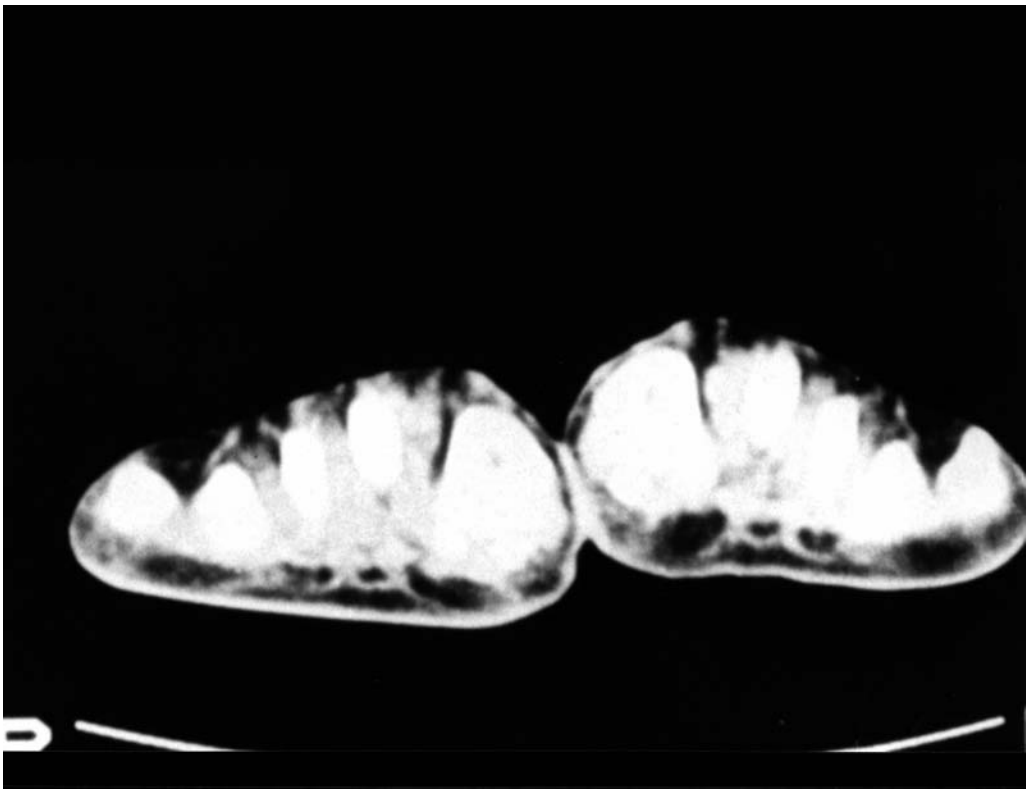

Fig. 75. CT demonstrates chronic changes after falaca: splay- and flat-foot deformities due to relaxed ligaments and aponeurosis. Reprinted from ref. *42* with permission from ecomed verlagsgesellschaft mbH.

Fig. 76. Multiple fractures of the calcaneous, sustained during falaca, now healed with residual deformity. Reprinted from ref. *42* with permission from ecomed verlagsgesellschaft mbH.

Fig. 77. "Knee capping." **A.** Photograph of a shotgun exit wound from a knee capping in Northern Ireland. **B.** Lateral radiograph of knee-capping wound just above the knee. Notice how the elastic skin contains many of the small shots. There is massive soft tissue and bony injury. Reprinted from Brogdon, BG, Forensic radiology (1998) with permission from CRC Press.

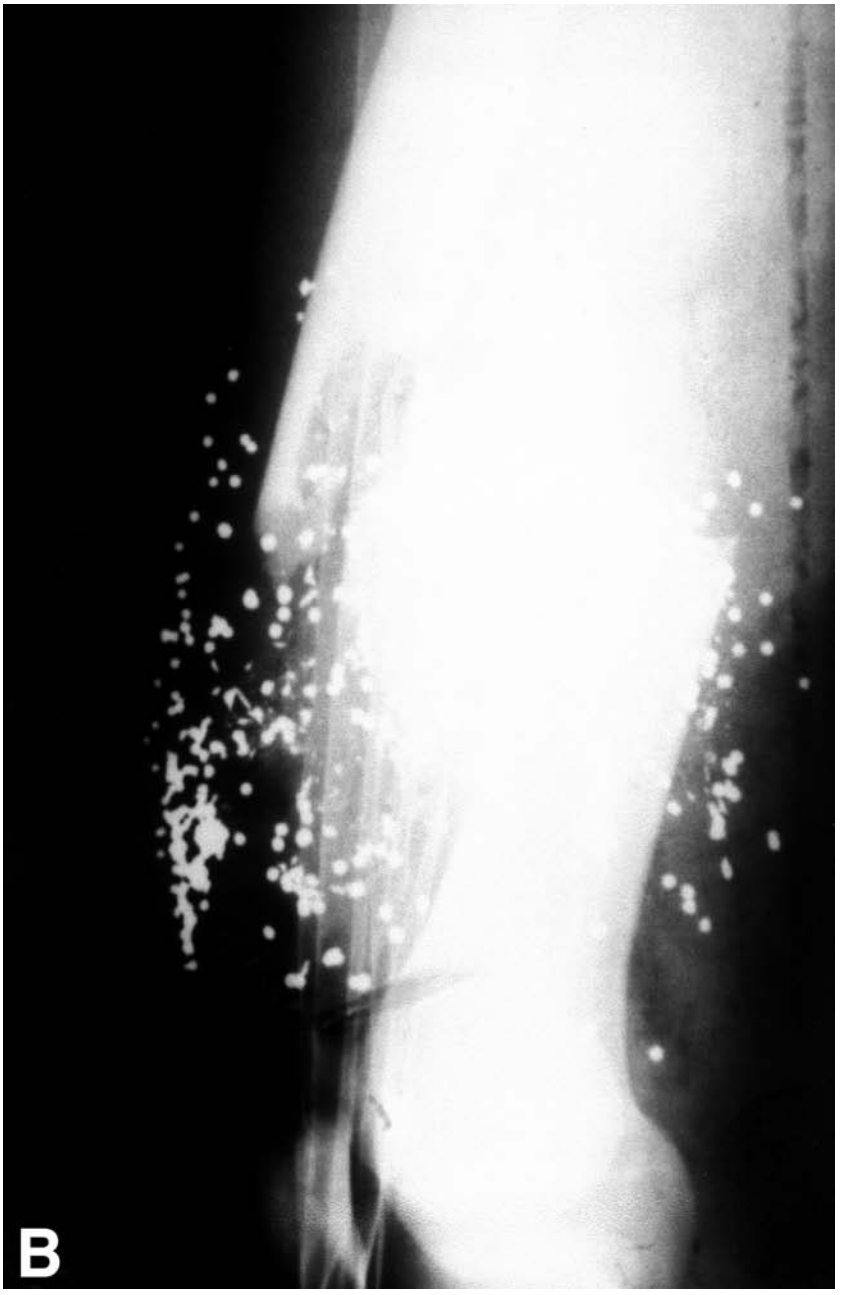

Fig. 77. *Continued.*

Fig. 78. A lateral radiograph shows total destruction of the subtalar joint. The anterior half of the talus is missing. Bullet fragments remain in the area. "Knee capping" in another major joint. Reprinted from ref. *42* with permission from ecomed verlagsgesellschaft mbH.

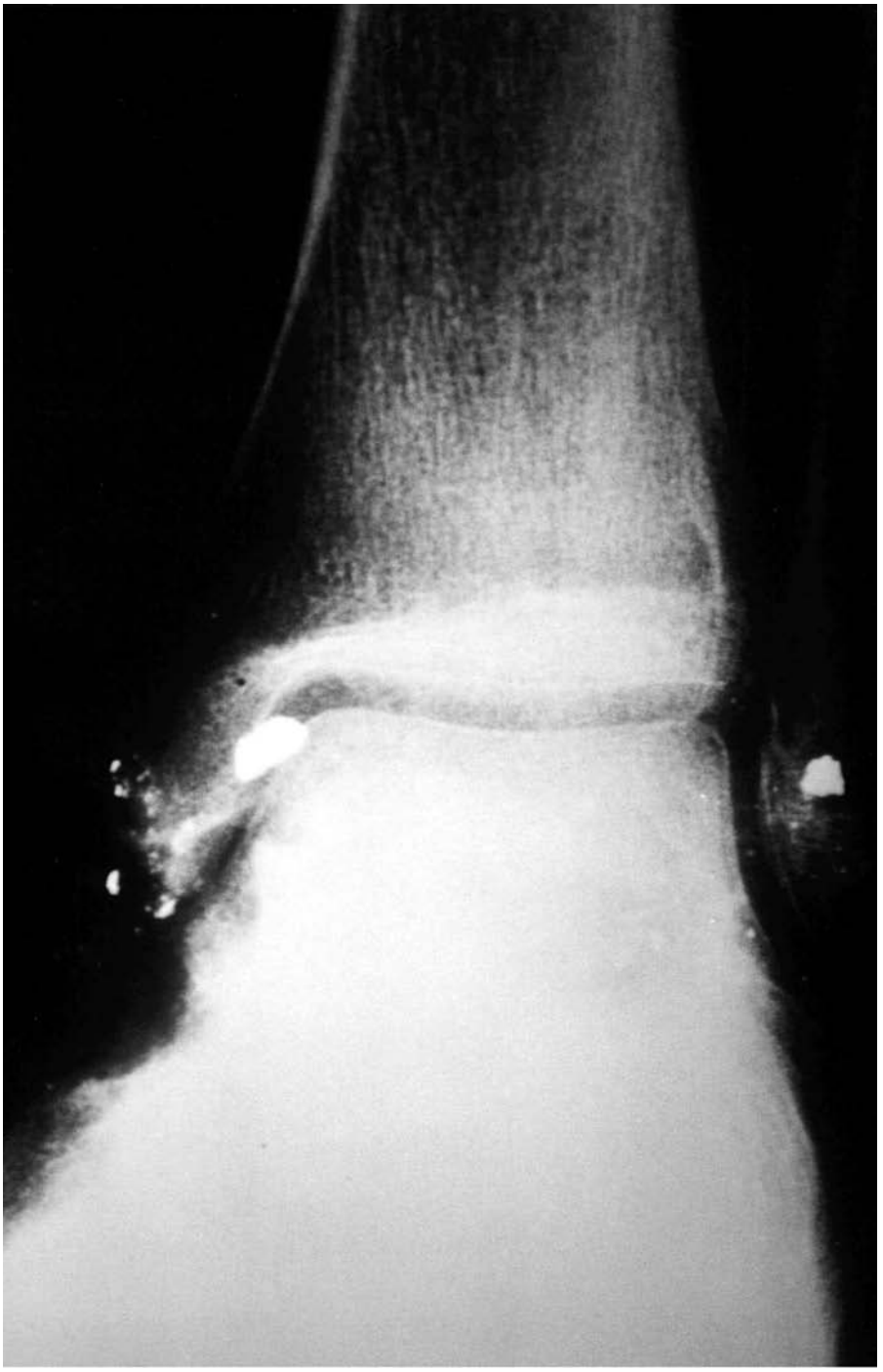

Fig. 79. AP view of an ankle shot with a low-velocity bullet as a punitive injury. Bullet fragments remain near the medial and lateral malleoli. Reprinted from ref. *42* with permission from ecomed verlagsgesellschaft mbH.

Fig. 80. High-velocity gunshot wound just above the elbow, producing massive destruction of the distal humerus. This is another punishment gunshot of the "knee-capping" variety. Reprinted from ref. *42* with permission from ecomed verlagsgesellschaft mbH.

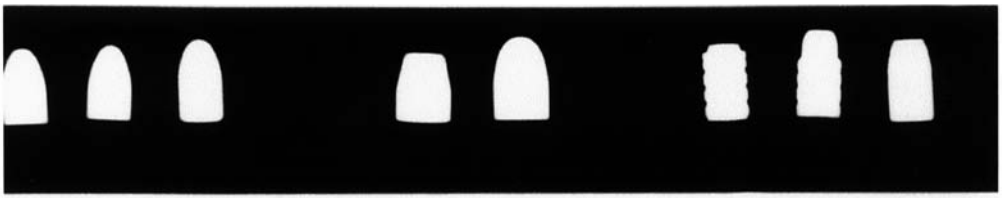

Fig. 81. Radiograph of several low-velocity bullets in profile shows a group of 9-mm bullets on the left; .45 caliber in the middle, and .38 caliber on the right. There is little difference in their size, and even with slight variation in magnification, the difference is very difficult, or impossible, to detect Reprinted from ref. *42* with permission from ecomed verlagsgesellschaft mbH.

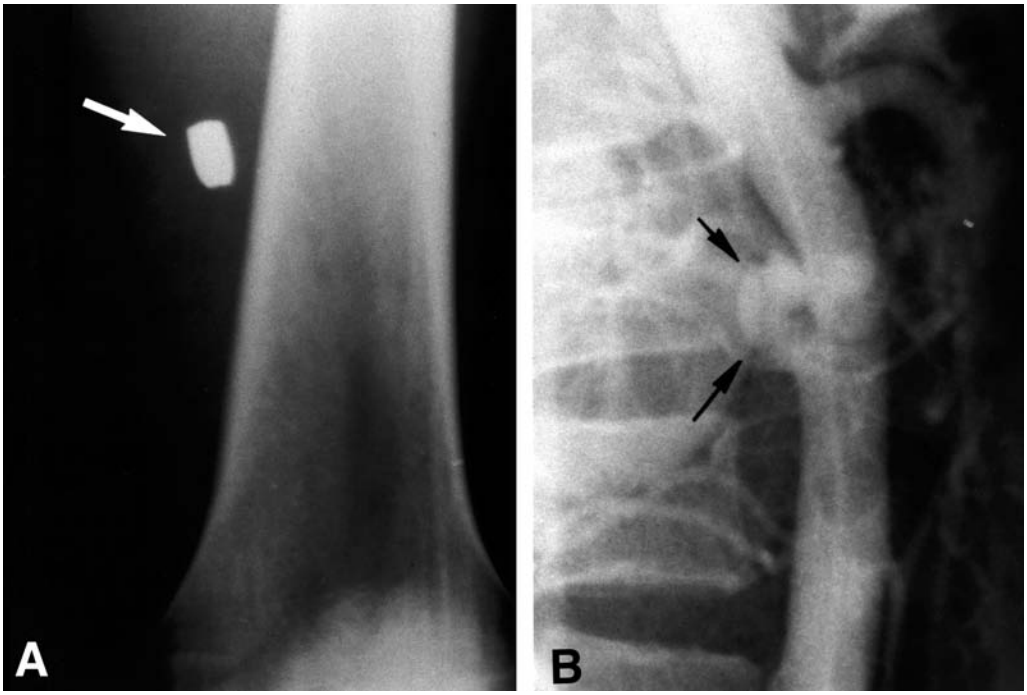

Fig. 82. This person sustained a gunshot wound in the left flank, but radiography of the area disclosed no bullet. **A.** The bullet was found after it obstructed blood flow to the lower extremity by lodging in the superficial femoral artery. **B.** Lateral aortogram shows a pseudoaneurysm (arrows) on the posterior wall of the aorta where the bullet entered the arterial flow. Reprinted from Brogdon, BG, Forensic radiology (1998) with permission from CRC Press.

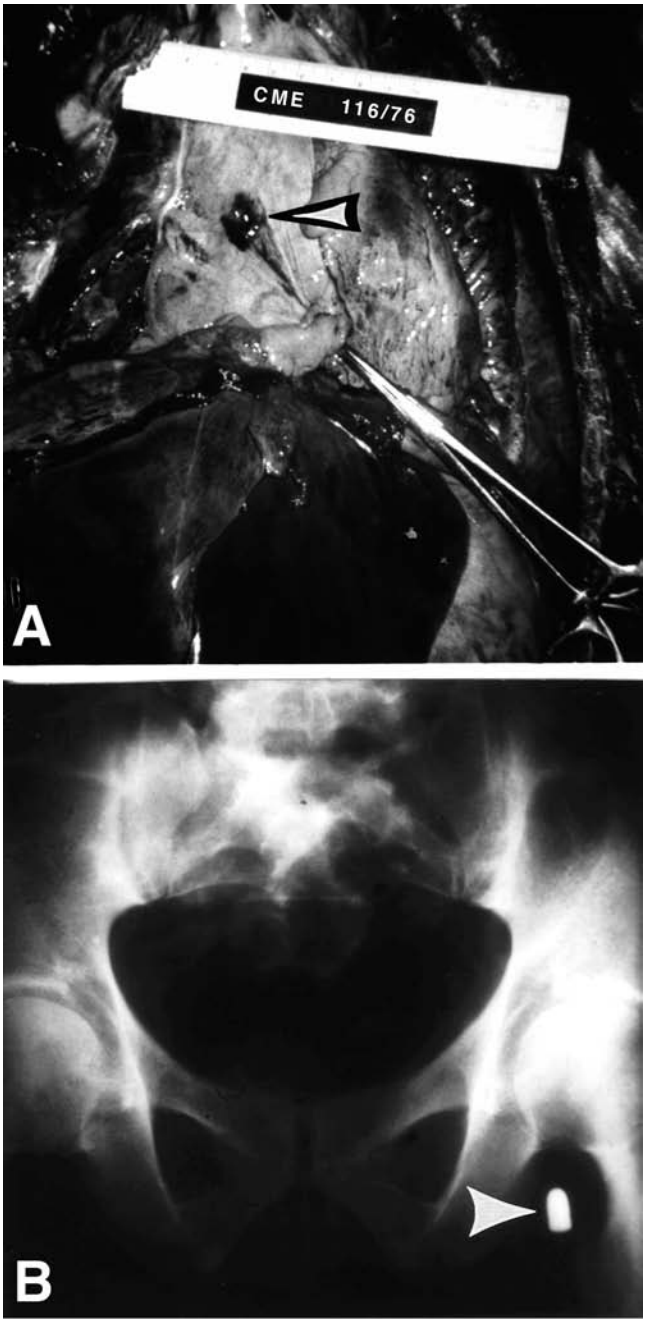

Fig. 83. A. A chest radiograph had revealed no bullet, but the autopsy showed a gunshot wound to the anterior surface of the heart (arrowheads). **B.** Radiographic search displayed the bullet in the left groin where dissection showed it to lie within the left femoral artery. Reprinted from ref. *65* with permission from the Radiological Society of North America.

Fig. 84. Radiograph of the shoulder shows a shattered upper humerus with scattered bone and lead fragments along the path of the bullet before it came to rest in the chest. Of interest is the less dense large piece of jacketing (arrowheads) lying next to the largest bullet fragment. This jacket fragment will contain valuable ballistic information. Reprinted from Brogdon, BG, Forensic radiology (1998) with permission from CRC Press.

Fig. 85. (A) A low-velocity gunshot wound through the femur shows a circular entry wound (arrowhead) with surrounding radial fractures. **(B)** The frontal view, somewhat enlarged, shows a small cloud of bone splinters extending into the soft tissues from the exit point of this fully jacketed bullet. Note that there are no metallic fragments. Reprinted from ref. *42* with permission from ecomed verlagsgesellschaft mbH.

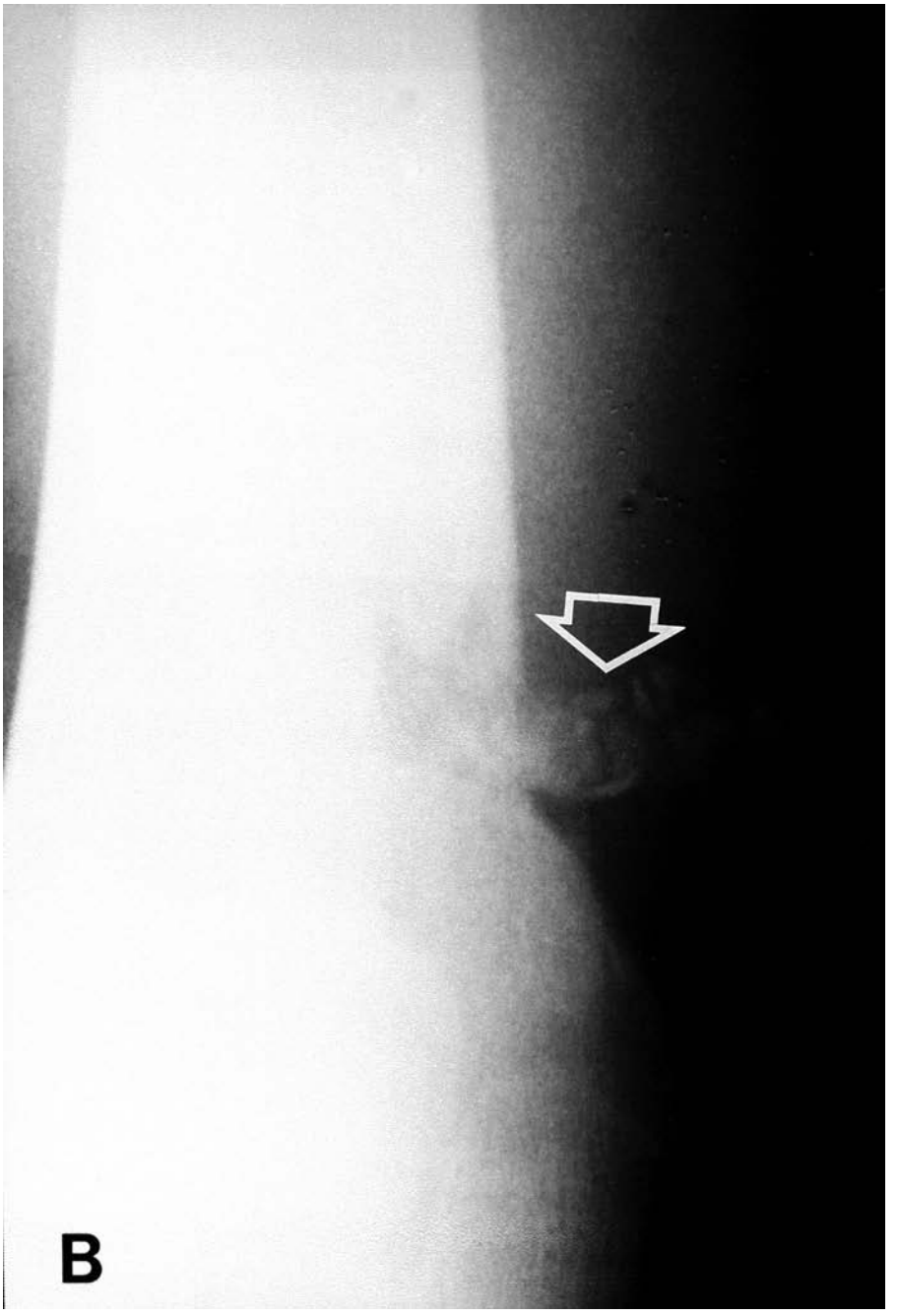

Fig. 85. *Continued.*

Fig. 86. A high-velocity jacketed bullet, fired from a military weapon, carried away almost the entire talus and a portion of the distal tibia, leaving no small bone or bullet fragments. Reprinted from ref. *42* with permission from ecomed verlagsgesellschaft mbH.

Fig. 87. A lateral view of the thigh shows two "rubber" bullets embedded in the soft tissues. One can differentiate the halo of the rubber coating surrounding the metallic core of the projectile. Reprinted from ref. *42* with permission from ecomed verlagsgesellschaft mbH.

Fig. 88. This totally shattered femoral shaft was hit with a ceramic bullet, which disintegrated into the tiny bright fragments seen among the less dense bone fragments. Reprinted from ref. *42* with permission from ecomed verlagsgesellschaft mbH.

Table 3
Technique Chart

Region	Projection	Thickness, cm	mAs	kVp	Grid	Distance, in
Hip	Frontal	15–20	40	76	Yes	40
		21–25	60	76		
		26–31	100	80		
Femur	Frontal	15–18	25	72	Yes	40
	Lateral	14–17	25	70	Yes	40
Knee	Frontal	10–13	20	60–70	Yes	40
	Lateral	9–12	20	62–66	Yes	40
Leg	Frontal	9–13	3	66–70	Yes	40
	Lateral	8–12	3	62–66	Yes	40
Foot/Ankle	Frontal	5/8	3	60–62	No	40
	Lateral	6–9	3	64–66	No	40

Note: For tissues filled with gas, or incinerated or dehydrated tissue decrease mAs by 30% or decrease kVp by 6-8 cm. Defleshed bones require mAs to be reduced by half and kVp to be reduced to 50 (non-grid). Modified from ref. *67*, with permission from CRC Press.

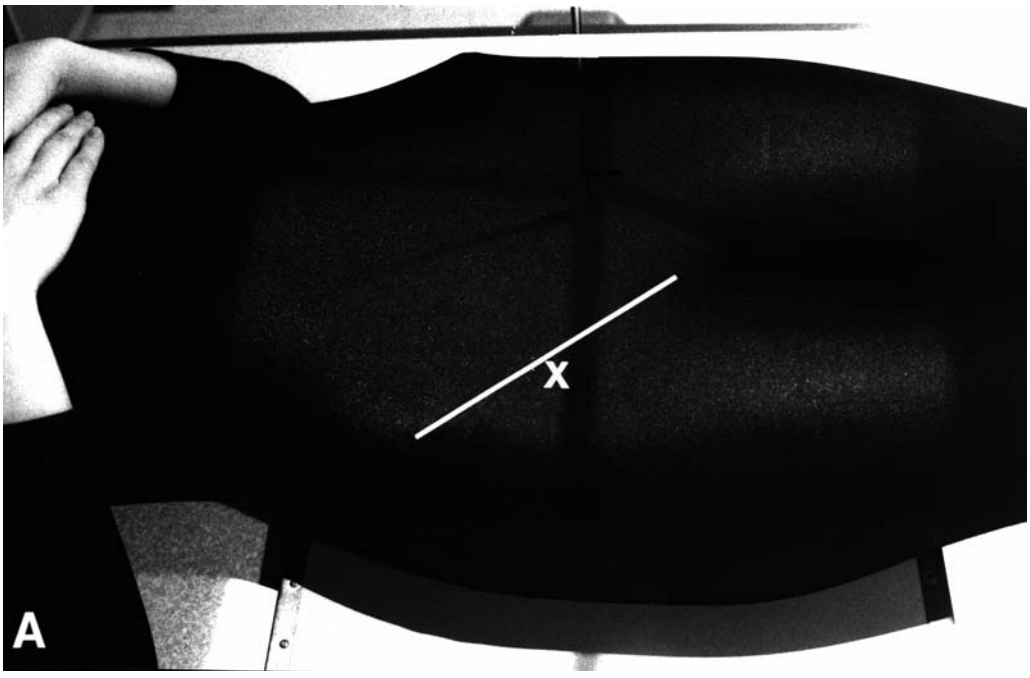

Fig. 89. **(A)** Position for frontal radiograph of the hip. The central ray should be directed at the midpoint (X) of the line drawn from the pubic symphysis to the anterior superior iliac spine. **(B)** Resultant radiograph. Reprinted from Brogdon, BG, Forensic radiology (1998) with permission from CRC Press.

Fig. 89. *Continued.*

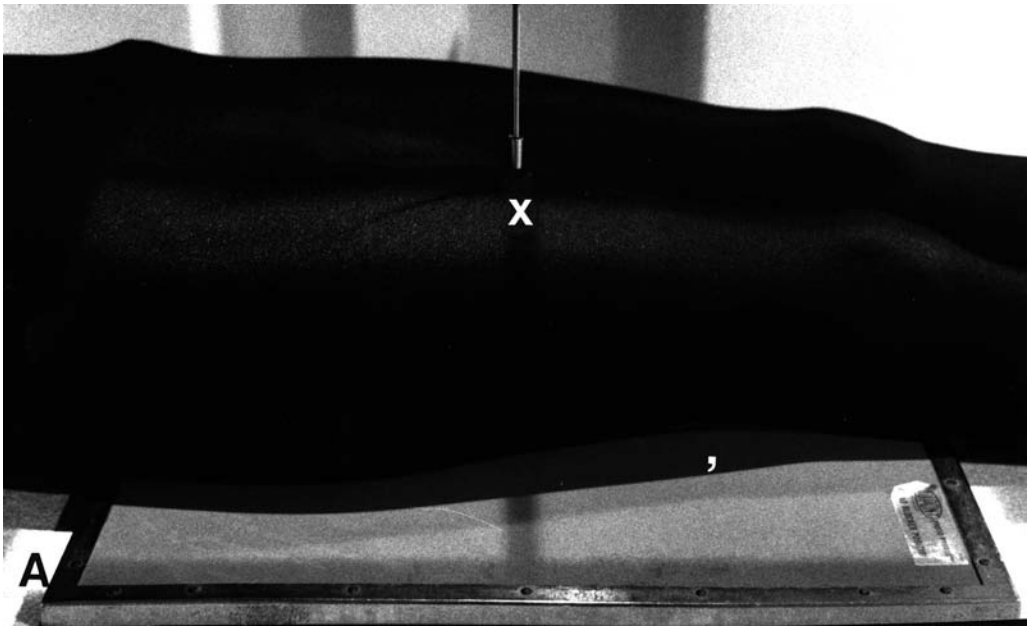

Fig. 90. (A) Position of the thigh, central beam, and cassette for a frontal view of the femur. **(B)** Resultant radiograph. Reprinted from Brogdon, BG, Forensic radiology (1998) with permission from CRC Press.

Fig. 90. *Continued.*

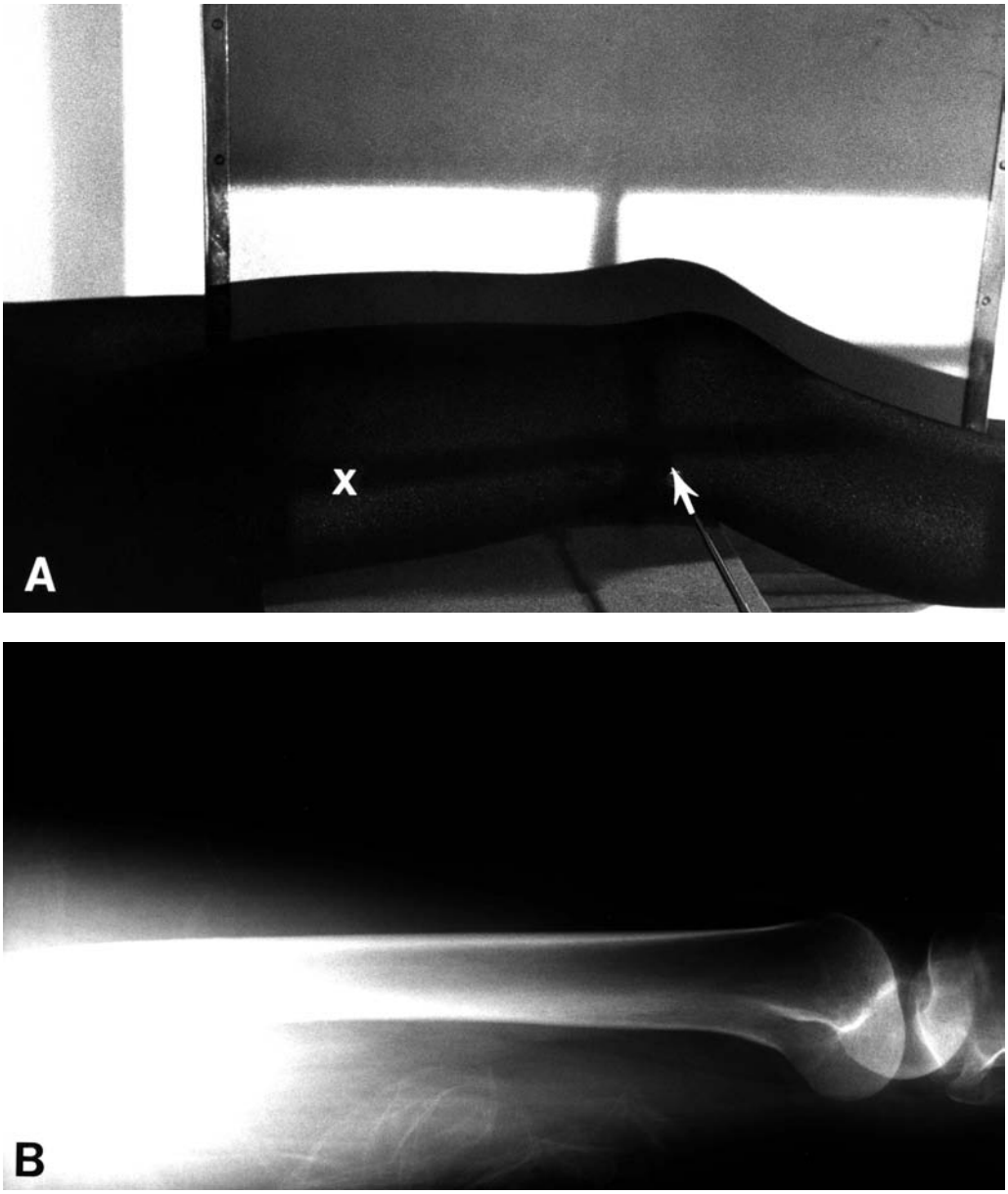

Fig. 91. **(A)** Positioning for a lateral view of the thigh or knee. For the thigh, the central beam should enter at the X and the cassette, standing upright, should be moved farther toward the patient's head than shown here. The cassette is in the proper position for a lateral knee view, with the central beam entering at the site of the arrow. **(B)** Lateral radiograph of the femur. **(C)** Lateral radiograph of the knee. Reprinted from Brogdon, BG, Forensic radiology (1998) with permission from CRC Press.

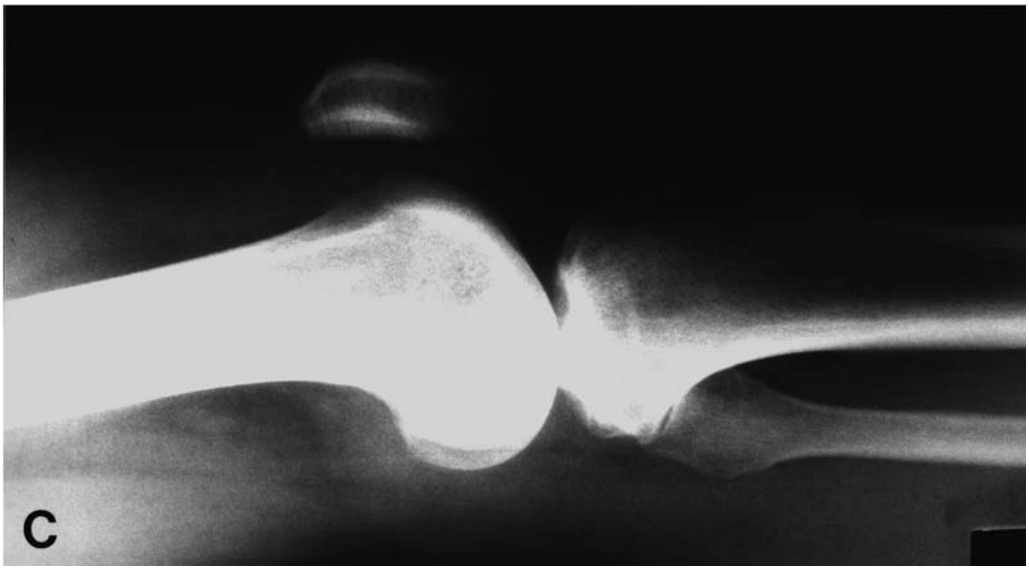

Fig. 91. *Continued.*

Fig. 92. **(A)** Positioning for frontal view of the knee. **(B)** Resultant radiograph. Reprinted from Brogdon, BG, Forensic radiology (1998) with permission from CRC Press.

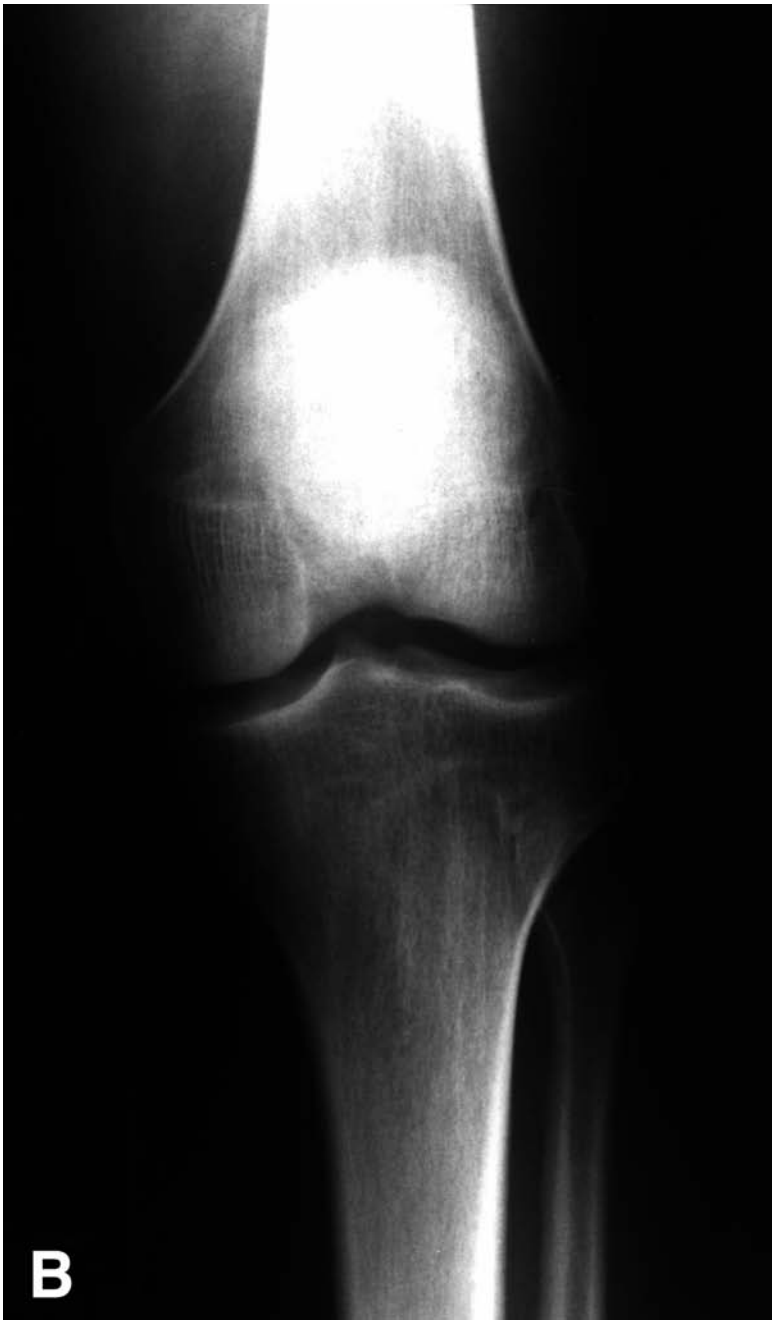

Fig. 92. *Continued.*

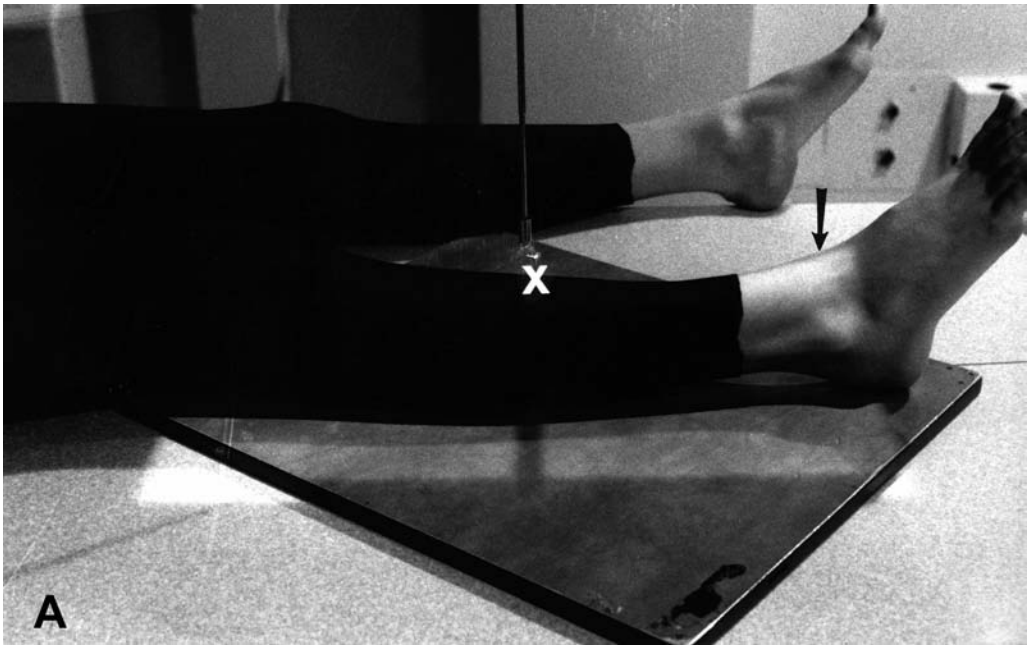

Fig. 93. Position for a frontal view of the leg with the central beam entering at point X. **(A)** Frontal view of the ankle could be obtained by moving the central beam to the arrow and the cassette downward appropriately. **(B)** Frontal radiograph of the leg. Frontal view of the ankle (arrow) would be better demonstrated if the central beam were directly over it, as shown by the position of the arrow in **(A)**. Reprinted from Brogdon, BG, Forensic radiology (1998) with permission from CRC Press.

Fig. 93. *Continued.*

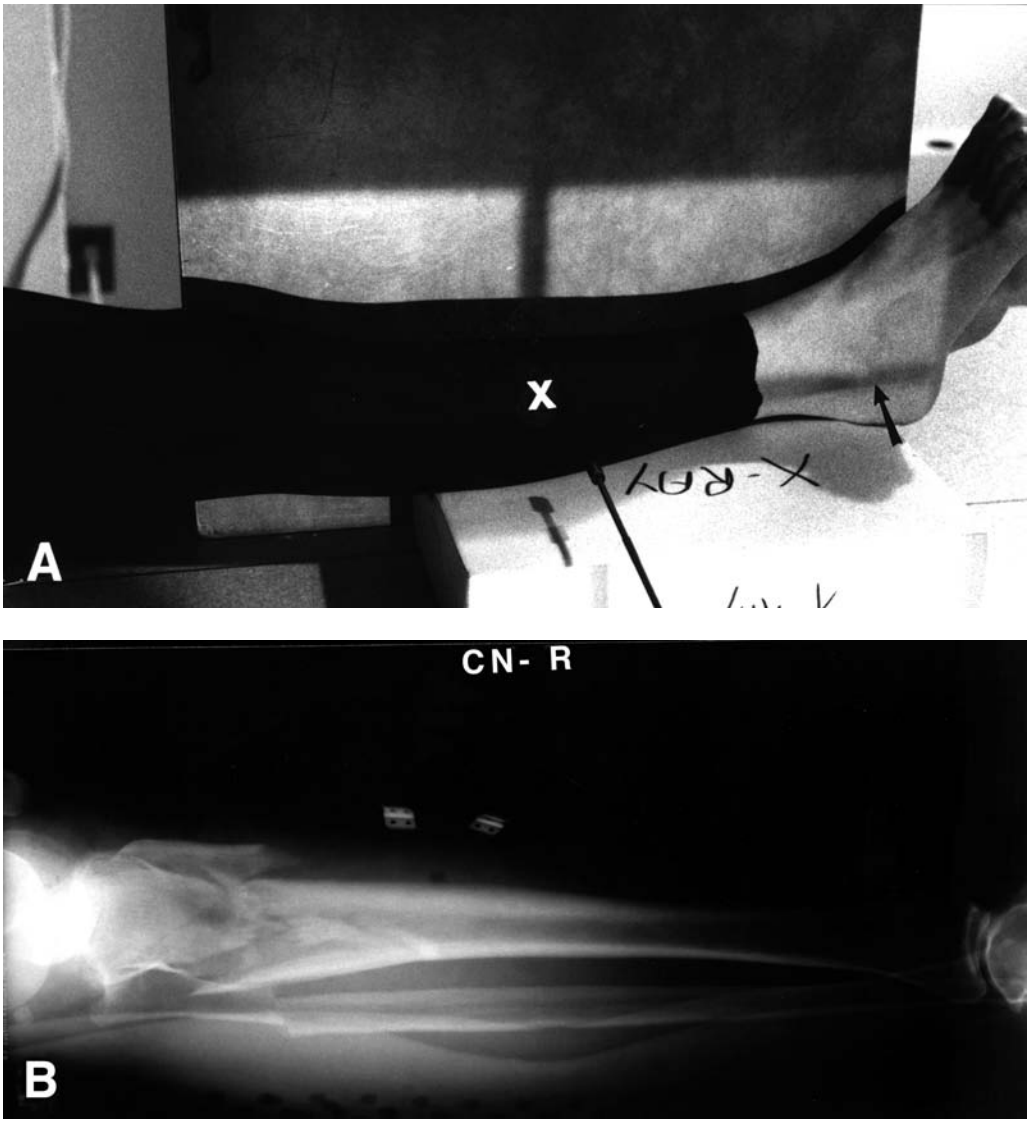

Fig. 94. **(A)** Positioning for a cross-table lateral view of the leg against an upright cassette with the central beam entering at point X. **(B)** Resultant radiograph shows a comminuted fracture of the proximal tibia. Reprinted from Brogdon, BG, Forensic radiology (1998) with permission from CRC Press.

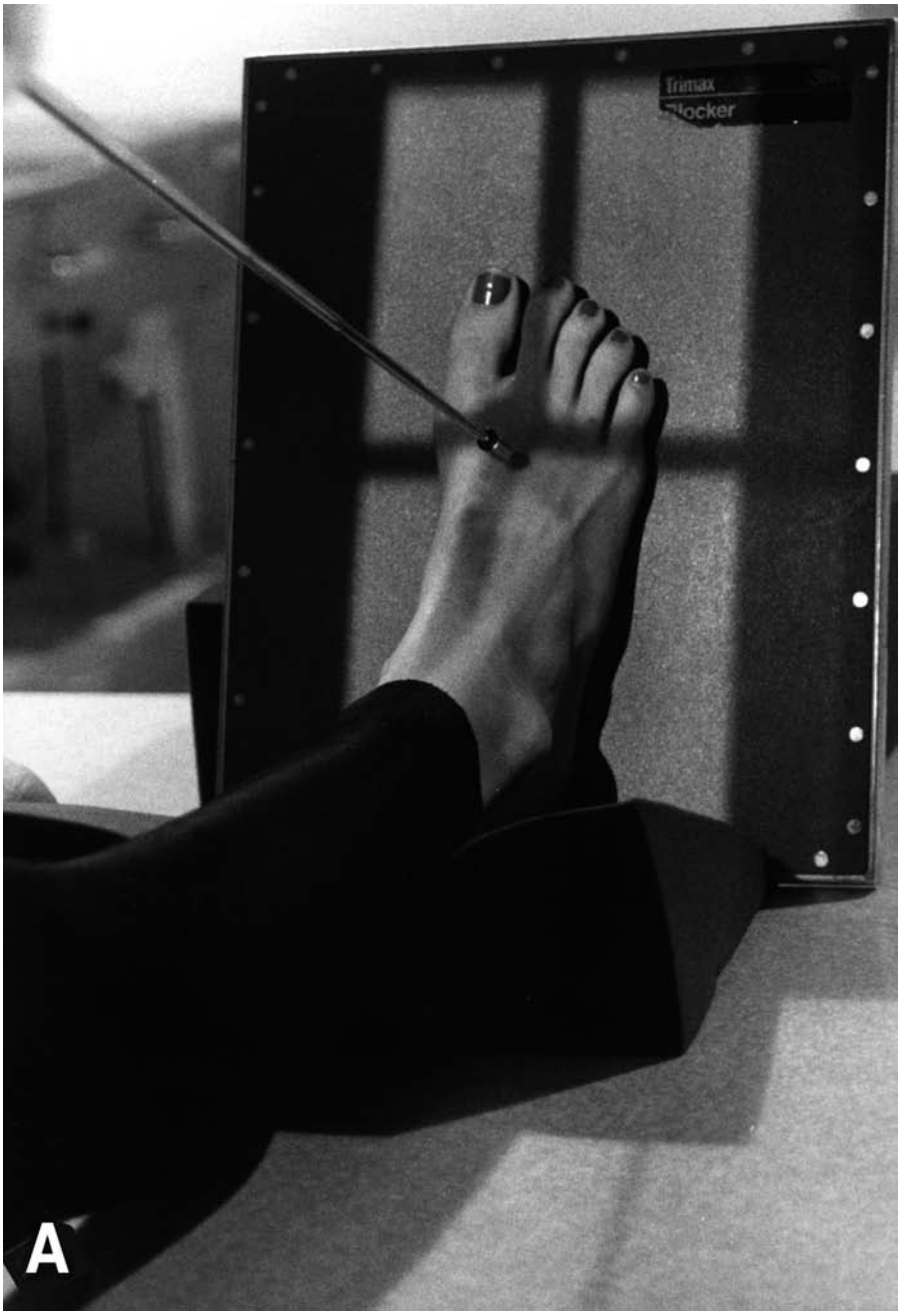

Fig. 95. **(A)** Positioning for frontal view of the foot. **(B)** Resultant radiograph. Reprinted from Brogdon, BG, Forensic radiology (1998) with permission from CRC Press.

Fig. 95. *Continued.*

Fig. 96. **(A)** Positioning for cross-table lateral view of the foot or ankle with the cassette held vertically. The central ray is directed at the mid-tarsal area (X) for optimal visualization of the foot. For optimal visualization of the lateral ankle, the central ray should be directed at the lateral malleolus (arrow). **(B)**. Lateral radiograph of the foot, showing a tarsal navicular fracture/dislocation. Reprinted from Brogdon, BG, Forensic radiology (1998) with permission from CRC Press.

Fig. 96. *Continued.*

References

1. Glasser O. Wilhelm Conrad Röntgen and the early history of the roentgen rays, Springfield, Ill: Charles C. Thomas, 1934.
2. Linton, OW. News of X-ray reaches America days after announcement of Roentgen's discovery. Am J Roent 165:471–472 (1995).
3. Brecher R, Brecher E. The rays: a history of radiology in the United States and Canada, Baltimore, Md: Williams and Wilkins, 1969.
4. Halperin EC. X-rays at the bar: 1986–1910. Invest Radiol 23:639–646(1988).
5. Cox J, Kirkpatrick RC. The new photography with report of a case in which a bullet was photographed in the leg. Montreal Med J 24:661 (1896).
6. Glasser O. First roentgen evidence. Radiology 17:789–791 (1931).
7. Anon. Literary digest. 12:707 (1896).
8. Collins VP. Origins of medico-legal and forensic roentgenology. In: Bruwer AJ, ed. Classic descriptions in diagnostic radiology. Vol. 2. Springfield, Ill: Charles C. Thomas, 1964:1578–1609.
9. Pear BL. The first year of X-rays in Colorado. Am J Roentgenol 165:1075–1078 (1995).
10. Withers S. The story of the first roentgen evidence. Radiology 17:99–103 (1931).
11. Anon. Associated Press release, Mobile Register, January 4, 1989, 1D.
12. Berlin L. Malpractice issues in radiology: the miasmatic expert witness. AJR 181:29–35 (2003).
13. Andrews HG. The medical and surgical aspects of aviation. London: Oxford University Press, 1919.
14. Glaister J, Brash JC. Medico-legal aspects of the Ruxton case. Baltimore: William Word and Co., 1937.
15. Rentoul E, Smith H, eds. Glaister's medical jurisprudence and toxicology. London: Churchill Livingston, 1997:90–98.

16. Caffey J. Multiple factures of the long bones in children suffering from chronic subdural hematoma. AJR 56:163–173 (1946).
17. Singleton AC. The roentgenological identification of victims of the "Noronic" disaster. AJR 66:375–384 (1951).
18. Evans KT, Knight B. Forensic radiology. London: Blackwell, 1981.
19. Brogdon BG. Preface. In: Forensic radiology. Brogdon BG, ed. Boca Raton: CRC Press, 1998.
20. Graham CB. Assessment of bone maturation: methods and pitfalls. Radiol Clin N Am 10:185–202 (1972).
21. Girdany BR, Golden R. Centers of ossification of the skeleton. Am J. Roentgenol 68:922–924 (1952).
22. Sontag IW, Snell D, Anderson, M. Rate of appearance of ossification centers from birth to the age of five years. Am J Dis Child 58:949–956 (1939).
23. Pyle SI, Hoerr NL. Atlas of skeletal development of the knee. Springfield: Charles C. Thomas, 1955.
24. Hoerr NL, Pyle SI, Francis CC. Radiologic atlas of the foot and ankle. Springfield: Charles C. Thomas, 1962.
25. Meschan, I. An atlas of anatomy basic to radiology. Philadelphia: Elsevier, 1975, p. 56.
26. Brogdon BG. Radiological identification: anthropological features. In: Forensic radiology. Brogdon BG, ed. Boca Raton: CRC Press, 1998:63–95.
27. Lawson JP. Clinically significant radiologic anatomic variants of the skeleton. Am J Roentgenol 163:249–255 (1994).
28. Krogman WN, Iscan MY. The human skeleton in forensic medicine. 2nd ed. Springfield: Charles C Thomas, 480–492.
29. Craig EA. Intercondylar shelf angle: a new method to determine race from the distal femur. J Forensic Sci 40:777–782 (1995).
30. Steinbach HL, Russell W. Measurement of the heal pad as an aid in diagnosis of acromegaly. Radiology 82:418–422 (1964).
31. Puckett SE, Seymour EQ. Fallibility in heel pad thickness in diagnosis of acromegaly. Radiology 88:982–983 (1967).
32. Trotter M, Gleser GC. A re-evaluation of estimation of stature based on measurements of stature taken during life and of long bones after death. Am J Phys Anthropol 15:79–123 (1958).
33. Jantz RL, Hunt DR, Meadows L. The measure and mismeasure of the tibia: implications in for stature estimation. J. Forensic Sci 40:758–761 (1995).
33a. Trotter, M. Estimation of stature from intact long limb bones. In: Personal identification in mass disasters. Steward TE, ed. Washington, DC: National Museum of Natural History, Smithsonian Institute; 1970:77.
34. Brogdon BG. Radiological identification of individual remains. In: Forensic radiology. Brogdon BG, ed. Boca Raton: CRC Press, 1998:149–187.
35. Bass WM, Driscoll PA. Summary of skeletal identification in Tennessee: 1971–1981. J Forensic Sci 28:159–168 (1983).
36. Murphy WA. Spruill FG, Gantner GE. Radiologic identification of unknown human remains. J Forensic Sci 25:727–735 (1980).
37. Fitzpatrick JJ, Macaluso J. Shadow positioning technique: a method for postmortem identification. J Forensic Sci 30:1226–1229 (1985).
38. Rich J, Tatarek NE, Powers RH, Brogdon BG, Lewis BJ, Dean DE. Using pre- and post-surgical foot and ankle radiographs for identification. J Forensic Sci 47:1319–1322 (2002).
39. Riddick L, Brogdon BG, Laswell-Hoff J, Delmar B. Radiographic identification of charred human remains through use of the dorsal defect of patella. J Forensic Sci 28:263–267 (1983).
40. Johnson JT, Brogdon BG. Dorsal defect of the patella: incidence and distribution. Am J Roentgenol 139:339–340 (1982).
41. Sudimack JR, Lewis BJ, Rich J, Dean DE, Fardal PM. Identification of decomposed human remains from radiographic comparison of an unusual foot deformity. J Forensic Sci 47:218–220 (2002).

42. Vogel, H. Gewalt im Röntgenbild. Landsberg/Lech: ecomed verlagsgesellschaft mbH, 1997.
43. Kahana T, Hiss J. Positive identification by means of trabecular bone pattern comparison, J Forensic Sci 39:1325–1330 (1994).
44. Brogdon BG, Silverstein GS, Lichtenstein JE. Mass casualty situations. In: A radiologic atlas of abuse, torture, terrorism and inflicted trauma. Brogdon BG, Vogel H, McDowell JD, eds. Boca Raton: CRC Press, 2003:267–278.
45. Liechtenstein JE. Radiology in mass casualty situations. In: Forensic radiology. Brogdon BG. Boca Raton: CRC Press, 1998:189–205.
46. Brogdon BG. Child abuse. In: Forensic radiology. Brogdon BG. Boca Raton: CRC Press, 1998:281–314.
47. Brogdon BG, Vogel H. Child abuse. In: A radiologic atlas of abuse, torture, terrorism and inflicted trauma. Brogdon BG, Vogel H, McDowell JD, eds. Boca Raton: CRC Press, 2003:3–44.
48. Brogdon BG. Forensic aspects of radiology. In: Medicolegal investigation of the death. 4th ed. Spitz, WU, ed. Springfield: CC Thomas, in press.
49. McDowell JD, Brogdon BG. Abuse of intimate partners. In: A radiologic atlas of abuse, torture, terrorism and inflicted trauma. Brogdon BG, Vogel H, McDowell JD, eds. Boca Raton: CRC Press, 2003:45–59.
50. McDowell JD, Brogdon BG. Spousal abuse and abuse of the elderly: an overview. In: Forensic radiology. Brogdon BG. Boca Raton: CRC Press, 1998:315–326.
51. Brogdon BG, McDowell JD. Abuse of the aged. In: A radiologic atlas of abuse, torture, terrorism and inflicted trauma. Brogdon BG, Vogel H, McDowell JD. Boca Raton: CRC Press, 2003:61–67.
52. Pinzur MS, Meyer PR Jr. Complete posterior dislocation of the talus. Clin Orthop 131:205–209 (1978).
53. Coltart WD. Aviator's astragalus. JBJS (B) 34:545–566 (1952).
54. Simson LR. Roentgenography in the human factors investigation of fatal aviation accidents. Aerospace Med 43:81–85 (1972).
55. Goosens M, Destoop N. Lisfranc's fracture–dislocations: etiology, radiology, and results of treatment. Clin Orthop 178:156–162 (1983).
56. Vogel H, Brogdon BG. Beating. In: A radiologic atlas of abuse, torture, terrorism and inflicted trauma. Brogdon BG, Vogel H, McDowell JD, eds. Boca Raton: CRC Press, 2003:109–118.
57. Petrow P, Page P, Vanel D. The hidden divot fracture: Brogdon's fracture. AJR 177:946–947 (2001).
58. Brogdon BG, Crotty JM. The hidden divot: a new type of incomplete fracture? AJR 172:789–790 (1999).
59. Vogel H. Other forms of torture. In: A radiologic atlas of abuse, torture, terrorism and inflicted trauma. Brogdon BG, Vogel H, McDowell JD, eds. Boca Raton: CRC Press, 2003:133–137.
60. Messmer JM. Radiology of gunshot wounds. In: Forensic radiology. Brogdon BG, ed. Boca Raton: CRC Press, 1998:209–224.
61. Messmer JM, Brogdon BG. Pitfalls in the radiology of gunshot wounds. In: Forensic radiology. Brogdon BG, ed. Boca Raton: CRC Press, 1998:225–248.
62. Messmer JM, Brogdon BG, Vogel H. Conventional weapons, including shotguns. In: A radiologic atlas of abuse, torture, terrorism and inflicted trauma. Brogdon BG, Vogel H, McDowell JD, eds. Boca Raton: CRC Press, 2003:161–178.
63. Messmer JM, Brogdon BG. Pitfalls in the radiology of gunshot wounds. In: A radiologic atlas of abuse, torture, terrorism and inflicted trauma. Brogdon BG, Vogel H, McDowell JD, eds. Boca Raton: CRC Press, 2003:179–194.
64. Vogel H, Brogdon BG. Unconventional loads and weapons. In: A radiologic atlas of abuse, torture, terrorism and inflicted trauma. Brogdon BG, Vogel H, McDowell JD, eds. Boca Raton: CRC Press, 2003:199–209.
65. Messmer JM, Fierro MF. Radiologic forensic investigation of fatal gunshot wounds. RadioGraphics 1986;6:457–473.

66. Newell CW, Jalkh CM, Brogdon BG. Radiographic equipment, installation and radiation protection. In: Forensic radiology. Brogdon BG, ed. Boca Raton: CRC Press, 1998:381–395.
67. Newell CH, Jalkh CM. Production of the radiographic image. In: Forensic radiology. Brogdon BG, ed. Boca Raton: CRC Press, 1998:443–462.
68. Newell CH, Jalkh CM. Radiographic positioning. In: Forensic radiology. Brogdon BG, ed. Boca Raton: CRC Press, 1998:397–441.

Part II

Trauma Analysis and Reconstruction

Chapter 7

Injuries to Children

A Surgeon's Perspective

Jonathan I. Groner, MD

1. Introduction

Trauma is the leading killer of children after the first year of life. Unlike trauma in the adult world, where penetrating injuries (mainly a result of firearms) predominate, pediatric trauma deaths are most commonly caused by blunt force injury (Table 1). Traumatic injuries and deaths do occur in children younger than 1 yr, however, congenital disease and prematurity claim more lives in that group and unintentional injuries are up to 15 times more common than injuries caused by abuse, although they tend to be less severe *(1)*. As will be demonstrated in this chapter, it is highly likely that an infant with the combination of a lower extremity fracture and virtually any other injury has been intentionally injured.

The Trauma Registry at Children's Hospital in Columbus, Ohio (a level-1 pediatric trauma center), records data on all children admitted for the treatment of injury, including those dying in the emergency department. Data from the registry reveal that among injured children of all ages with lower extremity fractures, 45% had femur fractures; 35% had fractures to the tibia, fibula, or both; and 19% had fractures involving the ankle, foot, or toes. Among patients with open wounds, 15% were in the hip or thigh; 48% were in the knee, leg, or ankle; and 28% were in the foot (Table 2).

The etiology of lower extremity injury varies widely with age. For example, the Trauma Registry reveals that among patients younger than 18 mo, 58% of lower extremity injuries were a result of assault (i.e., child abuse), 18% were because of falls, and 10% were because of motor vehicle crashes. In the 5- to 9-yr-old age group, only 15% of injuries were a result of assault, 18% a result of falls, 25% owing to pedestrian injuries, and 15% because

From: *Forensic Science and Medicine*
Forensic Medicine of the Lower Extremity: Human Identification and Trauma Analysis of the Thigh, Leg, and Foot
Edited by: J. Rich, D. E. Dean, and R. H. Powers © The Humana Press Inc., Totowa, NJ

Table 1
Cause and Age of Hospital Admissions (1998–2002) for Lower Extremity Injury From the Columbus, OH, Children's Hospital Trauma Registry

	Age									
Cause	<18 mo	18–23 mo	2–4Y	5–9Y	10–12Y	13–14Y	15Y	≥16Y	Total	%
Animal	2	0	5	8	3	8	0	1	27	2.2
Assault	39	1	4	0	1	0	0	0	45	3.6
Bike	0	0	7	56	33	25	3	4	128	10.2
Burn	0	0	1	0	0	0	0	0	1	0.1
Crush	0	0	2	2	3	1	0	0	8	0.6
Cut	0	0	5	7	4	0	2	0	18	1.4
Fall	12	6	37	65	61	30	13	10	234	18.7
FB	2	0	11	21	7	5	0	0	46	3.7
GSW	0	1	1	2	4	3	3	8	22	1.8
Hit by	0	0	2	5	2	2	0	0	11	0.9
MC	0	1	7	15	31	43	5	11	113	9.0
MVC	7	6	29	57	45	35	28	46	253	20.2
Other	5	2	14	30	15	8	3	1	78	6.2
PED	0	0	26	92	44	22	6	6	196	15.6
Sport	0	0	0	8	14	35	7	8	72	5.7
Stab	0	0	0	0	0	1	0	0	1	0.1
Total	67	17	151	368	267	218	70	95	1253	100.0
Percent	5.3	1.4	12.1	29.4	21.3	17.4	5.6	7.6		

Bike, injured while cycling on a nonmotorized bicycle; FB, foreign body; GSW, gun-shot wound; Hit by, struck by object (not a motor vehicle); MC, motorcycle; MVC, motor vehicle crash (injured while inside car); PED, pedestrian injury (struck by car); Sport, sports-related injury; Stab, penetrating trauma.

of motor vehicle crashes; 87% of all lower extremity injuries resulting from assault occurred in the children younger than 18 mo.

This chapter will focus primarily on the pathology of blunt injuries of the lower extremity in children. The chapter is divided into three sections: unintentional injuries, intentional injuries (i.e., child abuse), and disease processes that can mimic injury.

2. *Unintentional Injury*

The vast majority of unintentional injuries in children are caused by blunt trauma, in which the force applied to the tissue exceeds the strength of the tissue, resulting in injury. Skin and soft tissue can withstand a significant amount of direct force (such as a child struck by a car) with minimal damage, even though the underlying bone fractures. On the other hand, skin can sustain significant damage from a friction injury, even though the underlying bones may be unharmed. In some injury situations (e.g., when a child's leg is run over by a car), a combination of shearing (friction) and direct force can cause both severe soft tissue injury and fracture.

The leading causes of injury death in the Children's Hospital Trauma Registry are pedestrian–motor vehicle collisions, assaults, and motor vehicle crashes. Each of these mechanisms can cause injury to the lower extremity.

Table 2
Total Lower Extremity Fractures, Open Wounds, and Traumatic Amputations at the Columbus, OH, Children's Hospital Trauma Registry: 1998–2002

Lower Extremity Fractures:	
Femur	507
Tibia/Fibula	387
Ankle/Foot/Toes	207
Other/Multiple	2
Total	**1103**
Open Wounds:	
Hip/Thigh	39
Knee/Leg/Ankle	122
Foot	72
Toe	16
Other/Multiple	3
Total	**252**
Amputations:	
Toe/Foot	14
Leg	3
Total	**17**

A total of 253 motor vehicle-related lower extremity injuries occurred, including 101 in which the patient had been restrained by seat belt, 120 in which the patient had not been restrained by seat belt, and 32 cases in which the use of seat belts was not documented or unknown.

2.1. Pedestrian Trauma

Many older pediatric surgery or trauma textbooks refer to a constellation of injuries in pediatric pedestrians known as "Waddell's triad." The injury pattern consists of lower extremity fracture (from the bumper striking the upright child), abdominal injury (caused by the blunt force caused by the child being thrown onto the hood of the car), and head injury (caused by the head striking the windshield of the car). However, although lower extremity injuries (particularly midshaft femur fractures) do commonly occur when a child is struck by a car, the combination of head, abdominal, and lower extremity injury occurs in fewer than 2.5% of injured child pedestrians *(2)*. In fact, tibia–fibula fractures are more common than femur fractures, and lower extremity fractures are more commonly associated with ipsilateral upper extremity fractures in injured pediatric pedestrians *(3)*.

2.2. Motor Vehicle Crash Trauma

Pediatric motor vehicle occupants can sustain serious or fatal injuries in a crash, but fatal injuries usually involve severe central nervous system damage or intraabdominal hemorrhage and rarely involve the lower extremities. However, a patient with bilateral femoral fractures can develop hypovolemia and shock with minimal external signs of blood loss. Hip fractures and patella fractures are indications of a high-speed impact and are more common in unrestrained occupants. When small children are restrained by a

lap belt or lap belt–shoulder harness combination (instead of a booster seat), the belt tends to rest across the mid-abdomen instead of the bony pelvis. The violent deceleration of a head-on collision may result in the lap belt crushing against the spine, causing bowel injuries, chance fractures of the lumbar spine, and even transection of the lumbar spinal cord and thus lower extremity paralysis *(4)*.

2.3. Falls

Falls are a significant cause of lower extremity trauma in children. However, because children have a relatively high center of gravity, the relative rate of lower extremity injuries in children due to a free fall from a height is lower than in adults. One study of more than 700 cases of fall-related trauma found a lower extremity injury rate of 5.6% compared with an upper extremity injury rate of 6.2% *(5)*.

Low-altitude falls (e.g., a fall from a bed or couch) seldom cause lower extremity fractures. Research using biomechanical dummies suggests that the pelvis and lower extremities have the initial impact in a fall from a bed. However, the force imparted by such a fall is generally below the threshold for a lower extremity injury *(6)*. Unless there is an underlying bony or soft tissue disorder, children who sustain serious lower extremity trauma with a history of a fall from a bed or couch are likely to have suffered from intentional injury.

Although a nonambulatory infant with a femoral fracture is likely to have been a victim of child abuse, a possible exception is a distal femoral metaphyseal fracture extending through the growth plate owing to "activity center trauma." In a recent report of two infants with identical fractures who had been playing in a stationary activity center featuring a swiveling seat and a saucer-shaped base, investigators hypothesized that the twisting motion that resulted from the child rotating on the swivel seat transmitted enough force to the anterolateral aspect of the growth plate to initiate the fracture *(7)*.

Falls resulting from high-speed sports injuries (i.e., skiing, snowboarding, or sledding) tend to cause greater lower extremity trauma than falls from heights. One study found 10 lower extremity long-bone fractures among 25 patients hospitalized to treat sledding injuries *(8)*. Snowboarding and skiing both result in a high incidence of lower extremity trauma; Although snowboarding has become extremely popular among adolescents, a comparison of first-time snowboarders with first-time skiers revealed a higher incidence of lower extremity trauma in the skiers *(9)*. In another study, a much greater incidence of ligamentous knee injuries was observed in skiers than in snowboarders *(10)*.

Spontaneous fractures are rare, even in bedridden children. In a recent case report, spontaneous fractures in both femurs, tibias, and fibulas occurring secondary to osteopenia in a 4-yr-old child with cerebral palsy and spasticity were reported. The diagnosis was made postmortem after the child succumbed to pneumonia. Other causes of fractures, such as child abuse and metabolic disorders, were ruled out *(11)*.

2.4. Massive Soft Tissue Injury to the Lower Extremity ("Mangled Extremity")

Perhaps the greatest urban enemy of the lower extremity in children is the riding lawnmower. In the United States, it is estimated that eight children daily sustain injuries

while riding mowers *(12)*. In some cases, a child is struck in the leg by a mower because the operator does not see the child. The other (and more dangerous) injury occurs when the child is a passenger on a riding mower (i.e., in the operator's lap) and slides out of his seat and falls off the mower. In this case, the mower deck may pass completely over the child, often with fatal results. In one series of traumatic amputations in children, lawnmower injuries caused more amputations (22%) than motor vehicle crashes or gunshot wounds *(13)*. Lawn mower-related lower extremity amputations are massively contaminated with grass fibers and dirt, and the bones are frequently fractured at multiple levels.

The agricultural equivalent to the lawnmower is the high-powered, multi-spindled rotary cutting deck. This device is pulled behind a tractor while the tractor engine drives the cutting blades. One such device is manufactured by Bush Hog®; however, this name is often used generically by farm workers to refer to any agricultural mower. While these devices are less numerous than residential mowers—and, thus, are responsible for fewer injuries—they are nevertheless the cause of more serious and often fatal injuries. Again, a common mechanism involves a child riding as a passenger on the tractor, then slipping off his perch to be run over by the cutting deck. In addition to the grave danger of the rotating cutting blades, the typical "bush hog" also has a trailing wheel or wheels that are designed to stabilize the cutting platform. These wheels tend to keep any object (e.g., a child) that becomes caught under the cutting deck from rolling free.

The link between the bush hog (or other powered agricultural tool) to the tractor itself is called the "power take off" (PTO), which is essentially an extension of the engine's rotating drive shaft. It delivers high torque at more than 2000 rpm. PTOs are equipped with a protective shield, but these are often removed by farmers because the devices are cumbersome and slow maintenance chores. Injuries can occur when a child's clothing becomes ensnared in the rotating shaft of the PTO. Older children (adolescents) who operate farm equipment will sometimes straddle the PTO instead of walking around the machinery in order to save time. If the teenager's pants become ensnared in the PTO, they may well be ripped off entirely (particularly if the pants are old and worn). If the pants do not rip, the victim's legs will become wrapped around the PTO shaft, and a severe complex fracture and soft tissue injury to the lower extremity may result. The scale used to rate severe soft tissue injuries in children is called the mangled extremity severity score (MESS); this is a predictive score that is used to gauge the risk of salvage vs amputation for severe open fractures of the lower extremity *(14)*.

2.5. Animal Bites

Animal bites can cause lower extremity trauma in children. A consecutive series of more than 200 cat bites demonstrated a lower extremity injury rate of 13%. The overall infection rate for cat bites (in all locations) was 15% *(15)*. A series of more than 700 dog bites demonstrated an injury rate of 9.5% for bites in the thigh, 15.9% for the leg, and 1.7% for the foot and an overall wound infection rate of slightly more than 2% *(16)*. Although there are few reports of snakebites to the lower extremity in children, rattlesnake (North American Crotalid) bites in the lower extremity can cause intravascular hemolysis *(17)*.

3. Intentional Injury

3.1. Blunt Trauma

Lower extremity fractures are often associated with intentional injuries in children. In fact, child abuse accounts for 20% of pediatric femoral fractures. Each year, more than 1200 children in the United States die from child abuse. The failure of a primary care physician to diagnose child abuse in a patient increases the child's risk for further abuse and violent death; for the forensic pathologist, failure to diagnose child abuse on postmortem examination increases the risk that other children in the household will end up on the autopsy table. Therefore, the diagnosis of intentional injury should always be considered when a toddler presents with a lower extremity fracture.

Fractures are the second most common physical sign of child abuse after skin lesions, and approximately one-third of abused children will eventually be seen by an orthopedic specialist. The "classic metaphyseal lesion" (CML) of chronic myeloid leukemia is strongly correlated with intentional injury. However, there is no pathognomonic fracture pattern in abuse *(18)*. When evaluating a lower extremity fracture for the possibility of an intentional injury, the age of the child, the stated mechanism of injury, the presence of associated injuries, and various psychosocial issues must be considered before a final diagnosis is determined.

3.2. Penetrating Trauma

Penetrating trauma of the lower extremity is rare in children. However, the lower extremities are probably more easily penetrated by projectiles in children than in adults. Plastic bullets, often touted as "safer" by law enforcement authorities, are capable of causing major vascular injuries in the lower extremity in children. Twenty-three vascular injuries were reported in children wounded by plastic bullets during an Israeli–Palestinian conflict, including four isolated arterial injuries, three isolated venous injuries, and eight combination injuries *(19)*.

3.3. Thermal Injuries

Scald burns comprise a leading causing of admission to pediatric burn units and a significant cause of death in young children. Scald burns may be intentional or unintentional; however, burn injuries to the lower extremities, especially when they occur bilaterally, are thought to be virtually always a result of child abuse. Inflicted scald injuries are characterized by uniform burn depth and distinct borders, whereas unintentional injuries demonstrate irregular burns and splash marks from the child's attempts to struggle away from hot liquids.

Nevertheless, scald injuries to the lower extremity can be unintentional. In a series of three patients, all thought to be victims of child abuse, investigators discovered (on careful multidisciplinary investigation) that their injuries were owing to unintentional injuries occurring as a result of climbing into hot, water-filled sinks. In each case, a toddler used the toilet seat or a stool to climb into the sink and gain access the hot water supply *(20)*. Nevertheless, any toddler with a significant lower extremity scald, especially when combined with other injuries, is likely to have been intentionally injured. A thorough examination for other injuries (which may involve the use of a radiological skeletal survey, a computed tomography scan of the brain, and a retinal examination) should be considered in such cases.

4. Diseases That Mimic Traumatic Injury

4.1. Infectious Agents

Meningococcemia can manifest as a coagulopathy in the setting of overwhelming sepsis. Patients may have multiple ecchymotic lesions on the lower extremities and elsewhere that can be mistaken for traumatic injuries. The keys to the diagnosis of an infectious cause are the relatively uniform distribution of ecchymotic lesions throughout the body, no particular pattern or imprint mark, and no associated fractures. The author is personally acquainted with a case of traumatic origin: a patient under treatment for septic shock as a result of meningococcemia, who had ecchymotic lesions in multiple areas (including the lower extremities and abdomen), was found on closer scrutiny to have a perforated duodenum from intentional blunt traumatic injury.

In another case in the author's experience, an adolescent patient developed profound hypotension and severe vascular changes in the lower extremities (that initially looked similar to frostbite) following a spinal fusion. These changes advanced to a burn-like appearance with blistering and then to frank gangrene of the toes and eventually the feet. Blood cultures yielded *Yersinia*, and the infection source was ultimately traced to an intraoperative transfusion of contaminated blood. This child developed gangrene of both feet and eventually required bilateral below-knee amputations. Other reported cases of *Yersinia* sepsis have been fatal. A patient who develops symptoms and signs of septic shock or pronounced vascular changes in the lower extremities after a blood transfusion should be evaluated for possible *Yersinia* sepsis.

4.2. Bone Disorders

Osteogenesis imperfecta (OI) is a genetic disorder characterized by increased bone fragility. At least seven discrete types of OI are known, and the disease can range from mild to lethal. The cause of OI is extremely heterogeneous: in some types, defects in the genes encoding type I collagen have been found; in other types, defects in other proteins have been identified. Patients with OI have increased bone turnover rates, decreased bone mass, and a disturbed organization of bone tissue *(21)*. A radiograph of OI is provided in the chapter entitled *Radiology of the Lower Extremity*.

When there is no history of injury in patients with this disorder, OI and other metabolic bone disorders are always considered in the differential diagnosis of lower extremity fractures in children. However, these entities are extremely rare. In the author's personal experience, bone disease has never been diagnosed in a patient evaluated for a lower extremity fracture of unknown etiology. Not only is OI rare, but diagnoses of "temporary brittle bone disease" and "mild type IV OI" (a variant of OI said to lack extraskeletal findings) are so unusual (in fact, some authors believe that the former disease is purely hypothetical) that they are not acceptable diagnoses in small children *(22)*. Collagen analysis to search for mild forms of bone disease is generally not indicated in the vast majority of infants and children undergoing an evaluation for the possibility of child abuse *(23)*.

4.3. Other Diseases That Mimic Traumatic Injury

Epidermolysis bullosa (EB) is a form of genodermatosis (genetic disorder of the skin) that is characterized by sloughing of the dermal layers secondary to minimal trauma. EB is caused by a defect in collagen synthesis and occurs as a dominant or

Fig. 1. Epidermolysis bullosa mimics scalded skin from a hot liquid in this infant. The distribution of this disease mimics injury patterns that are usually found in children struggling to get away from the heat source. A bulla (blister) is also seen on the proximal thigh. Photo courtesy of Jonathan I. Groner, MD. *See* **Color Plate I**, following page 240.

recessive trait *(24)*. EB patients range from those with a relatively minor skin disorder to patients who are severely disfigured. In patients with severe disease, ill-fitting shoes, the application of a bandage, or even the use of an automated blood pressure cuff can cause skin damage.

Newborns with severe EB may present with peeling and blistering (bullae) of the skin at intrauterine pressure points, particularly the elbows, knees, and ankles (Fig. 1). The lesions look strikingly similar to partial thickness burns and are treated with protective dressings. In older children, trivial trauma, such as a fall, may lead to large areas of partial-thickness (and sometimes full-thickness) skin injury that may be confused with an intentional burn injury. Fortunately, many children with EB have both a family and a personal history of chronic cutaneous scarring from past injuries that allows for the appropriate diagnosis. Patients with EB who present with severe scarring will develop pseudosyndactyly of the digits. In longstanding cases (usually beyond childhood), squamous cell cancer can develop in the chronically damaged skin.

The dermatologic complications of Stevens-Johnson syndrome (SJS) are similar to those seen in patients with thermal injury *(25)*. SJS is induced by exposure to drugs or infections. Bacterial colonization of the skin can also result in sepsis. Frozen sections of denuded epidermis in SJS reveal full-thickness epidermal necrosis *(26)*. Conditions that may be confused with this disorder include staphylococcal scalded skin syndrome and

Fig. 2. Stevens-Johnson Syndrome in the distal lower extremity intraoperatively **(A)** and showing healed lesions **(B)**. These lesions mimic thermal trauma, such as that caused by cigarette burns or wounds induced with a heated implement. Photo courtesy of Jonathan I. Groner, MD. *See* **Color Plate II**, following page 240.

exfoliative erythroderma. Figure 2A, B illustrate acute and healed dermatologic sequelae of SJS in a child. Such lesions could be confused with cigarette burns or other thermal injury with an implement.

Fig. 2. *Continued.*

Children with Ehler-Danlos syndrome are not, in general, born with abnormal-appearing skin and do not develop burn-like lesions from trivial trauma. Patients with Ehler-Danlos do, however, develop large soft-tissue wounds in response to soft-tissue trauma. A blow to the tibial area (e.g., from a soccer opponent's kick or a bicycle pedal) may result in a large soft-tissue wound extending to the periosteum. The key to the diagnosis is an examination of the patient's knees: most children with Ehler-Danlos have multiple scars from previous trivial soft tissue trauma. In addition, a parent may be afflicted with the disease and have similar scarring.

Idiopathic palmoplantar eccrine hidradenitis (IPPH) is characterized by painful erythematous plantar nodules that may arise following intense physical activity. IPPH is not a truly traumatic lesion (microscopic examination demonstrates neutrophilic infiltrate around and within the eccrine sweat apparatus) and generally resolves after a few days' rest *(27)*.

5. *Hair Tourniquet Syndrome*

In an odd "twist," this chapter ends with a trauma that can be mistaken for a medical condition. The hair tourniquet syndrome can be defined as digital ischemia secondary to constricting thread or hair at the base of the digit. The resulting tourniquet effect causes venous congestion, usually in one or two toes. The affected toe becomes red and edematous, but in advanced cases may look profoundly ischemic. The syndrome is

more common in infants younger than 6 mo, and the diagnosis is often delayed 3 to 4 d *(28)*. The offending hair or thread is often concealed in natural skin wrinkles. A severely ischemic toe can be mistaken for an arterial embolism, which may arise in infants with congenital heart disease. Although complete necrosis of the toe is rare, a toe amputation has been required for some infants *(29)*.

Acknowledgments

The author gratefully acknowledges the assistance of Renae Kable and Wendi Lowell for providing data from the Children's Hospital Trauma Registry in Columbus, Ohio.

References

1. Rivara FP, Kamitsuka MD, Quan L. Injuries to children younger than 1 year of age. Pediatrics 81:93–97 (1988).
2. Orsborn R, Haley K, Hammond S, Falcone RE. Pediatric pedestrian versus motor vehicle patterns of injury: debunking the myth. Air Med J 18:107–110 (1999).
3. Brainard BJ, Slauterbeck J, Benjamin JB. Fracture patterns and mechanisms in pedestrian motor vehicle trauma: the ipsilateral dyad. J Orthop Trauma 6:279–282 (1992).
4. Rumball K, Jarvis J. Seat-belt injuries of the spine in young children. J Bone Joint Surg Br 74:571–574 (1992).
5. Wang MY, Kim KA, Griffith PM, et al. Injuries from falls in the pediatric population: an analysis of 729 cases. J Pediatr Surg 36:1528–1534 (2001).
6. Bertocci GE, Pierce MC, Deemer E, Aguel F, Janosky JE, Vogeley E. Using test dummy experiments to investigate pediatric injury risk in simulated short-distance falls. Arch Pediatr Adolesc Med 157:480–486 (2003).
7. Grant P, Mata MB, Tidwell M. Femur fracture in infants: a possible accidental etiology. Pediatrics 108:1009–1011 (2001).
8. Shorter NA, Mooney DP, Harmon BJ. Childhood sledding injuries. Am J Emerg Med 17:32–34 (1999).
9. O'Neill DF, McGlone MR. Injury risk in first-time snowboarders versus first-time skiers. Am J Sports Med 27:94–97 (1999).
10. Sacco DE, Sartorelli DH, Vane DW. Evaluation of alpine skiing and snowboarding injury in a north-eastern state. J Trauma 44:654–659 (1998).
11. Torwalt CR, Balachandra AT, Youngson C, de Nanassy J. Spontaneous fractures in the differential diagnosis of fractures in children. J Forensic Sci 47:1340–1344 (2002).
13. Kroening L, Davids JR. Management of lower extremity riding lawn mower injuries in children. Orthop Nurs 19:29–37 (2000).
13. Trautwein LC, Smith DG, Rivara FP. Pediatric amputation injuries: etiology, cost, and outcome. J Trauma 41:831–838 (1996).
14. Fagelman MF, Epps HR, Rang M. Mangled extremity severity score in children. J Pediatr Orthop 22:182–184 (2002).
15. Dire DJ. Cat bite wounds: risk factors for infection. Ann Emerg Med 20:973–979 (1991).
16. Dire DJ, Hogan DE, Riggs MW. A prospective evaluation of risk factors for infections from dog-bite wounds. Acad Emerg Med 1:258–266 (1994).
17. Gibly RL, Walter FG, Nowlin SW, Berg RA. Intravascular hemolysis associated with North American crotalid envenomation. J Toxicol Clin Toxicol 36:337–343 (1998).
18. Kocher MS, Kasser JR. Orthopaedic aspects of child abuse. J Am Acad Orthop Surg 8:10–20 (2000).
19. Schnitzer JJ, Fitzgerald D. Peripheral vascular injuries from plastic bullets in children. Surg Gynecol Obstet 176:172–174 (1993).

20. Titus MO, Baxter AL, Starling SP. Accidental scald burns in sinks. Pediatrics 111:E191–E194 (2003).
21. Zeitlin L, Fassier F, Glorieux FH. Modern approach to children with osteogenesis imperfecta. J Pediatr Orthop B 12:77–87 (2003).
22. Lund AM, Skovby F, Knudsen FU. [Child abuse and osteogenesis imperfecta. How do we distinguish?]. Ugeskr Laeger 162:1528–1533 (2000).
23. Ablin DS, Sane SM. Non-accidental injury: confusion with temporary brittle bone disease and mild osteogenesis imperfecta. Pediatr Radiol 27:111–113 (1997).
24. Horn HM, Tidman MJ. The clinical spectrum of dystrophic epidermolysis bullosa. Br J Dermatol 146:267–274 (2002).
25. Rzany B, Correia O, Kelly JP. et al. Risk of Stevens–Johnson syndrome or toxic epidermal necrolysis. N Engl J Med 333:1600 (1995).
26. Bastuji-Garin, Rzany B, Stern RS, et al. Clinical manifestation of cases of toxic epidermal necrolysis, Stevens–Johnson syndrome, and erythema multiforme. Arch Dermatol 129:92 (1993).
27. Ben-Amitai D, Hodak E, Landau M, Metzker A, Feinmesser M, David M. Idiopathic palmoplantar eccrine hidradenitis in children. Eur J Pediatr 160:189–191 (2001).
28. Harris EJ. Acute digital ischemia in infants: the hair-thread tourniquet syndrome—a report of two cases. J Foot Ankle Surg 41:112–116 (2002).
29. Leferink VJ, Klaase JM. [Toe tourniquet syndrome]. Ned Tijdschr Geneeskd 141:2499–2501 (1997).

Chapter 8

Skeletal Trauma Analysis of the Lower Extremity

Alison Galloway, PhD and Lauren Zephro, MA

1. Introduction

This chapter reviews the methods of forensic anthropological analysis in skeletal damage to the lower extremity and serves as an introduction for later chapters discussing the underlying physics and methodology used in engineering accident reconstruction. The discussion herein includes the interpretation of the mechanism of injury and the types of defects seen most commonly within forensic contexts. No such discussion can be comprehensive and each case must be assessed separately. Consistency with known patterns of damage can be stated, but in the majority of cases, the exact cause of injury cannot be determined. Analysis of lower extremity skeletal trauma requires an understanding of the movement patterns in which these bones have evolved, the capacity of the joints to absorb forces, the effects of forces beyond the capacity of bones and joints to withstand, and the resultant fracture patterns produced by excessive force.

Forensic anthropologists often analyze human remains that are removed from the context of death. Material may be partial, skeletonized, and weathered. Isolated bones of the leg may be encountered, and trauma must be assessed from the skeletal damage to these elements alone. Forensic interpretation must be grounded in the physical evidence embodied in the skeletal material. Conjecture beyond the physical evidence must be avoided. However, the types of cases seen by the forensic anthropologist differ markedly from those seen by the medical community, who report on survivors, and by forensic pathologists and coroners, who report on all fatalities that meet the criteria for examination. Forensic anthropologists are more likely to receive bodies of victims of homicide and suicide that lay in more remote areas, the remains of homeless individuals

From: *Forensic Science and Medicine*
Forensic Medicine of the Lower Extremity: Human Identification and Trauma Analysis of the Thigh, Leg, and Foot
Edited by: J. Rich, D. E. Dean, and R. H. Powers © The Humana Press Inc., Totowa, NJ

who have died accidentally or by natural causes but lain undiscovered, and occasionally victims of motor vehicle accidents (MVAs) or falls from heights. Although there are exceptions, the discrepancies among the populations sampled by the specialists in these various specialties must be emphasized.

Analysis of trauma from the perspective of the forensic anthropologist entails three distinct steps:

1. identification of the skeletal defects and establishment of the timing of injury;
2. interpretation of the biomechanical forces that produced the fractures or defects; and
3. linking fracture patterns to the anatomical context to understand the sequence of events that could have produced the observed defects.

2. Structural Features of the Lower Extremity

The lower extremity, as defined by this volume, consists of the femur, tibia, fibula, and the bones of the ankle and foot (Fig. 1). These lower limb long bones are the strongest within the human body, building on our evolutionary heritage of bipedal locomotion. The lower extremity has evolved to accommodate large amounts of compressive stress, a condition that has been compounded by modern life, with its hard surfaces and the potential for concentrated forces from certain types of footwear (e.g., "high heel" shoes). The hip joint provides for a wide circular range of movement with limitation of movement largely defined by the interference of soft tissue. The thigh angles inward so that pressure on the femur must be redirected into the hip joint. This structure leaves the femoral neck relatively weak, although it is well supported by the large muscles of the buttocks and thigh.

Below the hip, the knee joint is designed primarily as a loosely structured hinge joint with limited side-to-side movement. The side-to-side movement is constrained by the collateral ligaments. Unlike most quadrupedal animals, the joint is angled so the thighs can converge while the tibiae remain roughly parallel. For this reason, the medial condyle of the tibia is larger and lower, whereas the lateral condyle is smaller and higher. This joint is well suited for the normal levels of use under which humans have evolved, but poorly equipped for the high impacts encountered in modern traumatic settings. The distal femur generally bears compression well at the condyles but is prone to fractures in the supracondylar region. The proximal tibial plateau incorporates a significant quantity of trabecular bone and is prone to compression and fragmentation.

In contrast to the hip and knee, the ankle joint is more flexible, using the dorsiflexion and plantar flexion of the superior talar joint and the complex of joints between the tarsal bones. The foot itself is a relatively rigid structure with a tightly bound arch to absorb impacts during locomotion.

When viewed in terms of trauma analysis, the lower extremity presents long segments of the body that are designed to increase stride length and absorb compressive forces during walking and running, with some accommodation for uneven substrate in the ankle and foot. Almost one-third of our body weight and almost one-half of our height consists of the lower extremity, and the legs often bear the brunt of impacts from directed blows, falls, and MVAs. In addition, the indirect forces of rotation, bending, and shearing are often visible on these bones.

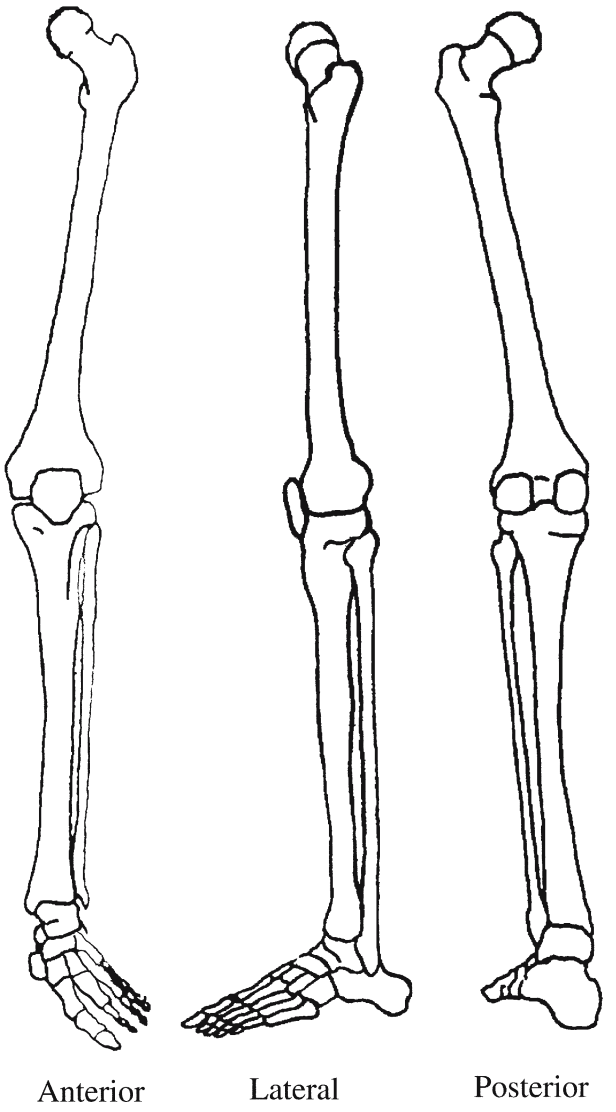

Fig. 1. Diagram of the bones of the lower extremity.

3. Methods of Analysis

Anthropological forensic cases should begin with documentation of the remains as they are first observed. Although some may be skeletonized on arrival, many are seen with varying levels of soft tissue remnants. All observable defects should be noted and photographed at this time, in part to guard against the possibility of defects being produced during the cleaning process *(1)*. From our experience, cleaning may be performed with water baths, according to the methodology described by Fenton *(2)*, or in a dermestid beetle colony *(3–5)*. Extreme care should be taken to minimize further damage to the bone; however, some postmortem defects may result. Special precautions should be taken to slow the

drying process because rapid dehydration can produce longitudinal fractures in bones. Similarly, immersing very hot bones in cold water or bones from the freezer in very hot water can produce minor fractures. Instruments used to clean the bones may also leave marks *(6)*. Finally, features having thin cortical bone (e.g., the tibial plateau) or extremely tough ligamentous attachments (as in the foot) may be damaged by overcooking *(7,8)*.

Once cleaned, all bones should be observed macroscopically and under low-power magnification and with oblique lighting *(9,10)*. Defects that may have been obscured by decomposing flesh or moisture are often revealed at this time. Low-power magnification and lighting techniques are particularly important in revealing sharp force injuries, incomplete fractures, and pathological fractures. Photo documentation with and without a scale is essential to show both the overall location and the close-up views of such defects, following the basic protocol set forth for other forensic disciplines *(11)*. Photographs should be taken at a 90° angle to the surface of the bone to minimize distortion. Close-up views are linked to the overall photos in which scales and labels are included. In addition, all bone abnormalities should be charted with notations of length and characteristics.

In some cases, fracture patterns cannot be understood without reconstructing the bone. Documentation of the fracture surfaces should be made prior to any reconstruction in order to record whether these occurred during the antemortem, perimortem or postmortem periods. If possible, reconstruction using a temporary bond such as tape is useful; however, this can be too difficult to maintain and gluing may be required. In addition to adhesives that will bond dry surfaces (i.e., Elmer's®, cyanoacrylate, Duco®, and Glyptal®), some epoxies are appropriate for adhering less pristine or greasy bone fragments (Quickshot®). Experimentation with adhesives on nonforensic bone is recommended prior to their use with active forensic material. When in doubt, use the least destructive and nonpermanent methods (clay, tape, photography).

For the purposes of this discussion, it is helpful to define specific terminology with which to describe these features. Inconsistent use of such terms, although seemingly minor, can produce damaging questioning on the witness stand where divergent definition of terms can be implied as lack of expertise. *Defects* are imperfections on the bone, failures or absences of bones, or bony features. *Fractures* are a specialized type of defect in which there is traumatic rupture of the integrity of the bone. A number of defects and fractures may result from one event, known as the *insult*; hence, clusters of defects can be linked to one insult. Within the context of the forensic anthropological report, *damage* can be defined as a pattern of defects, although these may not have occurred on a single occasion. For example, one could note rodent damage, although it consists of a multitude of small defects. The term *injury* can be interpreted as (1) the actual event in which the person suffered hurt or harm, or (2) the resulting damage inflicted by an external force. Within a medicolegal context, this term is best reserved for the combined information from the skeletal analysis, soft tissue observations at autopsy, and the pathologist's knowledge of the anatomical interrelationships involved in order to portray the overall effect of the trauma.

In the forensic anthropological examination, only after each defect has been described separately should the relationships among defects on the same or different bones be discussed. Variations in the anatomical positions of the deceased at the time of

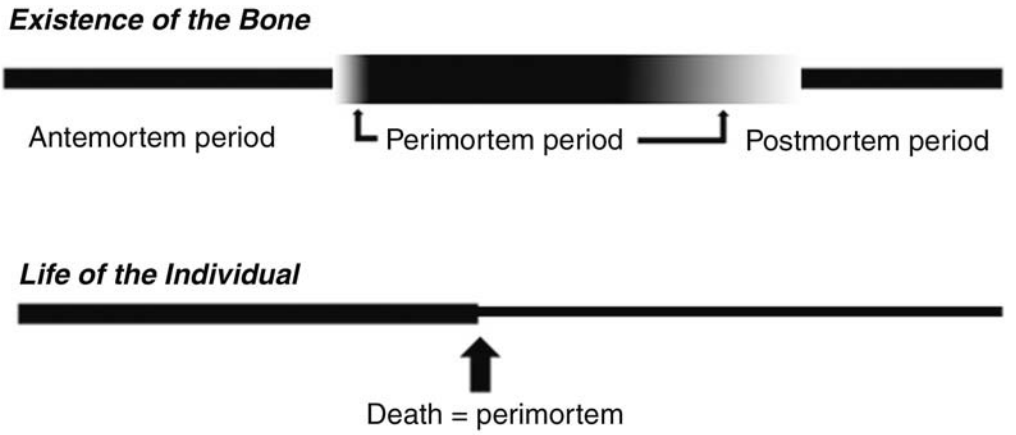

Fig. 2. Time line for ante-, peri-, and postmortem fractures contrasting the anthropological perspective, based on the bone with the more commonly held perspective of time of death.

injury are important to consider. Hypotheses and supporting observations linking insults to one or more possible positions of the victim should be included where appropriate.

4. Timing and Mechanism of Injury

Evidence of skeletal trauma in the forensic setting must be analyzed across two different axes. The first reflects the timing of the insult in relation to the death of the individual. The second reflects the forces involved and the mechanism of the insult itself.

Timing of skeletal trauma, as with most analyses of soft tissue defects, is broken down into ante-, peri-, and postmortem periods *(12)*. However, in contrast to the work of the forensic pathologist, the time frame under which the anthropologist works is not related to the time when the person breathed his or her last breath or thought his or her last thought, but to the time when the bone was first able to show skeletal signs of healing or lost the resiliency of living moist tissue (Fig. 2). The transition between ante- and perimortem defects is determined by the appearance of the first signs of healing—e.g., grooves around the fracture, active bone remodeling, callus formation, and edge resorption *(13)*—that in living adults may take up to 2 wk to appear after injury *(12–15)*. The transition between the peri- and postmortem occurs as bone loses moisture (desiccates), which changes the nature of the fracture pattern *(16)*. Due to the changing biomechanical properties of decomposing bone, postmortem fracture margins may appear jagged and splintery when compared with the fracture margins of fresh bone (Fig. 3). Depending on postmortem circumstances and conditions, this process may be relatively rapid or may be retarded. In addition, an examination of the fracture surface color may assist in perimortem vs postmortem determinations. In skeletonized remains, perimortem fractures are typically stained the same color as the surrounding cortical bone. In contrast, a recent postmortem bone fracture will differ in fracture margin color when compared to the surrounding bone, often being lighter. It must be emphasized that the biomechanical transition between antemortem, perimortem,

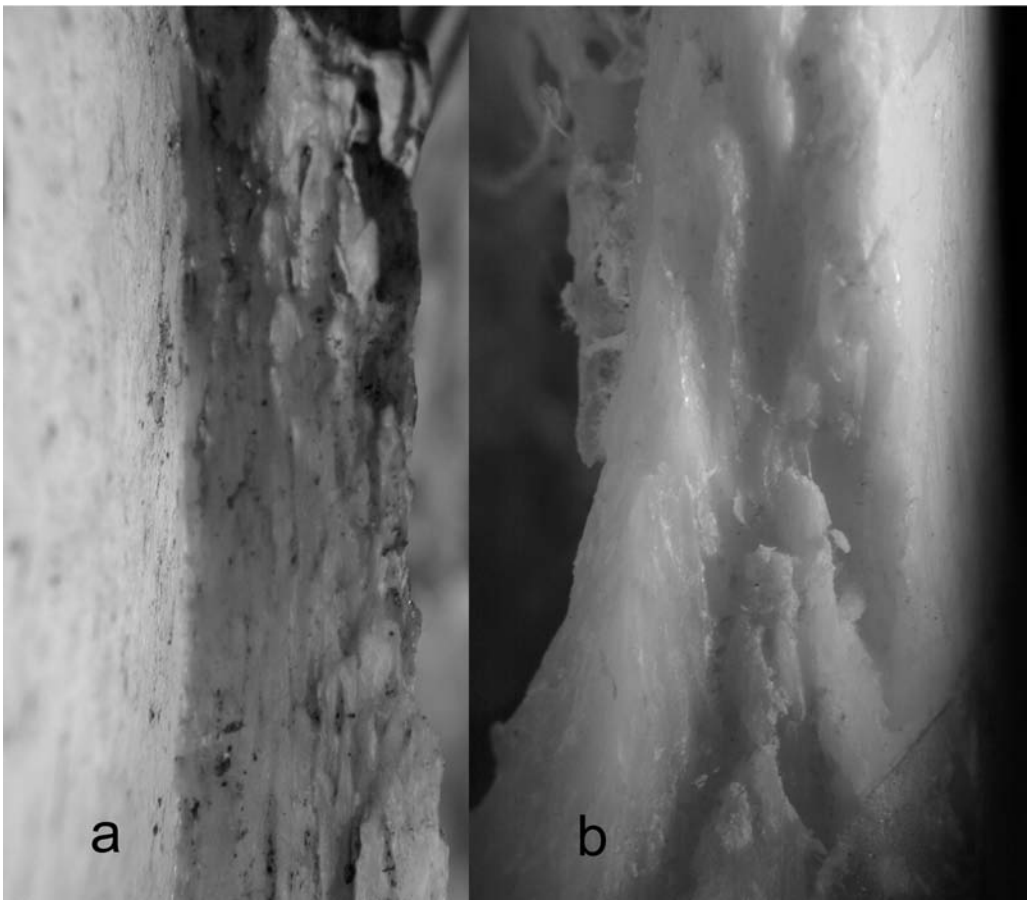

Fig. 3. Comparison of postmortem **(a)** and perimortem **(b)** fracture margins.

and postmortem, when based on the skeletal assessment, is not abrupt and varies with the individual, age, and the depositional environment.

Individual biological variation, sexual dimorphism, and age-related changes in leg bone size, cortical thickness, cross-sectional morphology, trabecular integrity, and resilience need to be considered in the forensic assessment. More gracile bones will be less resistant to fractures as will bones in which the endosteal surface has been resorbed as a result of age, hormonal influences, medical treatment, or the use of certain medications, alcohol, or illicit drugs *(17)*. For example, there is a bimodal distribution of subtrochanteric and distal femoral fractures with an initial peak in young adulthood associated with high energy impact and a second peak in older individuals, usually female, associated with relatively low-energy impact *(18,19)*. For this reason, it is difficult to estimate the actual force involved for the already damaged bone, although ranges can be produced from experimental situations in which the test bones are chosen to approximate the size and dimensions of the bone in question.

The ability of any product to accommodate the stress placed on it depends on its elastic qualities. Bone composition allows skeletal elements to bend under considerable

forces then return to the original shape. As the forces increase, the risk for permanent deformation followed by bone failure and fracture increases *(20,21)*. These forces can be seen at work in the damage that is produced. In blunt force trauma, bone is loaded relatively slowly and the fracture occurs after the bone has passed though its plastic phase. This process often results in bone fragments that are slightly misshapen and difficult to reconstruct. On the other hand, in cases of gunshot trauma, the bone experiences a high magnitude of stress for a short duration of time and responds like a more brittle material, permitting little or no plastic deformation before failure. Thus, bone fragmentation following a gun shot can be more extensive than that following blunt force trauma, causing little or no deformation in the bone fragments and making the reconstruction of the remains much easier *(22)*.

The forces that produce fractures are tension, compression, and shear. Tensile forces are poorly resisted by bony tissue, whereas compressive forces are handled relatively well. Shearing forces and rotational forces often move in directions to which bones are not adapted, but this varies considerably throughout the leg bones. Tube-shaped bones, such as the femoral shaft, will typically fracture in a more uniform pattern than more angular bones, such as the tibia *(23)*. The latter have varying areas of denser bone that redirect fractures toward those areas of least resistance.

Injuries can be produced by direct forces applied to the bone or the indirect effects of impacts somewhat distant from the point of failure. Direct impacts will produce fractures at the point where there is contact between a surface and the body. In the lower extremity, direct forces will largely produce transverse fractures, in which the fracture line lies approximately perpendicular to the long axis of the bone; these are also referred to as tapping fractures. Tapping fractures typically occur when a force in which the momentum has already peaked is applied over a small area *(24)*. Other examples of direct trauma include crush fractures, gunshot trauma, and sharp force trauma. Crushing fractures result in massive fragmentation of bone. In such cases, reconstruction can be difficult and will primarily show a broad area of impact. With gunshot trauma, forces imparted when a bullet strikes bone usually produce a shattering of the bone. Sharp force trauma indicates direct trauma where a cutting instrument was used directly on bone. The implements used in sharp force trauma can also induce elements of blunt force trauma. Further discussion of these defects will follow.

Indirect trauma includes compression, tension, angulation, and rotational fractures. The characteristics of the fractures themselves, as well as knowledge of the capacity of the bones to absorb energy, will help identify these fractures. Compression fractures involve the compaction of bone as the threshold for resilience is surpassed *(24)*. The most common sites for such fractures in the leg are in the areas of cancellous bone, such as the proximal tibia. In some cases, longitudinal or Y-shaped fractures can also be produced. Transverse fractures are produced under tension, but these are relatively rare. One tensile fracture that may be encountered is a transverse fracture of the patella caused by the knee being forcibly flexed while the extensor muscles are contracting. Twisting of the bone will produce spiral fractures, where the fracture line circles the bone before producing a longitudinal fracture to complete the separation. The most common situation for such breaks is when part of the body is turned while

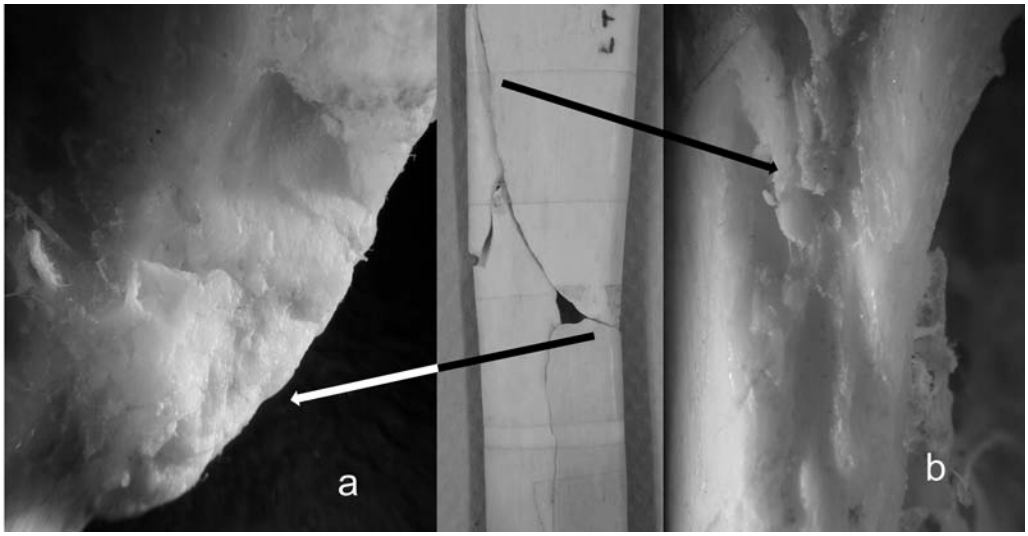

Fig. 4. Comparison of tensile fracture margin **(a)** and compressive fracture margin **(b)** from an axially loaded bone with lateral impact.

another portion is locked in position. The broken ends of true spiral fractures are long and pointed, in contrast to the ends of bones in oblique fractures, which are short, blunt and rounded.

Angulation fractures occur from bending, with fracture propagation caused by initial bone failure under tensile forces *(24)*. During bending, bone is placed under tension on the side of the convexity and under compression on the side of concavity, with a neutral plane located in between. Because bone is weaker under tension, bone failure is initiated on the convex side. On the side of compression, bone within the concavity may also fail, resulting in splintering. The propagation of the fracture from the site of tensile failure increases stress on the adjacent fibers, and the fracture may continue to fail in shear at an angle to the initial fracture line. This fracture commonly results in a triangular piece of bone (also known as a "butterfly" fracture), with the direction of force determined by the apex of the triangle (the apex represents the location where the bone initially failed under tension).

Microscopic examination of the fracture surfaces can offer some clues as to the types of forces involved in fracturing at specific sections of the bone (Fig. 4). Fracture surfaces usually have a billowy appearance and a transverse orientation at the site of tensile failure. On the other hand, bone that fails because of compression appears splintery and has a longitudinal alignment with the grain (long axis) of the bone *(25,26)*.

Although mechanisms can be identified for individual fractures, the pattern of fractures throughout the lower leg can often provide evidence of the sequence of events. For example, a driver of a vehicle will often have direct-impact injuries from the dashboard striking the knees, producing compression fractures in the distal femur and shearing fractures as the thigh is projected backwards past the hip joint. Therefore, although

documentation and description of individual fractures is important, the overall pattern of breakage sheds light on the sequence and explanation of events.

5. *Blunt Force Trauma*

The patterns of blunt force lower extremity injury depend on the mode of impact. Motor vehicles account for the majority of blunt force injuries, although victims of homicidal assault and falls are represented in the forensic samples. The anthropologist is frequently faced with bone where the context is under question. Did the individual die in an MVA, or was this a homicidal assault masquerading as an MVA? If it was an MVA, was the victim driving or was he or she a passenger? Where was the victim sitting at the time of the accident? Did a car hit the person or did that person fall off the cliff? How would the injuries differ if the person suffered these blows after he or she were already dead from some other cause? The following discussion is broken down into several modes under which injuries are encountered, including homicidal assault, MVAs, and falls. The goal in each case is to determine whether the injury patterns are so distinctive that other causes can be excluded.

5.1. Homicidal Assault

Fatal assault usually results from blows to the head *(27)* or torso; significant damage to the legs is less likely to occur owing to the density of the bones and the tendency to focus blows on more vulnerable portions of the body. A wide variety of objects can be used in assaults *(28–31)*, and in some cases, impressions of the instrument may be preserved on the bone *(32)*.

Fractures of the femoral diaphysis are relatively difficult to produce because of the density of the bone, given that this segment is one of the most heavily mineralized in the body *(33)*. However, femoral shaft fractures have been noted in homicidal assaults *(34)* and are usually associated with the use of some instrument, e.g., a bat or metal tool, which may produce tap or crush fractures at the point of impact. The characteristics of the fracture pattern are important for identifying angulation fractures of the leg and the direction of force (Fig. 5). Although death attributable solely to blunt force trauma of the extremities is not common, it may occur as a result of the disruption of major blood vessels, fat embolism, thromboembolism, rhabdomyolysis, coagulopathy, or wound infection.

Bone fragments should be cleaned and examined for the characteristics of the fracture surface. Reconstruction of the fracture pattern may also provide information on the general characteristics of the striking object, although any conclusion should be drawn with caution.

5.2. Child Abuse

Child abuse *(35,36)* results in traumatic injuries from being beaten, shaken, burned, thrown, purposefully dropped, or subjected to other physical assault. Although children may suffer abuse for many years, the most common age of occurrence is before 5 yr. Abuse-related fractures are most frequently seen in children younger than 12 to 18 mo *(37–40)*. The age distribution is significant, because children in this age range are less

Fig. 5. Angulation "butterfly" fracture of the left femur, with direction of force moving lateral to medial.

likely to suffer accidental fractures, being less mobile and not yet involved in sports activities.

Long-bone fractures are often associated with child abuse. Studies have documented that the extremities are involved in 60 to 77% of cases when skeletal trauma is identified with child abuse *(38,41)*. Indeed, approx 30% of limb injuries occurring early than age 3 are not accidental *(40)*. In another study, investigators found that in 79% of patients younger than 2 yr with femoral fractures, the injury was a result of child abuse; of this percentage, two-thirds had only femoral fractures as a result of abuse *(42)*. Much of this pattern is a result of the relative ease with which fracture occurs in the bones of very young children and should not be seen as an indication that abuse stops in older children.

One hallmark of child abuse is the repetition of fracture production *(17,43)*. The femora and tibiae may bear the marks of numerous fractures in various stages of healing from recent to well healed. For the forensic anthropologist, documentation of multiple fractures with varying stages of healing is crucial. A caution against relying on repeated

injury as the primary identifier of child abuse is that as many as 10% of abused children are killed by the second incident that brings them to the attention of the medical community *(44)*. Skeletal analysis may, however, show a number of unreported injuries. Evidence of skeletal trauma can be correlated with a medical history of poor ability to walk or crawl, complaints about pain when moving, or apparent developmental retardation. Repeated episodes of abuse may result in a child being unable to achieve normal landmarks of growth and development.

Radiographic fracture changes in children occur much faster than in adults. O'Connor and Cohen *(45)* suggest that new periosteal bone may be seen radiographically as early as 4 d after the injury, although gross skeletal manifestations may not be as apparent. Radiographic fracture line definition also is listed as beginning at 10 d after injury. In contrast, studies on dry bones from adults suggest the first changes occur approx 13 d after injury *(27)*.

Although the "battered baby" syndrome can be diagnosed from injuries in various stages of healing, the majority of child abuse deaths are a result of sudden, violent acts provoked by an often trivial event, although they may be part of an ongoing pattern of physical abuse *(39)*. In these cases, the child is often hit severely or thrown about the room.

A second hallmark of child abuse is the presence of bilateral injuries, which are rarely the result of accidental injury. Most abuse-related fractures of the leg, however, actually occur on only one side. Abuse fractures of the femur and tibia often occur at approximately the same height along the bone. These appear to have been produced when the child was held by the legs and thrown against a surface.

Abusive situations may be accompanied by neglect. In these cases, the long bones of the legs may reveal growth-arrest lines, also known radiographically as Harris lines. These radiodense lines are most commonly associated with growth interruptions in response to infection, malnutrition, or both *(46)*.

Among limb injuries, metaphyseal or epiphyseal fractures are included in the more classic signs of child abuse and result from indirect forces *(44,47)*. The legs are particularly vulnerable to being bent, yanked, or turned as the child is picked up or swung by their limbs. In the growing child, portions of the cartilagenous metaphyses of the long bones may be detached *(17,40,44,47,48)*. The most vulnerable area in the lower extremity is the proximal femur. Complete separation is classified as a "bucket-handle" defect and a partial separation is a "corner fracture." The result, should the child survive, can be stunting of growth in the limb. This may be seen as significant differences in limb length between right and left leg, or in differences in the lower leg between the length of the tibia and fibula. These types of fractures can occur accidentally in MVAs and falls from heights and so are not diagnostic. They are also less likely to be found in children aged more than 1 yr, as the strength of the metaphysis increases sufficiently to withstand the forces involved *(38)*.

Another leg injury considered diagnostic of abuse is fractures of the shafts of the femur or tibia *(44,49)*. These injuries can be spiral or oblique as the bone is twisted or, more commonly, transverse as the bone is bent *(39,47,48)* and are found four times more frequently than epiphyseal fractures. Worlock and associates *(37)* noted that infants tended to suffer leg fractures to a greater extent than toddlers. This suggests that infants are more prone to being lifted by the legs and that the risk decreases as the child becomes heavier and more awkward to lift with age.

Other fractures of the lower extremity may be encountered. Displacement of the femoral head may be induced during abuse *(49)*. Fractures of the feet and patella, however, are relatively rare.

For the anthropologist, reliance entirely on skeletal indicators for a diagnosis of child abuse may be problematic. Medical conditions that result in poor bone quality (e.g., osteogenesis imperfecta) must be excluded. Too frequently the "identifier" fractures are in low in incidence *(38)*. Instead, the patterns of multiple injuries or repeated injuries more strongly support the interpretation of abuse.

In cases in which child abuse is suspected, it is essential to clean the remains. If there is soft tissue, it should be inspected for signs of initial callus formation, which should be documented. When the body begins to decompose, however, full cleaning of the skeletal elements may reveal many injuries not evident at autopsy. Not only will well-healed fractures be evident, but the superficial remodeling associated with traumatic injury to the periosteum will also be seen (Fig. 6).

5.3. Motor Vehicle and Car–Pedestrian Accidents

MVAs are a leading cause of death at all ages in the United States *(17)*. Motor vehicles usually refer to automobiles, trucks, and motorcycles, but trains and various kinds of aircraft also produce blunt force trauma during crashes. The requirements of the anthropologist often will vary with the type of vehicle. In the deaths of presumed passengers in planes and trains, the primary analysis usually focuses on the identification of body elements leading to the establishment of a positive identification of the remains and reassociation of body segments. Injuries leading to each death are usually less central to the analysis, unless there is a question concerning a preceding incident, e.g., an assault. For vehicles used on road transportation, distinctions between driver and passenger may be central to the investigation, and the anthropologist's examination may bear weight on this determination. Vehicular homicide and suicide also should be considered by the medical examiner or coroner; therefore, the anthropologist must bring an open mind to the analysis.

Blunt force trauma suffered in such incidents often affects many areas of the body. With MVAs, the surrounding features of vehicle safety mechanisms, the type of impact (front impact, side-swipe, roll-over, rear impact) *(39)*, vehicular speed, and intrusive objects will all be factors in the development of the injury pattern. For the victim, body size and weight, age-related bone density, and awareness of the impending impact are further complications. Finally, there are the problems of human error, such as the failure to use restraints correctly or the decision to ride in nonpassenger areas of the vehicle. For these reasons, there is less consistency in the injury patterns than one would desire in order to quickly assess the position of the victim at impact.

Because of the massive forces involved in MVA, multiple fractures are common. Although no single injury is diagnostic of an MVA, the complex pattern of injuries can provide information on the various points of impact, the forces applied to the body, whether those forces were direct or indirect, and, in some cases, the location of the victim.

5.3.1. Automobile Drivers and Passengers

MVAs usually involve a frontal impact, with the vehicle striking another vehicle, a stationary object, or the ground when the vehicle drives off an elevated surface *(47)*.

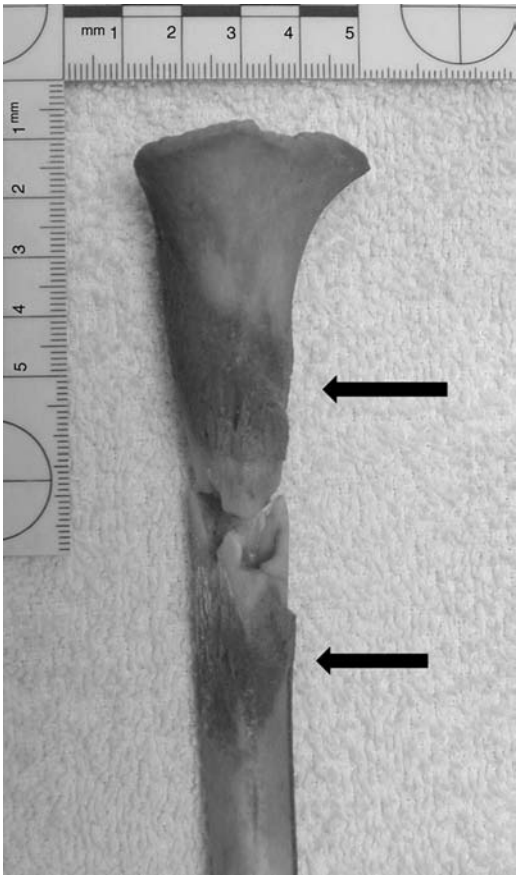

Fig. 6. Close-up of bone remodeling (arrows) to tibia associated with fracture.

Although some energy is absorbed by the vehicle—particularly in more modern cars and trucks, which are designed to crumple while protecting the passenger cabin—some of the impact may be passed along to the occupants. Fatal injuries usually involve the head and torso, but leg injuries are common as the structure collapses, portions of the vehicle are thrust inward (e.g., toe pan intrusion or interaction with pedals), or occupants are thrown against the interior features. The severity and location of injury will vary considerably with the location of the victim within the vehicle.

In the femur, fractures produced during an MVA are found throughout the bone. "Instrument panel syndrome" describes a complex of femoral- and knee joint injuries produced when the leg strikes the dashboard or instrument panel *(50,51)*. Proximally, fractures within the capsule of the hip joint usually result from posterior dislocation *(52)*. These fractures are produced when the dashboard or instrument panel is displaced into the knees, driving the femoral head against the posterior wall of the acetabulum. Associated pelvic fractures may be present, or fragments of acetabulum may be associated with the proximal femur. Subtrochanteric and intertrochanteric fractures are also found, despite the greater resistance to these injuries in younger individuals *(19,53)*. As the density of bone in the proximal femur declines significantly with age, proximal

femoral fractures are more common and comminution is often greater with aging. Drivers are particularly prone to this syndrome because they are often trying to apply the brakes at impact. Front seat passengers may suffer less damage because their hips may be more flexed and therefore driven downward and back so that less damage is sustained by the acetabulum.

Femoral shaft fractures are encountered in MVAs and are seen most frequently in drivers. These defects may take the form of relatively isolated transverse midshaft fractures with significant comminution *(54)*. Studies suggest that these injuries are a result of the leg striking the instrument panel and are more massive than attributable to impact alone. Muscular contraction and bracing of the legs for the crash appear to alter the stresses, producing fractures above the knee area.

Around the knee joint itself, the impact may shatter the patella and cause compression of the distal femur. Typical injuries at the knee include longitudinal or Y-shaped fracturing of the femoral shaft. Drivers tend to have a more upward movement of the femur because of the pressure they are placing on the brake at impact *(55)* bringing their knees into contact with rigid portions of the instrument panel.

Compression injuries to the foot and ankle occur as occupants of the vehicle press their feet on the floor or brake pedal *(30,47)*. As the vehicle itself compacts, the engine compartment and toe pan may be driven into the passenger area, producing twisting and wrenching injuries. These components may also crush the bones of the feet and ankles. Detaching seats may also trap the lower legs, causing the bones to break at the ankle. The impact and inward deformation of the vehicle frame can cause talar head and neck fractures, often known as "aviator's astragulus" *(56)*; this is more commonly found in drivers. This impact may also induce calcaneal fractures, as this bone is compressed by the straightened leg and the vehicle.

For the anthropologist who examines remains extracted from a vehicle or an accident scene, the pattern of injuries described above provides some guidance to the severity of damage inflicted. A primary concern, however, is to determine which of the victims was driving at the time of the accident. This proves much harder to do, because victims are often displaced within the vehicle or ejected on impact. Caution is advised in making any such assessment, however, because the pattern of injuries is highly variable.

Our research on fatal injury patterns shows that lower limb fractures occur in approximately one-fourth of drivers, but only one-tenth of front-seat passengers *(57)*. Rear-seat passengers may have been riding with legs stretched under the seats in front. At impact, an unrestrained backseat passenger can be thrown forward with feet still wedged under the front seat and the leg bending along the edge of the seat. Rear-seat passengers suffer lower limb fractures in almost 40% of cases. Therefore, although the intensity of damage may be expected to be greater in drivers, lower extremity fractures are not found solely in this group.

5.3.2. Motorcyclists

Motorcyclists are more vulnerable to injury because they travel without the protective framework and impact-absorbing devices commonly installed in an enclosed vehicle *(27, 47, 58)*. In our research, we found that motorcyclists tend to suffer from multiple impacts, aside from that with the road *(57)*. A common occurrence in mountainous areas is for the motorcyclist to lose control, leave the road, fly over an embankment

and down a steep hillside and into a tree or other fixed object. Intoxication and inexperience often play a role in these accidents *(59)*; our findings also emphasized the role of excessive speed in virtually all motorcycle accidents.

Lower limb fractures occur in approx 35% of fatal motorcycle accidents *(57)*. Although femoral fractures may occur, tibial fractures in the shaft are the more common event in fatal accidents involving motorcyclists. The seating arrangement on a motorcycle typically positions the driver with flexed knees, which make contact with the ground as the motorcycle tips over during the accident. The multiple leg injuries are often not noted at autopsy, often being grouped under "multiple fractures" in the body, but may be important for the anthropologist. Therefore, the presence of leg fractures is not diagnostic for motorcycle accidents any more than the absence of leg fractures is diagnostic that other causes were involved.

5.3.3. Car–Pedestrian Accidents

Skeletonized remains of car–pedestrian accidents may be received by the anthropologist when the body has been removed from the area for concealment of the incident or when the body was thrown by the car and not located immediately. Although there are often multiple fractures, impact injuries to the legs are often considered hallmarks of the car–pedestrian accident.

Accidents involving automobiles and pedestrians can involve victims of any age; however school-aged children and the elderly are disproportionately at risk *(58,60)*. The circumstances of the impacts vary. Some pedestrians are hit while on crosswalks or sidewalks, others crossing illegally or trying to retrieve items on roadways, still others are lying on the roadway. Variables to consider in the understanding of the injury pattern include the position of the victim, the height and weight of the victim, the size of the vehicle and shape of the impacting surface, and the speed of the vehicle. A number of pedestrians suffer subsequent impacts by cars following the initial vehicle. When faced with simply the skeletal remains, as the forensic anthropologist is, these overlapping factors must be kept in mind.

In the typical scenario, the victim's center of gravity is above the level of the hood of the vehicle and the impact on the legs flips the body up and onto the hood, windshield, or roof of the car. Many suffer significant injuries to the knees and legs as a result of the impact with the car bumper. Bumper fractures of the upper tibial shaft *(61)* or the lateral plateau *(62)* owing to direct horizontal or right-angle blows to the weighted leg by the car bumper are usually oblique or present "butterfly patterns" *(61)*. The fibula is often involved. Compression fractures may occur on the proximal tibia because it is may be compressed against the distal femur during impact. Secondarily, the proximal femur may be broken by impact as the body lands on the upper portion of the car or on the roadway. When the victims are not in a standing position or are relatively small (e.g., children). or if the vehicle has a relatively vertical fronted (e.g., a van), the vehicle may run over the victim and the legs may be broken by the weight of the car *(61)*.

Bumper fractures have received considerable attention in this type of accident. The height of these fractures will vary by the position of the victim, footwear, and angle of impact. If the victim is not standing upright, the impact may occur at a different height, and some types of footwear, such as boots, may displace the location of the fracture.

Braking action may drop the front end of the vehicle, thereby lowering the height of the impact and fracture. Bumper impact, therefore, cannot be assumed to be 90° to the long axis of the bone *(63)*.

Bicyclists who are hit by motor vehicles, like adult pedestrians, tend to be thrown over the vehicle, with the impact occurring when the cyclist lands on the hood, windshield, or roof of the car *(29)* and subsequently the roadway or other object(s). Unlike the pedestrian, however, bicyclists often suffer fewer leg injuries because the cyclist is not usually in a standing position at the time of impact.

More unusual instances of car–pedestrian accidents should also be borne in mind. The victim may have been "surfing" on the hood *(64)* or being pulled by the car while on a bicycle or skateboard. In these cases, leg fractures may occur as a result of a variety of mechanisms, including being run over or being thrown into surrounding objects. Victims who are hit while already lying on the roadway may be dragged for long distances, with abrasion occurring through the dependent portions of the body, including bones.

5.4. Train Accidents

Railroad injuries can be separated into two categories. First, there may be a train derailment followed by a crash, often with compaction and crushing of the cars. In these cases, the injuries will more closely resemble those seen in unrestrained automobile occupants, compounded by the greater weight of the vehicles involved. The second, more common, form involves individuals who are walking on the tracks or lying on the rails and are subsequently hit by trains. It is the latter category that is more likely to be brought to the attention of the forensic anthropologist.

Even a slow moving train is unable to come to an abrupt halt; therefore, unless the individual is thrown clear of the train on impact, the body is often caught beneath the vehicle and run over by subsequent portions. In these cases, the extent of the injuries will depend on the position and location of the victim *(65)*. Although some parallels with car–pedestrian accidents can be seen, in our experience the damage is usually more extensive *(28)*. Body segments can be strewn for long distances, with reported distances of up to 1 mile *(65,66)*. Tissue and body segments can be caught in the undercarriage of the train *(65)*. In cases of suicide, when the person lies across on the track, the rolling and tumbling of the body may be lessened, although leg amputation is expected.

One question that may be raised is whether the victim was deceased prior to being placed on the track. In some cases, preexisting fractures may be identifiable, but it is not likely that this will be the case in the lower extremity unless the mechanism of production is different, such as gunshot or sharp force trauma.

5.5. Plane Accidents

The severity of damage to occupants during aircraft crashes will vary with the angle at which the craft strikes the ground *(39)*. In very steep impacts, the craft and all passengers will be buried in a relatively small and high compacted area. Those components that weigh more decelerate more slowly, driving forward into and through the

intervening material, including human bodies. When the angle of impact is lower, the remains may be scattered over a larger area but the degree of fragmentation may be less. In-flight disintegration from explosions or collisions will result in the wide scatter of material, often over several miles. Falling material may also result in injury and death to those on the ground and the remains of both sources may be intermingled.

Light plane fatalities usually result in multiple fractures *(67)*, although the body may be held together by soft tissue until this decomposes. Similar to the mechanisms of injuries found in drivers of automobiles, compression of the ankle joint on impact can produce talar fractures (also known as "aviator's astragulus"), crushed calcanei, or even penetration of the pedal into the foot.

With commercial aircraft, the heavier plane and greater speeds lead to much greater fragmentation on impact *(30,68)*. The detachment of body segments is extreme and, in some cases, the largest portions found are only a few inches in length. The lower extremity is often divided into small parts with only sections recovered. A frequent recovery pattern is to find jointed bone fragments, longer bone segments having been shattered. In the lower extremity, isolated feet, knee, and hip joints are a common find. Identification as to side is relatively straightforward, but assessment of sex, age, and possibly stature can be tedious, time consuming, and fraught with error. Most final identifications of body segments are now done through DNA analysis.

Seatbelts may play a role in defining the patterns of body fragmentation, but the impact of the framework of the plane, as well as all the contents, complete the process. Flailing of the legs appears to produce a wide variety of femoral fractures *(69)*. Bracing seemed to increase the likelihood of femoral fractures.

Although helicopters do not travel at the very high rates of speed, impact after rapid altitude loss often results in fatalities. Segmental, comminuted fractures at the upper one-third of the tibia are commonly reported in helicopter pilots *(70)*, probably resulting from the impact transmitted through heavy boots worn while flying. Other lower extremity skeletal injuries accompanying these classic signs are tibial plateau fractures, mid-leg amputation, and rotational ankle fractures.

In many cases of plane or helicopter accidents, the impact-based fragmentation of the body is accompanied by extensive burning from the fuel. For the anthropologist, this may mean that additional fragmentation and bone loss because of thermal damage will limit the amount of bone left. For example, one colleague has reported finding only a single piece of bone at the scene of a light plane crash. Even when the remains are relatively intact, fire damage usually means loss of the distal portions of the extremities. Although other evidence should not be automatically excluded, most anthropological work in these situations focus on identification rather than analysis of trauma.

5.6. Falls

Falls are also a common cause of fractures, including those of the lower extremity *(17)*. Falls are usually divided into simple falls and falls from a height. Simple falls are defined as falling from a standing height onto normal terrain, whereas falls from a height involve acceleration and abrupt deceleration at impact beyond that encountered in simple falls. Although skeletal injuries in younger individuals occur as a result of

simple falls, they are rarely fatal. In older individuals, especially those older than 75 yr, a simple fall can lead to incapacitation and death *(71)*. In the leg, age-related and osteoporotic fractures cluster in the hip and increase dramatically in both sexes.

In contrast to simple falls, falls from heights can produce extensive damage but the pattern will vary according to the surface on which impact is made and with the position of the deceased upon impact. A complex of fractures—including basal skull, rib, and extremity fractures—has been designated "jumper syndrome," a term that is used to define the mechanism of injury rather than any suicidal motivation *(72)*. Because many fractures seen in MVAs can occur in falls from heights, information on fractures in other areas of the body (e.g., compression fractures in the spine or at the base of the skull) may be useful for identifying the cause of injury as a fall rather than a MVA.

Although landing on the arms, head, or buttocks after a fall from a height results in variable levels of lower extremity fracture, the most extreme damage comes from landing straight-legged on the feet. In these instances, the impact will compress the joints in the leg as it simultaneously drives the leg upward, producing a shearing action as the leg is driven past the more tightly locked hip joint *(30)*. Fractures in the area of the femoral angle are often produced, as well as subtrochanteric and intertrochanteric fractures *(19,53)*. As in motor vehicle drivers and pilots, landing on the feet after a fall from a height can produce massive fragmentation of the talus because the talus is compacted between the surface and the leg *(56)*. Calcaneal fractures also frequently occur in individuals who fall from a height *(56)*.

Children are less able to control their landing because of disproportionately heavy head and torso weights, and these areas tend to impact first. Fractures are found frequently in the limbs, including the long bones of the legs *(73,74)*, but are less likely to follow the more classic patterns described above.

Identification of victims of falls based on lower limb fractures alone may be problematic. Compression fractures may be noted if the landing was oriented along the vertical axis of the body, but such a landing cannot be assumed. Furthermore, many victims strike other objects during a fall from a height, sustaining impact injuries that may mimic those produced by other causes.

6. *Sharp Force Trauma*

Sharp force trauma refers to damage inflicted by an edged device that produced a stabbing or slicing movement on the bone. Common instruments include knives, scalpels, saws, axes, machetes, and cleavers. Sharp force trauma to the lower extremity is usually encountered by the forensic anthropologist in the context of body dismemberment.

Stabbing injuries are essentially puncture defects produced by the direct penetration of the instrument into the bone. The instrument may be moved back and forth while in the defect, thereby increasing the size of the stab mark. Although the width of the blade cannot be reliably determined, characteristics, such as double-edged or backed, can be seen from the profile. Backed knives or other instruments will produce a "squared-off" edge on one aspect. In contrast, double-edged instruments are pointed on both ends. Often

the sharp force defect is associated with fracturing produced by the "blunt force" of the blow or impact by portions of the instrument, such as the hilt.

Cut marks from slicing or hacking movements are usually thin, longitudinal marks that result from the passage of the sharp edge over the bone. The characteristics of the profile reflect the type of edge. Reichs *(75)* states that knife marks will show a narrow, smooth, V-shaped profile, with striations perpendicular to the *kerf floor* (the floor of a definable cut in the bone) and producing little loss of bone within the cut itself.

Experimentation with cut marks reveals that different edge forms will produce different characteristics, such that scalpel blades will produce noticeably different cut features that those of a knife *(76–78)*. Overlap between the cut marks that is attributable to the angle of the cut and force applied, however, make exact identification problematic. Scanning electron microscopy combined with quantitative methods are of value in analysis where a suspect weapon is known.

6.1. Dismemberment

Cut marks may be associated with damage that occurs after the death of the individual. Because of difficulties of body transport and disposal, the lower limbs may be dismembered *(79)*. In other cases, specific mutilation of the remains may entail separating portions of the body. Segmentation cuts on the bones usually have perimortem characteristics. These marks are distinguished by the location of the cuts in relation to joints or visualized body sections and can provide information on the dismembering. Cut marks usually are close to or at the joints and, in some cases, the attachment sites of the major muscles if the bones have been defleshed.

Dismemberment does not require anatomical knowledge, although such knowledge makes the segmentation of the body much easier. Knowledge of anatomical relationships between bones becomes apparent in the patterns of disarticulation and careful documentation of such cuts must be completed. An incorrect conception of the body segments, especially at the shoulder and hip joints, often leads to dismemberment attempts through the upper one-third of the humerus and femur rather than through the joint itself. Presumably this is triggered by the perpetrator seeing a slimming of the body segment above or below the joint itself and incorrectly assuming that this is the easiest portion to cut. False starts are common and can provide information on the sequence of tool types used during the dismemberment.

The scope of dismemberment is highly variable and portions of the body may distributed over wide areas *(80)*. The head and hands may be removed in order to hide identity. In the extreme, bodies can be put in tree chippers to destroy the evidence. If the body must be transported, segments may be made to make lifting and compacting of the body easier. In some instances, dismemberment is done to express complete destruction of the victim. Finally, as in archaeological instances, dismemberment may represent part of the processing of remains for later consumption.

The instruments of dismemberment include some of the items used in homicidal sharp force trauma, with a tendency to the larger range instruments such as saws, axes, and chainsaws. Saw marks are usually squared in nature, as the angled teeth on the cutting edge produce a wider area of bone destruction than a knife *(26,75)*. There are visible striations that run parallel to the kerf floor. Power saws may produce a series of ripples on

the cut surface known as harmonics. Careful examination of the cut surface can yield information on the blade and tooth size and shape *(26)*. Breakaway spurs are common, as the weight of the body segment causes the small remaining portion of the bone to break prior to completion of the cut. Axe marks are wide and V-shaped. As with knife marks, the striations are perpendicular to the kerf floor but are easily distinguished by the more significant bone damage and the frequent presence of breakaway spurs.

Careful cleaning and examination is critical to dismemberment analysis. If bone samples are to be taken and retained, which is recommended for re-examination possibilities, the samples should include several inches of the bone and should include both sides of the cut area *(75)*. The cut marks used to extract the sample should be marked. Making casts of the cut surface using vinyl polysiloxane, Microsil®, or other casting substances may be helpful to preserve the tool marks.

7. Gunshot Injuries

Gunshot injuries to the tubular bones of the lower extremity will usually result in severe fragmentation. The extent of the destruction will depend on the velocity, shape, and weight of the bullet at impact, as well as the quality of the bone itself. Distinctions between low-velocity bullets traveling under 1800 ft/s and high-velocity bullets traveling 1800 to 2000 ft/s are frequently evident. Low-velocity fracture patterns may mimic blunt force trauma, in that there may be more bone deformation and less fragmentation present than in high-velocity gunshot wounds *(22)*. One feature that is diagnostic of gunshot trauma is the presence of a *cone of percussion*—a cone-shaped transmission of the force that will displace a cone-shaped piece of bone that is wider internally than externally. In most cases, there will be at least some resemblance to the beveling effects seen in the skull. However, owing to the size of the bones in the leg, the beveling is often distorted. The cone of percussion that results in typical internal and external beveling will be confined to those rare occasions when a bullet impacts squarely on the shaft. More tangential shots may still produce massive fragmentation but with less evident conical spalls.

Fractures radiating from the impact area will move up, down, and around the shaft of the bone. The result is often bone shattering and extensive fragmentation *(81)*. The higher the velocity of the impact or the heavier the weight of the bullet, the greater the amount of fragmentation produced in the bone (Zephro L., unpublished data). In the living body, some bone fragments may be retained by adherence to soft tissue, whereas other fragments exit the body. Such expelled fragments at the scene may be useful in determining the location and orientation of the body when shot.

Fatal isolated gunshot injuries in the femur are usually a result of blood loss following trauma to the femoral artery and its branches *(82)*, because there are no internal organs in proximity. Damage to the arterial system in the thigh is most common when the injuries are anteromedial. Comminution is frequent in femoral gunshot injuries, because the energy of the shot is absorbed by the bone *(81)*.

As with all injuries to the body, the anthropologist is limited in what conclusions may be drawn from those derived directly from the bones. Injuries that show beveling

and fracturing typical of those seen with gunshot injuries are reported as being "consistent with gunshot injuries." Relationship to anatomical features may be noted, such as proximity to the femoral artery, but linking the skeletal injury to the soft tissue damage should be made by the medical examiner/coroner's office in consultation with a forensic pathologist.

8. Summary

The forensic anthropologist can play a crucial role in the medicolegal investigation of the skeleton. Anthropological evaluation requires careful preparation and documentation to include photographs, written records, and charts. The report must reflect the progress of the analysis, beginning with a descriptive list of perimortem defects, followed by a linking of defects by insults, an explanation of the biomechanics causing bone fracture, and culminating in the sequencing of defects and inference about body position (if possible). Antemortem and postmortem defects and damage must also be documented and reported.

There are significant limitations to the breadth of interpretation that can be applied to skeletal evidence. The forensic anthropologist must base his or her findings purely on the examination of skeletal material, without incorporating scenarios proposed by investigators or counsel. Therefore, anthropological discussions of insults in relation to actual events must be solely limited to observations of the skeleton. For example, one can discuss an impact on the lateral aspect of the left tibia and subsequent butterfly fracture, but the anthropologist cannot ascertain from bones alone whether a car hit the individual. For court presentation, however, it is often critical that skeletal evidence be consistent with scenarios. Only during court testimony under direct questioning should an exploration of whether skeletal defects are consistent with more specific events be addressed. To include these statements in the report will overly complicate the report, raise issues that may not be relevant to the case, and may add unnecessarily to the length of testimony at the risk of diluting the weight given the primary points. Moreover, it provides written evidence that the anthropologist knew of the possible cause prior to analysis and suggests that such knowledge may have caused him or her to be biased in the analysis to support the argument.

Forensic anthropologists act as consultants in the medicolegal process of postmortem examination. Unless specifically authorized within a coroner or medical examiner office (i.e., deputy coroner or death investigator), forensic anthropologists should not determine cause or manner of death. However, within the context of the entire investigation, the anthropological report can identify and document the occurrence of trauma, sequence insults, and help recognize types of forces involved.

Acknowledgment

The authors gratefully acknowledge Dr. John Hain for his editorial suggestions and insightful comments.

References

1. Maples WR. Trauma analysis by the forensic anthropologist. In: Forensic osteology: advances in the identification of human remains. Reichs KJ, ed. Springfield: Thomas, 1986:218–228.
2. Fenton TW, Birkby WT, Cornelison JA. Fast and safe non-bleaching method for forensic skeletal preparation. J Forens Sci 48:274–276 (2003).
3. Sommer HG, Anderson S. Cleaning skeletons with dermestid beetles: two refinements in the method. Curator 17:290–298 (1974).
4. Russell WC. Biology of the dermestid beetle with reference to cleaning. J Mammology 28:29–33 (1947).
5. Weichbrod RH. The dermestid beetle: a tiny laboratory worker. Lab Animal. 16:29–33 (1987).
6. Ubelaker DH. Human skeletal remains: excavation, analysis, interpretation. 2nd ed. Washington, DC: Taraxacum: Smithsonian Institute, 1989.
7. Krogman WM, Iscan MY. The human skeleton in forensic medicine. Springfield, Ill: Charles C. Thomas, 1986.
8. Hangay G. Biological museum methods. Vol 1. Orlando: Academic Press, 1985:326–365.
9. Galloway A. Broken bones: anthropological analysis of blunt force trauma. Springfield: Charles C. Thomas Publishers, 1999.
10. Ubelaker DH. The evolving role of the microscope in forensic anthropology. In: Forensic osteology: advances in the identification of human remains. Reichs KJ, ed. Springfield: C. Thomas, 1998:514–532.
11. Bodziak WJ. Footwear impression evidence: detection, recovery, and examination. 2nd ed. Boca Raton, Fla: CRC Press, 2000:27–58.
12. Sauer NJ. The timing of injuries and manner of death: distinguishing among antemortem, perimortem and postmortem trauma. In: Forensic osteology: advances in the identification of human remains. 2nd ed. Reichs, KJ, ed. Springfield: Charles C. Thomas Publishers, 1998:321–332.
13. Sledzik P, Kelley M. Initial osseous remodeling following trauma. [manuscript]
14. Ortner D. Identification of pathological conditions in human skeletal remains. 2nd Ed. London: Academic Press, 2003.
15. Buckwalter JA, Einhorn TA, Marsh JL. Bone and joint healing. In: Rockwood and Green's Fractures in adults. Vol 1. 5th ed. Bucholz RW, Heckman JD, eds. Philadelphia: Lippincott, Williams and Wilkins, 2001:245–271.
16. Johnson E. Current developments in bone technology. In: Advances in archaeological method and theory. MB Schiffer, ed. New York: Academic Press, 1985:157–235.
17. Rogers LF. Radiology of skeletal trauma. 2nd ed. New York: Churchill Livingstone, 1992.
18. Krettek C, Halfet DL. Fractures of the distal femur. In: Skeletal trauma: basic science, management, and reconstruction. 3rd ed. Browner BD, Jupiter JB, Levine AM, Trafton PG, ed. Philadelphia: WB Saunders, 2003:1957–2012.
19. Russell TA. Subtrochanteric fractures of the femur. In: Skeletal trauma: basic science, management, and reconstruction. 3rd ed. Browner BD, Jupiter JB, Levine AM, Trafton PG, ed. Philadelphia: WB Saunders, 2003:1832–1878.
20. Carter DR, Beaupre GS. Skeletal function and form: mechanobiology of skeletal development, aging and regeneration. Cambridge: Cambridge University Press, 2001.
21. Hipp JA, Hayes WC. Biomechanics of fractures. In: Skeletal trauma: basic science, management, and reconstruction. 3rd ed. Browner BD, Jupiter JB, Levine AM, Trafton PG, ed. Philadelphia: WB Saunders; 2003:90–119.
22. Smith OC. Ballistic bone trauma. In: Bones, bullets, burns, bludgeons, blunderers and why. Symes S ed. Workshop presented at: 48th Annual AAFS meeting, Nashville, Tenn, 1996.
23. Berryman H. Blunt trauma: cranial and tubular bone. In: Bones, bullets, burns bludgeons, blunderers and why. Symes S, ed. Workshop presented at: 48th Annual AAFS meeting, Nashville, Tenn., 1996
24. Harkess JW, Ramsey WC, Ahmadi B. Principle of fractures and dislocations. In: Fractures in adults. Vol 1, 3rd ed. Rockwood C, Green DP, Bucholz RW, eds. New York: JB Lippincott, 1991:1–21.

25. Symes S, Hugh E. Berryman HE, Smith OC, Moore SJ. Bone fracture III: microscopic fracture analysis of bone. Paper presented at: the American Academy of Forensic Sciences, Anaheim, Calif., 1991.
26. Symes S. Saw marks in bone: introduction and examination of residual kerf contour. In: Forensic osteology: advances in the identification of human remains. Reichs KJ, ed. Springfield: Charles C. Thomas, 1998:389–409.
27. Plueckhahn VD, Cordner SM. Ethics, legal medicine and forensic pathology. Melbourne, Australia: Melbourne University Press, 1991.
28. Gonzalez TA, Vance M, Helpern M, Umberger CI. Legal medicine, pathology, and toxicology. New York: Appleton-Century-Crofts, 1954.
29. Adelson L. Homicide by blunt violence: deaths caused by manual, pedal and instrumental assault and by motor vehicle crashes. In: The Pathology of Homicide: a Vade Mecum for Pathologist, Prosecutor and Defense Counsel. Springfield: Charles C. Thomas, 1974:378–520.
30. Spitz WU, Fisher RS. Medicolegal investigation of death: guidelines for application of pathology to crime investigation. Springfield: Charles C. Thomas, 1980.
31. Murphy GK. "Beaten to death": an autopsy series of homicidal blunt force injuries. Am J Forensic Med Pathol 12:98–101(1991).
32. Marks MK, Elkins SK. Craniofacial fractures: collaboration spells success. In: Broken Bones: Anthropological Analysis of Blunt Force Trauma.Galloway A, ed. Springfield: Charles C. Thomas, 1999:258–286.
33. Galloway A, Willey P, Snyder L. Human bone mineral densities and survival of bone elements: a contemporary sample. In: Forensic Taphonomy: the Post-Mortem Fate of Human Remains. Haglund W, Sorg M, eds. Boca Raton: CRC Press, 1997:295–317.
34. Court-Brown CM. Femoral diaphyseal fractures. In: Skeletal Trauma: Basic Science, Management, and Reconstruction. 3rd ed. Browner BD, Jupiter JB, Levine AM, Trafton PG, eds. Philadelphia: WB Saunders, 2003:1879–1883.
35. Caffey J. Multiple fractures in the long bones of infants suffering from chronic subdural hematoma. Am J Roentgenol Rad Ther. 56:163–173 (1946).
36. Kempe CH, Silverman FN, Steel J, et al. Battered child syndrome. JAMA 181:17–23 (1962).
37. Worlock P, Stower M, Barbor P. Patterns of fractures in accidental and non-accidental injury in children: a comparative study. BMJ 293:100–102 (1986).
38. Merten DF, Radkowski MA, Leonidas JC. The abused child: a radiological reappraisal. Radiology 146:377–381 (1983).
39. DiMaio DJ, DiMaio VJM. Forensic Pathology. New York: Elsevier, 1989.
40. Holter JC, Friedman SB. Child abuse: early case finding in the emergency department. Pediatrics 42:128–138 (1968).
41. King J, Diefendorf D, Apthorp J. Analysis of 429 fractures in 189 battered children. J Ped Orthoped 8:585–598 (1988).
42. Ander WA. The significance of femoral fractures in children. Annals of Emergency Medicine 11:174–177 (1982).
43. Kerley E. The identification of battered-infant skeletons. J Forensic Sci 223:163–168 (1978).
44. Green NE. Child abuse. In: Skeletal Trauma in Children.Green NE, Swiantkowski MF, eds. Philadelphia: WB Saunders, 1994:517–531.
45. O'Connor JF, Cohen J. Dating fractures. In: Diagnostic Imaging of Child Abuse. 2nd ed. Kleinman PK, ed. St. Louis: Mosby, 1987:168–177.
46. Skinner M, Anderson GS. Individualization and enamel histology: a case report in forensic anthropology. J Forensic Sci 36:939–948 (1991).
47. Knight B. Forensic Pathology. New York: Oxford University Press, 1991.
48. Cameron JM, Rae LJ. Atlas of the battered child syndrome. Edinburgh: Churchill Livingstone, 1975.
49. Cramer KE, Green NE. Child abuse. In: Skeletal Trauma in Children. Vol. 3. Green NE, Swiontkowski MF, eds. Philadelphia: WB Saunders, 2003:587–605.

50. Kulowski J. Interconnected motorist injuries of the hip, femoral shaft and knee. 5th Stapp Car Crash Conference 1961:105–124.
51. Walz F. Lower abdomen and pelvis, anatomy and types of injury. In: The Biomechanics of Impact Trauma. Aldman B, Chapon A, eds. Amsterdam: Elsevier Science Publishers; 1985:279–286.
52. Swiontkowski MF. Intracapsular hip fractures. In: Skeletal Trauma: Basic Science, Management, and Reconstruction. 3rd ed. Browner BD, Jupiter JB, Levine AM, Trafton PG, eds. Philadelphia: WB Saunders, 2003:1700–1775.
53. Baumgaertner MR. Intertrochanteric hip fractures. In: Skeletal Trauma: Basic Science, Management, and Reconstruction. 3rd ed. Browner BD, Jupiter JB, Levine AM, Trafton PG, ed. Philadelphia: WB Saunders, 2003:1776–1816.
54. Tencer AF, Kaufman R, Ryan K, et al, for the Crash Injury Research and Engineering Network (CIREN). Femur fractures in relatively low speed frontal crashes: the possible role of muscle forces. Accid Anal Prev 34:1–11 (2002).
55. Stewart MJ, Milford LW. Fracture-dislocation of the hip. J Bone Joint Surg Am 36:315–342 (1954).
56. Digiovanni CW, Benirschke SK, Hansen ST. Foot injuries. In: Skeletal Trauma: Basic Science, Management, and Reconstruction. 3rd ed. Browner BD, Jupiter JB, Levine AM, Trafton PG, ed. Philadelphia: WB Saunders, 2003:2375–2492.
57. Galloway A, Mason RT. Skeletal trauma in fatal impact injury: possibilities and limitations for interpretation. Proceedings from the American Academy of Forensic Sciences; Seattle, Wash; February 2001.
58. Waller JA. Injury control: a guide to causes and prevention of trauma. Lexington, Mass: Lexington Books; 1985.
59. Larsen CF, Hardt-Madsen M. Fatal motorcycle accidents in the county of Funun (Denmark). Forensic Sci Int 38:93–99 (1988).
60. O'Neill B. The statistics of trauma. In: The Biomechanics of Trauma. Nahum AM, Melvin J, eds. Norwalk, Conn: Appleton-Century-Crofts; 1985:17–30.
61. Spitz WU. The road traffic victim. In: Medicolegal Investigation of Death: Guidelines for the Application of Pathology to Crime Investigation. 3rd ed. Spitz WU, ed. Springfield: Charles C. Thomas; 1993.
62. Watson JT, Schatzker J. Tibial plateau fractures. In: Skeletal Trauma: Basic Science, Management, and Reconstruction. 3rd ed. Browner BD, Jupiter JB, Levine AM, Trafton PG, eds. Philadelphia: WB Saunders, 2003:2074–2130.
63. Eisele JW, Bonnell HJ, Reay DT. Boot top fractures in pedestrians: a forensic masquerade. Am J Forensic Med 4:181–184 (1983).
64. Kohr RM. Car surfing in Indiana: an unusual form of motor vehicle fatality. J Forensic Sci 37:1693–1696 (1992).
65. Watanabe T. Atlas of Legal Medicine. Philadelphia: JB Lippincott; 1972.
66. Cina SJ, Koelpin JL, Nichols CA, Sonradi SE. A decade of train–pedestrian fatalities: the Charleston experience. J Forensic Sci 39:668–673 (1994).
67. Shkrum MJ, Hurlbut DJ, Young JG. Fatal light aircraft accidents in Ontario: a five year study. J Forensic Sci 41:252–263 (1996).
68. Fulginiti L, Czuzak MH, Taylor, KM. Scatter versus impact during aircraft crashes: implications for forensic anthropologists. In: Broken Bones: Anthropological Analysis of Blunt Force Trauma. Galloway A, ed. Springfield: Charles C. Thomas; 1999:322–329.
69. Brownson P, Rowles JM, Wallace WA, Anton DJ. The mechanism of femoral fracture in an impact accident. Aviat Space Environ Med 69:971–974 (1998).
70. Dummit ES, Reid RL. Unique tibial shaft fractures resulting from helicopter crashes. Clin Orthop Rel Res 66:155–158 (1969).
71. Granek E, Baker SP, Abbey H, et al. Medications and diagnoses in relation to falls in a long-term care facility. J Am Geriatric Soc 35:503–511 (1987).
72. Scalea T, Goldstein A, Phillips T, et al. An analysis of 161 falls from a height: the 'jumper syndrome." J Trauma 26:706–712 (1986).

73. Smith MD, Burrington JD, Woolf AD. Injuries in children sustained in free falls: an analysis of 66 cases. J Trauma 15:987–991 (1975).
74. Barlow B, Niemirska M, Gandhi RP, Leblanc W. Ten years of experience with falls from a height in children. J Ped Surg 18:509–511 (1983).
75. Reichs KJ. Postmortem dismemberment: recovery, analysis and interpretation. In: Forensic Osteology: Advances in the Identification of Human Remains. Reichs KJ, ed. Springfield: C. Thomas; 1998:353–388.
76. Bartelink EJ, Wiersema JM, Demaree RS. Quantitative analysis of sharp-force trauma: an application of scanning electron microscopy in forensic anthropology. J Forensic Sci 46:1288–1293 (2001).
77. Humphrey JH, Hutchinson DL. Macroscopic characteristics of hacking trauma. J Forensic Sci 46:228–233 (2001).
78. Tucker BK, Hutchinson DL, Gilliland MFG, Charles TM, Daniel HJ, Wolfe LD. Microscopic characteristics of hacking trauma. J Forensic Sci 46:234–240 (2001).
79. Rajs J, Lundstrom M, Brobert M, Lindberg L, Lindquist O. Criminal mutilation of the human body in Sweden: a thirty-year medico-legal and forensic psychiatric study. J Forensic Sci 43:563–580 (1998).
80. Symes SA. Morphology of saw marks in human bone: identification of class characteristics. PhD dissertation, University of Tennessee, 1992.
81. Tornetta P, Tiburzi D. Anterograde interlocked nailing of distal femoral fractures after gunshot wounds. J Orthoped Trauma 8:220–227 (1994).
82. Shayne PH, Sloan EP, Rydman R, Barrett JA. A case-controlled study of risk factors that predict femoral arterial injury in penetrating thigh trauma. Ann Emerg Med 24:678–690 (1994).

Chapter 9

Biomechanics of Impact Injury

David J. Porta, PhD

1. Introduction

Physicians diagnose and treat. Engineers break and build. The field of biomechanics is a wonderful bridge between the two. Those who study the biomechanics of trauma get to work with fine people in both areas in an effort to elucidate mechanisms of injury. Presumably, definition of these mechanisms can lead to injury mitigation and perhaps even enhanced treatment outcomes. In the forensic arena, determination of injury mechanism can be a critical component in settling legal disputes, as illustrated by the case studies at the end of this chapter.

2. Basic Fracture Event

The complete fracture of a bone due to impact is a very quick event. In Fig. 1, the heavy cart is traveling a mere 7.8 m/s (17.5 mph) and the cadaveric foot is restrained only by the friction of the shoe with the concrete. During the impact, a force transducer situated between the two pipes records the resistance the cart encounters. At the instant that the leading 4.75-cm diameter steel pipe contacts the leg, the transducer is pinched between the pipes (the front pipe is connected to the rear by slide pins) and a signal analyzer captures force readings at up to 10,000 times per second. Figure 2 shows a sample plot of force (kN) vs time (ms) for these types of impacts. The tibia, fibula, and soft tissues store energy as they bend until the peak of the graph is reached. After this point, the bone fractures and the force drops off precipitously. The pipe contacts and pushes soft tissues for a short period of time as the leg wraps and then swings free, but the actual bone fracture event occurs in less than 0.001 s *(1)*.

When reconstructing an injury scenario, the extremely high speed of fracture propagation must be kept in mind. How can a victim or a witness be expected to know

From: *Forensic Science and Medicine*
Forensic Medicine of the Lower Extremity: Human Identification and Trauma Analysis of the Thigh, Leg, and Foot
Edited by: J. Rich, D. E. Dean, and R. H. Powers © The Humana Press Inc., Totowa, NJ

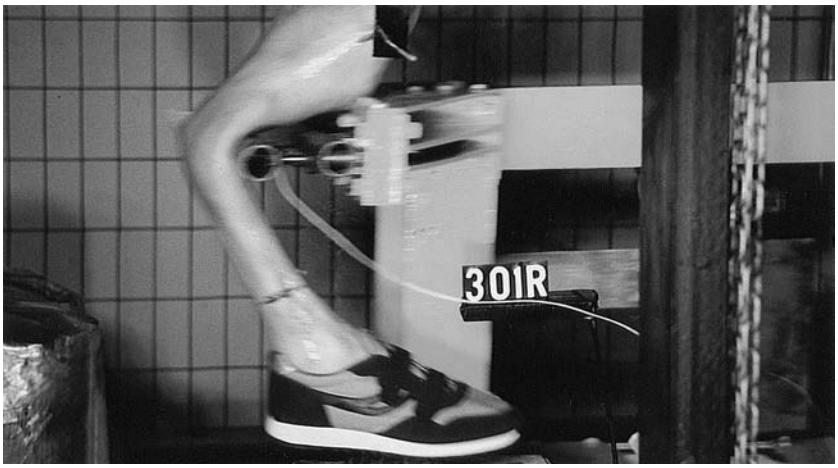

Fig. 1. Cadaver test simulating a pedestrian impact.

the precise position of a body part during an auto accident, attack, or slip-and-fall accident? What about the level of weight bearing? The precise angle of impact? In short, relying on the verbal history of a patient or witness is unwise. However, this hasn't stopped many a physician from rendering an opinion "to a high degree of medical certainty" that the injuries they treated were due to a particular accident or insult. On cross-examination, a skilled attorney can quickly separate the medical facts from hearsay. Often, the testifying physician is confused about his or her role. As the person who rendered medical care, he or she can testify to the extent of the injuries and usually the degree of impairment and potential disability. However, unless there is something remarkable about the nature of the injury (e.g., metal flakes were recovered from the fractured proximal tibia), the physician is generally unable to state with certainty that the cause of a particular injury was a bumper strike to the leg, for example. Treating thousands of patients with the same type of injury does not, in and of itself, qualify one to render opinions about the *cause* of a particular injury. Given proper questioning, the physician and court will soon realize that "medical certainty" does not apply when the rationale is based more on the timeline from the patient history than on the particulars of the injury. Imagine if patient history were the cornerstone of other medical opinions. Would there not be a large number of physicians testifying that toilet seats cause sexually transmitted diseases, given the histories reported by philandering husbands? Or perhaps obstetricians would support the stories of immaculate conceptions given the histories reported by impregnated 15-yr-olds.

Determination of the fracture mechanism related to impact should be based on scientific data and not on unreliable patient histories regarding an event that took place in a fraction of a second. Before introducing some basic tenets of that science, a review of bone composition is in order.

2.1. Bone Composition

It is assumed that persons reading this text will already be somewhat familiar with the basic composition of bone. However, in trying to convey the effects of the physics

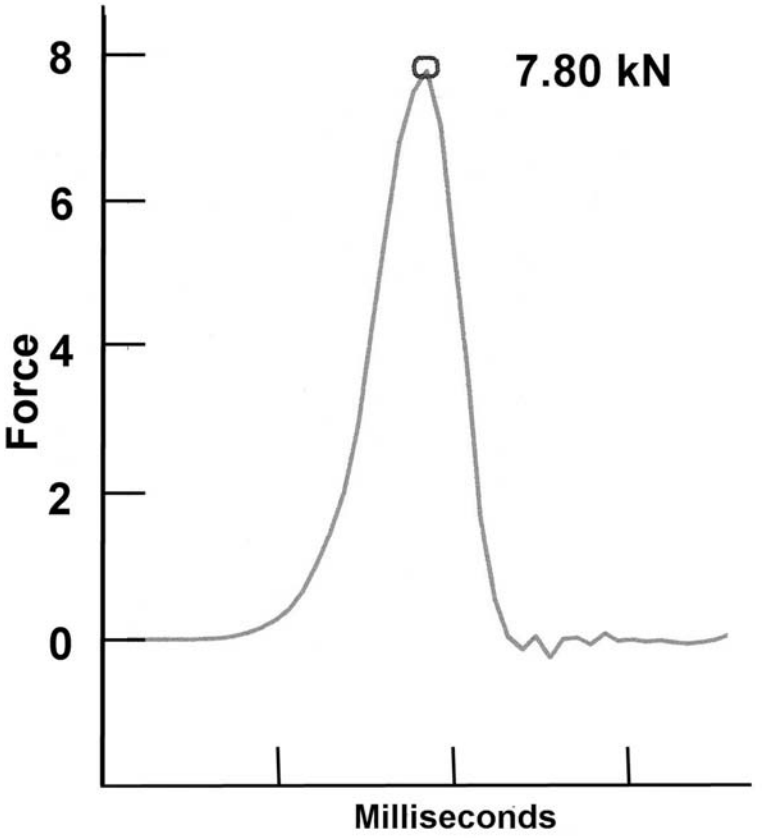

Fig. 2. Sample force plot from femur impact at 7.5 m/s.

involved in bone fracture, we must briefly revisit the materials of which bone is composed and discuss them in terms that engineers might use.

A bone is a nonhomogeneous, composite organ consisting of several types of tissue, although osseous connective tissue is dominant. Bone occurs in two forms: a low-density tissue (0.05–1.0 g/cc) termed cancellous, trabecular, or spongy bone; and a high-density form (1.8–2.0 g/cc) referred to as compact, cortical, or hard bone *(2,3)*. In long bones, both cancellous and compact osseous tissues are present, but their relative amounts vary by region. The epiphyses are large masses of cancellous bone covered by a thin layer of compact bone (and hyaline cartilage within the joint cavities). The diaphysis is a thickened tube of compact bone that has a thin layer of cancellous bone lining its medullary (marrow) cavity. The composition of the patella and tarsal bones is very similar to that of the epiphyses.

As with most connective tissues, the extracellular matrix is the defining feature, not the cells themselves. Water accounts for approx 25% of total bone weight. The remaining osseous connective tissue is generally described as roughly 50% organic and 50% inorganic by mass. The protein collagen accounts for about 95% of the organic extracellular matrix. Embedded in the matrix are the inorganic crystals of the mineral hydroxyapatite, $Ca_{10}(PO_4)_6(OH)_2$. The crystals are 50 to 100 angstroms (Å; where 1 Å = 10^{-7} mm) long

and provide bone with great compressive strength, while the collagen gives bone considerable tensile strength *(3–5)*.

Compact bone is arranged in functional units termed osteons or Haversian systems. Osteons take the form of small columns organized parallel to the long axis of a bone. Each osteon is approx 20 mm long and 200–400 μm in diameter *(6)*. At the center of each adult osteon is a small canal roughly 70 μm in diameter that transmits vascular components. Mature bone cells, or osteocytes, are arranged in concentric rings around each canal. The organic and inorganic components occupy the areas between osteocytes, such that each cell is enclosed in a small cave termed a lacuna. Tiny canaliculi serve as conduits for nutrients and waste transport between the lacunae and blood vessels in the larger central canal system. The concentric rings of cells are spaced according to very organized patterns of collagen and hydroxyapatite crystals. This composite of organic and inorganic materials, combined with nonuniform shapes, gives bone the property of being anisotropic. In terms of traumatic impact, this means bone behaves differently when the impact arrives from different angles. For example, bone is significantly more resistant to compressive forces along its long axis than when it is struck transverse to the axis. This is a product of the tendency of the osteonal structure to follow the long axis of the bone *(7)*. Additionally, it has been shown in cadaver studies that lower-extremity long bones offer greater resistance to anterior impacts than to medial, lateral, or posterior strikes, but there is no statistically significant difference between the breaking strength of left and right bones struck in the same plane *(1)*.

The next section serves as an introduction to biomechanics as it relates to bone. There are many excellent texts (e.g., *8–10*) devoted to biomechanics. However, the text by Lucas et al. *(11)* is highly recommended for anyone seeking an efficient discussion of details that cannot be covered in this single chapter. Their paperback text published in 1999 is particularly interesting and well organized. Each of the 17 chapters begins with a "Clinical Question," and the authors skillfully guide the reader (presumably an orthopedic resident) through some fairly complicated concepts that can only be introduced here.

2.2. The Physics of Movement

A brief review of any introductory physics text will remind one of the many ways in which scientists describe movement. *Scalar* quantities are the most basic variables. Each of these quantities has only one component—e.g., time is measured in seconds, length in meters, and mass in grams. When these scalar measures are combined, the resulting quantity is a bit more complex. For example, velocity (v) is the measure of distance traveled in a given length of time (recorded perhaps as m/s or mph). The energy of motion, termed kinetic energy (Ke), is dependent on velocity at a particular moment, and the higher the kinetic energy, the greater the risk of skeletal trauma. Kinetic energy is calculated by multiplying half the mass of a moving object by the square of its velocity ($Ke = 1/2\ mv^2$). Bearing both components in mind, it can be seen that a significant amount of potential energy is developed when a low-mass bullet is fired at a great velocity, or when a high-mass object travels at a relatively low rate of speed. Either can be sufficient to damage the lower extremity or any other body part.

A major cause of lower-extremity injury is motor vehicle accidents. Often the injurious motion of a vehicle is described in terms of its change in velocity or delta V (Δv).

However, further definition is necessary. A large change in velocity is not necessarily injurious. When one rides in a jet plane, the change in velocity during landing may be 400 mph, yet no passenger is injured. However, a car crash at 40 mph may result in serious injury or death for of all those aboard. The difference is quite simple. In an airplane, the change in velocity happens over several seconds or even minutes. This presents very little stress to the body. The car crash is a relatively instant change in velocity (probably over a period of 100–200 ms). The difference in this *pulse duration* is critical. Thus, when Δv is specified for a crash, it should be noted that this is a relatively instantaneous change in velocity.

The change in velocity *over time* is referred to as acceleration (often measured in m/s^2 or ft/s^2). One may also see "g" listed as a unit of acceleration. This refers to multiples of the earth's gravity, which pulls a body towards the earth's core at an acceleration of 9.80665 m/s^2. The use of acceleration is an improvement in the description of how a body acts when it is slowed (or sped up) to an injurious level. While acceleration is commonly utilized in describing neck injuries in car crashes, it also has a relationship to lower-extremity injuries. Extremities are often damaged during direct impact. Injurious impactors generally must have a fair amount of mass. Few people would mind having a lightweight foam ball accelerated to 90 mph against their leg. However, if the foam is replaced by a 5-oz baseball, the results could be serious. If the object in question is a 16-lb bowling ball, fracture surely would result.

The mass of an accelerated object exerts force. Force is a *vector* quantity, which must be described by two components: its magnitude and the direction of application. Sir Isaac Newton (1643–1727), in the second of his three laws regarding the motion of bodies, taught the world that force is the product of an impactor's mass and its acceleration ($F = ma$). In fact, the International System of Units (SI unit) for force ($kg \bullet m/s^2$) is termed a newton (N; 1 N = 0.225 lb of force [lbf]).

When a force is applied to a bone, it causes the bone to change its motion, size, and/or shape *(12)*. At this point, force may seem to be a fairly complicated but sufficient measure of an impact. However, force alone is woefully inadequate and often (particularly in a legal environment) misleading in describing an impact. To state that it takes 7.8 kN of force (1753 lbf) to break a leg (Fig. 2) is meaningless without describing the manner of application (especially the composition and shape of the impacting surface). Take, for example, the simple act of cutting a log. An axe of a given mass is accelerated towards the log such that the impact fractures the wood. Implicit in our understanding of this event is the fact that the sharp, thin edge of the axe was utilized. Imagine taking the same axe in hand and turning it 90 degrees, such that the wide side of the blade contacts the log. If it is accelerated in the same manner as before, the chance of cutting the log is almost nil. The force is equal, but the results are not. This difference reflects the engineering concept of stress, which is a more acceptable description of a traumatic force that will be explained in the next section. Although engineering publications may list results in terms of g or N, a quick look at the materials and methods section will invariably yield the impact parameters necessary to calculate more advanced concepts like stress and bending moment.

The manner of application of force or stress is critical when investigating injury mechanisms leading to bone fracture. In an effort to define the tolerance of the human

body to trauma, engineers have studied the material properties of bone. Just as biologists study the body by investigating its cells or molecules, engineers begin their study of structures by looking at the material and mechanical properties of finite elements. This approach is foundational of the field of biomechanics.

3. BIOMECHANICS

"In engineering, the design of failure-resistant structures requires three important pieces of information: (a) the geometry of the structure, (b) the mechanical properties of the materials from which the structure is made, and (c) the location and direction of the loads to which the structure is subjected in service." (3)

The biomechanics of bone has been thoroughly studied and presented by numerous authors (e.g., *13–16*). As noted previously, bone tissue is able to resist compressive forces while maintaining good tensile strength. In essence, there are numerous strong but brittle crystals embedded in a weaker, flexible mesh. From a material science standpoint, this provides a composite that is generally stronger per unit weight than a pure sample of either individual substance. Two factors are critical in defining material properties: strength and stiffness. To understand these factors, one must study the material under loading. The material properties of bone have been determined by the study of small samples of a standard length, width, and depth without regard for overall structural geometry. These milled cubes of bone were subjected to external pressure or Stress (σ).

Stress is a force applied per unit area and is usually expressed in terms of lb/in^2 (psi) or N/m^2, also referred to as a Pascal (Pa) in honor of the French scientist Blaise Pascal (1623–1662). In the previous example of force application, the properly swung axe (striking with the narrow portion of the head) imparts far greater stress and thus fractures the log. When the axe is turned 90 degrees, the stress is much lower and is completely tolerated by the log. When a bone is stressed sufficiently, it deforms. The change in length divided by the original length is the strain (ε) in the bone. This parameter has no units of its own but is occasionally expressed as a percentage. A plot of the results is termed a *stress–strain curve* (Fig. 3).

Many other material properties can be extracted from this curve *(16)*. The straight portion of the curve is termed the "elastic" region. When a force is applied per unit area, there will be a change in length; however, in this early phase, the change is temporary. The bone retains the ability to return to its original shape after removal of the external force. The slope of the line in the elastic region is known as the modulus of elasticity (E), or Young's modulus (named after Thomas Young, MD 1773–1829). This is essentially a measure of stiffness. Lucas *(7)* listed approximate stiffness values in gigaPascals (gPa) for cancellous bone (0.005–1.5 gPa), polymethylmethacrylate cement (1.2 gPa); cortical bone (12–24 gPa), and cobalt—chromium implant alloys (210 gPa). While other publications list similar data within a certain range *(16–19)*, the consistent finding is that spongy bone (found in the epiphyses) is much less stiff than cortical bone (found in the diaphysis). Perhaps the preponderance of epiphyseal fractures in falls that affect the lower extremity can be explained by the simple fact that the spongy bone in this area is less dense and has a lower value for E.

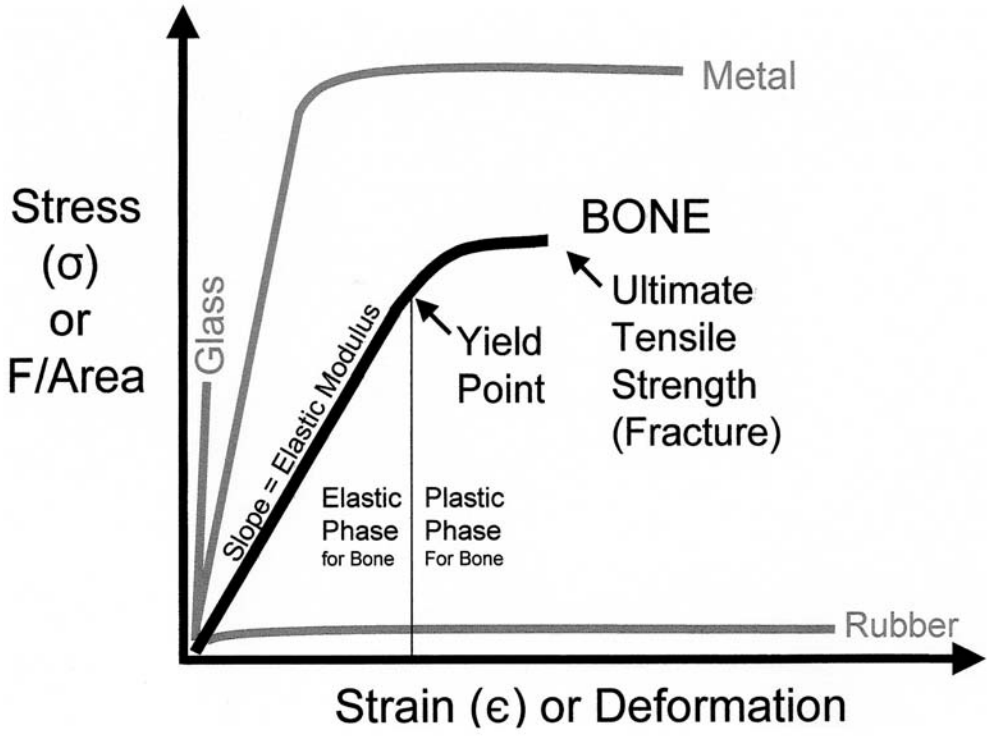

Fig. 3. Stress–strain curves for various materials.

At some point, the straight line on the stress–strain curve gives way to an actual curve. This is the yield point, and it marks the beginning of loading levels that will produce some permanent changes in the bone. From this point, loading results in "plastic" deformation. As the stress increases to the maximum the specimen can handle, the bone reaches its ultimate tensile strength (UTS) and failure becomes imminent. Continued loading results in fracture, and the bone specimen reaches its maximum deformation or strain. Note the theoretical differences between materials in Fig. 3. Some metals may be incredibly stiff, but with sufficient loading, they may have an extensive plastic phase (bending) prior to ultimate failure. The line for simple glass indicates a stiff material that has almost no plastic phase at all. Essentially, glass doesn't bend much before breaking, and when it does bend, it fractures. Application of slightly less stress or force does not elicit a plastic phase in this very brittle material. Thus, for safety, engineers cleverly glazed and layered windshield glass in an effort to help occupants remain inside a vehicle during a crash. Processing glass in this manner results in added strength and some ability for plastic deformation (of the windshield, not the individual pieces of glass). This is vividly demonstrated by the classic bulge in the windshield left by the head of an unbelted vehicle occupant after a frontal impact. Other material properties—such as energy, ductility, and toughness—can also be extrapolated from the stress–strain curve, but their discussion is unnecessary for this basic introduction. In summary, the

stress–strain curve for a material indicates the load it can bear until failure and the deformation before fracturing (both expressed as UTS for most bone).

Material properties calculated based on data from isolated cubes of cortical bone are interesting and important, but they serve merely as a starting point in understanding how an *entire* bone reacts to impact. Recall that a whole bone has varying levels of cortical and cancellous bone throughout its length. In addition to the strength and stiffness afforded by its composite nature, the anisotropic organization of the bone would surely lead to differing stress–strain curves depending on the orientation of a sample taken. Also, material properties vary according to the rate at which bone is loaded. A rapidly loaded bone has a greater modulus of elasticity and greater ultimate tensile strength (i.e., a steeper and taller stress–strain curve) than a slowly loaded bone. Some of the earliest studies supporting this property were performed by Mather in 1968 *(20)* with matched pairs of femurs. One was loaded quasi-statically (very slowly) and the other was loaded dynamically (impacted at speed). The energies were approx 50% higher in the dynamic loading cases. This property has come to be known as *viscoelasticity* and is a common feature of biologic tissues. Interestingly, Mather also noted that impact strength was unaffected by subject age, while static strength decreased with age.

3.1. Previous Research on Lower Extremity Impact Biomechanics

There are several published reviews of research into the tolerance of lower extremities to impact (e.g., *21–23*). However, the majority of the work has dealt with quasi-static testing of standardized specimens in order to determine material properties. In 1970, Yamada *(24)* published what is probably the most elaborate and thorough documentation of the mechanical properties of human and animal bones. Yamada noted that female tibias are approximately five-sixths as strong as those of males, and he found no significant differences in anterior versus lateral tests of small standardized samples of bone—not whole-bone impacts.

Melvin and Evans *(25)* and Nyquist *(21)* reviewed some of the earliest known biomechanical tests. In 1859, Weber performed static three-point loading tests of the mid-shaft region of human long bones. He applied 245-N (55-lb) increments of force to femurs fixed in place by supports placed 18.3 cm apart. Force applied over a distance is termed moment, which is often expressed in Newton–meters (Nm) or Foot–pounds (ft-lb). This is yet another improvement over force alone. The four male femurs failed at an average of 223 Nm (4.87 kN force), while the five female bones failed at 182 Nm (3.98 kN). Male tibias failed at 165 Nm (3.06 kN force) and female tibias failed at 125 Nm (2.33 kN force). In 1880, Messerer used a hydraulic test device that provided a much better resolution of 10 to 50 N. Positioned by supports placed 31.7 cm apart, 6 male femurs aged 24 to 78 yr were loaded laterally, resulting in an average bending moment of 310 Nm (3.92 kN). Six female femurs (28-cm support distance) aged 20 to 82 yr failed at an average of 180 Nm (2.58 kN). Male tibias (24.7-cm support distance) failed at 207 Nm (3.36 kN), and female tibias (22.2-cm support distance) failed at 124 Nm (2.24 kN). The direction of loading and impactor shape were not listed for most of the setups in either review. Since these early studies, numerous other static test results have been published. A discussion of these studies is beyond the scope of this chapter, but much of these data can be found in the engineering literature (e.g., the *Journal of Biomechanics*

Table 1
Organizations That Publish Injury Biomechanics Research

Organization	WebSite (http://www)	Publications
American Association of Automotive Medicine (AAAM)	.carcrash.org/	Annual Meeting Proceedings & Accident Analysis Prevention Journal and Journal of Crash Prevention and Injury Control
International Technical Conference on the Enhanced Safety of Vehicles (ESV)	-nrd.nhtsa.dot.gov/departments/nrd-o1/esv/esv.html	Biannual Conference Proceedings
International Research Council on the Biomechanics of impact (IRCOBI)	.ircobi.org/	Annual Conference Proceedings & Accident Analysis and Prevention journal
International Traffic Medicine Association (ITMA)	.trafficmedicine.org/	Traffic Injury Prevention journal
Society of Automotive Engineers (SAE)	.sae.org/servlets/index	Technical Papers, Textbooks, and Transactions Journal
Stapp Car Crash Conference	.stapp.org/index.htm	Annual Proceedings

and the *Journal of Biomechanical Engineering*). Table 1 lists the most relevant organizations publishing data on injury biomechanics, as opposed to the more academic pursuits found in traditional engineering journals or the treatment-oriented publications found in the medical literature.

In the most anatomically thorough discussion of tibial impact, Nyquist et al. *(21)* reported the results of subjecting 20 unembalmed cadaveric tibias to impact by a 32-kg impactor headed by a 25-mm cylinder. It is unclear whether the tests involved intact legs, because it indicates only that the skin was left in place. Specimens were struck on the anterior or lateral aspect at velocities ranging from 2.1 to 6.9 m/s (mean: 3.6 m/s). The distance between supports was 254 mm in most tests. Female bones failed at an average of 280 Nm and male bones failed at 320 Nm, regardless of direction of impact. In this study, cortex thickness was analyzed by computer to determine cross-sectional areas for further engineering calculations regarding moments of inertia. Bone samples were also subjected to ashing to determine mineral content. The authors concluded that the variability in bending moment could *not* be explained by correlations with cross-sectional area or classical strength of material beam bending theory. Furthermore, the variability in bending moments did not correlate with mineral content or impact velocity. The lack of correlation between various cortex measurements and breaking force was also seen in studies performed throughout the early 1990s *(1)*. The only information regarding fracture patterns in the Nyquist article was a listing of three degrees of comminution (comminuted, slightly

comminuted, and not comminuted). A serious emphasis on the anatomy of fracture patterns and their relationship to mechanism of injury is a relatively recent development.

4. Discussion of Fracture Patterns

In 1969, Klenerman *(26)* accurately noted that the appearance of a fracture during clinical examination is merely the end result of a series of events. These events are best understood by experimentally controlled fracture studies involving careful examination and documentation of posttest specimens. Only then can the true mechanism of injury be defined and ultimately mitigated. Fracture pattern is influenced by the specific mechanism of injury, the forces applied, and the physical properties of the bone *(27)*. When considering fracture propagation, the actual failure lines are said to be a record of energy dissipation *(28)*.

Numerous authors have attempted to list the mechanisms of loading that give rise to certain patterns of fracture. One of the most detailed listings was presented by Johner and Wruhs in 1983 *(29)*. Their system is a combination of the classifications made by the Swiss Association for the Study of Internal Fixation (AO/ASIF), the work of Muller in 1979 *(30)*, and the work of Muller and Nazarian in 1981 *(31)*. Long-bone fractures are classified generally as simple, butterfly, or comminuted. Within these classifications, several patterns of interest and their presumed mechanisms are listed: transverse fracture from pure bending, oblique fracture from uneven bending, nonfragmented wedge from low-speed bending with compression, fragmented wedge from high-speed bending with compression, segmental fractures by four-point loading, and massive comminution by crushing. Allum and Mabray *(32)* stated that a direct blow to an axially loaded bone gives rise to short oblique and wedge-type fractures. They attributed long oblique fractures to a combination of rotation, angulation, and axial compression. Levine *(33)* noted that wedge fractures result from indirect bending. Connolly *(34)* stated that "tapping force applied to the tibia" resulted in oblique fractures. He also noted that oblique fractures arise from "torsion with an upward thrust" and segmental fractures are due to direct violence at several locations. Numerous other authors have theorized that oblique fractures are due to a combination of rotational and transverse loading.

Although there is a consensus on the mechanisms that result in some patterns, there are clearly competing theories in the medical literature for others. Health care professionals benefit from the study of fracture patterns, because data from such work influences treatment and can be useful in predicting delayed union or nonunion *(27)*. However, determining the mechanism that results in particular patterns is better approached through experimentation rather than theorizing. Unfortunately, many unsubstantiated theories have been repeated and referenced for decades.

It is difficult to review older literature for detailed fracture pattern data, as nearly all the work was performed by engineers unfamiliar with anatomic terminology. Often thigh impacts are referred to as leg, upper leg, or femur tests, and it is unclear whether specimens were intact or bare bones. Likewise, leg impacts are referred to as tibial or lower-leg tests. Additionally, the precise site of impact was often unspecified. However, since 1989, Kress and Porta *(35–49)* have presented results from dynamic testing of more than 550 cadaveric lower-extremity components. The impact results shown in Fig. 1 were

part of that work. While many prior publications contain more engineering data, the more recent studies placed their major focus on ultimate fracture pattern and its relation to impact conditions. These data serve as the foundation for the content of the following section, in which mechanisms of injury related to specific fracture patterns are described.

4.1. How Bone Breaks

Bone may be subjected to several different types of force (alone or in combination) that exceed the structural integrity of the organ. A limb may be loaded in tension, bending, compression, and/or torsion. To a person in the health care field, these loading scenarios would equate to applying a force by traction (or distraction), transverse impact, axial loading, and/or twisting. Each will be discussed in the coming sections, with final comments on comminution and bone integrity to follow.

4.2. Tension

The most prominent example of a pure tensile force causing a break in a bone is the avulsion fracture. In the lower extremity, these are usually limited to the trochanters of the femur, the patella, the tibial tuberosity, and the ankle. All but the last one are usually due to a strong, rapid pull exerted by the muscle inserted on each area. During the complex motions associated with ankle injuries, it is possible for the collection of strong ligaments in the area to cause an avulsion in a malleolus during a particularly violent movement. Rarely, quick contraction of the quadriceps may result in a relatively pure tensile force acting on the patella, which tends to fracture transversely but may also cause a jagged fracture (Fig. 4) *(50)*.

Production of a pure tension-type fracture in the shaft of a normal lower-extremity long bone is difficult to imagine in the real world. Perhaps a *grossly* negligent traction setup could somehow apply sufficient tensile force to fracture a bone. A more likely scenario might involve a foot being caught in a type of machinery and then violently distracted. It is difficult to know where the injury would occur in this situation, because the force would be spread to virtually all the joints in the lower limb. This might result in dislocations and ligament damage before any fractures would be seen. However, this is speculation, as no reports of distraction-type injury mechanisms have been presented to date. If tension were applied to the long axis of a single bone, it is presumed the bone would fail with a transverse fracture based on materials property testing of bone samples. One cannot help but wonder, however, whether the fracture would occur at a metaphysis, given that it is a junctional zone between the dense cortical bone of the diaphysis and the less dense cancellous bone of the epiphysis. In short, studies of whole bones subjected to tension have not been published, and any discussion of a resultant fracture pattern is speculative.

4.3. Bending Fractures

Bending (or 3-point loading) is by far the most common mechanism of fracture for lower-extremity long bones. When a long bone is impacted transversely at the diaphysis, it reacts very much like a classic beam, in that it will bend (e.g., *7,17,51,52*). As it bends, the bone tissue at the site of the impact will become compressed. The tissue on the opposite side will be stretched (termed "tension"). This is often demonstrated with a standard yellow-painted wooden pencil. As one bends the pencil, the yellow paint on the concave side begins to buckle or bunch up—evidence of compression. The paint on the other

Fig. 4. Patellar fracture (anteroposterior and lateromedial radiographs).

side separates—evidence of tension. Another more dramatic example of tensile and compressive forces in the same tissue can be seen in a simple trick. In an uninflated balloon, the molecules of rubber are content to be in close proximity with each other. As the balloon is inflated many, but not all, of the molecules are put into tension. If the balloon is not fully inflated, it can be seen that the rubber closest to the inlet, and directly opposite of the inlet, are not being stretched (invariably the color is more intense—e.g., balloon will be "darker" in these spots because the balloon wall is thicker). Essentially these

Fig. 4. *Continued.*

molecules are in compression. A sharp wooden skewer poked into the side of the balloon would cause it to explode because the strength of the rubber was exceeded and the tensile forces were free to rip the balloon walls apart. However, if the skewer is carefully poked through the thicker areas of the balloon, the rubber molecules will compress around the stick and attempt to seal the hole; thus, the somewhat unintuitive results seen in Fig. 5. As with the balloon, failure of bone occurs in the areas of tension. The tensile forces lead to separation of the osseous tissue and propagation of a fracture line or lines.

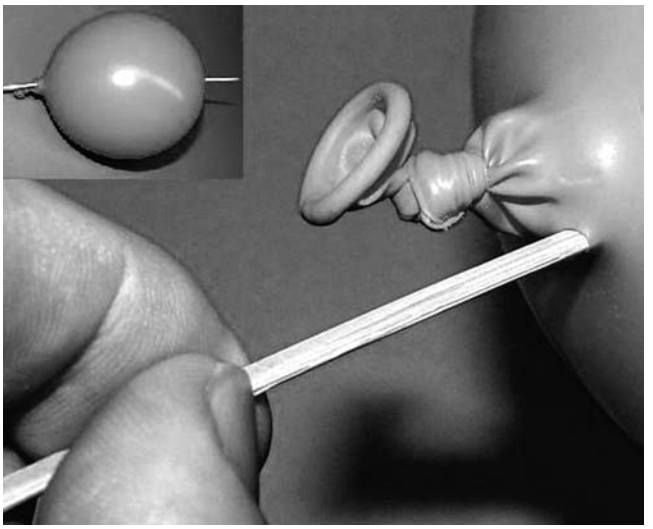

Fig. 5. Demonstration of tension and compression in a balloon.

Most sources agree that a transverse fracture can result from bending (Fig. 6). However, there is no consensus on oblique and wedge patterns (a.k.a. butterfly or delta fractures). Many authors assert that these patterns result from some form of combined loading (with compression or with twisting). In our simple 3-point loading of bare long bones, we routinely produced oblique, transverse, and wedge fracture patterns with absolutely no axial or torsional loading whatsoever. In nearly all cases of wedge fracture, the initial point of failure was on the tension side immediately opposite the point of impact (Fig. 7). This means that the point of the wedge is on the tension side of the bone, corroborating the work of Spitz *(53)*, who investigated pedestrian leg impacts that resulted in wedge fractures. He stated that the wedge often points in the direction of the movement of the vehicle.

In a stroke of serendipity, while cleaning fractured bone wedges for photographs, an interesting discovery was made. After being soaked in bleach, the bones were dried in an oven. The charred bleach revealed an amazing array of small fracture lines emanating from the initial tensile failure point (Fig. 8). The impact occurred at the bone surface facing the top of the photo. The solution had seeped into the cracks and then essentially burned when the heat was applied. Presumably heating of the solution also caused mild expansion of the cracks. This heat-treatment of bone may be an excellent method for elucidating or enhancing microfractures *(54)*. It was clear from this study that there are often many nondisplaced fracture lines in seemingly simple patterns. In later studies, the periosteum was carefully dissected away from transverse and oblique fracture fragments. In addition to the transverse and oblique fractures, tension lines are clearly visible (Fig. 9). The black arrows indicate the site of impact. Thus, it appears that all three of these patterns (transverse, oblique, and wedge) are actually slightly different manifestations of tensile failure. It is important to note that almost none of these tension lines were visible on plain radiographs. However, these lines may be helpful to the forensic pathologist or anthropologist examining postmortem specimens and attempting to determine a direction of impact.

Fig. 6. Radiograph of transverse fractures to the femur and tibia.

What determines whether a bending load will produce an oblique, transverse, or wedge pattern? It may be a feature of the tissue (inherent weakness in one plane) or the dynamic load (shape of impactor, slight variations in the angle or energy of impact, etc.), or some combination of factors. Perhaps the addition of compressive or torsional loads will have some effect on the pattern, but this is clearly not essential and should not be assumed when reconstructing an injury scenario from the fracture pattern.

Fig. 6. *Continued.*

One feature of bone that may influence fracture pattern and bending forces is the presence of stress-risers. "Stress-riser" (also referred to as stress raiser or stress concentrator) is an engineering term that describes a weak area or defect that when loaded, will tend to fail prior to surrounding areas *(55)*. This is analogous to the weakest link in

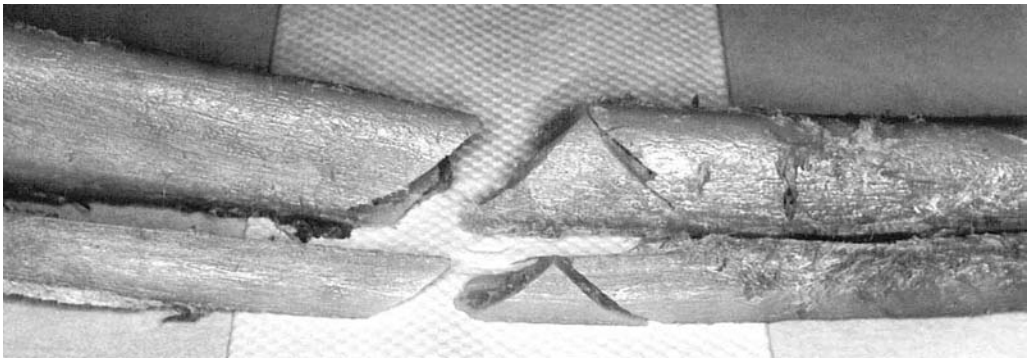

Fig. 7. Wedge fractures produced in a tibia and fibula from pure bending.

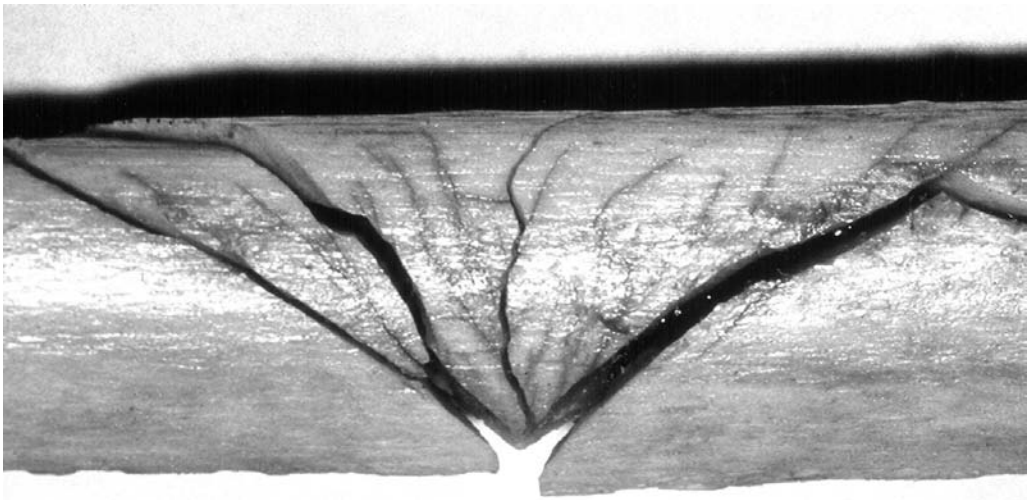

Fig. 8. Tension lines in a stripped, bleached, and heated wedge fracture.

a chain. An example of inducing a stress-riser would be the scoring of glass. When subjected to bending loads, glass will usually fail along the score or stress-riser. In some of our studies with bare bones, there was a concern that the bones could have been scored during retrieval and cleaning. To investigate this possibility, entire surfaces of several bones were scanned into a computer prior to testing. After fractures were produced, the images were examined under magnification with different software filtering applications *(56)*. No surface feature was found to influence the initiation or propagation of fracture lines. Since subtle or accidental scoring appeared to have no effect, an additional study of several bones was performed involving intentional scoring. In Fig. 10, a femur is shown with a pattern etched into the surface (up to 2 mm deep) by a Stryker saw. The bone was subjected to impact, and although this extreme level of etching influenced the initiation site of the fracture, it did not significantly affect the overall pattern. The tensile failure lines easily crossed the etching to give rise to a standard wedge pattern that would be expected from the indicated impact direction.

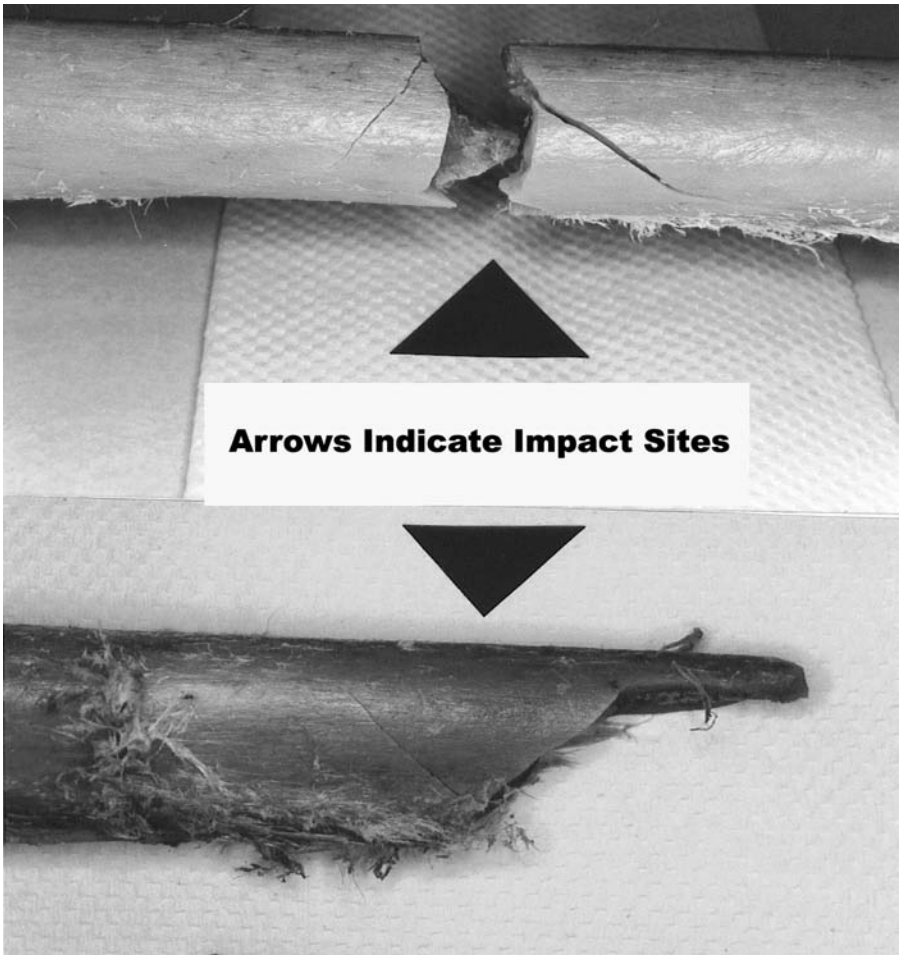

Fig. 9. Tension lines visible in transverse and oblique fractures.

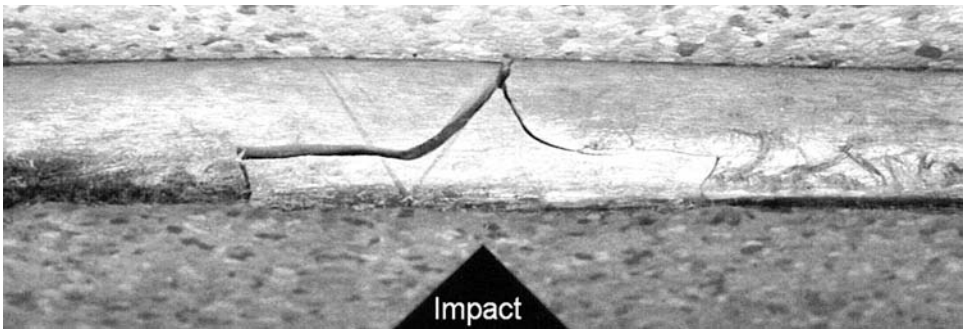

Fig. 10. Scoring bone had little effect on dynamically produced fracture pattern.

These studies of surface artifacts were too small to determine whether fracture force was affected. However, complete holes through the cortex have been shown to influence the strength and presumably the site of fracture initiation (e.g., previous fracture site or fixation

pins and screws). It has been reported that 3-mm holes can decrease tibial bending strength by 40% *(57)*. As reported by Brooks et al., Bechtol and associates (during the 1950s) drilled various sizes of holes into dog bones that were then subjected to bending loads. They found that holes in the area of the bone that was placed in tension reduced bone strength by 30%. Interestingly, as long as the ratio of the hole size to bone diameter was not more than 30%, the decrease in strength was not significantly different for holes of differing sizes. Holes in the area of the bone that was in compression had essentially no effect on strength *(57)*.

To this point, only artificial stress-risers have been discussed. It should be noted that internal weaknesses (due to pathology) can certainly affect fracture strength, pattern, and fragmentation levels *(50)*. Also, one cannot ignore the role that bone micro-architecture may play in fracture patterns. The difference between wedge, transverse, and oblique fracture patterns in bending may simply be due to the random alignment of Haversian and Volkmann canals, such that a certain impact parallel to these lines results in fracture energy dissipation along the canals. These natural stress risers should be explored more thoroughly.

4.4. Axial Loading Fractures

Cubes of cortical bone subjected to pure compression will often fail obliquely. Unfortunately, many authors have applied this material property data to whole bone. Some have even promulgated the idea that an oblique fracture arises from a bone subjected to pure compression or the combination of bending with axial loading. As noted in the previous section, oblique fractures will commonly arise from pure bending. In fact, given the anatomy of a whole bone such as the femur, an oblique fracture may result from apparent axial loading, but is more likely to occur because the bone actually bends. For example, the straw in Fig. 11 is subjected to axial loading, but the resultant force on the bone is bending (not the shear seen in cubes of bone). Add to this the fact that our long bones are not perfectly straight and it is easy to see that axial loading tends to enhance the curves (or compress the bow) in a bone. Thus, a fall onto a stiff limb may result in a bending fracture even though the loading is described as axial.

In the rare cases in which relatively pure axial loading is applied quickly to a lower extremity (as when an unrestrained passenger is involved in a frontal crash and the flexed knee strikes the dashboard), the result can be an impacted fracture, especially in the young (Fig. 12) and the very old. Note that bending fractures are still common (Fig. 13), and with high force levels there can be significant comminution, even in healthy bone. At lower levels of force or in particularly robust bone, acetabular and patellar fractures may occur without concomitant femur fractures, because the long bones are approx 50% stronger during compression (axial loading) vs bending *(58)*. However, if an impacted fracture is seen, there can be little doubt that the mechanism of injury involved significant axial loading of the bone. In these cases, the compact bone of the diaphysis is driven into the epiphysis. Presumably the less dense spongy bone is simply compacted within the epiphysis.

4.5. Torsional Fractures

When a twisting motion is applied to a long bone—e.g., when a ski tip is caught on the ice and acts as a moment arm for the lower extremity—the most elegant of fracture

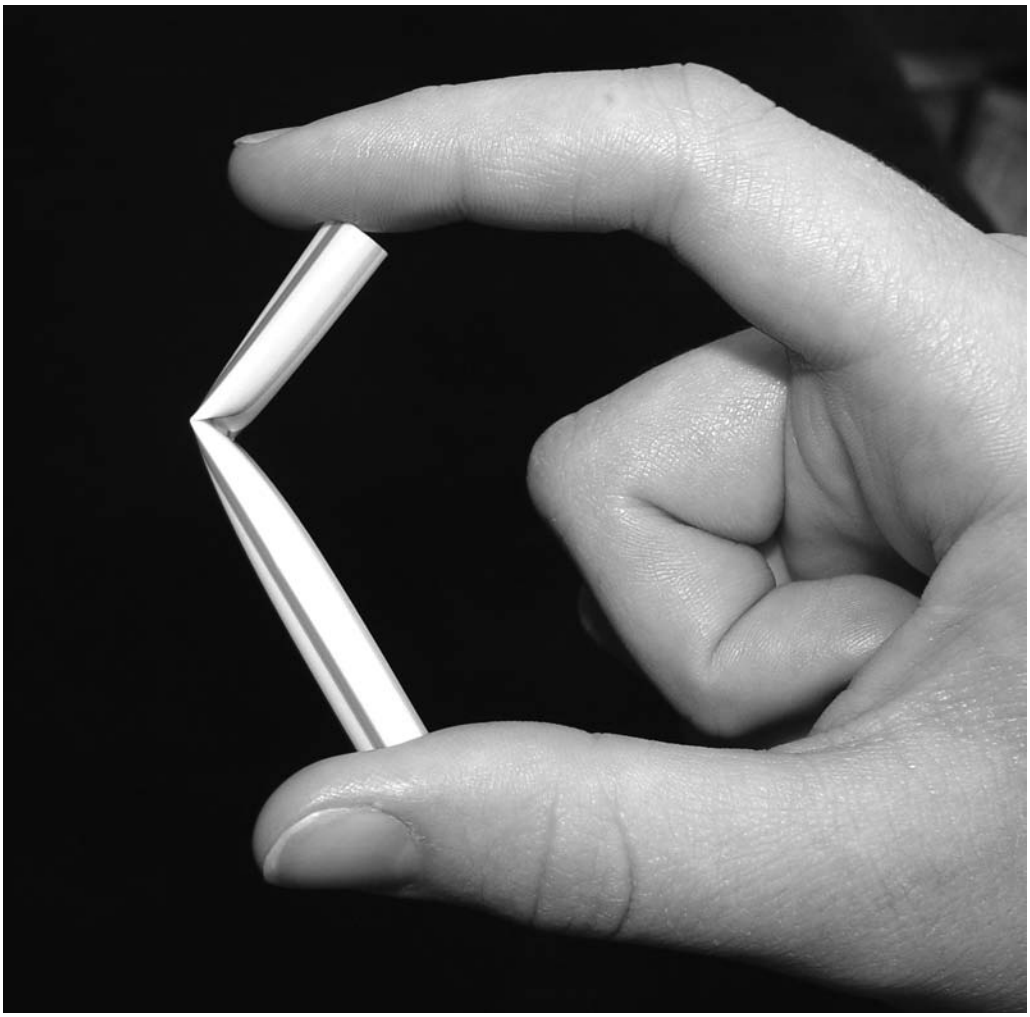

Fig. 11. Is this axial loading or bending?

patterns results: a spiral (Fig. 14). The pattern is completely unique and diagnostic of torsional force as the primary mechanism of injury. A fracture initiates at some point on the bone and then travels at an angle of approx 45 degrees (with respect to the long axis of the bone) around the shaft in the same direction as the applied torque. Once the fracture has completely encircled the bone, the shaft becomes so unstable that a longitudinal fracture line develops between the proximal and distal ends of the spiral. This can be easily demonstrated by twisting a piece of chalk. The fracture that results is essentially identical to what would be seen in bone. The precise propagation of the fracture line has been determined (Fig. 15) in more than 50 cadaveric bone experiments, and the longitudinal line or "hinge" (so called because it often acts like a hinge due to retention of the periosteum in this region) is the last component to form *(60–63)*. Bear in mind that although there is considerably more time involved in traveling along the lines in a spiral fracture than in other types, the amount of time for these fractures to develop is still very short: less than 2 ms. Figure 16 shows one radiographic view of a spiral fracture.

Fig. 12. Radiograph of an impacted distal femur fracture in a teenager.

With the aid of some simple tools (a bone model or an opaque tube with the four anatomic sides labeled, a sheet of clear plastic, and a marker) the direction of twist can often be determined using two high-quality orthogonal radiographs in six steps *(60)*:

1. Determine whether the hinge is located more on the lateral or medial side by looking at an A-P radiograph.
2. Define the position of the hinge as being more anterior or posterior by studying a lateral-medial radiograph.

Fig. 13. Comminuted fracture produced from dashboard-style axial impact.

3. Wrap the clear plastic sheet around the bone model or opaque tube and sketch the hinge on the plastic at the anatomic location determined from steps 1 and 2.
4. Use the radiograph with the clearest view of the hinge and determine the direction of the spiral as it radiates from one end of the hinge. Start at the same point on the plastic sheet to reproduce the spiral. Sketch the radiating spiral around the plastic until both ends of the hinge are connected.
5. The sketched pattern should be checked by separating the bone model from the plastic sheet and superimposing the rolled plastic over the radiographs. An accurate reproduction of the spiral fracture is confirmed if this three-dimensional sketch can be matched to the fracture lines in *both* radiographs.
6. To determine the direction in which the bone was twisted, first consider the logical choice for which end was torqued. In most cases, the torsion arises from the distal end of the bone, but evidence (e.g., witnesses or bruising pattern) and patient history should assist with this determination. Note which direction the spiral runs around the bone at the torqued end. That is the same direction in which the torque was applied to that end of the bone (if the opposite end of the bone was the site of torsion, then the direction will be opposite).

The spiral fracture is all too often the result of nonaccidental trauma. A frustrated caregiver may resort to twisting a limb to punish a child. When considering such a potential case of abuse, it may be important for the forensic expert to first distinguish between fracture patterns that result from bending vs twisting. Being able to determine the direction of twist might also prove helpful in finding inconsistencies in the story of a caregiver who is suspected of abusing a child.

The fact that two excellent X-rays are needed cannot be overemphasized. One is insufficient for any degree of certainty. In fact, a single view of a spiral fracture can be easily misinterpreted as a bending type of fracture (oblique or even a wedge), as seen in the humeri in Fig. 17.

Fig. 14. Photograph of spiral fracture fragments. (Courtesy of Patrick Besant-Matthews, MD)

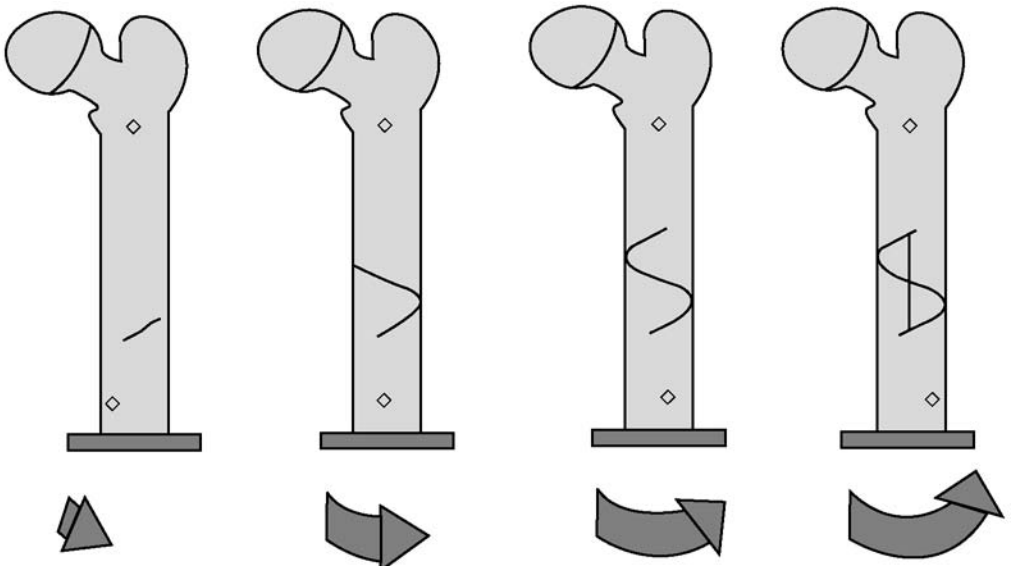

Fig. 15. Propagation of the spiral fracture pattern.

Fig. 16. Radiograph of a spiral fracture of the femur.

It was previously mentioned that the oblique fracture is often construed as the result of bending combined with simultaneous axial loading. Perhaps even more often, authors have noted that oblique fractures result from a combination of bending and twisting. Precious few studies have examined the effects of combined loading on fracture patterns. In 2003, Frick published the results of a study (an MS thesis) of matched

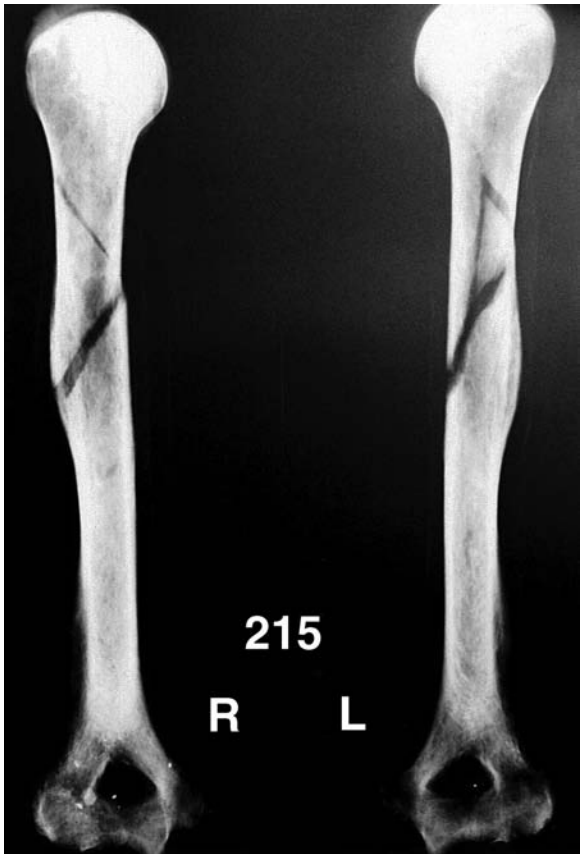

Fig. 17. Radiograph of a spiral fracture that could be confused for a wedge.

pairs of femurs *(64)*. One member was torqued to failure and the second was pre-torqued to either 30 or 70% of the torsional fracture threshold. That second bone was then struck with a steel pipe and fracture patterns were carefully documented. Frick found that oblique fractures may result from a combination of torsion and bending when bending is the dominant loading mechanism. If torsion is dominant and a bending force is added, the fracture is still spiral.

4.6. Effects of Impact Energy and Bone Integrity

As noted previously, when sufficiently stressed, bone will dissipate energy as it fractures. Many authors have noted that the higher the energy input, the greater the degree of fragmentation or comminution and the greater the potential for soft-tissue injury due to the displacement of fragments (Fig. 18). Aldman described fractures that resulted from low-speed impact as rather smooth, while those resulting from higher velocities gave rise to more "jagged and feathery" fracture patterns that are usually accompanied by a greater amount of soft-tissue damage (e.g., *65,66*). Today, orthopedic surgeons have a wide array of fixation devices, bone cements, and artificial replacements with which to repair almost any type of bone trauma. Thus, it is often the surrounding soft-tissue damage that ultimately determines the survival or demise of a limb.

Fig. 18. Comminuted fractures of the tibia and fibula.

Cancer, infection, or any of the multitude of diseases affecting bone metabolism will surely lead to decreased bone strength *(50)*. Unfortunately, the natural aging process also leaves our bones less able to resist external forces *(67)*. Regardless of the specific etiology, weakened bones are surely more prone to fracture. In general, fractures to osteoporotic bone, for example, will have a higher level of comminution than would

be seen in healthy bone. A relatively small impact on a weakened bone can result in a segmental fracture, normally the product of an impact from a large surface (e.g., a blunt vs pointed car bumper). High degrees of comminution will often completely obscure any particular pattern data. Weakened bones will also be more susceptible to secondary fractures in a traumatic event. For example, a young healthy person struck by a car may suffer only a broken tibia, fibula, or both. An older person with diabetes may have fractures in the leg, but also the thigh, pelvis, rib cage, and skull. In short, comminution will often negate the potential forensic value of fracture patterns.

5. Case Studies

The following case studies are provided to demonstrate the potential utility of a deeper understanding of fracture biomechanics and the resultant patterns. While they are similar to actual cases, they are not intended as direct representations.

5.1. Chiropractic Manipulation Causing Fracture?

At 2 AM, an obese 50-yr-old female called for an ambulance. The crew arrived quickly and transported her from her bathroom to the emergency department. After triage, she was sent for X-rays and was soon diagnosed with a transverse intertrochanteric fracture in the left femur. Orthopedic surgeons repaired the hip using an internal fixation device, and after appropriate rehabilitation, she was sent home. She subsequently experienced multiple failures of the fixation device and became frustrated with her constant setbacks. After hearing her grumble about malpractice, the orthopedist asked how the injury originally occurred. When informed that she had been to the chiropractor on the afternoon of the injury, the orthopedist suggested her injury was the result of chiropractic manipulation. The woman described a maneuver in which she was laid on her side and the left hip was twisted while the low back was held in place. Could the chiropractor have caused this injury?

There are several inconsistencies in the story. If the injury occurred in the afternoon, why didn't she call for an ambulance before 2 AM? Perhaps she had an extremely high tolerance for pain. How did she walk out of the office with a supposedly fractured hip? Perhaps it was an incomplete fracture (although there is no published record of an incomplete fracture being caused by manipulation and then spontaneously completing itself 12 h later). Why was she found in the bathroom? Perhaps she had to use the facilities and the hip fracture completed itself during her stroll.

While the story is highly suspicious, the only factual evidence is the fracture pattern. Both parties agree that the manipulation was a twist, yet the fracture pattern is one that results from bending (*see* Fig. 16 vs Fig. 6). She most likely fell and struck the tub or toilet while walking into the bathroom.

5.2. Pediatric Pedestrian Hit-and-Run Case

A teenaged boy lived in a small shotgun house on a busy downtown street. He was notorious for running into the street after his dog, which liked to chase cars. He has been nearly hit at least a dozen times. One cold winter morning, he was struck and killed by a car that was driven by a 26-yr-old woman who was taking medication for narcolepsy. There were no witnesses to the incident. The police accident reconstructionist

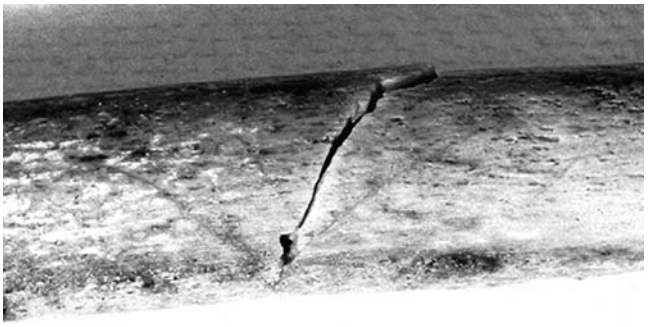

Fig. 19. Oblique fracture with tension lines evident.

determined that the boy was hit by the front of the vehicle, which was not braking at the time. The strike caused a right femoral fracture and he was thrown 35 ft. When he landed, his head struck the concrete and he died almost instantly from massive brain injuries. At autopsy investigators found no bruises or lacerations, aside from a small one on the top of the head. The superior portion of the cranium was massively depressed. Full body X-rays indicated an oblique fracture of the proximal left femur. The fragments were dissected out and are shown in Fig. 19. The driver did not stop at the scene. She later turned herself in to authorities after hearing the boy was killed. She claimed that as she was driving down the street, she saw the boy walking in the same direction on the side of the road. Just as her car was about to pass him, he turned as if to cross the street, stepped directly in front her, and was struck by the front grill on the passenger side of her car.

Who was at fault: the boy who ran into traffic? Or did the narcoleptic doze off and strike the boy? With no witnesses, the situation seems unlikely to be resolved. There are few if any surface markers on the boy, because he was dressed for a cold winter day. The head injury occurred on the vertex of the skull, and the angle of impact cannot be determined from that.

The femoral bone fragments are helpful. Although it is an oblique fracture (as one would expect in this transverse or bending-type impact), there were also tension lines visible on the bone after the periosteum was stripped away. The lines come to a point on the posterior edge (linea aspera) of the femur, indicating that the boy's femur was impacted on its anterior surface. This does not match the statement given by the young lady. The more likely scenario was that he was facing traffic when walking in the street and she fell asleep at the wheel just as she came upon the young man and struck him head on.

5.3. Transport Van Seatbelt Issue

A severely disabled boy in a wheelchair was rolled onto a van and his wheelchair was strapped into a side slot in the vehicle. A seatbelt was secured over the boy's lap, and he was ready for transport home after a visit to his endocrinologist. Just to the left of the boy was a steel post that ran from the floor to the ceiling of the van. While traveling, the van was involved in a minor frontal impact. Immediately afterwards, the driver exited to check on the damage to his front end and the small car he had bumped into. When he re-entered the van, he saw the boy lying on the floor moaning in pain. One

Fig. 20. Memorial to research donors.

other passenger said he was fumbling with his seatbelt and fell while straining to look out the front window. The other passenger said the boy's wheelchair spun around during the accident and then he fell to the ground. A third passenger indicated the boy was acting funny just before the accident and kept saying his belt was too tight, then "he got weirder" afterwards. The boy was taken to the hospital and found to have an impacted fracture of his left femur (Fig. 12), as well as low blood sugar. The boy's mother was very upset and decided to sue the van company, because she claimed her son's wheelchair was not properly restrained and that during the accident his chair spun violently and his left thigh slammed into the post, causing the fracture.

In this case, there were three witnesses (besides the driver and the boy), but their stores do not agree. If the chair was not restrained, it is possible that it could have spun and his leg could have hit the post. However, this would be a bending-type fracture, and the radiographs clearly show an impacted fracture. There is no doubt that he was somehow subjected to axial loading of his femur. The absence of injuries to his leg or any other body

part means it is highly likely he struck his knee in a somewhat stiff body position. It would seem the first and third witnesses were most accurate. Perhaps in a somewhat delirious state, he disconnected the belt in order to sit up to see what was going on in front of the van. In doing so, he leaned forward but his left foot was caught on the wheelchair footrest, and he landed on the hard metal van floor with all his weight on his left knee.

Acknowledgments

My sincere thanks to Bellarmine University and the University of Louisville Medical School for supporting my research over the past 14 yr. Even more importantly, I thank the kind souls who bequeathed their bodies so that others may learn (Fig. 20). Your ultimate gift is greatly appreciated.

References

1. Porta DJ. Anatomy and biomechanics of experimentally traumatized human cadaver lower extremity components [dissertation]. Louisville, KY: University of Louisville School of Medicine, 1996.
2. Fung YC. The application of biomechanics to the understanding of injury and healing. In:. Accidental injury: biomechanics and prevention. Nahum AM, Melvin J, eds. New York: Springer-Verlag Inc.; 1993:1–11.
3. Hayes WC. Biomechanics of cortical and trabecular bone: implications for assessment of fracture risk. In: Basic orthopaedic biomechanics. Mow VC, Hayes WC, eds. New York: Raven Press; 1991.
4. Viano DC. Biomechanics of bone and tissue: a review of material properties and failure characteristics. In: Biomechanics and medical aspects of lower limb injuries. Warrendale, PA: Society of Automotive Engineers, Inc.; 1986:33–64. SAE Technical Paper 861923. P-186.
5. Pope MH, Outwater JO. The fracture characteristics of bone substance. J Biomechanics 1972;5:457–465.
6. Peavy, DE. Endocrine regulation of calcium, phosphate, and bone homeostasis. In: Medical physiology. 2nd ed. Rhodes RA, Tanner GA, eds. Baltimore: Lippincott, Williams & Wilkins; 2003:634–648.
7. Lucas GL, Cooke FW, Friis EA. Strength of materials. In: A primer of biomechanics. New York: Springer-Verlag; 1999:36–52.
8. Cochran GVB. A primer of orthopedic biomechanics. New York Churchill Livingston; 1982.
9. Nahum AM, Melvin J, eds. Accidental injury: biomechanics and prevention. New York: Springer-Verlag Inc. 1993.
10. Burstein AM, Wright TM. Fundamentals of orthopaedic biomechanics. Baltimore: Williams & Wilkens; 1994.
11. Lucas GL, Cooke FW, Friis EA. A primer of biomechanics. New York: Springer-Verlag, 1999.
12. Lucas GL, Cooke FW, Friis EA. Mechanics. In: A primer of biomechanics. Lucas GL, Cooke FW, Friis EA, eds. New York: Springer-Verlag; 1999:1–22.
13. McElhaney JH, et al. Properties of human tissues and components. In: Handbook of Human Tolerance. Japanese Automotive Research Institute (JARI). 1976:57–123.
14. Carter DR. Biomechanics of bone. In: Nahum AM, Melvin J, eds. The biomechanics of trauma. 1985:135–165.
15. Nordin M, Frankel VH, eds. Basic biomechanics of the musculoskeletal system. 2nd ed. Philadelphia, Pa: Lea & Febiger; 1989.
16. Goldstein S, et al. Biomechanics of bone. In: Nahum AM, Melvin J, eds. Accidental injury: biomechanics and prevention. New York, NY: Springer-Verlag; 1993:198–223.
17. Tencer AF. Biomechanics of fractures and fixation. In: Bucholz RW, Heckman JD, eds. Rockwood and Green's fractures in adults. Vol. 1. Lippincott Williams & Wilkins. 2001.
18. Auteflage A. The point of view of the veterinary surgeon: bone and fracture. Injury Int J Care Injured 2000;31(suppl):C50–C55.

19. Hayes WC. Bone mechanics: material properties. In: Fracture healing: Bristol Myers/Zimmer Orthopedic Symposium. New York: Churchill Livingstone; 1987:97–104.
20. Mather BS. Observations of the effects of static and impact loading on the human femur. J Biomechanics 1968:1–4.
21. Nyquist GW. Injury tolerance characteristics of the adult human lower extremities under static and dynamic loading. In: Biomechanics and medical aspects of lower limb injuries. Warrendale, Pa: Society of Automotive Engineers, Inc.; 1986:79–90. SAE Technical Paper 861925.
22. SAE J885 APR80. Human Tolerance to Impact Conditions as Related to Motor Vehicle Design. Society for Automotive Engineers Information Report. 1980.
23. SAE J885 JUL86. Human Tolerance to Impact Conditions as Related to Motor Vehicle Design. Society for Automotive Engineers Information Report. 1986.
24. Yamada HE, ed. Strength of biological materials. Baltimore: Williams & Wilkins Co.; 1970.
25. Melvin JW, Evans FG. Extremities: experimental aspects. In: The biomechanics of trauma. Nahum AM, Melvin J, eds. Appleton and Lange. 1985:447–459.
26. Klenermann L. Experimental fractures of the adult humerus. Medical and Biological Engineering 7:357–364 (1969).
27. Levine RS. An introduction to lower limb injuries. In: biomechanics and medical aspects of lower limb injuries. Warrendale, Pa: Society of Automotive Engineers, Inc.; 1986:23–32.
28. Seligson D. Perspective on ski fractures on the leg and ankle. Clinics in Sports Medicine 1:253–262 (1982).
29. Johner R, Wruhs O. Classification of tibial shaft fractures and correlation with results after rigid internal fixation. Clinical Orthopedics 178:7–25 (1983).
30. Müller ME. Manual of the classification of fractures. AO Documentation (Verteilt an der AO-Herbsttagung CH-3008), 1979.
31. Müller ME, Nazarian S, Koch P, Schatzker J. Classification of fractures of long bones. Berlin: Springer-Verlag; 1990.
32. Allum RL, Mabray MAS. A retrospective review of the healing of fractures of the shaft of the tibia with special reference to the mechanism of injury. Injury 11:304–308 (1979).
33. Levine, Robert S. Injury to the extremities. In: Accidental injury: biomechanics and prevention. Nahum AM, Melvin J, eds. New York: Springer-Verlag; 1993:460–492.
34. Connolly, JF. Fractures and dislocations: closed management. Vol 1. Philadelphia: WB Saunders Co.; 1995.
35. Kress, Tyler A. Mechanical behavior of lower limbs in response to impact loading: facility development and initial results [masters thesis]. Knoxville, TN: The University of Tennessee Department of Engineering Science; 1989.
36. Kress TA, Snider JN, Fuller PM, Wasserman JF, Tucker GV, Sakamoto S. Automobile/motorcycle impact research using human legs and tibias. Society of Automotive Engineers, Inc. 1990:1–8. SAE Technical Paper 900746 (SP-827).
37. Kress T, Snider J, Porta D, Fuller D, Wasserman J, Tucker G. Human femur response to impact loading. Proceedings of the International Research Council on Biokinetics of Impact (IRCOBI) 1993:93–104.
38. Kress T, Porta D, Duma S, Snider J, Fuller P. An underwater impact biomechanics study to evaluate a boat motor cage-type propeller guard as a protective device. Proceedings of the Meeting of the International Research Council on the Biomechanics of Impact (IRCOBI) 1996:353–361.
39. Porta D, Kress T, Fuller P, Snider J. Biomechanics of impacting human cadaver thighs. The Anatomical Record 1993;(suppl 1):96.
40. Porta D, Fuller P, Kress T, Snider J. Impact studies of embalmed human cadaver thighs and femurs. Proceedings of the 14th International Technical Conference on the Enhanced Safety of Vehicles (ESV) 1:299–304 (1994).
41. Kress T, Porta D, Snider J, et al. Fracture patterns of human cadaver long bones. Proceedings of the International Research Council on the Biomechanics of Impact (IRCOBI) 1995:155–169.
42. Porta D, Kress T, Fuller P, Snider J. Fractures of experimentally traumatized embalmed versus unembalmed human cadaver legs. Biomedical Sciences Instrumentation 33:423–428 (1997).

43. Porta D, Kress T, Fuller P, Snider J. Fracture studies of male and female cadaver tibias subjected to anterior or lateral impact testing. The FASEB Journal 11:A622 (1997).
44. Porta D, Kress T, Fuller P. Pedestrian leg impact: kinematics as seen in experimental studies. Proceedings of the American Academy of Forensic Sciences 4:166–167 (1998).
45. Porta D, Frick S, Kress T, Fuller P. Transverse, oblique, and wedge fracture patterns: variation on the bending theme. Clin Anat 12:208 (1999).
46. Frick S, Fuller P, Porta D. Reconstruction of injury mechanisms using computer generated 3-D animations. Clinical Anatomy 12:435–436 (1999).
47. Porta D, Kress T. Enhancement of gross instruction via discussions of fracture mechanics with demonstrations on synthetic bones. The FASEB Journal 14:A801 (2000).
48. Kress T, Porta D. Characterization of pedestrian leg injuries from motor vehicle impacts. Proceedings of the 17th International Technical Conference on the Enhanced Safety of Vehicles (ESV) S-8 443:1–14 (2001).
49. Porta D, Kress T. Is distal friction (or entrapment) necessary to cause bending fractures of the leg at relatively low speeds? Clin Anat 14:462 (2001).
50. Lucas GL, Cooke FW, Friis EA. Biomechanics of pathology. In: A primer of biomechanics. New York, NY: Springer-Verlag; 1999:114–125.
51. Lucas GL, Cooke FW, Friis EA. Stresses in bending. In: A primer of biomechanics. New York, NY: Springer-Verlag; 1999:53–66.
52. Hyde AS. How we break and tear the stuff we are made of (i.e., biomechanics revisited). In: Crash injuries: how and why they happen. Key Biscayne, Fla: HAI Publishers; 1992:45–62.
53. Spitz WU, Russell SF. The road traffic victim. In: Medicolegal investigation of death: guidelines for the application of pathology to crime investigation. 2nd ed. Thomas Books Illinois; 1980:377–405.
54. Porta D, Kress T, Frick S, Fuller P. Post-mortem enhancement of long bone fractures: an aid to trauma reconstruction. Proceedings of the American Academy of Forensic Sciences 4:139 (1998).
55. Lucas GL, Cooke FW, Friis EA. Stress raisers, fracture, and fatigue. In: A primer of biomechanics. New York: Springer-Verlag; 1999:98–113.
56. Porta D, Tietjen W, Keeling B, Kress T, Fuller P. Surface morphology and fracture patterns in dynamically impacted femurs and tibia/fibulas. The FASEB Journal 8(5 pt 2):A823 (1994).
57. Brooks DB, Burstein AH, Frankel VH. The biomechanics of torsional fractures. The J Bone Joint Surg 52:507–514 (1970).
58. Lucas GL, Cooke FW, Friis EA. Tissue mechanics. In: A primer of biomechanics. New York: Springer-Verlag; 1999:257–280.
59. Lucas GL, Cooke FW, Friis EA. Stresses in torsion. In: A primer of biomechanics. New York: Springer-Verlag; 1999:67–78.
60. Porta D, Frick S, Kress T, et al. Spiral fracture: definition and determination of torsional direction from radiographs. Proceedings of the American Academy of Forensic Sciences 2:146 (1996).
61. Porta D, Kress T, Fuller P, Frick S, Klueber K, Snider J. Anthropometry and experimental spiral fractures. The FASEB Journal 10:A537 (1996).
62. Porta D, Frick S, Kress T, Fuller P. Production of spiral fractures in human cadaver long bones by use of a simple torsion machine. Biomedical Sciences Instrumentation 33:418–422 (1997).
63. Porta D, Frick S, Kress T, Fuller P. The fine points of spiral fractures. Clinical Anatomy 12:208 (1999).
64. Frick S. The effects of combined torsion and bending loads on fresh human cadaver femurs [masters thesis]. Louisville, KY: University of Louisville; 2003.
65. Aldman B. Limbs: kinematics, mechanisms of injury, tolerance levels and protection criteria for car occupants, pedestrians and two-wheelers. In: The biomechanics of impact trauma. Amsterdam: Elsevier Publishers; 1984:327–331.
66. Aldman B. Living tissue properties. In: The biomechanics of impact trauma. Amsterdam: Elsevier Publishers; 1984:81–84.
67. Kleerekoper M, Feldkamp LA, Goldstein SA. The effect of aging on the skeleton: implications for changes in tolerance. In: Biomechanics and medical aspects of lower limb injuries. Warrendale, PA: Society of Automotive Engineers, Inc.; 1986:91–96. SAE Technical Paper 861926.

Chapter 10

Injuries of the Thigh, Knee, and Ankle as Reconstructive Factors in Road Traffic Accidents

Grzegorz Teresiński, MD

1. Introduction

1.1. Global Burden of Traffic Accidents

Currently, traffic accidents comprise the most common cause of traumatic deaths throughout the world and the most common cause of death and disability in the 15- to 44-yr-old age group in developed countries. In 2002, about 1.2 million people were killed in road traffic accidents, and by the year 2020, according to WHO data *(1)*, this figure is projected to almost double, making traffic accidents the third (from the ninth) leading cause of death and disability worldwide (following ischemic heart disease and mental depression). Despite a large number of cars and accidents in high-income countries, however, the percentage of fatalities is low (Table 1). A good marker of the motorization progress in a particular country is the percentage of pedestrians among all victims of traffic accidents, e.g., high in the low-income countries and eastern Europe (due primarily to a lack of road infrastructure and the absence of a separation between pedestrian and car streams).

1.2. Legal Assessment of Traffic Accidents

1.2.1. The Need for Reconstruction

According to police statistics, only a small percentage of traffic accidents are the result of incidental factors or the poor conditions of vehicles. The most common causes of road collisions are errors by drivers and improper behavior of pedestrians who often are both the causes and victims of traffic accidents.

From: *Forensic Science and Medicine*
Forensic Medicine of the Lower Extremity: Human Identification and Trauma Analysis of the Thigh, Leg, and Foot
Edited by: J. Rich, D. E. Dean, and R. H. Powers © The Humana Press Inc., Totowa, NJ

Table 1
International Rates of Road Traffic Accidents in 2002 *(2)*

Country	Passenger Cars per 1000 Population	Road Traffic Accidents per 10,000 Population	Persons Killed per 1000 Accidents	Car-to-Pedestrian Accidents %
USA	776	69	22	3.9
Italy	583	41	28	6.7
Germany	541	44	19	9.3
Austria	494	54	22	11.0
France	492	18	69	14.8
Belgium	462	46	28	7.2
Sweden	452	19	33	9.4
Spain	455	24	54	11.8
Great Britain	448	39	15	16.9
Poland	289	14	109	33.7
Russian Federation	156	13	180	46.0

The basis of legal evaluation of the results of traffic accidents is the assessment of the participant's behavior and the road situation. To determine the degree of involvement of individual persons, traffic accidents should be reconstructed and testimony given by witnesses must be verified *(3–6)*. It is well known that when the driver is the only witness, he is likely to present the accident version that is more favorable for him (Fig. 1), e.g., a sudden intrusion of the pedestrian from the right side of the road at daytime and from the left lane at night (due to the light asymmetry and better lighting of the right side of the road). In car-to-bicycle accidents, depending on the road situation, the driver may claim that he hit the cyclist or the pedestrian walking with his bicycle.

Occasionally, the victim's body (injured or dead) is the only evidence available on which to base a reconstruction of the accident (e.g., in hit-and-run accidents and in the absence of other traces on the road or on the victim's clothes).

1.2.2. Reconstruction Parameters (Biological Markers)

From a medical point of view, a deduction of the circumstances of traffic accidents (e.g., determining the direction of hit or who was driving) depends on demonstrating certain injuries (biological markers) that reflect the type and direction of the external force *(7)*. Within more than 100 yr of motoring history, the evolution of vehicles has resulted in changes in the types of injuries sustained by victims, which, in turn, has made it necessary to consider new biological factors for reconstruction of the circumstances of accidents. For example, in the first decades of 20th century, the majority of fatalities from accidents involved pedestrians who were run over by vehicles with high bumpers that knocked pedestrians down after hitting them while they were in the erect position, thereby causing a secondary running-over of the victim. As the floor of the car was lowered and cars became fitted with low front bumpers, victims were thrown against the hood ("run under") and typical "bumper fractures" shifted typically to the shin diaphyses (the meaning of the term "bumper fracture" has also changed,

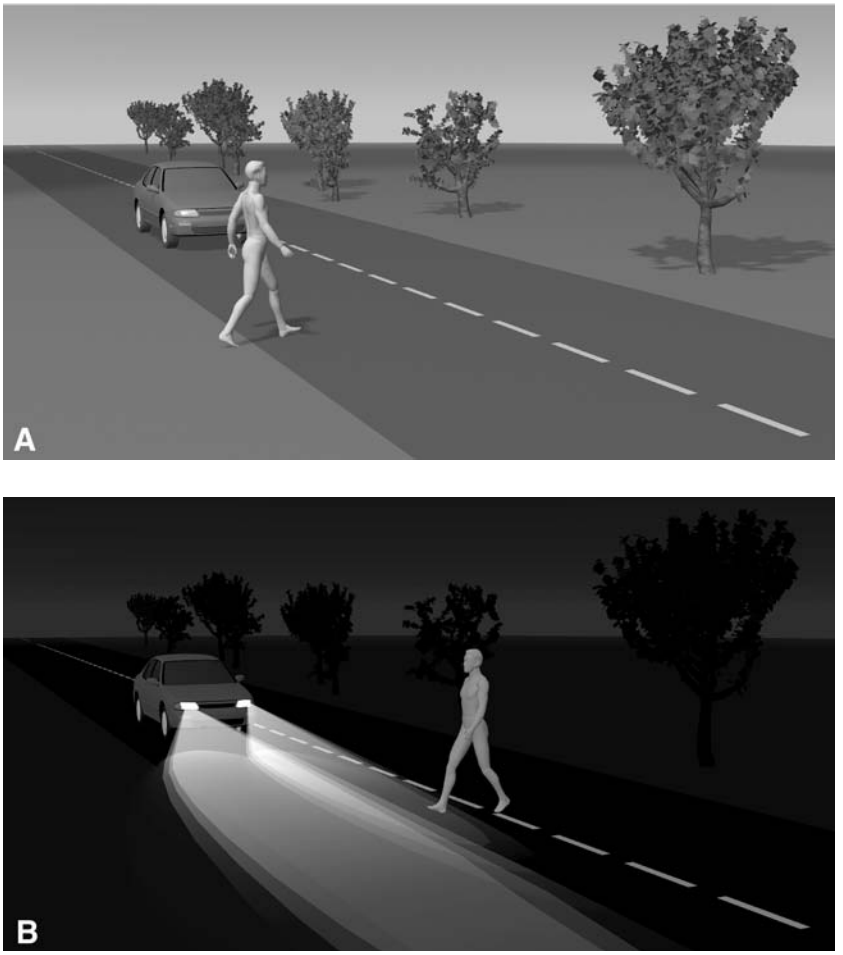

Fig. 1. The most dangerous directions of pedestrian intrusion by day and by night (the driver has the shortest time to react after noticing the pedestrian).

because it was first introduced during the 1930s by orthopedic surgeons as a synonym of tibial condyle fractures).

The biological markers for reconstruction must be associated with the first phase of the accident, i.e., the first contact with the victim's body by vehicular elements (e.g., "bumper injuries" in pedestrians and "dashboard injuries" in car occupants). The injuries should be detectable not only on autopsy but also by various imaging examinations in survivors.

1.2.3. Evidential Value of Biological Markers

From a legal point of view, each piece of evidence (both biological and technical) used in legal proceedings should be characterized by a precisely defined evidential value, especially by a strictly defined risk of error. Certain types of trauma will cause typical injuries only in some victims (this percentage makes it possible to make a deduction on the basis of a particular marker). Thus, from a medicolegal point of view, a lack of any typical injury often cannot be used as the evidence (negative),

i.e., the exclusion of a mechanism and thus a deduction should be based only on "positive" evidence. The percentage of cases with a defined injury pattern that indicates a mechanism different from the presumed one is an error risk for this marker *(7)*.

1.2.4. A Key Role of Lower Extremity Injuries in Some Aspects of Post-Crash Expertise

In various types of traffic accidents, the lower extremities are the first to come in contact with the body or interior of the vehicle (not only in pedestrians but also in cyclists, motorcyclists, drivers, and car occupants), and the injuries observed provide the best chance of proper forensic reconstruction of trauma circumstances *(4–6)*. The following circumstances are especially pertinent to pedestrian hits:

- location of pedestrian toward vehicle
- standing or recumbent position (important in "hit-and-run" accidents)
- impact direction (walking direction)
- type of collision (front, corner, sideswipe)
- moving phase (standing or moving)
- type of vehicle (in "hit-and-run" accidents)
- whether the vehicle was braked
- course of individual phases, particularly in complicated cases (e.g., hits in the standing position hits with subsequent running over by one or more vehicles)

In car crashes, it is most important to determine who was driving and whether the victim was wearing a seat belt. In motorcycle crashes, it is pertinent to determine whether the victims was the driver or passenger; and in car-to-bicycle accidents, it is important to determine whether the victim was the bicyclist or a pedestrian (and whether the individual was riding or walking along with bike) and the direction of impact.

Lower-extremity injuries are particularly relevant in car-to-pedestrian hits because they reflect the actual location of the pedestrian relative to the vehicle on collision, whereas the trunk, upper extremities, and head of the victim indicate the upper parts of the car that hit the body later, when the victim's body had already been rotated (Fig 25). Of note, there is no reliable method for evaluating crash speed in terms of biological markers *(5)*.

2. Lower-Extremity Injuries Useful for Reconstruction of Accidents

2.1. External Injuries

During the early years of motoring, forensic experts had already addressed the injuries characteristic of the recumbent body being run over. However, regular tire imprints on the victim's body are rarely observed and occur only at low speeds (e.g., when the victim is run over by a vehicle that is backing up). Contrary to popular belief, the most common traces found only resemble tire marks or are completely noncharacteristic (Fig. 2). The parallel, concentrated striae-like skin ruptures resulting from excessive pressure may also indicate the rolling of the victim's body by the wheel (Fig. 3). However, these signs are not specific for runover cases and are also likely to be caused by hitting the pedestrian in the standing position, because the rapid movement of the lower extremities may lead to similar skin tensions and ruptures, especially in groin region *(3,8,9)*.

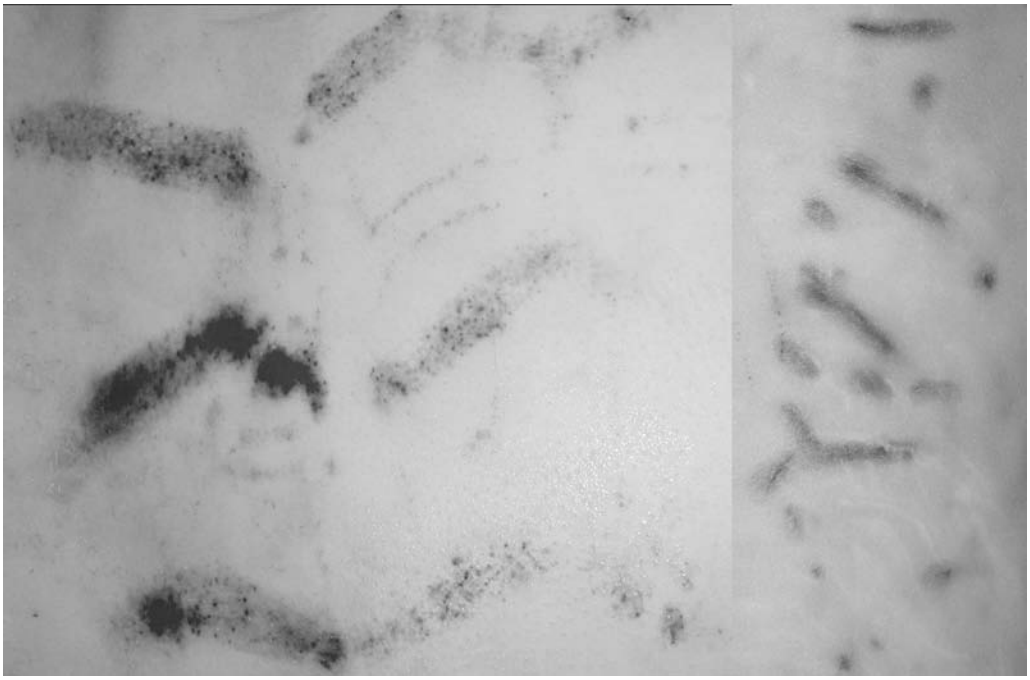

Fig. 2. Typical tire marks on the skin of victims run over by low- (left) and high-speed (right) vehicles.

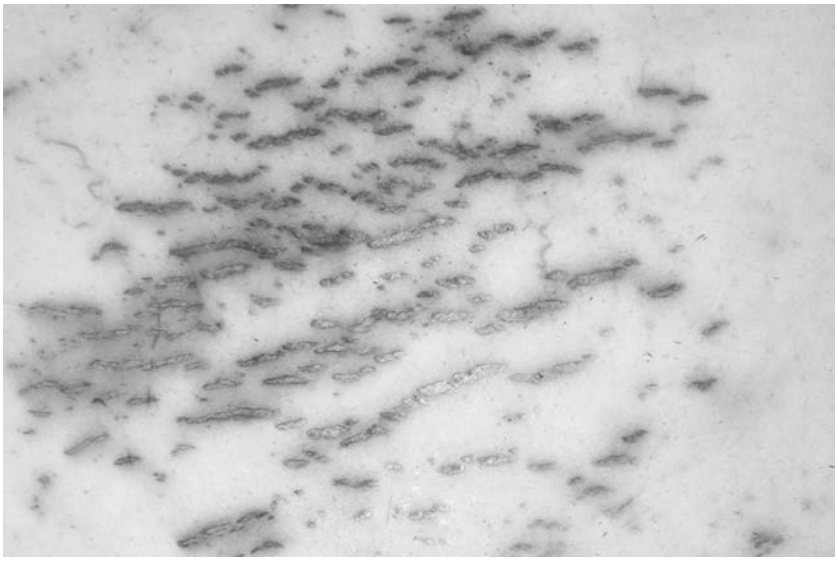

Fig. 3. Striae-like skin ruptures.

Until the 1970s, the reconstruction of impact direction in erect-pedestrian hits was based on a search for visible external "imprint" injuries, i.e. a "stamp" of the car's body elements on the victim's body (Fig. 4), similar to those observed in nonbelted car

Fig. 4. Imprint injuries in the pedestrian victim.

occupants when a bent knee hits the instrument panel (Fig. 5) *(3–5,9)*. However, the bodies (and interior) of modern vehicles are smooth, without edges or protruding elements and, thus, often do not cause any external injuries, even when internal injuries are extensive. Paint or dust chafing may be observed on the cloth of the trousers where the lower limbs contacted the car body (Fig. 6) *(4,9a)*. At present, the majority of external injuries (wounds, excoriations) found on the body of the pedestrian (or cyclist) victim are caused by further phases of the accident—impact and rubbing against the rough road surface (Fig. 7), rather than contact with the car body (except for those caused by glass chips). Only some open-extremity fractures are relevant for evaluation of the mechanism of injury *(9)* because the bone fragments often pierce the skin on the side opposite the injury (Fig. 8). If the victim dies directly after being hit, skin bruises are rarely observed; such bruises may occur in survivors, however, even few days after the injury due to the spread of deep bruises (*see also* Subheading 2.2).

2.2. Soft Tissue Injuries

Pedestrian- or cyclist-to-car hits usually cause extensive bruises and the crushing of deeper tissues, which can be detected within the organ by ultrasound and on autopsy only after extensive removal of the skin of the back and the entire circumference of extremities and deep-muscle incisions. In many cases, the location of bruises allows the investigator to determine the direction of impact and in hit-and-run accidents may also help the investigator determine the type of vehicle responsible for the injuries on the basis of the level at which bumper injuries are observed (Fig. 9). The injuries are usually located lower than the bumper level because the front part of the vehicle dips on braking.

Fig. 5. External injuries from a dashboard.

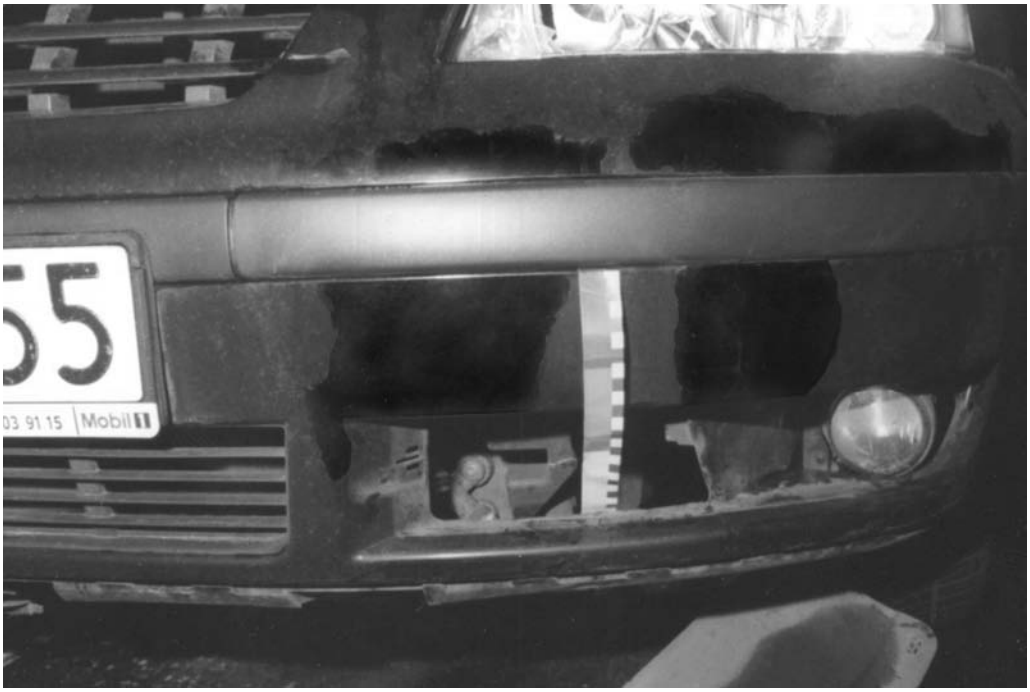

Fig. 6. Dust wipes on the bumper due to contact with both of the pedestrian's legs.

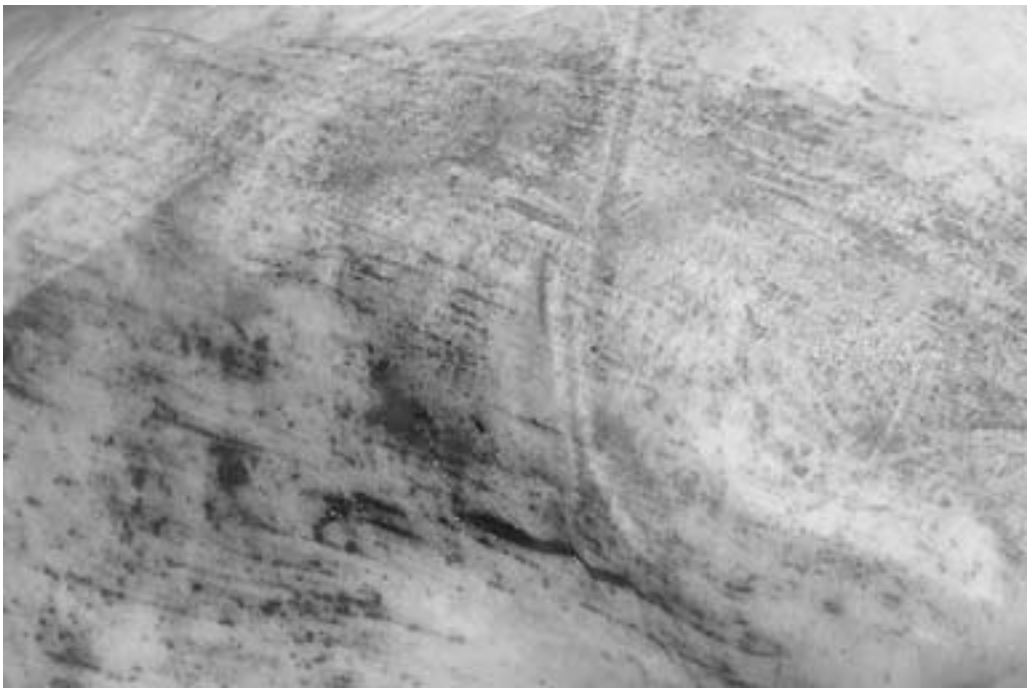

Fig. 7. Typical skin excoriations caused by being dragged along a rough road surface.

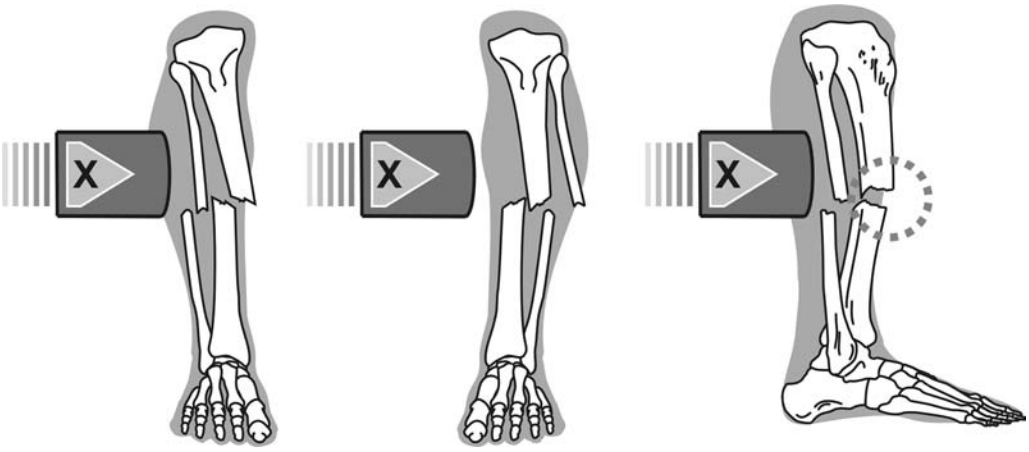

Fig. 8. Skin pierced by bone fragments on the side opposite to that on which the injury occurred (open fracture).

Moreover, heavy car loading and the height of the victim's shoes (especially important in women) may substantially lower the contact level. Injuries located only on one extremity may indicate that the victim was hit by the corner of the vehicle *(4,5,9)*.

Moreover, the skin preparation enables investigators to detect the areas in which the skin is torn from the muscle fascia as a result of the turning wheel rolling across the extremity ("decollement"); this usually involves most of the circumferences of the extremity (Fig. 10). Deeper injuries are usually more extensive on the side of the

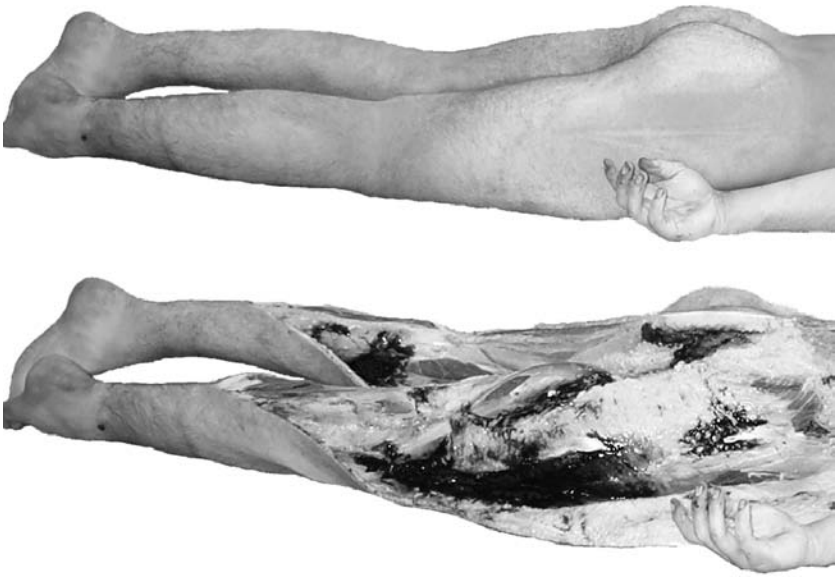

Fig. 9. Bruises in the muscles and subcutaneous tissue ("bumper injuries") revealed after skin preparation in the lower limbs.

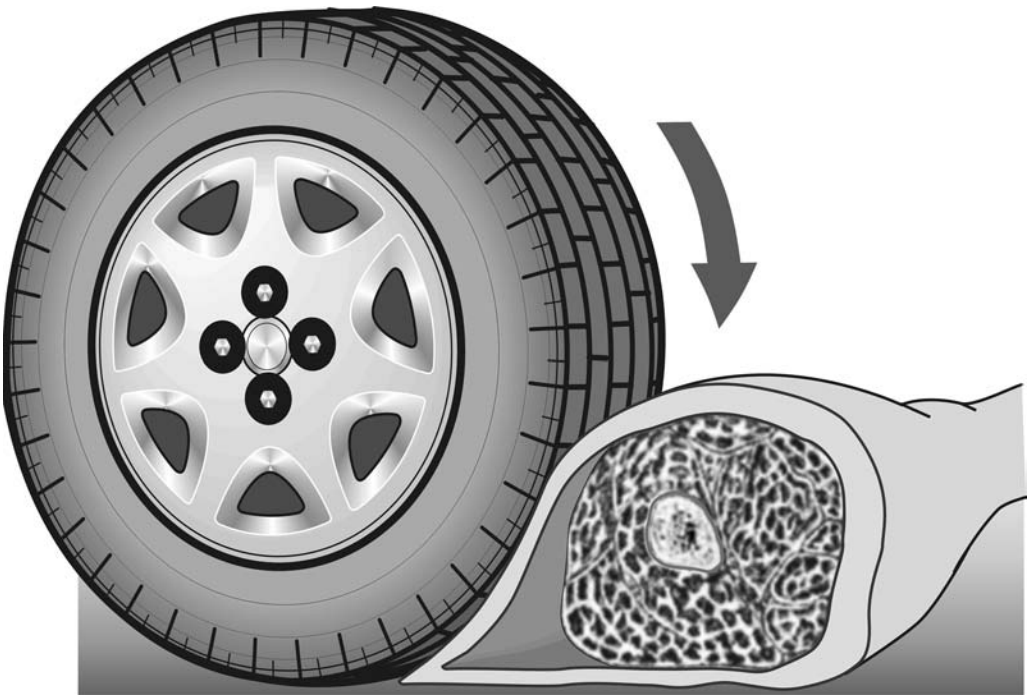

Fig. 10. The mechanism of the decollement type of skin detachment.

extremity towards which the vehicle was moving, and skin ruptures may lie transversely to the direction of the car. In most cases, however, the skin is not ruptured and a "subcutaneous pocket" forms, filled with blood and crushed fatty tissues *(3,5,9)*. Skin detachment is also likely to result from a tangential or oblique hit when the victim is in an erect position (when the corner or side of the vehicle only "brushes" the pedestrian's body) and occasionally by a perpendicular impact (especially in the elderly) as a result of the crushing of subcutaneous tissue, although in the latter case, they are usually much less extensive than in the cases involving being run over by the wheel *(10)*.

Modern vehicles are constructed to reduce the degree of traumatic injury in pedestrians by distributing the energy of primary trauma over larger surface area and by partially absorbing the energy into car body elements *(11)*. Therefore, in more and more cases typical "bumper injuries" cannot be detected or the "primary impact" injuries cannot be distinguished from secondary injuries occurring in subsequent phases of the accident. Such difficulties are even greater when the victim survives a relatively short time, because bruises tend to spread beyond their primary location within soft tissue; the infiltration of tissue with blood is particularly common around skeleton fractures, and bruises spread throughout (also due to gravity) loose connective tissue and interfascial spaces, especially when parenchymatous bleeding persists. In delayed postaccident deaths, which are increasingly common, the bruises undergo complete resorption before death.

2.3. Long-Bone Diaphyseal Fractures

Before the era of motorization, Messerer *(12)* had already performed experiments in long-bone diaphyseal fractures demonstrating that bones were less resistant to tearing than to compression forces. Thus, during bending, first the convex side of the bone is broken and fracture fissures run towards the concave side, forming a wedge-shaped bone fragment (Figs. 12, parts 1 and 2). During the 1960s, the rule formulated by Messerer concerning the so-called bending fractures—i.e., that the apex of the wedge-shaped fragment defines the direction of bending in bone—was adapted for use in reconstructing the direction of impact *(3,4,9,13)*. However, even a typical bending fracture, Messerer`s wedge indicates the direction of impact only when the bone was bent at the moment of impact, and not in a later phase of the accident.

Furthermore, bending fractures usually occur at a low speed of impact ("static" fractures; the lower the impact speed, the bigger the wedge base) *(14)*. At higher speeds of impact, "dynamic," noncharacteristic transverse or multifragment fractures are usually observed (more often in the elderly because of osteoporosis); in some cases, even "false" wedge-shaped fragments may be seen (i.e., the apex and not the base is directed towards the impact site, as is the case for crater-hole fractures created in the skull by bullets [Fig. 11]). However, the "true" Messerer's wedge always has a sharp apex and concave lateral edges (Fig. 12), whereas "false" triangular bone fragments often have an irregular apex and convex lateral edges *(3,15)*. Within the triangular section of the tibia, bending fractures are more likely to be caused by a hit to the flat back surface than to the lateral or medial side, and particularly from the front *(16)*.

Messerer's fractures are becoming increasingly rare, which is likely the result of changes in the shape of the front of modern passenger cars (especially the elimination

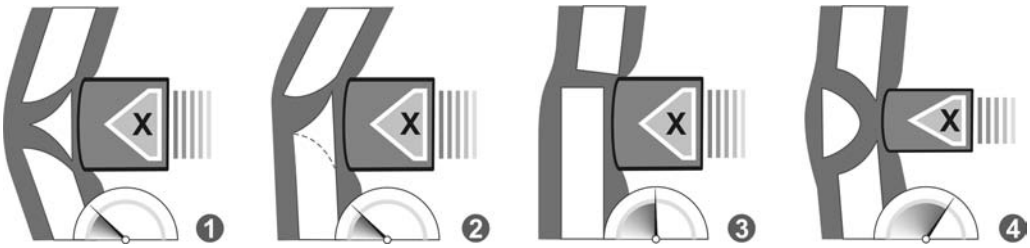

Fig. 11. Some patterns of long-bone diaphyseal fractures in pedestrian victims of traffic accidents: **(1)** "classic" bending fracture; **(2)** "incomplete" bone wedge; **(3)** "dynamic" transverse fracture with "phantom" wedges; and **(4)** "false" bone wedge.

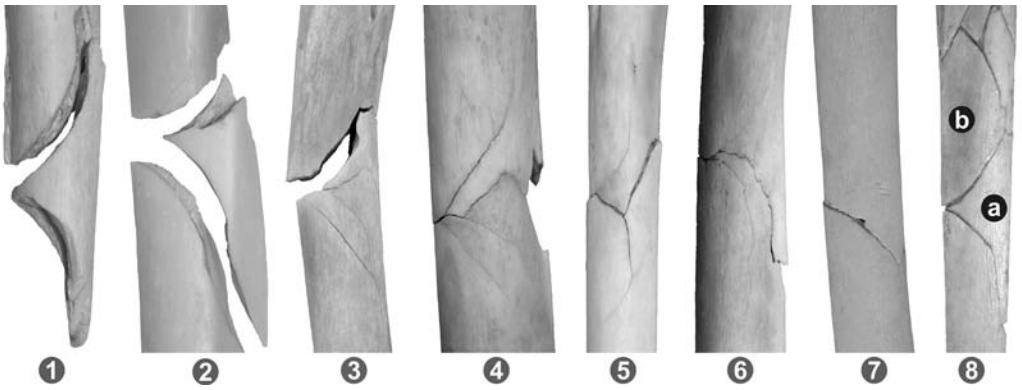

Fig. 12. Various patterns of "complete" **(1–2)** and "incomplete" **(3–7)** bending fractures. **(8)** "true" **(a)** and "false" **(b)** wedges. All impacts from right side of the figure.

of protruding bumpers) and the higher average speed on collision *(7,17)*. However, many apparently noncharacteristic oblique fractures are in fact "incomplete" bending fractures and the additional fissure of the fracture "supplementing" the wedge may be detected only on high-quality radiographs or after bone maceration (Fig. 12, part 3) *(16–18)*. Thus, if the oblique fracture fissure is clearly convex (i.e., it starts with a mild arch on one side of the bone and ends in a sharp angle on the opposite side), the direction of the external breaking force may be determined if one bears in mind that the edges of the Messerer's wedge must be convex in relation to its base (Fig. 12, parts 6 and 7) *(14,15)*. In many cases, after maceration of bones even the transverse fractures are found to be flexion fractures with so-called "phantom" wedges (Fig. 12, parts 4 and 5) *(17)*.

The spiral fractures (Fig. 13) are rare in victims of traffic accidents, because they are caused by torsional forces; e.g., from tangent hit of a pedestrian—i.e., sideswipes (author's personal observation). Being hit on the lateral body side of the body by the corner or side of a vehicle while walking along a road causes the body to rotate around the body mass-loaded lower limb *(4,5)*. A clockwise torsional load results in right-hand screw-like spiral fractures, whereas left-hand screw-like fractures are "counterclockwise" (looking up if the top of the bone is held and the bottom is twisted) *(18)*.

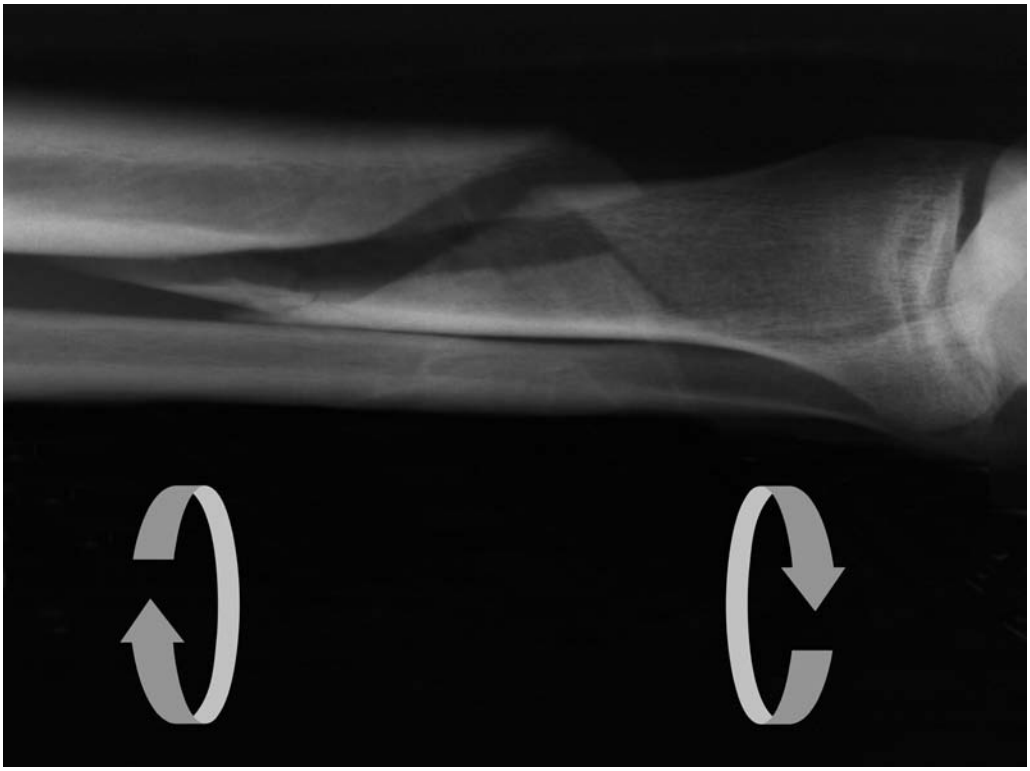

Fig. 13. Spiral fracture of tibial shaft.

In the case of axial loading (e.g., caused by dashboard injury to the femoral diaphysis area), the fracture fissures are often longitudinal (Fig. 14) *(19,20)*.

2.4. Knee Injuries

Mechanically, the knee joint is a modified hinge in which only flexion–extension and slight rotational movements are possible (the risk of injury is the highest when the knee is blocked in full extension). Unlike other joints, the shape of the joint surfaces does not ensure stability in the knee; instead, stability is provided by the menisci, as well as by ligaments and muscles. The lateral and medial walls of the joint capsule are strengthened by lateral collateral ligament (LCL) and medial collateral ligament (MCL). These ligaments are most tense in the extended knee, and they serve primarily to fix and stiffen the joint in this position and eliminate sideward movements. The knee joint has also two intraarticular ligaments—the anterior cruciate ligament (ACL) and the posterior cruciate ligament (PCL)—whose course and attachments allow them to tighten in almost all joint positions. The ACL mostly counteracts anterior tibial dislocation and internal rotation, whereas the PCL counteracts posterior tibial dislocation and external rotation *(21)*.

Knee-joint injuries form patterns (Fig. 15) according to the direction of the external force and any pathological dislocation within the joint *(21–24)*. Thus, injuries occur during hyperextension (i.e., when the position of tibial and femoral diaphyses exceeds the

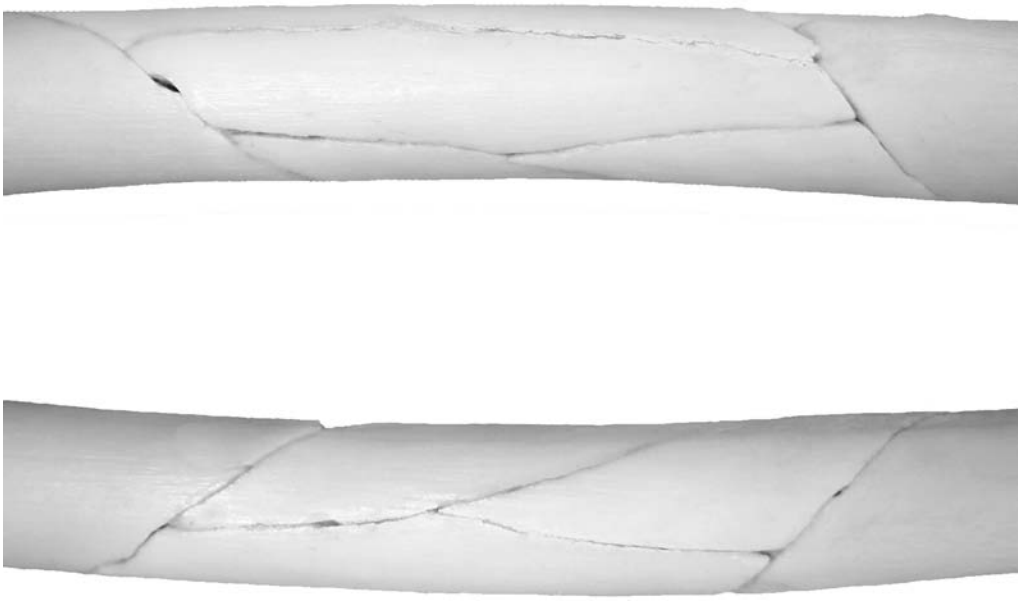

Fig. 14. Longitudinal fractures of femur shaft due to axial loading in dashboard-type injury.

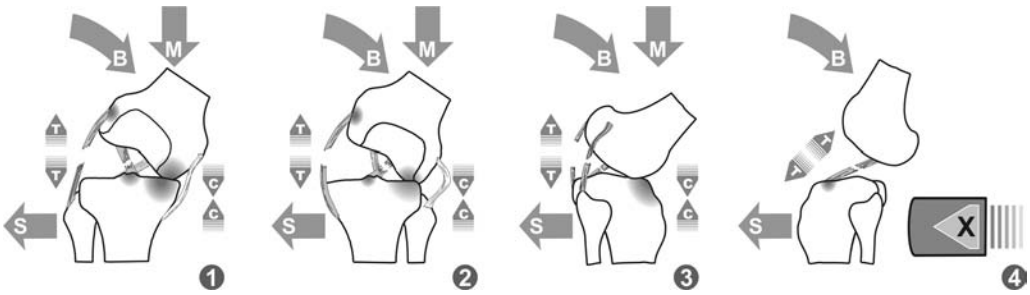

Fig. 15. The main mechanisms of knee joint injuries: **(1)** varus flexion; **(2)** valgus flexion; **(3)** hyperextension; **(4)** tibial translocation—bending force **(B)**, shearing force **(S)**, tearing force **(T)**, compression force **(C)**, limb load by body mass **(M)**, impact direction **(X)**.

normal range of physiological extension of the knee joint) and varus or valgus angulation (i.e., when the diaphyses bend in the frontal plane). Moreover, injuries to ligamentous structures may result from shearing forces (due to the dislocation of tibial and femoral diaphyses within the perpendicular plane). However, the isolated mechanism of dislocation is rare, because shearing force effects are masked by dominant bending injures. The only exceptions are isolated ACL injuries caused by hits from the rear that result in anterior dislocation of the proximal tibia relative to the femoral condyles (Fig. 15). The subsequent bending forces act in the natural range of articular movements ("pure" shearing effect) *(24,26)*.

Generally, the forces tearing the ligamentous structures act on one side of the joint while those crushing the bone act on the other side; the effects of these components are not always detectable simultaneously, however. In many cases, the only signs of ligamentous avulsion are the local bruises, which should be differentiated from the effects of direct

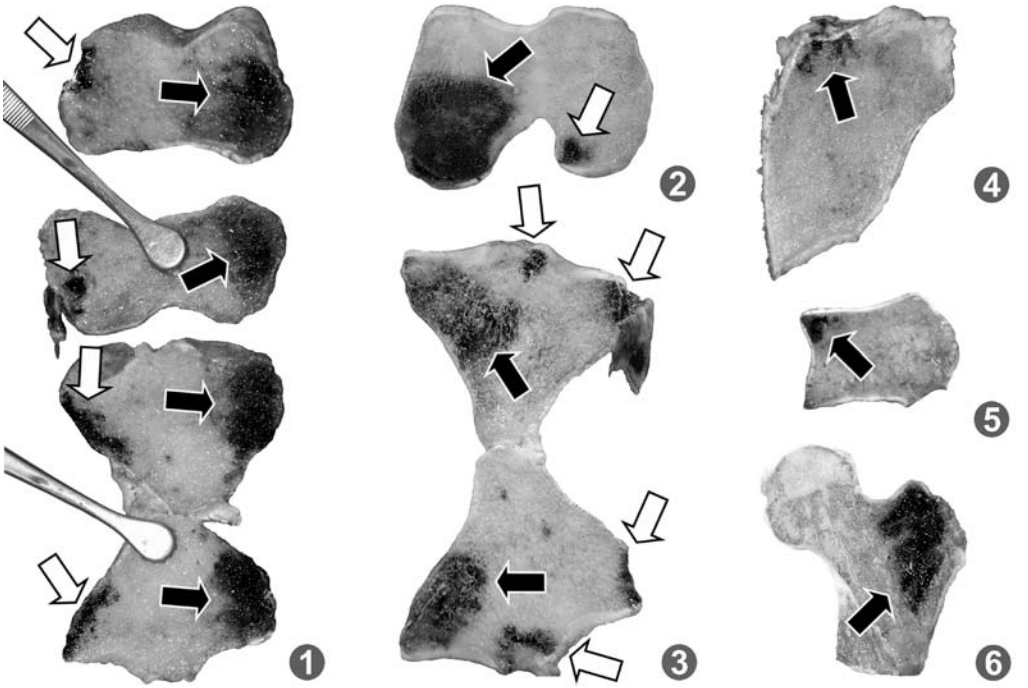

Fig. 16. (1–3) Bone bruises on tibial and femoral epiphysis frontal sections; **(4)** bruises at the anterior margin of tibial epiphysis sagittal section; **(5)** bruises on the trochlea tali section; **(6)** bruises on the femoral greater trochanter section (white arrows, ligament avulsion; black arrows, epiphysis compression).

trauma. To determine the mechanism of joint injury, it may be helpful to evaluate bone bruises; however, it is necessary to differentiate those caused by condylar compression from those resulting from tearing forces *(22–25)*. The former are usually extensive, located in the central and deep condyle structures, and reach under the articular surfaces of femoral and tibial condyles. They may be accompanied by macroscopically visible fissures of fractures or compression of bone trabeculae, occasionally with an indented or lowered condyle. On the other hand, the bone bruises resulting from avulsion (Fig. 16) are usually small and located peripherally within the lateral parts of the condyles (i.e., in the region of capsule attachments and collateral ligaments) or under the intercondylar prominence (in crucial ligament avulsions). They may be accompanied by small bone fragments tearing off at the site of ligamentous attachments. In living persons, bone bruises can be detected by magnetic resonance imaging (Fig. 17) *(22,23,25)*.

The characteristics of meniscus injuries (Fig. 18) vs fibular head fractures (Fig. 19) may be useful for differentiating the mechanisms of knee joint fractures.

2.5. Ankle Injuries

The upper portion of the ankle joint is a hinge articulation. Physiologically it allows only dorsal and plantar flexion around the axis running through the center of the trochlea tali. The compactness of this joint is ensured by the ligaments attached to the

Fig. 17. Magnetic resonance images of a bruise in the lateral femoral condyle (image courtesy of Marzena Janczarek, MD, from the Department of Interventional Radiology and Neuroradiology, Medical University of Lublin, Poland.

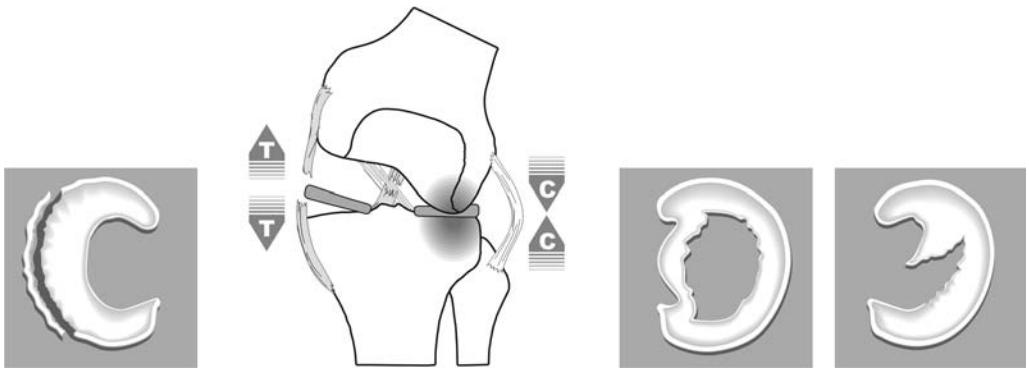

Fig. 18. The mechanism of meniscus injuries in valgus flexion of the knee: marginal separation (left) and "bucket handle" or "parrot beak" tears (right).

lateral and medial malleolus, while anteriorly and posteriorly the joint capsule is strengthened only by muscle tendons.

Similar to injuries to the knee joints, ankle injuries form patterns (Fig. 20) determined by the direction of the external force and dislocation of joint structures *(26–28)*. Thus, injuries occur when the distal tibial epiphysis lies beyond the range of physiological flexion (dorsal or plantar) and when excessive pronation or supination of the shins towards the fixed foot is observed (Table 2). Contrary to typical ankle sprains caused by improper positioning of the foot during running, jumping, or skidding, victims of traffic accidents often lack the rotational component and their injuries are caused by forces acting in one direction only. Injuries that occur during the first phase of trauma are usually caused by tearing forces, while those occurring during later phases of trauma are usually caused by crushing forces (the limb must be loaded by body mass). The site of compression may be indicated by bone bruises on the section of the trochlea tali whose

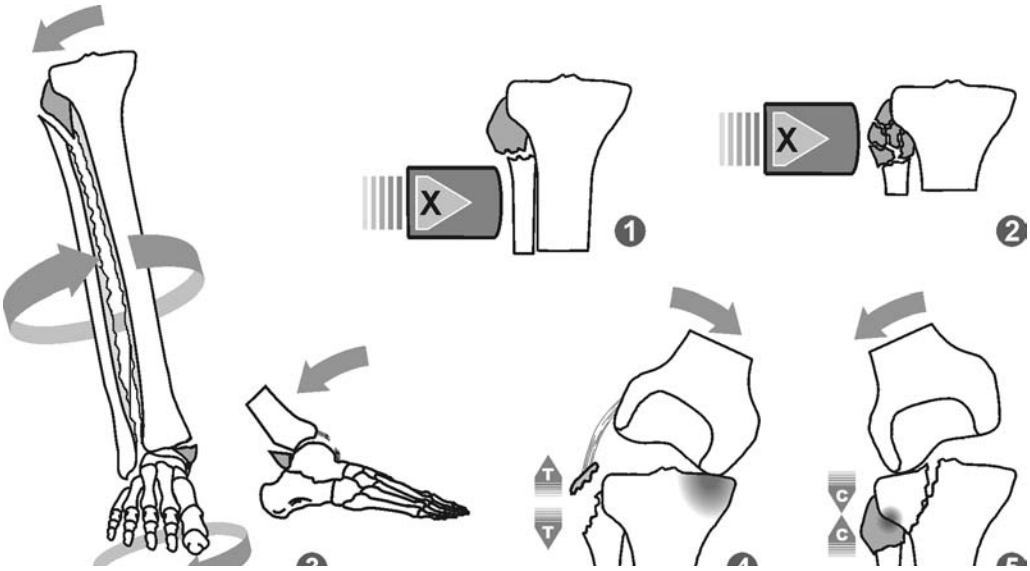

Fig. 19. Mechanisms of fibular head fractures: **(1,2)** direct injury; **(3)** pronation-rotation; Maisonneuve's fracture; **(4)** avulsion caused by varus flexion; **(5)** compression caused by valgus flexion.

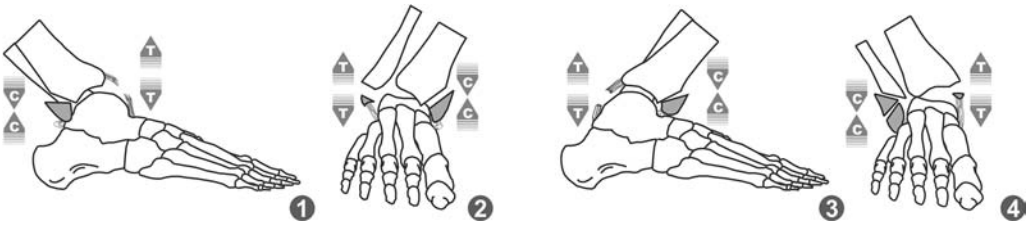

Fig. 20. The main direction of pathological dislocation of bone structures within the ankle joint in victims of traffic accidents: **(1)** plantar flexion; **(2)** supination; **(3)** dorsal flexion; **(4)** pronation.

edges press the lateral (pronation) or medial (supination) malleolus (Fig. 16, part 5). Avulsion of the collateral ligaments may disrupt the ligament or cause separation of the malleolus (*see also* Table 2). Because there are no ligaments strengthening the front and back of the joint capsule, avulsion of anterior or posterior edges of the distal epiphysis of the tibia is not observed (in fact, edge fractures are always caused by the compression mechanism).

2.6. Femoral Proximal Epiphysis Injuries

In injuries to the lateral side of the greater trochanter (Fig. 16, part 6), the victim may sustain bone bruises within the trochanter (Fig. 21) or more rarely in the femoral head and central fractures of the hip joint (or central dislocations when the femoral head is translocated into the interior of the pelvis) *(7,26)*. In car occupants central fractures or injuries to the posterior margin of the acetabulum may result from forces travelling along

Table 2
Mechanisms of Ankle-Joint Injuries in the Victims of Traffic Accidents

Injury Mechanism	Avulsion Phase	Compression Phase
Supination (inversion)	Horizontal fracture of lateral malleolus at or below the level of articular space or rupture of lateral malleolus ligaments	Vertical fracture of medial malleolus
Pronation (eversion)	Horizontal fracture of medial malleolus or rupture of deltoid ligament	Oblique fracture of lateral malleolus just above the level of ankle joint, often with displacement of a triangular fragment from the lateral surface of fibula
Dorsal flexion	Tearing off of the posterior joint capsule	Fracture of the anterior tibial edge
Plantar flexion	Tearing off of the anterior joint capsule	Fracture of the posterior tibial edge

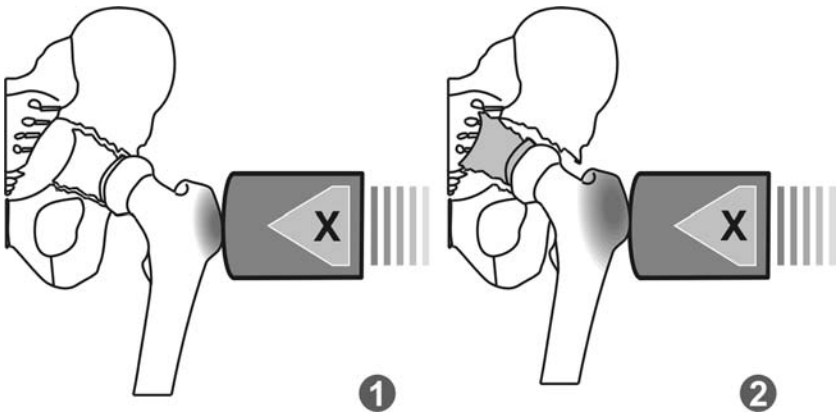

Fig. 21. The mechanism of bone-bruise onset in the great trochanter and central fracture (dislocation) of the hip joint (X, impact direction).

the axis of the femoral diaphysis (dashboard injuries), as well as during high-energy trauma while the thighs are in substantial adduction (e.g. when the passenger's legs are crossed) or abduction (e.g., when the passenger's thighs are kept apart). Under such circumstances, the femoral head may move outside the acetabulum (Fig. 22) *(3)*.

2.7. Mechanisms of Ankle and Knee Joint Injuries in Traffic Accidents

2.7.1. Car-to-Pedestrian Accidents

For many years, the efforts of researchers and car companies have been focused on reducing the degree of trauma in traffic-accident victims *(11,29)*. Changes in bumper

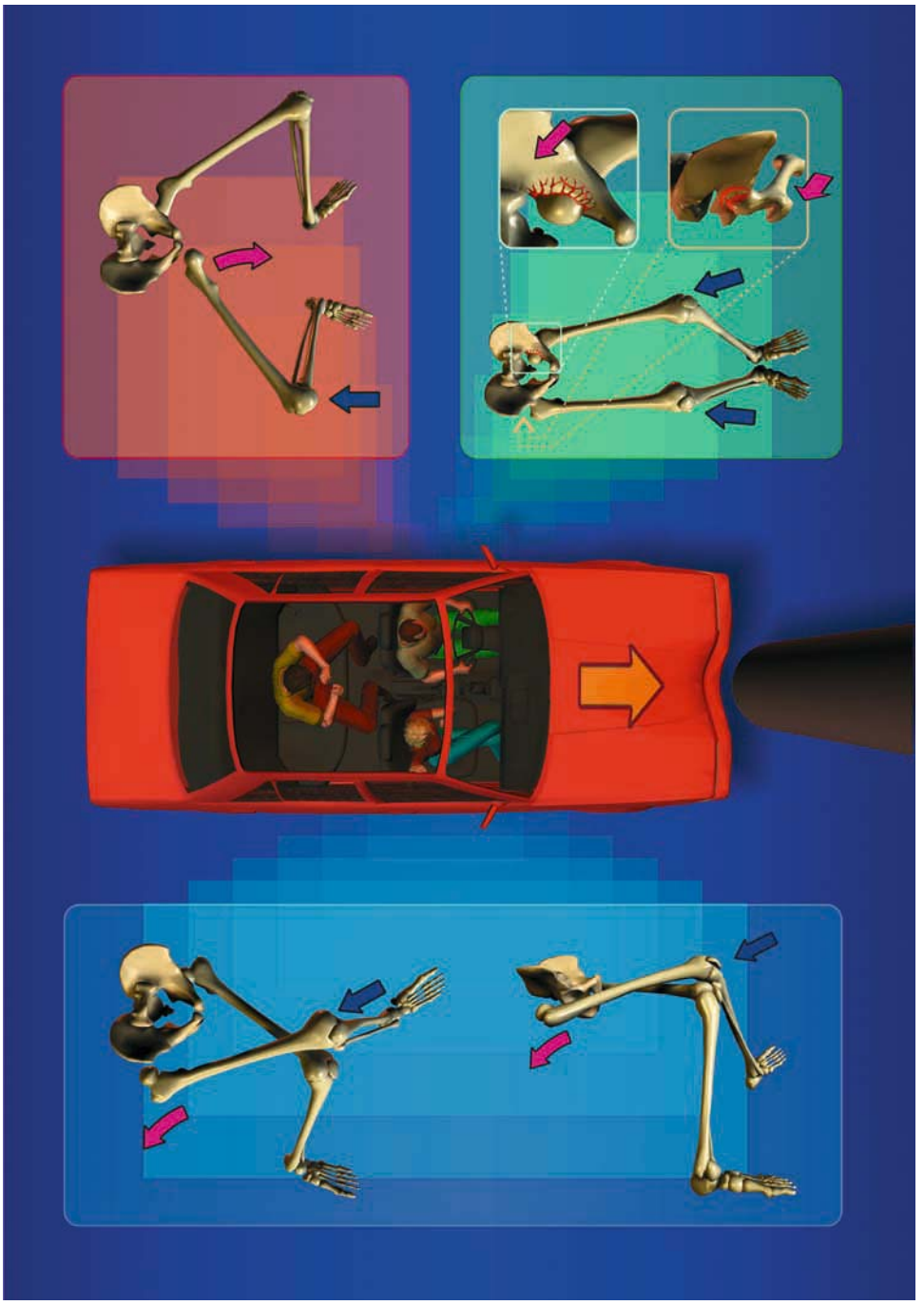

Fig. 22. The pattern of hip dislocation in a frontal collision depends on the initial sitting position of vehicle occupants. *See* **Color Plate III**, following page 240.

construction and the distribution of energy on impact over a larger surface have decreased the number of lower-extremity fractures in pedestrians hit by cars. Unfortunately, the redistribution of impact energy paradoxically has increased the risk of injury to joint structures, and ligament injuries have resulted in disability more often than even multisite diaphyseal fractures. By contrast, the low, protruding, and inflexible bumpers in older vehicles frequently caused fractures in the shins; this prevented the knee joint from absorbing the impact energy and, thus, protected it from the effects of trauma. In terms of forensics, however, the changes made in modern vehicles have increased the ability of investigators to reconstruct the accident based on the mechanism of trauma *(7,24)*.

The presence of ankle- or knee-joint injuries indicates that the pedestrian was hit while in an erect position, *(27)* as such injuries—especially those caused by the compression mechanism and resulting in bone bruises in the central parts of tibial and femoral condyles—occur only when the limb is loaded by body mass. When the victim is run over while in the recumbent position, the injuries are noncharacteristic and usually occur only when the wheel rolls directly over the ankle or knee. Running over of the pedestrian may cause external dislocations of the femoral head outside the acetabulum; such hip-related injuries are not normally observed in victims who were standing erect when hit *(7)*.

When a standing pedestrian is hit by a passenger car, protruding elements of the car hit much lower than the victim's center of gravity, causing the victim's upper body to rotate in the direction opposite that of the speed vector of the car. One or both ankles (depending on whether the victim was standing still or walking when hit) may twist along the rotation axis, causing the body to spread over the hood, in which case the thigh and hip regions are hit first, followed by the trunk and head *(4)*. In this hits caused by small- or medium-sized passenger cars of a trapezoidal or pontoon body, the site of primary impact is usually located in the middle or proximal part of the shins (medium-height victims). Large passenger cars and delivery vans hit at the level of the knee, and trucks with a high bumper may hit the proximal thigh or hip girdle (such a "high" impact is likely to knock the pedestrian down, which increases the risk of a secondary runover). During the first phase of the accident, the victim's body "adjusts" to the shape of the front of the vehicle, and the place of force application determines the type of pathological dislocation that will occur in the joint structures and consequently the mechanism of ankle and knee-joint injuries. On the other hand, injuries to proximal femoral epiphyses (the greater trochanter area) are good markers of an ipsilateral hit while the victim was in the erect position, no matter what the shape of body of the car *(7,26)*.

In contrast to passenger cars, trucks with a high bumper location often cause a reversed complex of injuries in both the knee and ankle joints (the lever principle; compare Fig. 23 and Table 3). Delivery vans, light trucks, sport utility vehicles, pickups, and large passenger cars usually cause a reversed complex of injuries in ankle joints only. Very low hits at the level of distal shin parts resulting in reversed injury complexes in the knee are rare (e.g., they are seen in tall victims and with intensive braking of the vehicles before the accident; particularly those vehicles with low floor and a wedge-shaped body). In short victims, the passenger-car hits resemble the delivery-van hits whereas in children they resemble the truck hits *(7,24,26,27)*.

Therefore, the mechanism of knee-joint injuries should always be considered within the context of every circumstance of the accident and the shape of car body.

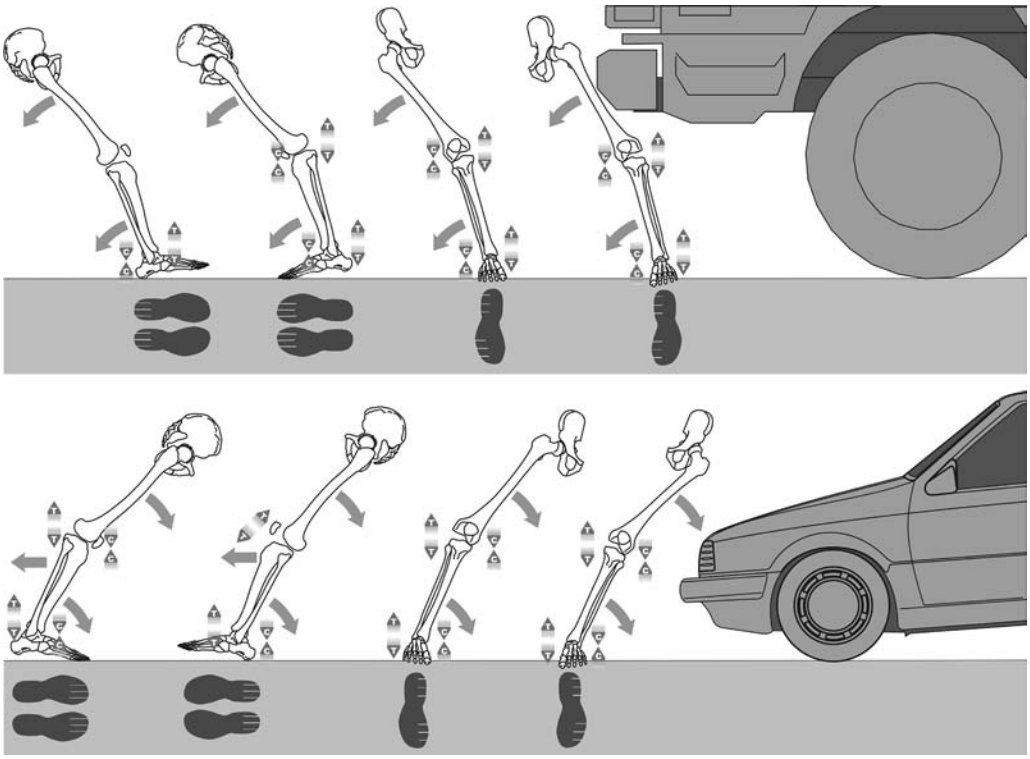

Fig. 23. The most common mechanisms of ankle and knee-joint injuries and the mechanisms of shoe–sole scratches in pedestrian hits caused by small passenger cars and trucks with a high bumper location. Compression forces (C); tension forces (T).

Table 3
The Most Common Mechanisms of Ankle- and Knee-Joint Injury in Pedestrians Hit by Vehicles With Various Vehicular Body Shapes

Joint	Vehicle Type	Impact Height	Mechanisms of Injury According to Hit Direction			
			Anterior	Posterior	Lateral	Medial
Ankle	Passenger	shin	dorsal flexion	plantar flexion	pronation	supination
	Van**	knee	plantar flexion	dorsal flexion	supination	pronation
	Truck	thigh	plantar flexion	dorsal flexion	supination	pronation
Knee	Passenger	shin	hyperextension	translocation*	valgus flexion	varus flexion
	Van**	knee	hyperextension	–	valgus flexion	varus flexion
	Truck	thigh	–	hyperextension	varus flexion	valgus flexion

*isolated injury to the ACL due to anterior translocation of the proximal tibial epiphysis in relation to the femoral condyles.

**also sport utility vehicles, pickups, or large passenger cars (non breaking).

ACL, anterior cruciate ligament.

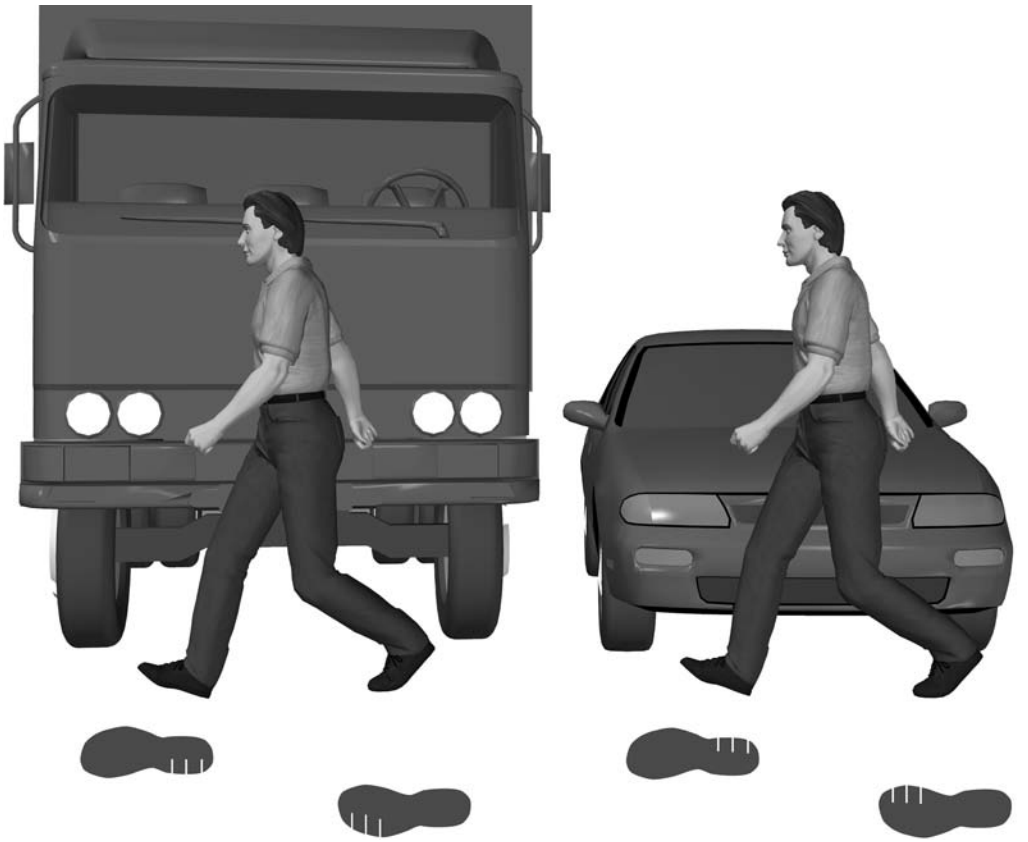

Fig. 24. The shoe-sole scratches indicate the impact direction and walking phase of the pedestrian.

However, when the impact direction is explicitly defined (e.g., on the basis of soft-tissue injuries), the findings in knee- and ankle-joint injuries may be used to determine the type of vehicle that was involved, particularly in hit-and-run accidents.

The mechanism of ankle-joint injury often correlates with scratches on the soles of the shoes *(28)* near the edge of the shoe. When a small passenger car is involved, these scratches are usually found on the side ipsilateral to the side of the vehicle that made contact with the body; when a truck with a high bumper is involved, they are usually found on the side of the shoe that is contralateral to the side of the body that was struck. In some cases, the location of these scratches can be used to determine the walking phase during which the individual was struck (Fig. 24).

In oblique pedestrian hits, mixed injury complexes are likely to occur in the region of ankle and knee joints, e.g., during dorsal flexion with the pronation component and during hyperextension with the valgus-flexion component in passenger-car anterolateral hits *(24,27)*. In corner hits (Fig. 25) or sideswipes, rotation may occur within the ankle joint, e.g., a corner of the car may rub against the lateral side of a pedestrian walking along the road, resulting in a pronation–rotation trimalleolar fracture (Fig. 19, part 3).

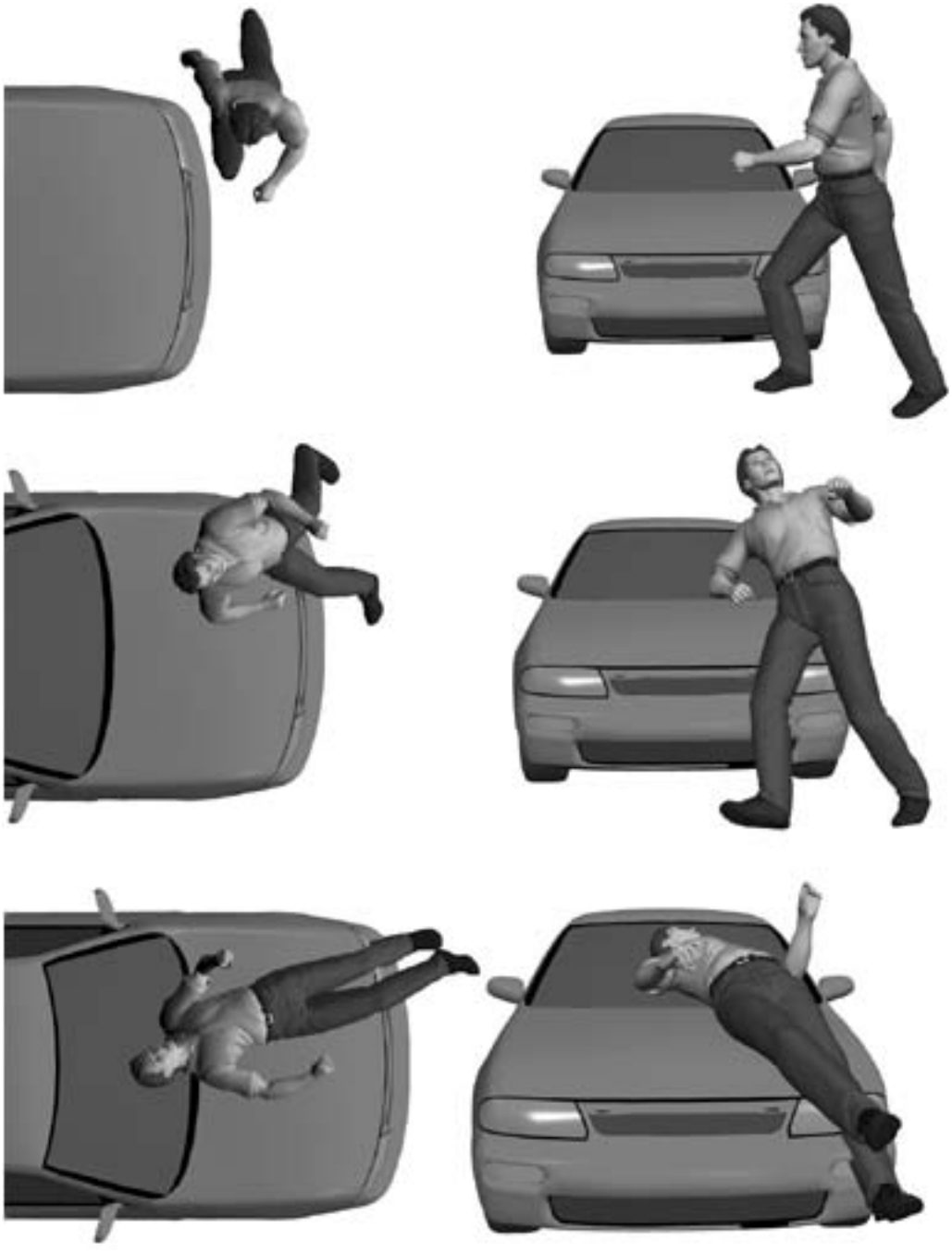

Fig. 25. Rotation of the victim's body in a car-to-pedestrian hit.

2.7.2. Car-to-Bicycle Accidents

Ankle- and knee-joint injuries are only slightly less common in cyclists than in pedestrians. This indicates that the pressure exerted on the bicycle pedals by the legs plays a role similar to that of body mass loading in the extremities in pedestrians.

In passenger-car-cyclist hits, the mechanisms involved in ankle-joint injuries (in back and lateral hits) are the same as those in similar pedestrian groups. Injuries to the knee joint are identical to those in pedestrians in lateral hits, only; in front and back hits, passenger cars cause primarily "reversed" injury complexes (Fig. 26). For example, hyperextension of the knee is a typical marker of a back hit in cyclists. Passenger cars usually do not cause knee joint injuries in front hits of cyclists, while almost all such hits cause hyperextension-related injuries in pedestrians (similar to cyclists hit in the front by a truck) *(26)*.

The relations described above may be used to distinguish the means by which a cyclist was hit vs a pedestrian walking with a bike. Bruises in the subcutaneous tissue beneath the medial aspects of the proximal femur (and the scrotal sac in men; Fig. 27) may be used for this purpose, since they are more common in cyclists (due to contact with the saddle) than in pedestrians *(26)*. In oblique passenger car-to-bicycle hits (usually at an angle of <30°) the cyclist's thighs and buttocks rotate the saddle in the direction opposite to the site of impact (Fig. 28), whereas in a perpendicular hit, the saddle rotates towards the striking vehicle (Fig. 29) *(30)*.

2.7.3. Inside-Car Casualties

Injuries to ankle joints and foot bones are common in car occupants and develop most often during front hits primarily as a result of floor intrusion (equally common in drivers and passengers), contact with pedals, and the foot becoming trapped under pedals (in drivers only, and more frequently in the right than in the left leg). The imprints of control pedals on the soles of shoes may be used to determine the circumstances responsible for injuries and to identify the driver. The mechanism of ankle-joint injuries consists of axial loading with simultaneous rapid dorsal flexion, supination, or pronation of the foot *(31)*.

Knee-joint injuries result from contact between the legs and the dashboard. Any of four different mechanisms may be involved (Fig. 30), based on the shape of the passenger compartment, the position of the passenger's seat, and the passenger's height, as well as whether the victim was belted or the occupant's compartment was compressed *(32)*. The determination of the site of contact between the legs and elements of the car's interior makes it easier to find trouser cloth that has rubbed off or melted into plastic dashboard elements. If the occupant's chamber was not compressed and the control panel was not translocated, the presence of dashboard injuries indicates that the victim was not belted on collision.

The most common contact is made between the front surface of a bent knee and the dashboard. This is likely to cause fractures between the patella and acetabulum (Fig. 30, part 1a–f, Fig. 31).

Such injuries are equally common in drivers and car occupants, and the nature of hip injuries may also indicate the position of the victim in his or her seat (compare Subheading 2.6 and Fig. 22).

In nonbelted occupants, the knee is more likely to be hyperextended (Fig. 30, part 4) in the front seat passenger when he is thrown from the car through the windscreen. On

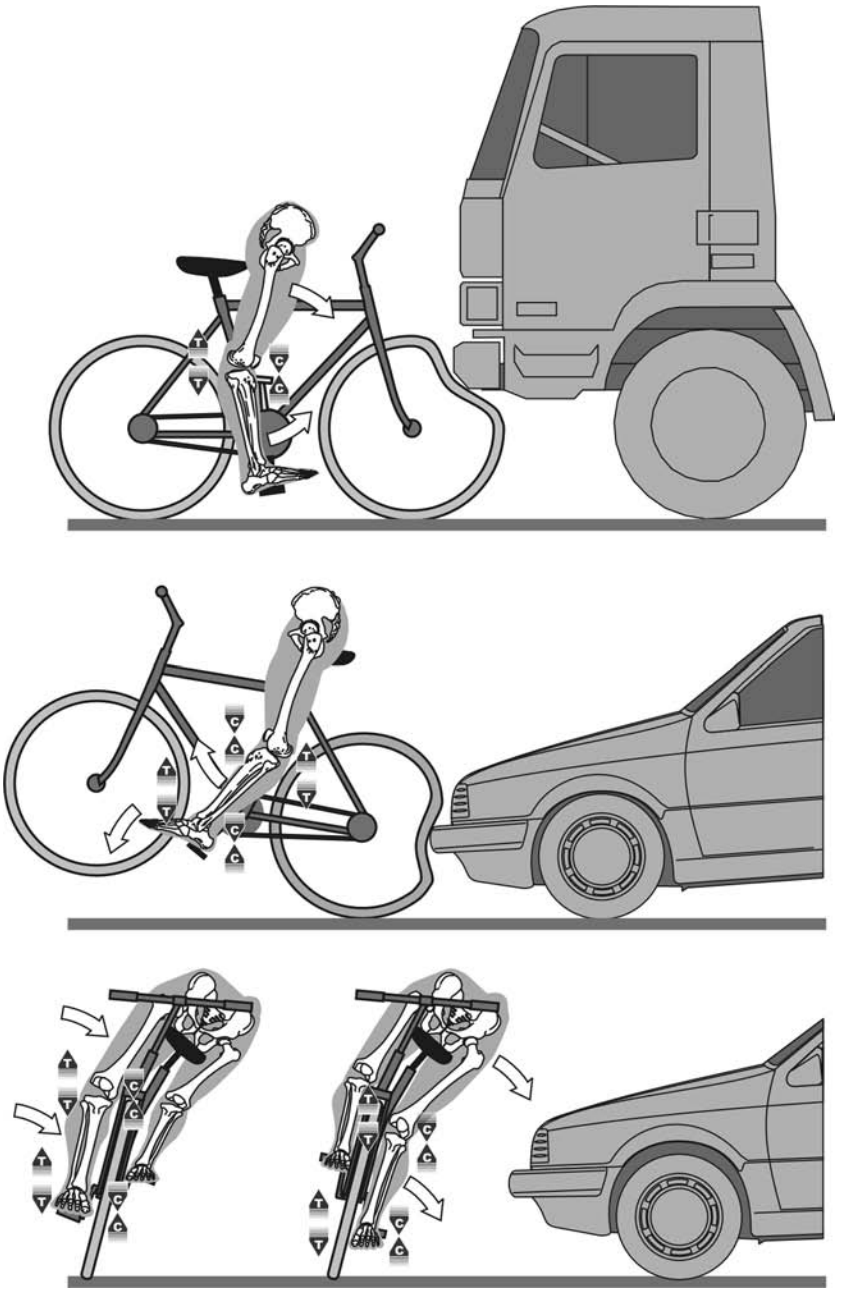

Fig. 26. The most common mechanisms of ankle and knee joint injuries in cyclists hit by passenger cars and a truck with a high bumper location.

the other hand, drivers are likely to experience splitting-compression fractures of the tibial plateau as a result of pressure on the femoral condyles when a leg is trapped between the floor and instrument panel (Fig. 30, part 3).

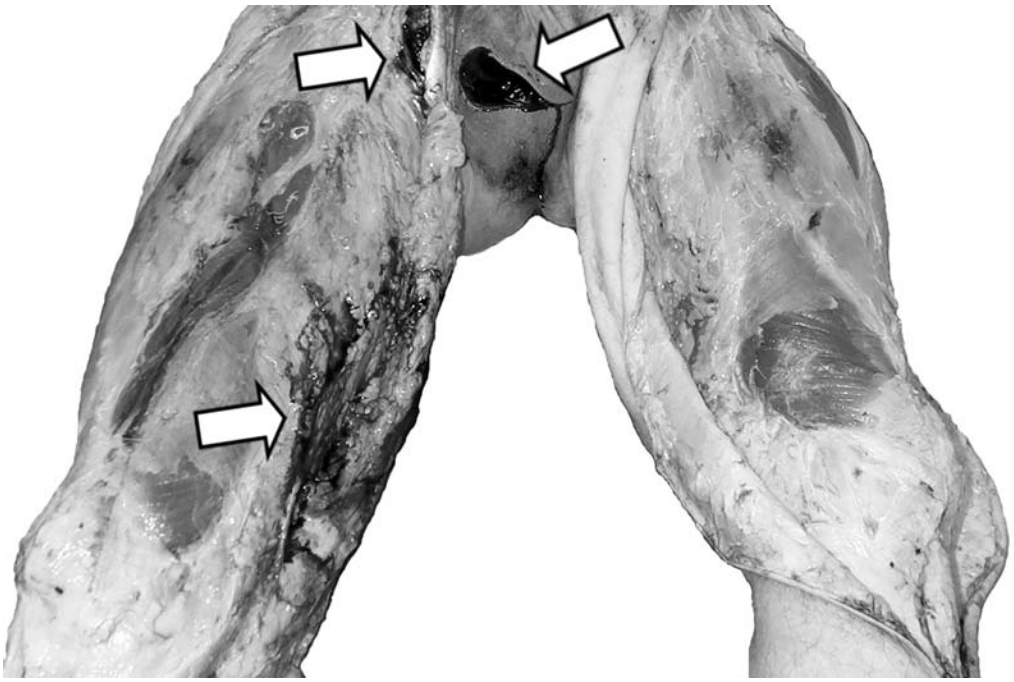

Fig. 27. Bruises in the perineum, scrotal sac (incised), and subcutaneous tissue of the medial surface of the right thigh and right groin in the cyclist caused by contact with the saddle.

Fig. 28. The direction of rotation of the saddle in car-to-bicycle collisions in the left oblique hit **(1)** and left perpendicular hit **(2)**.

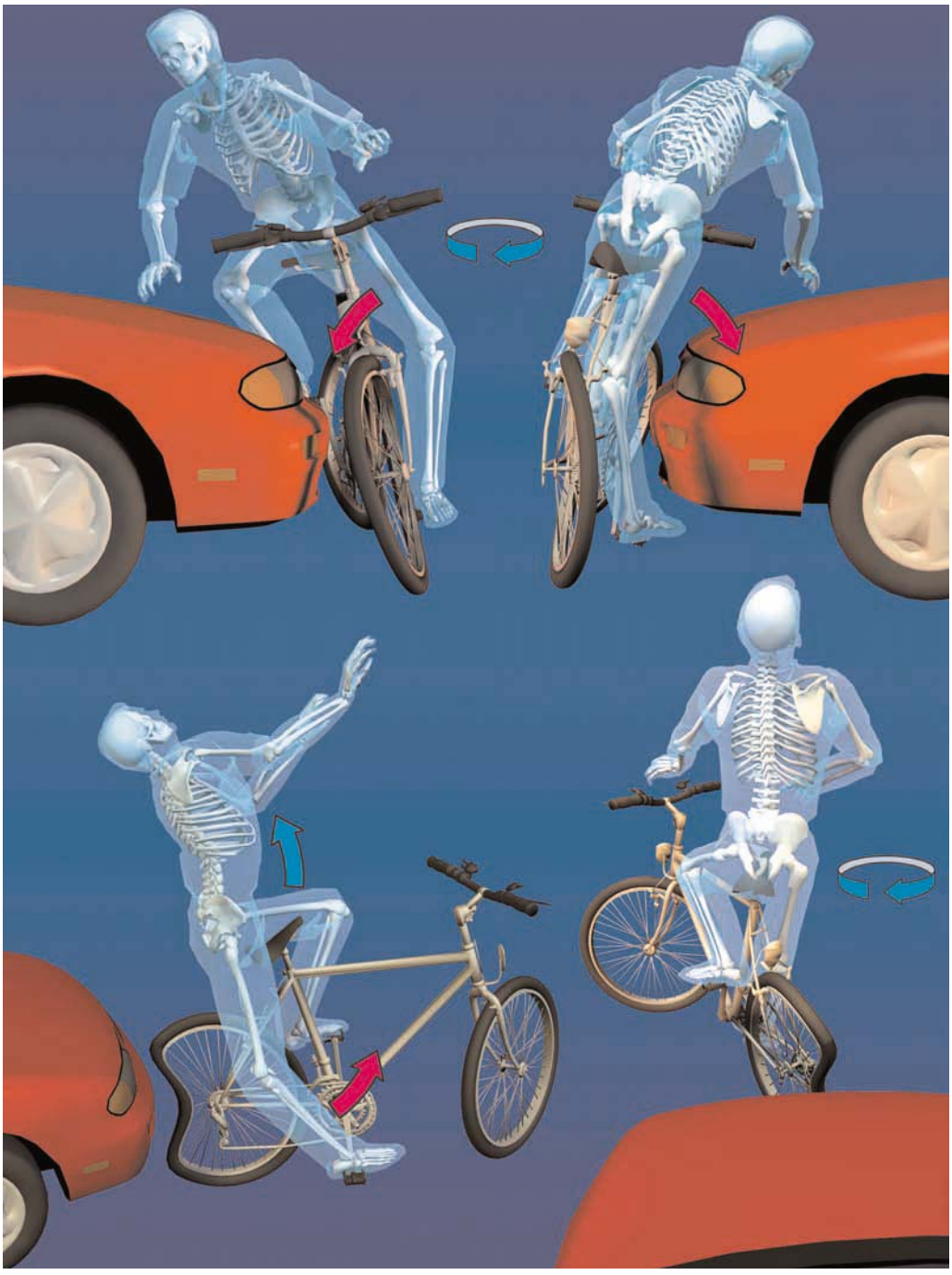

Fig. 29. The direction of knee joint dislocation and rotation of the saddle in car–bicycle collisions in relation to the direction of the impact. *See* **Color Plate IV**, following page 240.

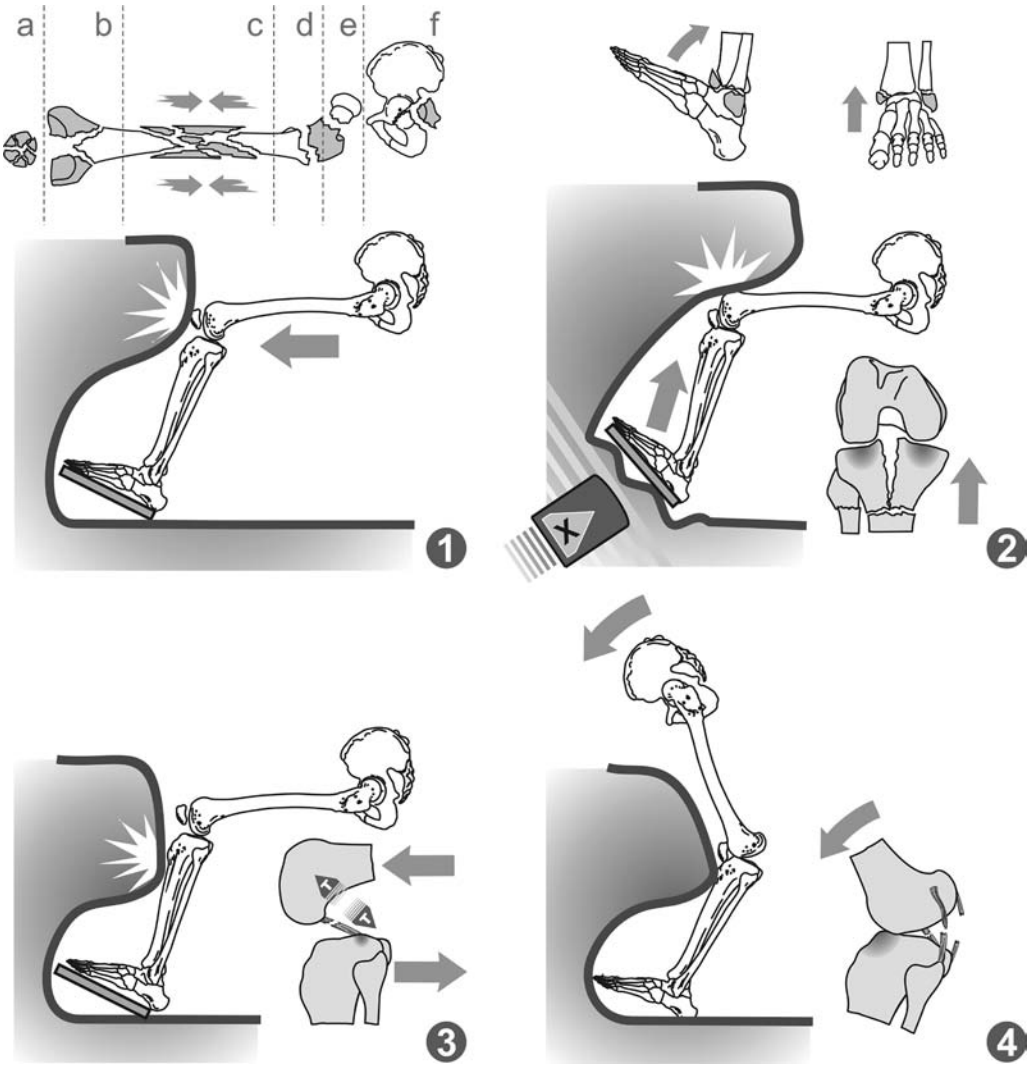

Fig. 30. Patterns of dashboard injuries in front collisions in nonbelted occupants.

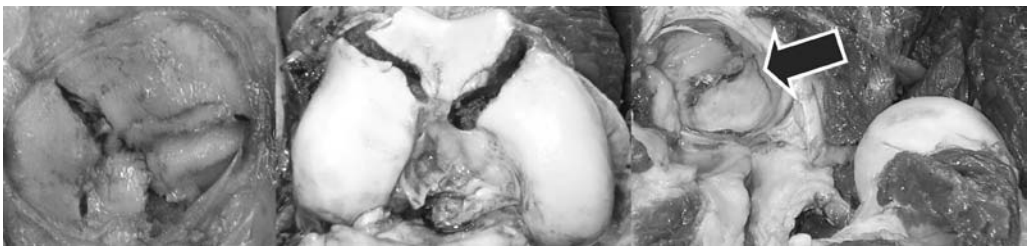

Fig. 31. The dashboard injury complex: "watch-glass-break"-type fracture of patella, femoral condyles splitting fracture, and acetabulum fracture.

2.7.4. Motorcycle Accidents

From the perspective of a forensic expert, the major difficulty in evaluating motorcycle accidents is to identify the motorcycle driver and passenger rather than to determine the impact direction (which is usually explicitly shown by the motorcycle damage).

The lateral car-to-motorcycle hits are similar to car-to-bicycle hits and may result in similar injuries to joint structures of the lower limbs (both in drivers and passengers). In frontal hits (both in high and low obstacles), the situation of motorcyclists is similar to that of car drivers and the motorcycle passenger is "protected" by the driver's body sustaining no serious lower limb injuries (moving along the driver's back, the passenger is thrown off the motorcycle and sustains some secondary injuries after hitting the road). The driver moving to the front due to inertia often hits the motorcycle elements with his knees sustaining injuries similar to the "dashboard" injuries in car occupants (also similar to the perineum injuries in cyclists). Moreover, the motorcycle driver is more bound than the bicycle rider to his vehicle and frequently sustains lower limb injuries when pressed by the motorcycle after collapsing or rubbing against the road surface *(33)*.

3. Trials Estimating the Speed of Vehicle at the Moment of Collision

So far attempts to determine the crash speed on the basis of the severity of injuries have brought no reliable (sufficiently precise and repeatable) methods of crash-speed determination *(5)*. The commonly used methods of injury scaling (AIS, ISS, CRIS) are useful only for statistical studies as they show a high level of error between the estimated extent of injury and the real collision speed in particular cases.

Studies *(8,29,34,35)* of car-to-pedestrian accidents have led only to some general conclusions (beside the obvious one, that the fracture frequency increases with the collision speed), e.g., the greater the lower limb body-mass load and the older the victim, the greater the risk of lower limb fractures. According to Spitz *(9)*, bumper fractures may occur at collision speeds above 20 km/h (14 mph) and the multi-fragment fractures as a rule are observed above 40 km/h (25 mph). At speeds higher than 90–100 km/h (60 mph) inguinal skin ruptures (Fig. 32) usually are present (they never occur below 50 km/h = 30 mph) and the limbs often get amputated (Fig. 33) as the limb is pulled under the front bumper of the car and disrupted due to the pulling by the upper body part thrown over the car-front (the disrupted distal limb may still be held by the skin or clothes and be completely severed during the "somersault" over the car—sometimes the limb is found very far from the hit site).

The injuries to knee and ankle joints are almost useless in estimating the collision speed, as they are caused by indirect bending mechanisms and occur even at low collision speeds. The ankle fractures result from the body-mass loaded shin–fixed foot translocation and often are found in accidental falls unrelated to traffic incidents. The main cause of knee joint injuries, however, is the pressure exerted by femoral and tibial joint structures, while the car is responsible only for pathological dislocation of these structures.

Thus, the determination of collision speed on the basis of the character of injuries can be only approximate, and the opinions should be left to traffic experts and their technical criteria (e.g., tire marks, throw distance, the area of glass scattering, wrap around distance).

Fig. 32. Inguinal skin rupture.

Fig. 33. Lower limb amputation in the pedestrian victim.

4. Examples of Reconstruction

4.1. Sample Case 1

An 81-yr-old pedestrian was hit by the front of a delivery van. The driver and passenger of Ford claimed that the pedestrian had run under the car from the right pavement. Although there were no other witnesses, it was determined that the pedestrian

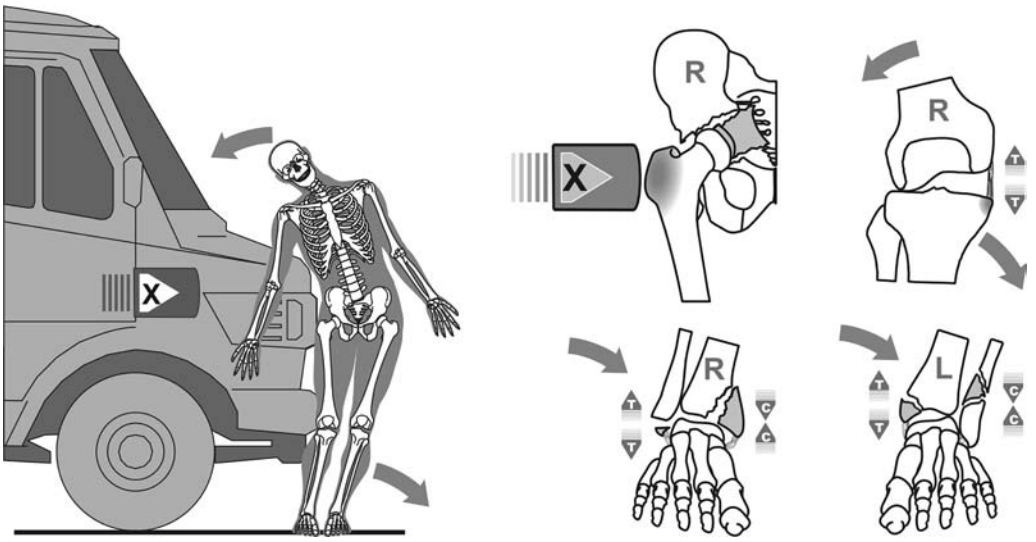

Fig. 34. The mechanism of ankle, knee, and right hip joint injuries in case 1.

had left home to go to church located on the right side of the road (looking from the driver's position, he would have crossed the road from the left to the right side). The autopsy revealed several injuries that support this (Fig. 34):

- damage to the lower attachment of the medial part of joint capsule due to valgus flexion of the right knee joint,
- a bimalleolar fracture of the right ankle due to the supination mechanism,
- a bimalleolar fracture of the left ankle due to the pronation mechanism,
- a central fracture of the right hip joint and bruises on the right greater trochanter section,
- injuries to the soft tissues and organs mainly located on the right body side and contralateral avulsion of the cervical spine ligaments.

4.2. Sample Case 2

A 20-yr-old injured man was found at the end of bloody marks indicating his having been dragged along the road for 1365 m. Without regaining consciousness, he died of brain injuries within 24 h. The next day a vehicle was found with a broken lower edge of the front plastic material under the front bumper and with some traces of victim's tissues and torn clothes on the chassis.

Beside the characteristic injuries of dragging along the rough surface (extensive epithelial excoriations and oval head wound with abraded external lamina of the right parietal bone), the autopsy revealed the injuries typical of an earlier front hit in the erect position: subcutaneous bruises in front surfaces of both shins with noncharacteristic fractures of both bones of the right shin, injuries to both knee joints characteristic of the hyperextension mechanism (disruption of the posterior part of the joint capsule with attachment bruises of both collateral ligaments; and on the right side, the patella fracture, disruption of both crucial ligaments and massive bone bruises within the region of

the anterior tibial edge), and injuries to the right ankle joint characteristic of the dorsal flexion mechanism (crushing of the anterior edge of the distal tibial epiphysis).

Those findings demonstrated that the earlier hit was caused by another vehicle because the car had no signs of any repairs. This hypothesis was confirmed by fiber examinations of the victim's clothes that revealed microtraces of glass particles and paint belonging to another car.

References

1. Peden M, Scurfield R, Sleet D, Mohan D, Hyder AA, Jarawan E, Mathers C, eds. World report on road traffic injury prevention. World Health Organisation, Geneva 2004. Available at: http://www.who.int/world-health-day/2004/informaterials/world_report/en/(accessed October 2004).
2. Statistics of road traffic accidents in Europe and North America 2004. Geneva: United Nations Economic Commission for Europe; 2002. Available at: http://www.unece.org/trans/main/wp6/transstatpub.html/(accessed October 2004).
3. Dürwald W. Gerichtsmedizinische Untersuchungen bei Verkehrsunfällen. Thieme: VEB Georg Leipzig; 1966.
4. Eubanks JJ, Hill PF. Pedestrian accident reconstruction and litigation, Lawyers & Judges Publishing Co.; 1999.
5. Mason JK, Purdue BN, eds. The pathology of trauma. 3rd ed. London: Arnold Publishing; 2000.
6. Siegel JA, Saukko PJ, Knupfer GC, eds. Encyclopedia of forensic sciences. Academic Press, 2000.
7. Teresiński G, Mądro R. Evidential value of injuries useful for reconstruction of the pedestrian–vehicle location at the moment of collision. Forensic Sci Int 128:127–135 (2002).
8. Karger B, Teige K, Bühren W, DuChesne A. Relationship between impact velocity and injuries in fatal pedestrian–car collisions, Int J Legal Med 113:84–88 (2000).
9. Spitz WU, Fisher RS, eds. Medicolegal investigation of death. 3rd ed. Springfield: Charles C. Thomas; 1993.

9a. Metter D. Spurenbefunde bei Fußgänger–Fahrzeugkollisionen und ihre Bedeutung für die Unfallrekonstruktion, Z Rechtsmedizin 91:21–32 (1983).

10. Metter D. Das Decollement als Anfahrverletzung, Z. Rechtsmedizin 85:211–219 (1980).
11. New Car Assessment Programme (NCAP) crash tests. Available at: http://www.euroncap.com.
12. Messerer OM. Über Elastizität and Festigkeit der menschlichen Knochens. Stuttgart: JG Cotta Verlag; 1880.
13. Karger B, Teige K, Fuchs M, Brinkmann B. Was the pedestrian hit in an erect position before being run over? Forensic Sci Int 119:217–220 (2001).
14. Sellier K. Zur mechanik des knochenbruchs. Dtsch Z Gerichtl Med 56:341–348 (1965).
15. Mittmeyer HJ, König HG, Springer E, Staak M. Die Unterschenkelfraktur verunglückter Fußgänger: Möglichkeiten und Grenzen der Unfallrekonstruktion. Z Rechtsmedizin 74:163–170 (1974).
16. Rabl W, Haid C, Krismer M. Biomechanical properties of the human tibia: fracture behavior and morphology. Forensic Sci Int 83:39–49 (1996).
17. Teresiński G, Mądro R. The patterns of diaphyseal fractures of the lower limbs in vulnerable participants in real world traffic accidents. Proceedings of the IRCOBI Conference, Graz 2004.
18. Kress TA, Snider JN, Psihogios JP, et al. Fracture patterns of human cadaver long bones. In: Biomechanics of impact injury and injury tolerances of the extremities. Backaitis SH, ed. Warrendale: Society of Automotive Engineers, Inc. 1996:453–467.
19. Klose H, Janik B. Frakturen und luxationen. Berlin: Walter de Gruyter; 1953.
20. Sjövall H. Die formen der frakturen der langen röhrenknochen. Zbl Chir 30:1234–1241 (1957).
21. Insall JN, ed. Surgery of the knee. 2nd ed. New York: Churchill–Livingstone; 1993.

22. Hayes CW, Brigido MK, Jamadar DA, Propeck T. Mechanism-based pattern approach to classification of complex injuries of the knee depicted at MR imaging. Radiographics 20:121–134 (2000).
23. Sanders TG, Medynski MA, Feller JF, Lawhorn KW. Bone contusion patterns of the knee at MR imaging: footprint of the mechanism of injury. Radiographics 20:135–151 (2000).
24. Teresiński G, Mądro R. Knee joint injuries as a reconstruction parameter in car-to-pedestrian accidents. Forensic Sci Int 124:74–82 (2001).
25. Mink JH, Reicher MA, Crues JV III, Deutsch AL, eds. Magnetic resonance imaging of the knee. 2nd ed. New York: Raven Press; 1993.
26. Teresiński G, Mądro R. A comparison of mechanisms of ankle, knee, pelvis and neck injuries in pedestrians and in cyclists according to the direction of impact and type of vehicle. Proceedings of the IRCOBI Conference; Lisbon, Portugal; 2003.
27. Teresiński G, Mądro R. Ankle joint injuries as a reconstruction parameter in car-to-pedestrian accidents. Forensic Sci Int 1118:65–73 (2001).
28. Teresiński G, Mądro R. Spuren an Schuhsohlenoberflächen von Fußgängerunfallopfern und Verletzungen der Sprunggelenke. Verkehrsunfall und Fahrzeugtechnik 39:190–197 (2001).
29. Bunketorp O, Aldman B, Thorngren L, Romanus B. Clinical and experimental studies on leg injuries in car–pedestrian accidents. In: Biomechanics of impact injury and injury tolerances of the extremities. Backaitis SH, ed. Warrendale: Society of Automotive Engineers, Inc.; 1996:699–710.
30. Wegner C, Otte D, Rau H. Deformationscharakteristik und Einflußparameter von Fahrrädern bei Kollisionen mit der Pkw-Front. Verkehrsunfall und Fahrzeugtechnik Heft 2, 32–38, Heft 3, 63–70 (2000).
31. Morgan RM, Eppinger RH, Hennessey BC. Ankle joint injury mechanism for adults in frontal automotive impact. In: Biomechanics of impact injury and injury tolerances of the extremities. Backaitis SH, ed. Warrendale: Society of Automotive Engineers, Inc.; 1996:525–534.
32. Nagel DA, Burton DS, Manning J. The dashboard knee injury. Clin Orthop 126:203–208 (1977).
33. Wagner K, Wagner HJ. Handbuch der Verkehrsmedizin. Berlin: Springer Verlag; 1968.
34. Rau H, Otte D, Schulz B. Pkw-Fußgängerkollisionen im hohen Geschwindigkeitsbereich. Ergebnisse von Dummyversuchen mit Kollisionsgeschwindigkeiten zwischen 70 und 90 km/h.Verkehrsunfall und Fahrzeugtechnik Heft 2:341–351 (2000).
35. Zivot U, Di Maio VJM. Motor vehicle–pedestrian accidents in adults: relationship between impact speed, injuries and distance thrown. Am J Forensic Med Pathol 14:185–186 (1993).

Chapter 11

Biomechanical Analysis of Slip, Trip, and Fall Accidents

Scott D. Batterman, PhD and Steven C. Batterman, PhD

1. Introduction

Traumatic injuries and deaths resulting from slip, trip, and fall accidents are a significant public health problem in the United States. The economic loss due to lost employment time is an important factor in many industrial settings and the likelihood of injuries resulting from slip, trip, and fall accidents is an increasing concern in general, particularly as the population ages. It is reported that in the year 2000, there were approx 8.1 million visits to emergency rooms as a result of accidental falls, which constitutes approx 20% of the total number of reported emergency room visits in that year *(1)*. Amongst the elderly living in the general population, it is reported that approx 30% of those over the age of 65 fall each year, and for those over 80 yr old, the rate is approx 40% *(2)*. Others estimate that on average more than 16,000 people die each year as a result of fall related injuries *(3)*. Injuries resulting from slip, trip, and fall accidents are not limited to a single region of the body and include injuries to the foot, ankle, knee, hip, and head. As a result of this epidemic in slip, trip, and fall-related injuries, numerous measures have been undertaken in an attempt to reduce the number of slip-and-fall accidents including, but not limited to, the use of slip-resistant materials on walkway surfaces and prescribed shoe outsole materials and patterns.

In addition, numerous researchers are studying the biomechanics of human walking and locomotion in order to identify the parameters that influence gait and the occurrence of the onset of slip. Various factors known to influence the likelihood of a slip have been quantified and ranked by numerous investigators. For the purposes of this chapter, a *slip* is defined as one that is large enough to be perceptible to the walker with an associated potential for a loss of balance.

From: *Forensic Science and Medicine*
Forensic Medicine of the Lower Extremity: Human Identification and Trauma Analysis of the Thigh, Leg, and Foot
Edited by: J. Rich, D. E. Dean, and R. H. Powers © The Humana Press Inc., Totowa, NJ

Much of the current work being done in the field of walkway safety is in the area of tribometry, i.e., the characterization and measurement of slip resistance of surfaces in contact using an instrument known as a tribometer. *Tribology* refers to the study of friction, lubrication, and wear of interacting surfaces that are in relative motion with respect to each other. Classical notions of slip resistance and the analysis of slip-and-fall accidents have typically revolved around Coulomb friction concepts, although these concepts do have acknowledged shortcomings when applied to deformable or compliant materials in contact. For hard, rigid, dry, material contact surfaces, Coulomb demonstrated that the magnitude of the friction force (F) acting on the contact surfaces in opposition to relative motion between the surfaces is proportional to the magnitude of the normal force (N). However, the constant of proportionality, μ, differs with the state of motion. For an impending slip at, or immediately prior to, relative motion between the surfaces, the magnitude of the friction force

$$F = \mu_s N$$

and for contact surfaces in relative motion, the magnitude of the friction force

$$F = \mu_k N$$

where μ_s is the coefficient of static friction and μ_k is the coefficient of kinetic (dynamic) friction. We note that μ_s is typically higher than μ_k and that μ_s and μ_k are functions of both materials in contact. In Coulomb friction theory, the friction force is independent of both the contact area and the relative speed of the materials in contact once relative motion of the surfaces has commenced. For compliant (deformable) materials in contact, such as shoe outsole and flooring materials, these are simplifying assumptions, which may not lead to an appropriate model in many circumstances. It is well known that the onset of a slip is a function of many factors, and the probability of a slip occurring cannot typically be based on a single quantity or parameter, such as the coefficient of friction, μ, or any other measure of the slip resistance alone. Anthropometric and gait specific parameters must also be considered when developing models and criteria to predict the onset of slip.

2. Remarks on Tribometry

The American Society for Testing and Materials (ASTM), through the F-13 committee on Safety and Traction for Footwear, has developed and continues to propose and develop numerous consensus standards intended to promote uniformity in the characterization and measurement of slip resistance. As a general rule, practitioners in the field of walkway safety consider a safe walkway surface to be one with a measured static coefficient of friction, μ_s, of 0.5, or higher. However, historically, the 0.5 value was defined in the ASTM standards specifically for testing performed with the James Machine. *See* Sacher *(4)* for a historical review of the development of the generally accepted 0.5 value for μ_s used to define a safe walkway. Utilizing a simple trigonometric model, Ekkebus and Killey *(5)* determined that for straight ahead forward walking on a level surface at moderate speeds, the required coefficient of friction necessary to prevent slip is typically on the order

of 0.30 to 0.45, which is consistent with some force plate measurements *(6)*. For some, this provided justification for the choice of $\mu_s = 0.5$ as a threshold value defining a safe walkway surface. More recent work by Powers et al. *(7)* suggests that the Ekkebus and Killey model may overestimate the amount of friction necessary to prevent slip. It is also noted, however, that for handicapped accessible walkways, compliance with the Americans With Disabilities Act (ADA) requires a minimum static coefficient of friction, μ_s, of 0.6 on level surfaces and 0.8 on ramps *(6)*.

Numerous tribometers are currently in use by practitioners to assess slip resistance, including, but not necessarily limited to, the James Machine, the Portable Articulated Strut Tribometer (PAST), the Portable Inclined Articulated Strut Tribometer (PIAST), the Variable Incidence Tribometer (VIT), the Sigler Pendulum Tester, the Horizontal Pull Slipmeter (HPS), and other drag-sled type devices. All of the aforementioned instruments are portable and can be brought to the subject walkway for use in field testing, with the exception of the James Machine, which is a nonportable laboratory machine that samples must be brought to for testing.

It is well known that the different types of tribometers yield different results on the same walkway surfaces, although the proponents of each all claim to be measuring the slip resistance of each surface. Some of the differences in results appear to arise, at least in part, from the fact that the different tribometers apparently measure different types of friction, i.e., some appear to measure static slip resistance while others appear to measure dynamic slip resistance. Differences also arise relating to the manner in which each device applies the load to the walkway surface during the testing, i.e., the time interval between the application of the normal and tangential surface loads. For example, for the HPS and other drag sled type devices, the device is placed on the test surface and the vertical load is, therefore, applied to the surface prior to the application of the tangential load. For the various pendulum, VIT, and articulated strut testers, the application of the vertical and tangential loads is essentially simultaneous and thus minimizes the effects of adhesion and/or "sticktion" during the testing process. It is well known that the residence time of the test device in contact with a walkway surface prior to the application of the tangential load can greatly affect the test results. This phenomenon can lead to erroneously high slip resistance results, particularly on wet surfaces. For wet testing, this phenomenon is often referred to as "sticktion." The term *adhesion* is typically used to describe the phenomenon on dry surfaces.

The lack of uniformity in testing devices, results, and procedures raises serious questions not only about current testing methodologies, but also about whether the Coulomb friction model alone is appropriate for modeling shoe (foot)—walkway interactions. It is noted that the Coulomb friction model was initially proposed to describe the behavior of hard rigid material bodies in contact and not the relatively soft compliant materials utilized in walkway and/or shoe outsole materials. A rigorous engineering model and analysis by Batterman et al. *(8)* based in part on using Coulomb friction as the slip resistance measure, although any other measure can be used, also incorporates other anthropometric and gait related factors. This model rigorously demonstrates that the onset of a slip is not only dependent on the chosen measure of slip resistance, μ, but is also strongly dependent on walking speed and stride length, as well as a newly defined Anthropometric Gait Index (AGI) introduced by Batterman et al. and discussed in detail

below. The newly defined AGI can vary significantly between individuals or similar anthropometric groupings of individuals.

It is noted for completeness that proponents of PIAST, VIT, and pendulum-type tribometers also claim that their devices produce reliable measures of slip resistance for fluid contaminated (wet) surfaces, with the rationale being that since the normal and tangential surface loads are essentially simultaneously applied to the wet walkway surface, the results account for the hydrodynamic effect of the fluid contaminant layer, as discussed above. However, due to the relatively more complicated dynamics involved in analyzing slip on a wet walkway surface, and taking proper tribology concepts into account, it has not been conclusively demonstrated that any of the aforementioned tribometers are truly suitable for wet testing. As shown by Batterman et al. *(8)*, slip on a wet surface is explicitly dependent on foot speed at contact, stride length, the area of shoe (foot) contact, the absolute viscosity of the fluid (η), the depth of the fluid contaminant layer, the appropriate AGI, and the amount of shoe/foot–walkway interaction. Furthermore, Medoff et al. *(9)* performed tests on wet and dry quarry and glazed tile surfaces using both VIT and PIAST tribometers. Tests were performed with each tribometer using both smooth and patterned test feet. Their results demonstrate that for wet testing, large variations in measured slip resistance are observed between smooth and textured test feet, even for the same tribometer. These results indicate that the interaction between the shoe and walkway surfaces is dependent upon the ability of the contacting surface of the shoe to penetrate and displace the fluid on shoe contact. Therefore, the occurrence of slip on a wet surface is also dependent upon the textured pattern on the heel and/or shoe outsole.

When analyzing a slip and fall accident, it is not enough to simply attempt to characterize the slip resistance of the shoe–walkway interface. Individual gait characteristics also influence the onset, or occurrence, of a slip. For instance, some people may be able to negotiate a walkway surface without incident, while others attempting to negotiate the same walkway in the same, or substantially similar, footwear may slip and fall. Even if a consensus was to be reached as to which tribometer and/or testing method most accurately characterizes the slip resistance of a given walkway, that number alone would have only limited utility in determining those individuals prone to slip and fall. This will be addressed in further detail below. Noting that each individual will have unique gait characteristics that will influence the propensity to slip, trip, and/or fall in any given situation, a brief but basic discussion of human gait follows.

3. *Human Gait*

Human walking is bipedal and is characterized by successive alternating periods of a single leg stance during which time the other leg is swinging forward, followed by a brief period when both feet are in contact with the ground. This is distinct from running, which does not involve any periods of time when both feet are in simultaneous contact with the ground. In fact, during running there are periods of time when neither foot is making ground contact. While both walking and running are highly dynamic processes, all of the discussions herein are limited to walking. McMahon *(10)* provides a description of the six determinants of normal gait originally presented by Saunders, Inman, and Eberhart *(11)*

in 1953. In this model, normal gait is broken into the following six determinants. Note that each determinant allows for the introduction of an additional degree of freedom.

- Compass gait: During compass gait, the stance leg remains stiff at all times and the trunk moves along an arc in the direction of motion. The radius of the arc is determined by the stiffened leg length.
- Pelvic rotation: This is the next level of complexity and allows for a rotational motion of the pelvis about a vertical axis during stepping. This allows the hip on the swing side to trace out a greater arc, allowing a longer step length.
- Pelvic tilt: By allowing the hip on the swing side to fall below the hip on the stance side, the arc traced out by the pelvis in the direction of motion (first described during compass gait) is flattened out, resulting in a more direct motion of the pelvis in the walking direction. The introduction of this determinant requires that flexion be allowed in the swing leg.
- Stance leg knee flexion: This determinant is added to further flatten out the arcs that are traced out by the center of the pelvis.
- Plantar flexion of the stance ankle: This ankle degree of freedom is added to allow the foot to rotate down during the transition from the double support phase (i.e., when both feet are in contact with the ground) to push-off (referred to as toe-off by some authors).
- Lateral displacement of the pelvis: Since load is alternately transferred from one leg to the other during walking, the body tends to rock from side to side during walking.

Further detail and additional references are provided in McMahon *(10)*.

At the conclusion of the swing phase, during a normal gait cycle the heel contacts the walkway surface, commonly referred to as *heel strike*. Immediately following heel strike, the foot (shoe) is decelerated to a zero forward velocity as it continues to roll down into complete ground contact (stance) and the push-off phase of the gait cycle. However, if sufficient friction force at the interface cannot be developed to decelerate the heel to a zero forward velocity, a heel slip occurs. Slips can also occur after the shoe (foot) rolls down into complete walkway surface contact and enters the push-off (toe-off) phase.

To better understand the force–time history of the ground reaction forces during the various phases of gait, Fig. 1 shows force plate measurements from walking experiments conducted in 1993 by members of the ASTM F-13 Committee on Safety and Traction for Footwear at the Center for Locomotion Studies, Pennsylvania State University. While the actual measured force traces will vary among individuals, these plots are shown simply to illustrate commonly observed trends. As shown in Fig. 1A, following heel strike the normal force rises rapidly to levels well in excess of body weight prior to reaching a maximum and starting to fall off, subsequently reaching a minimum during the double-support phase when both feet are in contact with the ground. At push-off, the normal force again begins to rise, reaching a second peak prior to a decrease in load and the commencement of the swing phase. Figure 1B shows the simultaneous force–time histories of the in-plane walking (anterior/posterior) direction and the lateral/medial force components. Note that the in-plane force components reverse direction during the loading history. This is not surprising and is, in fact, necessary for a normal gait cycle, particularly in the walking (anterior/posterior) direction. At heel strike, the foot is moving forward and must be decelerated to a zero forward

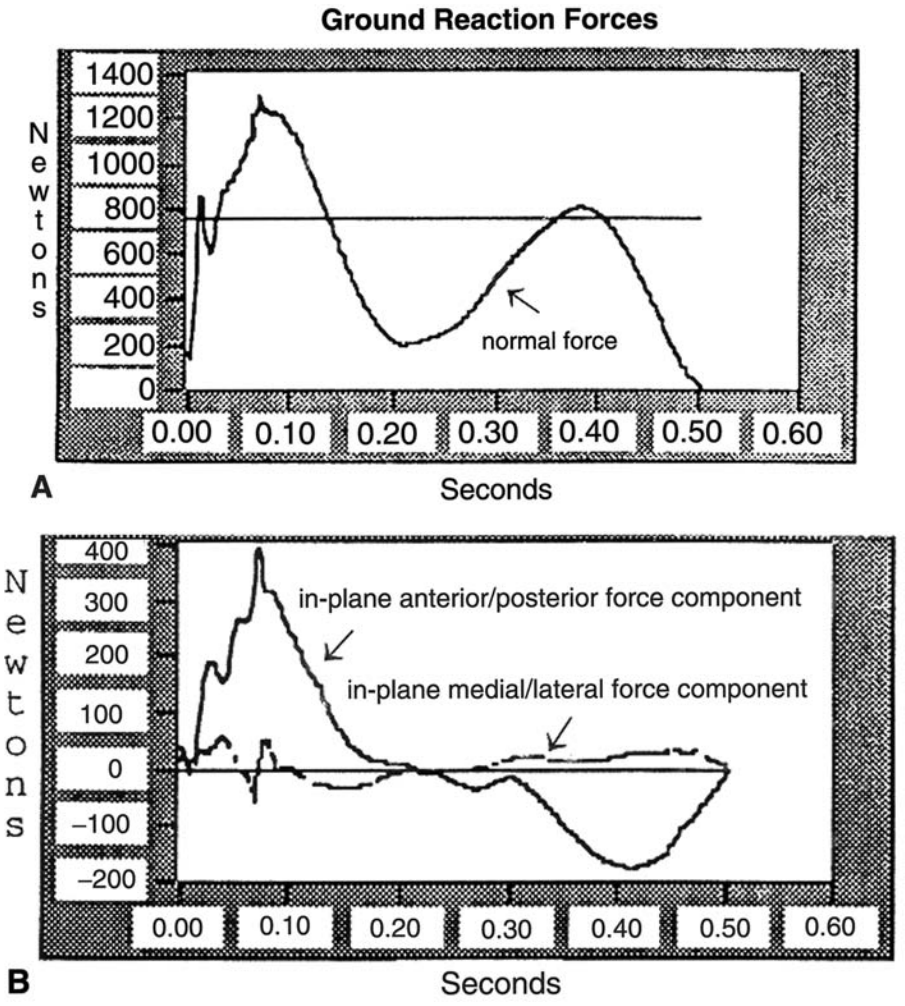

Fig. 1. Measured force–time histories for a 750-N (168.5 lb) individual stepping onto a force plate. Note that in **(A)** the peak normal force is well in excess of the body weight. In **(B)**, the in-plane forces are shown. Note the change in direction of the applied in-plane forces as the foot is decelerated and then pushes off.

velocity in order to prevent slip. Therefore, the in-plane forces must act in a direction to oppose the motion of the foot. On successful deceleration of the foot, the resultant in-plane force must be applied to the bottom of the foot in the direction of motion to continue the normal gait cycle. It is further noted for completeness that by Newton's third law of motion the forces acting on the shoe are equal and opposite to those acting on the floor, or force plate. Slip at heel strike occurs when the friction forces acting on the heel are insufficient to decelerate the foot to a zero forward velocity. Slip at push-off occurs when insufficient friction can be developed to prevent the shoe from slipping during push-off. Therefore, when modeling slip at heel strike, the relevant friction force is defined in terms of the coefficient of kinetic (dynamic) friction (μ_k). When modeling

slip at push-off, the foot or shoe in contact with the ground accelerates from a zero forward velocity. Therefore, for slip at push-off, the threshold friction force, defined by the coefficient of static friction (μ_s), must be overcome for slip to occur.

4. Mechanics of Macroslip

Batterman et al. *(8)* recently proposed a velocity dependent (or viscous) shear model for the prediction of the onset of macroslip, in which slip is predicted to occur when combinations of relevant factors known to affect the onset of slip combine to reach a threshold value. Macroslip is defined herein to be a slip that is large enough to be perceived by the walker, with a high probability of leading to a loss of balance. For the purposes of this chapter, the terms slip and macroslip are used interchangeably. Since slip occurs when sufficient friction forces cannot be developed at the shoe–floor interface to provide the ground reaction forces necessary to maintain normal gait, the threshold value is chosen to have units of force. Assuming that slip is a function of the mass of an individual, the horizontal walking speed at the center of mass, and the stride length, it follows from dimensional analysis that for the onset of slip on a hard, flat, dry, level surface the proposed criterion takes the following form:

$$F_\tau = \frac{C_{di} M V^2}{L}, \tag{1}$$

where F_τ is the threshold friction force defining the onset of macroslip; C_{di} is an experimentally determined dimensionless anthropometric constant, or Anthropometric Gait Index (AGI); $i = k$ for slip at heel strike; $i = s$ for slip at push-off; M is the mass of the individual; V is the forward (horizontal) walking speed at the center of mass of the individual; and L is the stride length. For the discussion herein, the stride length, L, is understood to be the step length.

As long as the maximum friction force generated at the shoe-floor interface, defined by the right side of equation 1, is below the threshold value (F_τ), a macroslip is not likely to occur. Slip is predicted to occur when the right side of equation 1 is greater than, or equal to, the threshold friction force, F_τ. For simplicity, and the purposes of this presentation, as well as to avoid any unnecessary controversy concerning a slip resistance measure, F_τ shall be defined utilizing Coulomb friction concepts, i.e.:

$$F_\tau = \mu_i N.$$

However, we again emphasize that any consistent slip resistance measure can be used in the model without any loss of generality. Furthermore, as demonstrated in Fig. 1, walking is a dynamic process with time-varying force components. In order to further simplify the analysis, as well as for the purpose of defining a threshold value for the onset of slip, the normal force N, is taken to be a constant equal to the weight, W, of the individual. It can then be demonstrated by a straight substitution of F_τ into equation 1 that the condition for the onset of slip on a dry, level surface can be written as follows:

$$\frac{C_{di} V^2}{gL} \geq \mu_i, \tag{2}$$

where g is the acceleration due to gravity. At the risk of being redundant, we note and emphasize that the utility of this model is independent of the testing method as long as the relevant coefficient of friction, or slip resistance measure, and anthropometric parameters are consistently defined throughout. For slip at heel strike (or push-off), for example, the AGI (C_{di}) can be experimentally determined by having test subjects in the same footwear negotiate a walkway surface of a predetermined μ_i and measuring the walking speed and stride length at increasingly faster walking speeds until a macroslip occurs at heel strike (or push-off). Equation 2 can then be rearranged and used to calculate the appropriate AGI for the combination of walking speed, V, and stride length, L, at which macroslip first occurs, i.e.:

$$C_{di} = \frac{\mu_i g L}{V^2}.$$

We parenthetically note that even for the same individual, the AGI on a given surface will likely be a function of the footwear.

Although mathematically more complex, the same methodology can be extended to model slip on a wet walkway surface. The fluid contaminant layer at the shoe-fluid-floor interface is modeled as a thin, continuous hydrodynamic film. In accord with hydrodynamic film theory, the pressure in the film does not vary with depth, and is a function of the horizontal position only. The composite behavior of the interface is modeled as a Bingham Plastic like fluid, and described by the following relationship.

$$\tau = \tau_y + \eta \dot{\gamma}, \tag{3}$$

where τ is the shear stress and τ_y is the critical shearing stress necessary to commence shearing deformation in the fluid contaminant layer. Although, there are numerous choices, the following form for τ_y is simple and captures the essential elements of the theory. The assumed form is as follows:

$$\tau_y = S_{fi} \mu_i \frac{W}{A_c} \cdot \tag{4}$$

τ_y arises as a result of the compliances and microtextures of both the walkway surface and the shoe outsole materials, as well as the depth of the fluid contaminant between the walkway and shoe outsole, and the speed of the foot at first contact. The shoe outsole, or heel, pattern will also likely influence the value of τ_y, as discussed above, and demonstrated by Medoff, et al. *(9)*. These effects are incorporated into the model through the S_{fi} factor, which represents the amount of surface-shoe interaction as a fraction of the coefficient of friction, (μ_i). W is the weight of the individual, and A_c is the contact area of the shoe (foot) with the wet walkway surface at the commencement of slip. It is noted that τ_y can be defined in terms of either μ_s or μ_k as long as S_{fi} is consistently defined. Note that for the case of pure hydroplaning τ_y is equal to zero. η is the absolute viscosity of the fluid (slope of the stress-strain rate curve) once shearing commences, and $\dot{\gamma}$ is the shear strain rate ($\partial v/\partial y$) through the fluid layer. For the prediction of slip on a wet walkway surface, equation 1 is modified as follows to yield the wet slip criterion:

$$\left(\tau_y + \eta\dot{\gamma}\right)A_c = \frac{C_{wi}MV_i^2}{L}, \tag{5}$$

where C_{wi} is the corresponding AGI to the one defined in the dry model. Here, as before, $i = k$ for slip at heel strike; $i = s$ for slip at push-off. V_i is the forward (horizontal) speed of the foot at first contact with the fluid/floor interface for $i = k$, and the forward (horizontal) speed of the center of mass of the individual for $i = s$, and all other quantities are as previously defined. For slip at push-off, the shoe (foot) commences slip from a zero forward velocity, with the shoe and trapped fluid contaminant layer considered to initially slip together relative to the walkway surface. Therefore, there is no velocity gradient through the fluid thickness and $\dot{\gamma} = 0$, initially. The threshold friction force, F_τ, therefore, becomes equal to $\tau_y A_c$. In this case, equation 5 reduces identically to the dry slip criterion (equation 1) and it follows that $C_{ws} = C_{ds}$. For the onset of slip at heel strike on a wet walkway surface it can be demonstrated that:

$$\frac{C_{wk}Mh^*\dot{x}^2}{A_cL} - \eta\dot{x} - \tau_y h^* = 0, \tag{6}$$

which is a quadratic equation in terms of the forward foot speed ($\dot{x}$) at heel strike. h^* is the depth of the fluid contaminant layer between the heel and the walkway surface at the point of maximum pressure in the fluid layer. All other terms are as previously defined. If the simplifying assumption is made that the forward foot speed ($\dot{x}$) is equal to the forward (horizontal) speed of the center of mass of the individual at the moment of heel strike, equation 6 may be rewritten in terms of the walking speed at the center of mass, V, as:

$$\frac{C_{wk}Mh^*V^2}{A_cL} - \eta V - \tau_y h^* = 0. \tag{7}$$

For the case where the aforementioned simplifying assumption cannot be made, it can be demonstrated that:

$$\frac{\dot{x}^2}{V^2} = \frac{C_{dk}}{C_{wk}}. \tag{8}$$

For illustrative purposes, consider an individual weighing 165 lb walking on a dry, μ_k = 0.50, surface who was found to commence a macroslip at heel strike at a walking speed, V = 4.4 ft/s, and a stride length, L = 2.5 ft. Using equation 2, the AGI for this individual is C_{dk} = 2.08. Curves can then be generated for the prediction of macroslip as a function of walking speed, V, and stride length, L, for various coefficients of friction, or other slip resistance measures and values of the AGI (Figs. 2 and 3). As shown in the figures, the proposed model not only defines the likelihood of a slip on a given walkway, but also quantifies the likelihood of a slip when stepping between surfaces with varying coefficients of friction, or slip resistances. Curves can also be generated which demonstrate and quantify the difference in slip potential for different individuals on the same walkway surface, or for the same individual on a walkway surface in differing footwear, i.e., differing values of the AGI on the same walkway (Fig. 4). Figures 5 and 6 compare

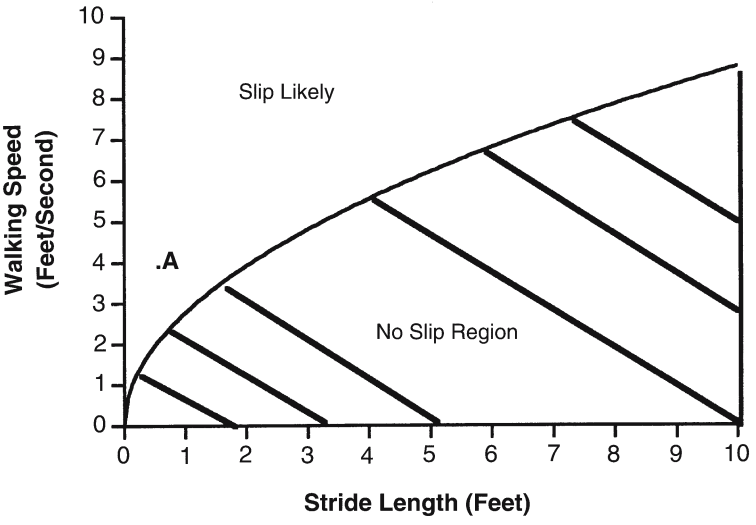

Fig. 2. Slip as a function of walking speed and stride length. Slip criterion for an exemplar individual. $\mu_k = 0.50$ and $C_{dk} = 2.08$. Note that point A denotes a point at which slip is likely to occur for this individual. Reprinted from ref. *8* with permission from Taylor & Francis and CRC Press.

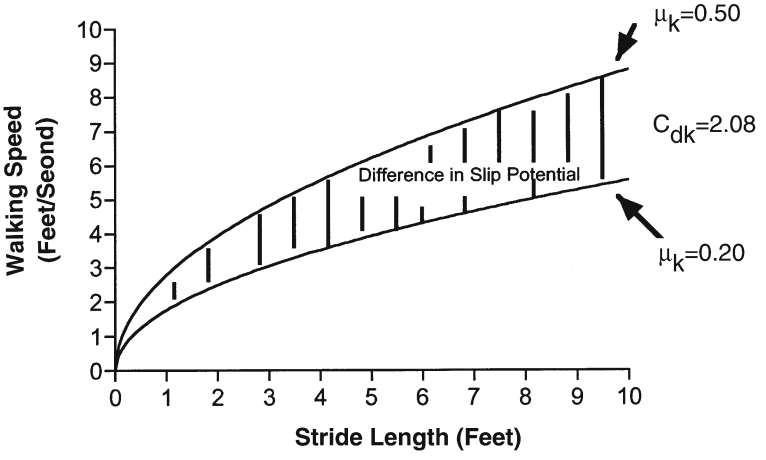

Fig. 3. Difference in slip potential for the same individual on two different walkway surfaces. Reprinted from ref. *8* with permission from Taylor & Francis and CRC Press.

the prediction of slip for the same individual on the same walkway surface under both wet and dry conditions for two different values of S_{fi}. The wet walkway conditions used in the figures are as follows:

absolute viscosity (η) = 2.09×10^{-5} lb-s/ft^2
fluid contaminant depth (h^*) = 0.01 in (8.33×10^{-4} ft)
wet contact area (A_c) = 1 in^2 (6.94×10^{-3} ft^2).

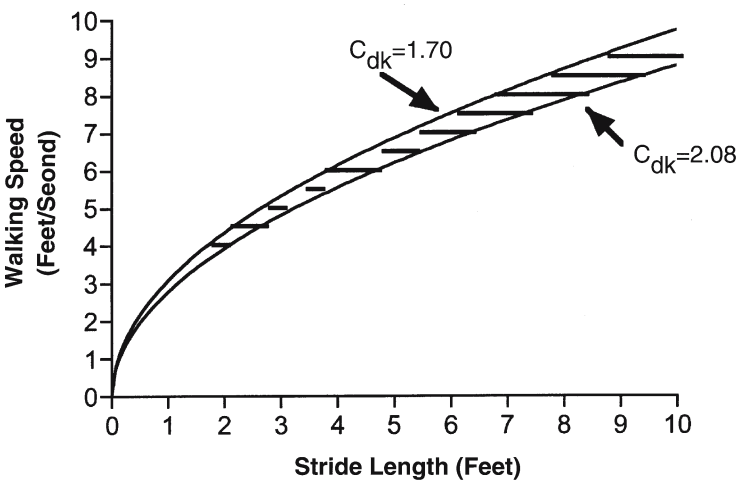

Fig. 4. Difference in slip potential for two values of the AGI on the same ($\mu_k = 0.50$) walkway surface. Reprinted from ref. *8* with permission from Taylor & Francis and CRC Press.

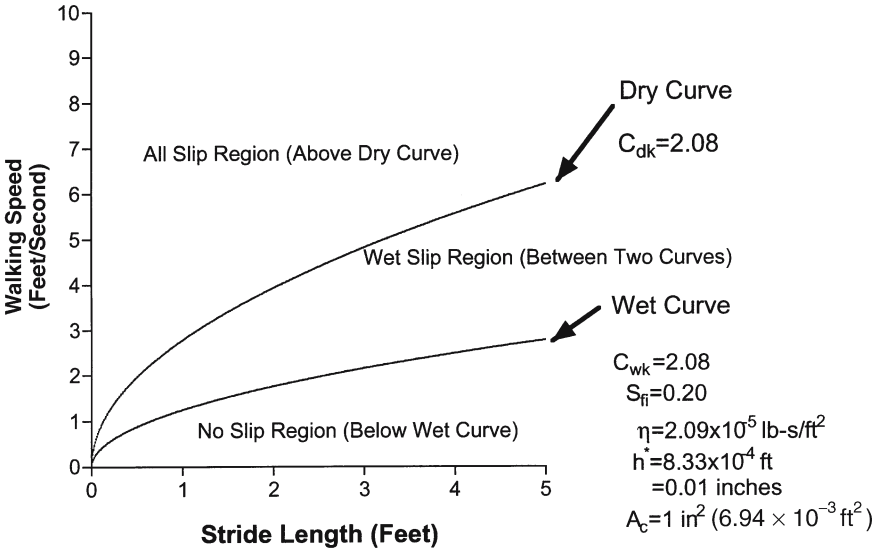

Fig. 5. Comparison of slip potential between wet and dry ($\mu_k = 0.50$) walkway surfaces. Reprinted from ref. *8* with permission from Taylor & Francis and CRC Press.

C_{dk} and C_{wk} are both taken to be 2.08, consistent with the simplifying assumption discussed above.As expected, the addition of a thin fluid film lowers the slip resistance, and it is also noted that for $S_{fi} = 1.0$, the predictions of the wet model reduce to those of the dry model.

Not all falls are precipitated by slips. Trips, for instance, result from a disruption in the motion of the swinging leg, typically by a raised obstruction, or misstep. During a tripping event the swinging leg is suddenly stopped, or slowed, resulting in a tendency

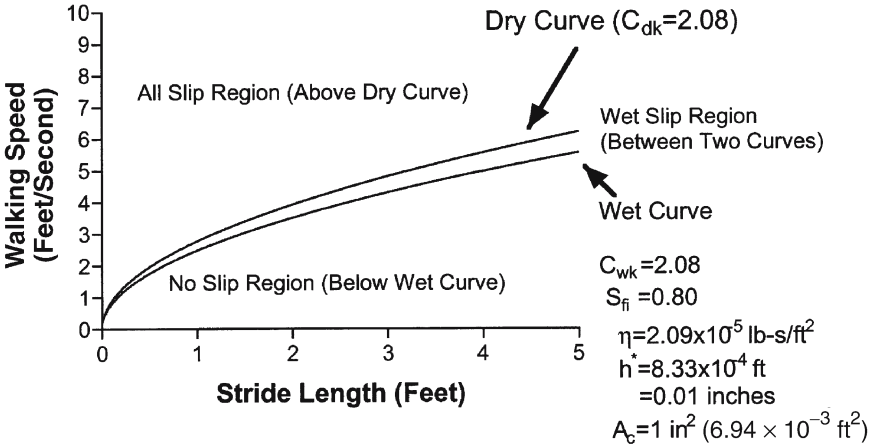

Fig. 6. Comparison of slip potential between wet and dry (μ_k = 0.50) walkway surfaces. Reprinted from ref. *8* with permission from Taylor & Francis and CRC Press.

for the walker to fall forward. Falls resulting from a slip at push-off will also often result in a tendency for the walker to fall forward, while a slip at heel strike will typically result in a tendency to fall backwards. Often, falls may result from a combined mechanism of slipping and tripping. For example, an event may kinematically begin as a slip with a partial recovery and a subsequent stumble and/or trip. Therefore, to properly identify the injury mechanism, it is important to biomechanically analyze the kinematics of the entire fall sequence.

5. Summary

Injuries and deaths resulting from slip, trip and fall accidents constitute a major public health concern in the United States and throughout the world. Major research efforts are currently underway to track, analyze, and prevent slip, trip and fall accidents. In this chapter, we have presented a brief overview of some of the methods used to measure walkway slip resistance and to analyze the probability of slip resulting in a fall. The biomechanical analysis of slip, trip, and fall accidents is a vast topic and the subject of ongoing research. For additional information, the reader is referred to the references at the end of the chapter, which is by no means an exhaustive list.

References

1. Injury Facts, 2002 Edition, National Safety Council.
2. Englander F, Hodson TJ, Terrerossa RA. Economic dimensions of slip and fall injuries. J Foren Sci 41:733-746 (1996).
3. Di Pilla S, Vidal K. State of the Art in Slip-Resistance Measurement A review of current standards and continuing developments, Professional Safety, June 2002.
4. Sacher A. Slip resistance and the James Machine 0.5 static coefficient of friction: sine qua non. ASTM Standardization News, August:52–59 (1993).

5. Ekkebus CF, Killey W. Measurement of safe walkway surfaces. Soap–Cosmetics–Chemical Specialties, February, 1973.
6. Marpet MI. On threshold values that separate pedestrian walkways that are slip resistant from those that are not. J Forensic Sci 41:747–755 (1996).
7. Powers CM, Burnfield JM, Lim P, Brault JM, Flynn JE. Utilized coefficient of friction during walking: static estimates exceed measured values. J Forensic Sci 47:1303–1308 (2002).
8. Batterman SD, Batterman SC, Medoff HP. Mechanics of Macroslip: A new phenomenological theory. In: McCabe PT, ed. Contemporary ergonomics. Boca Raton, Fla: CRC Press, 2004.
9. Medoff H, Fleisher DH, Di Pilla S. Comparison of slip resistance measurements between two tribometers using smooth and grooved neolite-test–liner-test feet: metrology of pedestrian locomotion and slip resistance: ASTM STP 1424. In: Marpet MI, Sapienza MA, eds. West Conshohocken, Pa: ASTM International, 2002.
10. McMahon TA. Muscles, reflexes, and locomotion. Princeton, NJ: Princeton University Press, 1984.
11. Saunders JB, Inman VT, Eberhart HD, The major determinants in normal and pathological gait. J Bone Joint Surg 35A:543–558 (1953).

Part III

Foot Identification Case Studies, Pedal Evidence, and Ongoing Research

Chapter 12

"The Game is Afoot!"*

Feet Help Solve Forensic Puzzles in the United States and Overseas

Julie Mather Saul, BA and Frank P. Saul, PhD, DABFA

1. The Role of the Foot in Death Investigation

Academic physical anthropologists are well aware of the importance of the foot (as more enduringly represented by its bony skeleton) in understanding human evolution, which is literally based on the acquisition of upright posture. The relative size of ancient calcanei and other tarsals, along with the curvature of the metatarsals that create the arches of the foot, provide direct clues as to the location and timing of the appearance of the "first" humans.

In our own research on the ancient Maya of Mexico and Central America, the bones of the foot yield interesting information about the activities these individuals engaged in *(1–4)*. Ubelaker *(5)* associated distal articular changes in metatarsals with habitual extreme upward and backward flexion of the toes, as occurs when kneeling with the toes bent back—perhaps to grind maize or when weaving. "Squatting facets"—flexion facets on the anterior surface of the distal tibia that are produced by frequent extreme dorsiflexion of the foot (Fig. 1)—may indicate a habitual squatting or "hunkering" posture or repeated climbing up steep hills and/or ladders *(6,7)*. Pathological findings—including healed fractures of metatarsals, sharply marked (even lipped) articular borders of tarsals, and osteoarthritic lipping of foot phalanges—reflect the difficulties inherent in moving about in rugged terrain *(6,7)*.

*apologies to Sir Arthur Conan Doyle

From: *Forensic Science and Medicine*
Forensic Medicine of the Lower Extremity: Human Identification and Trauma Analysis of the Thigh, Leg, and Foot
Edited by: J. Rich, D. E. Dean, and R. H. Powers © The Humana Press Inc., Totowa, NJ

Fig. 1. "Squatting facets" on distal tibiae. "Squatting facets" on the distal tibiae of an 18- to 24-yr-old woman from the Late Classic Maya site of Saki Tzul, located in the Maya Mountains of southern Belize, Central America. These facets represent extensions of the distal articulation of the tibia and are thought to be caused by frequent extreme dorsiflexion of the foot, as might result from "hunkering," squatting, or frequently climbing up and down steep hillsides. (Photo courtesy of K. Prufer, Maya Mountains Ritual Caves Project).

Fortunately, the weight bearing involved in upright posture and locomotion has not only influenced the basic structure of the bones of the foot and ankle, but has also increased the strength and density of the trabeculae within these bones, which helps them survive the hazards of taphonomy (i.e., what happens to the body after death) *(8,9)*.

The survival of tarsals, metatarsals, and phalanges as sources of information in modern forensic cases is further enhanced by our custom of wearing shoes and boots. Footwear serves as protective "armor" in crashes, explosions, fires, and similar situations, then continues to serve as literal storage containers for feet that would otherwise be exposed to other taphonomic events, such as insect and animal activity and weathering (Fig. 2). The skin of the foot may be breached by postmortem changes even when shoes are worn, but footgear helps to keep the foot bones "together" a while longer. The US Air Force took note of the identification potential of feet when they instituted a foot-printing program for flying personnel during the late 1950s *(10)*. It was observed as early as World War II that the heavy boots required to protect fliers against the extreme cold of high altitudes also protected the foot and its dermatoglyphics (friction ridges) in the event of a crash.

2. *The Role of the Anthropologist in Death Investigation*

A basic contribution of the forensic anthropologist in the standard forensic setting (coroner/medical examiner office) is to help create a biographic profile based on skeletal assessment of sex, age, ancestry, stature, etc., for the otherwise unidentified (including

Fig. 2. "He died with his boots on." These beautifully preserved cowboy boots protected the lower extremities of an individual found skeletonized in a wooded flood plane beside a stream. Much of the skeleton could not be located, and those bones that were recovered showed signs of animal activity. Some bones were found in the stream, leading us to suspect that bones not scavenged and removed by animals may have been washed downstream.

"unidentifiable") individual so that appropriate antemortem dental and medical radiographs and other means of identification can be obtained from a variably sized pool of missing persons for comparison. These profiles may also include fleshed characteristics, when available. (Of note, "unidentifiable" usually refers to skeletonized, burned, decomposed, fragmented, or otherwise damaged remains. However, even relatively fresh and intact bodies require more accurate age estimates than can be provided by visual inspection.)

In mass fatality incidents *(11,12)*, the situation is similar, but antemortem radiographs and other information can be immediately sought for a known relatively limited pool of presumed victims (i.e., passengers and crew on a flight manifest). The anthropologists create biographic profiles for each unit of remains, whether an intact body or a body fragment, such as a detached foot, so that when (and if) the antemortem radiographs arrive, potentially matching postmortem radiographs for each unit will be available for immediate comparison. Positive identification might then be based on an intact body or a disassociated body part, depending on availability.

The biographic profile of a unit is based primarily on the anthropologist's assessment of the skeletal remains within the unit. Aside from visualization using radiography, anthropologists may use appropriate dissection and cleaning techniques to obtain the biographic information stored in the bone. In addition to profile characteristics, the anthropologist will attempt to record side and other descriptive information that may later be used in considering whether to reassociate the unit with an incomplete set of remains with a similar biographic profile that is lacking that part. This descriptive information is also noted when DNA samples are taken.

Reassociation of units of fragmented remains with matching biographic profiles may be based on a positive identification of each unit to be reassociated. DNA is useful for this purpose, but its analysis is both expensive and relatively slow; therefore, fingerprints and dental and medical radiographs have been used most often for this purpose. In addition, a reassociation may be considered positive if fracture or joint articular surfaces can be physically linked and thereby matched. Strong presumptive reassociations may be based on surface morphology and radiographic comparisons (e.g., proportions and internal structure), as well as the process of elimination, which is sometimes based on well-defined age characteristics (i.e., immaturity) or sex (the only male present).

A qualified forensic anthropologist may compare antemortem and postmortem medical (non-dental) radiographs to establish a positive identification of the victim. Forensic radiologists are rare *(13)*; fortunately, forensic anthropologists are experienced in the potential variations of the human skeleton, usually including its radiology (especially growth and development). These non-dental radiographic identifications are based on human variation. Just as fingerprints (or noses or ears) of individuals are inherently different, bones are also dissimilar. Anthropologists not only look for obvious differences and similarities, such as healed trauma and surgical intervention, but also for such aspects as bone contours, density, cortical thickness, and trabecular patterns. As in dental identifications, any differences that cannot be explained by the passage of time or perimortem trauma result in a non-identification. Comparison of postmortem biographic profiles with antemortem information aids in the prevention of misidentifications.

In the examples that follow, we will demonstrate how we have used the lower extremities of victims to solve a series of forensic puzzles. In these cases, and in a variety of others (which include plane crashes, a train–truck crash, and a fireworks factory explosion), feet have provided us with information about the following:

- the identity of otherwise unidentifiable remains
- commingling of remains: peri- and postmortem
- reassociation of severed feet with appropriate individuals (including one survivor)
- who was flying a small plane that crashed
- taphonomic processes

2.1. A Fireworks Factory Explosion

A fireworks factory exploded in Osseo, Michigan, on December 11, 1998. The explosion destroyed all but the foundation of the building and resulted in the deaths of seven individuals *(12)*. After the explosion, six "bodies" were said to have been recovered by local emergency workers and Bureau of Alcohol, Tobacco, and Firearms agents. The seventh individual, who was believed to have been inside the building, was still unaccounted for when all the remains were brought to the Lucas County Coroner's Office in Toledo, Ohio, in 12 body bags.

Blast forces produced severe fragmentation of the building's occupants. Almost all the legs were fractured and the fractures were concentrated in the lower leg, reflecting the ground shock effects produced as the wave of energy passed through the solid floor. In some instances, the force of the explosion cleanly separated right and left hipbones from the sacrum by means of disarticulation of the sacroiliac joints.

The fragmented remains were commingled in the body bags. Body bag contents ranged from three bodies lacking some portions (three bags) through torsos lacking major portions (two bags); seven bags contained only commingled body parts. The bags containing "major" body parts also contained smaller fragments.

Dental remains provided the basis for positive identification (by a local odontologist) of portions of four victims based on the comparison of antemortem dental radiographs with radiographs obtained from the dental remains.

In a similar fashion, we positively identified portions of the other three individuals, including the "missing" seventh individual, by comparing antemortem medical and postmortem radiographs selected using matching biographic profiles. In two of these cases, right feet were sufficiently preserved to provide the identification. The frequency of sprained ankles and other foot and ankle trauma during life that require radiographic examination can be an advantage when a positive identification is needed. Radiographic comparisons of portions of the vertebral column and clavicles also produced positive identifications. A third individual was positively identified using radiographic comparisons of several portions of the vertebral column. Identified separated body parts (i.e., foot/ankle) could then in some cases be reassociated with other positively identified body parts, such as a torso that had been positively identified using dental radiographs. In addition, we reassociated a number of body parts having matching biographic profiles by linking fractures through direct matching of fracture surfaces and rearticulating joint surfaces. In some instances, presumptive associations were made using mirror imaging, sexual dimorphism (there was only one male among the victims), and proportions.

As an example, we positively identified a lower torso by comparing antemortem and postmortem radiographs (Fig. 3) of the attached right foot/ankle (the left thigh was also attached). This right foot was morphologically distinctive, with an unusually long great toe, enabling us to reassociate the lower torso and right leg with a separate left foot/ankle with a matching biographic profile and the same distinctive configuration, including an unusually long great toe. A separate upper torso with neck was also positively identified as this same individual by comparison of antemortem and postmortem radiographs of the cervical spine and shoulder. A body diagram (Fig. 4) illustrates the reassociation of these parts from three separate body bags. Unfortunately, there were some portions that could not be reassociated or positively identified by the above techniques and were therefore considered "common tissue" and buried in a common grave.

However, these procedures did enable us to locate and reassociate body parts from 11 separate body bags, thereby "rebuilding" and positively identifying the initially unaccounted-for seventh victim, whose family was then able to bury their loved one. This individual was one of those who suffered disarticulation at the sacroiliac joints and was so severely fragmented and widely dispersed about the scene that we suspect that he was close to the point of explosion.

2.2. The Comair Commuter Plane and the Korean Airlines Plane Crashes

Fragmentation is expected in explosions such as the previously mentioned fireworks factory explosion. It is also a frequent consequence of airplane and other high-energy impact crashes *(12,14,15)*. We first encountered this in the January 1997 crash of

Fig. 3. Radiographic identification of right leg and foot. **(A)** is the postmortem radiograph of the fractured right leg and foot of an unknown victim (H6) of a fireworks factory explosion. **(B)** is a transparent overlay tracing of the postmortem radiograph shown in **(A)** that was then superimposed on the antemortem radiograph of the known individual **(C)**. The circles on the overlay indicate locations of matching features on both radiographs, and there are no differences that cannot be explained. **(C)** is the antemortem radiograph of the right leg and foot of a known individual assumed to have been in the factory building at the time of the explosion.

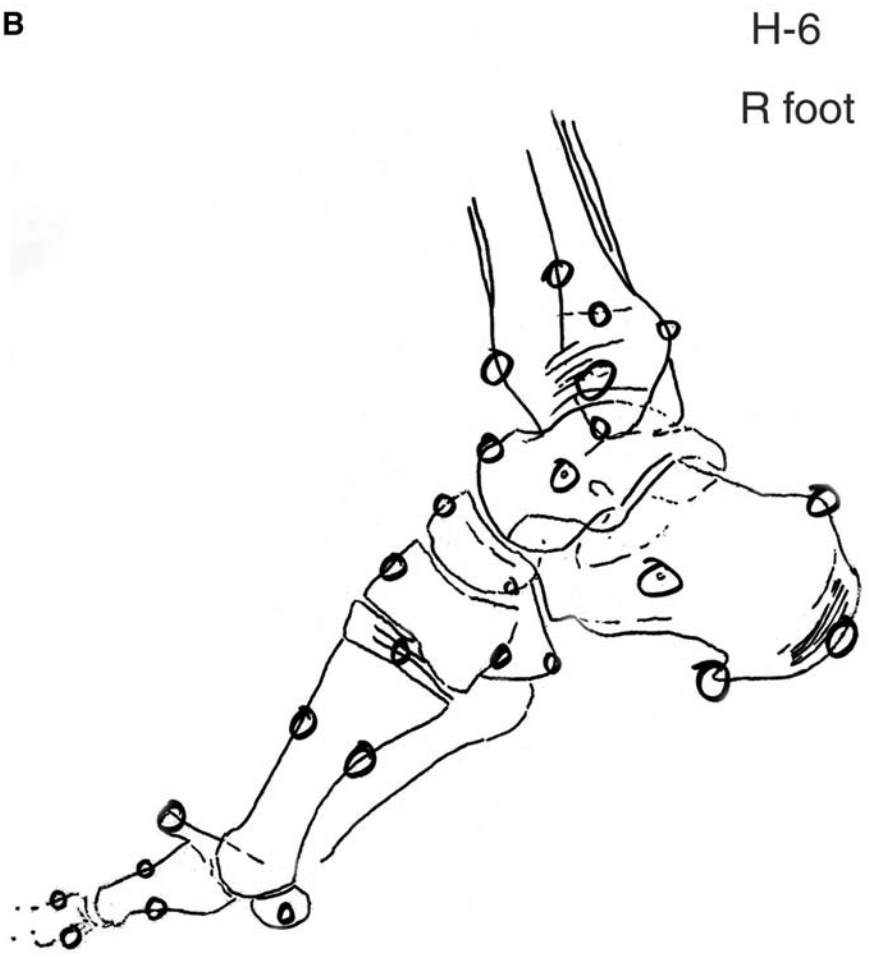

Fig. 3. *Continued.*

a Comair commuter flight en route from the Cincinnati, Ohio–Covington, Kentucky airport to the Detroit, Michigan airport. The aircraft had icing problems and plunged more or less straight down into frozen ground. This resulted in tremendous fragmentation of bodies, flaying of skin, and defleshing of bone. Twenty-nine identifications were obtained within less than a week, but priorities dictated that time was not available for reassociation of a number of dismembered feet and ankles that consequently became "common tissue" and were buried with other unidentified tissue in a common grave.

When Korean Air Lines Flight no. 801 made a "controlled-flight-into-terrain" (i.e., landed too soon and in the wrong place) on Guam, we made a special and at least partially successful effort to reassociate feet and ankles by keeping track of them from the beginning of the operation. Reassociations were made by matching biographic profiles and noting any lack of duplication plus morphological and other similarities of the contralateral part, followed by (preferably) separate positive identification via a

Fig. 3. *Continued.*

comparison of ante- and postmortem radiographs of the part in question, direct linkage of fractures, or articulation of joints.

In one notable case involving a separate female left foot and ankle with distinctive nail polish, we all were alerted to keep watch for a right foot with similar polish (hopefully attached to a body). Eventually, a female body was spotted with the toenails of the right foot coated with what appeared to be the same nail polish. The left foot was missing. Biographic profiles of both sets of remains were examined and were consistent. There was no duplication or overlapping of parts. Examination of both feet, side by side, showed strong similarities in size and configuration of feet, toes, and toenails. The nails were cut

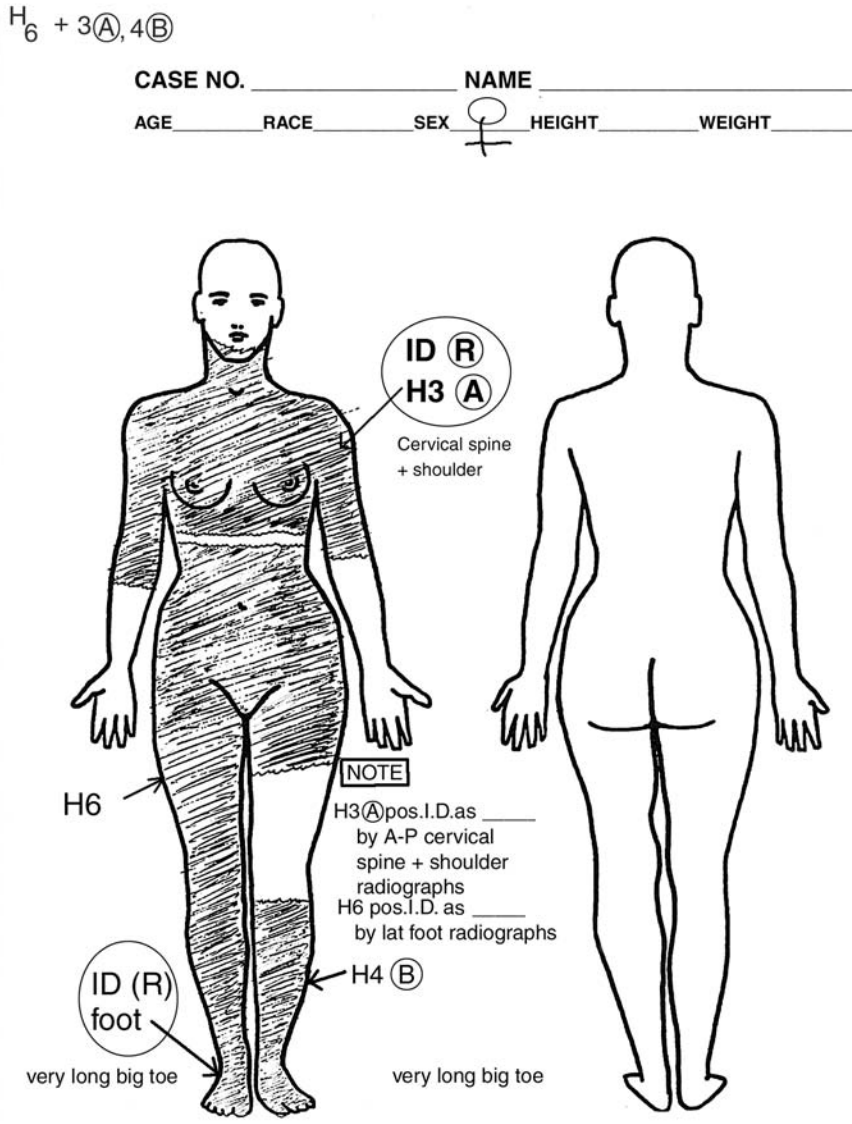

Fig. 4. Reassociation of "units." This "body diagram" illustrates the reassociation of three "units" (H6, H3A, and H4B) of remains recovered and brought to our morgue in separate body bags after a fireworks factory explosion. We positively identified the large unit consisting of the lower torso, left upper thigh, and right leg and foot by comparing antemortem and postmortem radiographs of the right foot and ankle (*see* Fig. 3). Comparison of antemortem and postmortem radiographs of the neck and left shoulder were used to positively identify an upper torso fragment as having come from the same woman. The left foot and ankle were linked by matching biographic profiles and a comparison of distinct morphological characteristics (i.e., unusually long "big toe") of the positively identified right foot and separate left foot.

and polished in an apparently identical manner. Fracture surfaces of the proximal ends of the left tibia and fibula fragments of the separate foot could not be fracture-linked to the distal ends of the left tibia and fibula attached to the body, due to destruction and loss of intermediate bone.

The young woman's body had been positively identified, so it might have been possible to compare antemortem clinical radiographs of her left foot with the postmortem radiographs of the separate left foot that we hoped to reassociate. Unfortunately, there were no antemortem clinical radiographs of either right or left lower leg and foot. We then retrieved postmortem radiographs of both the right and left feet and lower legs and examined them. Bone contours, trabecular bone patterns, density, cortical bone thickness of the left and right lower legs were essentially mirror images of each other. Based on all of these striking similarities (biographic profile, matching morphology of feet, toes and nails, matching polish, and nearly identical right and left postmortem radiographs), we proposed this to be a strong presumptive match, and with the agreement of the Medical Examiner the left foot was reassociated with the body.

In another instance, we were fortunately not led astray by bright red polish on the toenails of a victim. There is a tendency to assume that polished toenails will only be found on a female. In this case, we later learned that the male victim's toenails were painted at a bachelor party that he had attended the night before.

2.3. The Amtrak Train–Truck Crash

Our most unusual reassociation occurred as a consequence of the Amtrak train–truck crash in March 1999 *(12,15)*. The "City of New Orleans," en route from Chicago, IL, to New Orleans, LA, was proceeding normally until several hours after leaving Chicago, when it encountered a steel-laden truck that had failed to stop at a marked crossing in Bourbonnais, IL. Eleven passengers of various ages and origins died in the ensuing fiery crash.

Almost all of the recovered remains had been subjected to intense heat, ranging from charring on through calcined bone. Fragmentation was present to a lesser degree than occurs in plane crashes. Interestingly enough, several feet were separated from the leg by disarticulation at the tibio–talar joint. Some of these could be reassociated through matching biographic profiles and direct re-articulation.

When we arrived at the scene the day following the crash, we were handed remains that we identified as the distal (lower) part of the tibia of a child. We later learned that several female members of a family (grandmother, mothers, daughters, cousins) were returning from a wonderful weekend in Chicago that had included a visit to the American Girl Doll Store. They were in the sleeper car that had struck and become "draped" over one of the locomotives on impact and subsequently burned for several hours. The adults and two of the younger girls died, but one young girl suffered a traumatic amputation of her foot, after which a dining car attendant saved her life by removing her from the burning car.

We suspected a possible relationship between this incident and the distal tibia fragment found at the scene, and requested the presurgical amputation radiographs made by the local hospital. On the last day of recovery of the remains, a child's foot in a shoe was recovered at the crash site. The previously recovered distal tibia fragment

could be positively and directly articulated with this foot. The estimated age of the resulting foot and ankle was consistent with that of the young girl who "lost" her foot. Fracture linkage of the proximal end of the distal tibia fragment in hand and the distal end of the fractured tibia as seen in the presurgical radiograph provided the last link in the reassociation of the foot and lower tibia with a surviving victim.

There were concerns about how to handle this unusual situation, but we believed that this very courageous young lady, who had insisted on visiting the scene where her mother and other family members had died, might one day want to know where her foot was. It was deemed best to let her family make the final decision about disposition of the foot.

A newspaper clipping less than a year later informed us that she had made unusually rapid progress in her recovery and resumed playing soccer. A very resilient young lady, indeed.

2.4. A Small Plane Crash

A small plane crash resulted in the death of three individuals: the owner (who was a licensed pilot), his son, and the pilot employed by the plane's owner. The remains of one individual, who was later identified as the professional pilot, were fairly intact and collected in one body bag. The mangled and fragmented remains of the other two men, later identified as the owner and his son, were put into two separate body bags. Each set of remains was quickly and positively identified by comparison of antemortem and postmortem dental radiographs and returned to the two families. The authors' anthropological services were not used, inasmuch as the identifications appeared to be straightforward and provided rapid closure for the families.

Unfortunately, some time later, as aircraft and other insurance claims were being processed, a dispute arose between multiple opposing law firms as to whether or not the non-pilot son of the owner might have been flying the aircraft at the time of the accident rather than one of the two licensed pilots aboard. We were called in at that belated point. Fortunately, the Coroner's Office involved in the case had a policy of always taking full body radiographs—in this case, full body-bag radiographs were provided.

We were asked to answer the following questions:

1. Was there commingling of remains within the body bags?
2. Could we help determine who was flying the plane (who was at the controls) at the time that the plane crashed?

We were able to exclude the hired pilot from consideration, because his remains were found relatively intact and at some distance from the other two "sets" of remains. The radiographs of the single body bag containing these remains showed no signs of commingling. This was a helpful starting point, because the pilot, aged approx 20 yr, was about the same age as the nonpilot son.

Age differences served as our main basis for sorting the remains of the father and the son. We looked for signs of age differences that might indicate commingling, inasmuch as the father (identified as being in bag A-52) was aged approx 45 yr at death and the son (identified as being in bag A-53) was aged approx 20 yr at death.

Our review indicated that the torso remains (vertebral column, shoulder area, pelvis) labeled A-52 were indeed those of an older individual, while the torso remains

labeled A-53 were indeed those of a younger individual. These findings were based primarily on joint surface configuration and the radiographic presence or absence of persistent lines of density indicating recent epiphyseal union (sometimes called "growth plate scars"—not to be confused with "Harris lines," which are associated with growth arrest followed by growth augmentation).

However, we believed that commingling of lower legs and feet with torsos probably had occurred, as the articulated ankle and foot in bag A-52 (containing the torso of the father) showed recent fusion (a persistent line of epiphyseal union) in the distal tibia, suggesting that it belonged to someone in his early 20s. The disarticulated ankles and feet in bag A-53 (containing the torso of the son) showed no indications of recent immaturity, but rather were consistent with full maturity.

It is also possible that the articulated forearm and hand in bag A-52 ("the father") belonged to a younger individual (early 20s), based on the apparent presence of a persistent line of epiphyseal union in the distal radius suggestive of recent fusion, whereas the disarticulated hand and wrist in bag A-53 ("the son") showed no apparent signs of immaturity. The articulated hand and wrist in bag A-53 could not be evaluated, and the associated hand was consistent with that of a younger person (absence of joint surface changes).

Next, we considered the question of who was at the controls of the plane when it crashed. Although we felt that it was inappropriate for us to state who was or was not operating the controls, we felt that we were qualified to look for signs of trauma to hands and feet. The forensic pathologist could then interpret this information in the light of his own knowledge and experience.

In our report to the Coroner (8/07/95) we stated the following: "The important points would appear to be:

1. The foot associated with bag no. 52 ("the father") is fully articulated with the lower leg and shows minimal damage. It is inconsistent with being the father's foot because the distal tibia shows a radiographic line of density where the distal epiphysis of the tibia is located during adolescence i.e., a persistent epiphyseal surface line suggestive of recent immaturity. The foot probably belonged to a young adult (very late teens–early 20s) rather than to the father.
2. The feet associated with bag no. 53 ("the son") are both disarticulated from the lower legs (both show multiple fractures) and one foot shows fracturing. Neither the feet or the lower leg bones show any indication of immaturity, therefore they probably did not belong to the son."

In other words, the disarticulated and fractured feet were those of the older individual (the father, a licensed pilot), although they were located within the body bag containing other remains identified dentally as being the son. The damage present was consistent with that found in individuals "working" control pedals in both automobile and airplane crash situations. The foot of the younger individual (the son) showed minimal damage.

3. *Missing, Present, and Left Behind*

It is a common occurrence in our forensic practice to receive nearly intact remains that have been brought to us by law enforcement agents with varying numbers of small bones or fragments missing. The explanation for the incomplete recovery of skeletal

remains by nonspecialists is often failure to recognize the small bones (or fragments) as being human, or even as being bone at all.

Moreover, cases such as the partially skeletonized body of a young girl found wrapped in a sleeping bag in a field near Monroe, Michigan, and brought to us with several tarsals, metatarsals, and all but two foot phalanges missing suggested scavenger activity as the probable cause, rather than strictly problems of recognition and recovery. Protruding and therefore accessible toes and feet are very attractive to hungry scavengers and, like hands, are easily detached and transported for consumption, dispersal, or both. Even if they remain in the vicinity, they may be overlooked during recovery, particularly if they have been modified by gnawing *(16)*.

Taphonomic factors such as wind and water may sometimes play a part in "creating" incomplete remains. A number of years ago, a group of teenage boys retrieved several bags of human remains from the Maumee River in Toledo, Ohio. The bags contained 100 relatively fresh pieces of a female, ranging from the intact head on through squares of skin complete with underlying fatty layer, segments of bowel, and a torso with all the skin, fat, and muscle tissue neatly removed. The bags containing the pelvis and both lower legs and feet were not recovered. Her killer confessed that after dismembering her, he placed her remains into multiple plastic bags. He loaded them into her car and drove to a bridge spanning the Maumee River, which flows into Lake Erie. Throwing them into the river, he expected to see them disappear into the lake, but was undoubtedly startled to find that a strong wind from an unexpected direction brought most of them, other than the bags containing pelvis and lower legs (not found to this date), to the river shore like oddly shaped sailboats *(17)*.

Incompleteness was more or less "natural" in the former case and "accidental" in the latter, but in the following case it was deliberate. In eastern Ohio, a young woman disappeared shortly after her divorce around 1974. A confession by her former brother-in-law led to the recovery in 2000 of skeletal female remains that had been deposited in Indiana in 1980. These unidentified remains, lacking feet and ankles, were brought to us shortly thereafter. Our examination resulted in a biographic profile that was consistent with that of the missing woman. In the absence of antemortem dental and medical radiographs for comparison with those of the skeletal remains, DNA analysis was used for a positive identification. The former brother-in-law had confessed to seeing her remains in a wooden box some 5 yr after her disappearance. Our examination revealed that her lower legs had been deliberately severed about 3 in. below the knees, presumably to fit her into the box. With the addition of her lower legs and feet, she would have been too tall for the box. Although her former husband—now convicted of her murder—had stuffed the box with a great deal of her clothing, the detached lower legs (including feet) were nowhere to be found. To this day they have not been recovered and her former husband/murderer has not revealed what he did with them *(18)*.

The presence of even some of the small bones can yield important information. One sunny fall day, the incomplete skeletonized remains of a young man were found by a fisherman on a Maumee River flood plain. The young man had disappeared 3 yr earlier and last was seen some 30 mi upstream. Bones were scattered under the autumn leaves and tangled in weeds, and some were partially buried by repeated flooding of the area. Although several bones were never recovered, our ability to recognize and recover

several small bones of the hands and feet, as well as a few finger and toe nails, demonstrated that although it had traveled many miles and over a dam, his body was intact when it reached the floodplain *(19)*.

Occasionally we have seen the reverse, i.e., situations in which small bones or fragments ranging from femoral heads to carpals, tarsals, and phalanges have been recovered as isolated finds. We have experienced both situations in archaeologic and forensic contexts.

The explanation for isolated finds may be more complicated. It could involve such aspects of taphonomy as the animal activity discussed above, as well as erosion or even agricultural activity such as the tilling of fields or construction and development projects that involve the removal and dispersal of soil *(20,21)*. These processes are a frequent source of Native American and historic remains in many parts of the country, including Ohio and Michigan. It has also been noted in relation to the superficial burial of massacred Guatemalan peasants in recent times, whose remains were presumed to have been damaged by the agricultural process *(22)*.

A variation of the nonrecognition of small elements during recovery that actually serves the cause of justice involves attempts by the perpetrators to cover up individual and mass clandestine deaths by returning to the original deposition site some time afterwards. These remains "disappear" when they are moved elsewhere to avoid discovery or confound identification. During such a procedure, the easily seen and recognized bones are more likely to be collected, while less easily located and recognized small bones, fragments, and individual teeth may be left behind *(23)*. In some cases, this "collection" seems to have been followed by the disposal of the collected remains in several widely separated locations. Fortunately, these small, initially unrecognized bones and fragments that are often left behind bear witness to the original crime. Such instances of exhumation, reburial, and dispersal of victims of genocide have been documented in several countries, including Bosnia–Herzegovina *(23–25)*. Advances in DNA analysis have allowed these small bones and fragments to speak for the victims.

4. Summary

Academic physical anthropology has long recognized the importance of recovering and analyzing ancient foot bones in order to understand human evolution in relation to the acquisition of upright posture. In contrast, "traditional" forensic anthropology has focused on the informational potential of other portions of the skeleton, such as the skull and pelvis. The former yields information about such things as sex, ancestry, age, and trauma, and the latter is the most dependable guide to the sex of the individual while also yielding information such as age and parity. Information derived from teeth, long bones, ribs, and vertebrae has also been highlighted. Dentition is durable, assists in estimating age, and may provide clues to ancestry; it can also support positive identifications by the forensic odontologist. Long bones provide the basis for stature estimates. Ribs and vertebrae are examined for trauma as well as age information. Hand bones are examined for defense wounds. However, the usefulness of examinations of foot bones is underemphasized.

A recovery bias may be involved. Skulls, mandibles, and larger bones are more likely to be recognized by the public and brought to the attention of law enforcement. Searchers

(both law enforcement and volunteer) are also more likely to recognize and recover such distinctive bones while ignoring small bones that appear to be stones and twigs.

Hopefully the cases presented in this chapter (and of course this book) will remind the forensic community that foot and ankle remains are surprisingly durable and also have great forensic potential, particularly in regard to biographic profiles, identification, and activity in life.

Acknowledgments

We are grateful to the assistance, guidance, and inspiration of many: the archaeologists with whom we have worked in the Maya area (especially Drs. R. E. W. Adams, F. Valdez, N. Hammond, and K. Prufer), our colleagues in the Lucas County Coroner's Office (especially Dr. J. R. Patrick), the Wayne County Medical Examiner's Office (especially Dr. C. J. Schmidt), and fellow members of the DHS-FEMA-NDMS Mortuary Operational Response Team. Finally, we thank J. Meade for assistance with figures for this chapter.

References

1. Saul JM, Saul FP, Muñoz AR. Osteological analysis of burials from a small, non-elite site (RB-11, Programme for Belize). In: Abstracts of the 60th Annual Meeting of the Society for American Archeologists; 1995; Minneapolis, MN.
2. Saul FP, Saul JM. The people of Rio Azul. In: Adams REW, ed. Rio Azul Reports. The 1987 season. San Antonio, TX: Mesoamerican Archaeological Research Laboratory, University of Texas; 2000:240–254.
3. Saul JM, Saul FP. Maya Mountain rockshelter burials: nearer to the gods? In: Reconstructing Maya ritual and cosmology in the cave context. Prufer KM, Brady JE, eds. University of Colorado Press. In review.
4. Saul JM, Saul FP. Prehistoric burials in the far west bajo: Belize. In: Kunen, J. Ancient Maya Life in the Far West Bajo: Social and Environmental Change in the Wetlands of Belize. Tucson, Ariz: Anthropological Papers of the University of Arizona; 2004:147–155.
5. Ubelaker DH. Skeletal evidence for kneeling in prehistoric Ecuador. Am J Phys Anth 51:679–686 (1979).
6. Kennedy Kenneth AR. Skeletal markers of occupational stress. In: Mehmet Y, Iscan MY, Kennedy KAR. Reconstruction of life from the skeleton. New York, NY: Liss; 1989:129–160.
7. Capasso L, Kennedy KAR, Wilczak CA. Atlas of occupational markers on human remains. J Paleontol Mono Pub 1999;3:184.
8. Darwent CM, Lyman RL. Detecting the postburial fragmentation of carpals, tarsals and phalanges. In: Advances in forensic taphonomy: method, theory, and archaeological perspectives. Haglund WD, Sorg MH, ed. Boca Raton, Fla: CRC Press; 2002:355–377.
9. Ubelaker DH. Approaches to the study of commingling in human skeletal biology. In: Haglund WD, Sorg MH, eds. Advances in forensic taphonomy: method, theory, and archaeological perspectives. Boca Raton, Fla: CRC Press; 2002:331–351.
10. Anonymous. Military affairs: sole identification. In: Life Magazine, 12 January1959.
11. Saul FP, Sledzik PS, Saul JM. The Disaster Mortuary Operational Response Team (DMORT) model for managing mass fatality incidents (MFI) in the United States of America (with special emphasis on the role of the forensic anthropologist). Revista Colombiana de Sciencias Forense. 1:66–73 (2002).

12. Saul FP, Saul JM. Planes, trains and fireworks: the evolving role of the forensic anthropologist in mass fatality incidents. In: Steadman DW, ed. Hard evidence: case studies in forensic anthropology. NJ:Prentice-Hall, 2002:266–277.
13. Brogdon BG. Forensic radiology (preface). Boca Raton. Fla: CRC Press; 1998.
14. Saul FP, Saul JM. The evolving role of the forensic anthropologist, as seen in the identification of the victims of the Comair 7232 (Michigan) and the KAL 801 (Guam) aircrashes. Proceedings of the American Academy of Forensic Sciences 5:222 (1999).
15. Saul FP, Saul JM. The evolving role of the forensic anthropologist, as seen in the identification and reassociation of fragmented human remains. Proceedings of the American Academy of Forensic Sciences, 6:223 (2000), Reno, Nev.
16. Haglund WD. Dogs and coyotes: postmortem involvement with human remains. In: Haglund WD, Sorg MH, ed. Forensic taphonomy: the postmortem fate of human remains. Boca Raton, Fla: CRC Press; 1997:367–381.
17. Desley CW, Saul FP, Saul JM. Dismemberment: a cautionary tale. Abstract presented at: the 42nd Annual Meeting of the American Academy of Forensic Sciences; Cincinnati, Ohio; 1990:119.
18. Fleeman M. The stranger in my bed. New York, St Martin's Press, 2003:1–276.
19. Saul FP, Saul JM. Little things (can) mean a lot. Abstract presented at: the 44th Annual Meeting of the American Academy of Forensic Sciences; New Orleans, La; 1992:164.
20. Ubelaker DH. Taphonomic applications in forensic anthropology. In: Haglund WD, Sorg MH, eds. Forensic taphonomy: the postmortem fate of human remains. Boca Raton, Fla: CRC Press; 1997:77–90.
21. Haglund WD, O'Connor M, Scott DD. The effect of cultivation on human remains. In: Haglund WD, Sorg MH, ed. Advances in forensic taphonomy: method, theory, and archaeological perspectives. Boca Raton, Fla: CRC Press; 2002:133–150.
22. Schmitt S. Mass graves and the collection of forensic evidence: genocide, war crimes, and crimes against humanity. In: Haglund WD, Sorg MH, eds. Advances in forensic taphonomy: method, theory, and archaeological perspectives. Boca Raton, Fla: CRC Press; 2002:277–292.
23. Roksandic M. Position of skeletal remains as a key to understanding mortuary behavior. In: Haglund WD, Sorg MH, eds. Advances in forensic taphonomy: method, theory, and archaeological perspectives. Boca Raton, Fla: CRC Press; 2002:99–117.
24. Skinner MF, York HP, Connor MA. Postburial disturbance of graves in Bosnia–Herzegovina. In: Advances in forensic taphonomy: method, theory, and archaeological perspectives. Haglund WD, Sorg MH, eds. Boca Raton, Fla: CRC Press; 2002:293–308.
25. Klonowski EE, Mujkic M, Sarajlic N, Drukier P. Reassociation of skeletal remains recovered from graves in Bosnia and Herzegovina. Proceedings of the American Academy of Forensic Sciences; 2003; Chicago, Ill.

Chapter 13

The Role of Feet and Footwear in Medicolegal Investigations

John A. DiMaggio, DPM

1. Introduction

This chapter will serve as a practical treatise for evaluating pedal evidence (footwear and footprints) in forensic contexts. Extensive research is necessary to help validate identification markers between the foot and footwear. The reader is encouraged to review any unfamiliar terms in the appendix of this chapter.

The distinguished British anatomist, Frederick Wood Jones, ably described the human being's distinguishing characteristic:

> "Man's foot is all his own. It is unlike any other foot. It is the most distinctly human part of his whole anatomical makeup. It is a human specialization and, whether he is proud of it or not, it is his hallmark and so long as Man has been Man and so long as he remains Man it is by his feet that he will be known from all other members of the animal kingdom" *(1)*.

Moreover, in the last chapter of Sir Arthur Conan Doyle's Sherlock Holmes classic, *A Study in Scarlet*, Holmes recounts to Watson just how he solved the crime. Holmes states,

> "There is no branch of detective science which is so important and so much neglected as the art of tracing footsteps."

This text was first published in Beeton's Christmas Annual, London, in 1887. Furthermore, in his book on footwear identification, Cassidy says,

> "a podiatrist or orthopedic surgeon is a specialist who has the training to properly interpret the mark inside the shoe and present this form of evidence in court" *(2)*.

With an increased awareness of foot or foot-related evidence, most recently brought to the forefront with the O. J. Simpson case, the field of forensic podiatry has evolved.

From: *Forensic Science and Medicine*
Forensic Medicine of the Lower Extremity: Human Identification and Trauma Analysis of the Thigh, Leg, and Foot
Edited by: J. Rich, D. E. Dean, and R. H. Powers © The Humana Press Inc., Totowa, NJ

Forensic podiatry may be defined as the application of podiatric medical expertise to the legal system. Vernon and McCourt further define forensic podiatry as the

> "application of sound and researched podiatric knowledge in the context of forensic and mass disaster investigations. This may be for the purposes of person identification, to show the association of an individual with the scene of a crime, or to answer any other legal question concerning the foot or footwear that requires knowledge of the functioning foot" *(3)*.

2. Role of Forensic Podiatry

Footprint and footwear evidence is commonly present at a crime scene and must be discovered, recorded, and collected for further examination. When footprint analysis is required, the forensic podiatrist may act as an adjunct or a primary participant in the case. The foot is a complicated structure, and it requires years of experience to be able to distinguish all the intricacies—including soft tissue and skeletal pathologies—involved in its makeup and consequent evaluation. The use of unknowledgeable or simplistic approaches may have significant ramifications that can affect a person's freedom or even life itself.

2.1. History

There are numerous references in the literature to footwear evidence relative to footwear identification, the earliest recorded case dating back to 1876 in Scotland. However, a search of the literature on pedal cases is not replete with references relative to podiatry alone. The reader is encouraged to review the further reading section for historical references.

In the 1920s, Gerard published information and his thoughts about the foot and fingerprints, but apparently his ideas were either ahead of his time or unpopular because there is no further mention of his work. In 1935, Muir composed an article titled "Chiropody and Crime Detection," in which he offered his thoughts on a footprint case utilizing a forensic approach; however, Muir did not appear to be involved specifically in the case. One of the most infamous cases at the time was the Ruxton case, which occurred in Scotland in 1935 *(4)*. This forensic case involved placing dismembered feet from two profoundly mutilated individuals into the footwear of two missing persons: Mrs. Isabella Ruxton and her nursemaid. Mrs. Ruxton's chiropodist was employed for this purpose *(4)*.

In 1957, Sir Sidney Smith—although not a podiatrist but a police surgeon—wrote a well-known book called "Mostly Murder." Throughout his career, he investigated several crimes involving footwear. One of his best-known cases occurred in Falkirk, Scotland, in 1937. He gave the police a description of the perpetrator's locomotor system after reviewing the evidence and scrutinizing the footwear. The accuracy of his conclusions was uncanny, because he had not seen the perpetrator's feet before his evaluation and he demonstrated a thorough knowledge of podiatric medicine.

Lucock, a British chiropodist, published an article in 1980 in the *Chiropodist* titled "Identification from Footwear." It was the first article that included a discussion of the foot and observed wear patterns on shoes relative to pathologic and biomechanical imbalances in the feet. In 1982, Dr. Norman Gunn, a podiatrist, took plaster casts of foot impressions in sand at a murder scene in Canada, and the techniques used to match the impression to the suspect's foot convinced the suspect to change his plea to guilty.

Norman Gunn is a pioneer in the field and is well known for his extensive forensic involvement worldwide. Beginning in the late 1980s and early 1990s, several other podiatrists became active and have worked criminal cases and testified in court. In Canada, Keith Bettles has worked on several pedal cases and was featured on a forensic television production. Other podiatrists who have worked abroad in this field include Vernon and McCourt in England, Jones and Bennett in Australia, and Greg Coyle in New Zealand. In the United States, Christopher Smith testified at a trial and refuted the testimony of Louise Robbins on several issues *(5)*. Ronald Valmassy, Gerson Perry, Ivar Roth, Mario Campanelli, Robert Rinaldi, Henry Asin, and the author have all worked as forensic podiatrists in the United States.

2.2. Current Forensic Podiatry

Given the increased number and variety of applications of forensic podiatry, the field needed to be developed in an academically and scientifically robust manner similar to other disciplines, such as forensic anthropology and forensic odontology. Presently, podiatrists are active members of the American Academy of Forensic Sciences and Distinguished and Associate members of the International Association for Identification. They are also members of their forensic state societies and act as consultants to their local police departments. Podiatrists are also members of the Canadian Identification Society, British Association of Human Identification, Forensic Science Services, and the Centre for International Forensic Assistance.

The newly formed American Society of Forensic Podiatry promotes forensic sciences through continuing education for its members by means of educational seminars, research, publications, and through liaisons with other organized disciplines. An emphasis on statistically rigorous research in the forensic sciences is strongly encouraged. By virtue of training, podiatrists have a basic knowledge of footwear and significant experience with foot morphology, pathologic states, and biomechanical imbalances. The forensic podiatrist will attend and regularly participate in academic meetings and training seminars in the scientific community. This will give the podiatrist a sound indoctrination in other subjects related to law enforcement, criminal justice, and laboratory techniques. Working in the crime laboratory and with police departments is highly recommended. The podiatric medical educational system in the United States is in the process of developing forensic programs for podiatric medical students and postgraduate courses for practicing podiatrists. In 2000, Wesley Vernon became the first podiatrist to complete a PhD program in Forensic Podiatry in the United Kingdom.

3. The Crime Scene

Physical evidence can be defined as articles and materials found during an investigation that may establish the identity of suspects and the circumstances under which the crime was committed. Footprints are known as physical evidence, as are fingerprints. It is evidence that speaks for itself and requires no explanation, only identification.

Fingerprints are often discovered at the crime scene—but not always, because it is possible that nothing was touched or precautionary measures were taken (i.e., gloves

may have been worn to preclude identification). However, it is unlikely that an individual can enter and leave the crime scene without using his or her feet. Discovering pedal evidence can be difficult, however, and a conscious effort must be made to do so. The initial officer(s) must recognize the importance of footprint evidence and try to preserve the integrity of the scene. This task can be quite difficult when medical personnel or other persons inadvertently destroy potential evidence.

Foot impression evidence is most commonly discovered on ground surfaces, such as dirt, tile, concrete, and carpeting, but at times on counter-tops or other less common locations *(6)*. Prints that are transient in nature, such as in snow, must be addressed and processed immediately. A print that is latent or invisible means it can be overlooked. The importance of this evidence to crime scene personnel needs to be stressed. If one footprint is discovered, then logically there may be more. For example, if there is a homicide scene with copious amounts of blood, then the expert should anticipate a good number of prints; if not, one would need to determine why not. Perhaps the scenario was manufactured or was altered or cleaned to conceal the presence of pedal evidence.

General protocols regarding crime scenes are fairly universal. The main purpose is to discover evidence and recover it for scrutiny in the laboratory.

SECURE THE SCENE. The first step is to secure the scene. This may seem basic, but at times it is difficult to enforce because there are often extraneous individuals who try to enter. Because our interest is in pedal evidence, foot traffic should be limited.

RECORD THE SCENE. The most common methods of recording the scene are photography, sketching, and note taking. The use of video taping with commentary can be helpful and may negate the need for more time-consuming methods. The scene should be recorded as promptly as possible while it is in a relatively untouched state, especially when footprint evidence is being considered.

SEARCH THE SCENE (DISCOVER). A systematic approach is necessary when footprint evidence is suspected. Depending on the type of crime, certain approaches and paths through the scene may vary. For example, where was the point of entry? Is there blood or a substrate that might be efficacious in exhibiting footprints or foot impressions? Is there a major crime area or several different sites? Where is the point of exit? An examination of the immediate exterior may yield many impressions in dirt or foot/shoe prints on a concrete walkway.

COLLECT (RECORD) AND PACKAGE EVIDENCE. If footprints are visible, they must be photographed. This process includes proper positioning of the camera using a tripod, with the film parallel to the plane of the print or impression and directly over it, i.e., perpendicular to the impression. A scale should always be included so the photograph can be enlarged to reveal the natural size of the evidence, more commonly called 1:1, wherein 1 mm on the scale equals 1 mm. It is usually a good idea to take a similar photograph without a scale. As many photographs should be taken as possible, especially macro-views that will be used later for comparisons. It cannot be stressed enough how important accurate photographs are for a proper evaluation. Pedal impression evidence is often latent or poorly visible; therefore, various types of enhancement techniques must be used. Oblique lighting techniques using a strong white light are

implemented to highlight or detect footprints that may not be clearly visible to the naked eye. If there is a suspicion that there might be bloody footprints but they are not visible, then Luminol or some other method can be used. Luminol causes the heme portion of the erythrocyte to luminesce; the technique must be performed in complete darkness. The luminescent effect is usually very short lived; therefore, a chemical agent such as amido black is used to enhance and stabilize the erythrocyte in a blue-black color and the footprints can then be photographed.

An alternate light source, also known as a forensic light source, is an instrument that emits specific bands or wavelengths of light that are useful in detecting physical evidence. Depending on the device, the range can start at 365 nm (which is in the ultraviolet [UV] range) and extend through the visible spectrum to infrared capabilities in the 700-nm range and higher. This instrument can supply bright white light for the oblique technique and has capabilities for footprints often in the UV range. It is usually used to detect biological fluids, hairs, and fibers. Three-dimensional impressions of footprints are often discovered in dirt, mud, or some other impressible substrate and should be photographed first, then casts made, if possible. One recommended material for casting is dental stone, because it is more rigid and durable than plaster of Paris. It is not uncommon for plaster of Paris casts to break when in transit or while being examined by different individuals. A broken cast is not an adequate exhibit. Lifting techniques can be used for certain types of footprint evidence, using adhesive and gelatin lifters as are used for fingerprints *(7)*. If dust impressions are suspected, an electrostatic dust-lifting device can be used. It uses an electric charge to actually lift the dust print onto a foil surface that can be photographed and used for later evaluation.

General protocol is used for packaging the evidence; most importantly, items must be kept separate to prevent cross-contamination. Shoes should be individually wrapped in separate paper bags, as should plaster or dental stone casts.

SUBMIT EVIDENCE TO THE LABORATORY. The modern laboratory is equipped to handle most types of evidence. It is advantageous to acquire as much evidence as possible from the scene for transport to the laboratory for processing. This may involve removing a door, flooring, or plasterboard if it has foot or shoe prints. Evidence can be enhanced both photographically and chemically. For instance, the sock liner of a shoe may be viewed with an alternate light source, using laser or bright white light, to give the most accurate depiction of the foot image (Fig. 1). In this instance, the sock liner was treated in a fuming chamber of cyanoacrylate ester (superglue) for 30 min at 80% humidity. Basic yellow-40 solution was applied with a soft brush; the liner was then rinsed with water for 2 min and dried. Excitation was accomplished using a Crimescope-16 (SPEX Industries) at 455-nm. The camera used was a Crimescope VRM (SPEX Industries) with an orange long-pass filter or a 550-nm band-pass filter. In many cases, it takes experimentation to determine the best wavelength to get the best image because of the variability of the color of the sock-liner covering, which can be black, green, blue, white, or any of several other assorted colors.

Many departments are using digital photography, which has certainly made the task much simpler and less time-consuming for obvious reasons. Footwear evidence that is recovered should be photographed and then, at a minimum, examined for trace evidence. Blood on footwear may be collected for DNA analysis.

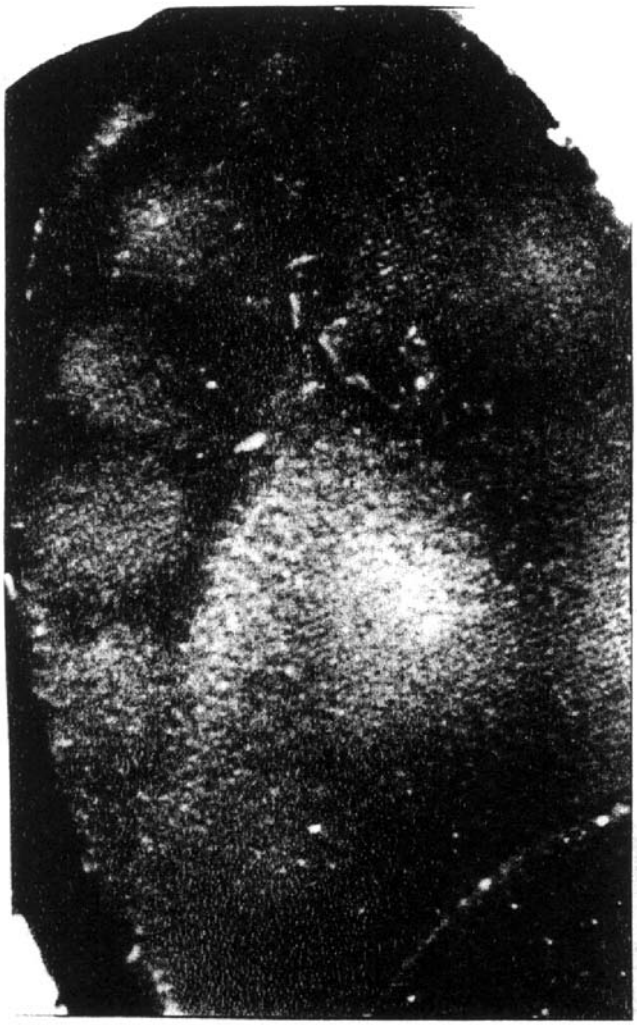

Fig. 1. Enhanced sock liner of a questioned foot image showing a fair representation of the toes and ball of foot area that can be used for comparison to a known standard.

A general overview of the crime scene and some techniques focusing on pedal evidence were presented. It is not comprehensive, and the reader should review the references and further reading section for more information.

4. Review of Foot Anatomy

The foot (Fig. 2) has 26 bones, plus at least two sesamoid bones located under the first metatarsal head. Thus, both feet contain a total of 28% of the 206 bones in the human body. What makes the human foot unique is that it is the only foot in nature with a heel bone that touches the ground, a straight-ahead (instead of a thumb-like) great toe (hallux), and an arch *(8)*. The bones are grouped into three different areas: the rearfoot

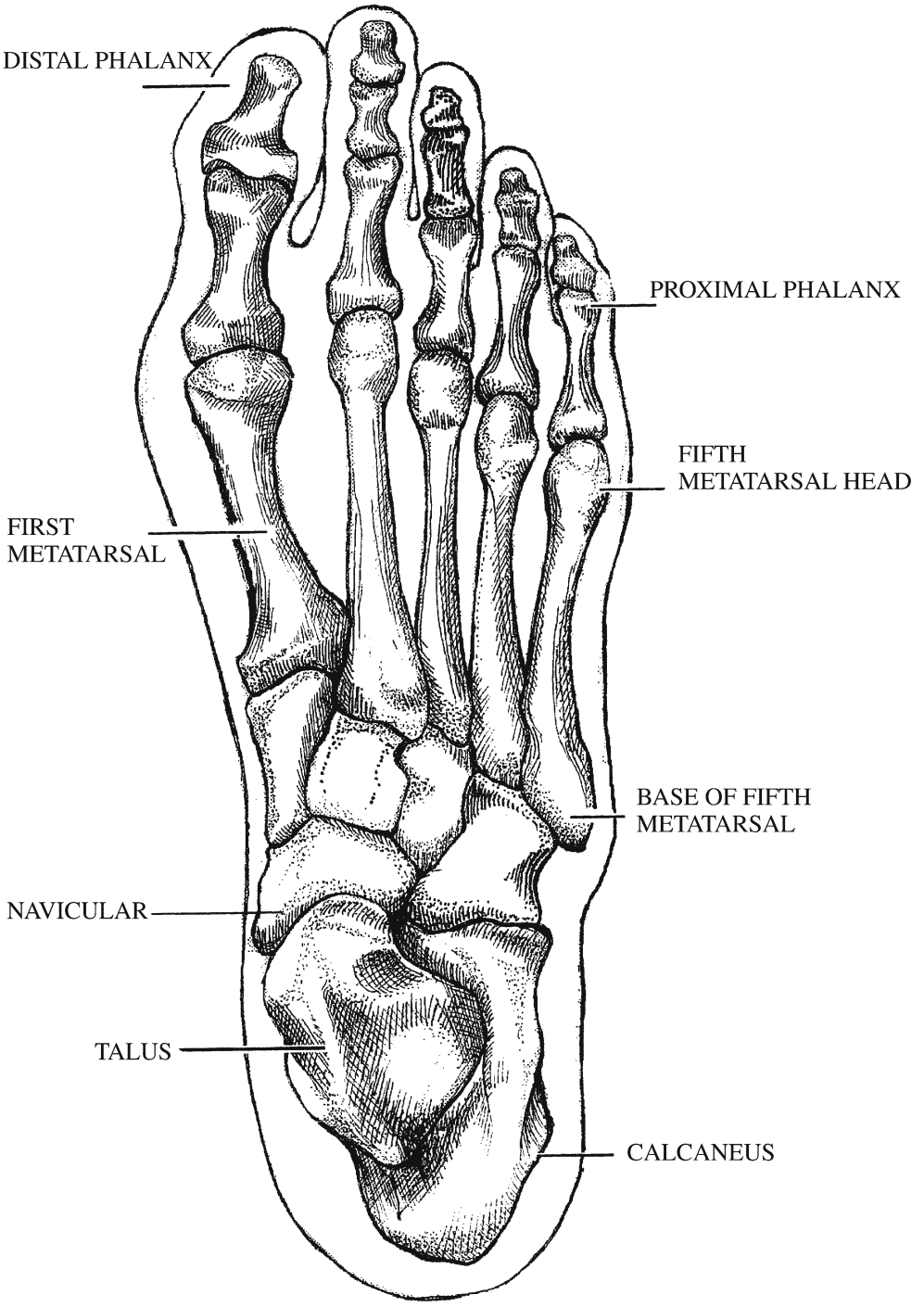

Fig. 2. Dorsal view of the 28 foot bones, (the two sesamoid bones located under the head of the first metatarsal are not shown), showing some anatomic regions that may have forensic implications.

(heel), midfoot (arch), and forefoot (ball and toes). The rearfoot is composed of the talus and calcaneus. The talus ("ankle bone") articulates with the lower end of the tibia and fibula and is responsible for dorsiflexion and plantar flexion of the foot. The calcaneus is known as the heel bone. The midfoot is composed of the three tarsal or cuneiform bones, the navicular bone, and the cuboid bone. The forefoot is composed of the five metatarsal bones and the phalanges. The second to fifth toes have three separate phalangeal bones and the great toe (hallux) has two phalangeal bones. The great toe is considered the first digit or toe number one; the fifth toe is also called the "little" toe.

The bony structure is held together by soft tissue elements known as the ligaments, of which there are 107. Muscles and tendons, 19 in number, comprise the other soft tissue elements that are responsible for locomotion. The foot has 38 articulations (joints); these are sites where two bones meet and various amounts of motion occur. A complex network of blood vessels and nerves supplies the foot *(8)*. The human foot presents an arch—the long arch along the inner border that is known as the inner or medial longitudinal arch. This is the most important arch in forensic applications, and it is commonly classified as either low, normal, or high. The arch is often depicted by a wide footprint for a low arch, a narrow footprint for a high arch, and a medium-width print for a normal arch. Moreover, it is possible to have what appears to be a "normal" arch (i.e., without a varus or valgus orientation) that still has a tendency towards hyperpronation (flat foot type), which can be explained in biomechanical terms, i.e., the arch height in these terms often is inaccurate or has no true meaning. In addition to the outer longitudinal arch, which is along the outside of the foot, there is a transverse arch, which is formed across the ball of the foot under the heads of the metatarsals. This arch flattens with weight bearing and has no real value in forensic podiatry.

Foot types are classified both morphologically and biomechanically. Morphological classification includes the structure and form of the foot. It is a combination of the bony configuration as well as the soft tissue, with the foot usually described as narrow, broad, long, or short. These designations are based solely on subjective opinion. A more scientific approach, proposed by Rossi in 1992, relies on anthropometrics (unpublished study of >600 subjects, per personal communication, WA Rossi). They have found that all human physiques fall into three main classifications:

- Ectomorph: tall, slender, long-boned, slim-muscled
- Mesomorph: stocky, muscular, heavy-boned
- Endomorph: fleshy, plump, small-boned, fatty

No body physique is entirely any one of these; however, although it is usually a combination of all three, one type in the combination is dominant. Significantly, the foot type will be in the same category as the body type. Thus, a dominantly mesomorphic physique will invariably have a mesomorphic (stocky, muscular, heavy-boned) foot. Also important, each foot type will have its own functional character. For example, the mesomorphic foot tends to have a lower arch and requires a wider shoe *(8)*.

This categorization may be helpful in forensic cases. If it can be determined that the footprint in question was made by a mesomorphic individual, then certain other physical characteristics can be determined that may be useful in suspect identification. It must be

remembered that the bare footprint is a representation of the bony structure pressing on the soft tissue underlying it. Noncontact areas are not shown, and that is why it is important to use the foot outline (Fig. 2) whenever possible to give the total morphological picture. It is possible to look at a bare footprint that appears to have a long second toe, when in actuality the first toe may be longer due to larger soft tissue expansion in that digit.

Another anatomical region of significance in forensic contexts is the skin of the plantar aspect (sole) of the foot. The skin is composed of a superficial layer, the epidermis, and the deeper dermis layer. The epidermis varies in thickness from 0.07 to 0.12 mm throughout most of the body. On the palms of the hands and the soles of the feet it measures 0.8 to 1.4 mm thick *(9)*. The sole, being 10 times thicker than the palmar aspect (palm) of the hand, presents a more durable integument capable of deforming a given surface. The plantar aspect of the foot contains eccrine glands, which secrete primarily water and some salts and traces of urea. A single foot has approx 60,000 sweat glands, which can account for the average adult foot perspiring approx 4 oz of water daily *(7)*. Perspiration can vary with the ambient temperature, humidity, and activity level *(8)*. The secretion of such quantities of water inside closed footwear can be of value in the forensic evaluation and will be discussed later in this chapter.

5. The Dynamic Foot

Foot dynamics or biomechanics deals with the foot in motion. As such, it is a complex phenomenon that has to propel the body and in effect prevent it from falling forward. The foot must adapt to the surface and compensate with change to allow the human being to walk in a straight line. There are variations in foot dynamics during the gait, and many activities that form a complex series of motions, when abnormal, lead to a pathologic change. No two feet are exactly the same in terms of anatomy and morphology. Neither are the rules of biomechanics the same for all feet, thus adding another means of forensic evaluation.

The dynamic foot, in addition to providing a base of support during a walking cycle, must be able to adapt to uneven terrain during initial contact with the ground and then change to a more rigid lever for push off. The gait cycle is a complex activity involving two phases. The stance phase accounts for 62% of the cycle and occurs when the foot is in contact with the ground; this includes heel contact, mid-stance, and propulsion *(8)*. The swing phase accounts for 38% and occurs when the foot is swinging through to recontact the ground *(8)*. Forensic considerations of the gait cycle relative to pedal evidence will be discussed later in this chapter.

We may classify the foot according to its morphologic appearance, as previously discussed. But how do we classify the functioning foot in biomechanical terms? Foot biomechanics is the application of mechanical laws to living structures, specifically the locomotor system of the human body. It pertains to the alignment of the rearfoot with the forefoot. This classification is based on the relationship between the standing calcaneal position and the nonweight forefoot-to-rearfoot position. It is logical in its approach and aims to be as objective as possible. The foot is characterized in four levels of cavus, a rectus foot (which is neutral), and four levels of planus. This classification system begins with type 1, with an inverted calcaneus and an everted forefoot (valgus). This is the most severe cavus deformity and is often considered the classic Pes Cavo-Varus deformity or

claw foot. Types two, three, and four represent diminishing degrees of severity of varus. Type 5 is the neutral foot, with the calcaneus perpendicular to the weight-bearing surface and the forefoot perpendicular to the rear foot; it is considered the "normal" foot. The subtalar joint is the position from which maximal function can occur. Types 6, 7, and 8 are increasing in degree of valgus, with type 9 being the classic Pes-Planus deformity or severe flatfoot. Further discussion of these pathologic entities is beyond the scope of this chapter, and pertinent references in the bibliography should be consulted *(10)*.

Pathologic change that is seen with different biomechanical foot types is well known, and although there can be deviations from the norm, for the most part assumptions can be made with a good degree of accuracy. The patient with a planus foot often presents in clinical practice with a complaint of arch pain, heel pain, hallux abductovalgus with bunion deformity, and hammer toe deformity. Other complaints may involve joints above the ankle level including the knee and hip joints. The patient with a cavus foot often presents with complaints of chronic lateral ankle instability, digital contracture, and metatarsophalangeal joint contracture, with increased declination of the metatarsal heads. Significant metatarsalgia with intractable plantar keratosis (deep, nucleated callus) formation may be a complaint in addition to medical concerns above the ankle. This biomechanical classification system with its inherent abnormalities in fact may lead to a better understanding of foot pathologies and how the complex system of dynamics influences pathologic entities. Entities known as subtalar or rearfoot varus or valgus deformity, forefoot varus or valgus deformity, and equinus deformity all may exist in a compensated or uncompensated form to some degree. Some of these entities are more common than others, but all may lead to an expected change in the footwear, gait pattern, or footprint. Therefore, without a keen knowledge of this subject matter, would be difficult to use in forensic contexts.

5.1. Pathology

In the physician's office, the clinical presentation of foot pain in many cases will be secondary to structural or biomechanical imbalances manifested by pathologic change. The deformities are often exacerbated by footwear, and pathologic change may be secondary to injury or disease. The foot undergoes many stresses during one's lifetime. The structure of the foot may be influenced by extrinsic factors, such as footwear, occupational stresses, and injury. Intrinsic factors may be genetically based or associated with biomechanical influences and may cause soft tissue and osseous pathology that may assist in identification efforts. Furthermore, juvenile foot problems, which are not uncommon, can lead to anatomical changes that can be translated into associated wear visible in their footwear.

A bunion deformity is an enlargement of the first metatarsal head, the presence of a bursa (fluid-filled sac), or both (Fig. 3). If there is also an arthritic component, the joint may be affected, with restriction of motion that may have some effect on foot dynamics as well. The bunion deformity may exist by itself or may include a lateral deviation of the hallux, which is called hallux abductovalgus. Juvenile hallux abductovalgus deformity, which is more common in females, can begin as early as 10 or 11 yr and may be fully matured by the mid-teens. The bunion is also a common deformity in adults that can be severe and is more common in females.

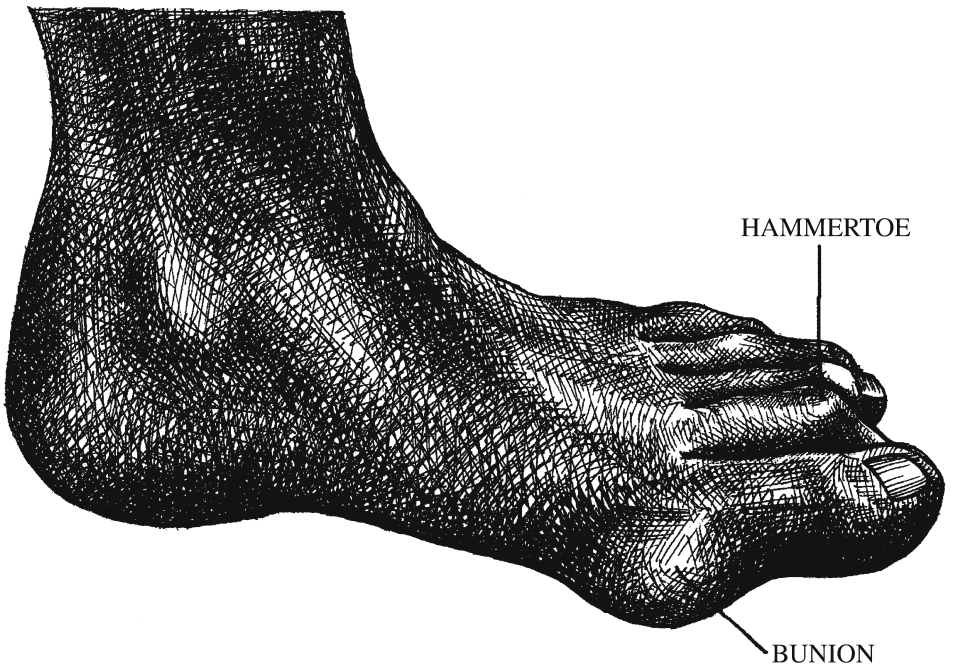

Fig. 3. Common foot deformities that will often leave their mark in footwear as wear on the inner liner and/or protrusion or bulge in the shoe upper.

Often associated with this problem is the hammer toe deformity (Fig. 3), which most commonly affects the second toe. This deformity at the proximal interphalangeal joint may have a contractural component at the metatarsophalangeal joint, which can apply a downward force on the metatarsal head. The increased downward force leads to increased pressure in that area, with or without callus formation under the metatarsal head. The second toe is longer than the first toe in 25 to 35% of the population (unpublished study by the author) and may be a component of the hammer toe deformity or not, but still has forensic implications either way. Hammer toes can affect the third and fourth toes, but more commonly the fifth toe is affected, though in a slightly different configuration. The fifth toe will, in many cases, be forced into or under the fourth toe, a condition that is specifically exacerbated by certain types of footwear. The toe is often rotated more laterally than medially and the boney prominence at the head of the proximal phalanx may develop the heloma durum ("corn") which is not uncommon.

A deformity that may be seen in younger individuals is a bunion deformity on the lateral aspect of the foot affecting the fifth metatarsal head, also known as tailor's bunion. The metatarsal head may be enlarged, with an inward deviation of the little toe. There may also be an outward bowing of the metatarsal shaft leading to more significant prominence laterally. Haglund's deformity affects the posterior aspect of the calcaneus by appearing as an enlargement in the back of the heel that tends to rub against the inner lining of the shoe counter, often creating an inflammation in that part of the foot. Prominence in the medial arch at the navicular bone is usually associated with

hyperpronation and is seen in younger individuals. Pain is present at that site and usually occurs secondary to footwear. Dorsal hypertrophy in the area of the base of the first metatarsal bone and medial cuneiform bone often leads to a large bump on the dorsum of the foot and is painful secondary to footwear. This is most frequently found in older individuals and is chronic in nature. Deformity may also exist as a result of injury. Congenital diseases, such as poliomyelitis, may also lead to foot deformity, and possibly at an early age.

For example, a pathologic change in one foot (e.g., a bunion) does not necessarily imply that the same problem exists to the same degree in the other foot. A deformity can also be present above the level of the foot, including problems with the knees, hips, or back. Limb-length discrepancy may be implicated in some of the pathologic changes noted. In most cases, the longer side will show more deformity, both structurally and biomechanically, and often in the flatter foot.

The wide array of pathologies in the feet can only be considered beneficial in forensic contexts. The pathologic change may be translated into the footprints and into footwear. The bunion prominence may deform that part of the shoe and may cause wear on the inside upper in that location. The same scenario applies to the hammer toe. Of note is the lack of statistical analyses regarding foot pathology. Some have been presented in the literature, but none by the podiatric or orthopedic communities specifically addressing forensic needs. Further research is warranted for addressing the commonality or lack thereof of foot pathologies and their use in forensic contexts.

5.2. Footwear

A chapter on pedal evidence would not be complete without a discussion of what houses the foot most of the time. The reader may gain a greater appreciation of the characteristics of footwear and how foot pathology may lead to identification. Footwear can often be found at or near the crime scene, recovered from a residence or vehicle, or taken from a suspect when taken into custody.

Footwear is considered by many to be important as a fashion statement, but little regard is given to its negative effect on the foot. Many individuals actually wear shoes that are too small for them. This occurs in some cases because of vanity but in many cases because of improper fitting. Currently, individuals order more merchandise, including footwear, through catalogs and the electronic media, which usually precludes measuring the feet properly. It is not uncommon for the foot to increase one-half (one-sixth of an inch) to one full size (two-sixths of an inch) as one ages. This increase can be attributed to arch breakdown, with elongation of the foot, and can be influenced by joints above the ankle including the knee, hip, and spinal column. The feet should always be measured each time shoes are purchased, and that includes both feet since they are often not exactly the same size. Because shoes may be purchased by the stated size, it is fairly common for shoes not to fit properly. Many shoes that are manufactured in foreign countries are usually shorter than the stated size. It is usually advised to purchase a shoe one-half to one full size larger than the measured foot size. As a general rule, there should be one-half to five-eighths of an inch between the end of the longest toe and the end of the shoe for a proper fit.

The size of feet in general has also changed over recent years. Men's feet appear to have remained stable, with perhaps a small percentage increase in larger sizes. The most common sizes for men's shoe range from 9 to 11. Size 11 usage has increased by approx 9% over the past 10 yr, and size 8 usage has decreased approx 3 to 4% for a similar period (unpublished study of author). Women's feet generally have increased in size, which has been noted in clinical practice over the past 10 to 15 yr. It appears women are wearing larger shoe sizes. The most common sizes are 7, 8, and 9 in approximately equal numbers. However, size 9 is approx 5% more common now than it was 10 yr ago (unpublished study by the author). The number of women wearing a size 10 has also increased by approx 6% over the past 10 yr (unpublished study by the author).

These shoe-size changes have forensic implications regarding footwear prints. It has also become more common for women to wear men's shoes, which are generally wider than women's footwear and give more room if they have a large foot. If they have a large foot, it is often difficult to find a good assortment of shoes in women's sizes that fit properly. A woman who wears a size 10 shoe can wear a men's size 8.0 to 8.5. The fact that it is also possible to wear a shoe two sizes smaller than one's normal size (but only for a short period of time) is of importance in some forensic contexts. When a footwear print is identified as a size 7 or 8 and it appears to be a men's shoe, we should also consider the possibility that a woman was wearing those shoes. Only a small percentage of men wear sizes 7 and 8, approx 6 and 9%, respectively (unpublished study by the author). The investigator may need to determine whether the foot impression/shoe print was produced by a man or woman and at times that may not be possible to absolute certainty. In the context of forensic evaluations, however, all of these factors—including improper shoe fit, biomechanical imbalances, and the subsequent pathologic changes in the foot—will make themselves known in the examination of the footwear.

While there are thousands of new shoe styles introduced to Americans each year, they are only variations of eight basic shoe types: the boot, pump, sandal, mule, clog, monk strap, moccasin, and oxford. Moreover, the latest of these styles—the oxford—is almost 300 yr old *(8)*. The basic shoe components have remained the same over the years, with changes in some components due to newer, more durable, and lighter-weight materials.

Shoe components are as follows:

1. The shoe upper. This is the visible part that covers the foot. The makeup will vary depending on the shoe style. Athletic type shoes (Fig. 4) may use cloth, nylon, or semi-synthetic materials. Dress/fashion/style-oriented shoes may be made in a large array of materials.
2. Insole board. This is the surface upon which the foot directly rests. It is necessary in shoes that are constructed using cement-lasted or Goodyear welt techniques, because it is the attachment for upper and lower components *(8)*.
3. Sock liner. Athletic footwear will often have a sock liner (Fig. 4), a piece of material placed over the top of the insole board *(11)*. It may be glued in position or it may be removable. In slip-lasted shoes, however, there is no insole board, and the sock liner lies directly on the midsole *(11)*. The sock liner decreases friction between the insole board and the plantar surface of the foot, assists in shock attenuation, and absorbs perspiration *(11)*. The ability to absorb perspiration and thereby leave an image of the foot is greatly aided by the large number of sweat glands on the plantar aspect of the foot as well as the forces applied with daily activity, shoe confinement, and body weight.

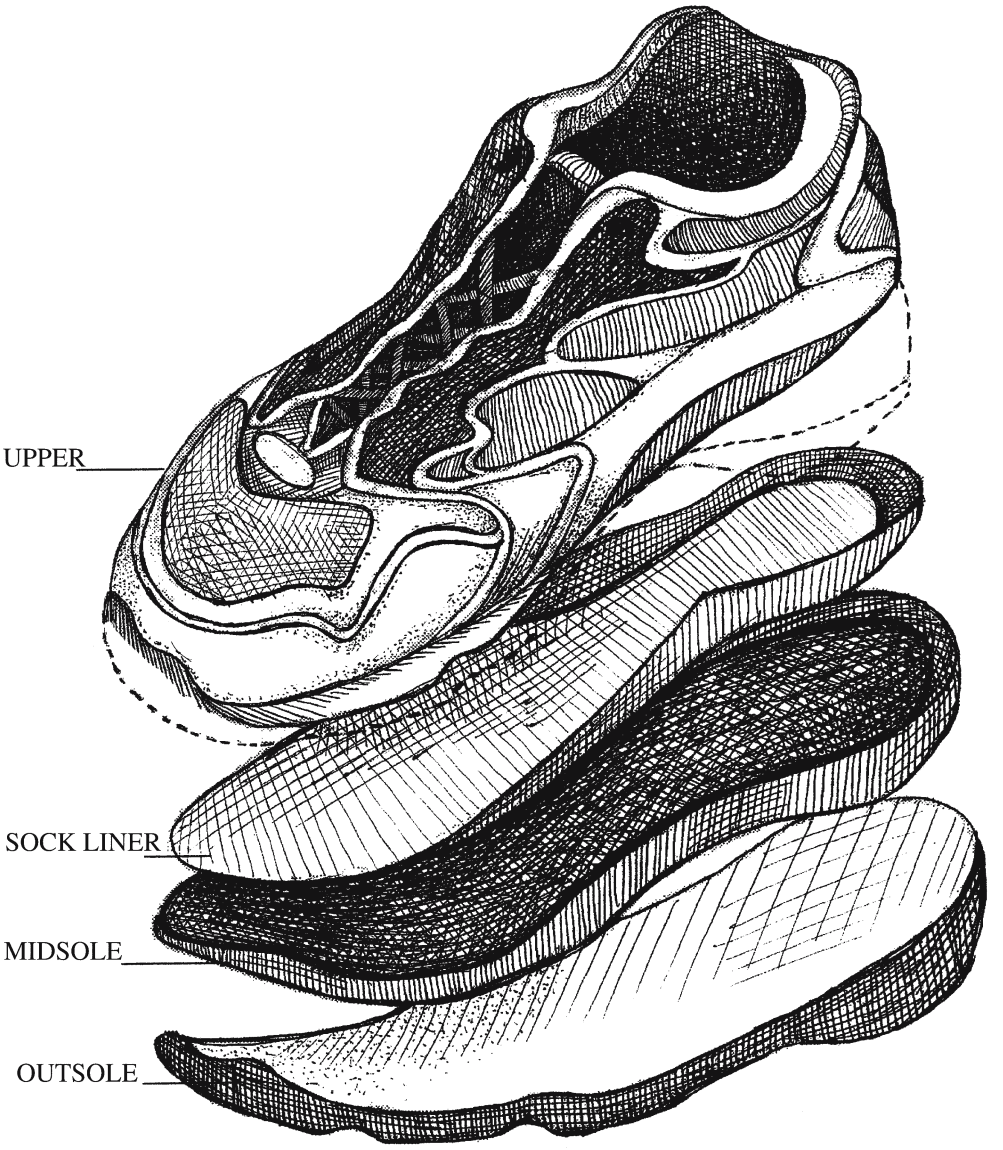

Fig. 4. Main shoe components of an athletic shoe. The sock liner is often the most important component in forensic identifications.

Many materials are used for the sock liner component. In the past, they were most often sponge rubber, vinyl, and latex materials covered with a very thin layer of terry cloth or nylon. More commonly in dress casual, running shoes, and many sports type shoes, where the materials are generally of a higher quality, the sock liner is removable from the shoe. The most common materials now used include closed-cell rubbers, open-cell polyurethane foam, and closed-cell polyethylene foam; ethylene vinyl acetate is also used. A potential advantage of these newer materials is that they are more durable, wear longer, and show a better foot image in both two and three dimensions. Other materials may wear faster and must be replaced on a regular basis, but can still

show a definable foot image. The foot image may be two-dimensional, three-dimensional, or a combination of the two. Some of the more impressible materials will show a depth impression of the foot, especially in the forefoot area (ball and digits). The foot image may be visualized, within a relatively short period, in some cases days, to the point that it may be of evidentiary value. This shoe component, the sock liner, in fact may be the most important part of the shoe forensically. If two individuals were supposed to have worn the same shoe, it may be possible to see a second image on the sock liner, but this depends greatly on how long the shoe was worn by the second individual and under what conditions.

4. Midsole. The midsole, which is a component of an athletic type shoe, is often made of polyurethane or ethylene vinyl acetate and may show some three-dimensional wear if the shoe is cut apart for examination.
5. Outsole. The outsole material varies according to shoe type. Athletic shoes commonly use carbon rubber or blown rubber, which are both durable and usually will not show appreciable wear for a long period except under extreme circumstances. Leather outsoles usually show the best wear patterns, and at times a clear image of the foot including the digits and ball area may be evident on the outsole. Other materials are available; for example, work shoes and dress casual shoes often use Vibram®, which is a popular soling material. This material may show wear fairly well, which may assist in forensic analysis.

As stated earlier, footwear is an important part of pedal evidence. There is a close association between the foot and shoe, in that they almost function as a single unit. The shoe is in a way an extension of the foot and functions in harmony with the foot during ambulation. The shoe is often a mirror image of the foot that it housed and much can be learned about the individual who wore it. In many cases, when perpetrators wear their shoes for a long period of time it generally leads to a good amount of wear both inside and outside, in fact, sometimes too much. There are times when the shoe is so worn it is of no value to the forensic evaluation.

6. Examination of Pedal Evidence

6.1. Types of Pedal Evidence

Pedal evidence comprises physical evidence relating to the human foot, with or without footwear. It may present in impression and print form. Impression evidence, being three-dimensional in nature, may be discovered in different materials and on varying surfaces. The substrate must be impressible to allow for depth, as well as length and width. Mud, sand, wet soil, and carpet, for example, may exhibit an impression. We expect to find barefoot impressions, sock-foot impressions, or shoe outsole impressions, but as we know, it takes a good investigator to discover them.

A three-dimensional impression may be evident on the sock liner of the shoe. Two-dimensional footprints or shoe prints are more prevalent on a hard surface, such as a tile floor or concrete walkway. A bloody trail can be most important and may present as a bare footprint, sock footprint, or footwear outsole print. The shoe may also be evaluated secondary to foot contact within, leading to wear on inner surfaces as well as very important wear on the sock liner or footbed component of the shoe. A bloody bare footprint with adequate friction ridge skin can be as identifiable as a fingerprint; unfortunately, such a find is a rare occurrence.

6.2. The Forensic Team

The forensic team may include a police officer or detective, a crime scene specialist or criminalist, a footwear examiner, and an attorney. A professional tracker may be of value in certain situations. If the team is working for the defense, it may include a private investigator, a criminalist from a private laboratory, other forensic specialists, and the attorney. The footwear examiner specializes in footwear evidence and is trained to make an identification that involves class characteristics or individual (random or accidental) characteristics on the outsole. This individual must have expert knowledge of manufacturing techniques for different shoes, which can often be an important part of the evaluation. Certification in the field is now available for those specializing in footwear evidence. The footwear examiner should be responsible for footwear-related evidence when the outsole evaluation is required and seeking appropriate podiatric medical consultation, if it is foot related.

7. The Basis of the Forensic Examination

A forensic evaluation leads to a determination of a common origin between two specimens and may establish positive identification. A questioned (unknown) specimen is used in a comparative analysis with a known specimen. To establish an identification, the morphology of the foot must be distinct from that of other individuals. The foot is genetically manufactured; therefore, even the anatomical, morphological, and biomechanical configuration of identical twins is different.

7.1. Class and Individual Characteristics

The forensic examination begins with an agreement of class characteristics. A class characteristic is something that is common to all specimens in a given group—in this instance, the group consists of feet. All feet have a size and shape, a heel or rearfoot region, an arch or midfoot area, and a forefoot area. The forefoot (as discussed earlier) is composed the metatarsophalangeal joint area (ball), including the five digits. An individual characteristic is typically something that is unique to one object and not present in other objects in a similar group, thereby leading to individualization and identification. In pedal evidence, the presence of a sixth toe or absence of a toe are extremely rare and would be considered individual characteristics because of their uncommonness.

In footwear, class characteristics include the tread pattern, logo, size, and shape of the outsole. Individual characteristics include things that are not normally part of the outsole, such as a pebble embedded in the outsole, a cut mark from a piece of glass, or a wear pattern suggestive of a foot problem. Some of these are considered accidental because of the way they are formed. Manufacturing characteristics that are present in a production run of shoes may also show randomness to help in the identification process. Similarly, a scar on the plantar aspect of the foot secondary to a laceration from a piece of glass or a puncture wound could be considered an accidental characteristic, but is still unique. The presence of unique characteristics in the foot is limited. What is known as an intermediate class characteristic falls between class and individual characteristics. Intermediate class characteristics relative to the foot include, for example, digital positioning secondary to pathologic abnormality, such as a hammer toe deformity (Fig. 3). One foot may have a significant

number of variations. Considering the digital positioning, size, and shape of just one toe, there is a significant number of possible differences. The aggregate number of intermediate class characteristics adds to the level of certainty of pedal evidence.

7.2. ACE-V

The acronym "ACE-V" (analysis, comparison, evaluation, and verification of evidence) denotes the scientific methodology used to arrive at a determination for identification purposes. ACE-V has weathered court scrutiny in fingerprint identification and can be applied to all disciplines where comparison techniques are used to make an identification. Common practice in most crime laboratories dictates that when a positive identification is made on a fingerprint, verification is required. This is also becoming a requirement in other forensic disciplines.

7.3. Analysis of the Questioned Item

The analysis involves the "dissection" of an item into its component parts, properties, and characteristics that can be directly observed and measured. The analysis of the questioned item is always performed before any examination on the known item. In pedal evidence, one is evaluating a bloody footprint or sock liner image to determine the quantity and quality of the image and whether it is sufficient for comparison purposes. A good number of marks or images may be present, but is there sufficient clarity (detail) to use them all? Every aspect must be evaluated and then recorded using photographs and casts of impressions, where applicable, as needed for comparison. Measurements can be taken to estimate, for example, possible height of the perpetrator, foot and/or shoe size. Once the findings are noted, they are compared with known standards to make a final determination.

7.4. Pedal Evidence and Forensic Considerations

The crime scene often involves serologic evidence, such as blood. A gait pattern may be visible in the blood, showing either a bare or socked foot. Many variations may present themselves at one crime scene: a full print of one or both feet or a partial print of, for instance, the forefoot area of one foot and the heel of the other. Some factors to be considered (again, depending on their presentation and the abilities of the evaluator) include step length, stride length, and foot plant. If there is a sufficient number of successive steps, it may be possible to determine, among other things, whether the suspect was walking or running.

Asymmetry in step length may be an indication of disability, limb-length discrepancy, or injury. We can determine the direction of travel, number of suspects, and whether the individual was walking backwards or back and forth. Out-toeing or in-toeing beyond the normal amount and other factors, which may not in themselves be conclusive, will add to the weight given to the ultimate identification. If a high-quality total-contact footprint is visible and the length can be measured, then height can be estimated, although not calculated exactly. Studies performed by Giles and Vallandigham *(12)* and Gordon and Buikstra *(13)* both include referencing the shoe size to height. Estimation of weight is more difficult to ascertain and has not proven very reliable.

Most footprints have to be considered as being made in a dynamic state or at least with body weight applied. In the weight-bearing foot, soft tissue expansion occurs. The amount of soft tissue between the underlying bone and the epidermis is quite uniform in most individuals and is relatively the same in both sexes. It is possible to estimate the shape of the foot and proper length of the digits from a bare bloody footprint, but there are always exceptions to the rule.

The foot image on the sock liner of the shoe is formed in both the static and dynamic state. Because the average individual takes approx 8000 steps daily, the image is more of a dynamic representation of the foot. Also distinguishable in a footprint are digital length, digital position, and the shape of the toes. Increased areas of pressure due to the presence of a plantar lesion—e.g., an intractable plantar keratosis, callus, or verruca plantaris (wart)—may leave an indentation in the sock liner. The quality of the print or impression is important, especially the clarity and sharpness of the identification lines (Fig. 5) such as the arch line, heel line, web ridge-line, and the web space outline (primarily visible on the sock liner). The web ridge-line is very individual and, depending on its quality, can be quite important. Whether it can be determined from the footprint if it was produced by a male or female is most commonly based on the size of the impression. Men's feet are generally longer and wider than women's feet. As previously stated, however, women's feet have generally increased in average size over the past few years, so at times a woman's footprint or shoe print is indistinguishable from a man's and, therefore, this parameter can only be used to infer the subject's gender.

If an item of footwear is involved, then the sock liner is analyzed in a similar manner to a bare footprint. The size of the shoe the individual is wearing can be correlated with height—again, within certain parameters. The upper of the shoe is evaluated for distinctive wear secondary to any pathologic change in the foot, such as a bunion deformity or hammer toe deformity, which will also show, in many cases, coincidental wear on the inside upper or actual bulging or deformity of the shoe in that area. Haglund's deformity, which is a bony enlargement on the posterior aspect of the calcaneus, commonly will result in wear in the center to lateral portion of the inside counter of the shoe. This deformity is also related to a biomechanical problem, specifically a compensated rearfoot varus deformity, which may be discovered in the suspect after biomechanical evaluation. The outsole is subject to both extrinsic and intrinsic influences. Wear can be influenced by occupation or certain activities that may put excessive weight on one part of the shoe or the other. For example, skate boarding may cause excessive posterior heel wear on one side or the other if the shoe is used for braking.

Environmental factors and poorly manufactured footwear may lead to altered or accelerated wear. Intrinsic wear is secondary to biomechanical influences and pathologic change. The outsole needs to be evaluated for a certain amount of normal wear first. Typically, wear is noted in the ball area of most shoes inferior to the second, third, and fourth metatarsal heads. Anticipated wear secondary to a moderate to severe cavus or valgus foot is not unusual. Asymmetric wear in most cases is caused by a limb-length discrepancy, disability, or injury. Different wear patterns are anticipated in a valgus type foot when there is abduction present vs no abduction. The composition of the outsole will also lead to a clear picture of different wear patterns and pathologic entities. The carbon

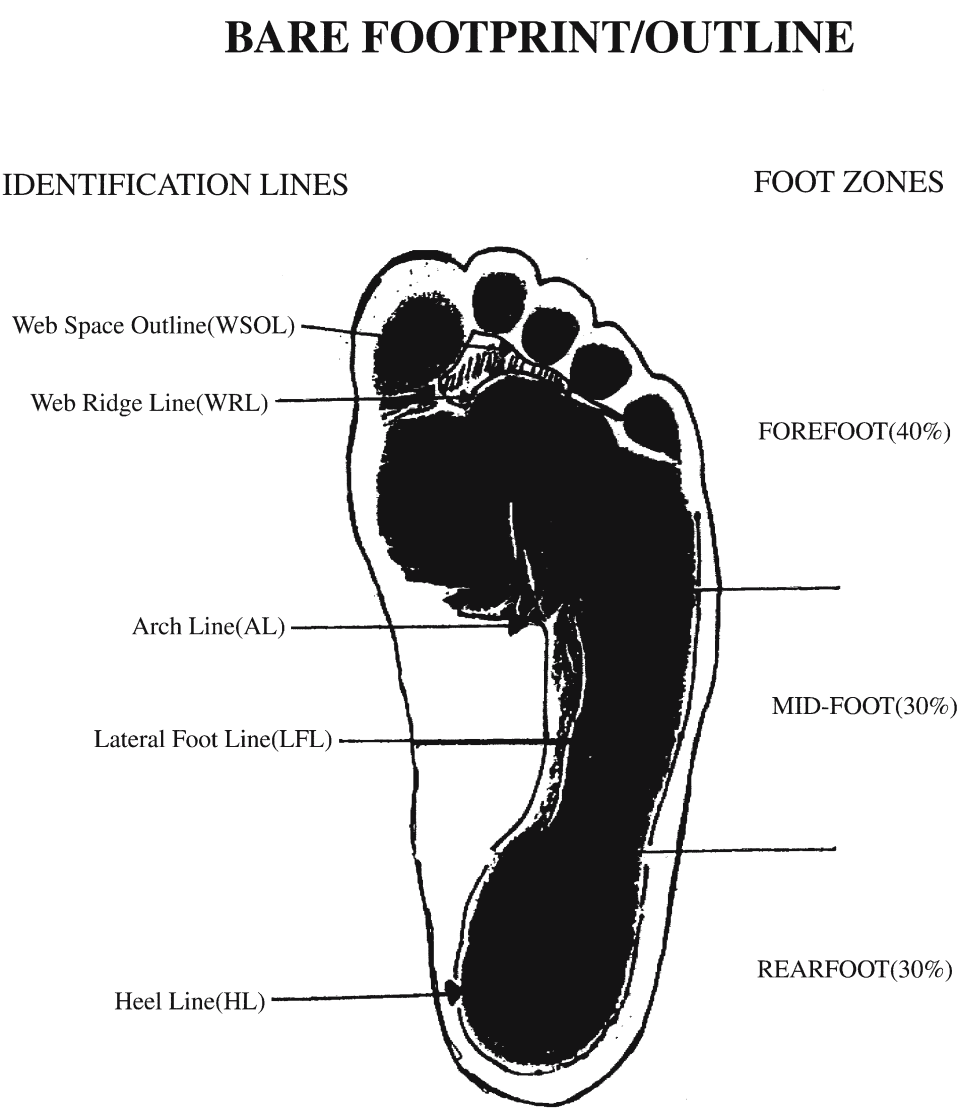

Fig. 5. Bare inked footprint with foot outline. The lines as indicated are very important in the comparative process, especially the web ridge line (WRL). The foot zones can be used in matching foot size between an unknown and known footprint or used to check proportional accuracy of an unknown or even to a known standard.

rubber outsole on many running shoes may not show appreciable wear for many miles of use and then wear may be minimal, especially if worn for general use. Typically, wear on a leather outsole is easier to visualize, and often the entire image of the foot is present.

7.5. Fabrication of Known Standards

An unknown fingerprint must be compared with the fingerprint of a known individual to make an identification. The same applies to pedal evidence. Any individual who is a suspect, in many cases already in police custody, or who left evidence of his

or her presence at the scene or some other related location, may need to be evaluated and required to give standards against which the unknown can be compared. If possible, the forensic podiatrist should be involved in this process. Although laboratory personnel are competent to perform many tasks, there are times when a specific technique and specialized medical expertise is required.

Photographs of the pedal evidence are taken of different positions, including the plantar aspect. Inked bare footprints, standing weight, or one step are taken with the soft tissue outlined with a thin lead pencil held perpendicular to the weight-bearing surface. This procedure is very important and needs to be performed accurately. Casting foam is used to create a weight-bearing impression, which may be taken in a step-down manner or after taking one step. These negative impressions will be filled with dental stone to create positive casts of the feet.

Radiographs, as discussed in detail in this text, represent an important tool for identification and may be taken at this time, if the circumstances warrant. An inked gait pattern is also important, especially if there is a walking pattern or some steps at the scene. However, it should always be made because it gives the most accurate representation of the dynamic foot that can be used in the comparison process. The gait pattern must be meticulously recorded. The gait pattern should be recorded at least three separate times, as should any other static or dynamic impression or print. This repetition will show the reliability of the technique and the reproducibility of the standards. The best technique is to apply black ink with a roller to the entire plantar aspect of the foot. White butcher-style paper or brown wrapping paper approximately 20 ft long and 3 ft wide is satisfactory. Most subjects will take eight to ten steps; usually the mid-pattern steps taken offer the best representation of the gait. The subject needs to be observed to ensure that there is no self-created change in foot plant, and step length. It is a good idea to ask questions such as, what is your date of birth, while the subject is performing this task for the purpose of taking their mind off what they are doing in case they are not cooperating or attempting to walk differently. Videotaping the entire process is also valuable, in case there are any discrepancies that need clarification later. A force-plate system yields more technical information, if needed. Specific areas of increased weight leading can be recorded and compared possibly to an area in the sock liner. In addition, the foot contact area can be compared with a bloody footprint, for example, to indicate how accurate our unknown is regarding the percentage of foot plant. Gait analysis can be further enhanced by using one of the portable in-shoe sensor systems. If bloody footprints are from a socked foot, then all standards are recorded with the subject wearing a sock or other type of hosiery.

Foot measurements can be taken with an appropriate measuring device. During these procedures, the podiatrist observes the individual, giving special attention to the weight-bearing attitude of the feet and anything that might be important in substantiating findings in the questioned evidence. During some of these procedures, the foot may be biomechanically evaluated, at a minimum to classify it in one of the biomechanical and morphological foot types.

If footwear is involved, then a representative sample of the subject's shoes must be obtained. It is best to recover shoes similar to those associated with the crime scene shoes. It is never appropriate for anyone to try on the unknown shoe for testing purposes. Photographs, foam outsole impressions that can be cast with dental stone to create a

positive model of the outsole, and inked outsole prints may be required and often will be best used by the footwear examiner. The sock liner, if exhibiting a three-dimensional impression, may be cast with a thin layer of dental stone to reproduce the indentations quite accurately. The sock liner needs to be photographed and enhanced by the laboratory. An examination quality photograph is then produced.

It may be necessary to create some test impressions using one's own feet to account for certain discrepancies or other things that might be evident in the crime scene prints in order to logically explain a certain activity that took place at the scene. The importance of recording accurate measurements cannot be overstressed.

7.6. Comparison and Evaluation

The comparison analysis is designed to determine whether the questioned specimen and known specimen were made by the same individual. Protocol calls for the known specimen to be compared with the questioned specimen. The overlay technique is commonly used to make a direct comparison of pedal evidence. A transparency of the known sock liner or inked footprint is compared with the questioned sock liner itself or a photograph of it. An examination-quality photograph, for example, of bloody footprints is compared with a transparency of the known standard.

Footprint and foot impression evidence presents in both two-dimensional and three-dimensional form, and it is best to compare known with unknowns of the same number of dimensions. If one recovers a foot impression in dirt that was cast with dental stone, then it is best to compare it to the known positive cast of the foot. A transparency overlay can be used to create a direct tracing of both specimens and to make a comparison. There are instances when a two-dimensional print may also be compared with a three-dimensional foot mold, but only with knowledge of tissue expansion and other factors can a valid comparison be made. The sock-liner impression can be three-dimensional; however, depending on its composition or duration of wear, the depth impression may be negligible. Other methods of comparison include measurement techniques. Direct measurements can be made using a ruler, but it's usually better to use a grid system. Random subjects' standards are also used. If, for example, we have an estimated size 10 male footprint, then a number of size 10 inked standards are used to show the many differences inherent in footprints taken from a data bank of exemplars. Standards taken from others, who perhaps lived with the victim or might have been at the scene for some reason, are compared with the questioned print and can be used to eliminate those individuals.

Medical or police personnel at a crime scene occasionally need to submit exemplars for exclusion purposes. We have performed the comparison and evaluation, and we must now make a determination or answer the question posed initially. For example, did this individual make the bloody bare footprint at the crime scene? Obviously, if there is a significant discrepancy that cannot be explained, we have an exclusion or a nonidentification. The forensic field is replete with differing opinions on how best to define the eventual determination or conclusion. For example, "possible," "very possible," "likely," "highly likely," "with reasonable medical certainty," and other terms are commonly used. Answering in the affirmative indicates an identification to some degree, but with an increasing number of intermediate class characteristics, one can

transcend to greater levels of certainty. If the opinion is in the negative, then it is a non-identification. An inconclusive determination can still be used. It is neither positive nor negative and might be applicable in a situation where a bloody footprint, for example, can neither be excluded nor identified satisfactorily.

7.7. Levels of Certainty

Level 1: Is it a footprint? If the answer is in the affirmative, subsequent questions may be as follows: Is it a partial or full, static or dynamic print or impression? Is there sufficient quantity or quality to continue? If the answer is still in the affirmative, then we proceed to the next level. If there is not an agreement in the response, it could lead to an inconclusive identification or nonidentification.

Level 2: General Agreement. Is there a general agreement in the size, shape, and position of the digits and foot zones? (Fig. 5). If the answer is in the affirmative, then we proceed to the next level.

Level 3: Identification Lines. Is there sufficient agreement of the web ridge line, arch line, lateral foot line, heel line, and web space outline? If the answer is in the affirmative, then we proceed to the next level.

Level 4: Intermediate characteristics. This is where the medical practitioner's clinical expertise and knowledge of pathological, morphological, and biomechanical imbalances or deviations are used. If the aggregate of findings are sufficient and can be verified, then we proceed to level 5.

Level 5: Individual characteristics are noted or level 4 with verification.

8. Case Presentation

TYPE OF CRIME: Homicide, 19-yr-old female

DATE OF OCCURRENCE: November 1996, Phoenix, Arizona

CASE HISTORY: Four female friends took an early morning drive in Phoenix, Arizona. After a failed attempt at strangling the victim, someone crushed her skull with a large rock, and the body was placed in a pond. Two different footwear impressions were discovered in soft dirt and photographed at the scene. The remaining three females, aged 15 to 18 yr, were arrested driving the victim's vehicle on November 20, 1996, and the shoes they were wearing were obtained by law enforcement for evaluation.

On November 21, 1996, four pairs of shoes were recovered from the victim's apartment.

On November 22, 1996, two pairs of shoes were recovered from the trunk of the victim's vehicle, along with other clothing items. The outsoles on these shoes gave impressions similar to those discovered at the scene, but could not be positively identified.

Subsequently, two pairs of the victim's shoes were given to the police by her parents to be used for the evaluation.

8.1. Objective

Can the following be determined from the evidence presented: (1) whether the suspects most likely wore the questioned shoes, and (2) who was the predominant wearer of each?

8.2. Methodology

Initial contact was in June 1998 by the case detective, at which time an evaluation of the questioned shoes was performed. There appeared to be sufficient quality and quantity of the footwear for podiatric medical evaluation to continue. The suspects were taken into custody and standards were collected including photographs, inked bare footprints with foot outlines, impressible foam foot impressions that were cast with dental stone to create positive molds of the feet, and foot measurements. Biomechanical and structural problems were observed at this time. The laboratory personnel produced examination quality photographs as requested, including photographically enhanced images of the sock liners of the questioned footwear. Eleven pairs of shoes were examined. The questioned shoes were a brand name canvas off-court casual sneaker size 5.5, and a designer athletic type shoe with a thick outsole, the left shoe measuring 5.0 and the right shoe measuring 5.5. Other shoes included two pairs known to belong to the victim, as well as several possibly belonging to the victim, and also some possibly belonging to one of the suspects, who had lived for a short period of time with the victim. Analysis of the questioned items was performed initially. A sock liner image was visible in each shoe, as well as some inner liner wear in the toe box area of one shoe.

The inked footprints and the foot molds were compared with the foot images present on the sock liners of the questioned shoes. The pair of shoes recovered from the trunk of the vehicle appeared to be the shoes that left the impressions at the crime scene. The suspects denied that these were their shoes. These shoes, in fact, were comparable to the foot size of the suspects. (The third suspect was not involved in the actual murder but was standing by at the car. She happened to be wearing a walking cast after sustaining a sprained ankle several days before the crime was committed and was wearing a shoe on her other foot. Her shoes were approximately two sizes larger than the questioned shoes.) Using comparisons of the known exemplars to the questioned sock liners and other footwear components, in addition to the biomechanical findings, foot measurements, and pathologic changes noted, a conclusion in the affirmative was made.

This case was particularly challenging because of the morphologic similarities of the suspects' feet. However, one suspect had a bunion developing and a long second toe that already had a fairly well-formed hammer toe. It was determined that the footwear recovered from the trunk of the victim's vehicle at the time of the arrest belonged to the two main suspects, each suspect being the predominant wearer of an individual pair of the questioned shoes. Moreover, one of the suspects was actually wearing a pair of the victim's shoes at the time of their arrest. Placing the suspects in their shoes, which were considered to be the shoes that left the impressions at the crime scene, was one piece of the circumstantial evidence that ultimately led to a conviction in this homicide.

APPENDIX

Foot:

Abduction. Movement of a body part (e.g., the foot) away from the midline of the body.

Adduction. Movement of a body part (e.g., the foot) towards the midline of the body.

Biomechanics. The application of mechanical laws to living structures, specifically to the locomotor functions of the human body.

Distal. Farthest away from the central location of the body or part in question, e.g., the toes are distal to the heel.

Dorsal. Toward the front. In the foot, the upper surface of the foot.

Dorsiflexion. Upward bending (flexion) of the foot.

Eversion. Tilting away from the midline of the body, e.g., the plantar surface tilts away from the midline of the body, thereby lowering the inner border of the foot.

Inversion. Tilting toward the midline of the body, e.g., the plantar surface tilts toward the midline of the body, thereby elevating the inner border of the foot.

Intractable plantar keratosis (IPK). A deeply nucleated keratotic lesion on the bottom of the foot that may leave its mark as an area of increased pressure on a receiving surface.

Lateral. Farther from the midline of the body.

Medial. Nearer to the midline of the body.

Metatarsalgia. A term denoting pain in the metatarsal area secondary to a variety of conditions. Often, the associated prominence of the metatarsal heads toward the plantar surface can lead to an area of increased pressure that can have forensic implications.

Plantar. Pertaining to the sole of the foot.

Plantar flexion. Downward bending of the foot.

Plantar verruca (plural, plantar verrucae). Plantar wart: lesion that appears on the bottom of the foot and leaves its mark as an area of increased pressure or a break in continuity on a receiving surface.

Pronation. A triplane motion of the foot consisting of abduction, dorsiflexion, and eversion of the calcaneus; often called a valgus (flat) foot type.

Proximal. Nearest to the central location of the body or the body part in question, e.g., the heel is proximal to the toes.

Rectus. Straight position.

Running. Double-float phasic gait.

Step length. The distance between one foot plant and the next, e.g., right foot to left foot.

Stride length. The distance between one foot plant and the next of the same foot, e.g., from a right foot plant to the next right foot plant.

Subtalar joint. Joint between the talus and calcaneus bones in the foot.

Supination. A tri-plane motion of the foot consisting of adduction, plantar flexion, and inversion of the calcaneus; often referred to as the cavus ("high arch") foot type.

Valgus. An abnormality or deformity characterized by foot turned or forced outward; used to describe a pronatory attitude ("flat foot").

Varus. An abnormality or deformity in which the foot is turned or forced inward; used to describe supination ("high arch").

Walking. Double-stance phasic gait.

Footwear and Miscellaneous:

Adhesive lifter. Adhesive-backed paper that can be used to "lift" a footprint from a given surface.

Amido black. Chemical agent that can be used to enhance bloody footprints.

CA fuming. Cyanoacrylate ester/superglue: A method used to detect and stabilize fingerprints; also used on the sock liner of the shoe for the same purpose.

EVA/CREPE (Ethylene vinyl acetate). A versatile lightweight soling material that is also used as a sock-liner component of shoe.

Gelatin lifter. Adhesive backed thin gelatin sheet used to "lift" a footprint from a hard surface.

Impression. A mark made by pressure.

Polyurethane (PU). A very versatile long-wearing material soling material also can be used for sock liner component and midsole component.

Print. An impression with ink.

Standard (exemplar). Any type model or example for comparison.

References

1. Weinstein F. Principles and practice of podiatry, Philadelphia: Lea and Febiger, 1968.
2. Cassidy MJ. Footwear identification. Salem, Ore: Lightning Powder Co., 1995:138.
3. Vernon DW, McCourt FJ. Forensic podiatry: a review and definition. Br J Podiatr 1999;2:45–48.
4. Rich J. Increasing the identification potential from human foot remains. J Forensic Sci 45;506–507 (2000).
5. Nirenberg MS. Forensic methods and the podiatric physician. J Am Podiatr Med Assoc 79;247–252 (1989).
6. Bodziak WJ. Footwear impression evidence. New York: Elsevier, 1990.
7. Hilderbrand DS. Footwear: the missed evidence. Temecula, Calif: Staggs, 1999.
8. Rossi WA, Tennant R. Professional shoe fitting. New York: National Shoe Retailers Association 1993:1–9.
9. Steen EB, Montagu A. Anatomy and physiology. New York: Barnes and Noble, 1969.
10. Valmassy RL. Clinical biomechanics of the lower extremity. St. Louis, Mo: Mosby–Year Book, Inc., 1996:86–93.
11. Cavanaugh PR. The running shoe book. Mountain View, Calif: Anderson World, Inc., 1980.
12. Giles E, Vallandigham, PH. Height estimation from foot and shoe-print length. J Forensic Sci 36:1134–1151 (1991).
13. Gordon CC, Buikstra JE. Linear models for the prediction of stature and boot dimensions. J Forensic Sci 37:771–782 (1992).

Further Reading

Abbott J. Footwear Evidence. Springfield: Charles C. Thomas; 1964.

Bowers MC, Bell GL. Manual of Forensic Odontology. 3rd ed. Ontario, Canada: Manticore; 1997.

Black HC. Black's Law Dictionary [abridged]. 6th ed. St. Paul, MN: West; 1991.

Bodziak WJ. Footwear Impression Evidence. New York: Elsevier; 1990.

Cantor JD, Benjamin J. The Role of the Expert Witness in a Court Trial. Belmont, Mass: Legal Evidence Photography Seminars; 1997.

Cassidy MJ. Footwear Identification. Salem, Ore: Lightning Powder Co.; 1995.

Cavanaugh PR. The Running Shoe Book. Mountain View, Calif: Anderson World, Inc.; 1980.

DiMaggio JA. Prints of Thieves. BioMechanics Magazine 2000;9:16–26.

DiMaggio JA. Forensic Podiatry and Barefoot Evidence. Presented at: the First International Conference on Forensic Human Identification in the Millennium; October 1999, London. Available at: www.fss.org.uk.

DiMaggio, JA. Forensic Podiatry: An Emerging New Field, J Forensic Identification, 1995;45:495–497.

Donatelli R. The Biomechanics of the Foot and Ankle. Philadelphia: FA Davis; 1990.
Doyle, Sir AC. A Study in Scarlet. In: Sherlock Holmes: The Complete Novels and Stories. Vol. 1. New York: Bantam Books, Inc.; 1986:100.
Eckert, WG. Introduction to Forensic Sciences. 2nd ed. Boca Raton: CRC Press, 1997.
Fisher, Barry A.J. Techniques of Crime Scene Investigation. Boca Raton: CRC Press, 1993.
Gerard WVM. Foot and Fingerprints. Pedic Items 1920; March:1–3.
Giles E, Vallandigham PH. Height estimation from foot and shoe-print length. J Forensic Sci 1991;36:4;1134–1151.
Gordon CC, Buikstra JE. Linear models for the prediction of stature and boot dimensions. J Forensic Sci 1992;37:771–782.
Gorman, M. If The Shoe Fits. Podiatry Today. 1997;9: 28–33.
Gunn N. Old and new methods of evaluating footprint impressions by a forensic podiatrist. Br J Podiatr Med Surg 1991;3:8–11.
Haglund WD, Sorg M. Forensic Taphonomy. Boca Raton, FL: CRC Press, Inc.; 1997.
Hilderbrand DS. Footwear, the missed evidence. Temecula, CA: Staggs; 1999.
Laskowski GE, Kyle VL. Barefoot impressions: a preliminary study of identification characteristics and population frequency of their morphological features. J Forensic Sci 1988;33:378–388.
Lesce, T. Forensic Podiatry: A New Field. *S.W.A.T.* 1992:70–73.
Lucock LJ. Identification from footwear. Med Sci Law 1979;19:225–230.
Matson, JV. Effective Expert Witnessing. Chelsea, MI: Lewis Publishers Inc, 1990.
McGlamary ED. Comprehensive textbook of foot surgery. Baltimore, MD: Williams and Wilkins; 1987.
Muir E. Chiropody in Crime Detection. The Chiropodist 1935;22:165–166.
Perry J. Gait analysis: normal and pathologic function. Thorofare, NJ: Slack Inc.; 1992.
Pickering RB, Bachman DC. The use of forensic anthropology. Boca Raton, FL: CRC Press, Inc.; 1997.
Rabinof MA, Holmes SP. The forensic expert's guide to litigation. Danvers, Mass: LRP Publications; 1996.
Root ML, Orien WP, Weed JH. Normal and abnormal function of the foot. Vol. 2. Los Angeles: Clinical Biomechanics Corporation; 1997.
Rossi WA, Tennant R. Professional shoe fitting, New York: National Shoe Retailers Association; 1984.
Rossi WA. Podometrics: a new methodology for foot typing. Contemporary Podiatric Physician 1992;128–39.
Sacks ME. An overview of the law: a guide for testifying and consulting experts. Danvers, Mass: LRP Publications; 1995.
Saferstein R. Criminalistics: an introduction to forensic science. 4th ed. Englewood Cliffs, NJ: Prentice-Hall, Inc.; 1999.
Sarrafian SK. Anatomy of the foot and ankle. Philadelphia: JB Lippincott; 1983.
Steen EB, Montagu A. Anatomy and physiology. New York: Barnes and Noble; 1969.
Ubelaker D. Bones: a forensic detectives casebook. New York: Harper Collins; 1992.
Valmassy RL. Clinical biomechanics of the lower extremity. St. Louis: Mosby–Year Book, Inc.; 1996.
Vernon DW, McCourt FJ. Forensic podiatry: a review and definition. Br J Podiatr 1999;2:45–48.
Weinstein F. Principles and practice of podiatry. Philadelphia: Lea and Febiger; 1968.

Chapter 14

Ongoing Research Into Barefoot Impression Evidence

Robert B. Kennedy

1. Introduction

Ongoing research in barefoot impression evidence will be discussed briefly. Further research is necessary to shed light on what constitutes a "unique" (individualizing) feature between barefoot and footwear evidence and to determine if these features are merely consistent with any individual or if they truly constitute an identification. Such research is critical because this evidence might not be accepted in some jurisdictions or may be at risk of not meeting the Daubert criteria in the United States and the Mohan standard in Canada.

In 1989, convicted murderer Alan Legere escaped from the Atlantic Institution in Renous, New Brunswick, Canada while being escorted to the hospital for an ear infection. During the next 6 months, he killed four people, spreading fear throughout the Miramichi region of New Brunswick. One of his victims, Father Smith, was found murdered in the rectory of a Catholic church in Chatham Head, New Brunswick. At the crime scene, bloody impressions from a pair of boots showed enough detail that they could be identified as the boots worn by the killer—if they could be found.

About a week after the murder, a pair of work boots that had been discarded was found behind a motel approx 60 mi from the murder scene and was subsequently matched to the crime scene by way of accidental characteristics on the outsole of the boots. The boots were cut apart in a search for any evidence that might link the owner of the boots to the scene. Barefoot weight-bearing impressions were evident on the insole of the boots, and it appeared that the impressions were of suitable quality for comparison with a suspect barefoot impression. Upon further examination of the inside

From: *Forensic Science and Medicine*
Forensic Medicine of the Lower Extremity: Human Identification and Trauma Analysis of the Thigh, Leg, and Foot
Edited by: J. Rich, D. E. Dean, and R. H. Powers © The Humana Press Inc., Totowa, NJ

Fig. 1. Nail in heel area of the footwear damaged the barefoot of Legere, as indicated by a dimple in the cast.

of the boot, a nail was found protruding through the heel area that appeared significant enough to cause damage to the foot.

When Legere was arrested in 1989, inked barefoot and molded impressions were taken of his feet. It appeared that a scar on the heel of Legere's foot was the same shape and in the same area as the nail protruding through the heel area of the boot (Fig. 1). The inked weight-bearing areas of Legere's bare foot were consistent with the weight-bearing barefoot impressions on the insole of the boot; this linked Legere to the boot and hence to the crime scene.

To get this barefoot morphology evidence introduced into a court of law, a detailed research project was undertaken by the Royal Canadian Mounted Police (RCMP) to prove that the inked weight-bearing areas of a human foot were unique to that person. A total of 1000 volunteers gave their inked barefoot impressions and all the relevant information was entered into a database. Each impression was searched through the database against all the others in the collection. No matches other than to that of the owner of the impression were found. The evidence was presented in court and Legere was found guilty.

2. OVERVIEW

Anyone committing a crime must walk around the crime scene, leaving footwear impressions and, at times, barefoot impressions, making the recovery of this type of evidence important. The human foot contains ridge detail similar to that found in a fingerprint. Forensic barefoot morphology involves the comparison of the weight-bearing areas of the bottom of a barefoot without such ridge detail, as in a fingerprint, to establish a link between the barefoot of an individual and an impression found in mud, blood, or some other medium at the crime scene or on the insole of a shoe that may have been linked to a crime scene. The elimination of an individual whose feet leave an impression that is not consistent with the crime scene impression is important to the judicial system.

2.1. History

The use of barefoot impression morphology in its current form by the RCMP had its origins in the Alan Legere case in 1989 *(1)*. Although extensive research into the individuality ("uniqueness") of barefoot impressions was not performed until last decade, barefoot comparisons were presented in court for many years.

2.2. Historical Cases

In 1948, two brothers—Donald and William Kett—were charged with a series of breaking-and-enterings in Canada. After Donald was convicted, William claimed he was innocent and that the shoes that were matched back to the crime scenes belonged to his brother. The shoes were cut open and the marks inside compared with the feet of the two brothers; it was determined that William, not Donald, had worn the shoes, and he was also convicted *(2)*.

In 1953, New Scotland Yard had a case in which a burglar left a pair of shoes behind at the scene of the crime. The main suspect denied ownership of the shoes and volunteered an old pair of his own boots for comparison. The outsole of the boots and the shoes exhibited the same unusual wear patterns. To compare the impressions on the inside, a casting material was poured into the shoes and boots, the casts were shown to be very similar, and the suspect was convicted *(3)*.

In 1962 in The Netherlands, a safecracker discarded the clothes he had worn while committing his crime by throwing them into a canal. The clothes, including a pair of shoes, were recovered and a prosecution expert compared the recovered shoes with the shoes from the suspect and concluded that they were worn by the same person. The defendant hired his own specialist, but was dismayed when his witness agreed with

the first expert. The defendant, who until this time had not agreed to have his feet photographed or printed, asked a third expert to examine his feet. Again to his dismay, this witness also agreed with the other two. The defendant was subsequently convicted *(4)*.

In a case in New Jersey in 1981, a bloody socked footprint found at the scene of a homicide was compared with the foot impressions of two suspects. One suspect had left a bloody fingerprint at the crime scene but was eliminated as the person leaving the bloody footprint. The second suspect's foot impression was compared and was found to be very similar to the print at the crime scene, leaving the expert to declare that there was a high probability that the second suspect left the impression at the murder scene. Both were convicted *(5)*.

3. Ongoing Barefoot Research

The purpose of the research described here is to study the outlines of footprints of persons walking and to determine whether one can prove that different people make verifiably distinct footprints. To support this hypothesis, a database of footprint outlines was compiled to provide a statistical basis for deciding whether the outlines of walking footprints of various people are distinguishable.

3.1. Potential of Bare Feet to Present Individualizing Features

In early casework, the individuality of human footprints was often assumed *(2,4,6,7)*, i.e., no two prints, even from the same individual, would be identical. RCMP research has shown that barefoot impressions from the same individual may remain unchanged over several years. Impressions from the insole of several pairs of footwear worn over a 25-year period were examined and showed little change in the weight-bearing areas of the foot. Impressions taken from individuals walking a distance of 20 feet show little or no change in the weight-bearing areas imprinted on paper. Barefoot impressions taken from several identical twins show that their barefoot impressions are distinct one from the other (Fig. 2).

A great deal of early research and casework in barefoot impressions was performed in India, probably because there people are more often barefoot or in sandals. For example, in 1965, Puri described his work of classifying and measuring barefoot impressions for comparison purposes *(8)*. In 1980, Qamra published the results of a preliminary study involving the measurement of the footprints of 725 individuals *(9)*.

3.2. Footprint Measurements

At its inception, footprint research involved an examination of anatomic characteristics such as stature. For example, Topinard estimated that on average a person's footprint length was equal to 15% of a person's height *(10)*. Gordon and Buikstra *(11)* analyzed the statures and foot lengths and widths of 867 soldiers in a combat boot-fitting study. Barker and Scheuer *(12)* investigated the Topinard estimate by collecting data from 105 seated and walking subjects.

Baba *(13)* studied 826 males and 1018 females to prove that there were significant differences in the ratios of breadth (i.e., ball width) to foot length and of ball girth to foot length between French and Japanese populations. The length of the foot was determined

Fig. 2. Barefoot impressions from identical twins show differences in placement of the toes and arch area.

to be the distance from the most posteriorly projecting point on the heel to the anterior tip of whichever toe gave the longest measurement. Hawes *(14)* studied ethnic differences between 513 Asian and 708 North American males. Their method of measurement was to have each subject place all of his weight on the right foot while the left foot was on a platform raised 25 cm higher than the one on the right. Calipers were used to measure the distance from the pternion to the tip of each toe, recording foot length as the maximum such measure. Breadth was measured between the first and fifth metatarsals in a plane perpendicular to the long axis of the foot. The reliability of foot measurements of

1197 Canadian subjects was studied, as well *(15)*. Kouchi and Mochimaru undertook a thorough study of 5000 Japanese footprints *(16,17)* and proved that there was a significant distinctive out-flaring of the Japanese foot, with a mean flexion angle of 8.4º. The individuality of feet was studied by Qamra *(9)*, Laskowski and Kyle *(18)*, Kennedy *(19–22)*, and Barker and Scheuer *(12)*.

The Federal Bureau of Investigation, specifically Special Agent William Bodziak, has presented evidence on barefoot morphology and has conducted research to help establish the potential individuality of barefoot impressions *(23)*. Bodziak's collection of impressions from 500 volunteers provided a starting point for studies of this nature. The RCMP has performed research regarding the individuality of barefoot impressions since 1989 and has extended this research considerably with the collection of samples from more than 12,000 volunteers who have given their barefoot impressions.

When the RCMP research began in 1989 *(21,22)*, impressions were traced by hand and measured with a ruler to obtain the 19 measurements needed. These measurements were entered into the database for each foot (e.g., overall length of foot from heel to longest toe, width of ball of foot, distance of toe pads from edge of heel). The system was capable of accepting these data and searching them against data already in the system to determine whether any other foot matched this set of data. With 5000 impressions in this database, no false matches were found. Each time, only the person being entered was found if his or her impression was already in the database. In 1994, this manual system was changed to an automated system in which the foot was scanned and automatically traced and measured by the computer. The number of areas measured went from 19 to approx 120 per foot (Fig. 3).

Initial research *(20,21)* indicates that bare feet have characteristics that may form the basis for identification and that these characteristics can be compared to eliminate or link a suspect to the scene of a crime. This research is statistical in nature and based on anatomic measurements; however, the actual forensic examination involves a comparison of the contours, shapes, and placements of parts of the foot, and the bare feet from different people may show a degree of individuality. In a study *(22)* based on the population from which our samples come, barefoot impressions show a high degree of individuality. The probability of a chance match was estimated to be less than 1 in 10^8. A subsequent analysis based on a larger sample size yielded a chance-match probability of 1 in 10^{11} (RB Kennedy et al., unpublished data). Of note, the mathematical database is used strictly for research purposes to establish the individuality of barefoot impressions.

The footprint impressions are collected from volunteers using a commercially available inkless pad and chemically treated paper. The pad is placed on the floor about one stride from the volunteer and the paper is placed approximately one stride ahead of the pad. The footprint impressions are taken in a one-step method not in a dynamic mode (i.e., walking mode). The volunteer walks toward the pad, steps on the inkless pad with one of his or her feet, and continues walking until that foot walks on the paper, creating a darkened impression. The process is repeated with the other foot so that we have a left and a right barefoot impression on each sheet of paper. The impressions are scanned and entered into a computer database. The computer program is capable of adding data to the

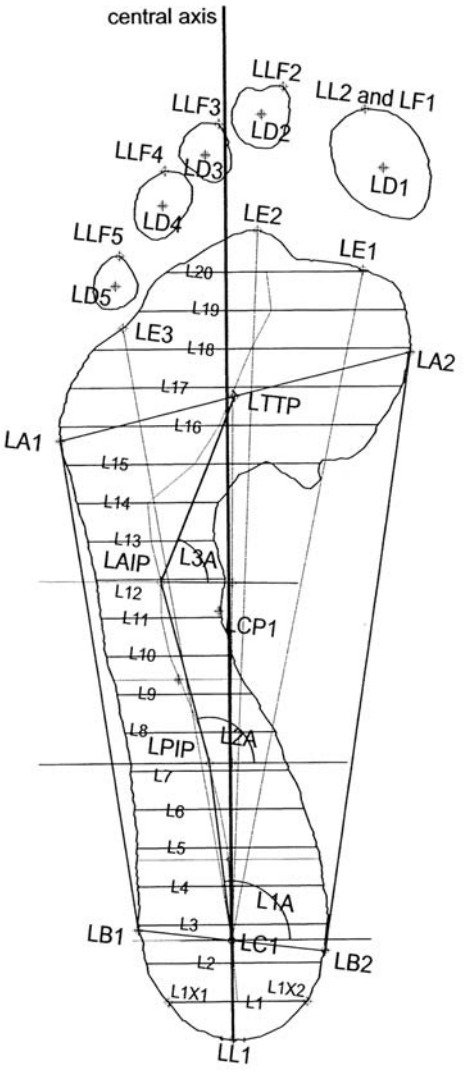

Fig. 3. Printout from the Royal Canadian Mounted Police database showing some of the areas measured during the processing of the barefoot impressions.

system and, as entry of new data takes place, it is searched against all the data presently in the system to determine whether a match exists. The system is capable of extracting data in any order for analysis by mathematicians and statisticians.

Damage or injury to the foot should be considered during the comparison process; it may explain a difference in impressions or produce an individualizing impression. Flexion creases on the foot can also be used to aid in the comparison and in sufficient number can be used to "individualize" the barefoot *(24)*. While partial impressions may not contain sufficient information to individualize a barefoot, they may still be useful evidence in a court of law and for the possible elimination of a suspect.

Fig. 4. Crime scene barefoot impression in dust.

4. Case Studies

4.1. Case Study 1

The investigation of a murder in Ontario, Canada, is an example of the comparison of a barefoot crime scene impression with a barefoot impression from a suspect.

Fig. 5. Inked barefoot impression from suspect.

The police received a report that a woman accidentally shot her husband as he tried to kill her. She contended that he went to the gun locker in the basement and returned to the bedroom carrying a rifle, with the intention of shooting her. She claimed that a struggle ensued and the rifle went off, killing him. The police found a set of barefoot impressions in dust on the concrete floor that led to the gun cabinet and then away. Barefoot

Fig. 6. Inked tracing of Fig. 6 overlaid on Fig. 5, the crime scene impression, showing consistency between the crime scene impression and the barefoot of the suspect.

impressions of the victim, his wife, and her sister were received and examined. It was determined that the barefoot impressions were too small to be the victim's and did not match the sister's, but did match the wife's barefoot impressions. These findings, along with other evidence gathered during the investigation, was presented in court, and she was subsequently found guilty of the murder (Figs. 4–6).

Fig. 7. Weight-bearing areas on the insole of two running shoes. Running shoes seized from the suspect with top removed **(A)** and running shoes (with the tops removed) found in the trash at the jail **(B).**

4.2. Case Study 2

A successful link between footwear from a crime scene and the accused was established in 1993, when an inmate in a prison in Quebec was found dead in his cell as a result of knife wounds in his neck and chest. Eighteen inmates lived in this section of the prison, providing a limited pool of suspects. Of the seventeen remaining prisoners, two brothers stood out as the prime suspects. The younger brother had only a short time left to serve, while the older brother, who then admitted to the killing, was serving a life sentence for murder.

A pair of blood-spattered running shoes, a pair of bloodstained jogging pants, and a nametag were found in the trash. The blood stains were eventually matched to the victim. Footwear and barefoot impressions were taken from both brothers and submitted, along with the running shoes found in the trash, to the Forensic Identification Research Services Section at RCMP Headquarters. The shoes were cut apart, and the impressions on the insoles were examined and compared with the barefoot impressions of the two suspects (Fig. 7). The older brother's impressions did not match those found in the running shoes, but the impressions of the younger brother were a good match. The case went to court, and the younger brother was found guilty and is presently serving a life sentence.

5. Summary

Barefoot morphology has been used successfully in jurisdictions to exclude or include a suspect as having been at the scene of a crime. This evidence is based on an evaluation of the shapes and placement of various weight-bearing parts of the foot. Although statistical research has been performed to establish the potential individuality of barefoot impressions to meet the stringent jurisprudence standards in the United States, Canada and elsewhere *(25)*, further studies may be necessary to help validate identification markers between the barefoot and shoe wear.

Acknowledgment

The author gratefully acknowledges Dr. Brian Yamashita for his helpful suggestions and critical review of the manuscript.

References

1. R vs Legere. Supreme Court of Canada. Fredericton, New Brunswick, Canada. October 1991.
2. Anonymous. Donald Delbert Kett and William Chester Kett. RCMP Gazette 11:17–20 (1949).
3. McCafferty JD. The shoe fits. The Police Journal, London 28:135–139 (1955).
4. Hofstede, JC. Convicted by his shoes. RCMP Gazette 27:6–11 (1965).
5. Smerecki CJ, Lovejoy CO. Identification via pedal morphology. Identification News 35:5–12 (1985).
6. Bodziak WJ. Footwear impression evidence. Boca Raton, Fla: CRC Press; 2000:381–411.
7. Cassidy MJ. Footwear identification. Ottawa, Canada: Canadian Government Printing Centre; 1980.
8. Puri DKS. Footprints. International Criminal Police Review 187:106–111 (1965).
9. Qamra SR, Sharma BR, Kaila P. Naked foot marks: a preliminary study of identification factors. Forensic Sci Int 16:145–152 (1980).
10. Topinard P. L'Anthropologie. Vol. 1, 2nd ed. Paris, France: Reinwald; 1877.
11. Gordon CC, Buikstra JE. Linear models for the prediction of stature from foot and boot dimensions. J Forensic Sci 37:771–782 (1992).
12. Barker SL, Scheuer JL. Predictive value of human footprints in a forensic context. Med Sci Law 38:341–346 (1998).
13. Baba K. Foot measurements for shoe construction with reference to the relationship between foot length, foot breadth, and ball girth. J Human Ergol 3:149–156 (1975).
14. Hawes MR, Sovak D, Miyashita M, Kang SJ, Yoshihuku Y, Tanaka S. Ethnic differences in forefoot shape and the determination of shoe comfort. Ergonomics 37:187–196 (1994).
15. Hawes MR, Sovak D. Quantitative morphology of the human foot in a North American population. Ergonomics 37:1213–1226 (1994).
16. Kouchi M. Analysis of foot shape variation based on the medial axis of foot outline, Ergonomics 38:1911–1920 (1995).
17. Mochimaru M, Kouchi M. Automatic classification of the medial axis of foot outline and its flexion angles, Ergonomics 40:450–464 (1997).
18. Laskowski GE, Kyle VL. Barefoot impressions: a preliminary study of identification characteristics and population frequency and their morphological features. J Forensic Sci 33:378–388 (1988).
19. Kennedy RB. Bare footprint marks. In: Siegel, JA, Saukko PJ, Knupfer GC, eds. Encyclopedia of forensic sciences. Vol 3. London: Academic Press; 2000:1189–1195.
20. Kennedy RB. Preliminary study on the uniqueness of barefoot impressions. Can Soc Forensic Sci J 29:233–238 (1996).
21. Kennedy RB. Uniqueness of bare feet and its use as a possible means of identification. Forensic Sci Int 82:81–87 (1996).

22. Kennedy RB, Pressman IS, Chen S, Petersen PH, Pressman AE. Statistical analysis of barefoot impressions. J Forensic Sci 48:55–63 (2003).
23. Bodziak WJ. Footwear Impression Evidence. Boca Raton: CRC Press; 2000:384.
24. Massey SL. Persistence of creases of the foot and their value for forensic identification purpose. J Forensic Identification 54:296–315 (2004).
25. Richard JC. Case Law: Ontario Superior Court, R vs Arcuri, Identification Canada 25:18–20 (2002).

Index

A

Adipocere, formation, 14
Age at death estimation,
  arthritic changes, 105
  bone remodeling, 103–105
  chemical changes, 105
  fetal measurements, 100, 101
  infancy through adolescents, 101, 102
  ossification center appearance
    and epiphyseal union, 102, 103
  overview, 99, 106
  radiography, 105
Amino acids, isomerization in age at death
  estimation, 105
Animal bites, children, 245
Ankle, *see also* Foot,
  structural features, 254
  traffic injury,
    mechanisms,
      pedestrian trauma, 327, 329–332
      bicycle accidents, 333
      drivers and passengers, 333, 334
      motorcycle accidents, 338
    reconstruction, 324–326
Arthritis, age at death estimation, 105
Autolysis, biochemical processes
  in decomposition, 6–11
Aviator's foot, radiography, 144, 197, 198

B

Barefoot impression evidence, *see* Forensic
  podiatry
Bicycle accidents, knee and ankle joint
  injury mechanisms, 333
Biomechanics,
  bone composition, 280–282
  falls,
    gait determinants, 346–349
    macroslip, 349–351, 354
    prospects for study, 354, 355
  foot types, 383, 384
  fracture patterns and injury mechanism,
    bone integrity effects, 303–305
    case studies, 305–308
    impact energy, 303
    loading scenarios,
      axial loading, 297
      bending, 289–297
      tension, 289
      torsion, 297–300, 302, 303
    overview, 288, 289
  historical perspective of lower extremity
    studies, 286–288
  pedestrian trauma example, 279, 280
  physics of movement, 282–284
  scoring and holing studies of bone
    strength effects, 294–297
  stress-risers, 294, 295
  stress–strain curve, 284–286
Blunt force trauma, *see also* Falls,
  child abuse, 246, 261–264
  homicidal assault, 261
  motor vehicle accidents,
    automobiles, 264–266
    children, 243, 244
    motorcycles, 266, 267
    pedestrian trauma, 243, 267, 268
  plane accidents, 268, 269
  skeletal trauma analysis, 269, 270
  train accidents, 268
Bone-in-bone phenomenon, radiography,
  151, 152
Bone island, radiography, 159–161
Bone remains, *see* Skeletal remains
Bone remodeling, age at death estimation,
  103–105
Bumper fracture, radiography, 145, 200
Bunions, forensic podiatry, 384, 385

C

Caffey's disease, radiographic findings, 191

Calcaneus, stature estimation, 74, 88
Child trauma,
  abuse,
    blunt trauma, 246, 261–264
    burns and scalds, 246
    mimicking conditions,
      bone disorders, 247
      dermatologic disease, 247–250
      infection, 247
      radiography, 142, 185–192
    penetrating trauma, 246
    radiography, 118, 140–142, 171–180
  causes and age of hospital admission 241, 242
  hair tourniquet syndrome, 250, 251
  lower extremities, 241–243
  unintentional injury,
    animal bites, 245
    falls, 244
    mangled extremity, 244, 245
    motor vehicle accidents, 243, 244
    overview, 242
    pedestrian trauma, 243
Chinese bound-foot deformity, radiography, 169
Chiropractor, case study of fracture, 305
Clubfoot deformity, identification of unknown remains, 136,, 141
Computed tomography (CT),
  falaca findings, 206
  palmatoria findings, 147, 202–205
CT, *see* Computed tomography

D

Decollement, skin detachment, 318, 319
Decomposition,
  adipocere formation, 14
  autolysis, 6–11
  factors affecting biochemical processes, 14
  liver mortis, 11, 12
  mummification, 14
  overview, 3–5
  putrefaction, 12–14
  rigor mortis, 11
  sequence, 5, 6
Dismemberment, skeletal trauma analysis, 271, 272

E

EB, *see* Epidermolysis bullosa
Ehlers-Danlos syndrome, dermatologic complications, 250
Elbow, capping in torture, 212
Elderly abuse, radiography, 143
Epidermolysis bullosa (EB), clinical features, 247, 248
Epiphyses, age at death estimation, 102, 103

F

Fabella, anatomy, 46–48
Falaca, radiographic findings, 147, 206, 207
Falls,
  biomechanics,
    gait determinants, 346–349
    macroslip, 349–351, 354
    prospects for study, 354, 355
  children, 244
  epidemiology, 343
  friction testing, 344–346
  slips, 343
  tribology, 344–346
Femur,
  age at death estimation,
    amino acid isomerization, 105
    bone remodeling, 104
    fetal body length estimation, 100
    infancy through adolescence, 101
    ossification center appearance in development, 102
  anatomy,
    articular surfaces, 34
    condyles, 34–36
    epicondyles, 36–38
    intercondylar notch, 38
    overview, 18, 33, 34
    popliteal surface, 38, 39
  bending fracture, 293, 294
  bone islands, 159–161
  fibrous cortical defects, 162, 163
  fracture and radiography, 164, 171, 174, 177
  fragmentary remains, 22, 24
  knee injury and stress evidence, 50, 53, 54
  Legg-Calvé-Perthe disease, 150
  length variation, 21
  osteogenic sarcoma, 157
  positioning for X-ray,
    anterior view, 223, 224, 226, 227
    lateral view, 225, 226
  race determination, 73, 74, 87
  sex determination, 84–86
  stature estimation, 76–78, 88–90, 92–94, 133
  stress tolerance, 286
  traffic injury reconstruction, 326, 327
Fibrous dysplasia, radiography, 158

Fibula,
anatomy, 19, 44
bending fracture, 295
fetal body length estimation, 100
ossification center appearance in development, 102
ossification center appearance in development, 102
pseudoarthrosis, 145
stature estimation, 92–94, 133
Foot,
anatomy, 19, 380–383
anthropology,
death investigation examples,
biographic profiling for identification, 360, 361
fireworks factory explosion, 362, 363
plane crashes, 363, 365, 366, 369–371
train crashes, 368, 369
historical perspective, 359, 360
bones, 19
developmental radiology, 127–130
fetal body length estimation from first metatarsal, 101
footwear and print evidence, *see* Forensic podiatry
heel pad thickness measurement, 132, 133
Madura foot, 153
melorheostosis of bones, 147
neurogenic destruction, 149
ossification center appearance in development, 102
pedal injury patterns, *see* Pedal injury patterns
plantar fascia attachment site calcification, 153
positioning for X-ray,
anterior view, 231, 232
lateral view, 233, 235
recovery of specimens, 370–372
sex determination from tarsals, 87
size trends, 387
stature determination from metatarsals, 89
structural features, 254
Forensic podiatry,
barefoot impression evidence,
boot matching with foot, 401–403
historical perspective, 403, 404
individualizing features, 404
measurement of footprints, 404–407
research prospects, 412
biomechanical foot types, 383, 384
case examples, 396, 397, 401–404, 407–411
crime scene handling guidelines, 377–380
evaluation principles,
ACE-V, 391
analysis of questioned item, 391
certainty levels, 396
class characteristics, 390, 391
comparison and evaluation, 395, 396
individual characteristics, 390, 391
known standard fabrication, 393–395
pedal evidence and forensic considerations, 391–393
evidence types, 389
foot anatomy and classification, 380–383
forensic team role, 390
glossary of terms, 397–399
historical perspective, 375–377, 403
pathology, 384–386
professional organizations, 377
shoe types and components, 387–389
Fracture, *see also specific bones and traumas,*
biomechanics, *see* Biomechanics
blunt force trauma in child abuse, 261–264
radiography, *see* Radiography
tension line visualization, 292, 295, 296
timing and mechanism of trauma, 257–261
Fractures,
child abuse, 118, 140–142, 171–180
radiography of healed fractures, 137, 164, 174
Fully method, stature estimation, 75

G

Gait, determinants, 346–349
Gunshot injuries,
radiographic findings,
caliber of bullets, 149, 150, 213
identification of bullet type and composition, 151, 155, 159, 215–220
localization, 150, 151, 213, 214
number of bullets, 149
skeletal trauma analysis, 272, 273

H

Hair tourniquet syndrome, features, 250, 251
Hammer toe deformity, forensic podiatry, 385

J

Juvenile rheumatoid arthritis, radiography, 155, 156

K

Kerley method, age at death estimation, 103, 104
Knee,
  bones, *see* Fabella; Femur; Patella; Tibia
  developmental radiology, 126
  intercondylar shelf angle, 131, 132
  osteopoikilosis, 148
  positioning for X-ray,
    anterior view, 223, 224, 226, 227
    lateral view, 225, 226
  skeletal evidence of injury and stress, 48–54
  traffic injury,
    mechanisms,
      bicycle accidents, 333
      drivers and passengers, 333, 334
      motorcycle accidents, 338
      pedestrian trauma, 327, 329–332
    reconstruction, 322–324
Knee capping, radiographic findings, 147, 149, 208–211

L

Lawnmower, pediatric injury, 244, 245
Legg-Calvé-Perthe disease, radiography, 150
Leukemia, radiographic findings, 192
Lisfranc lesion, radiography, 145, 199
Liver mortis, biochemical processes in decomposition, 11, 12

M

Madura foot, radiography, 153
Magnetic resonance imaging (MRI),
  bone island of femur, 160
  fibrous cortical defects of femur, 163
Meningococcemia, clinical manifestations, 247
Menkes disease, radiographic findings, 189
Messerer's fracture, traffic accidents, 320, 321
Metaphyseal cupping, radiography, 140, 176
Metaphyseal fracture, infant abuse, 172, 173
Motor vehicle accidents (MVAs),
  automobile drivers and passengers, 264–266
  children, 243, 244
  motorcycles, 266, 267
  pedestrian trauma, 243, 267, 268
Motorcycles, *see* Motor vehicle accidents
Motor vehicle accidents (MVAs),
  automobiles, 264–266
  bicycle collisions, *see* Bicycle accidents
  biological markers,
    evidential value, 313, 314
    lower extremity injury analysis findings, 314
  reconstruction parameters, 312, 313
  children, 243, 244
  collision speed determination from injuries, 338
  incidence, 311, 312
  knee and ankle joint injuries,
    mechanisms,
      bicycle accidents, 333
      drivers and passengers, 333, 334
      motorcycle accidents, 338
      pedestrian trauma, 327, 329–332
    reconstruction, 322–324
  lower extremity injury analysis in reconstruction,
    ankle injury, 324–326
    external injuries, 314–316
    femoral proximal epiphysis injury, 326, 327
    knee injury, 322–324
    long bone fracture, 320–322
    soft tissue injuries, 316, 318, 320
  motorcycles, 266, 267
  pedestrian trauma, *see* Pedestrian trauma
  physics of movement, 282–284
  seatbelt case study, 306–308
MRI, *see* Magnetic resonance imaging
Mummification, biochemical processes in decomposition, 14
MVAs, *see* Motor vehicle accidents

N

Natural objects, confusion of bones with, 22, 23, 26

O

OI, *see* Osteogenesis imperfecta
Osgood–Schlatter disease, skeletal analysis, 54, 67
Osteogenesis imperfecta (OI),
  radiography, 142, 185
  rarity, 247
  types and causes, 247
Osteogenic sarcoma, radiography, 157
Osteomalacia, radiographic findings, 187
Osteomyelitis,
  osteomyelitis of Garré, 154
  radiographic findings, 190

P

Palmatoria, radiographic findings, 147, 201–205

Patella,
anatomy, 18, 45, 46
dorsal defect, 136, 138–141
knee injury and stress evidence, 54
tension fracture, 289–291
Pedal injury patterns,
aviator's foot, 144, 197, 198
bumper fracture, 145, 200
classification, 143, 144
Lisfranc lesion, 145, 199
talar injury, 193–196
Pedestrian trauma,
biological markers,
evidential value, 313, 314
lower extremity injury analysis findings, 314
reconstruction parameters, 312, 313
cadaver study, 279, 280
case examples of reconstruction from injuries, 305, 306, 339–341
children, 243
collision speed determination from injuries, 338
incidence, 311, 312
knee and ankle joint injuries,
mechanisms, 327, 329–332
reconstruction, 322–324
lower extremity injury analysis in reconstruction,
ankle injury, 324–326
external injuries, 314–316
femoral proximal epiphysis injury, 326, 327
knee injury, 322–324
long bone fracture, 320–322
soft tissue injuries, 316, 318, 320
skeletal trauma analysis, 267, 268
Pediatrics, *see* Child trauma
Pelligrini-Stieda disease,
radiography, 169
skeletal analysis, 54, 60
Penetrating trauma,
child abuse, 246
skeletal trauma analysis, 270, 271
Plane accidents,
foot identification and analysis, 363, 365, 366, 369–371
skeletal trauma analysis, 268, 269
Putrefaction, biochemical processes in decomposition, 12–14

R

Race, determination from lower extremity analysis, 72–74, 87
Radiography,
age at death determination, 105, 122, 123, 125
equipment for X-rays,
cassettes, 168
film, 165, 168
mobile unit, 160
film,
documentation, 171
exposure, 171, 173, 221
handling, 165
processing, 168, 171
foreign bodies in bone, 139, 170
gunshot wounds,
caliber of bullets, 149, 150, 213
identification of bullet type and composition, 151, 155, 159, 215–220
localization, 150, 151, 213, 214
number of bullets, 149
historical perspective, 113–121
human versus animal remains, 122
identification of unknown remains,
developmental and congenital variations, 135, 136
disease or degenerative change, 137, 138
mass casualties, 139, 140
overview, 135
statistical considerations, 135
trabecular patterns and vascular grooves, 138
orthopedic materials, 138, 167
osteogenesis imperfecta, 142, 185
pattern injuries,
abuse,
adults, 142
child abuse, 118, 140–142, 171
elderly, 143
pedal injury patterns, 143–146, 194–200
torture and terrorism, 147–149, 201–212
positioning,
foot,
anterior view, 231, 232
lateral view, 233, 235
hip, 221, 222
lower leg,
anterior view, 228, 229
lateral view, 230
overview, 173
thigh or knee,
anterior view, 223, 224, 226, 227
lateral view, 225, 226

sex determination, 123, 125, 126, 130, 132
skeletal remains and documentation, 28, 29
spiral fractures, 298–300
Rigor mortis, biochemical processes in decomposition, 11
Rubella, radiographic findings, 186
Ruxton murder case, history of radiology, 118, 119

S

Scanogram, long bone length measurement, 134, 135
Scurvy, radiographic findings, 188
Sex, determination from lower extremity analysis, 70–72, 84–87, 123, 125, 126, 130, 132
Shoes,
components, 387–389
footwear evidence, *see* Forensic podiatry
proper sizing, 386, 387
types, 387
SJS, *see* Stevens-Johnson syndrome
Skeletal remains, *see also specific bones,*
age at death estimation,
arthritic changes, 105
bone remodeling, 103–105
chemical changes, 105
fetus, 100, 101
infancy through adolescents, 101, 102
ossification center appearance and epiphyseal union, 102, 103, 125
overview, 99, 106
radiography, 105
algorithm for forensic analysis, 22, 23
archaeologic findings, 26, 27
cleaning, 255, 256
confusion of bones with natural objects, 22, 23, 26
definitions,
damage, 256
defects, 256
fractures, 256
injury, 256
insult, 256
documentation, 28–30
heating and tension line visualization, 292, 295, 296
human versus animal remains, 26
missing person matching, 30
photography, 256
race determination, 72–74, 87
reconstruction, 256
recovery and transport, 27, 28
sex determination, 70–72, 84–87
stature determination, 74–83, 88–94
timing of trauma, 257–261
Skeleton, *see also specific bones*,
anatomy overview in forensics, 18, 19
bone composition, 280–282
embryology, 20–22
radiography, *see* Radiography
Slips, *see* Falls
Smith v. Grant, history of radiology, 115–117
Spiral fracture,
radiography and analysis, 298–300
traffic accidents, 321, 322
Stature, determination from bones,
aging loss considerations, 81, 82
decompositional process effects, 83
errors in living measurement and reporting, 79–81
fragmentary bone analysis, 79
Fully method, 75
lower extremity analysis, 75–79
overview, 74, 79–83
Stevens-Johnson syndrome (SJS), dermatologic complications, 248, 249
Stress–strain curve, generation and analysis, 284–286
Synovium, knee injury and stress evidence, 51
Syphylis, radiographic findings, 192

T

Thigh,
positioning for radiography,
anterior view, 223, 224, 226, 227
lateral view, 225, 226
structural features, 254
Tibia,
anatomy,
articular surfaces, 40, 41
condyles, 42, 43
overview, 18, 19, 39
posterior surface, 43, 44
tuberosity, 42
bending fracture, 293–295
fetal body length estimation, 100
fracture in child abuse, 178
fragmentary remains, 22, 25
knee injury and stress evidence, 50, 54
kyphoscoliosis, 145
length variation, 22
melorheostosis, 146
ossification center appearance in development, 102
periostitis in Caffey's disease, 191

positioning for X-ray,
anterior view, 228, 229
lateral view, 230
race determination, 73, 74
sex determination, 71, 86
stature estimation, 88, 90–94, 133
stress tolerance, 286, 287
Toddler's fracture, radiography, 141, 183, 184
Traffic accidents, *see* Bicycle accidents; Motor vehicle accidents; Pedestrian trauma
Train accidents,
foot identification and analysis, 368, 369
skeletal trauma analysis, 268
Tribometry, friction testing, 344–346

V

Viscoelasticity, definition, 286

X

X-ray, *see* Radiography